UNIVERZITA KARLOVA V PRAZE

LÉKAŘSKÁ FAKULTA V PLZNI

ŠIKLŮV ÚSTAV PATOLOGIE

DOKTORSKÁ DIZERTAČNÍ PRÁCE

VZÁCNÉ NÁDORY UROGENITÁLNÍHO TRAKTU, JEJICH BIOLOGICKÉ CHOVÁNÍ, MORFOLOGIE A CYTOGENETIKA

MUDr. KVĚTOSLAVA MICHALOVÁ

ŠKOLITEL: Prof. MUDr. ONDŘEJ HES, Ph.D.

PLZEŇ 2017

PŘEDMLUVA

Nádory ledvin se vyznačují velkou morfologickou heterogenitou, jsou tvořeny směsicí světlých, granulárních nebo vřetenitých buněk a jejich fenotyp se může s růstem tumorů dokonce měnit [1]. Vzhled tumorů tudíž nemusí odpovídat předpokládané progenitorové buňce a založit diagnózu pouze na morfologickém vzhledu se ukázalo být nespolehlivé [1]. Rozvoj genetiky umožnil porozumění molekulárním vlastnostem renálních nádorů, navíc začalo být jasné, že genetický podklad má vliv nejen na histopatologický vzhled tumorů, ale i na jejich biologické chování [1]. Heidelbergská klasifikace, publikována v roce 1997, byla historicky první klasifikací, která kromě morfologických vlastností zavzala též znaky molekulárně biologické [2]. Týkala se pouze epitelových tumorů a byla postavena na aktuálních genetických znalostech, které korelovala s histologickým obrazem. Obsahovala 8 nádorových jednotek a pro každou z nich se snažila zmapovat nejčastěji dokumentované genetické odchylky.

Krátce poté byla v roce 1998 publikována WHO klasifikace nádorů ledvin, navržená UICC (Union Internationale Contre le Cancer; International Union Against Cancer) a AJCC (American Joint Committee on Cancer). Zahrnovala 10 neoplastických jednotek a v podstatě nepřinesla žádné nové poznatky, byla velmi podobná Heidelbergské klasifikaci a nebyla nikdy přijata.

Od dob vzniku Heidelbergské klasifikace a WHO klasifikace 1998 bylo publikováno několik prací, které se zabývaly molekulárně genetickými vlastnostmi renálních tumorů. Avšak šlo povětšinou o práce publikované na malém souboru pacientů a s použitím omezené genetické metodiky, která byla toho času dostupná. Výsledky těchto prací byly proto nekonzistentní a genetické poznatky o nádorech ledvin nedostačující. Přesto však v oblasti renální nádorové patologie docházelo k obohacení poznatků a v roce 2004 byla vydána další WHO klasifikace nádorů ledvin. Ta již zahrnovala 12 nádorových jednotek. Přibližně od doby vzniku této klasifikace došlo k obrovskému rozvoji genetického a morfologického poznání vedoucího k popisu mnoha nových jednotek, variant a podtypů stávajících. Následující, čtvrtá edice WHO klasifikace, vyšla v roce 2016 a obsahuje již 16 nádorových jednotek.

Čím více poznatků získáváme z výzkumů publikovaných velkými institucemi na velkém souboru pacientů, tím více začíná být zřejmé, že snaha co nejpřesněji popsat a zmapovat podtypy renálních nádorů má pro pacienta prognostický význam. Hlubší poznání patogenetických mechanismů vzniku nádorových onemocnění spolu s pokroky molekulární genetiky umožnily v onkologii postupné zavádění nových léčebných metod. Ačkoliv protinádorová chemoterapie zůstává dodnes nepostradatelnou léčebnou metodou, je zaměřena převážně na proliferaci a apoptózu, a to nespecificky, neboť kromě patologického klonu postihuje i normální proliferující buňky. Tzv. targeted terapie cíleně zasahuje do patogenetických mechanismů specifických pro jednotlivé nádorové jednotky, a tyto patogenetické mechanismy mohou být identifikovány právě díky znalosti genetického podkladu nádorů [3]. Přes počáteční optimismus bohužel zatím targeted terapie nepřinesla očekávané výsledky, přesto věříme, že snaha co nejpřesněji popsat a zmapovat podtypy renálních nádorů má smysl a klinický potenciál.

V roce 2016 vyšla nová WHO klasifikace i pro nádory varlat. V této oblasti jsme zatím nezaznamenali tak výraznou syntézu genetiky a morfologie [4]. Převážná většina testikulárních tumorů je germinálního původu, sex-cord stromální tumory či epitelové tumory jsou raritní. Vzácnost a spletitost non-germinálních testikulárních tumorů z nich často činí i pro patologa se specializací na urogenitální oblast diagnosticky obtížné případy. Stejně jako v

jiných oblastech je však správná diagnóza stěžejní pro další léčebný postup a proto je důležité rozšiřovat znalosti i méně častých jednotek.

Doktorská dizertační práce se zabývá morfologií, molekulární genetikou a klinickým chováním neobvyklých tumorů urogenitálního traktu se speciálním zaměřením na nádory ledvin, ve snaze přesně definovat jednotlivé podskupiny. Téma bylo řešeno s využitím znalostí morfologických znaků vzácných nádorů urogenitálního traktu, na jejichž podkladě byly nádorové jednotky vybírány do studií a tyto byly dále vyšetřovány s použitím imunohistochemických a molekulárně genetických metod.

Výsledkem je 7 prvoautorských prací, z nichž většina se týká nádorů ledvin (5 prvoautorských publikací), zvláště v poslední době se autorka zaměřila i na problematiku nádorů varlat (2 prvoautorské publikace). Dále se autorka podílela jako spoluautor na 13 publikacích. Všech 20 prací bylo publikováno v zahraničních odborných časopisech s impact faktorem. Dizertační práce je vypracována formou souhrnu komentovaných publikací, všechny práce jsou samostatně krátce představeny. Od všech publikací je přiložena kopie reprintu (19 prací) nebo text práce s dokladem o přijetí k publikaci (1 práce).

První a rozsáhlejší část se týká nádorů ledvin, druhá nádorů varlat, přičemž prvoautorské publikace jsou spoluautorským předřazeny.

PROHLÁŠENÍ

Prohlašuji, že jsem dizertační práci zpracovala samostatně a řádně uvedla a citovala všechny použité zdroje. Souhlasím s trvalým uložením elektronické verze své práce v databázi UK LF Plzeň.

V Plzni, dne 25.7. 2017

ABSTRAKT

Doktorská dizertační práce popisuje biologické chování, morfologii a cytogenetiku neobvyklých tumorů urogenitálního traktu se speciálním zaměřením na nádory ledvin, které byly podkladem postgraduálního studia MUDr. Květoslavy Michalové (rozené Peckové) na Univerzitě Karlově v Praze, Lékařské fakultě v Plzni, v období let 2014 – 2017. Autorka se ve své publikační činnosti zaměřila na problematiku vzácných tumorů urogenitálního traktu. Výsledky tříletého výzkumu jsou prezentovány ve formě komentovaného souhrnu celkem 20 prací. Sedm prací vypracovala autorka jako hlavní autor a ve stručnosti je zde představuje.

První publikovaná prvoautorská práce „Renální karcinom s leiomyomatózním stromatem – další imunohistochemická a molekulárně genetická studie neobvyklé jednotky" se zabývala vztahem renálního karcinomu (RK) s leiomyomatózním stromatem (LS) k světlobuněčnému RK s reaktivním LS. Došla k závěru, že tyto dvě jednotky je možné odlišit pouze genetickou analýzou mutace genu *VHL*, *VHL* hypermetylace a ztráty heterozygozity na krátkém raménku 3. chromozomu (LOH 3p), přičemž "pravý" RK s LS tyto změny postrádá a světlobuněčný RK definují. "Pravý" RK s LS se zdá být indolentním tumorem s doposud nepopsaným agresivním případem, zatímco světlobuněčný RK je biologicky relativně nepříznivý a odlišení těchto dvou jednotek je důležité.

V druhé studii nazvané "Agresivní a neagresivní translokační t(6;11) renální karcinom: srovnávací studie 6 případů a přehled literatury" jsme na základě klinicko-patologických údajů, morfologických znaků, IHC, molekulární genetiky a rešerše literatury porovnávali neagresivní tumory s jedním agresivním. Zjistili jsme, že agresivní tumory se, na rozdíl od neagresivních, vyskytují u starší populace, mají makroskopicky viditelné nekrózy, často nemají morfologii typickou pro neagresivní tumory a molekulárně geneticky vykazují kromě translokace genu *TFEB* i jeho amplifikaci.

Ve třetí práci s názvem „Mucinózní tubulární a vřenetobuněčný renální karcinom: analýza chromozomálních aberací u low-grade, high-grade a morfologické varianty podobné papilárnímu renálnímu karcinomu" jsme se zaměřili na analýzu spektra chromozomálních aberací vyskytujících se u různých morfologických variant této vzácné jednotky. Zjistili jsme, že low-grade i high-grade varianta je cytogeneticky relativně uniformní (mnohočetné chromozomální ztráty), zatímco u některých případů napodobujících papilární RK jsme detekovali nadpočetné chromozomy 7 a 17 a u těchto jsme následně změnili diagnózu na papilární RK. U případů s atypickou morfologií, zvláště jedná-li se o tumory napodobující papilární RK, je tedy nezbytné provést chromozomální analýzu a v případě detekce nadpočetných chromozomů 7 a 17 by tyto tumory měly být překlasifikovány.

Do čtvrté studie s názvem „Chromofobní renální karcinom s neuroendokrinními znaky a znaky napodobujícími neuroendokrinní diferenciaci. Morfologická, imunohistochemická a ultrastrukturální studie a array komparativní genová hybridizace u 18 případů, přehled literatury" bylo vybráno 18 případů chromofobních renálních karcinomů (CHRK) s neuroendokrinními (NE) znaky, které byly na základě pozitivity/negativity NE markerů rozděleny do dvou skupin: 4 případy CHRK s „opravdovou" NE diferenciací a 14 případů CHRK se znaky napodobující NE diferenciaci. Je zřejmé, že ve většině případů CHRK s NE znaky se jedná pouze o růstovou variantu CHRK a nikoliv o pravou NE diferenciaci. Obě skupiny se liší molekulárně geneticky, ale i biologickým chováním („pravé" CHRK s NE diferenciací mají metastatický potenciál) a jejich odlišení tak má klinický význam.

Práce nazvaná „Cystický a nekrotický papilární renální karcinom: prognostický, morfologický imunohistochemický a molekulárně genetický profil 10 případů" je pátou

prvoautorskou studií v pořadí. Protože přítomnost nekrózy u RK (zvláště světlobuněčných) je všeobecně uznávána jako nepříznivý prognostický faktor, cílem této studie bylo demonstrovat, že papilární RK typu 1 se může vzácně prezentovat jako objemná cystická léze vyplněná hemoragickou/nekrotickou hmotou a že tento vzhled nic nemění na biologickém chování. Tato studie si však neklade za cíl ustanovit nová prognostická kritéria pro typ 1 papilární RK, jejím záměrem bylo vybrat skupinu morfologicky uniformních papilárních RK typu 1 s neobvyklými makroskopickými a mikroskopickými znaky a upozornit na fakt, ze nekróza u těchto typu tumorů nemá pravděpodobně prognostický význam.

Šestá a sedmá prvoautorská publikace se týká již nádorů varlat a obě souvisejí s jedním tématem, budou proto představeny najednou. Šestá publikace nazvaná "Primární stromální tumor varlete z prstenčitých buněk: studie 13 případů dokazující jejich fenotypickou a genotypickou obdobu s pankreatickým solidní pseudopapilárním tumorem" a sedmá s názvem "Solidní pseudopapilární tumor: nová nádorová jednotka ve varleti?-Odpověď" se zabývají problematikou analogie primárních stromálních tumorů varlete z prstenčitých buněk (PSTVPB) a solidních pseudopapilárních tumorů (SPT) pankreatu. Ve zkratce jde o to, že nás na základě jednoho případu tumoru varlete, který se histologicky skládal z komponenty identické jako solidní pseudopapilární tumor (SPT) pankreatu a komponenty identické jako PSTVPB napadlo porovnat tento případ se SPT pankreatu. Výsledkem byla imunohistochemická i molekulárně genetická shoda, což nás společně s morfologickým překryvem opravňovalo považovat tento tumor za "pankreatický analog solidního pseudopapilárního tumoru ve varleti" (PA-SPT) [5]. Díky přítomnosti komponenty identické s primárním stromálním tumorem varlete z prstenčitých buněk (PSTVPB) jsme se dále rozhodli zjistit, zda neexistuje spojitost i mezi PSTVPB a SPT pankreatu. V šesté publikaci jsme porovnali 13 případů PSTVPB s jedním případem PA-SPT a 19 případy SPT pankreatu. Jak imunoprofil, tak výsledky molekulární genetiky byly ve všech vyšetřovaných tumorech shodné, z čehož usuzujeme, že PA-SPT a PSTVPB reprezentují morfologické spektrum stejné jednotky a že obě skupiny mají vztah k SPT pankreatu. Náš koncept byl podpořen skupinou italských autorů, kteří reagovali na prvopopis PA-SPT. Formou dopisu editorovi přidali 2 případy testikulárních tumorů ve všech aspektech shodných s námi popisovanými případy a podpořili tak naši hypotézu, že PA-SPT a PSTVPB reprezentují distinktní jednotku analogickou SPT pankreatu. Sedmá publikace je odpovědí na tento dopis editorovi.

SUMMARY

Current doctoral thesis is dealing with biological behavior, morphology and cytogenetical features of rare urogenital tumors with a particular emphasis on renal tumors. Dr. Kvetoslava Michalova (birth name Peckova) was focused on this topic during her postgradual study at Charles University in Prague, Medical Faculty in Pilsen, in years 2014-2017. In her publication activity, the author focused on rare tumors of urogenital tract. The 20 publications published over a span of three years are presented in a form of a commentary. Seven of them are first-author papers and these are briefly introduced below.

The first paper entitled "Renal cell carcinoma with leiomyomatous stroma-further immunohistochemical and molecular genetic characteristics of unusual entity" dealt with the relationship between renal cell carcinoma (RCC) with leiomyomatous stroma (LS) and clear cell RCC with reactive LS. It led to the conclusion, that only genetic analysis of *VHL* gene mutation, *VHL* hypermatylation and chromosome 3p loss of heterozygosity can be used as a distinguishing tool. The „real" RCC with LS lack the above described genetic abnormalities which is in contrary to the clear cell RCC, which is characterized by them. The distinction between these two entities is of clinical importance, as the „real" RCC with LS seems to be an indolent tumor as no aggressive cases have been described to date whereas clear cell RCC may have unfavourable outcome.

In the second study termed „Aggressive and nonaggressive translocation t(6;11) renal cell carcinoma: comparative study of 6 cases and review of the literature" we compared nonaggressive tumors with one aggressive case. We based our conclusions on clinico-pathological data, morphological features, IHC, molecular genetics and literature review. Eventually, the conclusion was that aggressive tumors, in contrary to the nonaggressive cases, occur in older population, have grossly visible necroses, usually lack morphology typical for nonaggressive tumors and in addition to translocation of *TFEB* gene, they are also *TFEB* amplified.

The third study entitled „Mucinous spindle and tubular renal cell carcinoma: analysis of chromosomal aberration pattern of low-grade, high-grade, and overlapping morphologic variant with papillary renal cell carcinoma" was aimed to map the spectrum of chromosomal aberations occuring in different morphological variants of this rare antity. This study has shown that both low-grade and high-grade variant are cytogeletically relatively unifrom (multiple chromosomal losses). However, some cases resembling papillary RCC exhibited gains of chromosomes 7 and 17 and we consequently rediagnosed them as papillary RCC. Chromosomal analysis is thus essential in atypical cases, especially in those morphologically close to the papillary RCC. If polysomy 7 and 17 is found, such cases should not be classified as mucinous spindle and tubular RCC, but as papillary RCC.

Eighteen cases of chromophobe renal cell carcinoma (CRCC) with neuroendocrine (NE) features were selected to the fourth study named "Chromophobe renal cell carcinoma with neuroendocrine and neuroendocrine-like features. Morphologic, immunohistochemical, ultrastructural, and array comparative genomic hybridization analysis of 18 cases and review of the literature". The cases were divided into 2 groups based on their positivity/negativity with NE markers: 4 cases of CRCC with "true" NE differentiation and 14 cases of CRCC with features mimicking NE differentiation. It is evident, that the majority of CRCC with NE features represent just architectural variant and not real NE differentiation. Both groups have different genetic background and also biological behavior, which makes their distinguishing clinically important.

The study entitled "Cystic and necrotic papillary renal cell carcinoma: prognosis, morphology, immunohistochemical, and molecular-genetic profile of 10 cases" represents the fifth first-author paper. Because the presence of necrosis in RCC (especially in clear cell

RCC) is generally considered as an adverse prognostic feature, the goal of this study was to demonstrate that type 1 papillary RCC can present as a large hemorrhagic/necrotic unicystic lesion and that such appearance in this particular setting does not affect clinical course. However, the aim of the current study is not to establish the new prognostic criteria for type 1 papillary RCC, but rather to select morphologically uniform subset of type 1 papillary RCC with unusual gross and microscpic features and draw attention to the fact that necrosis in these tumor types does probably not have any prognostic significance.

The sixth and seventh publications are dealing with tumors of the testis and since they both are related to the same subject, they are discussed together. Sixth publication termed „Primary Signet Ring Stromal Tumor of the Testis: A Study of 13 Cases Indicating Their Phenotypic and Genotypic Analogy to Pancreatic Solid Pseudopapillary Neoplasm“ and seventh entitled „Solid Pseudopapillary Tumor: A New Tumor Entity in the Testis? Reply“ address the analogy between primary signet ring stromal tumors of the testis (PSRSTT) and solid pseudopapillary tumor (SPT) of the pancreas. Briefly, the fact that certain testicular tumors have an analogue in the pancreas became evident with the acquisition of one testiculart tumor, which was histologically composed of component identical to SPT of the pancreas and of component identical to PSRSTT. As a result, both IHC testing and molecular analysis of the testicular case revealed the same features as would be expected in pancreatic SPN which allowed us to consider this tumor „pancreatic analogue solid pseudopapillary tumor of the testis“ (PA-SPT) [5]. Owing to the very pronounced signet ring cell component in the PA-SPT we came to the idea that there might also be a connection between PSRSTT and SPT of the pancreas. In the 6th publication we compared 13 cases of PSRSTT with one case PA-SPT and 19 cases of pancreatic SPT. Both the immunoprofile anf molecular genetics were identical in all analyzable cases which led us to the conclusion that PA-SPT and PSRSTT represent the morphological spectrum of the same entity and that both of them are related to the pancreatic SPT. This concept was further strengthened by the group of italian authors who in the form of letter to editor reacted to the first description of PA-SPT. They reported another 2 cases of testicular tumors in all aspects identical to our cases and supported thus our hypothesis that PA-SPT and PSRSTT represent dictinct entity analogic to the pancreatic SPT. Seventh publication represents our reply to this letter to the editor.

OBSAH

PŘEDMLUVA ... 2

ABSTRAKT ... 4

SUMMARY ... 6

OBSAH ... 8

SEZNAM POUŽITÝCH ZKRATEK ... 10

SOUHRN KOMENTOVANÝCH PUBLIKACÍ ... 12

1. ČÁST ... 13

RENÁLNÍ KARCINOM S LEIOMYOMATÓZNÍM STROMATEM – DALŠÍ IMUNOHISTOCHEMICKÁ A MOLEKULÁRNĚ GENETICKÁ STUDIE NEOBVYKLÉ JEDNOTKY ... 14

AGRESIVNÍ A NEAGRESIVNÍ TRANSLOKAČNÍ t(6;11) RENÁLNÍ KARCINOM: SROVNÁVACÍ STUDIE ŠESTI PŘÍPADŮ A PŘEHLED LITERATURY ... 21

MUCINÓZNÍ TUBULÁRNÍ A VŘETENOBUNĚČNÝ RENÁLNÍ KARCINOM: ANALÝZA CHROMOZOMÁLNÍCH ABERACÍ U LOW-GRADE, HIGH-GRADE A MORFOLOGICKÉ VARIANTY PODOBNÉ PAPILÁRNÍMU RENÁLNÍMU KARCINOMU ... 29

CHROMOFOBNÍ RENÁLNÍ KARCINOM S NEUROENDOKRINNÍMI ZNAKY A ZNAKY NAPODOBUJÍCÍMI NEUROENDOKRINNÍ DIFERENCIACI. MORFOLOGICKÁ, IMUNOHISTOCHEMICKÁ A ULTRASTRUKTURÁLNÍ STUDIE A ARRAY KOMPARATIVNÍ GENOMOVÁ HYBRIDIZACE U 18 PŘÍPADŮ, PŘEHLED LITERATURY ... 36

CYSTICKÝ A NEKROTICKÝ PAPILÁRNÍ RENÁLNÍ KARCINOM: PROGNOSTICKÝ, MORFOLOGICKÝ, IMUNOHISTOCHEMICKÝ A MOLEKULÁRNĚ GENETICKÝ PROFIL 10 PŘÍPADŮ ... 45

LEIOMYOMATÓZNÍ STROMA V RENÁLNÍCH KARCINOMECH JE POLYKLONÁLNÍ A NIKOLIV SOUČÁSTÍ NEOPLASTICKÉHO PROCESU ... 54

SMÍŠENÝ EPITELOVÝ A STROMÁLNÍ TUMOR LEDVINY: MUTAČNÍ ANALÝZA *DICER 1* GENU U 29 PŘÍPADŮ ... 63

CYSTICKÝ RENÁLNÍ ONKOCYTOM A TUBULOCYSTICKÝ RENÁLNÍ KARCINOM: MORFOLOGICKÁ A IMUNOHISTOHEMICKÁ SROVNÁVACÍ STUDIE ... 69

„MUCIN“ SECERNUJÍCÍ PAPILÁRNÍ RENÁLNÍ KARCINOM: KLINICKOPATOLOGICKÁ, IMUNOHISTOCHEMICKÁ A MOLEKULÁRNĚ GENETICKÁ ANALÝZA SEDMI PŘÍPADŮ ... 78

WARTHINOVU TUMORU PODOBNÝ PAPILÁRNÍ RENÁLNÍ KARCINOM: KLINICKOPATOLOGICKÁ, MORFOLOGICKÁ, IMUNOHISTOCHEMICKÁ A MOLEKULÁRNĚ GENETICKÁ ANALÝZA 11 PŘÍPADŮ ... 89

BIFAZICKÝ SKVAMOIDNÍ ALVEOLÁRNÍ RENÁLNÍ KARCINOM. ZVLÁŠTNÍ PODTYP PAPILÁRNÍHO RENÁLNÍHO KARCINOMU? ... 99

SOLIDNÍ PAPILÁRNÍ RENÁLNÍ KARCINOM: KLINICKOPATOLOGICKÁ, MORFOLOGICKÁ A IMUNOHISTOCHEMICKÁ ANALÝZA 10 PŘÍPADŮ A PŘEHLED LITERATURY 113

MOLEKULÁRNĚ GENETICKÁ ANALÝZA JE NEZBYTNÁ PRO SPRÁVNOU DIAGNÓZU RENÁLNÍHO KARCINOMU NAPODOBUJÍCÍHO Xp11.2 TRANSLOKAČNÍ RENÁLNÍ KARCINOM 122

MORFOLOGICKÁ, IMUNOHISTOCHEMICKÁ A CHROMOZOMÁLNÍ ANALÝZA MULTICYSTICKÉHO CHROMOFOBNÍHO RENÁLNÍHO KARCINOMU, ARCHITEKTONICKY NEOBVYKLÉHO A DIAGNOSTICKY OBTÍŽNÉHO PODTYPU . 133

KOMPARATIVNÍ STUDIE MUTAČNÍ ANALÝZY GENU *TERT* MEZI VZORKY MOČI ZPRACOVANÝMI METODOU LIQUID BASED CYTOLOGIE A VZORKY TUMORŮ MOČOVÉHO MĚCHÝŘE ZPRACOVANÝMI STANDARDNÍ PARAFINOVOU TECHNIKOU 144

PŘÍTOMNOST PĚNITÝCH BUNĚK (NAPODOBUJÍCÍCH HIBERNOM) JE VZÁCNÝM RYSEM RENÁLNÍCH KARCINOMŮ 149

MOLEKULÁRNĚ GENETICKÉ ALTERACE V RENÁLNÍCH KARCINOMECH S TUBULOCYSTICKOU ARCHITEKTONIKOU: TUBULOCYSTICKÝ RENÁLNÍ KARCINOM, TUBULOCYSTICKÝ RENÁLNÍ KARCINOM S HETEROGENNÍ KOMPONENTOU A RENÁLNÍ KARCINOM ASOCIOVANÝ S HEREDITÁRNÍ LEIOMYOMATÓZOU. KLINICKOPATOLOGICKÁ A MOLEKULÁRNĚ GENETICKÁ STUDIE 15 PŘÍPADŮ. 160

2. ČÁST 171

PRIMÁRNÍ STROMÁLNÍ TUMOR VARLETE Z PRSTENČITÝCH BUNĚK: STUDIE 13 PŘÍPADŮ DOKAZUJÍCÍ JEJICH FENOTYPICKOU A GENOTYPICKOU OBDOBU S PANKREATICKÝM SOLIDNÍM PSEUDOPAPILÁRNÍM TUMOREM. 172

SOLIDNÍ PSEUDOPAPILÁRNÍ TUMOR: NOVÁ NÁDOROVÁ JEDNOTKA VE VARLETI? 200

CHORIOGONADOTROPIN POZITIVNÍ SEMINOM – KLINICKOPATOLOGICKÁ A MOLEKULÁRNĚ GENETICKÁ STUDIE 15 PŘÍPADŮ 203

ZÁVĚR 210

PODĚKOVÁNÍ 211

REFERENCE 212

SEZNAM POUŽITÝCH ZKRATEK

aCGH – array komparativní genová hybridizace

ACN – adultní cystický nefrom

AJCC - American Joint Committee on Cancer

AT – agresivní tumor

BSARK – bifazický skvamoidní alveolární renální karcinom

CGB – beta pojednotka lidského choriogonadotropinu

CHRK – chromofobní renální karcinom

CRCC - chromophobe renal cell carcinoma

EN – epiteloidní nefroblastom

FISH – fluorescenční in situ hybridizace

hCG – human chorionic gonadotropin; lidský choriogonadotropin

IHC – imunohistochemie, imunohistochemický

ISUP - International Society of Urological Pathology

LBC – liquid based cytologie

LOH 3p – ztráta heterozygozity (loss of heterozygozity) na krátkém raménku 3. chromozomu

LS – leiomyomatózní stroma; leiomyomatous stroma

MA – metanefrický adenom

MTVRK – mucinózní tubulární a vřetenobuněčný renální karcinom

NAT – neagresivní tumor

NE – neuroendokrinní; neuroendocrine

NOS – not otherwise specified

NGS – next generation sequencing

OPRK – onkocytický papilární renální karcinom

PA – papilární adenom

PA-SPT - pankreatický analog solidního pseudopapilárního tumoru paratestikulární oblasti

PCN – pediatrický cystický nefrom

PCR – polymerase chain reaction, polymerázová řetězová reakce

PRK – papilární renální karcinom

PSRSTT - primary signet ring stromal tumors of the testis

PSTVPB - primární stromální tumor varlete z prstenčitých buněk

RAT – renální angiomyoadenomatózní tumor

RCC – renal cell carcinoma

RK – renální karcinom

RKLS – renální karcinom s leiomyomatózním stromatem

RO – renální onkocytom

RT-PCR – polymerázová řetězová reakce spojená s reverzní transkripcí

SEST – smíšený epitelový a stromální tumor ledviny

SoPRK – solidní papilární renální karcinom

SoOPRK - solidní onkocytický papilární renální karcinom

SPRK – světlobuněčný papilární renální karcinom

SPT – solidní pseudopapilární tumor; solid pseudopapillary tumor

ST – syntitiotrofoblasty

TCRK – tubulocystický renální karcinom

TIL – tumor infiltrující lymfocyty

TRK – translokační renální karcinom

UICC - Union Internationale Contre le Cancer; International Union Against Cancer

WPRK – Warthinovu tumoru podobný (Warthin-like) papilární renální karcinom

SOUHRN KOMENTOVANÝCH PUBLIKACÍ

1. ČÁST

NÁDORY LEDVIN

RENÁLNÍ KARCINOM S LEIOMYOMATÓZNÍM STROMATEM – DALŠÍ IMUNOHISTOCHEMICKÁ A MOLEKULÁRNĚ GENETICKÁ STUDIE NEOBVYKLÉ JEDNOTKY

Renální karcinom s leiomyomatózním stromatem (RKLS) byl poprvé popsán skupinou italských autorů v roce 1993 pod názvem smíšený renální tumor s karcinomatózní a fibroleiomyomatózní komponentou [6]. Histologicky se jedna o bifazický tumor složený z epitelové a stromální komponenty. Epitelovou složku tvoří solidně, papilárně nebo tubulárně uspořádané blandní světlé buňky neodlišitelné od buněk konvenčního světlobuněčného renálního karcinomu (SRK), které jsou promíchány s nápadným leiomyomatózním stromatem.

Analýzou klonality bylo prokázáno, že leiomyomatózní stroma není součástí neoplastického procesu, ale pouze reaktivní příměsí [7]. RKLS nemá žádné specifické imunohistochemické znaky a k jeho diagnostice je nezbytné molekulárně genetické vyšetření. Absence mutace genu *VHL*, *VHL* hypermetylace a/nebo ztráta heterozygozity na krátkém raménku 3.chromozomu (LOH 3p) podporuje diagnózu RKLS. Z uvedeného je zřejmé, že RKLS je morfologicky identický jako SRK s reaktivním leiomyomatózním stromatem a jejich odlišení je možné pouze na základě molekulární genetiky, přičemž SRK výše popsané genetické odchylky obsahuje. Odlišení těchto dvou jednotek je klinicky důležité, protože SRK je maligní tumor a RKLS je považován za indolentní (doposud nebyl popsán agresivně se chovající případ). V nedávné době byl objeven tzv. *TCEB1* mutovaný renální karcinom, který je histologicky neodlišitelný od RKLS/SRK a geneticky je definován přítomností mutace genu *TCEB1*[8]. Biologické vlastnosti tohoto tumoru nejsou zatím příliš známé.

V přiložené publikaci jsme se problematikou výše popsané jednotky zabývali. Z plzeňského registru nádorů bylo vybráno 15 případů renálních karcinomů (RK) s leiomyomatózním stromatem, které byly následně hodnoceny morfologicky, imunohistochemicky a molekulárně geneticky. Všechny tumory se skládaly z hnízd světlých epitelových buněk low-grade vzhledu, promíchaných s hojným leimyomatózním stromatem.

Tato studie potvrdila, že RKLS nemá žádné specifické morfologické/imunohistochemické znaky. Leiomyomatózní stroma není pro tuto jednotku určující a může se vyskytovat i u jinak typických světlobuněčných RK (*TCEB1* mutovaný RK nebyl v době této publikace popsán a není proto zahrnut). Z našich výsledků vyplývá, že jako RKLS mohou být diagnostikovány pouze tumory, které postrádají jak mutace genu *VHL*, tak *VHL* hypermetylaci a LOH 3p. Vztah RK s nápadným leiomyomatózním stromatem k renálnímu angiomyoadenomatóznímu tumoru/světlobuněčnému papilárnímu renálnímu karcinomu není z naší studie zcela jednoznačný a k jeho objasnění je nezbytný další výzkum.

Annals of Diagnostic Pathology 18 (2014) 291–296

Contents lists available at ScienceDirect

Annals of Diagnostic Pathology

Renal cell carcinoma with leiomyomatous stroma—further immunohistochemical and molecular genetic characteristics of unusual entity

Kvetoslava Peckova, MD [a], Petr Grossmann, PhD [a], Stela Bulimbasic, MD, PhD [b], Maris Sperga, MD [c], Delia Perez Montiel, MD [d], Ondrej Daum, MD, PhD [a], Pavla Rotterova, MD, PhD [a], Bohuslava Kokoskova, MD [a], Pavla Vesela, MD [a], Kristyna Pivovarcikova, MD [a], Kevin Bauleth, MD [a], Jindrich Branzovsky, MD [a], Magdalena Dubova, MD [a], Milan Hora, MD, PhD [e], Michal Michal, MD [a], Ondrej Hes, MD, PhD [a,f,*]

[a] Department of Pathology, Charles University, Medical Faculty and Charles University Hospital, Plzen, Czech Republic
[b] Department of Pathology, University Hospital Dubrava, Zagreb, Croatia
[c] Department of Pathology, East University Riga, Latvia
[d] Department of Pathology, Institute Nacional de Cancerologia, Mexico City, Mexico
[e] Department of Urology, Charles University, Medical Faculty and Charles University Hospital, Plzen, Czech Republic
[f] Biomedical Centre, Faculty of Medicine in Plzen, Charles University in Prague, Plzen, Czech Republic

ARTICLE INFO

Keywords:
Kidney
Renal cell carcinoma
Leiomyomatous stroma
VHL gene mutation
LOH 3p
Clear cell carcinoma

ABSTRACT

Renal cell carcinoma (RCC) with leiomyomatous stroma (RCCLS) is a recently recognized entity with indolent biological behavior. The diagnostic implication of absence/presence of *VHL* gene mutation, *VHL* hypermethylation, or/and loss of heterozygosity of chromosome 3p (LOH 3p) is widely discussed. Criteria for establishing a diagnosis of RCCLS are still lacking. Fifteen RCCLSs were retrieved from our registry. The cases were studied with consideration to the morphology, immunohistochemistry, and molecular genetics. All cases were composed of low-grade epithelial cells with clear cytoplasm arranged in nests intermingled with abundant leiomyomatous stroma. Age range of the patients was 33 to 78 years. The tumor size ranged from 1.5 to 11 cm. Six of the patients were males, and 9, females. Of the 15 tumors sent for molecular genetic testing, only 12 cases were analyzable. All cases were analyzable immunohistochemically. Of 12 of these cases, 5 showed complete absence of *VHL* gene mutation, *VHL* hypermethylation, and LOH 3p. Of these 5 cases, 3 were positive for cytokeratin 7 (CK 7). All of the 5 cases were positive for carbonic anhydrase 9, vimentin, and CD10. The remaining 7 of 12 genetically analyzable cases were found to have had *VHL* hypermethylation, LOH 3p, *VHL* gene mutation, or a combination of the former 2 characteristics. These 7 cases were positive for vimentin. Variable reactivity was found for CK 7, carbonic anhydrase 9, α-methylacyl-CoA racemase, and CD10. In 1 of these 7 cases, gains on chromosomes 7 and 17 as well as hypermethylation of *VHL* gene were found. This case was considered as clear cell RCC with aberrant status of chromosomes 7 and 17. Conclusions: (1) Leiomyomatous stroma is not specific for the so called RCCLS. It can be seen also in otherwise typical clear cell RCCs. (2) There are no characteristic morphological/immunohistochemical features unique for "RCCLS." (3) Our results indicate that only tumors with the absence of the *VHL* gene mutation, hypermethylation, and LOH 3p can be diagnosed as RCCLS. (4) Relation of RCCs with a prominent smooth muscle stroma to the renal angiomyoadenomatous tumor/clear cell papillary (tubopapillary) RCC is not clearly evident from our study and has to be further analyzed on larger cohort of the patients.

1. Introduction

Renal cell carcinomas (RCCs) with a prominent smooth muscle stroma (RCCSMSs) are rare neoplasms, which were first described by Canzonieri et al in 1993 [1] and subsequently documented by Kuhn et al in 2006 [2] and other investigators [3-5]. Microscopically, RCCSMSs are composed of an intimate intermixture of 2 distinct components: epithelial and stromal. The epithelial component is represented by clear epithelial cells with mild nuclear atypia (mostly Fuhrman grade 2) arranged in adenomatous structures with predominantly nested or tubular pattern associated with focal papillary and solid areas.

Exact diagnostic criteria are not established. Morphology and immunohistochemical features (namely, cytokeratin 7 [CK 7] positivity among others) are variable in previous studies.

The role of absence/presence of *VHL* gene mutation, *VHL* hypermethylation, or/and loss of heterozygosity (LOH) of chromosome 3p (LOH 3p) for diagnosis is widely discussed [5].

* Corresponding author. Department of Pathology, Charles University, Medical Faculty and Charles University Hospital Plzen, Alej Svobody 80, 304 60 Plzen, Czech Republic.
E-mail address: hes@medima.cz (O. Hes).

http://dx.doi.org/10.1016/j.anndiagpath.2014.08.004
1092-9134/

We assembled a group of tumors with voluminous leiomyomatous stroma and clear cell morphology. The morphology, immunohistochemistry, and molecular biology of all tumors were examined as attempt to select RCCSMS from group of tumors with similar morphologic features.

2. Materials and methods

Of 17 700 renal tumors and tumor-like lesions in the institutional and consultation files of Sikl's Department of Pathology, Charles University, Plzen, Czech Republic, 15 cases of RCCs were retrieved. All were composed of epithelial cells with clear cytoplasm arranged in nests or tubules intermingled with abundant leiomyomatous stroma.

The tissue had been fixed in neutral formalin and embedded in paraffin; 4- to 5-μm-thick sections were cut and stained with hematoxylin and eosin.

2.1. Immunohistochemistry

The immunohistochemical study was performed using a Ventana Benchmark XT automated stainer (Ventana Medical System, Inc, Tucson, AZ). The following primary antibodies were used: CK 7 (OV-TL12/30, monoclonal, 1:200; DakoCytomation, Glostrup, Denmark), racemase/α-methylacyl-CoA racemase (AMACR) (P504S, monoclonal, 1:50; Zeta, Sierra Madre, CA), vimentin (D9, monoclonal, 1:1000; Neomarkers, Westinghouse, CA), carbonic anhydrase 9 (CANH 9) (rhCA9, monoclonal, 1:100; RD Systems, Minneapolis, MN), melanoma marker (HMB45, monoclonal, 1:200; Dako, Carpinteria, CA), and CD10 (56C6, 1:20; Novocastra, Burlingame, CA). Appropriate positive controls were used.

2.2. Molecular genetic study

2.2.1. Fluorescence in situ hybridization methods

Four-micrometer-thick section was placed onto positively charged slide. Hematoxylin and eosin–stained slide was examined for determination of areas for cell counting.

The unstained slide was routinely deparaffinized and incubated in the 1× target retrieval solution citrate pH 6 (Dako, Glostrup, Denmark) for 40 minutes at 95°C and subsequently cooled for 20 minutes at room temperature in the same solution. The slide was washed in deionized water for 5 minutes and digested in protease solution with pepsin (0.5 mg/mL) (Sigma Aldrich, St Louis, MO) in 0.01 M HCl at 37°C for 20 minutes. The slide was then placed into deionized water for 5 minutes, dehydrated in a series of ethanol solution (70%, 85%, and 96% for 2 minutes each), and air dried. Probes for aneuploidy detection of chromosomes 7 and 17 (Vysis; Abbott Molecular, Abbott Park, IL) (see Table 1) were mixed with water and Locus-Specific Identifier/Whole Chromosome Painting Hybridization buffer (Vysis) in a 1:2:7 ratio. An appropriate amount of probe mix was applied on specimen, covered with a glass coverslip, and sealed with rubber cement. The slide was incubated in the ThermoBrite instrument (StatSpin; Iris Sample Processing, Westwood, MA) with codenaturation parameters 85°C for 8 minutes and hybridization parameters 37°C for 16 hours. Rubber cemented coverslip was then removed, and the slide was placed in posthybridization wash solution (2× saline-sodium citrate/0.3% NP-40) at 72°C for 2 minutes. The slide was air dried in the dark, counterstained with 4′,6′-diamidino-2-phenylindole (Vysis), coverslipped, and immediately examined.

Fig. 1. Gross section of the kidney with 2 tumors. One was typical clear cell renal cell carcinoma (CCRCC) (yellow color), and the second was CCRCC (genetically confirmed) with abundant leiomyomatous stroma.

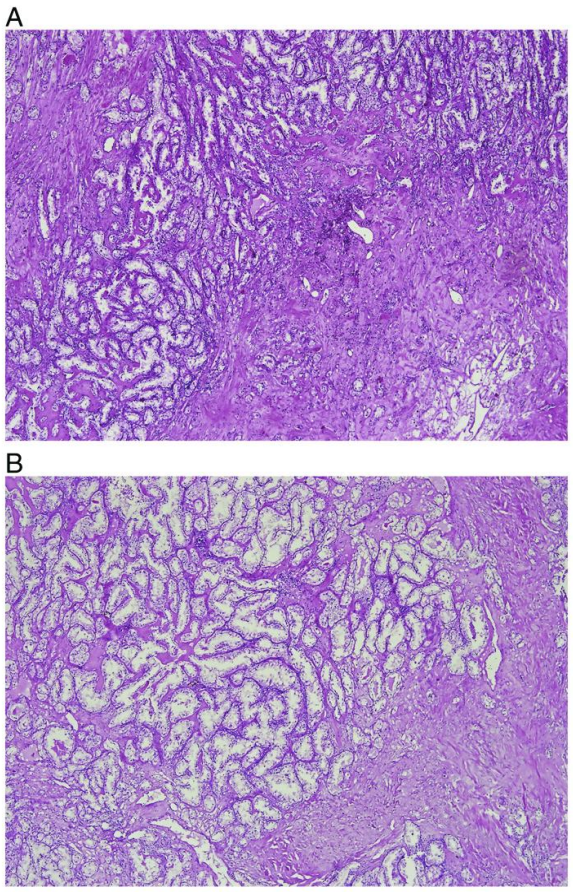

Fig. 2. Smooth muscle stroma was prominent in all cases. Epithelial component as well as stroma was identical in tumors, which were, after special examinations, considered as CCRCC (A), and in cases, which were diagnosed as "RCCLS" (B).

2.2.2. Fluorescence in situ hybridization interpretation

The section was examined with an Olympus BX51 fluorescence microscope (Olympus Corporation, Tokyo, Japan) using a ×100 objective and filter sets triple-band pass (4′,6′-diamidino-2-phenylindole/SpectrumGreen/SpectrumOrange) and single-band pass (SpectrumGreen/

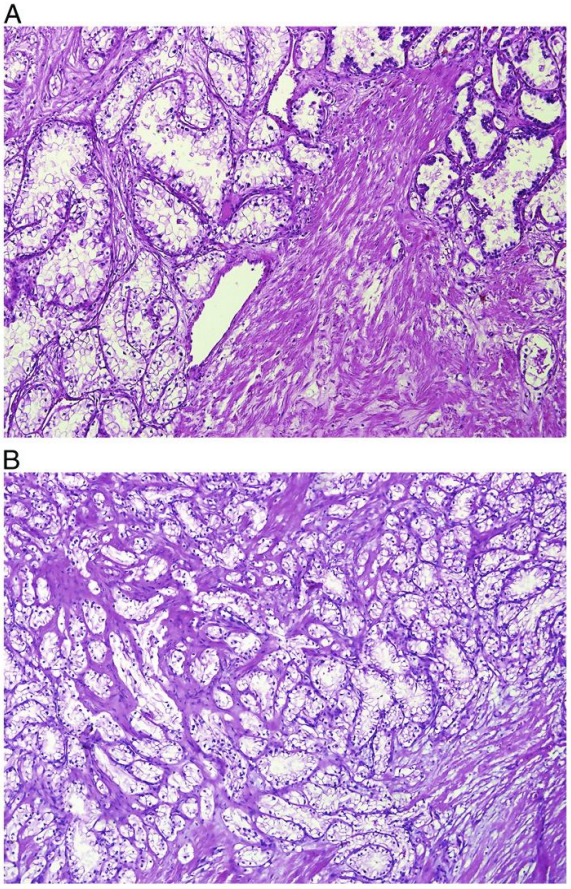

Fig. 3. Tumors were composed of voluminous clear cell elements with mostly low nucleolar Fuhrman grade. Clear cell RCCLS (A) and "RCCLS" (B).

SpectrumOrange). Scoring of aneuploidy was performed by counting the number of fluorescent signals in 100 randomly selected nonoverlapping tumor cell nuclei. The slide was independently enumerated by 2 observers (OH and PG). Monosomy and polysomy for studied chromosomes were defined as the presence of 1 signal per cell in more than 45% and 3 and more signals in more than 10% (mean + 3 SD in normal nonneoplastic control tissues), respectively.

2.2.3. DNA extraction and bisulfite DNA conversion

DNA for molecular genetic investigation was extracted from formalin-fixed, paraffin-embedded tissue. Several 5-μm-thick sections were placed on the slides. Hematoxylin and eosin–stained slides were examined for identification of neoplastic tissue. Subsequently, neoplastic tumor and nonneoplastic tissue from unstained slides were scraped, and DNA was isolated by the NucleoSpin Tissue Kit (Macherey-Nagel, Düren, Germany).

Table 1
Probes for aneuploidy detection of chromosomes 7 and 17

Chromosome	Probe
7	CEP 7 (D7Z1)/7p11.1-q11.1 Alpha Satellite DNA
17	CEP 17 (D17Z1)/17p11.1-q11.1 Alpha Satellite DNA

Table 2
Polymerase chain reaction primers used in mutation analysis of the *VHL* gene and designed in Primer3 software (14)

Gene/exon	Name	Primers (sequence 5′→3′)
VHL/exon 1	VHL e1-1	CGCGAAGACTACGGAGGT
	VHL e1-2	GTCTTCTTCAGGGCCGTA
	VHL e1-3	GAGGCAGGCGTCGAAGAG
	VHL e1-4	GCGATTGCAGAAGATGACCT
	VHL e1-5	GCCGAGGAGGAGATGGAG
	VHL e1-6	CCCGTACCTCCGTAGCTGT
	VHL e1-7	CCGTATGGCTCAACTTCGAC
	VHL e1-8	GCTTCAGACCGTGCTATCGT
VHL/exon 2	VHL e2-1	ACCGGTGTGGCTCTTTAACA
	VHL e2-2	TCCTGTACTTACCACAACAACCTT
VHL/exon 3	VHL e3-1	GCAAAGCCTCTTGTTCGTTC
	VHL e3-2	ACATTTGGGTGGTCTTCCAG
	VHL e3-3	CAGGAGACTGGACATCGTCA
	VHL e3-4C	CCATCAAAAGCTGAGATGAAAC

Bisulfite conversion of DNA was carried out using EZ DNA Methylation–Gold Kit (DNA input, 500 ng) (Zymo Research, Orange, CA).

All procedures were performed according to the manufacturers' protocols.

2.2.4. VHL gene analysis

Mutation analysis of exons 1, 2, and 3 of the *VHL* gene was performed using polymerase chain reaction (PCR) and direct sequencing. Polymerase chain reaction was carried out using primers shown in Table 2. The reaction conditions were as follows: 12.5 μL of HotStar Taq PCR Master Mix (Qiagen, Hilden, Germany), 10 pmol of each primer, 100 ng of template DNA, and distilled water up to 25 μL. The amplification program consisted of denaturation at 95°C for 15 minutes and then 40 cycles of denaturation at 95°C for 1 minute, annealing at 55°C for 1 minute, and extension at 72°C for 1.5 minutes for all amplicons. The program was finished by 72°C incubation for 7 minutes.

The PCR products were checked on 2% agarose gel electrophoresis.

Successfully amplified PCR products were purified with magnetic particles Agencourt AMPure (Agencourt Bioscience Corporation, A Beckman Coulter Company, Beverly, MA), both side sequenced using Big Dye Terminator Sequencing kit (Applied Biosystems, Foster City, CA), and purified with magnetic particles Agencourt CleanSEQ (Agencourt Bioscience Corporation) all according to the manufacturer's protocol and subsequently run on an automated sequencer ABI Prism 3130xl (Applied Biosystems) at a constant voltage of 13.2 kV for 20 minutes. All samples were analyzed in duplicates. Analyses of positive samples were repeated.

2.2.5. Analysis of VHL promoter methylation

Detection of promoter methylation was carried out via methylation-specific PCR as described by Herman et al [6]. Briefly, 100 ng of DNA or 2 μL of converted DNA was added to reaction consisted of 12.5 μL of HotStar Taq PCR Master Mix (Qiagen), 10 pmol of forward and reverse primer (Table 3), and distilled water up to 25 μL. The amplification program is composed of denaturation at 95°C for 14 minutes and then 40 cycles of denaturation at 95°C for 1 minute, annealing at 60°C for 1 minute, and extension at 72°C for 1 minute. The program was finished by incubation at 72°C for 7 minutes.

Table 3
Polymerase chain reaction primers used in methylation status of the *VHL* gene

Gene	Name	Primers (sequence 5′→3′)
VHL unmethylated	VHL-U-S	GTTGGAGGATTTTTTTGTGTATGT
VHL unmethylated	VHL-U-A	CCCAAACCAAACACCACAAA
VHL methylated	VHL-M-S	TGGAGGATTTTTTTGCGTACGC
VHL methylated	VHL-M-A	GAACCGAACGCCGCGAA

Table 4
PCR primers used in LOH analysis of chromosome 3

Marker	Name	Primers (sequence 5′→3′)
D3S666	D3S666-SK#15	CAAGGCATTAAAGTGGCCACGC
	D3S666- SK#16	GTTTGAACCAGTTTCCTACTGAG
D3S1270	D3S1270-F	TGGAACTGTATCAAAGGCTC
	D3S1270-R	TTGCATTAGNATTCTCCAGA
D3S1300	D3S1300SF	AGCTCACATTCTAGTCAGCCT
	D3S1300A	GCCAATTCCCCAGATG
D3S1581	D3S1581-F	CAGAACTGCCAAACCA
	D3S1581-R	GGGTAACAGGAGCGAG
D3S1597	D3S1597-F	AGTACAAATACACACAAATGTCTC
	D3S1597-R	GCAAATCGTTCATTGCT
D3S1600	D3S1600-F	ATCACCATCATCTGCCTGTC
	D3S1600-R	TGCTTGCCTTGGGATTTA
D3S1603	D3S1603-F	CCCTAACTCCACTTGAAAGC
	D3S1603-R	TCAGCGAACAGCAACAAAT
D3S1768	D3S1768SF	GGTTGCTGCCAAAGATTAGA
	D3S1768A	CACTGTGATTTGCTGTTGGA
D3S2338	D3S2338-F	GAAGCCAGCAGTTTCTC
	D3S2338-R	CTGTATTGTTTTCCAGGATAAG
D3S3630	D3S3630-F	AAGGGATAAGCTGCAAATCA
	D3S3630-R	ACCAAATACAATTCATGAGACCTGA

The PCR products were checked on 2% agarose gel electrophoresis.

A patient with known *VHL* mutation and fully methylated HeLa cell DNA was used as a positive control for *VHL* mutation analysis and promoter methylation analysis, respectively. As negative control, randomly selected healthy donor blood was used.

2.2.6. Loss of heterozygosity of chromosome 3p analysis

For LOH analysis of neoplastic tissue DNA, 10 short tandem repeat markers D3S666, D3S1270, D3S1300, D3S1581, D3S1597, D3S1600, D3S1603, D3S1768, D3S2338, and D3S3630 located on the short arm of chromosome 3 were chosen from the database (Gene Bank UniSTS). The primers are listed in Table 4. Polymerase chain reaction conditions were the same as mentioned above. Successfully amplified PCR products were mixed with GeneScan 500 LIZ dye Size Standard (Applied Biosystems) and run on an automated genetic analyzer ABI Prism 3130xl (Applied Biosystems) at a constant voltage of 15 kV for 20 minutes. A sample was considered LOH positive if the ratio of nontumor DNA to tumor DNA was greater than 1.5 or less than 0.66. All samples were analyzed in duplicates.

3. Results

Basic clinicopathologic data are summarized in Table 5. There were 15 patients, 6 males and 9 females. The age range of the patients was 33 to 78 years (mean, 60.5 years; median, 63 years), and the size of the lesions ranged from 1.5 to 11 cm (mean, 4.1 cm; median, 11.25 cm).

3.1. Gross and microscopic findings

Tumors were yellow, gray to brown, white color in cut section (Fig. 1). No grossly visible necroses or hemorrhagias were seen. Tumors were well circumscribed and nonencapsulated.

On microscopic examination, tumors were in all cases composed of an intimate admixture of stromal and epithelial component (Fig. 2). Stromal portion formed thick bundles of mature smooth muscle cells, which tend to merge with the wall of medium-sized blood vessels lined by normally looking endothelial cells. This vessel-related leiomyomatous proliferation was intermingled with an epithelial component arranged in nests, cords, and small cysts of epithelial cells with clear cytoplasm and hyperchromatic nuclei (Fuhrman modified nucleolar grade, mostly 2) (Fig. 3). There were no prominent atypias, mitoses, or necroses apparent in either of the components.

3.2. Immunohistochemistry

Immunohistochemical results are presented in Table 6. Briefly, the tumors showed variable reactivity for CK 7 and AMACR. CD10 expression was positive in most tumors (10/15 cases). Of 15 cases, 14 were positive for CANH 9, and all tumors were immunoreactive for vimentin.

All tumors (5 cases), which were further diagnosed (after complex analysis, including molecular genetic methods—see below) as RCCSMS, were positive for vimentin and for CANH 9. Of these 5 cases, 3 were positive for CK 7 (Fig. 4).

3.3. Molecular genetics

Molecular genetic characteristics are summarized in Table 7.

Of the 15 case, only 12 of them were genetically analyzable.

Of 12 of these genetically analyzable cases, 5 showed complete absence of *VHL* gene mutation, *VHL* hypermethylation, and LOH 3p. This subset of the tumors was considered as a group of "real" RCCSMS.

The remaining 7 of 12 genetically analyzable cases were found to have had *VHL* hypermethylation; LOH 3p; *VHL* gene mutation; or a combination of the former 2 characteristics, that is, *VHL* hypermethylation and LOH 3p. In 1 of these 7 cases, gains on chromosomes 7 and 17 were found altogether with hypermethylated status of *VHL* gene. This tumor, after complex morphologic and immunohistochemical analyses, was considered CCRCC with aberrant status of chromosomes 7 and 17.

Table 5
Basic clinicopathologic data

Case	Sex	Age (y)	Size (cm)	Color	Follow-up (y)
1	**M**	**53**	**Diam 3**	**Yellow**	**LE**
2	**M**	**63**	**NA**	**Yellowish**	**LE**
3	M	78	4 × 3.5 × 3	NA	LE
4	F	60	Diam 1.5	Yellow	LE
5	**F**	**69**	**Diam 1.5**	**Gray-brown**	**LE**
6	M	66	Diam 4	Gray with yellowish areas	CHT for colonic adenocarcinoma, multiple hepatic meta. Died in 2 y
7	F	59	Diam 11	White	LE
8	F	48	Diam 9.5	NA	LE
9	F	63	Diam 1.4	NA	LE
10	M	62	Diam 1.8	NA	LE
11	M	50	2. 2 × 2 × 1.8	Light brown to gray	No signs of recurrence and meta
12	F	73	Diam 4.8 and 1.8 (2 tumors, bigger typical CCRCC)	Tan to gray	No signs of recurrence or meta
13	F	48	11.5 × 10 × 12.5	NA	LE
14	**F**	**63**	**2.5 × 2 × 2.2**	**NA**	**LE**
15	**F**	**63**	**Diam 1.7**	**Yellow**	**0.5 AW**

Tumors diagnosed as RCCSMS are in boldface. Abbreviations: *M*, male; *F*, female; *NA*, not available; *LE*, loss of evidence; *Diam*, diameter; *AW*, alive and well; *meta*, metastasis; *y*, years; *CHT*, chemotherapy.

Table 6
Immunohistochemical examination

Case	CK 7	CANH 9	Vim	AMACR	HMB45	CD10
1	−	++	++	**+++foc.**	−	**+++foc.**
2	**++foc.**	++	++	**++foc.**	−	**+++foc.**
3	−	+++	+++	+++foc.	−	+++
4	+++foc.	+	+++	−	−	+++
5	**+++foc.**	**+++foc.**	+++	−	−	+++
6	−	+	+	−	−	+++
7	−	+++foc.	++	−	−	−
8	−	+++	+++	+++	−	+++
9	+++foc.	++	++	+++foc.	−	−
10	−	−	+++	−	−	−
11	+++foc.	++foc.	++	+++foc.	−	++foc.
12	+	+++	+	−	−	++foc
13	+++foc.	+	+++	−	−	+++foc.
14	**+++foc.**	**+++foc.**	+	−	−	+++
15	−	+++	+++	−	−	**+++foc.**

Tumors diagnosed as RCCSMS are in boldface. Abbreviations: *Vim*, vimentin; −, negative; +, weakly positive; ++, moderately positive; +++, strongly positive; *foc.*, focally.

4. Discussion

Leiomyomatous stroma can be encountered in several different renal tumors. The most common renal tumor with leiomyomatous component is angiomyolipoma. Angiomyolipoma is, in its typical form, characterized by an intimate admixture of tortuous thick-walled blood vessels devoid of elastic layer, mature adipose tissue, and bundles of smooth muscle. It is known from sporadic cases and cases associated with tuberous sclerosis complex [7].

Another tumor with leiomyomatous stroma is renal angiomyoadenomatous tumor (RAT)/clear cell papillary (tubopapillary) RCC (CCPRCC). Renal angiomyoadenomatous tumor and CCPRCC are 2 relatively recently described low-grade neoplastic entities with overlapping histologic features and so far considered as nonaggressive indolent neoplasias. Recently, RAT and CCPRCC have been, by some investigators, recognized as 2 separate entities; however, they have been thought of as 2 ends of a spectrum of 1 nosological entity by other authors [7]. Nevertheless, there are still no exact criteria for distinguishing of these 2 morphologic entities, and we will herein refer to them as RAT/CCPRCC.

Next group of renal tumors with leiomyomatous and/or fibroleiomyomatous component is unusual type of RCC composed of clear cells, which are intermingled with voluminous mostly leiomyomatous stroma. These tumors have been descriptively referred to as "RCC with smooth muscle stroma," "mixed renal tumor with carcinomatous and fibroleiomyomatous components," "RCC associated with prominent angioleiomyoma-like proliferation," or "CCRCC with smooth muscle stroma" [1-5].

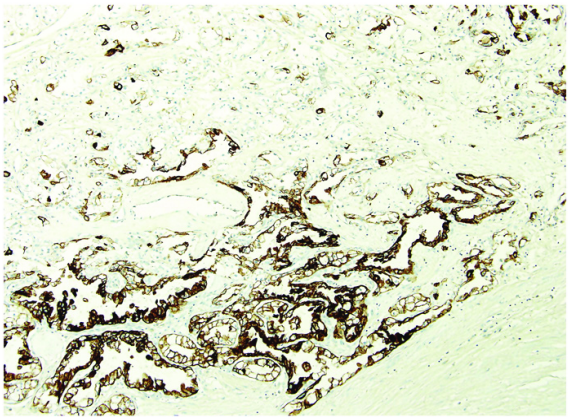

Fig. 4. Focal but strong CK 7 positivity was noted in 3 of 5 cases of "RCCLS."

These tumors constitute a heterogeneous group. Some of these cases obviously represented CCRCC, which produced smooth muscle stroma, and another part are, according our opinion, distinct renal neoplasms, which probably differ from CCRCC by their molecular genetic features and perhaps prognosis.

It was shown recently that the presence of a prominent smooth muscle stroma may be encountered not only in "RCC with smooth muscle stroma," CCRCC, and RAT/CCPRCC but also in papillary RCC. Moreover, this stroma is not part of the monoclonal, neoplastic proliferation but represents a reactive, polyclonal proliferation that is possibly derived from the smooth muscle cells of large caliber veins [8]. Another authors postulated that angioleiomyoma-like change is an epiphenomenon caused by overproduction of growth factors by epithelial neoplastic cells with inactivation of *VHL* gene [2,5]. Such a pathway could be an explanation for the production of the leiomyomatous stroma in CCRCC. It seems that there could be different pathways for stroma production in tumors such as papillary RCC, RAT/CCPRCC, and RCCSMS.

From the group of 15 RCC with leiomyomatous stroma (RCCLS) in our study, we were capable of identifying 5 tumors with normal status of *VHL* gene including LOH 3p, most (3/5) of which expressed CK 7 and which represented consequently, according to our opinion, real RCCSMS. Our research, hence, indicates that the CK 7 expression (diffuse or focal) is nonspecific even for RCCSMS. Besides RAT/CCPRCC, the CK 7 positivity can be found in up to 15% classic CCRCC [9]. Therefore, it is apparent that only molecular genetic examination, particularly *VHL* gene analysis and perhaps analysis of chromosomes 7 and 17, is crucial for differentiation of RCCSMS from CCRCC.

In our series of RCCLSs and *VHL* gene abnormalities, 1 case also showed gain of chromosomes 7 and 17. Morphologically, this tumor was CCRCC and, hence, not compatible with diagnosis of papillary RCC. Thus, we considered this case as a CCRCC with aberrant status of chromosomes 7 and 17.

It remains unclear whether RCCSMS and RAT/CCPRCC have in common something more than similar morphology, immunohistochemistry, and some of genetic features.

Renal angiomyoadenomatous tumor and CCPRCC share almost equal morphology and immunophenotype. Both types are characterized by the presence of fibroleiomyomatous stroma and CK 7 positivity; they also bear similar molecular genetic attributes (lack of *VHL* gene abnormalities) [10-13]. Presumably, the difference between them inheres in stromal component, in the sense that RAT exhibits a voluminous stromal component and CCPRCC, in contrast, usually features a much less prominent smooth muscle stroma. Therefore, the presence of the abundant fibroleiomyomatous stroma has been becoming a mark of distinction between RAT and CCPRCC, and hence, these 2 entities are regarded as related tumors and viewed as 2 ends of spectrum of 1 nosologic entity [5].

It was pointed out by Martignoni et al [5] that RCCSMS is a tumor distinct from CCRCC and that these tumors could be related to RAT/CCPRCC. Our results indicate, at least on the morphologic and immunohistochemical levels, that there are some differences between RCCSMS and RAT/CCPRCC. Further studies with a larger cohort of patients should be performed to confirm any possible link between RCCSMS and CCPRCC/RAT.

The question remains whether these tumors have an aggressive potential and whether the biological treatment (antiangiogenic drugs) may be applicable for such types of renal tumor. Up to date, no aggressive behavior and local recurrences of metastases have been documented; nevertheless, both the number of the cases and the available follow-up information are too meager to conclude explicit prognostic outcomes.

Table 7
Molecular genetic findings

Case	Chr 7	Chr 17	VHL	methylVHL	LOH 3p
1	**norm**	**norm**	**−**	**−**	**−**
2	**norm**	**norm**	**−**	**−**	**−**
3	norm	norm	−	−	+
4	norm	norm	−	−	+
5	**norm**	**norm**	**−**	**−**	**−**
6	norm	norm	−	+	+
7	NA	NA	NA	NA	NA
8	NA	NA	NA	NA	NA
9	norm	norm	+	−	−
10	NA	NA	NA	NA	NA
11	gain	gain	−	+	−
12	norm	norm	−	+	+
13	norm	norm	−	+	−
14	**norm**	**norm**	**−**	**−**	**−**
15	**norm**	**norm**	**−**	**−**	**−**

Tumors diagnosed as RCCSMS are in boldface. Abbreviations: *Chr*, chromosome; *VHL*, *VHL* gene mutation; *methylVHL*, methylation status of *VHL* gene; −, negative; +, positive; *NA*, not analyzable; *norm*, normal status.

Being able to rigorously separate RCCSMS from clear cell RCCLS, we would subsequently get group of nonaggressive, possibly benign/indolent tumors. Such information would be beneficial both for the patients and for our clinical colleagues.

5. Conclusions

Our study highlights the following conclusions:

1. Leiomyomatous stroma is not specific for RCCSMS and can be also seen in otherwise typical CCRCC.
2. There are no morphological/immunohistochemical features unique for RCCSMS, and merely molecular genetic analysis can reliably separate RCCSMS from variants of CCRCC with reactive smooth muscle stroma.
3. From our results, it seems that only tumors with the absence of *VHL* gene mutation and/or hypermethylation and LOH 3p can be diagnosed as RCCSMS.
4. Relation of RCCSMS to the RAT/CCPRCC is not clearly evident from our study and has to be further analyzed on larger cohort of the patients.

Disclosure of conflict of interest

All authors declare no conflict of interest.

The study was supported by the Charles University Research Fund (project number P36) and by the project CZ.1.05/2.1.00/03.0076 from European Regional Development Fund.

References

[1] Canzonieri V, Volpe R, Gloghini A, Carbone A, Merlo A. Mixed renal tumor with carcinomatous and fibroleiomyomatous components, associated with angiomyolipoma in the same kidney. Pathol Res Pract 1993;189:951–6 [discussion 7-9. PubMed PMID: 8302716].
[2] Kuhn E, De Anda J, Manoni S, Netto G, Rosai J. Renal cell carcinoma associated with prominent angioleiomyoma-like proliferation: report of 5 cases and review of the literature. Am J Surg Pathol 2006;30:1372–81 [PubMed PMID: 17063076].
[3] Shannon BA, Cohen RJ, Segal A, Baker EG, Murch AR. Clear cell renal cell carcinoma with smooth muscle stroma. Hum Pathol 2009;40:425–9 [PubMed PMID: 18789480].
[4] Iczkowski KA, Shanks JH, Burdge AH, Cheng L. Renal cell carcinoma with clear cells, smooth muscle stroma, and negative for 3p deletion: a variant of renal angiomyoadenomatous tumour? A case report. Histopathology 2013;62:522–4 [PubMed PMID: 23339367].
[5] Martignoni G, Brunelli M, Segala D, Gobbo S, Borze I, Atanesyan L, et al. Renal cell carcinoma with smooth muscle stroma lacks chromosome 3p and VHL alterations. Mod Pathol 2014;27:765–74 [PubMed PMID: 24201123].
[6] Herman JG, Graff JR, Myohanen S, Nelkin BD, Baylin SB. Methylation-specific PCR: a novel PCR assay for methylation status of CpG islands. Proc Natl Acad Sci U S A 1996;93:9821–6 [PubMed PMID: 8790415. Pubmed Central PMCID: 38513].
[7] Srigley JR, Delahunt B, Eble JN, Egevad L, Epstein JI, Grignon D, et al. The International Society of Urological Pathology (ISUP) Vancouver Classification of Renal Neoplasia. Am J Surg Pathol 2013;37:1469–89 [PubMed PMID: 24025519].
[8] Petersson F, Branzovsky J, Martinek P, Korabecna M, Kruslin B, Hora M, et al. The leiomyomatous stroma in renal cell carcinomas is polyclonal and not part of the neoplastic process. Virchows Arch 2014;465:89–96 [PubMed PMID: 24838683].
[9] Gatalica Z, Miettinen M. Consistent expression of cytokeratin 7 in papillary renal-cell carcinoma. J Urol Pathol 1995;3:205–11.
[10] Gobbo S, Eble JN, Grignon DJ, Martignoni G, MacLennan GT, Shah RB, et al. Clear cell papillary renal cell carcinoma: a distinct histopathologic and molecular genetic entity. Am J Surg Pathol 2008;32:1239–45 [PubMed PMID: 18594469].
[11] Rohan SM, Xiao Y, Liang Y, Dudas ME, Al-Ahmadie HA, Fine SW, et al. Clear-cell papillary renal cell carcinoma: molecular and immunohistochemical analysis with emphasis on the von Hippel-Lindau gene and hypoxia-inducible factor pathway-related proteins. Mod Pathol 2011;24:1207–20 [PubMed PMID: 21602815].
[12] Michal M, Hes O, Havlicek F. Benign renal angiomyoadenomatous tumor: a previously unreported renal tumor. Ann Diagn Pathol 2000;4:311–5 [PubMed PMID: 11073338].
[13] Michal M, Hes O, Nemcova J, Sima R, Kuroda N, Bulimbasic S, et al. Renal angiomyoadenomatous tumor: morphologic, immunohistochemical, and molecular genetic study of a distinct entity. Virchows Arch 2009;9:89–99.

AGRESIVNÍ A NEAGRESIVNÍ TRANSLOKAČNÍ t(6;11) RENÁLNÍ KARCINOM: SROVNÁVACÍ STUDIE ŠESTI PŘÍPADŮ A PŘEHLED LITERATURY

MiT rodina translokačních RK, zařazená do WHO klasifikace nádorů ledvin v roce 2004, obsahuje renální karcinomy nesoucí genové fúze *TFE3* nebo *TFEB*. Do této skupiny patří častější Xp11.2 translokační renální karcinom, charakterizován chromozomální translokací způsobující fúzi genu *TFE3* s různými fúzními partnery. Druhým základním typem je translokační t(6;11) renální karcinom nesoucí *MALAT1-TFEB* genovou fúzi, která je způsobena onkogenní aktivací genu *TFEB*. Oba typy MiT translokačních renálních karcinomů se vyskytují převážně u mladých jedinců [4].

t(6;11) translokační renální karcinom poprvé popsal v roce 2001 Argani et al [9]. Jedná se o velmi vzácný tumor, ve světové literatuře s doposud publikovanými přibližně 50 případy. Histologicky jsou tyto tumory charakteristické bifazickou morfologií: velké epiteloidní buňky, tvořící většinu tumoru, jsou promíchány s malými epiteloidními buňkami obklopujícími materiál bazální membrány a tvořícími tak pseudorozety. Narozdíl od Xp11.2 translokačních RK, jejichž prognóza se příliš neliší od konvenčního SRK, byly t(6;11) renální karcinomy do nedávné doby považovány za indolentní tumory. Byly však již popsány agresivně se chovající případy s metastázami a díky vzácnosti tohoto tumoru je zřejmé, že klinicko-patologické spektrum této jednotky bude širší, než se myslelo, a že stojí za to ho prozkoumat.

V této studii jsme porovnali 5 neagresivních tumorů (NAT) s jedním agresivním tumorem (AT). Ke komparaci jsme využili klinicko-patologické údaje, morfologické znaky, imunohistochemii (IHC) a molekulární genetiku. Dále jsme prostudovali všechny 4 doposud publikované agresivní případy t(6;11) renálních karcinomů a porovnali je s jedním naším případem a mezi sebou.

Závěrem studie lze konstatovat, že:

- AT se v porovnání s NAT vyskytují u starší populace.
- Tři z pěti případů nevykazovaly morfologii typickou pro NAT: ve dvou případech nebyly přítomny pseudorozety a jeden byl morfologicky blíže světlobuněčnému renálnímu karcinomu.
- Makroskopicky viditelné nekrózy byly detekovány pouze u agresivních případů a mohou tak sloužit jako potencionální nepříznivý prognostický faktor.
- Molekulárně geneticky vykazovaly NAT translokaci *TFEB* genu, přičemž u AT byla kromě této detekována i amplifikace genu *TFEB*.

V nedávno publikované práci dal Argani et al. do souvislosti amplifikaci genu *TFEB* a agresivní klinické chování. Do studie bylo zahrnuto 8 případů high grade t(6;11) translokačního renálního karcinomu, z nichž všechny vykazovaly amplifikaci genu *TFEB* a nepříznivé biologické chování [10].

Annals of Diagnostic Pathology 18 (2014) 351–357

Contents lists available at ScienceDirect

Annals of Diagnostic Pathology

Aggressive and nonaggressive translocation t(6;11) renal cell carcinoma: comparative study of 6 cases and review of the literature

Kvetoslava Peckova, MD [a], Tomas Vanecek, PhD [a], Petr Martinek, MSc [a], Dominic Spagnolo, MD [b], Naoto Kuroda, MD [c], Matteo Brunelli, MD, PhD [d], Semir Vranic, MD, PhD [e], Slavisa Djuricic, MD, PhD [f], Pavla Rotterova, MD, PhD [a], Ondrej Daum, MD, PhD [a], Bohuslava Kokoskova, MD [a], Pavla Vesela, MD [a], Kristyna Pivovarcikova, MD [a], Kevin Bauleth, MD [a], Magdalena Dubova, MD [a], Kristyna Kalusova, MD [g], Milan Hora, MD, PhD [g], Michal Michal, MD [a], Ondrej Hes, MD, PhD [a,h,*]

[a] Department of Pathology, Faculty of Medicine, University Hospital Plzeň, Charles University, Pilsen, Czech Republic
[b] Department of Pathology, PathWest Laboratory Medicine WA, Nedlands, Australia
[c] Department of Diagnostic Pathology, Kochi Red Cross Hospital, Kochi, Japan
[d] Department of Pathology and Diagnostic, University of Verona, Verona, Italy
[e] Department of Pathology, Clinical Center of the University of Sarajevo, Sarajevo, Bosnia and Herzegovina
[f] Department of Pathology, Mother and Child Health Institute of Serbia, Belgrade, Serbia
[g] Department of Urology, Faculty of Medicine in Plzeň, Charles University in Prague, Pilsen, Czech Republic
[h] Biomedical Centre, Faculty of Medicine in Plzen, Charles University in Prague, Pilsen, Czech Republic

ARTICLE INFO

Keywords:
Kidney
Translocation renal cell carcinoma
t(6;11)
Aggressive
Nonaggressive
Immunohistochemistry
Molecular biology

ABSTRACT

t(6;11) renal cell carcinoma (RCC) has been recognized as a rare and mostly nonaggressive tumor (NAT). The criteria for distinguishing aggressive tumors (AT) from NATs are not well established. A total of 6 cases were selected for the study. Five cases of t(6;11) RCCs behaved nonaggressively, and 1 was carcinoma with aggressive behavior. The tumors were analyzed morphologically using immunohistochemistry and by molecular-genetic methods. The specimen of aggressive t(6;11) RCC was from a 77-year-old woman who died of the disease 2.5 months after diagnosis. The specimens of nonaggressive t(6;11) RCCs were from 3 women and 2 men whose ages range between 15 and 54 years. Follow-up was available in all cases (2.5 months-8 years). The tumor size ranged from 3 to 14 cm in nonaggressive t(6;11) RCC. In the aggressive carcinoma, the tumor size was 12 cm. All tumors (6/6) were well circumscribed. Aggressive t(6;11) RCC was widely necrotic. Six (100%) of 6 all tumors displayed a solid/alveolar architecture with occasional tubules and pseudorosettes. Pseudopapillary formations lined by bizarre polymorphic cells were found focally in the aggressive t(6;11) RCC case. Mitoses, though rare, were found as well. All cases (AT and NAT) were positive for HMB-45, Melan-A, Cathepsin K, and cytokeratins. CD117 positivity was seen in 4 of 5 NATs, as well as in the primary and metastatic lesions of the AT. mTOR was positive in 2 of 5 NATs and vimentin in 4 of 5 NATs. Vimentin was negative in the primary lesion of the AT, as well as in the metastasis found in the adrenal gland. Translocation t(6;11)(*Alpha-TFEB*) or *TFEB* break was detected in 4 of 5 NATs and in the AT case. Aggressive tumor showed amplification of *TFEB* locus. Losses of part of chromosome 1 and chromosome 22 were found in 1 of 5 NATs and in the AT. Conclusions: (1) Aggressive t(6;11) RCCs generally occur in the older population in comparison with their indolent counterparts. (2) In regard to the histologic findings in ATs, 3 of 5 so far published cases were morphologically not typical for t(6;11) RCC. Of the 3 cases, 2 cases lacked a small cell component and 1 closely mimicked clear cell–type RCC. (3) Necroses were only present in aggressive t(6;11) RCC. (4) Amplification of *TFEB* locus was also found only in the aggressive t(6;11) RCC.

1. Introduction

t(6;11) translocation renal cell carcinoma (t(6;11) (TRCC) has been recognized as a new entity by the International Society of Urological Pathology 2012 conference and has subsequently been considered as a part of MiT family translocation carcinomas [1]. Regrouping TFEB and TFE3 translocation carcinomas together under the category of "MiTF/TFE family translocation carcinomas" was first suggested by Argani and Ladanyi [2–4], because the reason for regrouping of t(6;11) RCC and Xp11 TRCCs was similar morphologic, immunohistochemical, and molecular-genetic features. Translocation involving *TFEB* and *TFE3* induces the overexpression of these proteins and can be specifically identified by immunohistochemistry, where nuclear

* Corresponding author. Department of Pathology, Faculty of Medicine, Charles University Hospital Plzeň, Charles University, Alej Svobody 80, 304 60 Pilsen, Czech Republic. Tel.: +420 377104643; fax: +420 377104650.
E-mail address: hes@medima.cz (O. Hes).

http://dx.doi.org/10.1016/j.anndiagpath.2014.10.002
1092-9134/

labeling for TFEB is specific to t(6;11) RCC and nuclear positivity of TFE3 is specific to Xp11.2 translocations. However, recent articles have shown the limited reliability of immunohistochemical evaluation of TFE3 protein [5].

Together with the TFEB and TFE3, MiT family also involves MITF and TFEC, all of which have overlapping transcriptional activities [6]. The variations of the clinicopathologic spectrum of these tumors have yet to be determined. Contrary to the Xp11.2 TRCCs, where aggressive clinical behavior has frequently been documented, the t(6;11) TRCC presented mostly with a nonaggressive clinical course, thus having come to be considered as indolent, usually low-stage and low-grade tumors [7–9].

Up to date, 49 cases of t(6;11) TRCC have been reported, most without signs of aggressive behavior. [5,10,11]. Only 4 cases with aggressive behavior have been reported thus far (8%) [11–14].

In our study, we have compared 5 nonaggressive tumors (NAT) with 1 previously unreported aggressive metastazing tumor (AT), using the morphology, immunohistochemistry, and molecular-genetic examinations. Extensive research of the literature written in English has been undertaken to elucidate all known facts about aggressive t(6;11) TRCC that have been described so far.

2. Materials and methods

Out of 17 700 renal tumors and tumor-like lesions in the institutional and consultation files of Sikl's Department of Pathology, Charles University, Plzen, Czech Republic, 6 cases of t(6;11) RCC were identified. Four cases have been reported [15,16], and 2 new unpublished cases (including 1 aggressive metastazing case) have been added. The tissues were fixed in neutral formalin and embedded in paraffin and were cut into 4 to 5 μm thin sections and stained with hematoxylin and eosin.

2.1. Immunohistochemistry

The immunohistochemical study was performed using a Ventana Benchmark XT automated stainer (Ventana Medical System, Inc, Tucson, Arizona) on formalin-fixed, paraffin-embedded tissue. The following primary antibodies were used: cytokeratins (CAM 5,2, monoclonal, 1:200; Becton-Dickinson, San Jose, California), AE1-AE3 (monoclonal, 1:1000; BioGenex, San Ramon, California), CD10 (56C6, 1:20; Novocastra, Burlingame, California), c-kit (CD 117, polyclonal, RTU; DakoCytomation, Glostrup, Denmark), racemase/AMACR (P504S, monoclonal, 1:50; Zeta, Sierra Madre, California), vimentin (D9, monoclonal, 1:1000; NeoMarkers, Westinghouse, California), anti-melanosome (HMB45, monoclonal, 1:200; DakoCytomation), PAX8 (polyclonal, 1:25; Cell Marque, Rocklin, California), cathepsin K (3F9, monoclonal, 1:100; Abcam, Cambridge, UK), S100 (polyclonal, 1:400; DakoCytomation), Melan-A (A103,monoclonal, RTU; DakoCytomation), TFE3 (monoclonal, MRQ-37, RTU; Cell Marque), tyrosinase (polyclonal, 1:100; NeoMarkers, Westinghouse, Fremont California), mTor (monoclonal, Ser 2448, 49F9, 1:50; Cell Signaling, Danvers, Massachusetts). The primary antibodies were visualized using the supersensitive streptavidin-biotin-peroxidase complex (BioGenex). Appropriate positive controls were used.

2.2. Molecular-genetic study

Detection of *Alpha-TFEB* genomic junction, *Alpha-TFEB* fusion transcript, and chromosomal numerical changes was performed by polymerase chain reaction (PCR; case 2), reverse transcriptase PCR (cases 2 and 6), and array comparative genomic hybridization (aCGH) (case 2), respectively. All these methods were described in Petersson et al [15]. Fluorescence in situ hybridization (FISH) analysis was performed in cases 1, 3, 4, 5, and 6 using break apart probe *TFEB* ba (6p21) consisting of BAC probes RP11-328M4 a RP11-533O20 (BlueGnome, Cambridge, UK). In cases 5 and 6, FISH analysis of chromosomal loci 1p36 and 22q was performed using probes 1p36/1q25 and LSI 22BCR (VYSIS/Abbott Molecular, Des Plaines, Illinois). The tumor areas of the specimens were examined with an Olympus BX51 fluorescence microscope using a ×100 objective and filter sets Triple Band Pass (DAPI/Spectrum Green/Spectrum Orange) and Single Band Pass (Spectrum Green, Orange, and Aqua). Scoring was performed by counting the number of fluorescent signals in 100 randomly selected, nonoverlapping tumor cell nuclei. The slide was independently enumerated by 2 observers (P.M. and T.V.). Cutoff values for monosomy were set at 35% and 37% for 1p36 and 22q probes, respectively, and for polysomy at 10% for both probes. Cutoff for *TFEB* ba probe was set at 10%.

3. Results

3.1. Clinical features

The basic clinicopathologic data are summarized in Table 1. Cases 1 to 4 have been already reported [15,16]. In brief, the patients were 4 women and 2 men (all Caucasian) with age ranging from 15 to 77 years (mean, 35.3 years; median, 23 years). Follow-up was available for all patients (ranging from 2.5 months to 8 years; mean, 3.37; median, 3 years). Clinical data from the 2 new patients were as follows:

Case 5: a 15-year-old boy was referred to the hospital because of a palpable painless swelling of the abdomen. No hematuria was detected. Radical nephrectomy was performed; no adjuvant oncologic treatment was administered.

Case 6: tumor was found in a 77-year-old women. The patient complained of increasing back pain and renal colic. Computed tomographic (CT) scan revealed a tumor of the left kidney measuring 16.5 × 12.3 × 16.7 cm. The patient died of disease 2.5 months after diagnosis with metastases to ipsilateral adrenal gland (histologically confirmed) and lung (determined using CT and positron emission tomography/CT scanning).

3.2. Pathological findings

3.2.1. Gross pathology

Nonaggressive tumors were well circumscribed, largely encapsulated, and displayed gray to tan cut surface with focal hemorrhage. Focal cystic change was present in 1 case. There were no grossly visible foci of necrosis. Tumor size ranged from 3 to 14 cm (median, 5 cm). In all cases, the tumors were confined to the kidney. Hence, there was no infiltration of the perirenal or sinusoidal fat, neither was there renal vein invasion.

Aggressive tumor was partially encapsulated, well circumscribed with voluminous, mostly centrally located hemorrhagic necrosis. Cut surface was brown. Tumor measured 12 × 11.5 × 9 cm (Fig. 1).

3.2.2. Morphology

3.2.2.1. Cases 1 to 5 (NATs). On low power, all tumors displayed a solid or solid/alveolar architecture. The tumors were mostly surrounded by a fibrous pseudocapsule. Although only focally, groups of entrapped

Table 1
Main clinicopathologic data

Case	Age (y)	Sex	Size (cm)	Clinical manifestation	Follow-up
1	22	M	3	Incidental finding	8 y AW, then LE
2	24	F	14	Palpable mass	3 y AW, then LE
3	20	F	9.5	Incidental finding	5 y AW, than LE
4	54	F	7	Increasing pain right hip (nephrectomy)	AW 3 y after dg, then LE
5	15	M	10	Palpable mass	AW 1 y
6	77	F	12	Increased back pain, renal colic	DOD 2.5 mo after dg

Abbreviations: M, male; F, female; AW, alive and well; LE, lost of evidence; DOD, dead of disease; dg, diagnosis.

Table 2
Results of immunohistochemical examinations: nonaggressive cases

Case	HMB45	Melan-A	TFE3	CD10	CD117	Tyros	mTor	CAM 5.2	AE1/AE3	Cath	Vim	PAX8	MIB1
1	+++	++	−	+	++	+	−	Foc ++	−	+++	+	−	1-2/hpf
2	+++	++	−	Foc +	++	Foc +	Foc+	++	++	+++	+	Foc weak+	1-2/hpf
3	+++	−	−	Foc +	−	+ −	Foc+	Foc+	−	+++	+	++	0-1/hpf
4	++ focal	++	−	0	Foc ++	Not done	−	−	−	+++	Not done	Foc +	0-1/hpf
5	+++	+++	−	Foc ++	Foc ++	Foc+	−	Foc ++	Foc ++	+++	+	Foc ++	5-8/hpf

Abbreviations: Cath, Cathepsin-K; MIB1, antibody against Ki-67 antigen; Tyros, tyrosinase; vim, vimentin; hpf, high-power field; foc, focal.
"+" = weak positivity; "++" = moderate positivity; "+++" = strong positivity; "−" = negative.

tubules at the edge of the tumor were found. Degenerative changes were noted in 2 of the 4 cases. Microscopic foci of necrosis and fibrosis were seen in cases 1 and 2. All tumors contained areas with discohesive neoplastic cells. Some of these areas displayed tubulary architecture, whereas other areas showed a more solid architecture. The pseudorosettes were present in all tumors (Fig. 2). These pseudorosettes were formed by smaller lymphocyte-like cells, grouped around collagenous spheres, formed by basement membrane material. The small lymphocyte-like cells had scanty cytoplasm and round nuclei (Fuhrman grade 1). The pseudorosettes frequently contained areas with signet ring–like change or conspicuous clear cell change. In some tumors (cases 1, 3, and 4), the pseudorosettes were already apparent at low magnification. In case 2, the pseudorosettes were less apparent and discernible only at higher magnification and after serial sectioning. In the same case, there were long branching narrow tubules that were already very conspicuous at low-power magnification. These tubules were rimmed by one row of neoplastic cells with granular cytoplasm, having the nuclei aligned on the basement membrane, thus giving these structures a resemblance to glandular epithelium. Infrequently, areas with solid growth and moderate atypia (corresponding to Fuhrman nucleolar grade 2 or rarely 3) were observed (Fig. 3). Most of the neoplastic cells had abundant eosinophilic, slightly granular, and sometimes "feathery" cytoplasm. Populations of larger cells with voluminous clear to slightly eosinophilic cytoplasm were present in all tumors. In 2 cases (cases 1 and 2), we found areas with hyalinization formed by basal membrane material. Mitotic figures were exceptionally rare in 1 case (case 2), and atypical mitoses were absent. In addition to the above-described morphologic characteristics, small foci with morphologic features strongly resembling another translocation associated renal tumor, the ASPL-TFE3 renal carcinoma (Xp11.2 group), were detected in 1 case (case 2). In this area, alveolar and tubulopapillary structures were lined by large cells having voluminous clear to slightly eosinophilic cytoplasm. The nuclei in these areas were Fuhrman nucleolar grade 3.

3.2.2.2. Case 6 (AT). Tumor was mostly solid to solid-alveolar, composed of larger eosinophilic cells with the occasional presence of lymphocytes in the interstitium (Fig. 4). There were voluminous necrotic and hemorrhagic areas. Occasionally, large tubules and pseudotubules were scattered through tumorous mass. Cells were mostly voluminous, weakly eosinophilic with "cloudy" appearance. Nuclei were of grade 2 and 3 according to Fuhrman nucleolar grade. Pseudorosettes were located mostly within large pseudotubules. Only few mitotic figures were noted, no atypical mitoses were encountered. Foci of pseudopapillary to papillary formations were rarely noted. Papillae were lined by large, bizarre polymorphic cells with Fuhrman nucleolar grade 3 and 4 (Fig. 5).

3.2.3. Immunohistochemistry

3.2.3.1. NATs (cases 1-5). The immunohistochemical findings of NATs are summarized in Table 2. All of them were diffusely positive for Cathepsin K, HMB-45 (Fig. 6A), and Melan-A. Vimentin was positive in all cases, although positivity was weak. Expression of cytokeratins CAM 5.2 and AE1-AE3 was variable (Fig. 6B). CD10 and tyrosinase were weakly and focally positive in 4 of 5. Two of 5 cases were weakly and focally immunoreactive for mTOR. Four of 5 NATs were positive strongly but focally for CD117. PAX8 immunoreactive pattern was variable with negative (1/5) to moderate positive staining (1/5). Mostly tumors were focally positive (3/5). There was no diffuse expression of TFE3 in any of the tumors.

3.2.3.2. AT (case 6). The complete results of immunohistochemical examinations of primary aggressive t(6;11) RCC and metastatic lesion are summarized in Table 3. Both showed a strong, diffuse immunoreactivity for HMB-45, Melan-A, and Cathepsin-K. CAM 5.2 and CD10 were moderately positive. CD117 was positive in both primary and metastatic lesions. PAX8 was focally positive in primary and metastatic tumor. The neoplastic cells did not express TFE3, tyrosinase, mTOR, AE1/AE3, and vimentin in both primary and metastatic tumor.

3.3. Molecular-genetic findings

Results of molecular-genetic findings are summarized in Table 4. *TFEB* gene rearrangement or *Alpha-TFEB* translocation was found in 5 of 6 cases. One was unanalyzable. In AT, *TFEB* gene break was accompanied by its amplification. In 2 of 3 analyzed cases, including AT, loss of 1p36 and 22q was also detected.

4. Discussion

t(6;11) TRCC is recognized mostly as a low-grade NAT. This is in contrast to Xp11.2 TRCC. Most of Xp11.2 TRCCs are considered to be highly aggressive, high-stage, and high-grade tumors [1,16].

There are no well-established prognostic criteria predicting biological behavior that are applicable for t(6;11) TRCC.

t(6;11) TRCC is usually described as neoplasm with a distinctive biphasic pattern, comprising larger and smaller epithelioid cells, with the latter often clustered around basement membrane material; however, the full spectrum of the morphologic appearances of the t(6;11) TRCC is probably more variable [17–19]. The t(6;11) TRCCs express Cathepsin K, HMB-45, Melan-A, and usually PAX8. Nuclear labeling for TFEB protein by IHC is supposed to be a sensitive and specific assay for

Table 3
Results of immunohistochemical examinations—aggressive case

	HMB45	Melan-A	TFE3	CD 10	CD 117	Tyros	mTor	CAM 5.2	AE1/AE3	Cath	Vim	PAX8	MIB1
Prim	+++	+++	0	++	Foc ++	0	0	++	0	+++	−	Foc +	0-5/hpf
Meta	+++	+++	0	Foc ++	Foc ++	0	0	++	0	+++	−	Foc +	8-12/hpf

Abbreviations: Cath, Cathepsin-K; MIB1, antibody against Ki-67 antigen; Tyros, tyrosinase; Vim, vimentin; hpf, high-power field; Prim, primary tumor; Meta, metastasis to suprarenal gland; foc, focal.
"+" = weak positivity; "++" = moderate positivity; "+++" = strong positivity; "−" = negative.

Table 4
Molecular-genetic analysis

Case	Numerical changes	Translocation		
	aCGH or FISH (1p36 and 22q probes)	FISH *TFEB* ba probe	RT-PCR *Alpha-TFEB*	PCR *Alpha-TFEB*
1	NP	NA	NP	NP
2[a]	Loss 1p35.1 to p36.21 (aCGH) Loss 22q (aCGH)	NP	Positive	Positive
3	NP	Positive	NP	NP
4	NP	Positive	NP	NP
5	Negative (FISH)	Positive	NP	NP
6	Loss 1p36 (FISH) Loss 22q (FISH)	Positive (amplification)	Positive	NP

Abbreviations: RT, reverse transcriptase; NP, not performed; NA, not analyzable.
[a] Translocation t(X;17) (ASPL-TFE3) was analyzed in case 2 with negative result.

these neoplasms; however, there are many false-positive/negative staining as a result of fixation, autolysis, and other steps related to the tissue processing [5,20]. Furthermore, CD117 was found to be another potential distinguishing marker between the t(6;11) TRCC and Xp11.2 TRCC. CD117 is usually positive in t(6;11) TRCC, but not positive in most of Xp11.2 TRCCs [11]. In our series, one of the NATs was negative for CD117. Generally, positivity for CD117 was moderate, but mostly focal. In the AT, focal membranous positivity for CD117 was noted both in the primary tumor and in metastasis. Immunoreactivity with PAX8 was highly variable (negative to moderately positive) in our cases.

Fluorescence in situ hybridization assay for *TFEB* gene break or PCR-based analysis for the presence of *Alpha-TFEB* fusion is currently available even for paraffin-embedded material, which seems a more robust technique than immunohistochemical examination [1,21].

t(6;11) TRCC has long been considered as NAT. Even so, the possible late recurrence, similar to the behavior reported of Xp11.2 TRCC, and metastatic potential have been observed. Up to date, 4 aggressive cases of t(6;11) TRCC have been reported. The overview of 4 aggressive t(6;11) TRCC described in the literature and summary of our new case is outlined in Table 5[11,14].

The first case was described by Martignoni et al [12] in 2005. The tumor was found in 42-year-old woman who presented with paratracheal and pleural metastases 3 years after the surgery. However, later the question was raised, whether this tumor was indeed t(6;11) TRCC, Xp11.2 TRCC, or an unusual variant of TRCC with overlapping features between Xp11.2 and t(6;11) TRCC (Dr. Guido Martignoni and Dr. Matteo Brunelli's personal communication).

The second aggressive case of t(6;11) TRCC was reported by Camparo et al [13] in 2008. The size of the tumor was 20 cm, and it presented as an abdominal mass in a 36-year-old man who died after 3 months after the diagnosis with widespread metastatic disease.

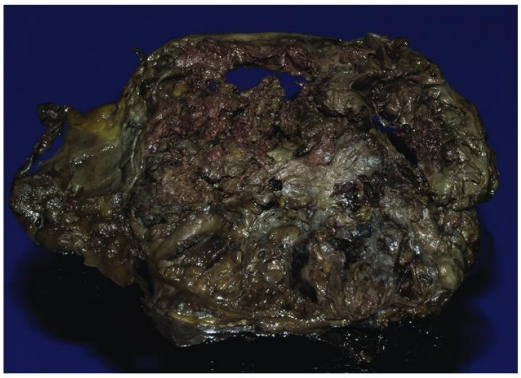

Fig. 1. Huge area of mostly centrally located necrosis was present on gross section of aggressive case.

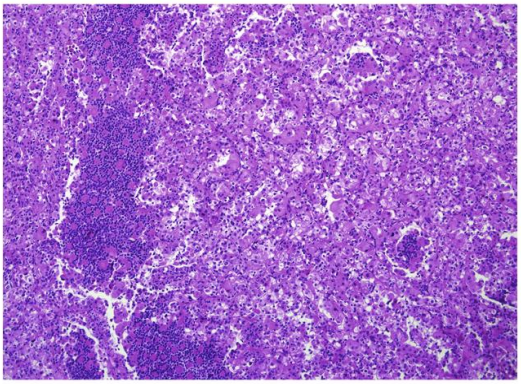

Fig. 2. In typical cases of nonaggressive cases, the pseudorosettes were formed by smaller lymphocyte-like cells grouped around collagenous spherules.

Third malignant t(6;11) TRCC was described by Inamura et al [14] in 2012. A 37-year-old man had undergone a total nephrectomy in 1989. Eight years later, he presented with lung and mediastinal lymph node metastases. The renal tumor was originally diagnosed as clear cell–type RCC. Subsequently, he underwent a lymph node dissection and

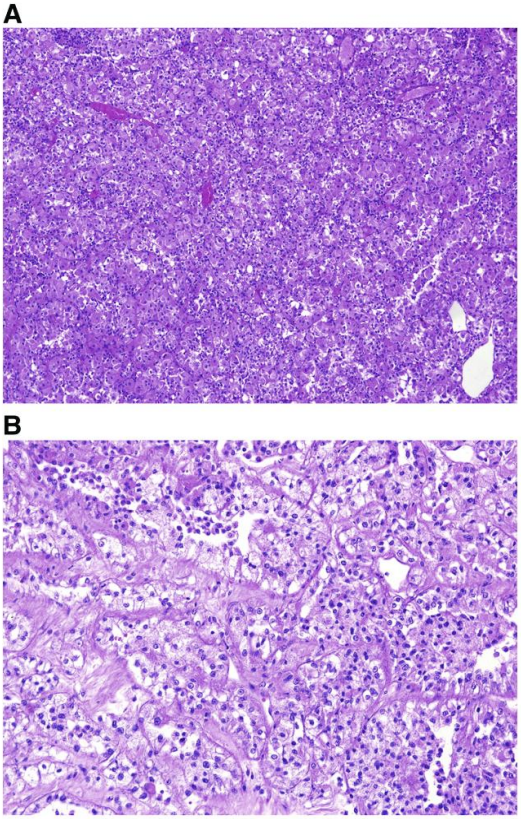

Fig. 3. Areas with solid growth and moderate atypia were observed both in nonaggressive cases (A) and in aggressive cases (B).

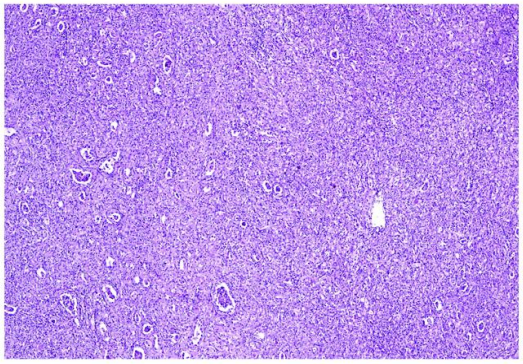

Fig. 4. Pseudorosettes in aggressive case were less conspicuous comparing with typical nonaggressive cases.

partial resection of the lung for the metastatic tumor measuring 4.5 cm. Karyotyping of the tumor revealed a t(6;11) (p21.1;q12 ~ 13) chromosomal rearrangement, a characteristic of the t(6;11) TRCC. Thirty months after second surgery, the patient died of multiple metastases to the lung and bone.

The fourth case was described by Smith et al [11] in January 2014. The tumor was found in a 34-year-old man. The patient developed rib metastasis 8 years after resection of the primary tumor.

The fifth case (currently described case) differs clinically from previously reported ATs mainly by age of the patient. The size of the tumor was relatively large; however, substantially larger NATs have been reported. Our patient died of disease 2.5 months after surgery.

Summarizing all available clinical data dealing with aggressive t(6;11) RCC cases, a few mutual characteristics have been observed. As regards clinicopathologic features, the aggressive t(6;11) TRCC appears to affect older population (mean, 45.2 years; median, 37 years) than nonaggressive cases (mean, 31.5 years; median, 30.5 years). Previously described ATs metastasized into the pleura (case 1), lung (cases 3 and 5), mediastinal lymph nodes (cases 1 and 3), bones (cases 3 and 4), and adrenal gland (case 5) (Fig. 7). The same 8-year interval between resection of the primary tumor and metastasis was observed in cases 3 and 4 (Table 5).

Size of the ATs was bigger (mean, 11.67 cm; median, 20 cm) than that of the NATs (mean, 7.43 cm; median, 4.75 cm).

Microscopic foci of necrosis were described in 1 nonaggressive case only [13]; however, it is not possible to get more information about presence/absence of necrotic foci from the previous literature. Grossly visible necrotic areas were present in 2 of 5 malignant tumors only.

Probably, the presence of grossly visible necrosis could be a possible adverse prognostic factor in t(6;11) TRCC. Mitotic figures were observed in 2 of 49 NATs and in 1 AT. However, presence/absence of mitotic activity has been seldom mentioned in the literature.

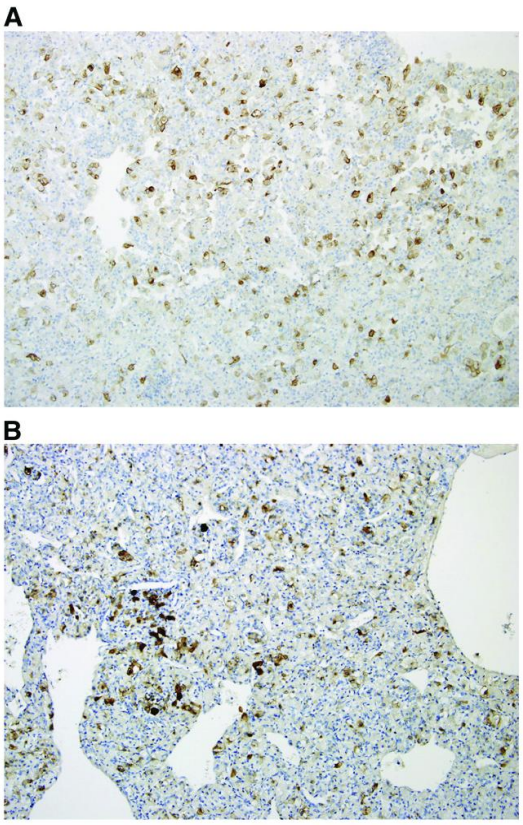

Fig. 6. All cases were positive for HMB45 (A) and cytokeratins (CAM 5.2 shown in case 2) (B).

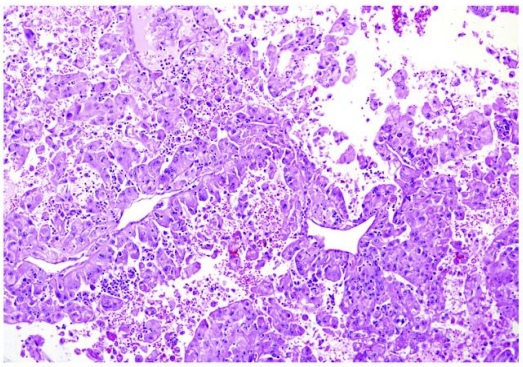

Fig. 5. In aggressive case, it was possible to find foci with papillary/pseudopapillary structures composed of bizarre atypical cells.

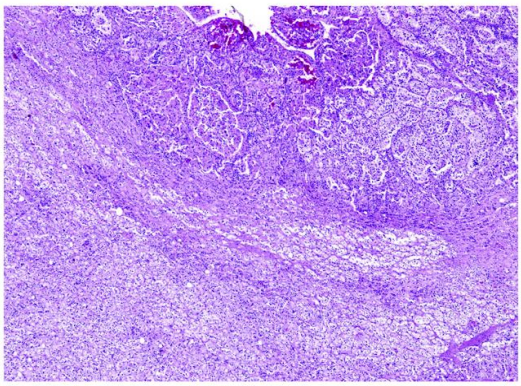

Fig. 7. Metastasis of t(6;11) RCC to the ipsilateral adrenal gland.

Table 5
Overview of the aggressive cases in the literature and current case

Case	Age (y)	Size (cm)	Necrosis	Vimentin	Mitoses	Atypical mitoses	TFEB rearrangement	Meta
Case 1: Martignoni et al Martignoni et al [12]	42	NA	None	+	None	None	NP	Paratracheal lymph nodes, pleura
Case 2: Camparo et al [13]	36	20	+ (5%)	+	Not known	Not known	NA	Not known (deceased)
Case 3: Inamura et al [14]	37	NA	Not known	+	Not known	Not known	+	Lung, mediastinal lymph node, bone
Case 4: Smith et al [11]	34	3	Not known	Not known	Not known	Not known	+	Rib
Case 5: currently described new case	77	12	+ (40%)	−	+	None	+	Adrenal gland and lung

Abbreviations: NP, not performed; NA, nonavailable; Meta, metastasis; y, years.
"+" = positive; "−" = negative.

Histologically, 2 ATs (cases 2 and 4; Table 5) lacked a small cell component. One AT (case 3; Table 5) showed features of unusual morphology for t(6;11) TRCC and was initially diagnosed as clear cell–type RCC. Morphology in the current aggressive case (case 5; Table 5) was compatible with the usual features of t(6;11) TRCC; however, some minor variations were noted (for further details, see the Results section). Papillary and pseudopapillary formations lined by high-grade cells were not described in any of NATs according to the literature. However, similar focal architecture has been described in 1 NAT but with low-grade neoplastic cells.

Aggressive tumor (case 5; Table 5) showed amplification of *TFEB* locus. No information about copy number changes of TFEB loci is mentioned in previous articles dealing AT; however, as this phenomenon was found in our set only in AT, it could be a genetic hallmark of aggressive t(6;11) RCC. Analysis of other ATs is, however, necessary to confirm this hypothesis.

Translocation t(6;11) (Alpha-TFEB) or *TFEB* break was detected in 4 NATs and 1 AT.

Losses of part of chromosomes 1 and 22 were found in our AT. However, identical findings were shown in nonaggressive case (case 2 in the original series) published previously [15]. Thus, chromosomal aberration pattern does not seem to predict/rule out potential aggressive behavior.

Regarding the histopathologic differential diagnosis, the morphology and immunohistochemical pattern of t(6;11) TRCC could mimic Xp11.2 TRCC. The most distinctive histologic pattern of the Xp11 TRCC is presence of both clear/eosinophilic cells, mostly papillary architecture and, in some cases, abundant psammoma bodies. However, Xp11.2 TRCCs can also produce pattern or unusual morphology mimicking other types of RCCs [22]. The biphasic morphologic variant with population of larger polygonal cells mixed with smaller cells clustering around hyaline material has been already described in Xp11.2 TRRCC. Such cases can simulate t(6;11) TRCC. On the other hand, the t(6;11) TRCC can mimic Xp11.2 TRCC as well [22]. The Xp11 TRCC is distinguished by chromosomal translocations with breakpoints involving the *TFE3*, which maps to the Xp11.2 locus. Differential diagnosis between both basic types of translocation carcinomas is complicated in difficult cases. Analysis of the morphology, together with immunohistochemical examination (TFE3, TFEB—if available, CD117, HMB-45, and Melan-A), should be supported by the molecular-genetic analysis.

Another tumor, which should be ruled out during the differential diagnostic process, is angiomyolipoma (AML), especially its epithelioid/oncocytic variety. Both t(6;11) TRCC and AML are positive for HMB-45 and Melan-A. It is important to note that some AMLs, as well as t(6;11) TRCC, may show only scattered HMB-45–positive cells. Angiomyolipoma is frequently composed, at least in part, of voluminous cells with slightly eosinophilic cloudy cytoplasm resembling in some aspects the neoplastic cells in t(6;11) TRCC. Angiomyolipoma frequently contains lipocytes, which are usually absent in t(6;11)-associated RCCs. Voluminous prominent vascular structures characteristic for AML could be present/absent in t(6;11) TRCC. Thus, it is not possible to use this morphologic feature for differential diagnosis. Moreover, the epithelioid variant of AML lacks usually lipocytic component (or it is inconspicuous), and vascular component could be less prominent [23]. The so-called oncocytic variant of AML is composed of large cells with voluminous eosinophilic cytoplasm arranged in solid arrangements [1,24]. Again, in unusual challenging cases, a good sampling is necessary and, in more difficult cases, analysis of translocation and/or TFEB protein performed by molecular-genetic techniques would be helpful.

5. Conclusions

We have compared all, to date reported, malignant cases of t(6;11) translocation carcinomas with one another and have tried to find some mutual features.

1. Aggressive t(6;11) RCCs generally occur in older population in comparison with their indolent counterparts.
2. In regard to the histologic findings in ATs, 3 of 5 cases were morphologically slightly different from nonaggressive t(6;11) RCC. Of the 3 cases, 2 cases lacked a small cell component and 1 closely mimicked clear cell–type RCC.
3. Grossly visible necroses were present in aggressive t(6;11) RCC only and could be potentially taken as a adverse prognostic factor.
4. Amplification of *TFEB* locus was also found only in aggressive t(6;11) RCC.

Further genetic and clinicopathologic investigations with additional new cases can further highlight this rare and peculiar variant of RCC.

Disclosure of conflict of interest

All authors declare no conflict of interest.

The study was supported by the Charles University Research Fund (project number P36) and by the project by the project CZ.1.05/2.1.00/03.0076 from European Regional Development Fund.

References

[1] Srigley JR, Delahunt B, Eble JN, Egevad L, Epstein JI, Grignon D, et al. The International Society of Urological Pathology (ISUP) Vancouver Classification of Renal Neoplasia. Am J Surg Pathol 2013;37(10):1469–89 [PubMed PMID: 24025519].
[2] Argani P, Ladanyi M. Recent advances in pediatric renal neoplasia. Adv Anat Pathol 2003;10(5):243–60 [PubMed PMID: 12973047].
[3] Argani P, Ladanyi M. Distinctive neoplasms characterised by specific chromosomal translocations comprise a significant proportion of paediatric renal cell carcinomas. Pathology 2003;35(6):492–8 [PubMed PMID: 14660099].
[4] Argani P, Ladanyi M. The evolving story of renal translocation carcinomas. Am J Clin Pathol 2006;126(3):332–4 [PubMed PMID: 16880145].
[5] Argani P, Yonescu R, Morsberger L, Morris K, Netto GJ, Smith N, et al. Molecular confirmation of t(6;11)(p21;q12) renal cell carcinoma in archival paraffin-embedded material using a break-apart TFEB FISH assay expands its clinicopathologic spectrum. Am J Surg Pathol 2012;36(10):1516–26 [PubMed PMID: 22892601].
[6] Medendorp K, van Groningen JJ, Schepens M, Vreede L, Thijssen J, Schoenmakers EF, et al. Molecular mechanisms underlying the MiT translocation subgroup of renal cell carcinomas. Cytogenet Genome Res 2007;118(2-4):157–65 [PubMed PMID: 18000366].
[7] Kuiper RP, Schepens M, Thijssen J, van Asseldonk M, van den Berg E, Bridge J, et al. Upregulation of the transcription factor TFEB in t(6;11)(p21;q13)-positive renal

cell carcinomas due to promoter substitution. Hum Mol Genet 2003;12(14):1661–9 [PubMed PMID: 12837690].
[8] Davis IJ, Hsi BL, Arroyo JD, Vargas SO, Yeh YA, Motyckova G, et al. Cloning of an Alpha-TFEB fusion in renal tumors harboring the t(6;11)(p21;q13) chromosome translocation. Proc Natl Acad Sci U S A 2003;100(10):6051–6 [PubMed PMID: 12719541. Pubmed Central PMCID: 156324].
[9] Geller JI, Argani P, Adeniran A, Hampton E, De Marzo A, Hicks J, et al. Translocation renal cell carcinoma: lack of negative impact due to lymph node spread. Cancer 2008;112(7):1607–16 [PubMed PMID: 18278810].
[10] Rao Q, Liu B, Cheng L, Zhu Y, Shi QL, Wu B, et al. Renal cell carcinomas with t(6;11)(p21;q12): a clinicopathologic study emphasizing unusual morphology, novel alpha-TFEB gene fusion point, immunobiomarkers, and ultrastructural features, as well as detection of the gene fusion by fluorescence in situ hybridization. Am J Surg Pathol 2012;36(9):1327–38 [PubMed PMID: 22895266].
[11] Smith NE, Illei PB, Allaf M, Gonzalez N, Morris K, Hicks J, et al. t(6;11) renal cell carcinoma (RCC): expanded immunohistochemical profile emphasizing novel RCC markers and report of 10 new genetically confirmed cases. Am J Surg Pathol 2014;38(5):604–14 [PubMed PMID: 24618616].
[12] Martignoni G, Tardarico R, Pea M, Pecciarini L, Gobbo S. t6;11 renal cell tumor. A clinicopathological study of two cases in adults. Mod Pathol 2005;18(Suppl 1):155A.
[13] Camparo P, Vasiliu V, Molinie V, Couturier J, Dykema KJ, Petillo D, et al. Renal translocation carcinomas: clinicopathologic, immunohistochemical, and gene expression profiling analysis of 31 cases with a review of the literature. Am J Surg Pathol 2008;32(5):656–70 [PubMed PMID: 18344867].
[14] Inamura K, Fujiwara M, Togashi Y, Nomura K, Mukai H, Fujii Y, et al. Diverse fusion patterns and heterogeneous clinicopathologic features of renal cell carcinoma with t(6;11) translocation. Am J Surg Pathol 2012;36(1):35–42 [PubMed PMID: 21959307].
[15] Petersson F, Vanecek T, Michal M, Martignoni G, Brunelli M, Halbhuber Z, et al. A distinctive translocation carcinoma of the kidney; "rosette forming," t(6;11), HMB45-positive renal tumor: a histomorphologic, immunohistochemical, ultrastructural, and molecular genetic study of 4 cases. Hum Pathol 2012;43(5):726–36 [PubMed PMID: 22051379].
[16] Hora M, Urge T, Travnicek I, Ferda J, Chudacek Z, Vanecek T, et al. MiT translocation renal cell carcinomas: two subgroups of tumours with translocations involving 6p21 [t (6; 11)] and Xp11.2 [t (X;1 or X or 17)]. SpringerPlus 2014;3:245 [PubMed PMID: 24877033. Pubmed Central PMCID: 4032393].
[17] Argani P, Lae M, Hutchinson B, Reuter VE, Collins MH, Perentesis J, et al. Renal carcinomas with the t(6;11)(p21;q12): clinicopathologic features and demonstration of the specific alpha-TFEB gene fusion by immunohistochemistry, RT-PCR, and DNA PCR. Am J Surg Pathol 2005;29(2):230–40 [PubMed PMID: 15644781].
[18] Argani P, Lae M, Ballard ET, Amin M, Manivel C, Hutchinson B, et al. Translocation carcinomas of the kidney after chemotherapy in childhood. J Clin Oncol 2006;24(10):1529–34 [PubMed PMID: 16575003].
[19] Suarez-Vilela D, Izquierdo-Garcia F, Mendez-Alvarez JR, Miguelez-Garcia E, Dominguez-Iglesias F. Renal translocation carcinoma with expression of TFEB: presentation of a case with distinctive histological and immunohistochemical features. Int J Surg Pathol 2011;19(4):506–9 [PubMed PMID: 19687027].
[20] Martignoni G, Bonetti F, Chilosi M, Brunelli M, Segala D, Amin MB, et al. Cathepsin K expression in the spectrum of perivascular epithelioid cell (PEC) lesions of the kidney. Mod Pathol 2012;25(1):100–11 [PubMed PMID: 21874011].
[21] Zhong M, De Angelo P, Osborne L, Keane-Tarchichi M, Goldfischer M, Edelmann L, et al. Dual-color, break-apart FISH assay on paraffin-embedded tissues as an adjunct to diagnosis of Xp11 translocation renal cell carcinoma and alveolar soft part sarcoma. Am J Surg Pathol 2010;34(6):757–66 [PubMed PMID: 20421778].
[22] Argani P, Olgac S, Tickoo SK, Goldfischer M, Moch H, Chan DY, et al. Xp11 translocation renal cell carcinoma in adults: expanded clinical, pathologic, and genetic spectrum. Am J Surg Pathol 2007;31(8):1149–60 [PubMed PMID: 17667536].
[23] Nese N, Martignoni G, Fletcher CD, Gupta R, Pan CC, Kim H, et al. Pure epithelioid PEComas (so-called epithelioid angiomyolipoma) of the kidney: a clinicopathologic study of 41 cases: detailed assessment of morphology and risk stratification. Am J Surg Pathol 2011;35(2):161–76 [PubMed PMID: 21263237].
[24] Martignoni G, Pea M, Bonetti F, Brunelli M, Eble JN. Oncocytoma-like angiomyolipoma. A clinicopathologic and immunohistochemical study of 2 cases. Arch Pathol Lab Med 2002;126(5):610–2 [PubMed PMID: 11958671].

MUCINÓZNÍ TUBULÁRNÍ A VŘETENOBUNĚČNÝ RENÁLNÍ KARCINOM: ANALÝZA CHROMOZOMÁLNÍCH ABERACÍ U LOW-GRADE, HIGH-GRADE A MORFOLOGICKÉ VARIANTY PODOBNÉ PAPILÁRNÍMU RENÁLNÍMU KARCINOMU

Mucinózní tubulární a vřetenobuněčný renální karcinom (MTVRK) je histologicky charakterizován proliferací tubulárně uspořádaných kuboidálních buněk, které jsou promíchány s low grade vřetenitými buňkami a myxoidním stromatem [6]. Morfologie těchto tumorů se často překrývá s papilárním renálním karcinomem (PRK), vzácněji se vyskytují i případy s high-grade histopatologickými znaky [11]. MTVRK patří mezi vzácné tumory s incidencí menší než 1% ze všech renálních neoplazií.

V přiložené publikaci jsme se zaměřili na analýzu spektra chromozomálních aberací vyskytujících se u různých morfologických variant této cytogeneticky málo prozkoumané jednotky. Do studie bylo zahrnuto 16 případů MTVRK, které byly dle morfologie rozděleny na 3 skupiny: klasické, low-grade MTVRK (5 případů), high-grade MTVRK (5 případů) a tumory napodobující PRK (6 případů). Cílem studie bylo zmapovat spektrum chromozomálních aberací na velkém souboru případů a porovnat genetické odchylky s morfologickými variantami MTVRK. Skupina klasických MTVRK vykazovala ztráty chromozomů 1,4,8,9,14,15 a 22 a žádné nadpočetné chromozomy, skupina high-grade tumorů měla ztráty chromozomů 1,4,6,8,9,13,14,15 a 22 a rovněž žádné nadpočetné chromozomy a tumory napodobující PRK se prezentovaly ztrátami chromozomů 1,4,6,8,9,10,14,15 a 22. Z této skupiny měly 2 případy nadpočetné chromozomy včetně 7,17, tyto byly následně překlasifikovány na PRCC.

Na základě této práce lze říci, že MTVRK má relativně uniformní chromozomální numerické aberace. U případů s atypickou morfologií, převážně se jedná o tumory napodobující PRK, je nezbytné provést chromozomální analýzu a v případě detekce nadpočetných chromozomů 7 a 17 by tyto tumory měly být překlasifikovány na papilární renální karcinom.

Annals of Diagnostic Pathology 19 (2015) 226–231

Contents lists available at ScienceDirect

Annals of Diagnostic Pathology

Mucinous spindle and tubular renal cell carcinoma: analysis of chromosomal aberration pattern of low-grade, high-grade, and overlapping morphologic variant with papillary renal cell carcinoma☆,☆☆

Kvetoslava Peckova, MD [a], Petr Martinek, MSc [a], Maris Sperga, MD [b], Delia Perez Montiel, MD [c], Ondrej Daum, MD, PhD [a], Pavla Rotterova, MD, PhD [a], Kristýna Kalusová, MD [d], Milan Hora, MD, PhD [d], Kristýna Pivovarcikova, MD [a], Boris Rychly, MD [e], Semir Vranic, MD, PhD [f], Whitney Davidson, MD [g], Josef Vodicka, MD, PhD [h], Magdaléna Dubová, MD [a], Michal Michal, MD [a], Ondrej Hes, MD, PhD [a,i,*]

[a] Department of Pathology, Charles University, Medical Faculty and Charles University Hospital Plzen, Pilsen, Czech Republic
[b] Department of Pathology, East University Riga Riga, Latvia
[c] Department of Pathology, Instituto Nacional de Cancerologia, Mexico City, Mexico
[d] Department of Urology, Charles University, Medical Faculty and Charles University Hospital Plzen, Pilsen, Czech Republic
[e] Cytopathos, Bratislava, Slovak Republic
[f] Department of Pathology, University Clinical Centre, Sarajevo, Bosnia and Hercegovina
[g] Department of Pathology and Laboratory Medicine, University of Kansas Medical Center, Kansas City, KS
[h] Department of Surgery, Charles University, Medical Faculty and Charles University Hospital Plzen, Pilsen, Czech Republic
[i] Biomedical Centre, Charles University, Medical Faculty and Charles University Hospital Plzen, Pilsen, Czech Republic

ARTICLE INFO

Keywords:
Kidney
Mucinous spindle and tubular cell carcinoma
Chromosomal aberration
aCGH

ABSTRACT

The chromosomal numerical aberration pattern in mucinous tubular and spindle renal cell carcinoma (MTSRCC) is referred to as variable with frequent gains and losses. The objectives of this study are to map the spectrum of chromosomal aberrations (extent and location) in a large cohort of the cases and relate these findings to the morphologic variants of MTSRCC. Fifty-four MTSRCCs with uniform morphologic pattern were selected (of 133 MTSRCCs available in our registry) and divided into 3 groups: classic low-grade MTSRCC (Fuhrman nucleolar International Society of Urological Pathology grade 2), high-grade MTSRCC (grade 3), and overlapping MTSRCC with papillary renal cell carcinoma (RCC) morphology. Array comparative genomic hybridization analysis was applied to 16 cases in which DNA was well preserved. Four analyzable classic low-grade MTSRCCs showed multiple losses affecting chromosomes 1, 4, 8, 9, 14, 15, and 22. No chromosomal gains were found. Four analyzable cases of MTSRCC showing overlapping morphology with PRCC displayed a more variable pattern including normal chromosomal status; losses of chromosomes 1, 6, 8, 9, 14, 15, and 22; and gains of 3, 7, 16, and 17. The group of 4 high-grade MTSRCCs exhibited a more uniform chromosomal aberration pattern with losses of chromosomes 1, 4, 6, 8, 9, 13, 14, 15, and 22 and without any gains detected. (1) MTSRCC, both low-grade and high-grade, shows chromosomal losses (including 1, 4, 6, 8, 9, 13, 14, 15, and 22) in all analyzable cases; this seems to be the most frequent chromosomal numerical aberration in this type of RCC. (2) Cases with overlapping morphologic features (MTSRCC and PRCC) showed a more variable pattern with multiple losses and gains, including gains of chromosomes 7 and 17 (2 cases). This result is in line with previously published morphologic and immunohistochemical studies that describe the broad morphologic spectrum of MTSRCC, with changes resembling papillary RCC. (3) The diagnosis of MTSRCC in tumors with overlapping morphology (MTSRCC and PRCC) showing gains of both chromosomes 7 and 17 remains questionable. Based on our findings, we recommend that such tumors should not be classified as MTSRCC but rather as PRCC.

1. Introduction

Mucinous spindle and tubular renal cell carcinoma (MTSRCC) is a relatively rare but distinctive subtype of renal cell carcinoma (RCC). The tumor is characterized by proliferation of cuboidal and spindle cells of low nuclear cytology which are arranged in cords and tubules,

☆ The study was supported by the Charles University Research Fund (Project No. P36) and by the project CZ.1.05/2.1.00/03.0076 from European Regional Development Fund.
☆☆ Disclosure of conflict of interest: All authors declare no conflict of interest.
* Corresponding author at: Department of Pathology, Charles University, Medical Faculty and Charles University Hospital Plzen, Alej Svobody 80, 304 60 Pilsen, Czech Republic. Tel.: +420377104643; fax: +420377104650.
E-mail address: hes@medima.cz (O. Hes).

http://dx.doi.org/10.1016/j.anndiagpath.2015.04.004
1092-9134/

typically within a myxoid background [1]. Some cases seem to show certain morphologic similarities to papillary RCC (PRCC) [2–4]. The chromosomal numerical aberration pattern in MTSRCC is usually referred to as variable with frequent gains and losses. However, few studies have been published, thus far, making it difficult to establish a precise description of the genetic profile [2, 5–10]. The objectives of this study were to map the spectrum of chromosomal aberrations (extent and location) in a large cohort of cases and to relate these findings to the morphologic variants of MTSRCC; special emphasis was placed on the differential diagnosis between PRCC and MTSRCC.

2. Materials and methods

Fifty-four cases of MTSRCC with uniform morphologic pattern were selected of 133 MTSRCCs available in the Pilzen Tumor Registry. Pathologic examination of routine hematoxylin-eosin–stained sections was performed on each case by at least 2 pathologists (K.P. and O.H.). Cases were reevaluated and further histologic patterns were described. For each case, 1 to 4 tissue blocks were available for further study. All cases were divided into 3 groups: classic low-grade (CLG; Fuhrman International Society of Urological Pathology [ISUP] nucleolar grade 2), high-grade (HG; Fuhrman nucleolar ISUP grade 3), and cases with morphologic features overlapping with PRCC morphology (OPM). Array comparative genomic hybridization (aCGH) analysis was applied to 16 cases with well-preserved DNA.

2.1. Molecular study

Tumor areas of the formalin-fixed, paraffin-embedded samples were determined using hematoxylin-eosin–stained slides and macrodissected. The procedures of DNA purification, integrity control, array CGH, and fluorescent in situ hybridization (FISH) analysis were described previously [11]. Required integrity of DNA was 400 base pairs. Array CGH analysis was performed using CytoChip Focus Constitutional (Illumina, San Diego, California). Several chromosomal aberrations from each group were confirmed by FISH analysis.

3. Results

The clinical and pathological features of the cases are summarized in Table 1. All 16 cases were divided into 3 groups: CLG mucinous spindle cell and tubular RCC (Fuhrman ISUP nucleolar grade 2), OPM, and HG (Fuhrman ISUP nucleolar grade 3) MTSRCC.

The group of 5 analyzable CLG MTSRCCs was composed of 4 men and 1 woman, with ages ranging from 51 to 60 years (mean, 56.4 years; median, 57 years). Tumor size ranged from 3.2 to 12.5 cm (mean, 6.44 cm; median, 6 cm). Follow-up information was available for 2 patients, both of which were alive and well at last clinical examination. Histologically, the tumors showed a predominantly tubular architectural pattern composed of tubules and cords lined by cuboidal cells with pale to eosinophilic cytoplasm admixed with spindle cell proliferation foci, all set in a loose fibrotic and, in 2 of 5 cases, myxoid stroma. Tumor cells of both cuboidal and spindle cell populations were generally bland in appearance. The nuclei were uniform in size, with rounded contours and occasional distinct nucleoli. Mitoses were infrequently observed and abnormal mitotic figures were not identified. None of the tumors displayed necrosis (Fig. 1A + B).

The group of 6 OPM MTSRCCs included 3 male and 3 female patients, with ages ranging from 47 to 71 years (mean, 57.83 years; median, 56.5 years). The tumor size ranged from 1.2 to 11 cm (mean, 4.62 cm; median, 3.5 cm). Follow-up was available for 2 patients with no signs of progression at the last clinical examination in either case. Histologically, the tumors showed areas compatible with the diagnosis of MTSRCC, composed of elongated tubules and streams (Fig. 2A + B). There was both a spindle cell component and a cuboidal cell component within the myxoid stroma. Neoplastic cells were generally of low to intermediate grade; however, cells with larger nucleoli, consistent with grade 3 (Fuhrman nucleolar), were also observed. In some areas, structures strongly resembling PRCC with predominantly papillary architecture, rare foamy macrophages, and occasional psammoma bodies were also seen. Myxoid changes in the interstitium were present in 2 of 6 cases.

Table 1
Basic clinicopathologic data

Case number	Age (years)	Sex	Size (cm)	Follow up (years)	Myxoid changes in interstitium
1	59	M	6	LE	Present
2	51	M	4.5	6 AW	Present
3	55	M	12.5	LE	Absent
4	60	F	6	LE	Absent
5	57	M	3.2	6 AW*	Absent
6	59	F	11	1 AW	Present focally
7	51	F	6.5	LE	Present
8	54	F	2	5 AW	Absent
9+	65	M	4	1 AW	Absent
10+	71	M	1.2	LE	Absent
11	47	M	3	5 AW	Absent
12	60	F	5.5	5 AW	Present
13	40	F	3.4	6 AW	Present
14	42	M	1.3	2 AW	Absent
15	57	M	??	5 AW	Absent
16	83	M	5.6	9 AW	Absent

Yellow represents classic MSTRCC; green, overlapping morphology between MSTRCC and PRCC; blue, HG MSTRCC; +, tumors were reevaluated as PRCC.
Abbreviations: AW, alive and well; LE, lost of evidence.
[a]Patient subsequently underwent kidney transplantation.

The third group included 5 cases of MTSRCC with HG morphology. Patient age (3 men and 2 women) ranged from 40 to 83 years (mean, 56.4 years; median, 57 years), and tumor size ranged from 1.3 to 5.6 cm (mean, 3.95 cm; median, 4.45 cm). Follow-up was available for all 5 patients, all of whom were alive with no evidence of disease. Tumors were morphologically characterized by the intermixing of spindle and cuboidal cells within predominantly loose, fibrous stroma. Myxoid stromal changes were present in 2 of 5 cases. The architecture was similar to that of the low-grade group (Fig. 3). Nevertheless, in some areas, neoplastic cells showed HG nuclear features, that is, nuclear pleomorphism and enlarged nucleoli (Fuhrman nucleolar grade 3).

3.1. Molecular study

Results of the aCGH are summarized in Table 2. The aCGH analysis was successful for 4 of 5 CLG MTSRCCs. In these 4 cases, aCGH data indicated multiple losses, mostly involving chromosomes 1, 4, 8, 9, 14, 15, and 22, with no detected gains in any of the studied tumors (Fig. 4A).

From the group of 6 cases designated as OPM MTSRCCs, 4 were analyzable. Array comparative genomic hybridization analysis revealed a more variable pattern in this group: 1 case showed a normal chromosomal status; 1 case presented with losses of chromosomes 1, 4, 6, 8, 9, 10, 14, 15, and 22; and in 2 cases, multiple gains (chromosomes 3, 7, 16, and 17) were detected (Fig. 4B).

Array comparative genomic hybridization results from 4 analyzable cases of HG MTSRCC demonstrated a more uniform chromosomal aberration pattern with losses of chromosomes 1, 4, 6, 8, 9, 13, 14, 15, and 22. There were no areas of gain detected in any of these cases (Fig. 4C).

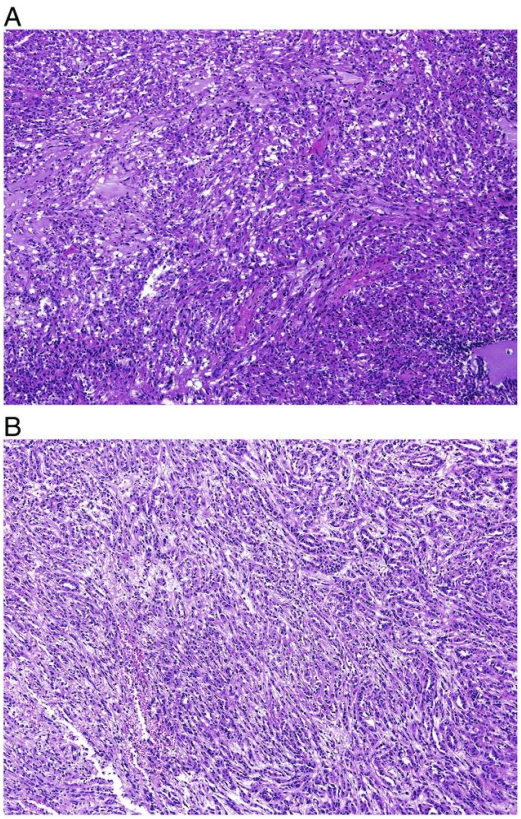

Fig. 1. (A + B) Typical low-grade MTSRCC with myxoid (mucinous) stroma and low-grade cytologic features.

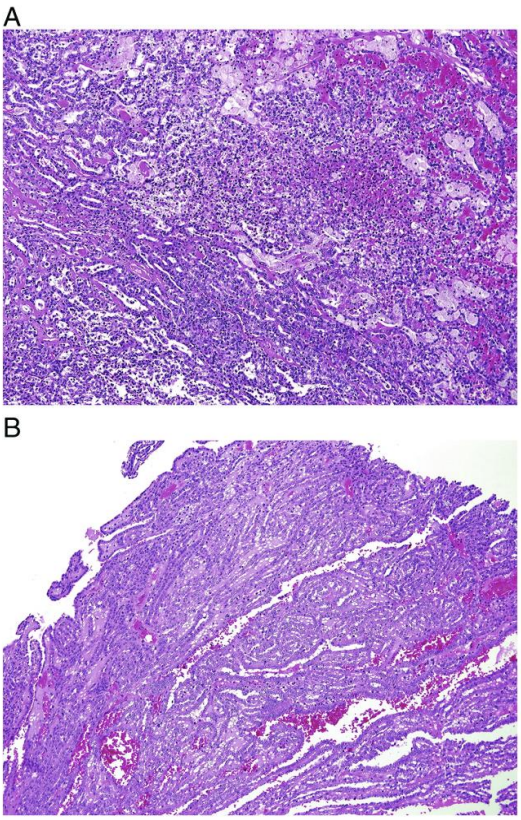

Fig. 2. (A + B) MTSRCC with overlapping features with PRCC.

4. Discussion

Mucinous tubular and spindle cell carcinoma is a relatively new and rare entity accepted as a distinct type of RCC by the recent World Health Organization classification 2004. Mucinous spindle and tubular renal cell carcinoma is generally considered a low-grade neoplasm with an indolent clinical course [6]. Nevertheless, occasional cases with local recurrence [8], metastases to regional lymph nodes [6, 10, 12, 13], and even distant metastases with fatal outcome have been published [6, 10, 12, 14–16]. The tumor mostly occurs in adults, and previous reports highlighted a remarkable female predominance (3 to 4:1) [1]. We have not observed a female predominance in our study, probably due to the selection of cases based on uniform morphology and DNA quality. Grossly, tumors were mainly well circumscribed, but noncapsulated, large, but usually in the pT1/pT2 stage according to the seventh AJCC TNM staging. The diagnoses were made predominantly based on morphologic features. The classic histologic profile of this tumor shows 2 cell populations set within a myxoid stroma: an admixture of tubules or cords composed of weakly eosinophilic spindle cell proliferations and cuboidal to short cylindrical cells with mostly pale to weakly eosinophilic cytoplasm. Low-grade nuclear features are typical for most cases of MTSRCC [1]. Initially, the morphologic and ultrastructural resemblance to loop of Henle was thought to indicate distal nephron differentiation. However, consequent attempts to confirm this theory using immunohistochemistry showed inconsistent results [4, 8, 17]. Furthermore, the largest immunohistochemical analysis performed so far suggests proximal nephron differentiation; the analyzed MTSRCC showed positive staining for AMACR, EMA, and CK7, which is identical to the profile of PRCC [4]. Given the lack of confirming evidence, the true origin of MTSRCC remains to be elucidated.

The molecular genetic features of MTSRCC were initially described by Rakozy et al [8] and subsequently by several other researchers [2, 5–7, 10]. Rakozy et al [8] studied chromosomal numerical aberrations in MTSRCCs using comparative genomic hybridization. They found consistent genetic alterations in 6 analyzed tumors, in particular,

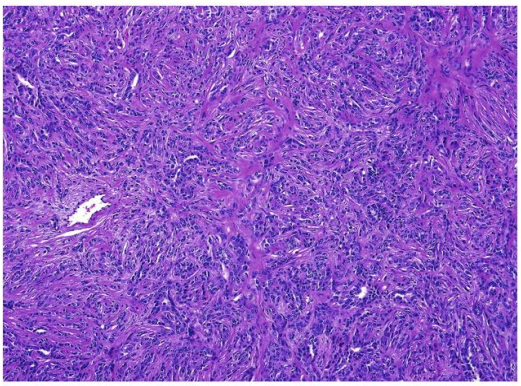

Fig. 3. High-grade MTSRCC with Fuhrman (ISUP) nucleolar grade 3.

Table 2
Results of aCGH

Case number	ArrayCGH
1	−1, −4, −6, −8, −9, −13, −14, −15, −22
2	−1,−4,−6,−8,−9,−10,−13,−14,−15,−22
3	NA
4	−1,−4,−8,−9,−14,−15,−22
5	−1,−14,−15
6	Normal
7	−1,−4,−6,−8,−9,−10,−13,−14,−15,−22
8	NA
9+	+3,+7,+13, +16,+17,+20
10+	+3,+7,+16,+17
11	NA
12	−1,−4, −6,−8,−9, −13,−14,−15, −22,
13	−1p,−4, −6, −8, −9, −13, −14, −19, −22
14	−1, −4, −6, −9, −14, −15,−18, −22, −Y
15	−1,−4,−6,−8,−9,−13,−14,−15,−22
16	NA

Yellow represents classic MSTRCC; green, overlapping morphology between MSTRCC and PRCC; blue, HG MSTRCC; −, loss of chromosome; +, gain of chromosome; + (first column), tumors were reevaluated as PRCC.
Abbreviation: NA, not analyzable.

multiple losses of chromosomes 1, 4, 6, 8, 9, 13, 14, 15, and 22. Furthermore, loss of the X-chromosome was detected in 3 tumors. In 2003, Weber et al [7] studied 11 tumors by CGH and obtained similar results to the aforementioned study; they found multiple losses of chromosomes 1, 4, 6, 8, 9, 13, and 14. However, CGH also revealed gains of chromosome 17 in 3 cases, but consequent FISH analysis of the same cases failed to confirm this finding. Brandal et al [9] presented genomic characteristics of 3 cases using a wide scale of molecular genetic investigative techniques. Two of their cases showed disomic chromosomal populations, while one of them was a nearly triploid neoplasm. Results of this study were compared with all available molecular genetic analyses from previous reports, and the authors concluded that all chromosomes were affected by aberrations. Molecular genetic analysis of MTSRCC has been consequently performed by other investigators with similar results [2, 5, 10].

From the above-mentioned data, it is evident that it is very difficult to establish a "typical" chromosomal aberration pattern for MTSRCC. In addition, the results may be biased by the fact that MTSRCC morphology may vary and substantially overlap with that of PRCC.

In our study, we have selected 5 cases of low-grade, morphologically typical MTSRCC. They all showed "classic" morphology, mostly owing to the presence of characteristic myxoid stroma accompanying the typical tubular and spindle cell components. In this group, we found losses of chromosomes 1, 4, 8, 9, 14, 15, and 22. Gains were not detected in any of the examined tumors. Renal tumors characterized by multiple losses are traditionally designated as chromophobe RCC, with losses frequently involving chromosomes 1, 2, 6, 10, 13, 17, and 21 [1]. However, recent studies have revealed a wider spectrum of chromosomal abnormalities including not only multiple losses but also numerous gains [11, 18, 19]. From the genetic point of view, one may speculate the existence of a histogenetic link between MTSRCC and CHRCC. Nevertheless, although both entities exhibit some overlap in chromosomal aberration pattern, upon more detailed exploration, they harbor different genetic profiles. Losses of chromosomes 2, 10, and 17 are usually found in CHRCC but not in MTSRCC. Moreover, morphologic and immunohistochemical differences between these neoplasms nearly exclude the possibility of a mutual origin.

Our study is essentially in concordance with the research done by Cossu-Rocca [20] in which FISH was applied to 10 MTSRCC cases to further investigate the tumor's chromosomal pattern. They did not prove trisomy of 7 or 17 in any tested tumor, but showed that MTSRCC was mostly disomic in chromosomes 7, 17, and Y. Our results are also more or less in agreement with those of Rakozy et al [8] and Weber et al [7], which demonstrated multiple chromosomal losses and no gains.

The second group of our study included cases with morphology overlapping that of PRCC. This group showed a more variable genetic pattern. Areas exhibiting features of classic MTSRCC were admixed with areas reminiscent of PRCC, insomuch as they demonstrated focal papillations, aggregates of foamy cells, and/or psammoma bodies. This unusual pattern has been described in a comprehensive study conducted by Fine et al [21]. The differential diagnosis between MTSRCC and PRCC is considered to be the most challenging in similar tumors. The tubular cells of MTSRCC mimic the basophilic type (type 1) PRCC cells and the spindle cell component may be confused with the solid, trabecular, and compact papillary areas of PRCC. Moreover, these 2 entities share a relatively similar immunohistochemical profile [4]. Because both neoplasms show histomorphologic overlap in some cases, molecular genetic analysis could serve as the most important tool for definitive diagnosis. Several studies have previously demonstrated that MTSRCC lacks the gains of chromosomes 7 and 17 and losses of chromosome Y that are prevalent in PRCC [20]. The results of our study further support and confirm that even tumors with morphologic overlap between PRCC and MTSRCC show multiple chromosomal losses (chromosomes 1, 4, 6, 8, 9, 10, 14, 15, and 22) and no gains. In the 2 cases of OPM MTSRCC showing multiple gains, including those of chromosomes 7 and 17, a careful morphologic reevaluation was performed. The final diagnosis of PRCC was established in both of these cases based on morphologic and immunohistochemical reexamination (detailed results are not shown).

The spectrum of nonclassic morphologic variants of MTSRCC, apart from the overlapping characteristics with PRCC, appears to be very wide. The "mucin-poor" and predominantly tubular and/or spindle cell variants, as well as the otherwise typical MTSRCC with neuroendocrine differentiation, sarcomatoid differentiation, or unusual differentiation toward clear cell RCC, have been described in previous studies [22, 21, 10, 23, 16, 24, 25]. It is critical for the pathologist to be aware of morphologic variability within MTSRCC. Adequate sampling, careful histologic examination, and focusing on the combination of morphologic features (including low-grade cytology and the presence of transition areas between tubular and spindled morphology) aid in reaching the correct diagnosis [21]. In difficult cases, examination of chromosomal aberration pattern appears to be essential.

In the third series, we included tumors with morphology typical for MTSRCC but with high Fuhrman nucleolar grade (grade 3). Although MTSRCC with HG features has already been reported by some investigators, it is a rare phenomenon [21, 5, 10, 23, 26]. The aCGH analysis in this group revealed multiple losses including chromosomes 1, 4, 6, 8, 9, 13, 14, 15, and 22. Contrary to the cytogenetic studies of HG MTSRCC done by Dhillon et al [10] and Kuroda et al [5], our cases demonstrated

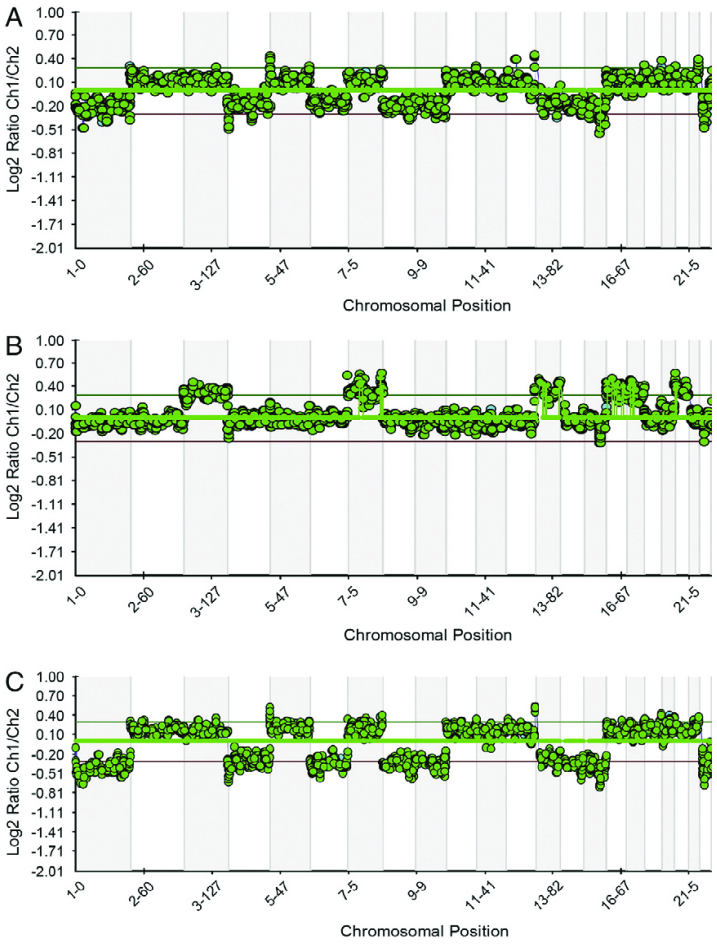

Fig. 4. Array comparative genomic hybridization fused chart of MTSRCC from each group. (A) Low-grade MTSRCC with losses of chromosomes 1, 4, 6, 8, 9, 13, 14, 15, and 22. (B) MTSRCC with overlapping features with PRCC showing gains of chromosomes 3, 7, 13, 16, 17, and 20. (C) HG MTSRCC with losses of chromosomes 1, 4, 6, 8, 9, 13, 14, 15, and 22.

no chromosomal gains. Notably, we observed a disomic status of chromosomes 7 and 17. According to cytogenetic results, chromosomal aberrations in HG MTSRCC are comparable with those demonstrated in low-grade MTSRCC.

Our results revealed multiple chromosomal losses and no gains in both low-grade MTSRCC and HG MTSRCC. Specifically, both groups demonstrated losses of chromosomes 1, 4, and 15. According to these findings, nuclear grade may not imply genetic diversity between otherwise classic forms of MTSRCC. Our results in cases with morphology reminiscent of PRCC are consistent with those of previously reported studies regarding MTSRCC with PRCC-like features. These tumors show a more heterogeneous genetic profile with losses, gains, and normal chromosomal status. However, 2 of our cases also showed gains of chromosomes 7 and 17, raising questions about the diagnosis of MTSRCC. In both cases with these specific chromosomal gains, after careful morphologic reevaluation, the final diagnosis of PRCC not otherwise specified was established.

5. Conclusions

From our results, it is clear that the chromosomal aberration pattern of classic MTSRCC is relatively uniform. In less typical cases, namely, those with overlapping features of PRCC, analysis of chromosomes 7 and 17 could be helpful in establishing the correct diagnosis.

Owing to the paucity of cytogenetically analyzed MTSRCC, our study contributes to mapping the spectrum of chromosomal aberrations that occur in particular morphologic variants of this rare entity.

References

[1] Srigley JR, Delahunt B, Eble JN, Egevad L, Epstein JI, Grignon D, et al. The International Society of Urological Pathology (ISUP) Vancouver classification of renal neoplasia. Am J Surg Pathol 2013;37(10):1469–89 [PubMed PMID: 24025519].

[2] Alexiev BA, Burke AP, Drachenberg CB, Richards SM, Zou YS. Mucinous tubular and spindle cell carcinoma of the kidney with prominent papillary component, a non-classic morphologic variant. A histologic, immunohistochemical, electron microscopic and fluorescence in situ hybridization study. Pathol Res Pract 2014;210(7):454–8 [PubMed PMID: 24702883].

[3] Argani P, Netto GJ, Parwani AV. Papillary renal cell carcinoma with low-grade spindle cell foci: a mimic of mucinous tubular and spindle cell carcinoma. Am J Surg Pathol 2008;32(9):1353–9 [PubMed PMID: 18670354].

[4] Paner GP, Srigley JR, Radhakrishnan A, Cohen C, Skinnider BF, Tickoo SK, et al. Immunohistochemical analysis of mucinous tubular and spindle cell carcinoma and papillary renal cell carcinoma of the kidney: significant immunophenotypic overlap warrants diagnostic caution. Am J Surg Pathol 2006;30(1):13–9 [PubMed PMID: 16330937].

[5] Kuroda N, Naroda T, Tamura M, Taguchi T, Tominaga A, Inoue K, et al. High-grade mucinous tubular and spindle cell carcinoma: comparative genomic hybridization study. Ann Diagn Pathol 2011;15(6):472–5 [PubMed PMID: 21106420].

[6] Ferlicot S, Allory Y, Comperat E, Mege-Lechevalier F, Dimet S, Sibony M, et al. Mucinous tubular and spindle cell carcinoma: a report of 15 cases and a review of the literature. Virchows Arch 2005;447(6):978–83 [PubMed PMID: 16231179].
[7] Weber A, Srigley J, Moch H. Mucinous spindle cell carcinoma of the kidney. A molecular analysis. Pathologe 2003;24(6):453–9 [PubMed PMID: 14605851, Muzinoses, tubulares und spindelzelliges Nierenkarzinom. Eine molekulare Analyse].
[8] Rakozy C, Schmahl GE, Bogner S, Storkel S. Low-grade tubular-mucinous renal neoplasms: morphologic, immunohistochemical, and genetic features. Mod Pathol 2002;15(11):1162–71 [PubMed PMID: 12429795].
[9] Brandal P, Lie AK, Bassarova A, Svindland A, Risberg B, Danielsen H, et al. Genomic aberrations in mucinous tubular and spindle cell renal cell carcinomas. Mod Pathol 2006;19(2):186–94 [PubMed PMID: 16258504].
[10] Dhillon J, Amin MB, Selbs E, Turi GK, Paner GP, Reuter VE. Mucinous tubular and spindle cell carcinoma of the kidney with sarcomatoid change. Am J Surg Pathol 2009;33(1):44–9 [PubMed PMID: 18941398].
[11] Sperga M, Martinek P, Vanecek T, Grossmann P, Bauleth K, Perez-Montiel D, et al. Chromophobe renal cell carcinoma—chromosomal aberration variability and its relation to Paner grading system: an array CGH and FISH analysis of 37 cases. Virchows Arch 2013;463(4):563–73 [PubMed PMID: 23913167].
[12] Hes O, Hora M, Perez-Montiel DM, Suster S, Curik R, Sokol L, et al. Spindle and cuboidal renal cell carcinoma, a tumour having frequent association with nephrolithiasis: report of 11 cases including a case with hybrid conventional renal cell carcinoma/spindle and cuboidal renal cell carcinoma components. Histopathology 2002;41(6):549–55 [PubMed PMID: 12460208].
[13] Larkin J, Fisher R, Pickering L, Thway K, Livni N, Fisher C, et al. Metastatic mucinous tubular and spindle cell carcinoma of the kidney responding to sunitinib. J Clin Oncol 2010;28(28):e539–40 [PubMed PMID: 20679595].
[14] Arafah M, Zaidi SN. Mucinous tubular and spindle cell carcinoma of the kidney with sarcomatoid transformation. Saudi J Kidney Dis Transpl 2013;24(3):557–60.
[15] Lee JH, Oh MH, Cho HD, Kim YS. Mucinous tubular and spindle cell carcinoma of the kidney with aggressive behaviour: an unusual renal epithelial neoplasm. A case report. Korean J Pathol 2010;44:211–5.
[16] Bulimbasic S, Ljubanovic D, Sima R, Michal M, Hes O, Kuroda N, et al. Aggressive high-grade mucinous tubular and spindle cell carcinoma. Hum Pathol 2009;40(6):906–7 [PubMed PMID: 19442792].
[17] Parwani AV, Husain AN, Epstein JI, Beckwith JB, Argani P. Low-grade myxoid renal epithelial neoplasms with distal nephron differentiation. Hum Pathol 2001;32(5):506–12 [PubMed PMID: 11381369].
[18] Vieira J, Henrique R, Ribeiro FR, Barros-Silva JD, Peixoto A, Santos C, et al. Feasibility of differential diagnosis of kidney tumors by comparative genomic hybridization of fine needle aspiration biopsies. Genes Chromosomes Cancer 2010;49(10):935–47 [PubMed PMID: 20629095].
[19] Tan MH, Wong CF, Tan HL, Yang XJ, Ditlev J, Matsuda D, et al. Genomic expression and single-nucleotide polymorphism profiling discriminates chromophobe renal cell carcinoma and oncocytoma. BMC Cancer 2010;10:196 [PubMed PMID: 20462447, Pubmed Central PMCID: 2883967].
[20] Cossu-Rocca P, Eble JN, Delahunt B, Zhang S, Martignoni G, Brunelli M, et al. Renal mucinous tubular and spindle carcinoma lacks the gains of chromosomes 7 and 17 and losses of chromosome Y that are prevalent in papillary renal cell carcinoma. Mod Pathol 2006;19(4):488–93 [PubMed PMID: 16554730].
[21] Fine SW, Argani P, DeMarzo AM, Delahunt B, Sebo TJ, Reuter VE, et al. Expanding the histologic spectrum of mucinous tubular and spindle cell carcinoma of the kidney. Am J Surg Pathol 2006;30(12):1554–60 [PubMed PMID: 17122511].
[22] Thway K, du Parcq J, Larkin JM, Fisher C, Livni N. Metastatic renal mucinous tubular and spindle cell carcinoma. Atypical behavior of a rare, morphologically bland tumor. Ann Diagn Pathol 2012;16(5):407–10 [PubMed PMID: 21684183].
[23] Simon RA, di Sant'agnese PA, Palapattu GS, Singer EA, Candelario GD, Huang J, et al. Mucinous tubular and spindle cell carcinoma of the kidney with sarcomatoid differentiation. Int J Clin Exp Pathol 2008;1(2):180–4 [PubMed PMID: 18784804, Pubmed Central PMCID: 2480554].
[24] Kuroda N, Nakamura S, Miyazaki E, Hayashi Y, Taguchi T, Hiroi M, et al. Low-grade tubular-mucinous renal neoplasm with neuroendocrine differentiation: a histological, immunohistochemical and ultrastructural study. Pathol Int 2004;54(3):201–7 [PubMed PMID: 14989744].
[25] Kuroda N, Tamura M, Hes O, Michal M, Kawada C, Shuin T, et al. Renal cell carcinoma with extensive clear cell change sharing characteristics of mucinous tubular and spindle cell carcinoma and papillary renal cell carcinoma. Pathol Int 2009;59(9):687–8 [PubMed PMID: 19712140].
[26] Pillay N, Ramdial PK, Cooper K, Batuule D. Mucinous tubular and spindle cell carcinoma with aggressive histomorphology—a sarcomatoid variant. Hum Pathol 2008;39(6):966–9 [PubMed PMID: 18400251].

CHROMOFOBNÍ RENÁLNÍ KARCINOM S NEUROENDOKRINNÍMI ZNAKY A ZNAKY NAPODOBUJÍCÍMI NEUROENDOKRINNÍ DIFERENCIACI. MORFOLOGICKÁ, IMUNOHISTOCHEMICKÁ A ULTRASTRUKTURÁLNÍ STUDIE A ARRAY KOMPARATIVNÍ GENOMOVÁ HYBRIDIZACE U 18 PŘÍPADŮ, PŘEHLED LITERATURY

Chromofobní renální karcinom (CHRK) je v typickém případě složen ze solidně uspořádaných světlých buněk s výraznou cytoplazmatickou membránou a hrozinkovitě tvarovaným jádrem s perinukleárním projasněním [6]. CHRK může velmi vzácně vykazovat neuroendokrinní diferenciaci, která je histologicky definována příměsí malých uniformních buněk uspořádaných kribriformně, gyriformně, do pseudorozet, hnízdovitých struktur či palisádujících pruhů. K průkazu pravosti neuroendokrinní diferenciace je nutné tento morfologický obraz podpořit imunohistochemickým vyšetřením, konkrétně expresí neuroendokrinních markerů v malobuněčné komponentě. Pokud jsou tyto v malobuněčné komponentě negativní, jedná se o CHRK se znaky napodobujícími neuroendokrinní diferenciaci a nikoliv o pravou neuroendokrinní diferenciaci. CHRK je považován za indolentní tumor. Není zcela jisté, zda přítomnost neuroendokrinní diferenciace ovlivňuje klinický průběh a prognózu pacienta; CHRK s neuroendokrinními znaky je extrémně vzácný a proto málo prozkoumaný tumor, doposud byla publikována pouze hrstka případů [12-15].

Cílem této studie bylo porovnat skupinu CHRK s neuroendokrinní diferenciací s CHRK se znaky pouze napodobujícími neuroendokrinní diferenciaci. Bylo vybráno 18 případů CHRK s neuroendokrinními znaky, které byly na základě pozitivity/negativity neuroendokrinních markerů rozděleny do dvou skupin: 4 případy CHRK s „opravdovou“ neuroendokrinní diferenciací a 14 případů CHRK napodobující neuroendokrinní diferenciaci.

Výsledky studie lze shrnout takto:

- Ve většině případů CHRK s morfologickými znaky určujícími neuroendokrinní diferenciaci se jedná pouze o růstovou variantu CHRK a nikoliv o pravou neuroendokrinní diferenciaci.
- Obě skupiny se mírně liší molekulárně geneticky; ztráty chromozomů 1,2,6 a10 byly zastiženy převážně ve skupině CHRK s neuroendokrinní diferenciací, zatímco skupina CHRK se znaky napodobujícími neuroendokrinní diferenciaci vykazovala jak mnohočetné chromozomální ztráty, tak i nadpočetné chromozomy.
- 2/4 případů CHRK s neuroendokrinní diferenciací měly metastatický potenciál naznačující skutečnost, že přítomnost pravé neuroendokrinní diferenciace může mít negativní vliv na prognózu. Nicméně, z takto malého počtu případu nelze vyvozovat jednoznačné prognostické závěry a naše pozorování bude muset být podpořeno dalšími výzkumy.

Annals of Diagnostic Pathology 19 (2015) 261–268

Contents lists available at ScienceDirect

Annals of Diagnostic Pathology

Chromophobe renal cell carcinoma with neuroendocrine and neuroendocrine-like features. Morphologic, immunohistochemical, ultrastructural, and array comparative genomic hybridization analysis of 18 cases and review of the literature ☆

Kvetoslava Peckova, MD [a], Petr Martinek, MSc [a], Chisato Ohe, MD [b], Naoto Kuroda, MD [c], Stela Bulimbasic, MD, PhD [d], Enric Condom Mundo, MD [e], Delia Perez Montiel, MD [f], Jose I. Lopez, MD [g], Ondrej Daum, MD, PhD [a], Pavla Rotterova, MD, PhD [a], Bohuslava Kokoskova, MD [a], Magdalena Dubova, MD [a], Kristyna Pivovarcikova, MD [a], Kevin Bauleth, MD [a], Petr Grossmann, PhD [a], Milan Hora, MD [h], Kristyna Kalusova, MD [h], Whitney Davidson, MD [i], David Slouka, MD, PhD [j], Sulc Miroslav, MD [k], Petr Buzrla, MD [l], Mirka Hynek, MD, PhD [m], Michal Michal, MD [a], Ondrej Hes, MD, PhD [a,n,*]

[a] Department of Pathology, Charles University, Medical Faculty and Charles University Hospital Plzen, Plzen, Czech Republic
[b] Department of Diagnostic Pathology, Kansai Medical University, Hirakata Hospital, Osaka, Japan
[c] Department of Diagnostic Pathology, Kochi Red Cross Hospital, Kochi, Japan
[d] Department of Pathology, University Hospital Dubrava, Zagreb, Croatia
[e] Department of Pathology, Bellvitge University Hospital, Barcelona, Spain
[f] Department of Pathology, Instituto Nacional de Cancerologia, Mexico City, Mexico
[g] Department of Pathology, Cruces University Hospital, Barakaldo, Spain
[h] Department of Urology, Charles University, Medical Faculty and Charles University Hospital Plzen, Plzen, Czech Republic
[i] Department of Pathology and Laboratory Medicine, University of Kansas Medical Center, Kansas City, KS
[j] Department of Otorhinolaryngology, Charles University, Medical Faculty and Charles University Hospital Plzen, Plzen, Czech Republic
[k] Bioptical Laboratory Chomutov, Chomutov, Czech Republic
[l] Department of Pathology, University Hospital Ostrava, Ostrava, Czech Republic
[m] Department of Radiology, Medical Faculty and Charles University Hospital Plzen, Plzen, Czech Republic
[n] Biomedical Centre, Charles University, Medical Faculty and Charles University Hospital Plzen, Plzen, Czech Republic

ARTICLE INFO

Keywords:
Kidney
Chromophobe renal cell carcinoma
Neuroendocrine differentiation
Immunohistochemistry
Chromosomal numerical aberrations
aCGH

ABSTRACT

Chromophobe renal cell carcinoma (CRCC) with neuroendocrine differentiation (CRCCND) has only recently been described. Eighteen cases of CRCC with morphologic features suggestive of neuroendocrine differentiation were selected from among 624 CRCCs in our registry. The tissues were fixed in neutral formalin, embedded in paraffin, cut into 4- to 5-μm-thick sections, and stained with hematoxylin and eosin. As CRCC with neuroendocrine features, tumors with following morphology were suggested: (1) trabecular/palisading/ribbon-like, gyriform, insular, glandular, and solid pattern; (2) uniform polygonal cells formed in small islets; and (3) cribriform pattern in combination with palisading. Selected cases were further analyzed using immunohistochemistry, electron microscopy, array comparative genomic hybridization, and fluorescence in situ hybridization. Cases were classified as CRCCND or CRCC with neuroendocrine-like features (CRCCND-L) based on the immunohistochemical expression of neuroendocrine markers: CRCCND, 4 cases, age range 49 to 79 years, size ranged from 2.2 to 22 cm, and CRCCND-L, 14 cases, age range 34 to 74 years, size range 3.8 to 16.5 cm. Follow-up information was available for 11 of 18 patients aged 0.5 to 12 years. Two of 4 CRCCNDs showed aggressive clinical course with metastatic spreading. Chromophobe renal cell carcinomas with neuroendocrine differentiation were focally positive for CD56 (4/4), synaptophysin (4/4), chromogranin A (1/4), and neuron-specific enolase (3/4). All 14 CRCCND-Ls were mostly negative or very weakly focally positive for some of the aforementioned markers. All 18 tumors were positive for cytokeratin 7 and CD117. Ultrastructural analysis showed poorly preserved neuroendocrine granules only in 2 of 4 analyzed CRCCNDs. Losses

☆ The study was supported by the Charles University Research Fund (project no. P36) and by the project CZ.1.05/2.1.00/03.0076 from European Regional Development Fund.
* Corresponding author at: Department of Pathology, Charles University, Medical Faculty and Charles University Hospital Plzen, Alej Svobody 80, 304 60 Plzen, Czech Republic.
E-mail address: hes@medima.cz (O. Hes).

http://dx.doi.org/10.1016/j.anndiagpath.2015.05.001

of chromosomes 1, 2, 6, and 10 were found in all analyzable CRCCNDs, whereas multiple losses (chromosomes 1, 2, 6, 10, 13, 17, and 21) and gains (chromosomes 4, 11, 12, 14, 15, 16, 19, and 20) were found in CRCCND-L.

1. Introduction

Chromophobe renal cell carcinoma (CRCC) represents approximately 5% of renal carcinomas. Microscopically, these tumors are described as mostly solid or solid alveolar; however, the morphologic spectrum has expanded to include microcystic, adenomatoid, and focal papillary arrangements [1-4].

Chromophobe renal cell carcinoma with true neuroendocrine differentiation (CRCCND) and CRCC with a neuroendocrine-like pattern (CRCCND-L) have only recently been described; a limited number of cases have been reported [5-7].

In this study, we attempt to distinguish and compare true neuroendocrine differentiation in CRCC to CRCC with a neuroendocrine-like pattern and to evaluate the biological nature of both forms.

2. Materials and methods

The tissues were fixed in neutral formalin, embedded in paraffin, cut into 4- to 5-μm-thick sections, and stained with hematoxylin and eosin.

We selected 18 cases of CRCC with morphologic features suggestive of neuroendocrine differentiation from among 624 CRCCs in our files. As CRCCs with neuroendocrine features, tumors with following morphology were suggested: (1) palisading/ribbon-like, gyriform patterns; (2) insular pattern; and (3) cribriform/pseudorosettoid pattern or small cell islets in combination with palisading.

Selected cases were further analyzed using immunohistochemistry (IHC), electron microscopy, array comparative genomic hybridization (aCGH), and fluorescence in situ hybridization (FISH).

3. Immunohistochemistry

The immunohistochemical study was performed using a Ventana Benchmark XT automated stainer (Ventana Medical System, Inc, Tucson, AZ) on formalin-fixed, paraffin-embedded (FFPE) tissue. The following primary antibodies were used: cytokeratin 7 (CK7) (OV-TL12/30, monoclonal, 1:200; DakoCytomation, Glostrup, Denmark), c-kit (CD 117, polyclonal, RTU; DakoCytomation), CD56 (1B6, monoclonal, 1:100; Leica Biosystems, Newcastle, UK), Ki-67 (MIB1, monoclonal, 1:1000; Dako, Glostrup, Denmark), synaptophysin (polyclonal, 1:350; LabVision, Fremont, CA), chromogranin A (monoclonal, DAK-A3, 1:600; DakoCytomation), CD99 (O13, monoclonal, 1:200; Ventana, Mannheim, Germany), cytokeratin 20 (CK20) (Ks20.8, monoclonal, 1:250; DakoCytomation). The primary antibodies were visualized using the supersensitive streptavidin-biotin-peroxidase complex (Biogenex, Fremont, CA). Appropriate positive and negative controls were used.

4. Ultrastructure

Electron microscopy evaluation was performed on 7 cases. Small pieces of FFPE from 3 cases of CRCCND and 4 cases of CRCCND-L were deparaffinized and further routinely processed for ultrastructural analysis. Semithin sections of epoxy-embedded tissue were stained with toluidine blue and examined by light microscopy. Ultrathin sections from representative areas were cut, stained with uranyl acetate and lead citrate, and examined with a Jeol (Tokyo, Japan) JEM 1400 Transmission Electronic Microscope.

Table 1
Clinicopathologic features

Case	Age	Sex	Site	Size (cm)	Color	Pattern	Follow up (y)
CRCCND							
1.[a]	79	M	Right	22 × 12 × 10	Brownish	SCI	3.5 AWD (CT scan, lymph nodes mediastinum)
2.	66	F	Left	12 cm	Yellow	SCI	Metastatic spreading in time of diagnosis, 0.5 AWD (local recurrence and bone meta)
3.	67	M	Right	5.6	Yellowish	PSC	LE
4.[a]	49	M	Left	Diam. 2.2	Beige	SCI	1 AW after partial nephrectomy
CRCCND-L							
1.	70	M	Right	2.6 × 3 × 2.3	Brown	P	AW 8/2014
2.	69	F	NA	12 × 5	Brown	PSC	NA
3.	74	F	Right	16.5	Yellow hemorrhagic, atrophic kidney	PSC	LE
4.	47	F	NA	3.8	NA	PSC	NA
5.	67	F	Left	7.3 × 6.8	Grayish	SC PR	LE
6.	46	M	Left	10 × 8 × 2	Grayish	SCI	3 y AW, then LE
7.	51	M	Left	8 × 7 × 6	Brownish	PSC	LE
8.	72	M	NA	NA	NA	SCPR	LE
9.	72	F	left	6.4	Pink to tan	PSC	AW 8/2014
10.	51	M	Left	Diam. 5	Yellow	PSC	AW 8/2014
11.	34	F	Left	14 × 11 × 10.5	Yellow	P	AW 8/14
12.	70	M	Right	13 × 10 × 9	Brown	P	AW 8/2014
13.	63	M	Left	Diam. 5.5	Brown	PSC	AW 2010, then LE
14.	49	F	NA	Diam. 13	NA	P	AW 9/14

Abbreviations: M, male; F, female; SCI, small cell islets; PSC, palisading and small cell areas; P, palisading; SCPR, small cells and pseudorosettes; AWD, alive with disease; CT, computed tomography; meta, metastasis; LE, loss of evidence; Diam., diameter; AW, alive and well; NA, not available.

[a] Cases have been published previously.

5. Molecular genetic methods

5.1. DNA extraction

DNA from FFPE tumor and nontumor tissues (when available) of each case was extracted using QIAsymphony DNA Mini Kit (Qiagen, Hilden, Germany) on automated extraction system (QIAsymphony SP; Qiagen) according to the manufacturer's supplementary protocol for FFPE samples (purification of genomic DNA from FFPE tissue using the QIAamp DNA FFPE Tissue Kit and Deparaffinization Solution). Concentration and purity of isolated DNA were measured using Nanodrop ND1000 (NanoDrop Technologies, Inc, Wilmington, DE). DNA integrity was examined by amplification of control genes in multiplex PCR, producing fragments from 100 to 600 base pairs (bp). Only cases with DNA integrity equal to or higher than 400 bp were used for further analysis by aCGH.

5.2. Fluorescence in situ hybridization

For each specimen, a 4-μm-thick, FFPE section was placed on a positively charged slide. The hematoxylin and eosin–stained slide was examined for determination of areas for cell counting. Another unstained slide was routinely deparaffinized and incubated in the 1× Target Retrieval Solution Citrate pH 6 (Dako) for 40 minutes at 95°C and subsequently cooled for 20 minutes at room temperature in the same solution. The slide was washed in deionized water for 5 minutes, and the tissue was digested in protease solution with pepsin (0.5 mg/mL) (Sigma Aldrich, St Louis, MO) in 0.01 M HCl at 37°C for 15 minutes. The slide was then immersed in deionized water for 5 minutes, dehydrated in a series of ethanol solutions (70%, 85%, and 96% for 2 minutes each), and air dried. Fluorescence in situ hybridization probes, shown in Table 1 (VYSIS/Abbott Molecular, Des Plaines, IL), were mixed with water and hybridization buffers according to the manufacturer's protocol. An appropriate amount of probe mix was applied to the specimen, covered with a glass cover slip, and sealed with rubber cement. The slide was then incubated in a ThermoBrite instrument (StatSpin/Iris Sample Processing, Westwood, MA) with codenaturation at 85°C for 8 minutes and hybridization at 37°C for 16 hours. The rubber-cemented cover slip was removed, and the slide was placed in posthybridization wash solution (compounded of saline-sodium citrate buffer (SSC) and detergent nonyl phenoxypolyethoxylethanol (NP-40) at a ratio of 2× SSC/0.3% NP-40) at 72°C for 2 minutes. Finally, the slide was air dried in the dark, counterstained with 4′,6-diamidino-2-phenylindole (DAPI I; VYSIS), cover slipped, and immediately examined.

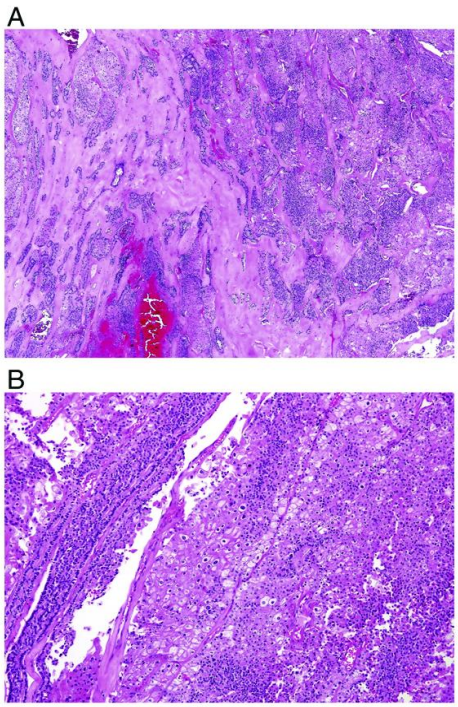

Fig. 2. Tumorous cells arranged in palisading structures in a background of dense fibrotic stroma in a case of CRCC with neuroendocrine differentiation (CRCCND case 1) (A). Cords of small neoplastic cells crossing areas composed of otherwise typical large polygonal cells with raisinoid nuclei (CRCCND case 3) (B).

5.3. Fluorescence in situ hybridization interpretation

The areas of the specimen with tumor were examined on an Olympus BX51 fluorescence microscope using an objective ×100 and filter sets triple bandpass (DAPI/Spectrum Green/Spectrum Orange) and single bandpass (Spectrum Green and Spectrum Orange). Scoring of aneuploidy was performed by counting the number of fluorescent signals in 100 randomly selected, nonoverlapping

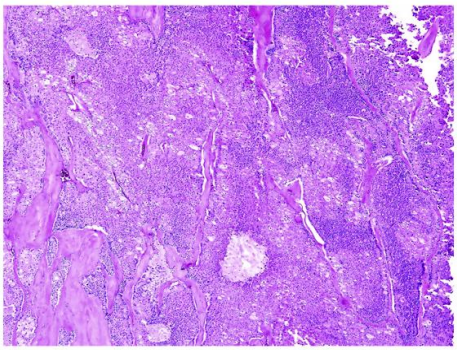

Fig. 1. Low-power view showing solid alveolar architecture of CRCC with neuroendocrine differentiation. Areas of small uniform cells are clearly visible in the right side of the picture (CRCCND case 4).

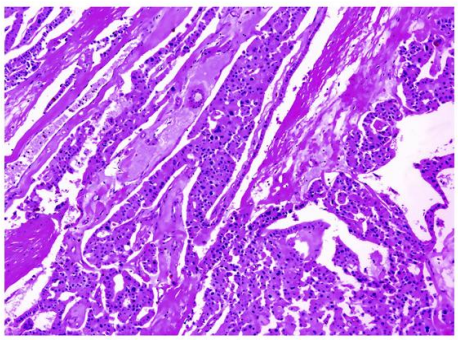

Fig. 3. Cords of neoplastic cells with inconspicuous palisading architecture in case of chromophobe RCC with neuroendocrine-like differentiation (CRCCND-L case 5).

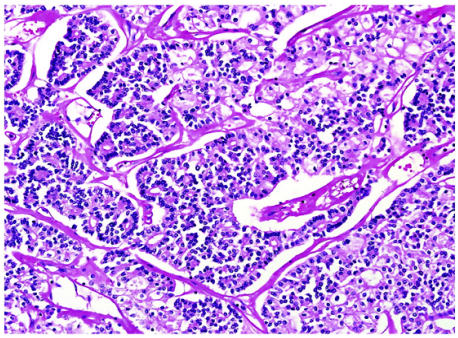

Fig. 4. Cribriform pattern in CRCC with neuroendocrine-like differentiation (CRCCND-L case 8).

tumor cell nuclei. Each slide was independently enumerated by 2 observers (PM and PG). The cut-off values used for each probe were established in a previous study [8].

5.4. Array comparative genomic hybridization

A CytoChip Focus Constitutional (BlueGnome Ltd, Cambridge, UK) microarray processor was used for analysis. CytoChip Focus Constitutional uses BAC technology and covers 143 regions of known significance with 1-Mb spacing across a genome. Probes are spotted in triplicates. First, 400 ng of gDNA was labeled using the Fluorescent Labeling System (BlueGnome Ltd). The procedure consisted of Cy3 labeling of a test sample and Cy5 labeling of a reference sample. MegaPool Reference DNA of opposite sex was used as a reference sample (Kreatech Diagnostics, Amsterdam, The Netherlands). Each labeled pair was mixed, dried, and hybridized overnight at 47°C using ArrayIt hybridization cassettes (Arrayit Corporation, Sunnyvale, CA). Posthybridization washing was done using SSC buffers with increasing stringency. Dried microarrays were scanned with InnoScan 900 (Innopsys, Carbonne, France) at a resolution of 5 μm.

5.5. Image and data analyses

Scanned images were analyzed and quantified using BlueFuse Multi software (BlueGnome Ltd). BlueFuse Multi uses Bayesian algorithms to generate intensity values for each Cy5- and Cy3-labeled spot on the array according to an appropriate .gal file. The reported changes were browsed and interpreted using BlueFuse Multi as well. Cut-off values were set to a log 2 ratio of −0.193 for loss and 0.170 for gain.

6. Results

Tumors were defined as CRCCND or CRCCND-L based on morphologic, immunohistochemical, and ultrastructural examinations.

The clinicopathologic features of the 4 patients with CRCCND are summarized in Table 1. Three of the patients were male, and 1 was female with ages ranging from 49 to 79 years (mean, 65.25 years; median, 66.5 years). Tumor size ranged from 2.2 to 22 cm in greatest dimension (mean, 10.45 cm; median, 8.8 cm); the cut surface of the tumor was yellow/yellowish in 2 cases and brownish/beige in 2 cases. Follow-up data were available for 3 of 4 patients with follow-up period ranging from 0.5 to 3.5 years. Tumors in the CRCCND group exhibited aggressive behavior in 2 of 3 patients for whom follow-up information was available.

The second group included 14 patients with CRCCND-L tumors; clinicopathologic data are available in Table 1. Within this group, there were 7 males and 7 females whose ages ranged from 34 to 74 years (mean, 59.64 years; median, 65 years). Tumor size ranged from 3.0 to 16.5 cm in greatest dimension (mean, 9.0 cm; median, 8 cm), and the cut surface of the tumor was brown/brownish in 5 cases, yellow/yellowish in 3 cases, grayish in 2 cases, and pink to tan in 1 case. Information regarding tumor color and consistency was not available in the 3 remaining cases. Follow-up information was available for 8 of 14 patients with no evidence of aggressive clinical course discovered in any of the cases of CRCCND-L.

6.1. Morphology

The morphologic patterns are summarized in Table 1. A typical dual cell population was found in every examined case. Characteristic raisinoid nuclei and perinuclear clearing were observed in all cases, albeit only focally in some cases. Regarding CRCCND, islets of small neoplastic cells were found in 3 of 4 tumors (Fig. 1), whereas palisading and small cell areas were detected in 1 of 4 tumors (Fig. 2A and B). As for CRCCND-L, we observed palisading and small cell areas in 7 of 14 cases (Fig. 3), palisading/ribbon-like pattern in 4 of 14 cases, small cell areas in 2 of 14 cases, and small cells with cribriform pattern/pseudorosettes (Fig. 4) in 1 of 14 cases.

Table 2
Results of immunohistochemical examination

Case	chrom	Syn	NSE	CD56	CK7	CD117	Ki-67	CD99	CK20
CRCCND									
1	−	Weak Foc++	Foc+++	Foc+++	+++	+++	8-10/HPF	−	−
2	−	+++	+++	Foc+	Foc++	+++	10-12/HPF	−	−
3	Foc+	Foc+++	Foc+++	Foc+	+++	+++	10-12/HPF	SC	−
4	−	+++	Foc+++	+++	+++	+++	10-12/HPF	−	−
CRCCND-L									
1	−	−	+	Foc+	Foc+++	+++	6-10/HPF	−	−
2	−	−	−	−	Foc++	++	4-5/HPF	−	−
3	−	−	−	−	+++	++	3-5/HPF	−	−
4	−	Foc+	−	−	+++	+++	6-7/HPF	−	SC
5	−	−	Foc+++	−	+++	+++	5-7/HPF	−	−
6	−	−	Foc+++	−	+++	+++	10-14/HPF	−	−
7	−	−	Foc+++	−	+++	+++	2-5/HPF	−	−
8	−	−	−	−	+++	+++	10-12/HPF	−	−
9	−		Foc++	−	+++	+++	8-10/HPF	−	−
10	−	−	−	−	Foc++	+++	3-7/HPF	−	−
11	−	−	+++	−	−	++	5-8/HPF	−	−
12	−	−	−	−	Foc++	++	4-6/HPF	−	−
13	−	−	−	−	+++	+++	2-5/HPF	NP	NP
14	−	−	Foc+++	−	+++	+++	1-2/HPF	NP	NP

Abbreviations: −, negative; +, weak positivity; ++, moderate positivity; +++, strong positivity; Foc, focal; NP, not performed; HPF, high-power field; SC, single cells; chrom, chromogranin; syn, synaptophysin.

6.2. Immunohistochemistry

The results of immunohistochemical examination are summarized in Table 2 (CRCCND and CRCCND-L). All of the tumors in the CRCCND group expressed markers considered to be typical for CRCC (CD117 and CK7) and were negative for vimentin (single positive cells). All tumors classified in this group were immunoreactive for synaptophysin, CD56, and neuron-specific enolase (NSE), although the positivity was often focal. A single case was focally and weakly positive for chromogranin A (Fig. 5A, B and C). Concerning the CRCCND-like group, all but 1 of the tumors were reactive for CD117 and CK7. Generally speaking, they were negative for neuroendocrine markers (synaptophysin, CD56, and NSE) or displayed variable positivity for NSE (7/14 cases). None of these tumors was positive for chromogranin A.

6.3. Ultrastructure

Electron-dense structures (granules) were found within the cytoplasm in 2 of 3 cases of CRCCND; however, the exact origin of such structures cannot be fully elucidated due to the presence of fixation artifacts. Such structures were not present in the 4 analyzed cases of CRCCND-L.

6.4. Array comparative genomic hybridization

Complete results of aCGH and FISH are summarized in Table 3. Losses of chromosomes 1, 2, 6, 10, and 17 were the most frequent finding in CRCCND (Fig. 6), whereas multiple losses (chromosomes 1, 2, 6, 10, 13, 17, and 21) and gains (chromosomes 4, 11, 12, 14, 15, 16, 19, and 20) were most frequently found in CRCCND-L (Fig. 7).

Table 4 summarizes comparative features of both CRCCND and CRCCND-L.

7. Discussion

Chromophobe renal cell carcinoma is a renal cell neoplasm, typically described as a solid alveolar tumor. These tumors are often composed of a dual population of cells, large leaf-like cells with abundant pale cytoplasm and well-defined borders variably intermixed with smaller eosinophilic cells embedded in a fine reticular setting. Large wrinkled nuclei, usually referred to as "raisinoid," are another characteristic feature of these tumors. One relatively common subtype of CRCC is the eosinophilic variant, which is composed mostly of smaller eosinophilic cells and is distinguished from classic CRCC according to the proportion of cell populations [9]. Additional variants of CRCC including those with microcystic, pigmented, and oncocytic morphologies have also been described [1,2,10,11].

Neuroendocrine differentiation within CRCC has been described only recently [5-7]. The histologic features of this extremely rare variant of CRCC are characterized by an admixture of classical and eosinophilic cells with regions of features consistent with neuroendocrine differentiation. These features include the formation of tubular, glandular, and insular patterns with rosettoid formations, intense granular eosinophilic cytoplasm, and dense hyaline stroma. In these areas, the neuroendocrine differentiation can be confirmed by immunohistochemical positivity for chromogranin, synaptophysin, CD56, and NSE, whereas the typical CRCC regions do not express these neuroendocrine markers.

Although sarcomatoid features can be observed in all types of renal cell carcinoma (RCC), 1 study suggests that CRCC is the most common RCC subtype with such dedifferentiation [12]. Clinically, this differentiation represents high-grade transformation of relatively indolent CRCC into a neoplasm with aggressive course and unfavorable prognosis. The neoplastic cells in sarcomatoid areas mostly express epithelial markers, and their epithelial origin can be immunohistochemically and ultrastructurally confirmed [12]. This sarcomatoid component may mimic or even differentiate into several different types of heterologous mesenchymal tumors such as osteosarcoma, rhabdomyosarcoma, chondrosarcoma, or liposarcoma [13-17].

One case report even describes the combination of CRCC, collecting duct RCC, and sarcomatoid differentiation within the same tumor [18].

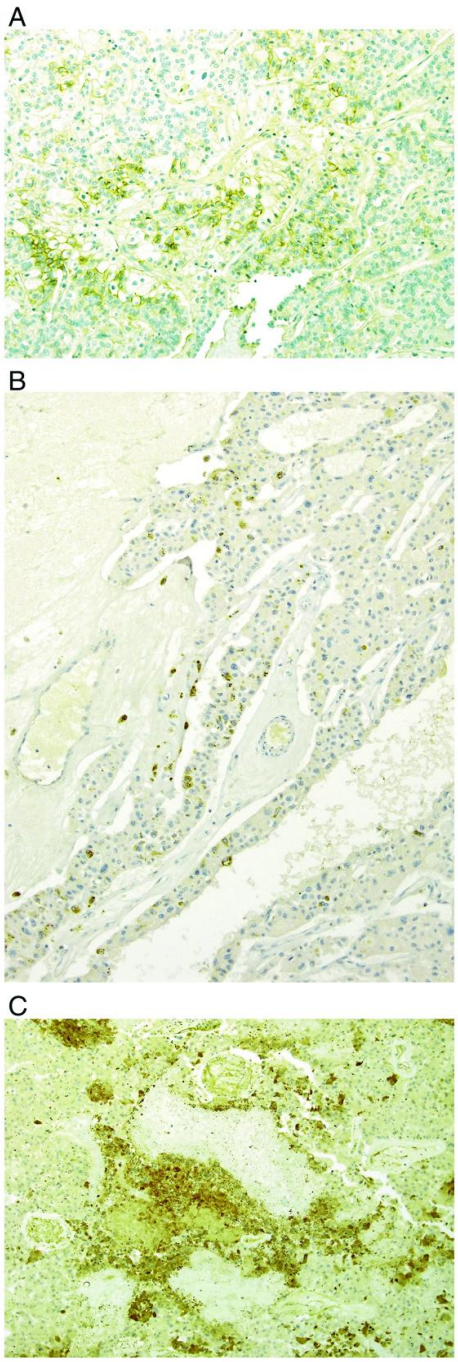

Fig. 5. Immunohistochemical examination of CRCC with neuroendocrine differentiation disclosed focal positivity for CD56 (A), synaptophysin (B), and NSE (C).

In this study, we have focused on the changes occurring in the epithelial component of certain CRCC subtypes. Only 1 of the 18 cases studied included areas of sarcomatoid differentiation. This particular case was CRCC with neuroendocrine differentiation and has also been published in previous studies [6,7]. Microscopically, the tumor was composed of 3 histologic components: an area of typical CRCC, a neuroendocrine carcinoma component, and a sarcomatoid component. The area with neuroendocrine differentiation was purely epithelial with no signs of sarcomatoid differentiation. The remaining 17 tumors analyzed were CRCC without areas of sarcomatoid transformation.

Neuroendocrine differentiation is a well-known phenomenon and occurs in tumors such as gastrointestinal adenocarcinoma, small and large cell carcinoma of the lung, urothelial carcinoma, prostatic adenocarcinoma, ovarian carcinosarcoma, and certain breast carcinomas [19-23].

The morphologic features suggesting neuroendocrine differentiation consist of organoid growth patterns characterized by trabecular, insular, palisading, ribbon, and rosette-like architecture. The tumor cells are uniform and polygonal with finely eosinophilic cytoplasm. Nuclei are round to oval with haphazardly distributed nuclear chromatin (frequently with a "salt and pepper" pattern), inconspicuous nucleoli, and scant to moderate cytoplasm. Necrosis is usually absent. Highly vascularized fibrovascular stroma, stromal hyalinization, cartilage, or bone formation as well as the presence of amyloid can be observed [24].

The morphologic features of CRCCND should be supported by IHC and/or ultrastructural examinations. Chromogranin A, synaptophysin, CD56, and NSE are often used as IHC markers of neuroendocrine differentiation with chromogranin A and synaptophysin being the most common. Both of the aforementioned markers are specific to neuroendocrine differentiation, although synaptophysin manifests much higher sensitivity than chromogranin A. CD56 is not a specific neuroendocrine marker and should not be considered as confirmation of neuroendocrine differentiation in the absence of synaptophysin/chromogranin positivity. Neuron-specific enolase, despite its name, is also not specific for neuroendocrine cells/tumors [24]. Ultrastructurally, the presence of neurosecretory or endosecretory granules is sometimes helpful. In this study, all available CRCCs with patterns suggesting possible neuroendocrine differentiation were examined by IHC with selected cases also being analyzed by ultrastructure. Of 18 cases, we confirmed real neuroendocrine differentiation in only 4 of them. The remaining 14 tumors exhibiting morphology compatible with neuroendocrine differentiation turned out to be examples of architectural/morphologic variability only.

Table 3
Results of molecular genetic analysis

Case	aCGH	FISH
CRCCND		
1	−1, −2, −6, −10, −17, −21	n7, −17
2	−1, −2, −3, −6, +7, −9, −10, −11, −13, −14, −17	+7, n17
3	NA	NT
4	−1, −2, −4, −5[a], −6, −9, −10, −13, −16p, −17, −21	NT
CRCCND-L		
1	No changes	NT
2	+11, +14	NT
3	−1, −2, +3, +4pter-4q31.21, −4q31.21-qter, −5, −6, +7, −8pter-8q13, −8q24.22, +8q13-8qter, +9pter-9q21.13, +9q21-9qter, −10, −11, +12, −13, −14, +15, +16, −17, +18, +19, +20, −21, +22	+7, −17
4	NT	NT
5	−1, −2, −6, −10, −13, −17, −21	n7, −17
6	+4, +5, +8, +11, +12, +14, +15, +16, +19, +20	+8, n10
7	NT	NT
8	−1, −3, −6, −10, −17, −21	NA
9	NA	NT
10	NT	NT
11	NT	NT
12	−1, −2, −6, −10, −13, −17, −18, −21	NA
13	NT	NT
14	NT	NT

Abbreviations: NT, not tested; NA, not analyzable; +, gain of chromosome; −, loss of chromosome; n, normal status (disomy).
[a] Only in area with neuroendocrine differentiation.

The presence of multiple losses of chromosomes 1, 2, 6, 10, 13, 17, and 21 has been considered a genetic hallmark of both classic and eosinophilic CRCCs. Although the presence of multiple chromosomal gains in CRCC has also been reported [10,25], these findings have been regarded as an uncommon phenomenon with CRCC generally believed to have a hypodiploid genome with the chromosomal losses described above. However, recent articles in which larger cohorts of cases were analyzed have described a more variable genetic pattern with multiple losses as well as with multiple gains. In these studies, chromosomal gains were most frequently detected on chromosomes 4, 7, 15, 19, and 20 [8,26,27]. These findings indicate that the molecular-genetic abnormalities in CRCC can encompass a considerably broader spectrum than was previously suggested. Our study reveals losses of chromosomes 1, 2, 6, and 10 in all analyzable neuroendocrine CRCC with multiple losses (chromosomes 1, 2, 6, 10, 13,

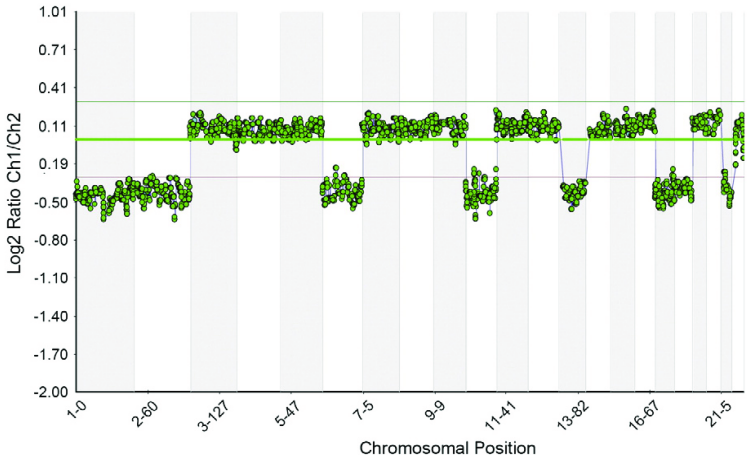

Fig. 6. Array comparative genomic hybridization fused chart of CRCC with neuroendocrine differentiation case with losses of chromosomes 1, 2, 6, 10, 13, 17, 18, and 21.

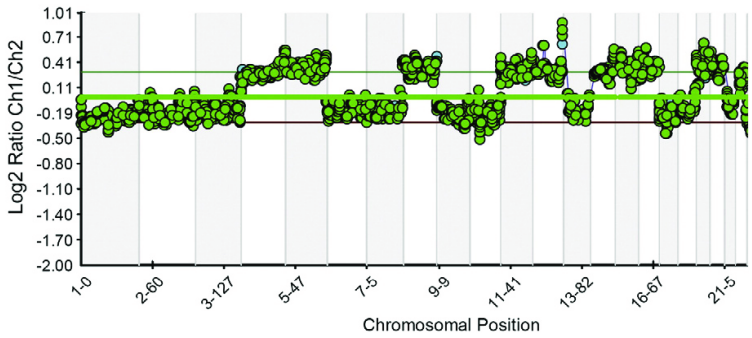

Fig. 7. Array comparative genomic hybridization fused chart of CRCCND-L with gains of chromosomes 4, 5, 8, 11, 12, 14, 15, 16, 19, and 20.

17, and 21) and gains (chromosomes 4, 11, 12, 14, 15, 16, 19, and 20) in neuroendocrine-like CRCC. These findings further enrich the spectrum of chromosomal anomalies on CRCC.

Chromophobe RCC has generally been regarded as an indolent tumor with a more favorable prognosis than other common RCCs. As for CRCCND, it remains unclear whether neuroendocrine differentiation influences clinical course and prognosis; the rarity of CRCCND makes it difficult to assess clinical outcomes, and few cases have been published to date [5-7].

Two cases (nos. 1 and 4) from our series were previously reported by Kuroda et al [6] and Ohe et al [7]. One of these new patients (case 2) presented with a 12-cm primary tumor and metastatic spreading at the time of diagnosis. She is alive with disease with 0.5 years of follow-up revealing local recurrence and bone metastasis. The second patient (case 3) presented with a 5.6-cm tumor with no available follow-up data. Chromophobe renal cell carcinoma with neuroendocrine differentiation exhibited aggressive behavior with relatively large tumor size (12 and 22 cm) in 2 of our 4 cases. Although few cases have been reported and follow-up information is not always complete, our data are in concordance with the hypothesis that neuroendocrine differentiation may represent advanced tumor stage [6]. Some authors have suggested a possible link between loss of chromosomes 4, 5, and 16p and neuroendocrine differentiation in CRCC; however, this finding was not confirmed in our series [7]. It appears that CRCCND may represent a more aggressive tumor than conventional CRCC, but further large-scale study is needed to elucidate this issue.

Most RCC patients are treated surgically following the discovery of a renal mass by modern imaging techniques, but in certain cases, a core biopsy is indicated. In such cases, making a definitive diagnosis from such limited material is often difficult. The most problematic tumors in the differential diagnosis are carcinoid, transitional cell carcinoma (TCC) with neuroendocrine features, and outside metastases.

Primary renal carcinoid tumors are rare, and their histogenesis within the kidney remains uncertain. Although malignant, the biological behavior of renal carcinoid tumors is considered to be more indolent than that of most RCC [24]. Microscopically, the tumors are composed of monomorphic round to polygonal cells with round to oval nuclei showing evenly distributed chromatin. These cells are arranged in trabecular, ribbon-like, gyriform, insular, glandular, and solid patterns. Immunohistochemically, tumor cells demonstrate variable positivity for neuroendocrine markers such as chromogranin A, synaptophysin, and NSE. In addition, renal carcinoids frequently display immunoreactivity for CD99. Ultrastructurally, the neoplastic cells contain abundant dense core neurosecretory granules [24]. Raisinoid nuclei and perinuclear clearing (halo) are not characteristics of renal carcinoid. The presence of such findings, along with immunohistochemical examination, could help to resolve diagnostic problems. However, the neuroendocrine component in CRCCND can mimic carcinoid features, especially if only limited material is available. In such cases, immunoreactivity for CD99 can be especially useful, as it has not been observed in CRCCND.

Transitional cell carcinoma can also feature neuroendocrine differentiation [20], exhibiting overlapping morphologic characteristic with CRCCND and making differential diagnosis complicated. The typical microscopic pattern of this variant of TCC is a mosaic arrangement of tumor cells resembling Merkel neuroendocrine carcinoma of skin. The dual cell population with raisinoid nuclei and perinuclear clearing found in CRCCND can be a helpful morphologic distinction. Immunohistochemically, CK20 can be used for distinction between these 2 entities, although other immunostaining qualities tend to be similar. However, in unusual TCC or in cases with high grade, CK20 is usually only weakly positive or entirely negative. CD117 is reported as negative in TCC, which may serve as another immunohistochemical marker for differentiation between TCC and CRCCND. In cases where a whole kidney specimen is available, well-performed sampling is nearly always helpful. It is usually possible to find areas where the urothelial origin of the lesion is obvious and it is not necessary to apply extensive immunohistochemical examination. Careful sampling of the renal pelvis in deeply located tumors can also help to find TCC in situ or

Table 4
Summary of morphologic, immunohistochemical, ultrastructural, and molecular genetic features of CRCCND and CRCCND-L

	CRCCND	CRCCND-L
Morphology/pattern	SCI, PSC	SCI, PSC, P, SC PR
Immunohistochemistry	Chrom−+, Syn +, CD56+, NSE+	Chrom−, Syn−+, CD56−+, NSE+
Ultrastructure[a]	Neurosecretory granules +	Neurosecretory granules −
Chromosomal numerical aberrations	Loss of chromosomes 1, 2, 6, 10, 17	Multiple losses of chromosomes 1, 2, 6, 10, 13, 17, 21 and gains of chromosomes 4, 11, 12, 14, 15, 16, 19, 20

Abbreviations: −+, focally, weakly positive in single case; +, positive; −, negative.
[a] Ultrastructural study was performed on limited number of the cases.

to discover the transition from more typical TCC to areas with neuroendocrine differentiation.

Finally, metastases of neuroendocrine carcinomas from other organs can also cause diagnostic difficulties. The morphology, immunohistochemistry, and ultrastructure of such lesions can resemble the neuroendocrine component in CRCCND making it important to look carefully for the chromophobe component. Definitive resolution usually requires clinical and radiologic correlation in these cases.

8. Conclusions

1. Morphologic features suggestive of neuroendocrine differentiation are rarely seen in CRCC. In the majority of such cases, true neuroendocrine differentiation cannot be demonstrated; thus, these features often simply represent an architectural growth pattern variant.
2. True CRCCND is distinguished from CRCCND-L based on the expression of neuroendocrine markers and the presence of neuroendocrine granules.
3. Chromosomal losses (chromosomes 1, 2, 6, and 10) are mostly found in CRCCND, whereas some CRCCND-L cases show both losses and gains of multiple chromosomes.
4. CRCCND appears to have metastatic potential based on the fact that 2 of 4 reported cases behaved aggressively. Nevertheless, further research with additional cases is required to highlight this rare and peculiar variant of RCC.

Disclosure of conflict of interest

All authors declare no conflict of interest.

References

[1] Michal M, Hes O, Svec A, Ludvikova M. Pigmented microcystic chromophobe cell carcinoma: a unique variant of renal cell carcinoma. Ann Diagn Pathol 1998;2:149–53 [PubMed PMID: 9845733].
[2] Hes O, Vanecek T, Perez-Montiel DM, Alvarado Cabrero I, Hora M, Suster S, et al. Chromophobe renal cell carcinoma with microcystic and adenomatous arrangement and pigmentation—a diagnostic pitfall. Morphological, immunohistochemical, ultrastructural and molecular genetic report of 20 cases. Virchows Arch 2005;446:383–93 [PubMed PMID: 15756595].
[3] Dundr P, Pesl M, Povysil C, Tvrdik D, Pavlik I, Soukup V, et al. Pigmented microcystic chromophobe renal cell carcinoma. Pathol Res Pract 2007;203:593–7 [PubMed PMID: 17658700].
[4] Kuroda N, Iiyama T, Moriki T, Shuin T, Enzan H. Chromophobe renal cell carcinoma with focal papillary configuration, nuclear basaloid arrangement and stromal osseous metaplasia containing fatty bone marrow element. Histopathology 2005;46:712–3 [PubMed PMID: 15910607].
[5] Parada DD, Pena KB. Chromophobe renal cell carcinoma with neuroendocrine differentiation. APMIS 2008;116:859–65 [PubMed PMID: 19024610].
[6] Kuroda N, Tamura M, Hes O, Michal M, Gatalica Z. Chromophobe renal cell carcinoma with neuroendocrine differentiation and sarcomatoid change. Pathol Int 2011;61:552–4 [PubMed PMID: WOS:000294976700009. English].
[7] Ohe C, Kuroda N, Keiko M, Tomoki K, Masatsugu M, Shun S, et al. Chromophobe renal cell carcinoma with neuroendocrine differentiation/morphology: a clinicopathological and genetic study of three cases. Hum Pathol Case Rep 2014;1:31–9.
[8] Sperga M, Martinek P, Vanecek T, Grossmann P, Bauleth K, Perez-Montiel D, et al. Chromophobe renal cell carcinoma–chromosomal aberration variability and its relation to Paner grading system: an array CGH and FISH analysis of 37 cases. Virchows Arch 2013;463:563–73 [PubMed PMID: 23913167].
[9] Thoenes W, Storkel S, Rumpelt HJ, Moll R, Baum HP, Werener S. Chromophobe renal cell carcinoma and its variants. A report on 32 cases. J Pathol 1988;155:277–87.
[10] Brunelli M, Eble JN, Zhang S, Martignoni G, Delahunt B, Cheng L. Eosinophilic and classic chromophobe renal cell carcinomas have similar frequent losses of multiple chromosomes from among chromosomes 1, 2, 6, 10, and 17, and this pattern of genetic abnormality is not present in renal oncocytoma. Mod Pathol 2005;18:161–9 [PubMed PMID: 15467713].
[11] Kuroda N, Tanaka A, Yamaguchi T, Kasahara K, Naruse K, Yamada Y, et al. Chromophobe renal cell carcinoma, oncocytic variant: a proposal of a new variant giving a critical diagnostic pitfall in diagnosing renal oncocytic tumors. Med Mol Morphol 2013;46:49–55 [PubMed PMID: 23338778].
[12] Akhtar M, Tulbah A, Kardar AH, Ali MA. Sarcomatoid renal cell carcinoma: the chromophobe connection. Am J Surg Pathol 1997;21:1188–95 [PubMed PMID: 9331291].
[13] Magro G, Lopes M, Amico P, Puzzo L. Chromophobe renal cell carcinoma with extensive rhabdomyosarcomatous component. Virchows Arch 2005;447:894–6 [PubMed PMID: 16021511].
[14] Itoh T, Chikai K, Ota S, Nakagawa T, Takiyama A, Mouri G, et al. Chromophobe renal cell carcinoma with osteosarcoma-like differentiation. Am J Surg Pathol 2002;26:1358–62 [PubMed PMID: 12360051].
[15] Quiroga-Garza G, Khurana H, Shen S, Ayala AG, Ro JY. Sarcomatoid chromophobe renal cell carcinoma with heterologous sarcomatoid elements. A case report and review of the literature. Arch Pathol Lab Med 2009;133:1857–60 [PubMed PMID: 19886723].
[16] Anila KR, Mathew AP, Somanathan T, Mathews A, Jayasree K. Chromophobe renal cell carcinoma with heterologous (liposarcomatous) differentiation: a case report. Int J Surg Pathol 2012;20:416–9 [PubMed PMID: 22134633].
[17] Petersson F, Michal M, Franco M, Hes O. Chromophobe renal cell carcinoma with liposarcomatous dedifferentiation—report of a unique case. Int J Clin Exp Pathol 2010;3:534–40 [PubMed PMID: 20606735, Pubmed Central PMCID: 2897100].
[18] Husain A, EBJ, Trpkov K. Composite chromophobe renal cell carcinoma with sarcomatoid differentiation containing osteosarcoma, chondrosarcoma, squamous metaplasia and associated collecting duct carcinoma: a case report. Anal Quant Cytol Histol 2014;36:235–40.
[19] Dittus CFC, Saha D, Magee A. A rare case of ovarian carcinosarcoma with neuroendocrine differentiation. J Community Support Oncol 2004;12:71–4.
[20] Eble JN, Sauter G, Epstein JI, Sesterhenn I. WHO Classification of Tumours. Tumours of the urinary system and male genital organs. Pathology and GeneticsLyon: IARC Press; 2004.
[21] La Rosa SSF. High-grade poorly differentiated neuroendocrine carcinomas of the gastroenteropancreatic system: from morphology to proliferation and back. Endocr Pathol 2014;52:193–8.
[22] Caplin ME, Baudin E, Ferolla P, Filosso P, Garcia-Yuste M, Lim E, et al. Pulmonary neuroendocrine (carcinoid) tumors: European Neuroendocrine Tumor Society expert consensus and recommendations for best practice for typical and atypical pulmonary carcinoids. Ann Oncol 2015;2 [PubMed PMID: 25646366].
[23] Rekhtman N. Neuroendocrine tumors of the lung: an update. Arch Pathol Lab Med 2010;134:1628–38 [PubMed PMID: 21043816].
[24] Kuroda N, Tanaka A, Ohe C, Mikami S, Nagashima Y, Inoue K, et al. Review of renal carcinoid tumor with focus on clinical and pathobiological aspects. Histol Histopathol 2013;28:15–21 [PubMed PMID: 23233056].
[25] Gunawan B, Bergmann F, Braun S, Hemmerlein B, Ringert RH, Jakse G, et al. Polyploidization and losses of chromosomes 1, 2, 6, 10, 13, and 17 in three cases of chromophobe renal cell carcinomas. Cancer Genet Cytogenet 1999;110:57–61 [PubMed PMID: 10198624].
[26] Vieira J, Henrique R, Ribeiro FR, Barros-Silva JD, Peixoto A, Santos C, et al. Feasibility of differential diagnosis of kidney tumors by comparative genomic hybridization of fine needle aspiration biopsies. Genes Chromosomes Cancer 2010;49:935–47 [PubMed PMID: 20629095].
[27] Tan MH, Wong CF, Tan HL, Yang XJ, Ditlev J, Matsuda D, et al. Genomic expression and single-nucleotide polymorphism profiling discriminates chromophobe renal cell carcinoma and oncocytoma. BMC Cancer 2010;10:196 [PubMed PMID: 20462447, Pubmed Central PMCID: 2883967].

CYSTICKÝ A NEKROTICKÝ PAPILÁRNÍ RENÁLNÍ KARCINOM: PROGNOSTICKÝ, MORFOLOGICKÝ, IMUNOHISTOCHEMICKÝ A MOLEKULÁRNĚ GENETICKÝ PROFIL 10 PŘÍPADŮ

Přítomnost nekrózy u renálních karcinomů je všeobecně uznávána jako nepříznivý prognostický faktor, ačkoliv její význam je pevně ustanoven pouze u světlobuněčných renálních karcinomů a zde platí, že pouze koagulační nekróza má prognostický vliv [16-18]. Význam přítomnosti nekrózy u papilárního renálního karcinomu (PRK) není zatím zcela objasněn; doposud publikované studie prokazují nekonzistentní výsledky.

Do této studie jsme zařadili 10 cystických a rozsáhle nekrotických PRK, které se dle dostupných klinických informací chovaly biologicky příznivě (bez agresivního chování a metastáz). Zaměřili jsme se na precizní morfologická kritéria a zařadili pouze jednotné tumory: sférické, cystické, obklopené fibrózním pouzdrem a vyplněné hemoragickou/nekrotickou tekutinou. Na vnitřní části pouzdra byl u všech tumorů tenký lem neoplastických buněk, které odpovídaly typu 1 PRK. Všechny případy byly imunohistochemicky pozitivní s AMACR, OSCAR, CAM5.2, HIF-2 a vimentinem. Molekulárně genetický profil byl taktéž ve všech případech kompatibilní s diagnózou PRK. Abnormality *VHL* genu nebyly v žádném z tumorů zjištěny.

Cílem naší studie bylo demonstrovat, že papilární renální karcinom typu 1 se může vzácně prezentovat jako objemná cystická léze ohraničená silným fibroleiomyomatózním pouzdrem a vyplněná hemoragickou/nekrotickou hmotou. Nekróza, která ve všech případech měla kolikvační charakter, neměla vliv na biologické chování tumorů a pokud se tato vyskytne PRK typu 1, neměla by být automaticky považována za nepříznivý prognostický faktor. Tato studie si však neklade za cíl ustanovit nová prognostická kritéria pro typ 1 PRK, jejím záměrem bylo vybrat skupinu morfologicky uniformních PRK typu 1 s neobvyklými makroskopickými a mikroskopickými znaky (cystická léze s nekrotickým obsahem) a upozornit na fakt, ze kolikvační nekróza u těchto typu tumorů nemá pravděpodobně prognostický význam.

Annals of Diagnostic Pathology 26 (2017) 23–30

Contents lists available at ScienceDirect

Annals of Diagnostic Pathology

Cystic and necrotic papillary renal cell carcinoma: prognosis, morphology, immunohistochemical, and molecular-genetic profile of 10 cases☆,☆☆

Kvetoslava Peckova, MD [a], Petr Martinek, PhD [a], Kristyna Pivovarcikova, MD [a], Tomas Vanecek, PhD [a], Reza Alaghehbandan, MD [b], Kristyna Prochazkova, MD [c], Delia Perez Montiel, MD [d], Milan Hora, MD, PhD [c], Faruk Skenderi, MD [e], Monika Ulamec, MD, PhD [f], Pavla Rotterova, MD, PhD [g], Ondrej Daum, MD, PhD [a], Jiri Ferda, MD, PhD [h], Whitney Davidson, BS [i], Ondrej Ondic, MD [a], Magdalena Dubova, MD [a], Michal Michal, MD [a], Ondrej Hes, MD, PhD [a,*]

[a] Department of Pathology, Charles University, Medical Faculty and Charles University Hospital Plzen, Czech Republic
[b] Department of Pathology, University of British Columbia, Royal Columbian Hospital, Vancouver, Canada
[c] Department of Urology, Charles University, Medical Faculty and Charles University Hospital Plzen, Czech Republic
[d] Department of Pathology, Instituto Nacional de Cancerologia, Mexico City, Mexico
[e] Department of Pathology, University Clinical Center, Sarajevo, Bosnia and Herzegovina
[f] "Ljudevit Jurak" Pathology Department, Clinical Hospital Center "Sestre milosrdnice,", Zagreb, Croatia
[g] Biopticka Laborator, Plzen, Czech Republic
[h] Department of Radiodiology, Charles University, Medical Faculty and Charles University Hospital Plzen, Czech Republic
[i] Department of Pathology, The University of Kansas School of Medicine, Kansas City, KS

ARTICLE INFO

Keywords:
Kidney
Papillary renal cell carcinoma
Cystic
Necrosis
Necrotics
Molecular genetics

ABSTRACT

Conflicting data have been published on the prognostic significance of tumor necrosis in papillary renal cell carcinoma (PRCC). Although the presence of necrosis is generally considered an adverse prognostic feature in PRCC, we report a cohort of 10 morphologically distinct cystic and extensively necrotic PRCC with favorable biological behavior. Ten cases of type 1 PRCC with a uniform morphologic pattern were selected from the 19 500 renal tumors, of which 1311 were PRCCs in our registry. We focused on precise morphologic diagnosis supported by immunohistochemical and molecular-genetic analysis. Patients included 8 men and 2 women with an age range of 32-85 years (mean, 62.6 years). Tumor size ranged from 6 to 14 cm (mean, 9.4 cm). Follow-up data were available in 7 patients, ranging from 0.5 to 14 years (mean, 4 years). All tumors were spherical, cystic, and circumscribed by a thick fibrous capsule, filled with hemorrhagic/necrotic contents. Limited viable neoplastic tissue was present only as a thin rim in the inner surface of the cyst wall, consistent with type 1 PRCC. All cases were positive for AMACR, OSCAR, CAM 5.2, HIF-2, and vimentin. Chromosome 7 and 17 polysomy was found in 5 of 9 analyzable cases, 2 cases demonstrated chromosome 7 and 17 disomy, and 1 case showed only chromosome 17 polysomy. Loss of chromosome Y was found in 5 cases, including 1 case with disomic chromosomes 7 and 17. No *VHL* gene abnormalities were found. Papillary renal cell carcinoma type 1 can present as a large hemorrhagic/necrotic unicystic lesion with a thick fibroleiomyomatous capsule. Most cases showed a chromosomal numerical aberration pattern characteristic of PRCC. All tumors followed a nonaggressive clinical course. Large liquefactive necrosis should not necessarily be considered an adverse prognostic feature, particularly in a subset of type 1 PRCC with unilocular cysts filled with necrotic/hemorrhagic material.

1. Introduction

Papillary renal cell carcinoma (PRCC) accounts for 15% to 20% of renal carcinomas and is a heterogeneous disease with histologic subtypes and variations in clinical behavior and outcome. It is traditionally subclassified as type 1, which is a distinct entity (morphologically, immunohistochemically, and genetically), and type 2, which is composed of more heterogeneous group of diseases [1]. Grossly, PRCCs are usually well circumscribed and may contain foci of necrosis and

☆ Disclosure of Conflict of Interest: All authors declare no conflict of interest.

☆☆ The study was supported by the Charles University Research Fund (Project No. P36), by the Ministry of Health of the Czech Republic—Conceptual Development of Research Organization (Faculty Hospital in Pilsen, 00669806), and by SVV 260283.

* Corresponding author at: Department of Pathology, Charles University, Medical Faculty and Charles University Hospital Plzen, Alej Svobody 80, 304 60 Pilsen, Czech Republic.
E-mail address: hes@medima.cz (O. Hes).

http://dx.doi.org/10.1016/j.anndiagpath.2016.10.007
1092-9134/

hemorrhage. Nonetheless, unilocular cystic tumors within type 1 PRCC are rather uncommon.

We describe a cohort of PRCC, morphologically consistent with type 1 according to the Delahunt classification, which were large unilocular cystic tumors surrounded by thick-wall fibrous capsule and filled with hemorrhagic/necrotic contents, demonstrating long-term favorable clinical outcome [1,2]. The purpose of this study was to describe a unique subpopulation of type 1 PRCC with an unusual gross and histologic presentation (cystic lesion with necrotic content) to enhance our understating of the prognostic significance of tumor necrosis (TN) in these tumors.

2. Materials and methods

This study design was approved by local ethical committee (Charles University, Medical School Plzen).

Of 19 500 renal tumors and tumor-like lesions (including 1311 PRCCs) in the institutional and consultation files of the Sikl's Department of Pathology at Charles' University, Plzen, Czech Republic, 10 cases of cystic and largely necrotic type 1 PRCC were retrieved. The tissue had been fixed in neutral formalin, embedded in paraffin, 3- to 4-μm-thick sections were cut and stained with hematoxylin and eosin.

All tumors were large cystic lesions encapsulated by a thick, mostly fibrotic tissue. In 2 cases, the tumor capsule was histologically composed of so-called phenomenon inflammatory pseudotumor, for which one of them has already been reported [3]. Cysts were filled with sanguinolent necrotic material, whereas viable neoplastic structures were identified only in the inner surface of the cyst wall. Cases were further examined by immunohistochemistry and analyzed by molecular-genetic methods.

2.1. Immunohistochemistry

The immunohistochemical study was performed using a Ventana Benchmark XT automated stainer (Ventana Medical System, Inc, Tucson, AZ). The following primary antibodies were used: cytokeratin AE1/3 VM (AE1/AE3/PCK26, monoclonal; Ventana-Roche, Mannheim, Germany, RTU), wide-spectrum keratin (OSCAR, monoclonal, 1:2000; Covance, Princetown, NJ), cytokeratin (CAM 5,2 monoclonal, 1:200; Becton-Dickinson, San Jose, CA), racemase/AMACR (P504S, monoclonal, 1:50; Zeta, Sierra Madre, CA), vimentin (D9, monoclonal, 1:1000; Neomarkers, Westinghouse, CA), carbonic anhydrase IX (rhCA9, monoclonal, 1:100; RD Systems, Abingdon, GB), CD31 (JC70A, monoclonal, 1:50; DakoCytomation, Glostrup, Denmark), CD34 (QBEnd-10, monoclonal, 1:100; DakoCytomation), c-kit (CD 117, polyclonal; DakoCytomation, RTU), cathepsin K (monoclonal, 3F9, 1:100; Abcam, Cambridge, UK), PAX-8 (polyclonal rabbit, 1:25; Cell Marque–Medac/RNDr. A. Manthey, Rocklin, CA), TFE3 (polyclonal, 1:100; Abcam), HIF-1α (ESEE122, 0.5:150; Abcam), HIF-2α (ep190b, 1:30; Abcam), and phospho-mTOR (Ser2448, 1:80; Cell Signaling Technology, Danvers, MA). Appropriate positive and negative controls were used.

2.2. Molecular-genetic study

2.2.1. Fluorescence in situ hybridization methods

Four-micrometer-thick section was placed onto a positively charged slide. Hematoxylin and eosin–stained slide was examined for the cell counting area determination.

The unstained slide was routinely deparaffinized and incubated in the 1× Target Retrieval Solution Citrate pH 6 (Dako, Glostrup, Denmark) for 40 minutes at 95°C and subsequently cooled for 20 minutes at room temperature in the same solution. The slide was washed in deionized water for 5 minutes and digested in protease solution with Pepsin (0.5 mg/mL; Sigma-Aldrich, St Louis, MO) in 0.01 M HCl at 37°C for 20 minutes. The slide was then placed into deionized water for 5 minutes, dehydrated in a series of ethanol solution (70%, 85%, and 96% for 2 minutes each), and air-dried. Probes for aneuploidy detection of chromosomes 7 and 17 (Vysis/Abbott Molecular, Des Plaines, IL; see Table 1) were mixed with water and LSI/WCP (Locus-Specific Identifier/Whole Chromosome Painting) Hybridization buffer (Vysis) in a 1:2:7 ratio. An appropriate amount of probe mix was applied on the specimen, covered with a glass coverslip and sealed with a rubber cement. The slide was incubated in the ThermoBrite instrument (StatSpin/Iris Sample Processing, Westwood, MA) with co-denaturation parameters 85°C for 8 minutes and hybridization parameters 37°C for 16 hours. Rubber-cemented coverslip was then removed and the slide was placed in a posthybridization wash solution (2× SSC/0.3% NP-40) at 72°C for 2 minutes. The slide was air-dried in the dark, counterstained with DAPI (Vysis), coverslipped and immediately examined.

2.2.2. Fluorescence in situ hybridization interpretation

The section was examined with an Olympus BX51 fluorescence microscope (Olympus Corporation, Tokyo, Japan) using a ×100 objective and filter sets Triple Band Pass (DAPI/SpectrumGreen/SpectrumOrange) and Single Band Pass (SpectrumGreen/SpectrumOrange). Scoring of aneuploidy was performed by counting the number of fluorescent signals in 100 randomly selected nonoverlapping tumor cell nuclei. The slide was independently enumerated by 2 observers (OH and PG). Monosomy and polysomy for studied chromosomes were defined as the presence of one signal per cell in greater than 45% and 3 and more signals in greater than 10% (mean + 3 SD in normal nonneoplastic control tissues), respectively.

2.2.3. DNA extraction and bisulfite DNA conversion

DNA for molecular-genetic investigation was extracted from formalin-fixed, paraffin-embedded tissue. Several 5-μm-thick sections were placed on the slides. Hematoxylin and eosin–stained slides were examined for identification of neoplastic tissue. Subsequently, neoplastic tumor and nonneoplastic tissue from unstained slides were scraped and DNA was isolated by the NucleoSpin Tissue Kit (Macherey-Nagel, Düren, Germany).

Bisulfite conversion of DNA was carried out using EZ DNA Methylation–Gold Kit (DNA input 500 ng; Zymo Research, Orange, CA).

All procedures were performed according to the manufacturer's protocols.

2.3. VHL gene analysis

Mutation analysis of exons 1, 2, and 3 of the *VHL* gene was performed using polymerase chain reaction (PCR) and direct sequencing. Polymerase chain reaction was carried out using primers shown in Table 2. The reaction conditions were as follows: 12.5 μL of HotStar Taq PCR Master Mix (Qiagen, Hilden, Germany), 10 pmol of each primer, 100 ng of template DNA, and distilled water up to 25 μL. The amplification program consisted of denaturation at 95°C for 15 minutes and then 40 cycles of denaturation at 95°C for 1 minute, annealing at 55°C for 1 minute, and extension at 72°C for 1.5 minute for all amplicons. The program was finished by 72°C incubation for 7 minutes.

The PCR products were checked on 2% agarose gel electrophoresis.

Successfully amplified PCR products were purified with magnetic particles Agencourt AMPure (Agencourt Bioscince Corporation, A Beckman Coulter Company, Beverly, MA), both side sequenced using Big Dye Terminator Sequencing kit (Applied Biosystems, Foster City, CA) and purified with magnetic particles Agencourt CleanSEQ (Agencourt Bioscince Corporation) all according to the manufacturer's protocol, and subsequently run on an automated sequencer ABI Prism 3130xl (Applied Biosystems) at a constant voltage of 13.2 kV for 20 minutes. All samples were analyzed in duplicates. Analyses of positive samples were repeated.

Table 1
Clinicopathologic data

Case	Age (y)	Sex	Size (cm)	Follow-up (y)	Follow-up (clinical information)
1	40	M	6 × 5.5 × 3.5	0.5	Open resection; pT1b. AW, without recurrency
2	67	F	6.5 × 5.5 × 5.5	2	Right kidney resection; pT1b; duplicate malignancy-brest cancer. AW, without recurrency
3	67	M	9 × 7.5 × 4	NA	NA
4	37	M	NA	NA	NA
5	65	F	9 × 7 × 6	4	AW
6	83	M	14 × 11.5 × 7	0.5	Nephrectomy with appendectomy; pT2. Epidermoid lung carcinoma. Died in 2008 of lung carcinoma. No autopsy
7	69	M	9 × 11 × 11	14	Nephrectomy with appendectomy; AW, without progression
8	85	M	9.5 × 7.5 × 5	NA	NA
9	32	M	NA	4	Marsupialization of "renal cyst"; pT2. Died in 2007 of hepatic failure. No autopsy
10	81	M	10 × 8 × 4	3	Nephrectomy. Died 3 y later of unknown causes. Suspect malignant tumor diagnosed from needle biopsy.

Abbreviations: AW, alive and well; F, female; M, male; NA, not available.

2.3.1. Analysis of VHL promoter methylation

Detection of promoter methylation was carried out via methylation-specific PCR as described by Herman et al [4]. Briefly, 100 ng of DNA or 2 μL of converted DNA was added to reaction consisted of 12.5 μL of HotStar Taq PCR Master Mix (Qiagen), 10 pmol of forward and reverse primer (Table 3), and distilled water up to 25 μL. The amplification program comprised denaturation at 95°C for 14 minutes and then 40 cycles of denaturation at 95°C for 1 minute, annealing at 60°C for 1 minute, and extension at 72°C for 1 minute. The program was finished by incubation at 72°C for 7 minutes.

The PCR products were checked on 2% agarose gel electrophoresis.

A patient with known *VHL* mutation and fully methylated HeLa cell DNA were used as a positive control for *VHL* mutation analysis and promoter methylation analysis, respectively. As a negative control, randomly selected healthy donor blood was used.

3. Results

3.1. Clinical features

Clinicopathologic data of the patients under study are summarized in Table 1. Of 10 patients, 8 were men and 2 were women, with age ranging from 32 to 85 years (mean, 62.6 years; median, 67 years). The tumor size ranged from 6 to 14 cm (mean, 9.4 cm; median, 9.3 cm). Follow-up data were available for 7 patients and ranged from 5 months to 14 years (mean, 4 years; median, 3 years). Three patients died of conditions unrelated to renal tumor progression (ie, lung cancer and hepatic failure). The remaining 7 patients were alive and well without disease progression or metastasis at the time of study.

3.2. Gross and microscopic findings

Grossly, tumors were large, with size up to 14 cm in greatest dimension (case 6). The tumors grew expansively, were well demarcated, and did not invade into adjacent structures (Fig. 1A + B). All tumors presented as unilocular cystic mass encapsulated by thick whitish fibrous tissue. The inner surface of the capsule was mainly covered by a very thin layer of brownish friable tissue, and the whole cyst was usually filled with hemorrhagic and necrotic material (Fig. 2). No grossly identifiable neoplastic tissue was noted within the entire tumor.

Microscopically, all cases showed similar basophilic morphologic appearance with low-grade nuclear features consistent with type 1 PRCC. In most cases, there was only very limited amount of viable neoplastic tissue present lining the inner surface the cyst (Fig. 3A + B). This residual viable neoplastic tissue focally formed short papillae/tubulopapillary structures mostly lined by a single-cuboidal or low-columnar epithelial cells with scant cytoplasm and relatively uniform nuclei (Fig. 4A + B). Occasionally, more complex papillary structures were encountered. Histologic grade 2 was found in 8 cases, 3 in 2 cases (International Society of Urological Pathology [ISUP] nucleolar grading).

All tumors were well circumscribed, with a prominent fibrous capsule showing a thickness up to 2 cm. In 2 cases (cases 9 and 10), the capsule wall comprised rather cellular tissue composed mostly of fibroblasts with focally dense lymphocytic infiltration. Such a phenomenon was morphologically consistent with the diagnosis of inflammatory pseudotumor (Fig. 5A + B). Cysts were filled with hemorrhagic and necrotic material.

3.3. Immunohistochemistry

The immunohistochemical findings are summarized in Table 2. All of the examined tumors were diffusely positive for AMACR, OSCAR, CAM 5.2, anti–HIF-2 and vimentin (Fig. 6). CD117 and anti HIF-1 were weakly positive. MIA was diffusely positive in 9/10 cases, and in one case (case 8) the positivity was focal. 7 of 10 tumors diffusely reacted with PAX 8, and the remaining 3 cases were focally positive. There was no expression of CANH and TFE3 in any case. Expression of CD34, CD31, mTor, Cathepsin K, and AE1-AE3 was variable. ALK-1 was negative both in pseudocapsules and in the neoplastic tissue in all cases.

3.4. Molecular-genetic findings

Findings of molecular-genetic analyses are summarized in Table 3. Tumors were analyzed for chromosomal copy number variation using array comparative genomic hybridization (aCGH) and fluorescence in

Table 2
Immunohistochemical findings

Case	CD117	CD31	CD34	Cath	AMACR	OSCAR	Vim	AE 1/3	CAM 5.2	MIA	TFE 3	CANH	PAX 8	Anti–HIF-1	Anti–HIF-2	mTOR	ALK 1[a]
1	+	−	−	−	+++	+++	+++	foc +++	++	+++	−	−	+++	+	+++	foc +++	−
2	+	+	+	−	+++	+++	+++	foc ++	++	+++	−	−	++	+	+++	foc +++	−
3	+	+	+	−	+++	+++	+++	foc +++	++	+++	−	−	++	+	+++	foc +++	−
4	+	+	−	−	+++	+++	+++	+++	+++	+++	−	−	+++	++	+++	foc +++	−
5	+	+	+	−	+++	+++	+++	foc +++	+++	+++	−	−	+++	+	+++	+	−
6	+	+	−	−	+++	+++	+++	+++	++	+++	−	−	++	++	+++	−	−
7	+	−	−	−	+++	+++	+++	foc +++	++	+++	−	−	foc +++	+	+++	foc +++	−
8	+	+	+	+	+++	+++	+++	+++	++	foc +++	−	−	foc +++	++	+++	foc +++	−
9	+	+	+	−	+++	+++	+++	+++	++	+++	−	−	foc +++	++	+++	foc ++	−
10	+	+	+	+	+++	+++	+++	foc ++	++	+++	−	−	+++	+	+++	+	−

Abbreviations: Cath, cathepsin K; foc, focally; Vim, vimentin; −, negative; +, weakly positive; ++, moderately positive; +++, strongly positive.
[a] Assessed in the capsule only.

Table 3
Molecular-genetic analyses

Case	Sex	aCGH	CEP 7	CEP 17	CEP XY	LOH 3p	VHL	VHLM
1	M	+9,+12,+20,−Y	D	D	X-	Neg	Neg	Neg
2	F	+12,+13,+16,+17,−21	D	P	XX	Neg	Neg	Neg
3	M	No changes	NA	NA	NA	Neg	Neg	Neg
4	M	NP	P	P	X-	NA	NA	Neg
5	F	NP	NP	NP	NP	NP	NP	NP
6	M	+7,+17	P	P	X-	Neg	Neg	Neg
7	M	+(7pter-7q22.1),+17,−Y	P	P	X-	NA	Neg	Neg
8	M	No changes	D	D	XY	Neg	Neg	Neg
9	M	+2,+3,+7,+12,+16,+17,+20,+21,+22	P	P	XY	Neg	Neg	Neg
10	M	NP	P	P	X-	NA	Neg	Neg

situ hybridization. Seven cases were analyzable by aCGH. Chromosome 7 and 17 polysomy was found in 5 cases (Fig. 7). No chromosomal numerical aberrations were found in 2 cases. In case 1, both chromosomes 7 and 17 were disomic with loss of chromosome Y detected by aCGH and subsequently confirmed by fluorescence in situ hybridization. Polysomies of chromosomes 9, 12, and 20 were found in the same tumor (case 1). Case 2 exhibited gains of chromosomes 12, 13, 16, and 17; chromosome 21 was monosomic and chromosome 7 was disomic.

No *VHL* gene abnormalities including mutations, hypermethylation of *VHL* promoter, and loss of heterozygosity of 3p locus were found in analyzable cases (Table 3).

4. Discussion

It has been evident since the so-called Heidelberg classification in 1997 that renal tumors represent a highly heterogeneous group of neoplasms not only morphologically but also from molecular-genetic perspectives [5]. In the 2004 World Health Organization classification of genitourinary tumors, 4 new subtypes of renal tumors were introduced [6]. In the 2012 ISUP Vancouver Renal Tumor Classification, further 5 new renal tumors were included and 3 more were recognized as "emerging" renal tumors [6]. The recent 2016 World Health Organization classification fully accepts the proposals of the 2012 ISUP Vancouver classification and one of the "emerging entities," succinate dehydrogenase deficient renal cell carcinoma (RCC), has been added as a new entity [7]. It is evident from these ever-evolving classifications that the morphologic and genetic variability of renal tumors are enormous and that one can reasonably anticipate different clinical outcomes in particular tumor types. Therefore, prognostic criteria and predictor factors can play a crucial role in providing individual risk profiles with a suitable aftercare conception [8]. It would be challenging to apply prognostic morphologic criteria to RCCs owing to vast tumor heterogeneity and the diverse biological pathways that exist in various tumors [8,9].

Type 1 PRCC is currently considered a distinct entity with relative uniform gross, histologic, and immunohistochemical features as well as similar molecular-genetic profile. Our cohort is constituted of a homogenous subset of type 1 PRCC presenting with large unilocular cystic necrotic tumors.

Papillary renal cell carcinoma, the second most common RCCs, was initially classified as 2 morphologic groups of so-called type 1 and type 2 by Delahunt and Eble [2]. Papillary renal cell carcinomas are generally immunoreactive for vimentin, cytokeratins AE1-AE3, CAM5.2, high-molecular-weight cytokeratins, EMA, CD10, and AMACR. Type 1 PRCC is more frequently positive for CK7. Genetic abnormalities in PRCC most commonly include trisomy/polysomy of chromosomes 7, 12, 16, 17, and 20 and loss of the Y chromosome. Several studies have

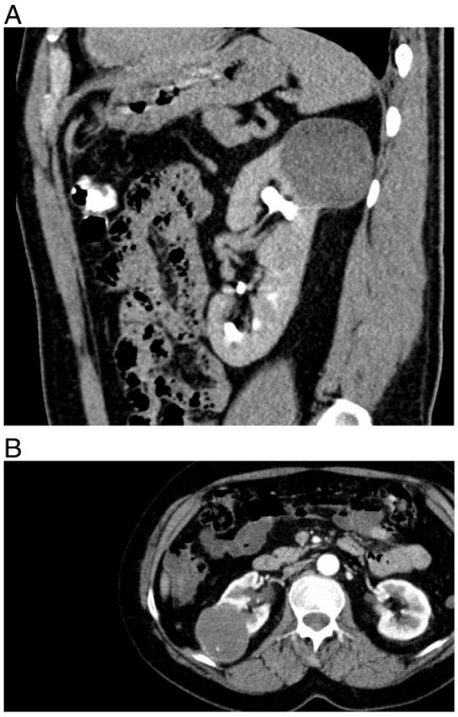

Fig. 1. (A) Case 2. Postcontrast computed tomography (CT), excretory phase, sagittal section. A round-shape tumor of the upper pole of the left kidney. Postcontrast density 17-61 HU. Necrotic center of the tumor is clearly visible. (B) Case 3. Postcontrast CT, arterial phase, axial section. Tumor of the right kidney, round shape with large central necrosis, postcontrast density 25-68 HU.

Fig. 2. Thick-walled cyst with thin, mostly necrotic rim of neoplastic tissue on the inner surface.

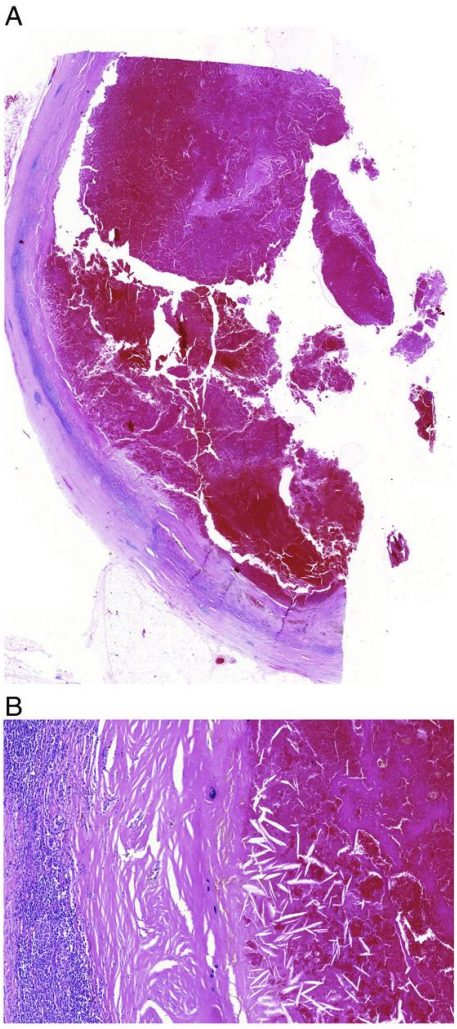

Fig. 3. (A + B) A limited amount of the vital neoplastic tissue lined the inner wall of the cyst. (A) Scanning magnification showing a large portion of thick-walled cyst. (B) Large areas of inner surface of the cyst were covered by necrotic material only.

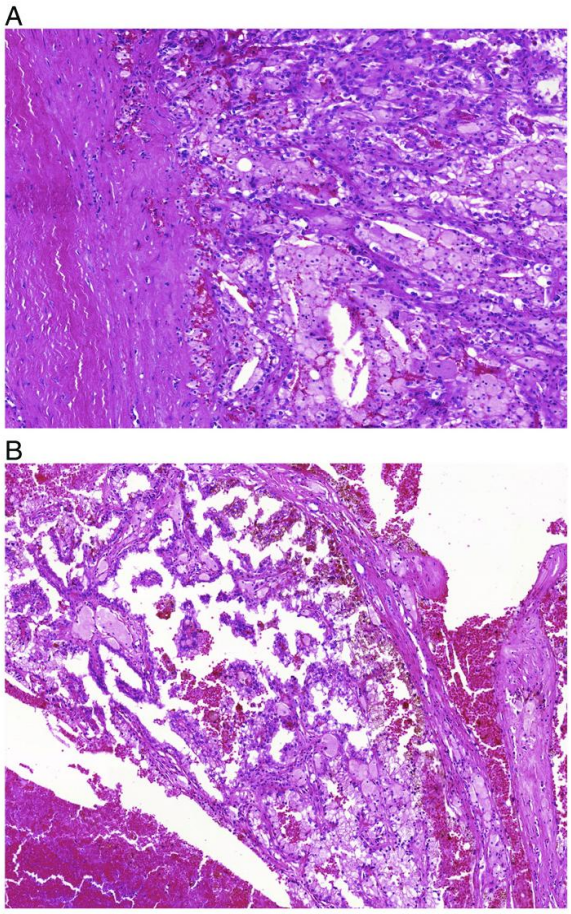

Fig. 4. Viable neoplastic tissue focally formed tubulopapillary (A) or short papillary (B) structures mostly lined by single-cuboidal or low-columnar epithelial cells with scant cytoplasm and uniform nuclei.

suggested genetic differences between type 1 (morphologically basophilic) and type 2 (morphologically eosinophilic) subtypes [6].

The increasing number of reported cases and the development of new diagnostic techniques have demonstrated that PRCC, as a group, is more diverse morphologically and genetically than previously thought.

Papillary renal cell carcinomas sometimes display overlapping morphologic features of type 1 and type 2, which can pose significant diagnostic difficulties in differentiating between the 2 types [10]. Several distinct variants of PRCC that are different from type 1 and type 2 have been described in the literature [11-14]. It should be noted that types 1 and 2 PRCCs are shown to be clinically and biologically distinct. Alterations in the MET pathway are associated with type 1, and activation of the NRF2-ARE pathway is described with type 2 [15]. Type 1 tumors often harbor gains of chromosomes 7p and 17p, whereas type 2 tumors contain an allelic imbalance of one or more chromosomes, namely, chromosomes 1p, 3p, 5, 6, 8, 9p, 10, 11, 15, 18, and 22 [6,15].

In our study, we attempted to assemble a uniform cohort of PRCC tumors that were consisted of large cystic necrotic/hemorrhagic tumors encapsulated by thick fibrous tissue. Morphologically and immunohistochemically, all lesions corresponded with type 1 PRCC. We noted that the tumors contained only scarce amounts of viable neoplastic tissue, mainly in the inner surface of the cyst wall, with most of tumor volume consisting of necrotic sanguinolent material.

The molecular-genetic profile was also expectedly consistent with type 1 PRCC (in 5/9 analyzable cases). Two of our cases demonstrated disomy in chromosomes 7 and 17, but also showed additional chromosomal abnormalities. Gains of chromosomes 9, 12, and 20 were found in 1 case (case 1), with a second case (case 6) exhibiting normal chromosome 7 and 17 status as well as disomy of all other chromosomes.

The prognosis of RCCs in general is attributed to several clinical and pathological factors such as symptomatic cancer, TNM classification, histologic grade, and presence/absence of a sarcomatoid differentiation [22]. The presence of TN has also been proposed repeatedly as an independent prognostic factor. Tumor necrosis appears to represent an interesting parameter in prognostic assessment owing to its easy and reproducible identification in routine histopathologic examination. However, there are several conflicting aspects that challenge the notion

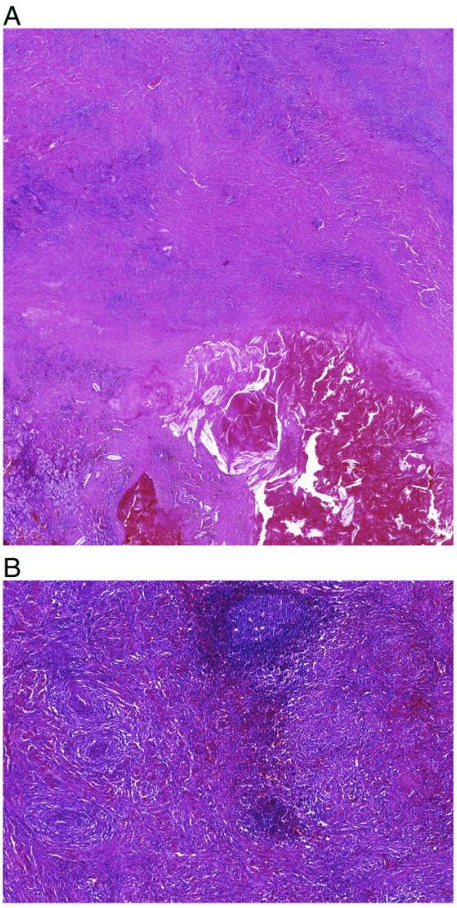

Fig. 5. Thick capsule resembling inflammatory pseudotumor was present in 2 cases. Scanning magnification (A) and detailed view (B).

of TN as a prognostic parameter. First, the prognostic significance of necrosis in RCCs remains controversial because the studies published to date have shown conflicting results [9,16,17]. This may be explained by the fact that no uniform consensus on assessing TN exists. Some researchers evaluate necrosis from gross specimens only [16,18], whereas others use radiologic or microscopic findings [9,17,19]. Klatte et al suggested that classification based solely on the presence or absence of necrosis is unsatisfactory. Conversely, they recommended a scoring system based on the extent of necrosis as a part of every pathological examination [33]. However, this concept is not currently accepted as part of standard reporting.

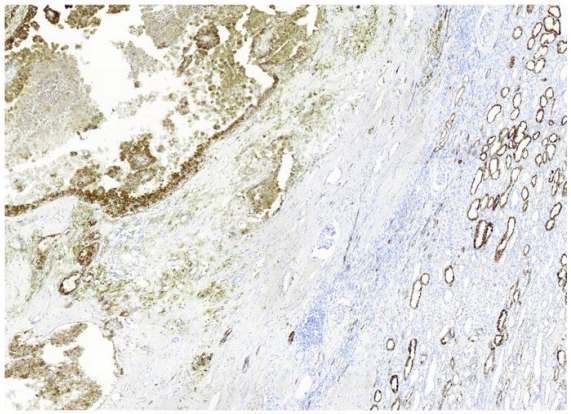

Fig. 6. All tumors were positive for AMACR.

Although TN is often reported as an adverse prognostic factor, its significance is only well established in clear cell RCC [6,20-22]. Furthermore, according to a recently proposed grading system for clear cell RCC, only coagulative-type necrosis is considered as a significant prognostic marker. It should be noted that no such criteria have been established for PRCC. Coagulative-type necrosis is characterized by preserved architecture of dead tissues and firm texture, with neoplastic cells showing no nuclei with limited structural damage, giving the appearance of so-called "ghost cells."

On the other hand, liquefactive necrosis is characterized by digestion of the dead cells resulting in transformation of the tissue into a liquid viscous mass [23]. We consider the necrosis within our cohort to be liquefactive type, as a substantial part of the tumor was transformed into a liquid viscous, largely hemorrhagic mass in all cases.

Considering that PRCCs are composed of a diverse and heterogeneous group of tumors, the determination of prognostic factors would even be more difficult to ascertain. The situation is further complicated by the fact that the incidence of PRCC is much lower than that of clear cell RCC, and a relatively limited number of studies dealing with prognostic factors in PRCC have been published [24]. One of the strengths of our series is that all the cases were uniformly and exclusively composed of type 1 PRCC according to Delahunt classification. It is worth noting that studies assessing clinical outcomes in PRCC may have generated inconsistent conclusions simply due to heterogeneous nature of PRCCs. Hence, numerous researchers have made an effort to determine the most useful method of histologic assessment in establishing meaningful prognostic factors. Onishi et al [25] studied clinicopathologic features of 42 PRCCs and their influence on prognosis. They suggested that the presence or absence of foam cells, pseudocapsule, solid architecture, cytologic appearance, stage, and nuclear grade were meaningful prognostic factors. In addition, they observed that the prognosis of patients with PRCC was similar to those with clear cell RCC. They did not include TN among the list of prognostic parameters, assuming that TN simply indicates poor tumor vascularization and that would be clinically irrelevant. However, because PRCC refers to a rather diverse heterogenous group of tumors and no further subclassifications of PRCC were provided by the authors, it would be difficult to determine which prognostic factors would have been attributed to different types of PRCC. Several other studies also reached a similar conclusion to that of Onishi et al, not considering TN to be an adverse prognostic parameter in PRCC [9,25-28]. In contrast, a number of studies reported TN to be associated with an adverse clinical course. In this regard, it is thus understandable that some researchers have designated TN as an adverse prognostic factor for PRCC [24,29-32].

However, it is of note that the subclassifying of PRCC into the type 1 and type 2 was not taken into consideration in some of these studies [8,26,28,33,34], whereas it was included in others [9,16,29,31]. For this reason, it is unclear whether it would be possible to compare the results from studies dealing with such a heterogeneous cohort of tumors. For instance, some PRCCs (ie, familiar leiomyomatosis associated [papillary] RCC) are clinically aggressive tumors, and that it would be inappropriate to objectively assess the prognostic value of TN in PRCCs without further subtyping.

This study is one of its kind to address this issue in an objective fashion. In our series of 10 largely necrotic type 1 PRCCs, none of the tumors demonstrated an aggressive or metastatic behavior. However, we would like to point out that our study has no ambition to establish prognostic criteria for type 1 PRCC or to evaluate presence/absence of

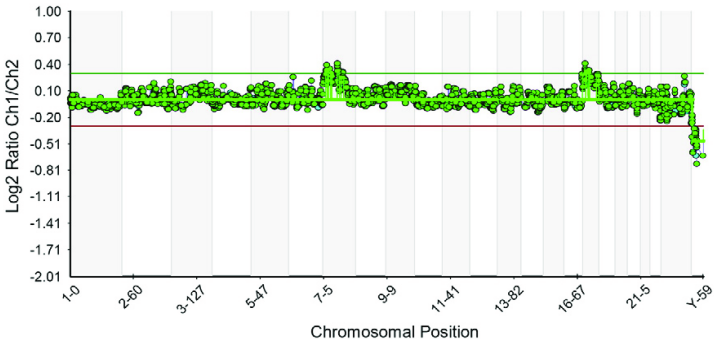

Fig. 7. Array CGH profile of case 7 revealing gains on chromosomes 7 (7pter-7q22.1) and 17, and a loss of chromosome Y.

necrosis as an adverse/ambivalent prognostic feature. The aim of this study was to describe a subpopulation of type 1 PRCC characterized by uniform, albeit unusual gross and histologic features.

An interesting phenomenon was documented in cases 9 and 10 of our series where the tumor capsule was composed of fibrous tissue, indistinguishable from inflammatory pseudotumor histologically. Therefore, it is very important to carefully examine the capsule and to distinguish myofibroblastic proliferation from sarcomatoid differentiation or even from sarcoma arising in an inflammatory pseudotumor. Inflammatory pseudotumors may express ALK-1 and cytokeratin immunostains, which can be helpful in differentiating ambiguous entities [33,34]. Neither ALK-1 nor cytokeratins showed a positive reaction in any tumor capsule in our series including the above-mentioned 2 cases. The capsules reminiscent of inflammatory pseudotumor in the above-mentioned cases exhibited identical immunohistochemical reaction against ALK-1 and cytokeratins as tumors with a "simple" fibrous capsule.

According to some authors, the presence of a fibromuscular pseudocapsule is rather characteristic of and more prominent in clear cell RCC, less frequently present in chromophobe RCC, and rarely in PRCC [34]. Fibromuscular pseudocapsules are characterized by a complex architecture including both connective tissue and smooth muscle fibers with thicker capsules sometimes containing vasculopathy. The presence of a pseudocapsule may be helpful to resolve diagnostic difficulties in challenging cases. The core biopsy specimen from patients with a high Bosniak type might be composed predominantly of fibromuscular tissue and only scant tumor fragments [34]. This kind of biopsy finding should lead to recommend additional tissue sampling. The designation of such a specimen as a nonrepresentative or even nonneoplastic biopsy should be considered with caution. According to some authors, radiologic and/or pathologic presence of a pseudocapsule/fibromuscular tissue may raise suspicion for RCC, with a higher probability of clear cell type [34]. The cases described in our study clearly show that a thick pseudocapsule can also be found in low-grade PRCC type 1.

5. Conclusions

Type 1 PRCC can present as a large unicystic lesion with necrotic/hemorrhagic content and surrounded by thick fibroleiomyomatous capsule. Most of our cases contained a chromosomal numerical aberration pattern characteristic of PRCC. All tumors followed a nonaggressive clinical course. Large liquefactive necrosis should not necessarily be considered an adverse prognostic feature, at least in a subset of type 1 PRCC with unilocular necrotic cystic presentation. Adequate tissue sampling in such tumors is crucial to arrive at accurate diagnosis, because most of these tumors contain limited viable neoplastic tissue lining the inner cyst wall.

Abbreviations: CEP, centromeric enumeration probe; F, female; LOH 3p, loss of heterozygosity of chromosome 3p; M, male; NA, not analyzable; Neg, negative; NP, not performed; P, polysomy; VHL, mutation analysis of VHL; VHLM, methylation of VHL; X-, loss of chromosome Y

References

[1] Moch H, Humphrey PA, Ulbright TM, Reuter VE. WHO classification of tumours of the urinary system and male genital organs; 2016.
[2] Delahunt B, Eble JN. Papillary renal cell carcinoma: a clinicopathologic and immunohistochemical study of 105 tumors. Mod Pathol 1997;10:537–44.
[3] Hes O, Hora M, Havlicek F, Chudacek Z, Klecka J, Michal M. Papillary renal cell carcinoma surrounded by unusual fibrotic reaction resembling inflammatory pseudotumour—a case report. Cesk Patol 2004;40:112–6.
[4] Herman JG, Graff JR, Myohanen S, Nelkin BD, Baylin SB. Methylation-specific PCR: a novel PCR assay for methylation status of CpG islands. Proc Natl Acad Sci U S A 1996; 93:9821–6.
[5] Kovacs G, Akhtar M, Beckwith BJ, Bugert P, Cooper CS, Delahunt B, et al. The Heidelberg classification of renal cell tumours. J Pathol 1997;183:131–3.
[6] Srigley JR, Delahunt B, Eble JN, Egevad L, Epstein JI, Grignon D, et al. The International Society of Urological Pathology (ISUP) Vancouver classification of renal neoplasia. Am J Surg Pathol 2013;37:1469–89.
[7] Agaimy A. Succinate dehydrogenase (SDH)-deficient renal cell carcinoma. Pathologe 2016;37:144–52.
[8] Pflanz S, Brookman-Amissah S, Roigas J, Kendel F, Hoschke B, May M. Impact of macroscopic tumour necrosis to predict survival of patients with surgically resected renal cell carcinoma. Scand J Urol Nephrol 2008;42:507–13.
[9] Sengupta S, Lohse CM, Leibovich BC, Frank I, Thompson RH, Webster WS, et al. Histologic coagulative tumor necrosis as a prognostic indicator of renal cell carcinoma aggressiveness. Cancer 2005;104:511–20.
[10] Allory Y, Ouazana D, Boucher E, Thiounn N, Vieillefond A. Papillary renal cell carcinoma. Prognostic value of morphological subtypes in a clinicopathologic study of 43 cases. Virchows Arch 2003;442:336–42.
[11] Argani P, Netto GJ, Parwani AV. Papillary renal cell carcinoma with low-grade spindle cell foci: a mimic of mucinous tubular and spindle cell carcinoma. Am J Surg Pathol 2008;32:1353–9.
[12] Cantley R, Gattuso P, Cimbaluk D. Solid variant of papillary renal cell carcinoma with spindle cell and tubular components. Arch Pathol Lab Med 2010;134:1210–4.
[13] Hes O, Brunelli M, Michal M, Cossu Rocca P, Hora M, Chilosi M, et al. Oncocytic papillary renal cell carcinoma: a clinicopathologic, immunohistochemical, ultrastructural, and interphase cytogenetic study of 12 cases. Ann Diagn Pathol 2006;10:133–9.
[14] Val-Bernal JF, Gomez-Roman JJ, Vallina T, Villoria F, Mayorga M, Garcia-Arranz P. Papillary (chromophil) renal cell carcinoma with mucinous secretion. Pathol Res Pract 1999;195:11–7.
[15] Linehan WM, Spellman PT, Ricketts CJ, Creighton CJ, Fei SS, Davis C, et al. Comprehensive molecular characterization of papillary renal-cell carcinoma. N Engl J Med 2016;374:135–45.
[16] Leibovitch I, Lev R, Mor Y, Golomb J, Dotan ZA, Ramon J. Extensive necrosis in renal cell carcinoma specimens: potential clinical and prognostic implications. Isr Med Assoc J 2001;3:563–5.
[17] Zubac DP, Bostad L, Gestblom C, Kihl B, Seidal T, Wentzel-Larsen T, et al. Renal cell carcinoma: a clinicopathological follow-up study after radical nephrectomy. Scand J Urol Nephrol 2007;41:191–7.
[18] Sabo E, Boltenko A, Sova Y, Stein A, Kleinhaus S, Resnick MB. Microscopic analysis and significance of vascular architectural complexity in renal cell carcinoma. Clin Cancer Res 2001;7:533–7.
[19] Tollefson MK, Thompson RH, Sheinin Y, Lohse CM, Cheville JC, Leibovich BC, et al. Ki-67 and coagulative tumor necrosis are independent predictors of poor outcome for patients with clear cell renal cell carcinoma and not surrogates for each other. Cancer 2007;110:783–90.

[20] Delahunt B. Advances and controversies in grading and staging of renal cell carcinoma. Mod Pathol 2009;22(Suppl. 2):S24–36.
[21] Delahunt B, Bethwaite PB, Nacey JN. Outcome prediction for renal cell carcinoma: evaluation of prognostic factors for tumours divided according to histological subtype. Pathology 2007;39:459–65.
[22] Delahunt B, Bethwaite PB, Miller RJ, Sika-Paotonu D, Srigley JR. Re: Fuhrman grade provides higher prognostic accuracy than nucleolar grade for papillary renal cell carcinoma: T. Klatte, C. Anterasian, J. W. Said, M. de Martino, F. F. Kabbinavar, A. S. Belldegrun and A. J. Pantuck. *J Urol* 2010;183:2143-2147. J Urol 2011;185:356–7 [author reply 357-358].
[23] Kumar V, Abbas AK, Fausto N, Aster JC. Robbins and Cotran pathologic basis of diseases. , 3-42 Philadelpia: Saunders Elsevier; 2010.
[24] Sukov WR, Lohse CM, Leibovich BC, Thompson RH, Cheville JC. Clinical and pathological features associated with prognosis in patients with papillary renal cell carcinoma. J Urol 2012;187:54–9.
[25] Onishi T, Ohishi Y, Goto H, Suzuki M, Miyazawa Y. Papillary renal cell carcinoma: clinicopathological characteristics and evaluation of prognosis in 42 patients. BJU Int 1999;83:937–43.
[26] Moch H, Gasser T, Amin MB, Torhorst J, Sauter G, Mihatsch MJ. Prognostic utility of the recently recommended histologic classification and revised TNM staging system of renal cell carcinoma: a Swiss experience with 588 tumors. Cancer 2000;89:604–14.
[27] Kim H, Cho NH, Kim DS, Kwon YM, Kim EK, Rha SH, et al. Renal cell carcinoma in South Korea: a multicenter study. Hum Pathol 2004;35:1556–63.
[28] Cheville JC, Lohse CM, Zincke H, Weaver AL, Blute ML. Comparisons of outcome and prognostic features among histologic subtypes of renal cell carcinoma. Am J Surg Pathol 2003;27:612–24.
[29] Fu Z, Sun L, Huang Y, Zhang J, Zhang Z, Wang L, et al. A type 2 papillary renal cell carcinoma presenting as an intracystic necrotic lesion: a case report. Mol Clin Oncol 2013;1:318–20.
[30] Pichler M, Hutterer GC, Chromecki TF, Pummer K, Mannweiler S, Zigeuner R. Presence and extent of histological tumour necrosis is an adverse prognostic factor in papillary type 1 but not in papillary type 2 renal cell carcinoma. Histopathology 2013;62:219–28.
[31] Pichler M, Hutterer GC, Chromecki TF, Jesche J, Kampel-Kettner K, Rehak P, et al. Histologic tumor necrosis is an independent prognostic indicator for clear cell and papillary renal cell carcinoma. Am J Clin Pathol 2012;137:283–9.
[32] Klatte T, Remzi M, Zigeuner RE, Mannweiler S, Said JW, Kabbinavar FF, et al. Development and external validation of a nomogram predicting disease specific survival after nephrectomy for papillary renal cell carcinoma. J Urol 2010;184:53–8.
[33] Chan JK, Cheuk W, Shimizu M. Anaplastic lymphoma kinase expression in inflammatory pseudotumors. Am J Surg Pathol 2001;25:761–8.
[34] Roquero L, Kryvenko ON, Gupta NS, Lee MW. Characterization of fibromuscular pseudocapsule in renal cell carcinoma. Int J Surg Pathol 2015;23:359–63.

LEIOMYOMATÓZNÍ STROMA V RENÁLNÍCH KARCINOMECH JE POLYKLONÁLNÍ A NIKOLIV SOUČÁSTÍ NEOPLASTICKÉHO PROCESU

Některé typy renálních epiteliálních neoplazií se vyznačují přítomností variabilního množství leiomyomatózního stromatu (LS). Mezi tyto tumory lze zařadit světlobuněčný papilární renální karcinom (SPRK)/renální angiomyoadenomatózní tumor (RAT), světlobuněčný renální karcinom (SRK) a renální karcinom s leiomyomatózním stromatem (RKLS). Pro upřesnění je třeba dodat, že SPRK a RAT jsou identické tumory tvořící 2 konce morfologického spektra jedné jednotky a v současné WHO klasifikaci byly sloučeny do jedné jednotky nesoucí název světlobuněčný papilární renální karcinom [4]. Doposud nebylo stanoveno, je-li LS součástí neoplastického procesu či jeho pouze reaktivní příměsí.

V přiložené studii jsme za použití human androgen receptor assay (HUMARA) zkoumali klonalitu epitelové a leiomyomatózní komponenty u 14 renálních karcinomů; skupina vybraných tumorů zahrnovala 4 SPRK, 5 SRK s leiomyomatózním stromatem, 2 papilární renální karcinomy (PRK) a 3 SRK s bohatým leiomyomatózním stromatem. Ve všech analyzovatelných případech (8/14) byla zjištěna polyklonalita leiomyomatózní komponenty. Na základě této studie lze vyvodit, že:

- Leiomyomatózní stroma se může nacházet nejen u SPRK/RAT, SRK a RKLS, ale vyskytuje se například i u PRK.
- Hladkosvalové stromální buňky jsou polyklonální a nejsou tedy součástí neoplastického procesu, nýbrž pouze reaktivní příměsí pocházející pravděpodobně ze stěny renálních žil, jakožto jediného zdroje hladké svaloviny v ledvinách.

Virchows Arch (2014) 465:89–96
DOI 10.1007/s00428-014-1591-9

ORIGINAL ARTICLE

The leiomyomatous stroma in renal cell carcinomas is polyclonal and not part of the neoplastic process

Fredrik Petersson · Jindrich Branzovsky · Petr Martinek · Marie Korabecna · Bozo Kruslin · Milan Hora · Kvetoslava Peckova · Kevin Bauleth · Kristyna Pivovarcikova · Michal Michal · Marian Svajdler · Maris Sperga · Stela Bulimbasic · Xavier Leroy · Boris Rychly · Sandra Trivunic · Bohuslava Kokoskova · Pavla Rotterova · Miroslav Podhola · Saul Suster · Ondrej Hes

Received: 27 February 2014 / Revised: 18 April 2014 / Accepted: 6 May 2014 / Published online: 18 May 2014

Abstract Some renal epithelial neoplasms, such as renal angiomyoadenomatous tumor, clear cell papillary renal cell carcinoma and renal cell carcinoma with smooth muscle stroma, contain a variably prominent smooth muscle stromal component. Whether or not this leiomyomatous stroma is part of the neoplastic proliferation has not been firmly established. We studied the clonality status of 14 renal cell carcinomas with a prominent smooth muscle stromal component (four renal angiomyoadenomatous tumors/clear cell papillary carcinomas, five clear cell carcinomas, two papillary carcinomas, and three renal cell carcinomas with smooth muscle rich stroma) using the human androgen receptor assay (HUMARA). We found the leiomyomatous stromal component in all analyzable (8/14) cases to be polyclonal and therefore reactive rather than neoplastic. Based on morphological observations, we propose that the non-neoplastic leiomyomatous stromal component is likely derived from smooth muscle cells of large caliber veins located at the peripheral capsular region or within the collagenous septae of the tumors.

Keywords Kidney · Renal cell carcinoma · Leiomyomatous stroma · Stroma origin · HUMARA · Reactive stroma

F. Petersson
Department of Pathology, National University Health System Hospital, Singapore, Singapore

F. Petersson · J. Branzovsky · P. Martinek · K. Peckova · K. Bauleth · K. Pivovarcikova · M. Michal · M. Svajdler · B. Kokoskova · P. Rotterova · O. Hes (✉)
Department of Pathology, Medical Faculty and Charles University Hospital Plzen, Charles University, Alej Svobody 80, 304 60 Pilsen, Czech Republic
e-mail: hes@medima.cz

M. Korabecna
Institute of Biology and Medical Genetics, First Faculty of Medicine and General University Hospital, Charles University, Prague, Czech Republic

B. Kruslin
Department of Pathology, University Hospital Sestre Milosrdnice, Zagreb, Croatia

M. Hora
Department of Urology, Medical Faculty and Charles University Hospital Plzen, Charles University, Prague, Czech Republic

M. Sperga
Department of Pathology, East University, Riga, Latvia

S. Bulimbasic
Department of Pathology, University Hospital Dubrava, Zagreb, Croatia

X. Leroy
Department of Pathology, Lille University Hospitals, Lille, France

B. Rychly
Cytopathos, Bratislava, Slovak Republic

S. Trivunic
Department of Pathology, University Hospital Novi Sad, Novi Sad, Serbia

M. Podhola
Department of Pathology, Medical Faculty and Charles University Hospital Hradec Kralove, Charles University, Praque, Czech Republic

S. Suster
Department of Pathology, Medical College of Wisconsin, Milwaukee, WI, USA

Introduction

Some renal epithelial neoplasms contain a variably prominent smooth muscle stromal component. This is regularly seen in renal angiomyoadenomatous tumor (RAT), but has also been described in clear cell papillary renal cell carcinoma (CCPRCC) and is a conspicuous feature in a specific subset of renal cell carcinoma—"renal cell carcinoma with smooth muscle stroma" (RCCSMS), as previously described by several investigators [3, 6, 7, 12]. Apart from being diagnostically relevant (as an inherent component of RAT) and also as a potentially confusing histomorphological feature (obscuring the neoplastic epithelial cells, especially on a core biopsy), the biological nature of this leiomyomatous stroma has not been firmly established. In this study, we characterize 14 renal cell carcinomas of various types harboring a prominent leiomyomatous stroma with focus on clonality analysis, i.e., we aim at determining whether the stromal component is a part of the (monoclonal) neoplastic proliferation or not.

Materials and methods

Out of 17,000 renal tumors in the Plzen Tumor registry, we identified 27 cases which contained a prominent fibroleiomyomatous stromal component. We selected those cases in which the fibroleiomyomatous component formed at least 10 % of the estimated tumor volume. As we intended to use a clonality assay based on identifying a non-random inactivation pattern of the human androgen receptor located on the X-chromosome (HUMARA), cases occurring in males (13) were excluded from further study. The remaining 14 cases in females were classified as RAT/CCPRCC, RCCSMS, papillary RCC (PRCC), and clear cell RCC (CRCC). As RCCSMS, we diagnosed tumors with clear cell neoplastic elements, admixed with huge and thick bundles and cords of leiomyomatous stroma. None of the RCCSMS contained mutations of the *VHL* gene or loss of heterozygosity (LOH) of 3p (results not shown).

Immunohistochemistry

The immunohistochemical study was performed using a Ventana BenchMark XT automated stainer (Ventana Medical System, Inc., Tucson, AZ, USA) on formalin fixed, paraffin embedded tissue. The following primary antibodies were employed: vimentin (D9, monoclonal, NeoMarkers, Westinghouse, CA, 1:1000), smooth muscle actin (1A4, monoclonal, Cell Marque, Rocklin, CA, RTU), desmin (D33, monoclonal, Dako, Glostrup, Denmark, 1:200), caldesmon (E89, Cell Marque, RTU), and CD34 (QBEnd10, monoclonal, Dako, 1:1000). Appropriate positive controls included normal kidney cortex tissue for vimentin and CD34, human heart tissue for smooth muscle actin, and uterus for caldesmon.

Molecular genetic analysis

Microdissection

Eight micrometer-thick sections were cut from each FFPE block, placed on Frame Slides (PET membrane, 1.4 μm, Leica, Wetzlar, Germany), deparaffinized with xylene, and stained with nuclear red. Microdissection, to separate tumor stroma, neoplastic epithelial cells, and non-tumor tissue, was performed by Laser Capture Microdissection, LMD 6500 (Leica, Wetzlar, Germany).

DNA extraction

DNA from microdissected tissue was extracted using a QIAsymphony DNA Mini Kit (Qiagen, Hilden, Germany) on automated extraction system (QIAsymphony SP, Qiagen) according to the manufacturer's supplementary protocol for FFPE samples (purification of genomic DNA from FFPE tissue using the QIAamp DNA FFPE Tissue Kit and Deparaffinization Solution).

The lysate was manually transferred to clean tubes to get rid of the microdissection membranes. Concentration and purity of isolated DNA were measured using NanoDrop ND-1000 (NanoDrop Technologies Inc., Wilmington, DE, USA). DNA integrity was examined by amplification of control genes in a multiplex PCR [19].

Analysis of clonality using human androgen receptor assay

Clonality analysis was performed according to a previously described method based on the digestion of differentially methylated X chromosomal DNA with methylation-sensitive restriction enzyme followed by PCR amplification of a CAG repeat located in human androgen receptor (AR, HUMARA) [1]. DNA samples were digested by restriction enzyme HhaI and amplified as described previously [1].

PCR products were examined by a fragment analysis on Abi3130*xl*. Peak heights of the two alleles were measured for each sample (stroma, neoplastic cells, non-tumor). A corrected ratio (CR) was assessed by dividing the ratio (allele 1/allele2) of the digested sample by the ratio (allele1/allele 2) of the undigested sample. A final clonality ratio of the neoplastic epithelial cell samples was determined by dividing the CR of the neoplastic cell DNA by the CR of the non-tumor DNA. An analogous calculation was used to get a clonality ratio of stromal sample. The sample was considered monoclonal if the final ratio was higher than 1.5 or lower than 0.66.

Table 1 Basic clinicopathological data

Case	Age	Sex	Size	Histology
1	74	F	Diam 10 cm	RAT-CCPRCC
2	80	F	Diam 2.3 cm	RAT-CCPRCC
3	59	F	Diam 1.9 cm	RAT-CCPRCC
4	63	F	2.5×2×2.2 cm	RCCSMS
5	33	F	NA[a]–	RCCSMS
6	57	F	9×7×5 cm	PRCC
7	48	F	11.5×12×10.5 cm	CCRCC
8	64	F	Diam 1.2 cm	RAT-CCPRCC
9	73	F[b]	Diam 1.8 cm	CCRCC
10	69	F	Diam 1.5 cm	CCRCC
11	60	F	Diam 1.5 cm	RCCSMS
12	24	F	12×10×9 cm	CCRCC
13	67	F	6×5×5 cm	PRCC
14	65	F[c]	Diam 1 cm	CCRCC

F female, *Diam* diameter, *RAT-CCPRCC* renal angiomyoadenomatous tumor/clear cell papillary renal cell carcinoma, *RCCSMS* renal cell carcinoma with smooth muscle stroma, *PRCC* papillary renal cell carcinoma, *CCRCC* clear cell renal cell carcinoma, *NA* not available

[a] Multicentric lesion

[b] Bilateral tumor, contralateral lesion was typical CCRCC

[c] Bilateral tumor, contralateral lesion was sarcomatoid CCRCC

Results

Basic clinicopathologic data are summarized in Table 1.

Briefly, four cases were diagnosed as RAT/CCPRCC, five cases as CRCC, two cases as PRCC, and three cases as RCCSMS. The age of the patients ranged from 24 to 80 years (mean 59.7 years, median 63.5 years). The size of the tumors ranged from 1 to 12 cm (mean 4.8 cm, median 10.0 cm).

Cases diagnosed as RAT/CCPRCC were composed of areas with leiomyomatous stroma admixed with elongated, variably open and collapsed tubules lined by a single layer of columnar-shaped clear cells with basally located low-grade nuclei, apical snouts composed of cytoplasm at the luminal aspect, and a prominent peritubular capillary network (Fig. 1).

Cases diagnosed as PRCC were predominantly composed of well-formed papillary structures, e.g., finger-like fibrovascular cores lined by basophilic to eosinophilic small, neoplastic epithelial cells exhibiting round, low-grade nuclei characteristic of type-1 PRCC intermingled with a prominent fibroleiomyomatous stroma (Fig. 2).

Cases diagnosed as RCCSMS displayed neoplastic epithelial cells with clear cytoplasm arranged in small nest, cords, or tubules admixed with a conspicuous smooth muscle stroma (Fig. 3).

Cases diagnosed as CCRCC were composed of neoplastic clear cells arranged in solid alveolar nests surrounded by a rich capillary network. The neoplastic epithelial nests were surrounded by a prominent fibroleiomyomatous stroma (Fig. 4).

The stromal component constituted from 10 to 30 % of the tumor volume. Histologically, the stroma was rather uniform with little variation between tumors. The stroma was composed of more or less well-formed fascicles of smooth muscle-like spindle cells with mildly eosinophilic cytoplasm and without significant nuclear atypia. The cellularity was generally low, and there was a variable component of frequently edematous collagenous extracellular matrix containing blood vessels of different caliber, some of which appeared to have

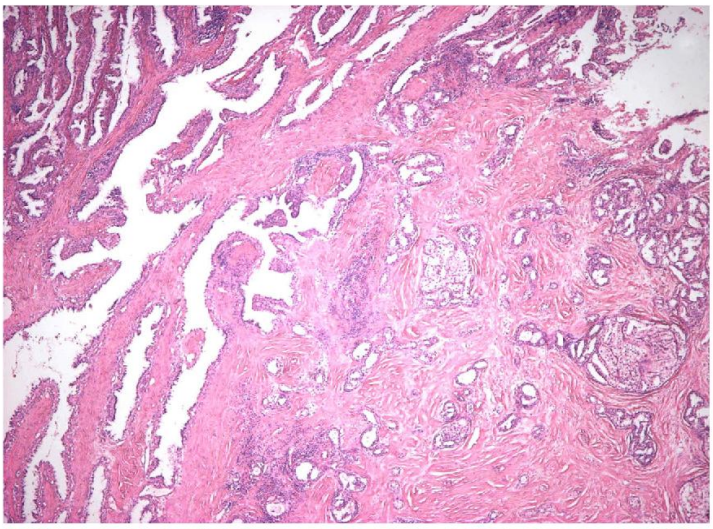

Fig. 1 RAT/CCPRCC composed of areas with leiomyomatous stroma admixed with elongated tubules

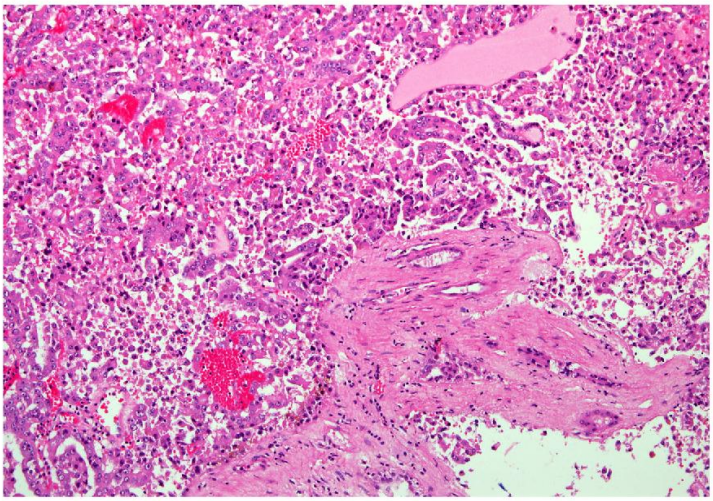

Fig. 2 PRCC predominantly composed of well-formed papillary structures lined by basophilic to eosinophilic epithelial cells intermingled with a prominent fibroleiomyomatous stroma

collapsed or have inadequately developed lumina ("abortive vessels") (Fig. 5). In most instances (10/14), the stromal component seemed to merge with the muscle layer of veins located at the periphery/capsular regions of the tumors (Fig. 6).

Immunohistochemistry

The results of the immunohistochemical study are presented in Table 2. Briefly, the stromal cell in all cases displayed moderate or strong expression of smooth muscle actin, vimentin, and caldesmon, whereas the expression of desmin was variable and only few cases showed weak expression of CD34.

HUMARA

Six cases could not be analyzed due to insufficient quantity or poor quality of the DNA of one of the three samples. The remaining eight cases showed a monoclonal pattern of the neoplastic epithelial cell samples, whereas all tumor stromal samples revealed a polyclonal pattern, e.g., random inactivation of the androgen receptor on the X-chromosome (Table 3). A polyclonal pattern was also detected in all samples from non-neoplastic renal parenchyma.

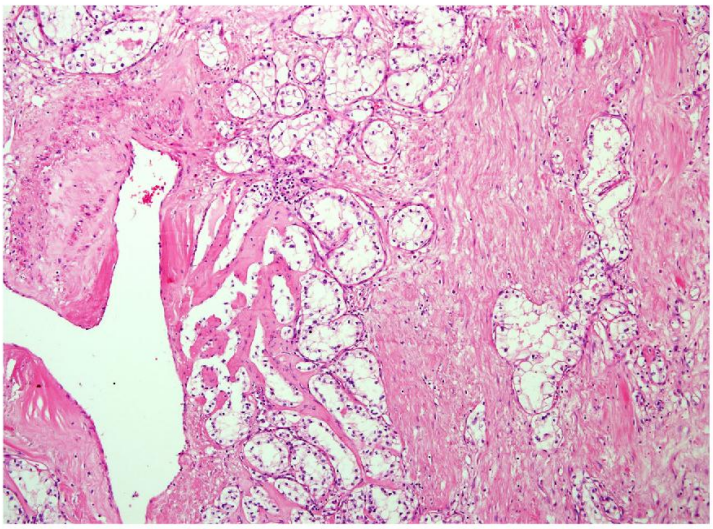

Fig. 3 RCCSMS showing neoplastic epithelial cells with clear cytoplasm arranged in small nest, cords, or tubules admixed with a conspicuous smooth muscle stroma

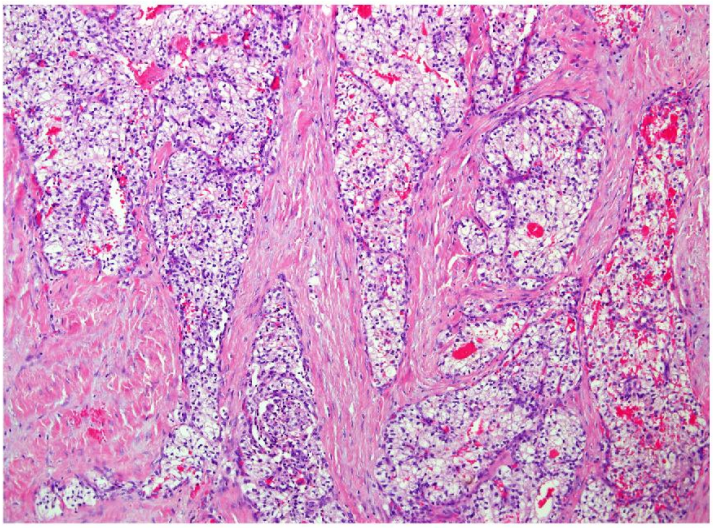

Fig. 4 CCRCC composed of neoplastic clear cells arranged in solid alveolar nests surrounded by a prominent fibroleiomyomatous stroma

Discussion

The rare existence of renal cell carcinomas with a prominent smooth muscle-rich stroma (RCCSMS) was first pointed out by Canzonieri et al. in 1993 [3] and was further substantiated by Rosai and Kuhn in 2006 [6] and subsequently by other researchers [4, 7, 12]. These tumors have been descriptively referred to as "renal cell carcinoma with smooth muscle stroma", "mixed renal tumor with carcinomatous and fibroleiomyomatous components", "renal cell carcinoma associated with prominent angioleiomyoma-like proliferation", or "clear cell renal cell carcinoma with smooth muscle stroma". A possible relationship between RCCSMS and CCPRCC/RAT has been discussed recently [7]. Both types of RCC express CK 7, contain fibroleiomyomatous stroma, and share similar genetic features. Whether or not they constitute different forms of one nosologic entity remains unclear. In contrast to the rare presence of leiomyomatous stroma in the majority of renal carcinomas, this is an inherent feature of RAT and has also been described in CCPRCC [2]. RAT and CCPRCC may be perceived as two ends of a spectrum, where the presence of a leiomyomatous stromal component is the defining feature of, and hence separates, RAT from CCPRCC. This position was adopted by the ISUP meeting at Vancouver,

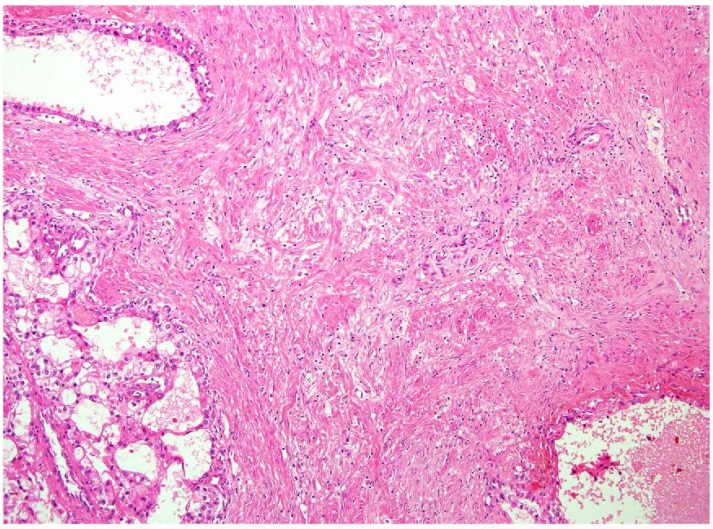

Fig. 5 Mostly hypocellular stroma with edematous collagenous extracellular matrix

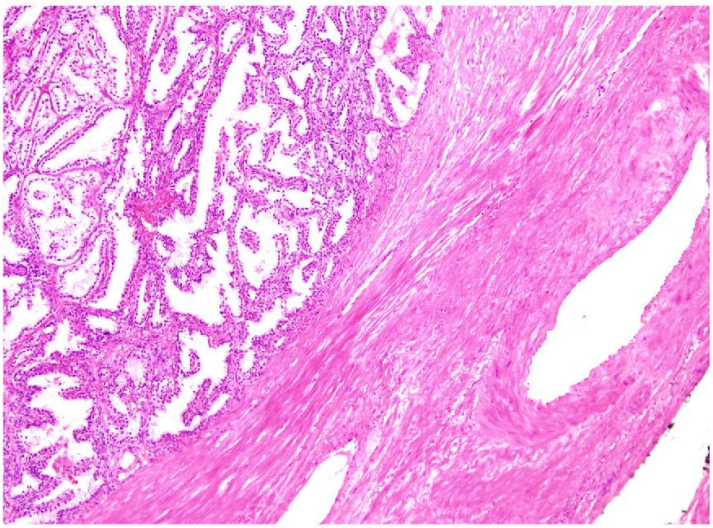

Fig. 6 Example of a RAT/CCPRCC with a stromal component merging with the muscle layer of veins located at the periphery/capsular regions of the tumors

Canada in 2012 [16]. There is no consensus about exact amount of leiomyomatous stromal component in RAT. Mostly, tumors with a thick fibroleiomyomatous capsule and voluminous stromal component are designated as RAT and cases with less prominent capsular and stromal component as CCPRCC. However, in particular cases, it is extremely difficult to draw the line between these two entities/ends of the spectrum. Apart from the nosological aspects pertaining to the presence of smooth muscle rich/leiomyomatous stroma, an abundant presence of such a stromal component may give rise to diagnostic problems, especially when limited tissue is available for histopathological examination, e.g., on a core biopsy. This may be particularly problematic when the stromal component is as conspicuous as in RCCSMS, where the

Table 2 Immunohistochemical reactivity of the stromal component

Case	Actin	CD34	Desmin	Vimentin	Caldesmon
1	+++	+–	–	+++	+++
2	++/+++	–	+	+++	++
3	++	+	–	+++	+++
4	+++	+–	+	+++	+++
5	+++	+–	+/++	+++	+++
6	+++	–	–	+	–
7	+++	–	+	++	++/+++
8	+++	–	+foc	+++	++
9	++	NA	NA	+++	NA
10	+++	+	+++	+++	+++
11	+++	–	++	+++	+++
12	+++	–	–	+++	++
13	+++	–	–	+++	+++
14	+++	–	+++	++	++

+ weakly positive, ++ moderately positive, +++ strongly positive, – negative, *NA* not analyzed, *foc* focally

Table 3 Results of clonality analysis of neoplastic and stromal samples (data for non-neoplastic samples not shown)

Case #	Sample	Interpretation
1	T	POS
	S	NEG
2	T	POS
	S	NEG
3	T	POS
	S	NEG
4	T	NA
	S	
5	T	NA
	S	
6	T	NA
	S	
7	T	NA
	S	
8	T	NA
	S	
9	T	NA
	S	
10	T	POS
	S	NEG
11	T	POS
	S	NEG
12	T	POS
	S	NEG
13	T	POS
	S	NEG
14	T	POS
	S	NEG

S stromal sample, *T* neoplastic sample, *POS* positive, *NEG* negative, *NA* non analyzable

neoplastic/malignant epithelial component is very limited. Based on the literature, however, this appears to be a very rare event as reflected in our series, in which in none of the cases the stromal component exceeded 30 % of the tumor volume.

The smooth muscle-like cells of the stroma exhibited moderate or strong expression of SMA, vimentin, and caldesmon, whereas the expression of desmin was variable. This is not surprising since smooth muscle cells may alternate between synthetic and contractile phenotypes [11, 17], and the shift between these phenotypes corresponds to changes in the cellular content of a number of proteins, such as vimentin, desmin, smooth muscle actin, and tropomyosin both in vivo and in vitro [14, 18]. Moreover, different types of blood vessels exhibit differences in their cytoskeletal intermediate filament content [9, 10, 13], and it is well known that human smooth muscle tumors such as leiomyomas, leiomyosarcomas, and Epstein-Barr virus-associated smooth muscle tumors not infrequently are negative for or exhibit weak focal expression of desmin. Likewise, in RAT, the leiomyomatous stroma reacted positively and strongly with antibodies to caldesmon, calponin, vimentin, and smooth muscle actin in all cases, whereas immunostaining for desmin was patchy and weak [8].

The nature and origin of this smooth muscle-rich stroma are closely related questions. Our study clearly indicates that the smooth muscle-like cells are not part of the monoclonal neoplastic epithelial process. The clonality assay (HUMARA) exploits the fact that monoclonal proliferations exhibit a non-random inactivation pattern of the androgen receptor on the X-chromosome and that polyclonal proliferations do not. Although monoclonality does not equate to neoplasia, it is, however, a sine qua non for a biological process to be labeled as a neoplasm. Our findings thus strongly support a reactive, polyclonal origin of the leiomyomatous stroma in renal neoplasms.

Morphologically, we found the stromal component to be closely connected to the muscle layer of large caliber veins located at the capsular region and in the fibrous septae within the tumor. This justifies our proposal to consider these vessels as the source of the stromal proliferation. The proliferation of vessel-derived smooth muscle cells may be related to hypoxia-induced factors as suggested by Kuhn et al. [6]. However, based on the data presented on RCCSMS, by Martignoni et al. [7], it seems that at least the hypoxia-related *VHL* pathway is not activated in this group of neoplasms. Interestingly, using LOH for the *TSC2* region on chromosome 16p13, a dual composition of both neoplastic and non-neoplastic vessels has been documented in angiomyolipomas in patients with lymphangioleiomyomatosis [5]. No evidence of leiomyomatosis associated with renal tumors was found in any of our patients.

On a final note, some investigators have suggested that different stromal-vascular patterns in human cancers ("tumor vessel or stromal vessel phenotype") may be predictive of clinical response to ("anti-angiogenetic") drugs targeting the VEGF pathway [15]. Our data may contribute to this discussion.

Conclusions

Our data support the following conclusions: (1) the presence of a prominent smooth muscle containing stroma may be encountered not only in "renal cell carcinoma with smooth muscle stroma", clear cell renal cell carcinoma, and clear cell papillary renal cell carcinoma/renal angiomyoadenomatous tumor but also in papillary renal cell carcinoma, and (2) the smooth muscle cells constituting this stroma are polyclonal and represent a reactive proliferation possibly derived from smooth muscle cells of large caliber veins located at the peripheral capsular region or within the collagenous septae of the tumors.

Acknowledgments This study was supported by the Charles University Research Fund (project number P36) and by Charles University Grant SVV 260051/2014.

Conflict of interest All authors declare no conflict of interest.

References

1. Allen RC, Zoghbi HY, Moseley AB, Rosenblatt HM, Belmont JW (1992) Methylation of HpaII and HhaI sites near the polymorphic CAG repeat in the human androgen-receptor gene correlates with X chromosome inactivation. Am J Hum Genet 51:1229–1239
2. Aydin H, Chen L, Cheng L, Vaziri S, He H, Ganapathi R, Delahunt B, Magi-Galluzzi C, Zhou M (2010) Clear cell tubulopapillary renal cell carcinoma: a study of 36 distinctive low-grade epithelial tumors of the kidney. Am J Surg Pathol 34:1608–1621
3. Canzonieri V, Volpe R, Gloghini A, Carbone A, Merlo A (1993) Mixed renal tumor with carcinomatous and fibroleiomyomatous components, associated with angiomyolipoma in the same kidney. Pathol Res Pract 189:951–956
4. Iczkowski KA, Shanks JH, Burdge AH, Cheng L (2013) Renal cell carcinoma with clear cells, smooth muscle stroma, and negative for 3p deletion: a variant of renal angiomyoadenomatous tumour? A case report. Histopathology 62:522–524
5. Karbowniczek M, Yu J, Henske EP (2003) Renal angiomyolipomas from patients with sporadic lymphangiomyomatosis contain both neoplastic and non-neoplastic vascular structures. Am J Pathol 162: 491–500
6. Kuhn E, De Anda J, Manoni S, Netto G, Rosai J (2006) Renal cell carcinoma associated with prominent angioleiomyoma-like proliferation: report of 5 cases and review of the literature. Am J Surg Pathol 30:1372–1381
7. Martignoni G, Brunelli M, Segala D, Gobbo S, Borze I, Atanesyan L, Savola S, Barzon L, Masi G, Tardanico R, Zhang S, Eble JN, Chilosi M, Bohling T, Cheng L, Delahunt B, Knuutila S (2014) Renal cell carcinoma with smooth muscle stroma lacks chromosome 3p and VHL alterations. Mod Pathol, in press

8. Michal M, Hes O, Nemcova J, Sima R, Kuroda N, Bulimbasic S, Franco M, Sakaida N, Danis D, Kazakov DV, Ohe C, Hora M (2009) Renal angiomyoadenomatous tumor: morphologic, immunohistochemical, and molecular genetic study of a distinct entity. Virchows Arch 454:89–99
9. Nanaev AK, Shirinsky VP, Birukov KG (1991) Immunofluorescent study of heterogeneity in smooth muscle cells of human fetal vessels using antibodies to myosin, desmin, and vimentin. Cell Tissue Res 266:535–540
10. Osborn M, Caselitz J, Puschel K, Weber K (1987) Intermediate filament expression in human vascular smooth muscle and in arteriosclerotic plaques. Virchows Arch A Pathol Anat Histopathol 411: 449–458
11. Owens GK (1995) Regulation of differentiation of vascular smooth muscle cells. Physiol Rev 75:487–517
12. Shannon BA, Cohen RJ, Segal A, Baker EG, Murch AR (2009) Clear cell renal cell carcinoma with smooth muscle stroma. Hum Pathol 40: 425–429. doi:10.1016/j.humpath.2008.05.021
13. Schmid E, Osborn M, Rungger-Brandle E, Gabbiani G, Weber K, Franke WW (1982) Distribution of vimentin and desmin filaments in smooth muscle tissue of mammalian and avian aorta. Exp Cell Res 137:329–340
14. Skalli O, Bloom WS, Ropraz P, Azzarone B, Gabbiani G (1986) Cytoskeletal remodeling of rat aortic smooth muscle cells in vitro: relationships to culture conditions and analogies to in vivo situations. J Submicrosc Cytol 18:481–493
15. Smith NR, Baker D, Farren M, Pommier A, Swann R, Wang X, Mistry S, McDaid K, Kendrew J, Womack C, Wedge SR, Barry ST Tumor stromal architecture can define the intrinsic tumor response to VEGF-targeted therapy. Clin Cancer Res 19:6943–6956
16. Srigley JR, Delahunt B, Eble JN, Egevad L, Epstein JI, Grignon D, Hes O, Moch H, Montironi R, Tickoo SK, Zhou M, Argani P (2013) The International Society of Urological Pathology (ISUP) Vancouver Classification of Renal Neoplasia. Am J Surg Pathol 37:1469–1489
17. Thyberg J, Hedin U, Sjolund M, Palmberg L, Bottger BA (1990) Regulation of differentiated properties and proliferation of arterial smooth muscle cells. Arteriosclerosis 10:966–990
18. Travo P, Weber K, Osborn M (1982) Co-existence of vimentin and desmin type intermediate filaments in a subpopulation of adult rat vascular smooth muscle cells growing in primary culture. Exp Cell Res 139:87–94
19. van Dongen JJ, Langerak AW, Bruggemann M, Evans PA, Hummel M, Lavender FL, Delabesse E, Davi F, Schuuring E, Garcia-Sanz R, van Krieken JH, Droese J, Gonzalez D, Bastard C, White HE, Spaargaren M, Gonzalez M, Parreira A, Smith JL, Morgan GJ, Kneba M, Macintyre EA (2003) Design and standardization of PCR primers and protocols for detection of clonal immunoglobulin and T-cell receptor gene recombinations in suspect lymphoproliferations: report of the BIOMED-2 Concerted Action BMH4-CT98-3936. Leukemia 17:2257–2317

SMÍŠENÝ EPITELOVÝ A STROMÁLNÍ TUMOR LEDVINY: MUTAČNÍ ANALÝZA *DICER 1* GENU U 29 PŘÍPADŮ

Skupina smíšeného epitelového stromálního tumoru ledviny zahrnuje spektrum tumorů od predominantně cystických (cystický nefrom adultního typu, ACN) k tumorům, které vykazují variabilní solidní složku (smíšený epitelový a stromální tumor, SEST) [4]. Tyto tumory se vyskytují především u dospělých pacientů. Cystický nefrom dětského věku (PCN) je prokazatelně odlišná jednotka od skupiny SEST a v nové WHO klasifikaci z roku 2016 [6] je termín cystický nefrom vyhrazen pouze pro pediatrické případy, zatímco termín smíšený epitelový a stromální tumor zahrnuje výše zmíněné tumory dospělého věku (ACN, SEST). V dalším textu je v souladu s WHO používán pro skupinu SEST/ACN pouze název SEST.

Většina PCN je geneticky definována přítomností mutace genu *DICER 1* [19]. Jelikož nám nebyla známá studie zabývající se přítomností mutace genu *DICER 1* u SEST, stanovili jsme si tuto problematiku za cíl naší studie. Analyzovali jsme 28 případů benigních a jeden případ maligního SEST. U žádného ze studovaných tumorů nebyla prokázána mutace genu *DICER 1* v hot-spot kodónech 1705, 1709, 1809, 1810, 1813 a 1814.

Na základě výsledků této studie a dalších výzkumů provedených dříve je možné říci, že:

- Absence mutace *DICER 1* genu v SEST v naší studii a její prokázaná přítomnost u PCN v předchozích studiích [19] dělí tyto skupiny tumorů do dvou odlišných skupin. Kromě molekulárně genetických charakteristik se navíc PCN a SEST liší i morfologicky.
- Termín cystický nefrom by měl být vyhrazen pouze pro pediatrické případy a neměl by být považován za synonymum k SEST u dospělých pacientů *(práce vyšla před publikací WHO 2016, pozn. aut.)*

Mixed Epithelial and Stromal Tumor of the Kidney: Mutation Analysis of the *DICER 1* Gene in 29 Cases

Tomas Vanecek, PhD, Kristyna Pivovarcikova, MD,* Tomas Pitra, MD,† Kvetoslava Peckova, MD,* Pavla Rotterova, MD, PhD,* Ondrej Daum, MD, PhD,* Whitney Davidson, MD,‡ Delia Perez Montiel, MD,§ Kristyna Kalusova, MD,† Milan Hora, MD, PhD,† Ondrej Ondic, MD,* Magdalena Dubova, MD,* Michal Michal, MD,* and Ondrej Hes, MD, PhD*‖*

Abstract: Cystic nephroma (CN) and mixed epithelial stromal tumor (MEST) of the kidney have been considered as synonymous terms describing a single nosologic entity in adult patients. Cystic nephroma in pediatric patients (PCN) is, apparently, a completely different nosologic entity. Although the presence of *DICER 1* mutations is well established in PCN, nothing is currently known about the *DICER 1* gene status in adult MEST/CN. About 33 cases of MEST/CN were selected from the Plzen Tumor Registry; 4 cases were later excluded from the study due to low DNA quality. About 28 of the studied tumors displayed a benign morphology, whereas 1 was diagnosed as a malignant MEST/CN with sarcomatoid differentiation of the stromal component. All 29 samples analyzed using polymerase chain reaction and direct sequencing, including the case with the malignant morphology, were negative for mutation in *DICER 1* hot-spot codons 1705, 1709, 1809, 1810, 1813, and 1814. Our results show that MEST/CN has no relation to PCN on a molecular genetic level. On the basis of our findings and the established morphologic differences between PCN and MEST/CN, we conclude that the term CN should be used for pediatric cases only and should be avoided in adult cases of MEST.

Key Words: kidney, mixed epithelial and stromal tumor, cystic nephroma, pediatric cystic nephroma, *DICER 1* gene mutation

(*Appl Immunohistochem Mol Morphol* 2015;00:000–000)

Received for publication May 18, 2015; accepted July 22, 2015.

From the Departments of *Pathology; †Urology, Charles University, Medical Faculty and Charles University Hospital Plzen; ‖Biomedical Centre, Faculty of Medicine in Plzen, Charles University in Prague, Plzen, Czech Republic; §Department of Pathology, Instituto Nacional de Cancerologia, Mexico City, Mexico; and ‡Department of Pathology and Laboratory Medicine, University of Kansas Medical Center, Kansas City, KS.

Supported by the Charles University Research Fund (project number P36) and by the project CZ.1.05/2.1.00/03.0076 from the European Regional Development Fund.

The authors declare no conflict of interest.

Reprints: Ondrej Hes, MD, PhD, Department of Pathology, Charles University, Medical Faculty and Charles University Hospital Plzen, Alej Svobody 80, Pilsen 304 60, Czech Republic (e-mail: hes@medima.cz).

The term mixed epithelial stromal tumor (MEST) of the kidney was established in 1998 by Michal and Syrucek,[1] whereas the whole concept of MEST was proposed by Michal[2] in 2000 and confirmed later the same year by Adsay et al.[3] Several studies have been published since 2000 that discuss at length the relationship between cystic nephroma (CN) and MEST. The current theory is that CN of adult onset and MEST are the same tumor: 2 ends of the morphologic spectrum of 1 entity. This concept is supported not only by clinical data but also by morphology and molecular genetic analyses.[4–10] The molecular genetic study of MEST and CN has been performed by Zhou et al.[7] Unsupervised clustering of mRNA expression profiles in their report demonstrated that MEST and CN had very similar expression profiles that were distinct from other renal tumors.

The currently preferred term for this entity is MEST.[11] Cystic nephroma in pediatric patients (PCN) is a completely different tumor[7] (for further reference, see below). Unfortunately, the name CN is currently used to describe these distinct entities; however, this will no longer be the case in the new upcoming WHO classification 2016, and the term CN will be preserved for pediatric tumors only (O.H., unpublished data). PCN is a tumor characterized by a multicystic architecture with septa lined by flat to cuboidal epithelial cells. The majority of the tumors occur before the fifth year of life.[12,13] The relation of PCN to Wilms tumor and cystic partially differentiated nephroblastoma is mentioned in the literature.[14,15]

DICER 1 is located on chromosome 14q32.13 and encodes proteins belonging to the RNase III family. It acts as an endoribonuclease, cleaving double-stranded RNA, and is required mainly by the RNA interference pathway to produce active miRNA and siRNA molecules that play a role in a gene repression.[16]

PCN bears biallelic alteration of the *DICER 1* gene. Although the role of *DICER 1* mutations is well recognized in PCN, no data are available regarding the presence/absence of *DICER 1* mutations in adult MEST/CN. In this study, we analyzed mutation hot spots of the *DICER 1* gene in a series of MEST/CN cases.

MATERIALS AND METHODS

A total of 33 cases of MEST/CN were retrieved from among more than 19,500 renal tumors in the files of

the Pilsen Tumor Registry. One to 33 blocks were available for each case. The tumors were reevaluated by at least 2 pathologists (Kristyna Pivovarcikova, O.H.). Tissue for light microscopy was fixed in 10% buffered formalin, embedded in paraffin, cut into 5-μm sections, and stained with hematoxylin and eosin.

The quality of DNA was evaluated, and 4 cases were excluded from further molecular genetic study on the basis of low DNA quality.

MOLECULAR GENETICS

DNA was extracted using the QIAsymphony DNA Mini Kit (Qiagen, Hilden, Germany) on an automated extraction system (QIAsymphony SP, Qiagen) according to the manufacturer's supplementary protocol for paraffin embedded, formalin fixed (FFPE) samples (purification of genomic DNA from FFPE tissue using the QIAamp DNA FFPE Tissue Kit and deparaffinization solution). The concentration and the purity of the extracted DNA were measured using the NanoDrop ND-1000 (NanoDrop Technologies Inc., Wilmington, DE).

For hot-spot mutation analysis [codons 1705, 1709, 1809, 1810, 1813, and 1814, all localized in the RNaseIIb domain of *DICER1*,[23] 50 ng of DNA was added to a reaction that consisted of 12.5 μL of HotStar Taq polymerase chain reaction Master Mix (Qiagen), 10 pmol of each primer (Table 1), and distilled water up to 25 μL. The amplification program was as follows: denaturation at 95°C for 14 minutes, 40 cycles of denaturation at 95°C for 1 minute, annealing at 60°C for 1 minute, extension at 72°C for 1 minute, and finally, incubation at 72°C for 7 minutes.

Successfully amplified polymerase chain reaction products were purified with magnetic particles Agencourt AMPure (Agencourt Bioscience Corporation, A Beckman Coulter Company, Beverly, MA). Products were then sequenced bidirectionally using a Big Dye Terminator Sequencing kit (PE/Applied Biosystems, Foster City, CA) and purified with magnetic particles Agencourt CleanSEQ (Agencourt Bioscience Corporation) according to the manufacturers' protocols before being run on an automated sequencer ABI Prism 3130xl (Applied Biosystems) at a constant voltage of 13.2 kV for 20 minutes.

All sequences were compared with reference sequence NG_016311.1 by BLAST (http://blast.ncbi.nlm.nih.gov/Blast.cgi).

TABLE 1. Primer Pairs for Hot-Spot Mutation Analysis of the *DICER 1* Gene[17]

Primer Name	Sequence 5′-3′	Analyzed Codons
DICER1-hs1F	TGGGGATCAGTTGCTATGTG	1705, 1709
DICER1-hs1R	CGGGTCTTCATAAAGGTGCT	
DICER1-hs2F	TGGACTGCCTGTAAAAGTGG	1809, 1810, 1813, 1814
DICER1-hs2R	ATGTAAATGGCACCAGCAAG	

RESULTS

The basic clinicopathologic data are summarized in Table 2. The patients studied included 5 men and 28 women whose ages ranged from 33 to 92 years (mean, 58.79; median, 59 y). The tumor size was measured in the greatest dimension and ranged from 0.9 to 25 cm (mean, 7.34; median, 6.5 cm). Of the 33 MEST in our study, 31 showed no morphologic signs of aggressive behavior, whereas the other 2 displayed characteristics most consistent with the diagnosis of malignant MEST. A review of corresponding pathology reports revealed that all of the neoplasms were described as well-circumscribed but not encapsulated. Benign tumors were characterized primarily by a multicystic and solid architecture with ovarian (Müllerian)-type stroma and cysts lined by hobnail-shaped epithelial cells (Figs. 1A–C). In cases of malignant neoplasms, tumors were multicystic, with a stromal component containing polymorphic, spindled cells and occasional mitotic figures; the epithelial component in both of these tumors lacked malignant morphologic features. The first malignant case was diagnosed as low-grade sarcoma not otherwise specified arising in MEST (case 25), whereas the second case was diagnosed

TABLE 2. Basic Clinicopathologic Features and Results of *DICER 1* Gene Molecular Genetic Analysis

Case	Sex	Age (y)	Side	Size (cm)	DICER1—Hot-Spots
1	F	47	U	U	–
2	F	72	U	U	–
3	F	39	U	1.0	–
4	F	52	U	3.5	–
5	M	48	U	U	–
6	F	89	L	2.0	–
7	F	74	U	U	–
8	F	63	U	8.0	–
9	F	49	U	9.0	–
10	F	62	U	6.0	–
11	F	71	U	25.0	–
12	F	58	U	8.5	–
13	F	53	R	5.0	–
14	F	44	R	U	–
15	F	36	R	13.0	–
16	F	33	L	U	–
17	F	59	U	13.0	–
18	M	92	L	0.9	–
19	F	64	U	9.0	–
20	F	47	R	6.5	–
21	F	59	R	5.5	–
22	F	65	R	6.0	Not analyzable
23	F	37	R	U	–
24	F	49	U	10.0	–
25*	F	75	U	2.5	–
26	F	74	U	U	–
27	F	78	R	U	Not analyzable
28	M	64	U	8.0	–
29	F	48	L	8.0	–
30	F	53	R	6.0	–
31	M	50	U	3.0	–
32*	M	69	U	9.5	Not analyzable
33	F	67	U	U	Not analyzable

Size denotes the tumor size in the greatest dimension.
*Malignant.
F indicates female; L, left kidney; M, male; R, right kidney; U, unknown; –, negative.

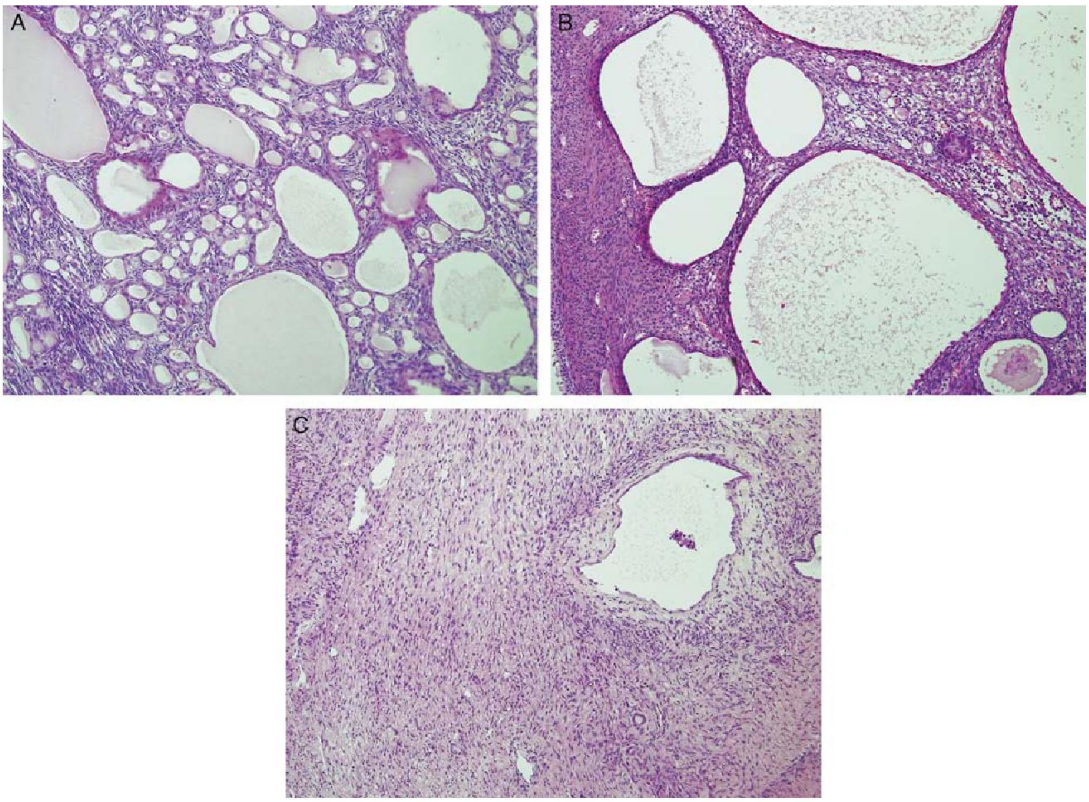

FIGURE 1. MEST/CN is a tumor characterized by both multicystic and solid architecture (A) with the overall appearance depending on the proportion of cystic and solid components (B). The lesional stroma is described as ovarian (Müllerian) type and cysts are lined by epithelium with variable morphology (C).

as spindle cell sarcoma not otherwise specified arising in MEST (case 32) (Figs. 2A, B).

DICER 1 gene mutation hot-spot analysis was performed successfully on 29 of the 33 cases of MEST/CN. All 28 benign samples and the single analyzable malignant sample were negative for mutation in codons 1705, 1709, 1809, 1810, 1813, and 1814 (Table 2).

DISCUSSION

CN was first described by Edmunds in a case report in 1892. His report included a single, hand-drawn plate of an encapsulated cystic tumor in an 18-year-old girl; no microscopic picture of the lesion or histologic description was part of the report. It is very unlikely that the tumor presented by Edmunds was either PCN or MEST/CN; it would be extremely unusual for these tumors to occur in an 18-year-old patient and they do not normally have a well-formed capsule such as that described in Edmunds' paper. It remains a mystery as to which tumor was being described in the above-mentioned case report, but the name CN has since been used many times and has been associated with at least 2 different entities.[18]

MEST/CN has a strong female predilection (up to 8:1) and occurs mostly in perimenopausal women. A few reports have proposed an association with estrogen therapy (the majority of the male cases). Radiologically, MEST/CN are a complex of solid tumor and multicystic lesions, mostly classified as Bosniak 3 or 4.[19] The vast majority of the reported cases follow a benign clinical course, although a few cases have been described as aggressive malignant tumors with sarcomatoid differentiation or carcinomatous change within the epithelial component.[17,20]

MEST/CN is a tumor characterized by both a multicystic and a solid architecture with the overall appearance depending on the proportion of cystic and solid components. The lesional stroma is described as ovarian (Müllerian) type, and cysts are lined by an epithelium with a variable morphology. Most commonly, the epithelial cells have a hobnail appearance, but tumors with a columnar to cylindrical morphology resembling the cervical, the colonic,

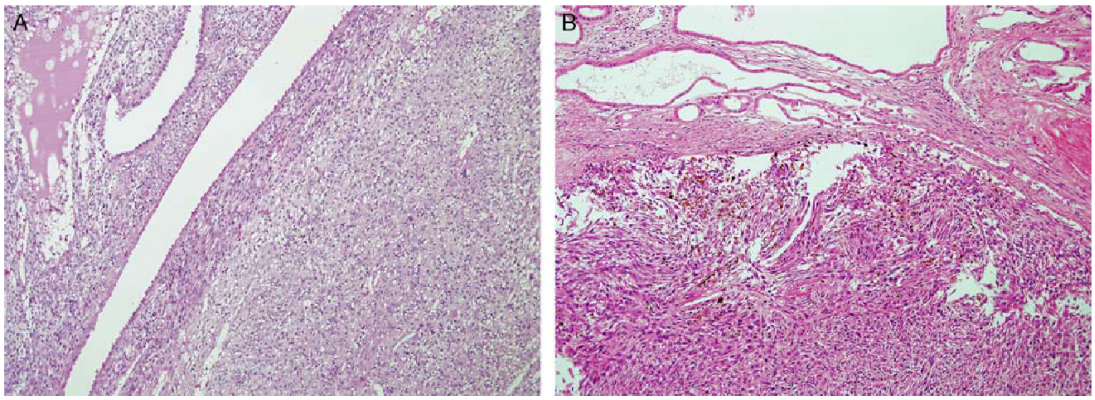

FIGURE 2. A, The first malignant case was diagnosed as low-grade sarcoma NOS arising in MEST. B, The second case was diagnosed as spindle cell sarcoma NOS arising in MEST.

or even the tubular type of epithelium have been documented. Structures resembling corpus albicans in the ovary, lipomatous differentiation, and structures identical to ovarian adenofibromas have also been reported.[21]

PCN is a tumor characterized by its occurrence in pediatric patients, with the majority arising before the fifth year of life and a strong male predominance (up to 4:1).[18,22] PCN are typically expansile, noncapsulated masses that are well demarcated from the normal kidney parenchyma. Most of these tumors are solitary; however, cases of bilateral lesions have been described. Tumors are typically multicystic with septa lined by flattened, cuboidal epithelial cells; the septal stroma is composed mostly of spindle cell elements. PCN, cystic partially differentiated nephroblastoma, and cystic Wilms' tumor are thought to represent a spectrum of a single etiological entity, with PCN at the benign end, cystic Wilms tumor at the malignant end, and cystic partially differentiated nephroblastoma occupying the intermediate position. PCN and stage 1 cystic partially differentiated nephroblastoma are often treated with surgery alone. The International Society of Pediatric Oncology (SIOP) protocols for Wilms' tumor advocate preoperative chemotherapy, which may be unnecessary and potentially harmful in PCN and in pT 1 cystic partially differentiated nephroblastoma.[15]

Doros and colleagues studied PCN and cystic partially differentiated nephroblastomas, including cases of sarcoma with morphologic features of pleuropulmonary blastoma arising in PCN. They found that *DICER1* mutations are a major genetic event in the development of PCN, and also that PCN and pleuropulmonary blastoma have similar *DICER1* loss of function and "hotspot" missence mutation rates. The relationship between PCN, medulloepithelioma, Sertoli-Leydig cell tumors, and pleuropulmonary blastoma, on a molecular genetic level, has also been proposed by others.[23,24] Cases of familial PCN have also been documented.[25–27]

We are not aware of any previous study describing the role of *DICER 1* gene mutations in MEST/CN. In our study, we analyzed 28 cases of benign MEST/CN with DNA suitable for *DICER 1* gene mutation analysis. None of the cases were positive for mutations within hot-spot regions of the *DICER 1* gene. Only 1 malignant MEST/CN from our cohort was suitable for genetic analysis. Even in this case, we were not able to find mutations within hot-spot regions of the *DICER 1* gene. Our findings can thus be considered as another argument for a strict differentiation between PCN and tumors from the MEST/CN group occurring in adult patients.

On the basis of the results of our study and others performed previously, it is possible to conclude that MEST/CN is a tumor that has no relation to PCN on the morphologic or the molecular genetic level. The term CN should be used for pediatric cases only and should be avoided as a synonym for adult cases of MEST.

REFERENCES

1. Michal M, Syrucek M. Benign mixed epithelial and stromal tumor of the kidney. *Pathol Res Pract*. 1998;194:445–448.
2. Michal M. Benign mixed epithelial and stromal tumor of the kidney. *Pathol Res Pract*. 2000;196:275–276.
3. Adsay NV, Eble JN, Srigley JR, et al. Mixed epithelial and stromal tumor of the kidney. *Am J Surg Pathol*. 2000;24:958–970.
4. Jevremovic D, Lager DJ, Lewin M. Cystic nephroma (multilocular cyst) and mixed epithelial and stromal tumor of the kidney: a spectrum of the same entity? *Ann Diagn Pathol*. 2006;10:77–82.
5. Bisceglia M, Galliani CA, Senger C, et al. Renal cystic diseases: a review. *Adv Anat Pathol*. 2006;13:26–56.
6. Turbiner J, Amin MB, Humphrey PA, et al. Cystic nephroma and mixed epithelial and stromal tumor of kidney: a detailed clinicopathologic analysis of 34 cases and proposal for renal epithelial and stromal tumor (REST) as a unifying term. *Am J Surg Pathol*. 2007;31:489–500.
7. Zhou M, Kort E, Hoekstra P, et al. Adult cystic nephroma and mixed epithelial and stromal tumor of the kidney are the same disease entity: molecular and histologic evidence. *Am J Surg Pathol*. 2009;33:72–80.
8. Mohanty SK, Parwani AV. Mixed epithelial and stromal tumors of the kidney: an overview. *Arch Pathol Lab Med*. 2009;133:1483–1486.

9. Lane BR, Campbell SC, Remer EM, et al. Adult cystic nephroma and mixed epithelial and stromal tumor of the kidney: clinical, radiographic, and pathologic characteristics. *Urology*. 2008;71:1142–1148.
10. Montironi R, Mazzucchelli R, Lopez-Beltran A, et al. Cystic nephroma and mixed epithelial and stromal tumour of the kidney: opposite ends of the spectrum of the same entity? *Eur Urol*. 2008;54:1237–1246.
11. Srigley JR, Delahunt B, Eble JN, et al. The International Society of Urological Pathology (ISUP) Vancouver Classification of Renal Neoplasia. *Am J Surg Pathol*. 2013;37:1469–1489.
12. Boybeyi O, Karnak I, Orhan D, et al. Cystic nephroma and localized renal cystic disease in children: diagnostic clues and management. *J Pediatr Surg*. 2008;43:1985–1989.
13. Luithle T, Szavay P, Furtwangler R, et al. Group SGS. Treatment of cystic nephroma and cystic partially differentiated nephroblastoma–a report from the SIOP/GPOH study group. *J Urol*. 2007;177:294–296.
14. Joshi VV, Banerjee AK, Yadav K, et al. Cystic partially differentiated nephroblastoma: a clinicopathologic entity in the spectrum of infantile renal neoplasia. *Cancer*. 1977;40:789–795.
15. van den Hoek J, de Krijger R, van de Ven K, et al. Cystic nephroma, cystic partially differentiated nephroblastoma and cystic Wilms' tumor in children: a spectrum with therapeutic dilemmas. *Urol Int*. 2009;82:65–70.
16. Hannon GJ, Rossi JJ. Unlocking the potential of the human genome with RNA interference. *Nature*. 2004;431:371–378.
17. Sukov WR, Cheville JC, Lager DJ, et al. Malignant mixed epithelial and stromal tumor of the kidney with rhabdoid features: report of a case including immunohistochemical, molecular genetic studies and comparison to morphologically similar renal tumors. *Hum Pathol*. 2007;38:1432–1437.
18. Michal M, Hes O, Kuroda N, et al. What is a cystic nephroma? *Am J Surg Pathol*. 2010;34:126–127. Author reply 7.
19. Hora M, Hes O, Michal M, et al. Extensively cystic renal neoplasms in adults (Bosniak classification II or III)—possible "common" histological diagnoses: multilocular cystic renal cell carcinoma, cystic nephroma, and mixed epithelial and stromal tumor of the kidney. *Int Urol Nephrol*. 2005;37:743–750.
20. Svec A, Hes O, Michal M, et al. Malignant mixed epithelial and stromal tumor of the kidney. *Virchows Arch*. 2001;439:700–702.
21. Michal M, Hes O, Bisceglia M, et al. Mixed epithelial and stromal tumors of the kidney. A report of 22 cases. *Virchows Arch*. 2004;445:359–367.
22. Madewell JE, Goldman SM, Davis CJ Jr, et al. Multilocular cystic nephroma: a radiographic-pathologic correlation of 58 patients. *Radiology*. 1983;146:309–321.
23. Doros LA, Rossi CT, Yang J, et al. DICER1 mutations in childhood cystic nephroma and its relationship to DICER1-renal sarcoma. *Mod Pathol*. 2014;27:1267–1280.
24. Schultze-Florey RE, Graf N, Vorwerk P, et al. DICER1 syndrome: a new cancer syndrome. *Klin Padiatr*. 2013;225:177–178.
25. Bahubeshi A, Bal N, Rio Frio T, et al. Germline DICER1 mutations and familial cystic nephroma. *J Med Genet*. 2010;47:863–866.
26. Bal N, Kayaselcuk F, Polat A, et al. Familial cystic nephroma in two siblings with pleuropulmonary blastoma. *Pathol Oncol Res*. 2005;11:53–56.
27. Ashley RA, Reinberg YE. Familial multilocular cystic nephroma: a variant of a unique renal neoplasm. *Urology*. 2007;70:179.e9–179.e10.

CYSTICKÝ RENÁLNÍ ONKOCYTOM A TUBULOCYSTICKÝ RENÁLNÍ KARCINOM: MORFOLOGICKÁ A IMUNOHISTOHEMICKÁ SROVNÁVACÍ STUDIE

Renální onkocytom (RO) je charakterizován velkými eosinofilními buňkami uspořádanými nejčastěji solidně nebo ve formě solidních hnízd rozptýlených v řídkém hypocelulárním stromatu [4]. Architektonika i cytologické vlastnosti RO jsou však značně variabilní a v malém procentu případů může RO růst cysticky a vést tak snadno k záměně za tubulocystický renální karcinom (TCRK), zvláště pokud není k dispozici dostatek materiálu (nedostatečný sampling, punkční biopsie).

Nedávno publikovaná rozsáhlá klinickopatologická studie potvrzuje benigní povahu RO; u 109 studovaných případů nebyla prokázána lokální recidiva, vzdálená metastáza ani smrt pacienta zapříčiněná tumorem (průměrný follow-up 51 měsíců) [20]. TCRK je považován za nízce maligní tumor, který má potenciál chovat se agresivně. Má proto klinický význam umět tyto dva tumory odlišit, na což jsme se zaměřili v této studii. Porovnali jsme 24 cystických RO a 15 TCRK na základě architektoniky, charakteru stromatu, cytomorfologie, ISUP nukleolárního grade, přítomnosti nekróz, mitotické aktivity a IHC vlastností (použité protilátky: AE1-AE3, OSCAR, CAM5.2, CK7, vimentin, CD10, CD117, AMACR, CA-IX, MIA, EMA a Ki-67).

RO vykazoval ve všech případech alespoň fokálně solidní růst, stroma bylo řídké, hypocelulární, ISUP nukleolární grade byl nižší (převážně 1 a 2), nekrózy a mitózy nebyly přítomné. Imunohistochemicky byly všechny RO silně pozitivní s CD117 a negativní nebo slabě pozitivní v průkazu vimentinu, negativní v reakci s CD10 a AMACR. Narozdíl od RO, TCRK nevykazoval solidní růst, stroma mělo fibrózní charakter, ISUP grade byl vyšší (převážně 2 a 3), fokálně byly přítomné nekrózy a mitózy. Immunohistochemický průkaz CD 117 byl ve 14/15 TCRK negativní (1 případ se barvil slabě pozitivně). Vimentin reagoval silně a difuzně pozitivně, CD10, CK7 a AMACR byly pozitivní difuzně nebo fokálně. Protilátky AE1-AE3, OSCAR, CAM5.2, CA-IX, MIA a EMA byly bez diskriminačního významu.

Ačkoliv se cystický RO a TCRK mohou morfologicky překrývat, při důkladném zhodnocení lze oba tumory odlišit se zaměřením na histologické znaky v kombinaci s imunohistochemií: přítomnost/absence solidního růstu, mitotické aktivity a nekrózy, typ stromatu, nukleolární grade, společně s aplikací IHC panelu zahrnujícího vimentin, CD117, CD10, CK7, AMACR a Ki67 jsou dobrým vodítkem ke správné diagnóze.

Cystic Renal Oncocytoma and Tubulocystic Renal Cell Carcinoma: Morphologic and Immunohistochemical Comparative Study

Faruk Skenderi, MD, MSc, Monika Ulamec, MD, PhD,† Semir Vranic, MD, PhD,* Nurija Bilalovic, MD, PhD,* Kvetoslava Peckova, MD,‡ Pavla Rotterova, MD, PhD,‡ Bohuslava Kokoskova, MD,‡ Kiril Trpkov, MD,§ Pavla Vesela, MD,‡ Milan Hora, MD, PhD,‖ Kristyna Kalusova, MD, MSc,‖ Maris Sperga, MD,¶ Delia Perez Montiel, MD,# Isabel Alvarado Cabrero, MD, PhD,** Stela Bulimbasic, MD, PhD,†† Jindrich Branzovsky, MD,‡ Michal Michal, MD,‡ and Ondrej Hes, MD, PhD‡ ‡‡*

Abstract: Renal oncocytoma (RO) may present with a tubulocystic growth in 3% to 7% of cases, and in such cases its morphology may significantly overlap with tubulocystic renal cell carcinoma (TCRCC). We compared the morphologic and immunohistochemical characteristics of these tumors, aiming to clarify the differential diagnostic criteria, which facilitate the discrimination of RO from TCRCC. Twenty-four cystic ROs and 15 TCRCCs were selected and analyzed for: architectural growth patterns, stromal features, cytomorphology, ISUP nucleolar grade, necrosis, and mitotic activity. Immunohistochemical panel included various cytokeratins (AE1-AE3, OSCAR, CAM5.2, CK7), vimentin, CD10, CD117, AMACR, CA-IX, antimitochondrial antigen (MIA), EMA, and Ki-67. The presence of at least focal solid growth and islands of tumor cells interspersed with loose stroma, lower ISUP nucleolar grade, absence of necrosis, and absence of mitotic figures were strongly suggestive of a cystic RO. In contrast, the absence of solid and island growth patterns and presence of more compact, fibrous stroma, accompanied by higher ISUP nucleolar grade, focal necrosis, and mitotic figures were all associated with TCRCC. TCRCC marked more frequently for vimentin, CD10, AMACR, and CK7 and had a higher proliferative index by Ki-67 (> 15%). CD117 was negative in 14/15 cases. One case was weakly CD117 reactive with cytoplasmic positivity. All cystic RO cases were strongly positive for CD117. The remaining markers (AE1-AE3, CAM5.2, OSCAR, CA-IX, MIA, EMA) were of limited utility. Presence of tumor cell islands and solid growth areas and the type of stroma may be major morphologic criteria in differentiating cystic RO from TCRCC. In difficult cases, or when a limited tissue precludes full morphologic assessment, immunohistochemical pattern of vimentin, CD10, CD117, AMACR, CK7, and Ki-67 could help in establishing the correct diagnosis.

Key Words: kidney, renal oncocytoma, tubulocystic renal cell carcinoma, overlap, immunohistochemistry

(*Appl Immunohistochem Mol Morphol* 2016;24:112–119)

Renal oncocytoma (RO) is considered a benign renal neoplasm originating from the intercalated cells. It comprises approximately 5% of all renal tumors and has an excellent prognosis.[1] RO is known for its variations in architecture and cytology, and several renal neoplasms may mimic RO, such as chromophobe renal cell carcinoma, oncocytic variant of papillary renal cell carcinoma, granular cell variant of clear cell renal cell carcinoma, or hybrid oncocytic/chromophobe tumors.[2–5] Less frequently (3% to 7%), RO may exhibit a pattern composed of tubules and cysts, combined with a variable component of small cell islands, with a background of loose or hypocellular stroma.[6–9] Tubulocystic renal cell carcinoma (TCRCC) has been recently recognized as a distinct entity by the International Society of Urological Pathology (ISUP) Vancouver Classification.[10] TCRCC is composed of tubules and cysts of variable size and scant fibrous stroma. The cysts are lined by 1 or more epithelial cell layers, which demonstrate abundant eosinophilic

Received for publication August 26, 2014; accepted October 1, 2014.

From the *Department of Pathology and Cytology, Clinical Center of the University of Sarajevo, Sarajevo, Bosnia and Herzegovina; †Ljudevit Jurak Department of Pathology, Sestre milosrdnice Clinical Hospital Center; ††Department of Pathology, University Hospital Dubrava, Zagreb, Croatia; Departments of ‡Pathology; ‖Urology, Charles University, Faculty of Medicine and University Hospital Plzeň; ‡‡Biomedical Centre, Faculty of Medicine in Plzen, Charles University in Prague, Plzen, Czech Republic; §Department of Pathology and Laboratory Medicine, Calgary Laboratory Services and University of Calgary, Calgary, AB, Canada; ¶Department of Pathology, East University Riga, Riga, Latvia; #Department of Pathology, Institute Nacional de Cancerologia; and **Department of Pathology, Centro Medico, Mexico City, Mexico.

Supported by the Charles University Research Fund (project number P36) and by the project CZ.1.05/2.1.00/03.0076 from European Regional Development Fund.

The authors declare no conflict of interest.

Reprints: Ondrej Hes, MD, PhD, Department of Pathology, Medical Faculty and Charles University Hospital Plzen, Charles University, Alej Svobody 80, 304 60 Pilsen, Czech Republic (e-mail: hes@medima.cz).

cytoplasm and prominent nucleoli.[11] The overlapping morphologic features of the cystic variant of RO (CRO) and TCRCC may represent a diagnostic challenge, particularly when limited tissue sample is available for assessment. RO is considered a benign tumor despite the presence of atypical features.[6,9,12–14] In contrast, TCRCC represents a low-grade carcinoma, which sometimes may demonstrate an aggressive behavior. Therefore, the distinction and the correct diagnosis of these tumors are of clinical relevance and impact the patient prognosis and management. In this study, we compared the morphologic and immunohistochemical (IHC) characteristics of CRO and TCRCC, with an aim to clarify the diagnostic and the differential diagnostic features of these tumors.

MATERIALS AND METHODS

Case Selection

Twenty-four CRO with at least 50% of the tumor demonstrating tubulocystic architecture have been selected from a total of 645 ROs (3.7% of available RO). CRO otherwise showed morphology of round-to-polygonal cells with finely granular, eosinophilic cytoplasm with round to oval nuclei consistent with diagnosis of RO. Fifteen TCRCCs have also been retrieved from the in-house and consultation files of the same registry. TCRCC typically demonstrated well-formed, small to medium-sized tubules and cysts, lined by large cells, usually demonstrating abundant eosinophilic cytoplasm. The lining cells showed focal hob-nail shape with high nuclear grade with prominent nucleoli. For each case, 1 to 49 tissue blocks (mean 5.6) were available for review. The diagnosis was rendered by 3 pathologists (F.S., M.U., O.H.) and was supported by the IHC analysis.

The tissue was fixed in 4% buffered formalin, embedded routinely into paraffin, and 5 μm sections were cut and stained with hematoxylin and eosin. The sections were evaluated by light microscopy for the following histologic features: visually estimated percentage of cystic, solid, and island patterns, epithelial lining of the cysts (single, pseudopapillary, multilayered), presence of papillary protrusions in the cysts, hemorrhage within the cysts or stroma, extent and composition of the stroma, cytologic features including nuclear ISUP nucleolar grade, mitotic activity, and presence of microscopic necrosis.

IHC

IHC examination was performed in 37 of 39 cases. Only selected markers were stained in 2 ROs and 2 TCRCCs because of limited tissue availability. Assays were performed using the Ventana Benchmark XT automated stainer (Ventana Medical System Inc., Tucson, AZ). The following primary antibodies were used: epithelial membrane antigen (EMA) (E29, monoclonal; Dako, Carpinteria, CA; 1:1000), cytokeratins (CAM5.2, monoclonal; Becton-Dickinson, San Jose, CA; 1:200), Pan Ab-1 (AE1-AE3, monoclonal; BioGenex, San Ramon, CA; 1:1000), cytokeratin 7 (OV-TL12/30, monoclonal; Dako; 1:200), cytokeratin OSCAR (OSCAR, monoclonal; Covance, Princetown, NJ; 1:2000), racemase/AMACR (P504S, monoclonal; Zeta, Sierra Madre, CA, 1:50), vimentin (D9, monoclonal; NeoMarkers, Westinghouse, CA; 1:1000), Ki-67 (MIB1, monoclonal; Dako, Glostrup, Denmark; 1:1000), carbonic anhydrase IX (CA-IX; rhCA9, monoclonal; RD systems, Abingdon, GB; 1:100), antimitochondrial antigen (MIA, monoclonal; BioGenex; 1:100). CD10 (56C6, monoclonal; Novocastra, Newcastle, UK; 1:50), c-kit (CD117, polyclonal; DakoCytomation, Glostrup, Denmark; RTU). Appropriate positive and negative controls were used for all IHC assays. The pattern of staining was scored *negative*, if no staining was observed; *scattered positive*, if single or few cells were clearly positive throughout the tumor; *focal positive*, if large groups of cells were clearly positive (< 50%); and *diffuse positive*, if majority (> 50%) of tumor cells were positive.

Statistical Analysis

The data were analyzed using SPSS version 19 (Chicago, IL). χ^2 test was used to analyze the differences regarding the morphologic criteria and IHC staining patterns and intensity. The Fisher exact test was used for dichotomous variables and Student *t* test was used to compare mean Ki-67 percentages. *P* value of <0.05 was considered significant.

RESULTS

Clinicopathologic Data

Basic clinical and pathologic data were available for 38 of 39 cases and are summarized in Tables 1 and 2. The mean age of patients with RO was 68.7 years (range, 51 to 85 y), in contrast to the mean age of 59.8 years for TCRCC (range, 29 to 78 y). Male to female ratios were 2.4:1 in CRO and 2:1 in TCRCC. The mean size of CRO was 2.5 cm, demonstrating brown cut surface with numerous small to large, often hemorrhagic cysts, but without grossly visible necrosis. TCRCCs had a twice larger mean size of 5 cm, with white to gray "bubble wrap" gross appearance, and demonstrated focal hemorrhage in about half of the cases; necrosis was uniformly absent on gross examination.

The follow-up data for 10/24 patients who underwent surgery for CRO were available (Tables 1 and 2) and all the followed patients were alive and well at the time of the study. Eleven of 13 patients who underwent surgery for TCRCC were followed up. One patient died of disease, 1 died of life event, and the remaining 9 were alive and well at the time of study (Tables 1 and 2).

Morphologic Characteristics

Microscopic characteristics of CRO and TCRCC are summarized in Table 3. Both tumor types presented with dominant tubular and cystic architecture (76.8% in CRO vs. 86.7% in TCRCC, both mean % of total tumor volume) (Figs. 1A, B). Cell islands and solid areas were present in all cases of CRO, with a mean of 12% and

TABLE 1. Clinicopathologic Details of the CRO and TCRCC Cases

CRO						TCRCC					
Case #	Age (y)	Sex	Size (cm)	Follow-up (y)	Clinical Manifestation	Case #	Age (y)	Sex	Size (cm)	Follow-up (y)	Clinical Manifestation
1	77	F	2.7	1 AW	Back pain	1	62	M	2	9 AW	Incidental
2	73	M	3.8	NA	NA	2	44	M	8	NA	NA
3	64	F	1.7	1 AW	Incidental	3	68	M	2.5	6 AW	NA
4	65	M	2.4	2 AW	CRI, regular check	4	78	M	2.8	NA	NA
5	72	M	1.4	2 AW	CRI, regular check	5	31	F	5.1	NA	NA
6	77	M	3.7	NA	NA	6	72	M	6.5	4 AW	Incidental
7	70	M	1.3	1 AW	Incidental	7	29	M	3.6	1 DOD	Skeletal metastasis, back pain
8	72	M	2.8	2 AW	Incidental	8	60	M	2.2	4 AW	Back pain
9	61	F	4	2 AW	Incidental	9	49	F	3	4 AW	NA
10	70	M	3.5	NA	NA	10	63	M	9	3 AW	Hematuria
11	62	M	1	4 AW	Surgery for feochromocytoma, incidental	11	75	M	9	3 AW	CRI
12	59	M	NA	NA	NA	12	60	M	2.5	1 AW	Incidental
13	82	F	2	NA	NA	13	61	F	5	7 AW, then LE	Routine examination
14	65	M	2	4 AW	Follow-up checkup for lung adenocarcinoma	14	71	F	4.5	1.5 AW	Abdominal pain
15	85	M	1.3	NA	NA	15	74	F	10	NA	NA
16	76	F	4.7	NA	NA						
17	65	M	2.7	NA	NA						
18	54	M	3	NA	NA						
19	60	M	3.2	NA	NA						
20	72	M	1.4	NA	NA						
21	68	F	NA	NA	NA						
22	51	M	1.5	9 AW	NA						
23	NA	F	4	NA	NA						
24	80	M	2.2	NA	NA						

AW indicates alive and well; CRI, chronic renal insufficiency; CRO, cystic renal oncocytoma; F, female; M, male; NA, not available; TCRCC, tubulocystic renal cell carcinoma.

10.7% of the total tumor volume, respectively (Fig. 2). Cell islands and solid cell areas were found in only 8/15 of TCRCCs, demonstrating only a 1.8% and 2% of the total tumor volume, respectively ($P = 0.002$ and 0.001) (Table 3). CRO presented with loose stroma in 22/24 cases (91.6%); in 2 cases, minor fibrotic areas were present. In contrast, predominantly compact fibrotic stroma was present in 14/15 TCRCCs (93.3%) and only 1 case contained a minor loose stromal component. CRO typically showed nuclear grades 1 and 2, and only 1 case showed nuclear grade 3 (1/24, 4.2%), in contrast to TCRCC, in which 10/15 (66.7%) cases presented with nuclear grade 3 ($P < 0.001$). No mitotic figures and necrosis were found microscopically in CRO, whereas they were found in 26.7% and 38.4% TCRCCs, respectively ($P = 0.024$ and 0.007, respectively). The tubules and cysts in CRO were frequently lined by single cell layer (20/24, 83.3%), whereas less than half of TCRCCs (6/15, 40%) showed a single cell lining, as illustrated in Figure 3A. The remaining TCRCCs demonstrated focal pseudopapillary (40%) or multilayered lining (20%) (Fig. 3B). Slender and isolated papillary/micropapillary buddings within the cysts appeared less frequently in CRO (3/24, 12%), compared with TCRCC, in which they were noted in more than half of the cases (9/15, 60%) ($P = 0.013$).

TABLE 2. Summary of the Clinical and Macroscopic Data

	CRO	TCRCC
Total (n)	24	15
Female (n)	7	5
Male (n)	17	10
Mean age (range) (y)	68.7 (51-85)	59.8 (29-78)
Mean tumor size (range) (cm)	2.5 (1.0-4.7)	5 (2.0-10.0)
Mean follow-up duration (y)	2.8 (1-9)	4.2 (1-9)

CRO indicates cystic renal oncocytoma; TCRCC, tubulocystic renal cell carcinoma.

IHC Findings

The results of the IHC evaluation are summarized in Table 4 and Figure 4. We found no significant differences in the reactivity of wide-spectrum cytokeratins (AE1/AE3, OSCAR, and CAM5.2), MIA, and EMA, with both tumors showing similar reactivity. Significant differences in immunoreactivity were, however, found for vimentin, CD10, AMACR, CD117, CK7, CA-IX, and Ki-67. Vimentin was either negative (9/22, 40%) or scattered positive (12/22, 55%) in CRO, in contrast to TCRCC, in which majority of the cases exhibited diffuse reactivity (11/13, 84.6%) (Figs. 5A, B). Similarly, CD10 stained TCRCC either focally or diffusely in 69.1% of cases, but only 1 CRO (1/23, 4%) showed focal reactivity; the remaining CRO cases were typically negative or

TABLE 3. Morphologic Characteristics of the CRO and TCRCC

Tumor Type/Morphologic Characteristic	CRO (N = 24)	TCRCC (N = 15)	*P*
Architecture			
Tubules/cysts (mean volume %)	76.8	86.7	0.057
Solid (mean volume %)	10.7	2.0	**0.001**
Islands/nests (mean volume %)	12.0	1.8	**0.002**
Papillary/micropapillary buddings in the cysts [n (%)]			
Yes	3 (12)	9 (60)	**0.013**
No	21 (88)	6 (40)	
Lining of the cysts [n (%)]			
Single	20 (83.3)	6 (40)	**0.042**
Pseudopapillary	2 (8.3)	6 (40)	
Multilayered	2 (8.3)	3 (20)	
Hemorrhage [n (%)]			
None	3 (12.5)	5 (33.3)	
Tubules/cysts	17 (70.8)	3 (20)	**0.003**
Tubules/cysts and stroma	4 (16.7)	3 (20)	
Stroma	0 (0.0)	4 (26.7)	
Type of stroma [n (%)]			
Loose	19 (79.2)	1 (6.7)	**< 0.001**
Loose and fibrotic	3 (12.5)	2 (13)	
Fibrotic	2 (8.3)	12 (80)	
Amount of stroma			
Scant	12 (50.0)	13 (86.7)	0.103
Moderate	9 (37.5)	2 (13.3)	
Abundant	3 (3.0)	1 (6.7)	
Cytology [n (%)]			
Dominant oncocytic	24 (100)	9 (60)	**< 0.001**
Focal oncocytic	0 (0.0)	6 (4140)	
Nucleolar grade [n (%)]			
1	13 (54.2)	1 (6.7)	
2	10 (41.7)	5 (33.3)	**< 0.001**
3	1 (4.2)	9 (60)	
4	0 (0.0)	0 (0.0)	
Mitotic figures [n (%)]			
Yes	0 (0.0)	4 (26.6)	**0.024**
No	24 (100)	11 (73.3)	
Necrosis [n (%)]			
Yes	0 (0.0)	4 (26.7)	**0.007**
No	24 (100)	11 (73.3)	

$P < 0.05$ was considered significant.
CRO indicates cystic renal oncocytoma; TCRCC, tubulocystic renal cell carcinoma.

scattered positive. AMACR immunoreactivity was also more frequently diffusely positive in TCRCC (10/13, 77%), in contrast to CRO (3/23; 13%). CK7 was either negative or scattered positive in 22/23 (96%) of CRO cases, whereas a focal or diffuse staining pattern was present in 9/13 (69.2%) TCRCC cases. CD117 was positive in all CROs with cytoplasmic and membranous positivity (23/23), whereas all but 1 TRRCC (14/15, 93.3%) were completely negative. One case (case 8) was weakly positive for CD117 within cytoplasm. The proliferative activity (MIB1/Ki-67) was much lower in CRO (mean < 5%), in contrast to TCRCC, in which a higher proliferative activity was observed (mean > 15%). CA-IX was positive in 1/19 (5%) cases of CRO, whereas 6/14 (43%) cases of TCRCC were either focally or diffusely positive.

DISCUSSION

RO is a benign renal neoplasm, which may show a spectrum of atypical features, such as vascular or fat tissue extension, hemorrhage, presence of small oncocytic cells (so-called oncoblasts), microscopic necrosis, pleomorphic nuclei, or rare mitoses.[6,9,12–14] Although reports of its malignant behavior have been published in the older literature,[15,16] a recent large contemporary study confirmed the benign nature of RO, because no local recurrence, distant metastasis, or death due to tumor occurred during the median follow-up of 51 months.[9]

RO is well known for its ability to mimic malignant renal tumors particularly when solid and nested growth patterns are seen (49% to 89% cases[9]), which are also present within a group of other oncocytic/eosinophilic renal tumors, such as granular variant of clear cell renal cell carcinoma, chromophobe renal cell carcinoma, hybrid oncocytic/chromophobe tumors, and oncocytic variant of papillary renal cell carcinoma. Less commonly, RO presents with tubulocystic architecture (3% to 7%),[9,17,18] a morphology that may simulate a TCRCC.

The histologic features of TCRCC have been first described by MacLennan and colleagues in 1997 who

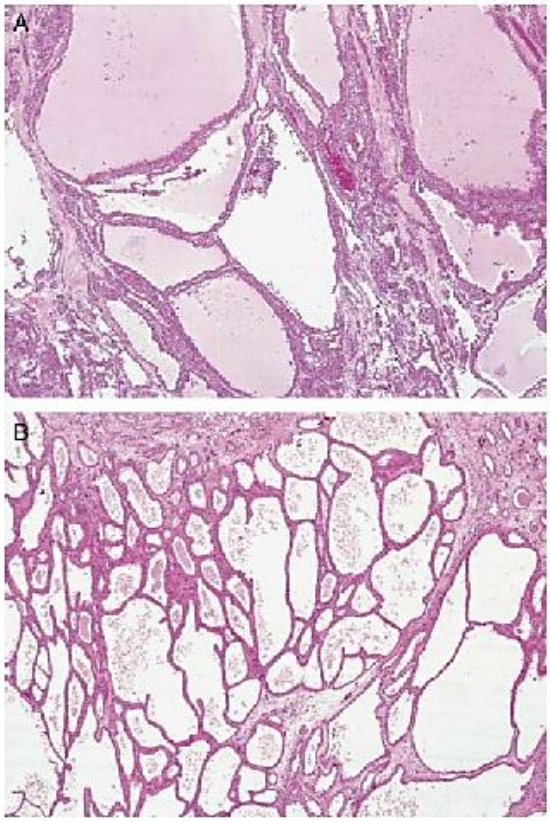

FIGURE 1. Low-power magnification showed predominantly cystic architecture in both CRO (A) and TCRCC (B) (hematoxylin and eosin).

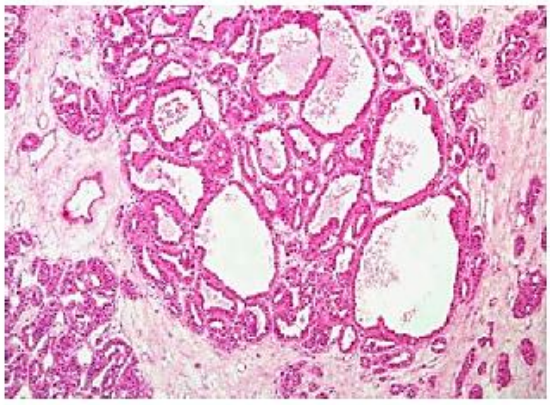

FIGURE 2. Areas of prominent stroma with isolated islands of oncocytic cells are more typical for CRO (hematoxylin and eosin).

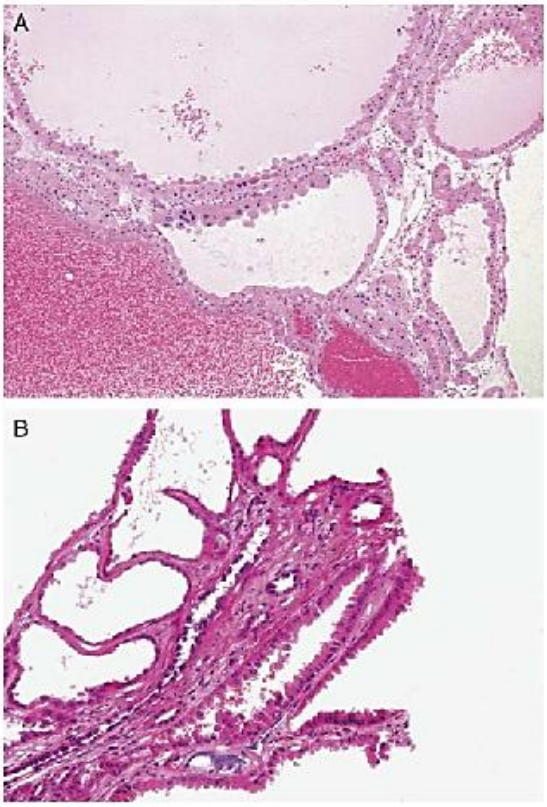

FIGURE 3. Cells lining cysts are relatively uniform, voluminous, cuboidal arranged in a single row in CRO (A), whereas in TCRCC they are usually more elongated, cylindrical, arranged in a single row and/or in a pseudostratified pattern (B) (hematoxylin and eosin).

labeled the tumor "low-grade collecting duct carcinoma"; however, part of the cases from the original series were later recognized as mucinous tubulary and spindle cell carcinoma.[19–21] The results of recent studies suggested distinct pathologic characteristics of this tumor, which led to its recognition as a separate entity in the recent ISUP Vancouver Classification of Renal Neoplasia.[10] To date, about 80 cases of this rare tumor have been reported in the literature.[22]

In this study, we compared the morphologic features and the IHC profile of 24 CROs and 15 TCRCCs to establish the most useful features that help to distinguish between these 2 entities. The gross appearance of CRO, mostly solid with scattered cysts, contrasts the TCRCC cystic appearance resembling "bubble wrap." The color on gross examination (brown vs. tan-gray, respectively) may also aid in arriving at the correct diagnosis. On microscopy, the presence of at least focal solid nests or islands of tumor cells, which were observed in all cases of CRO in this study, were much less common and quite

TABLE 4. Comparison of Immunohistochemical Profile of CRO and TCRCC

Tumor Type/IHC Marker	CRO [n (%)]	TCRCC [n (%)]	*P*
CK7			
Negative	1/23 (4)	3/13 (23)	
Scattered positive	22/23 (96)	1/13 (7.7)	**< 0.001**
Focal positive	0/23 (0)	8/13 (61.5)	
Diffuse positive	0/23 (0)	1/13 (7.7)	
AE1/AE3			
Negative	0/22 (0)	0/13 (0)	
Scattered positive	4/22 (17)	0/13 (0)	0.16
Focal positive	13/22 (57)	8/13 (61.5)	
Diffuse positive	5/22 (22)	5/13 (38.4)	
CAM5.2			
Negative	0/21 (0)	0/13 (0)	
Scattered positive	0/21 (0)	0/13 (0)	0.23
Focal positive	0/21 (0)	1/13 (7.7)	
Diffuse positive	21/21 (100)	12/13 (92.3)	
OSCAR			
Negative	0/22 (0)	0/13 (0)	
Scattered positive	0/22 (0)	0/13 (0)	> 0.05
Focal positive	0/22 (0)	0/13 (0)	
Diffuse positive	22/22 (100)	13/13 (100)	
Vimentin			
Negative	9/22 (40)	1/13 (7.7)	
Scattered positive	12/22 (55)	0/13 (0)	**< 0.001**
Focal positive	1/22 (5)	1/13 (7.7)	
Diffuse positive	0/22 (0)	11/13 (84.6)	
CD10			
Negative	20/23 (87)	4/13 (30)	
Scattered positive	2/23 (9)	0/13 (0)	**< 0.001**
Focal positive	1/23 (4)	3/13 (23)	
Diffuse positive	0/23 (0)	6/13 (46.1)	
AMACR			
Negative	14/24 (58)	2/13 (15.3)	
Scattered positive	2/24 (8)	0/13 (0)	**< 0.001**
Focal positive	5/24 (21)	1/13 (7.7)	
Diffuse positive	3/24 (13)	10/13 (77)	
CD117			
Negative	0/23 (0)	14/15 (93.3)	
Scattered positive	0/23 (0)	1/15 (6.7)	**< 0.001**
Focal positive	0/23 (0)	0/15 (0)	
Diffuse positive	23/23 (100)	0/15 (0)	
CA-IX			
Negative	18/19 (95)	8/14 (57)	
Scattered positive	0/19 (0)	0/14 (0)	**0.03**
Focal positive	1/19 (5)	5/14 (36)	
Diffuse positive	0/19 (0)	1/14 (7)	
MIA			
Negative	1/24 (4)	0/13 (0)	
Scattered positive	0/24 (0)	0/13 (0)	0.71
Focal positive	2/24 (8)	1/13 (7.7)	
Diffuse positive	21/24 (88)	14/13 (92.3)	
EMA			
Negative	2/22 (9)	3/13 (23)	
Scattered positive	2/22 (9)	0/13 (0)	0.52
Focal positive	10/22 (45)	5/13 (38.5)	
Diffuse positive	8/22 (36)	5/13 (35.5)	
Ki-67 mean %	4.91	17.93	**0.001**

$P < 0.05$ was considered significant.
AMACR indicates α-methylacyl-CoA racemase; CA-IX, carbonic anhydrase 9; EMA, epithelial membrane antigen; MIA, antimitochondrial antigen.

limited in TCRCC and may also help differentiate between these tumors. The type of intervening stroma can be another helpful morphologic feature, because loose stroma was regularly seen in CRO, whereas TCRCC usually contained fibrotic and more compact stromal component. In addition, no mitotic figures were found in any of the CROs and the majority of them demonstrated lower nucleolar grades (1 or 2). In contrast, TCRCC showed focal mitotic figures in about a quarter of the cases and nucleolar grade 3 was present in 60% of TCRCC. Microscopic necrosis was not seen in any CRO, but was found in about a third of TCRCC.

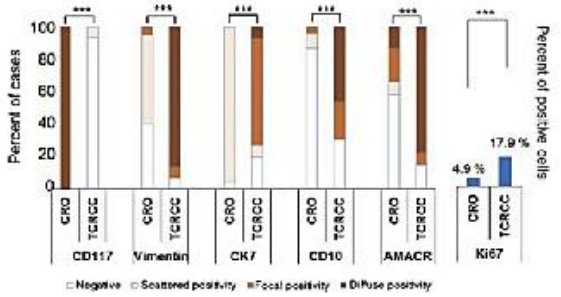

FIGURE 4. Markers useful for differential diagnosis between CRO and TCRCC. CD117 was positive in all the CRO cases, whereas negative in all but 1 case of TCRCC. CK7, vimentin, CD10, and AMACR were negative or scattered positive in majority of CRO cases, whereas they were focally or diffusely positive in most of the TCRCC cases. CRO indicates cystic renal oncocytoma; TCRCC, tubulocystic renal cell carcinoma; ***$P < 0.001$.

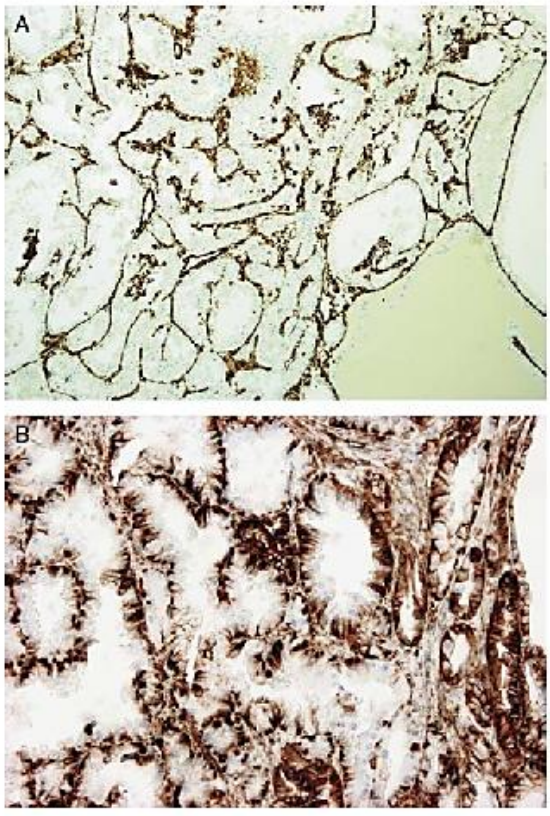

FIGURE 5. Immunoreactivity for vimentin in CRO (A) and TCRCC (B) showing diffuse positivity in TRCC and negative staining in cells of CRO (vimentin, clone D9).

The development of radiologically guided percutaneous needle biopsies, which provide small amounts of tissue or cellular material for assessment of renal masses, has introduced novel diagnostic challenges for the pathologist. In such circumstances, many morphologic features may not be available for assessment in the limited tissue and the ancillary IHC may help establish the correct diagnosis. In this study, none of the evaluated antibodies showed exclusive specificity for either CRO or TCRCC, although CD117 was highly discriminative, as all CROs were diffusely positive, whereas only 1 case of TCRCC showed weak cytoplasmic staining. We found TCRCC to be more frequently positive for vimentin, CD10, AMACR, and CK7 and had a higher proliferative index by Ki-67 (> 15%). Vimentin was very useful, as it was either negative or scattered cell positive in CRO, in contrast to TCRCC, in which it was strongly and diffusely expressed. Pattern of vimentin positivity in RO was described in detail by Hes et al in 2007. In their series, 72.6% of RO showed scattered strong positivity (single cells or small groups of cells).[14] Vimentin positivity is described as diffuse in all TCRCCs.[23,24] Results of our study are in concordance with above-mentioned data (55% of CRO with scattered positivity and 84.6% of TCRCC with diffuse strong positivity). CD10 and AMACR were both often negative in CRO, whereas diffuse or focal positivity was observed in TCRCC. CRO also consistently expressed CK7 in an isolated cells or scattered pattern, much less than observed in TCRCC. Proliferation activity in CRO was also lower (< 5% cells), whereas TCRCC demonstrated higher expression (> 15% cells). CA-IX was of limited utility as it was predominantly negative in both TCRCC and CRO. The remaining markers (AE1/AE3, CAM5.2, OSCAR, MIA, EMA) were also of limited diagnostic value.

Performing additional studies for differentiation of these tumors, including genetic and molecular, may rarely be necessary, but it may be helpful in most difficult cases. Cytogenetic changes found most frequently in RO include losses of chromosome 1 or Y and balanced translocation of the 11q13 breakpoint region.[9] Most frequent cytogenetic change in TCRCC includes gain of chromosome 7, although occasionally gains of both chromosomes 7 and 17 may occur.[11]

In conclusion, although CRO and TCRCC may present with significantly overlapping morphology, a careful morphologic assessment for the presence of solid tumor growth or islands, the type of tumor stroma, nucleolar grade, mitotic activity, and necrosis, and aided by a limited immunopanel that includes vimentin, CD10, CD117, AMACR, CK7, and Ki-67, will lead to establishing a correct diagnosis. This is important to bear in mind when faced with limited material (core biopsy or inadequate sampling) from a low-grade renal neoplasm composed of oncocytic cells arranged in a predominantly tubulary pattern.

REFERENCES

1. Eble JN, Sauter G, Epstein A, et al. *Pathology and Genetics. Tumors of the Urinary System and Male Genital Organs*. Lyon: IARC Press; 2004.
2. Kuroda N, Tanaka A, Yamaguchi T, et al. Chromophobe renal cell carcinoma, oncocytic variant: a proposal of a new variant giving a

critical diagnostic pitfall in diagnosing renal oncocytic tumors. *Med Mol Morphol*. 2013;46:49–55.
3. Hes O, Brunelli M, Michal M, et al. Oncocytic papillary renal cell carcinoma: a clinicopathologic, immunohistochemical, ultrastructural, and interphase cytogenetic study of 12 cases. *Ann Diagn Pathol*. 2006;10:133–139.
4. Mai KT, Kohler DM, Robertson SJ, et al. Oncocytic papillary renal cell carcinoma with solid architecture: mimic of renal oncocytoma. *Pathol Int*. 2008;58:164–168.
5. Petersson F, Gatalica Z, Grossmann P, et al. Sporadic hybrid oncocytic/chromophobe tumor of the kidney: a clinicopathologic, histomorphologic, immunohistochemical, ultrastructural, and molecular cytogenetic study of 14 cases. *Virchows Arch*. 2010;456:355–365.
6. Amin MB, Crotty TB, Tickoo SK, et al. Renal oncocytoma: a reappraisal of morphologic features with clinicopathologic findings in 80 cases. *Am J Surg Pathol*. 1997;21:1–12.
7. Xiao GQ, Ko HB, Unger P. Telangiectatic oncocytoma: a previously undescribed variant of renal oncocytoma. *Am J Clin Pathol*. 2013;140:103–108.
8. Kuroda N, Toi M, Hiroi M, et al. Review of renal oncocytoma with focus on clinical and pathobiological aspects. *Histol Histopathol*. 2003;18:935–942.
9. Trpkov K, Yilmaz A, Uzer D, et al. Renal oncocytoma revisited: a clinicopathological study of 109 cases with emphasis on problematic diagnostic features. *Histopathology*. 2010;57:893–906.
10. Srigley JR, Delahunt B, Eble JN, et al. The International Society of Urological Pathology (ISUP) Vancouver classification of renal neoplasia. *Am J Surg Pathol*. 2013;37:1469–1489.
11. Yang XJ, Zhou M, Hes O, et al. Tubulocystic carcinoma of the kidney: clinicopathologic and molecular characterization. *Am J Surg Pathol*. 2008;32:177–187.
12. Petersson F, Sima R, Grossmann P, et al. Renal small cell oncocytoma with pseudorosettes: a histomorphologic, immunohistochemical, and molecular genetic study of 10 cases. *Hum Pathol*. 2011;42:1751–1760.
13. Hes O, Michal M, Boudova L, et al. Small cell variant of renal oncocytoma—a rare and misleading type of benign renal tumor. *Int J Surg Pathol*. 2001;9:215–222.
14. Hes O, Michal M, Kuroda N, et al. Vimentin reactivity in renal oncocytoma: immunohistochemical study of 234 cases. *Arch Pathol Lab Med*. 2007;131:1782–1788.
15. Amin R, Anthony P. Metastatic renal oncocytoma: a case report and review of the literature. *Clin Oncol*. 1999;11:277–279.
16. Oxley JD, Sullivan J, Mitchelmore A, et al. Metastatic renal oncocytoma. *J Clin Pathol*. 2007;60:720–722.
17. Perez-Ordonez B, Hamed G, Campbell S, et al. Renal oncocytoma: a clinicopathologic study of 70 cases. *Am J Surg Pathol*. 1997;21:871–883.
18. Arguelles Salido E, Marcilla Plaza D, Medina Lopez R, et al. Renal oncocytoma. Review of our 22 patients. *Actas Urol Esp*. 2006;30:583–590.
19. MacLennan GT, Farrow GM, Bostwick DG. Low-grade collecting duct carcinoma of the kidney: report of 13 cases of low-grade mucinous tubulocystic renal carcinoma of possible collecting duct origin. *Urology*. 1997;50:679–684.
20. MacLennan GT, Bostwick DG. Tubulocystic carcinoma, mucinous tubular and spindle cell carcinoma, and other recently described rare renal tumors. *Clin Lab Med*. 2005;25:393–416.
21. Hora M, Urge T, Eret V, et al. Tubulocystic renal carcinoma: a clinical perspective. *World J Urol*. 2011;29:349–354.
22. Bhullar JS, Varshney N, Bhullar AK, et al. A new type of renal cancer—tubulocystic carcinoma of the kidney: a review of the literature. *Int J Surg Pathol*. 2013;22:297–302.
23. Skinnider BF, Folpe AL, Hennigar RA, et al. Distribution of cytokeratins and vimentin in adult renal neoplasms and normal renal tissue: potential utility of a cytokeratin antibody panel in the differential diagnosis of renal tumors. *Am J Surg Pathol*. 2005;29:747–754.
24. Alexiev BA, Drachenberg CB. Tubulocystic carcinoma of the kidney: a histologic, immunohistochemical, and ultrastructural study. *Virchows Arch*. 2013;462:575–581.

„MUCIN“ SECERNUJÍCÍ PAPILÁRNÍ RENÁLNÍ KARCINOM: KLINICKOPATOLOGICKÁ, IMUNOHISTOCHEMICKÁ A MOLEKULÁRNĚ GENETICKÁ ANALÝZA SEDMI PŘÍPADŮ

Přítomnost intersticiálního hlenu je typická mucinózní tubulární a vřetenobuněčný renální karcinom (MTVRK). Vzácně však může být mucin zastižen i v jiných typech primárních renálních tumorů než je MTVRK, jmenovitě v papilárním renálním karcinomu (PRK), světlobuněčném renálním karcinomu (SRK), renálním onkocytomu (RO) nebo papilárním adenomu (PA). Distribuce hlenu je nicméně odlišná, u posledně jmenovaných tumorů se jedná o intracytoplazmatický a/nebo intraluminální mucin, nikoliv intersticiální. Obecně však lze říci, že nález hlenového materiálu v RK vzbuzují (vyjma MTVRK) spíše podezření na sekundární neoplazii, zvláště uroteliálního či kolorektálního origa. Mucikarmin, empiricky užívané histochemické barvení na hlen a hlenu podobný materiál, je dokonce některými patology v papilárních tumorech ledvin využíváno na vyloučení renálního původu [21]. Cílem této studie bylo prokázat, že vzácně existují i mucikarmin pozitivní primární PRK.

Z plzeňského registru nádorů jsme na základě klíčových slov mezi 1311 PRK vybrali 7 mucikarmin pozitivních (intracytoplazmaticky a/nebo intraluminálně) případů PRK, které byly dále analyzovány morfologicky, histochemicky, imunohistochemicky a molekulárně geneticky (aCGH, FISH). Morfologicky (papilární architektonika) a imunohistochemicky (koexprese AMACR, vimentin, CK7) zapadaly všechny tumory do vzorce PRK, převážně typu 1. Molekulárně genetické znaky nebyly u případu 1 a 5 typické pro PRK, avšak kombinace typické morfologie a imunoprofilu nám dovolila zařadit je mezi PRK.

V této studii daváme výraz mucin do uvozovek nebo používáme termín mucinu podobný materiál, jelikož imunohistochemické rysy „hlenu“ nebyly uniformní: 5/7 případů byly silně difúzně nebo fokálně pozitivní v reakci s MUC1, 2/7 slabě fokálně pozitivní s MUC5AC, průkaz MUC2,MUC4 a MUC6 byl u všech případů negativní. Uvedené výsledky svědčí o heterogenitě hlenového materiálu.

„Mucin“ secernující PRK jsou velmi vzácné tumory, které je však dobré vzít na vědomí z důvodu možné záměny za sekundární novotvar.

MTVRK lze od „mucinózního“ PRK snadno odlišit mimojiné distribucí hlenového materiálu.

Virchows Arch (2016) 469:71–80
DOI 10.1007/s00428-016-1936-7

ORIGINAL ARTICLE

"Mucin"-secreting papillary renal cell carcinoma: clinicopathological, immunohistochemical, and molecular genetic analysis of seven cases

Kristyna Pivovarcikova[1] · Kvetoslava Peckova[1] · Petr Martinek[1] · Delia Perez Montiel[2] · Kristyna Kalusova[3] · Tomas Pitra[3] · Milan Hora[3] · Faruk Skenderi[4] · Monika Ulamec[5] · Ondrej Daum[1] · Pavla Rotterova[1] · Ondrej Ondic[1] · Magdalena Dubova[1] · Romuald Curik[1] · Ana Dunatov[6] · Tomas Svoboda[7] · Michal Michal[1] · Ondrej Hes[1,8]

Received: 28 December 2015 / Revised: 9 March 2016 / Accepted: 28 March 2016 / Published online: 12 April 2016

Abstract Mucin and mucin-like material are features of mucinous tubular and spindle renal cell carcinoma (MTS RCC) but are rarely seen in papillary renal cell carcinoma (PRCC). We reviewed 1311 PRCC and identified 7 tumors containing extracellular and/or intracellular mucinous/mucin-like material (labeled as PRCCM). We analyzed these using morphological, histochemical, immunohistochemical, and molecular genetic methods (arrayCGH, FISH). Clinical data were available for six of the seven patients (five males and one female, age range 61–78 years). Follow-up was available for four patients (2–4 years); one patient died of widespread metastases. Tumor size ranged from 3 to 5 cm (mean 3.8). Of all cases, histological architecture showed a predominantly papillary pattern. Mucin or mucin-like was extracellular in one, intracellular in three, and both intra/extracellular in three cases. All tumors were positive for AMACR, vimentin, and OSCAR, while CK7 was positive in four. Mucicarmine stain was positive in all cases, PAS in six and Alcian blue in three cases. Five tumors were positive for MUC 1, but none were positive for MUC 2, MUC 4, or MUC 6. In only four cases, genetic analysis could be performed. Gain of chromosomes 7 and 17 was found in two cases; gain of 17 only was found in one case. Loss of heterozygosity of 3p was found in one case together with polysomy of chromosomes 7 and 17. No abnormalities of *VHL*, *fumarate dehydrogenase*, and *TFE3* genes were detected. We conclude that PRCCM is a rare but challenging subtype of RCC that deserves to be further studied. In all the tumors, the mucin-like material was found in those stained with mucicarmin, but other conventional and immunohistochemical stains did not reveal consistent features of a single mucin. The molecular-genetic profile of these tumors was most consistent with that of typical papillary RCC, although one case had mixed genetic features of papillary and clear RCC. PRCCM has metastatic potential, as evidenced by one case with widespread metastases. It remains to be determined whether PRCCM represents a unique tumor subtype, deserving to be distinguished from other subtypes of PRCC.

Keywords Kidney · Papillary renal cell carcinoma · Mucin · Mucin-like secretion · Immunohistochemistry · Array CGH · FISH

✉ Ondrej Hes
hes@medima.cz

[1] Department of Pathology, Medical Faculty, Charles University and Charles University Hospital Plzen, Alej Svobody 80, 304 60 Pilsen, Czech Republic

[2] Department of Pathology, Instituto Nacional de Cancerologia, Mexico City, Mexico

[3] Department of Urology, Medical Faculty, Charles University and Charles University Hospital Plzen, Prague, Czech Republic

[4] Department of Pathology, University Hospital Sarajevo, Sarajevo, Bosna and Hercegovina

[5] Pathology Department, Clinical Hospital Center, Sestre milosrdnice, Zagreb, Croatia

[6] Department of Pathology, University Hospital Split, Split, Croatia

[7] Department of Oncology, Medical Faculty, Charles University and Charles University Hospital Plzen, Prague, Czech Republic

[8] Biomedical Centre, Faculty of Medicine in Plzen, Charles University in Prague, Plzen, Czech Republic

Introduction

Interstitial mucin is an almost constant feature of mucinous tubular and spindle RCC (MTS RCC) [1]. Other renal cell

tumors with mucin production, including mucinous papillary renal cell carcinoma (PRCC), renal papillary adenoma (RPA), renal oncocytoma (RO), and clear cell RCC (CCRCC), are rare, and most of them have been reported in the literature as case reports or a short series of cases. Mucin deposits in MPRCC, RPA, and CCRCC have been described as intracytoplasmic and intraluminal [2–5]. In RO, mucin was described in the lumen of scattered tubules but not intracytoplasmic [6].

Mucicarmine, an empirical stain for mucin and mucin-like material, has been occasionally used by pathologists to exclude renal origin in case of a papillary carcinoma with unknown primary [7]. However, rare cases of mucicarmine-positive papillary renal cell carcinomas have been reported. We therefore decided to determine how common mucicarmine-positive PRCC are and whether or not they represent a distinct clinicopathological entity. To this end, we reviewed 1311 PRCC in our files and identified 7 cases that were mucicarmine positive. This paper presents characteristics of these tumors.

Material and methods

Ten renal tumors matching keywords "unclassified, papillary, mucin, renal cell carcinoma" were retrieved out of 1311 PRCC from the Plzen Tumor Registry. All cases were reviewed by two pathologists (KPi, OH), who compared the features with the index cases. Finally, 7 cases were selected. There were 1–13 blocks available for each case; 1–2 representative blocks of each case were selected for immunohistochemical and molecular genetic study.

Tissue for light microscopy had been fixed in 4 % formaldehyde and embedded in paraffin using routine procedures. Tissue sections (4 μm) were cut and stained with hematoxylin and eosin (H&E). As special staining techniques for mucin, we used mucicarmine, Periodic Acid-Schiff (PAS), and Alcian blue at pH 2.5.

Immunohistochemical staining was performed using primary antibodies against the following antigens: racemase/AMACR (13H4, monoclonal, DAKO, Glostrup, Denmark, 1:200), carbonic anhydrase IX (rhCA9, 303123, monoclonal, RD Systems, Abingdon, GB, 1:100), vimentin VM (D9, monoclonal, NeoMarkers, Westinghouse, CA, 1:1000), MUC 1 (Ma695, monoclonal, Leica, Newcastle, UK, 1:200), MUC 5 AC (CLH2, monoclonal, Leica, 1:400), MUC 2 (Ccp58, monoclonal, Novocastra,Newcastle upon Tyne, UK, 1:400), MUCIN 4 (8G7, monoclonal, Santa Cruz Biotechnology, Dallas, TX, 1:50), MUC 6 (CLH5, monoclonal, Novocastra, 1:300), OSCAR (OSCAR, 1:500, Covance, Herts, UK, 1:500), PAX-8 (polyclonal rabbit, Cell Marque, Rocklin, CA, 1:25), CDX2 (CDX2-88, monoclonal, BioGenex, San Ramon, CA, 1:150), cytokeratin 7 (OV-TL12/30, monoclonal, DakoCytomation, Carpenteria, CA, 1:200), cytokeratin 20 (Ks20.8, monoclonal, DakoCytomation, 1:100), and cytokeratin (AE1-AE3, monoclonal, BioGenex, 1:1000). Bound antibodies were visualized using a supersensitive streptavidin-biotin-peroxidase complex (Biogenex). Appropriate positive controls were employed.

DNA extraction

DNA from macro-dissected formalin-fixed paraffin-embedded (FFPE) tissue was extracted using a QIAsymphony DNA Mini Kit (Qiagen, Hilden, Germany) on an automated system (QIAsymphony SP, Qiagen) according to the manufacturer's supplementary protocol for FFPE samples (purification of genomic DNA from FFPE tissue using the QIAamp DNA FFPE Tissue Kit and Deparaffinization Solution). Samples were then purified using Qiaquick kit (Qiagen) and eluted in EB buffer. Concentration and purity of isolated DNA was measured using NanoDrop ND-1000 (NanoDrop Technologies Inc., Wilmington, DE, USA). DNA integrity was examined by amplification of control genes in multiplex PCR [8].

Array comparative genomic hybridization

CytoChip Focus Constitutional (BlueGnome Ltd., Cambridge, UK) array was used for array comparative genomic hybridization (aCGH) analysis. It uses BAC technology and covers 143 regions of known significance with 1 Mb spacing across a genome. Probes are spotted in triplicate. First, 400 ng of DNA was labeled using a Fluorescent Labeling System (BlueGnome Ltd., Cambridge, UK). The procedure included Cy3 labeling of a test sample and Cy5 labeling of a reference sample. Commercially produced reference of the opposite sex was used when no reference sample was available (MegaPool Reference DNA Male/Female, Kreatech Diagnostics, Amsterdam, Netherlands). The labeled reference and the test sample were mixed, dried, and hybridized overnight at 47 °C using Arrayit hybridization cassette (Arrayit Corporation, California, U.S.A.). Post-hybridization washing was done using SSC buffers with increasing stringency. Dried microarrays were scanned with InnoScan 900 (Innopsys, France) at a resolution of 5 μm. Scanned images were analyzed and quantified by BlueFuse Multi software (BlueGnome Ltd., Cambridge, UK). The software uses Bayesian algorithms to generate intensity values for each Cy5 and Cy3 labeled spot on the array according an appropriate gal file. Cutoff values for log 2 ratio are preset to −0.3 for loss and to 0.3 for gain by BlueFuse software. All genomic coordinates were based on the March 2009 assembly of the reference genome GRCh37.

Fluorescent in situ hybridization (FISH)

FFPE tissue sections (4 μm) were placed onto a positively charged glass slide. The target area, corresponding to what was marked on a H&E stained slide, was circled with a diamond pen. The section was routinely deparaffinized, incubated in the 1× Target Retrieval Citrate Solution (DAKO, Glostrup, Denmark; pH 6 for 40 min at 95 °C) then cooled in the same solution (20 min at room temp). The slide was washed in deionized water and digested in protease solution with Pepsin (0.5 mg/ml in 0.01 M HCl; Sigma Aldrich, St. Louis, MO, USA) at 37 °C for 15 min. The slide was then immersed in deionized water for 5 min, dehydrated in a series of ethanol solutions (70, 85, and 96 %, 2 min each), and air-dried. Fluorescent in situ hybridization (FISH) probes CEP 7 Spectrum Orange (D7Z1), CEP 17Spectrum Orange, CEP X (DXZ1) Spectrum Green/CEP Y (DYZ3), and Spectrum Orange (Vysis/Abbott Molecular, Des Plaines, Illinois) were mixed with water and hybridization buffers according to the manufacturer's protocol. The slide was incubated in a ThermoBrite instrument (StatSpin/Iris Sample Processing, Westwood, Massachusetts) with codenaturation (85 °C for 8 min) and hybridization (37 °C for 16 h). Post-hybridization wash was performed in 2× SSC/0.3 % NP-40 solution (72 °C for 2 min). The section was counterstained with DAPI I (Vysis) and stored in the dark at −20 °C until examined. FISH signals were assessed using an Olympus BX51 fluorescence microscope. Scoring of aneuploidy was performed by counting the number of fluorescent signals in 100 randomly selected, non-overlapping tumor cell nuclei. The slide was independently enumerated by two observers (PG, TV). Cutoff values were set for each probe as shown in previous study [9].

Results

Clinical data were available for six of the seven cases (Table 1). These included five males and one female, age range 61 to 78 years (median 74 years, mean 71.17 years). Tumor size ranged from 3 to 5 cm in the greatest dimension (median 3.5 cm, mean 3.8 cm). One tumor was found in the left kidney and two in the right kidney; no information about laterality was available for four cases. On gross section, the tumors were yellowish to gray-white to grayish-brown, with visible hemorrhages in two cases.

Follow-up was available for four patients (range 2 to 4 years, mean 2.75 years, median 2.5 years). One patient died of disease 4 years after diagnosis despite treatment (sunitinib). One patient died of colorectal adenocarcinoma 2 years after diagnosis. Two patients are alive and well without signs of recurrence or metastasis, although for one patient, only basic and limited information was available. Other patients were lost to follow-up.

Histological findings

The histopathological features are summarized in Table 2. All seven cases showed at histological examination a papillary pattern architecture (Fig. 1). In two cases, a prominent tubulopapillary component (cases 4 and 5) was noted (Fig. 2). Cases 2 and 3 contained smaller areas with a solid pattern. Bluish to eosinophilic mucin-like material was present to a variable extent in all cases (Fig. 3a, b). This was only extracellular in one case; in three cases, it was only intracellular; and in three cases, it was present both intracellularly and extracellularly in H&E-stained sections.

Extracellular material presented as a bluish to eosinophilic deposit of mucin-like material in the interstitium between tumor cells or within papillary stalks. Intracellular material presented as a mucin-like substance in the cytoplasm as larger or smaller clear vacuoles. Some of these cells had the features of signet-ring cells (Fig. 4a, b) and they were present in five cases. In all cases, mucin-like material was positive for mucicarmine (Fig. 5), and in six cases, it was PAS positive (Fig. 6). In three cases, the cells were reactive with Alcian blue, and this was designated as PAS and Alcian blue co-staining. The intracellular mucin-like material was positive either for mucicarmine or for PAS in two of the cases containing cells with signet-ring

Table 1 Basic clinicopathological data

Case	Sex	Age (years)	Size (cm)	Site	Stage	Color	Follow-up
1	F	78	3 × 2 × 1.5	NA	pT1a (TNM09)	NA	NA
2	M	77	3 × 3.5 × 1.5 and 2 × 1.5 × 1	Right	pT1a (TNM09)	Ochroid	2 years, AW
3	M	76	3.5 × 2.5 × 3	Right	pT1 (TNM09)	Yellowish	Dead of disease 4 years after dg.
4	M	63	Diameter 5	NA	NA	NA	NA
5	NA	NA	NA	NA	NA	NA	NA
6	M	61	3 × 3.7 × 4	NA	NA	Gray-white	3 years, A, no information about health condition
7	M	72	NA	Left	NA	Grayish-brown	Dead 2 years after dg.—other malignant disease

M male, *F* female, *NA* not available, *AW* alive and well, *A* alive

Table 2 Histopathological features

Case	Papillary	Tubulopapillary	Solid	Extracellular mucin-like secretion	Intracellular mucin-like secretion	Signet-ring morphology	Hibernoma-like changes	Psammoma bodies	Siderophages	Foamy macrophages	Giant cells	Heamorrhage	Fuhrman grade (ISUP)	Type
1	+	–	–	+ (intraluminal)	+	+	–	–	–	–	–	–	2	1
2	+	–	+ (10 %)	+ (papillary stroma)	+	–	–	–	–	+	–	+	2	1
3	+	–	+ (20 %)	–	+	+	+	+	+	+	+	+	4	NOS
4	+	+ (80 %)	–	+ (papillary stroma)	–	–	–	–	–	+	–	–	2	1
5	+	+	–	+ (intraluminal)	+	+	–	–	–	+	–	–	3	NOS
6	+	–	–	–	+	+	–	–	+	+	+	+	3	2
7	+	–	–	–	+	+	+	–	+	+	+	+	3	2

+ = present, – = absent, *NOS* not otherwise specified

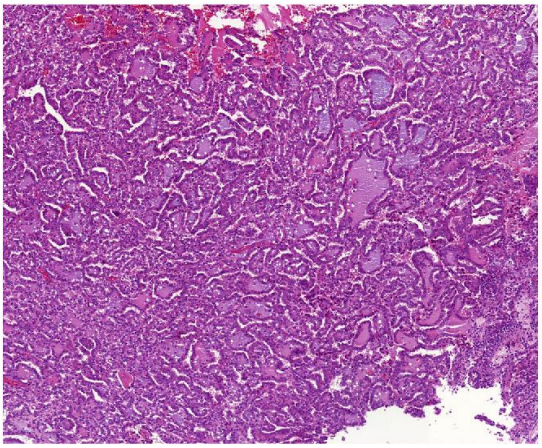

Fig. 1 All 7 cases were arranged in papillary pattern

morphology. In three of the cases, cells with signet-ring morphology did not react with mucicarmine nor PAS. Four tumors contained hemorrhagic areas. Foamy macrophages were found in six cases. Hemosiderophages were observed in three cases and in two cases (cases 3 and 7) clear cell-like areas, containing cells with foamy cytoplasm and microvacuolated appearance resembling macrophages or hibernoma cells (Fig. 7). These tumors both contained also giant multinucleated neoplastic cells.

In addition to these morphological features, we found a focus with epithelial cells in pseudorosette formation in case 3, numerous extracellular eosinophilic globules, and larger pools of eosinophilic material in case 5 and in case 6 abundant giant multinucleated cells and foamy macrophages.

Nuclear grades according to the "Fuhrman (ISUP) nucleolar" grading system was 4 (one case), 3 (three cases), and 2 (three cases). No relationship or direct connection with renal pelvis or calyces was seen.

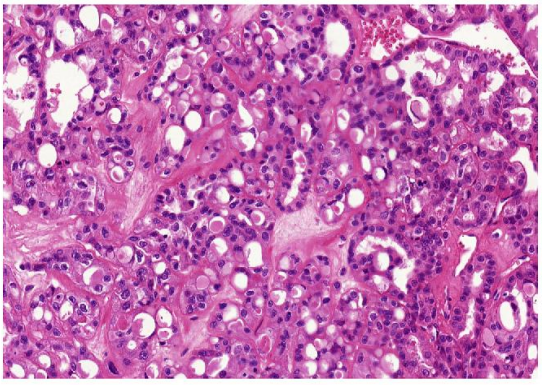

Fig. 2 Focus of tubulopapillary architecture was noted in 2 cases

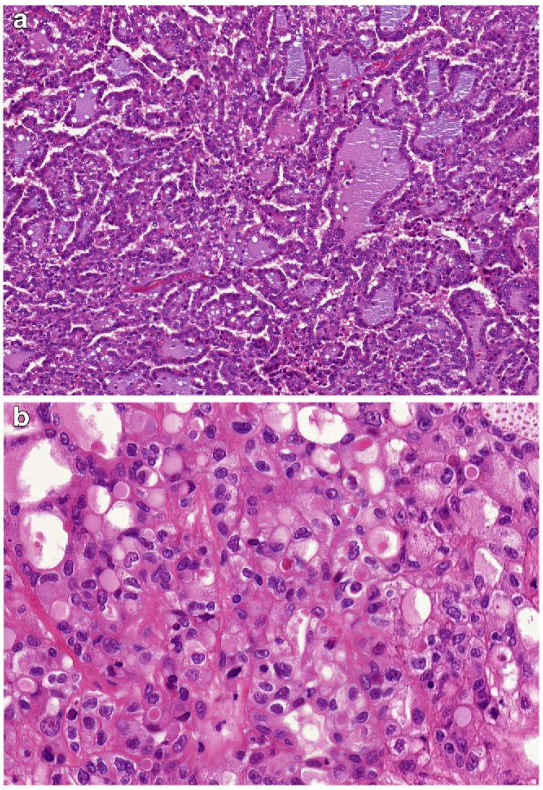

Fig. 3 Bluish to eosinophilic mucin-like secretion was variably present in all cases in the intersticium (**a**) or in intracellular vacuoles (**b**)

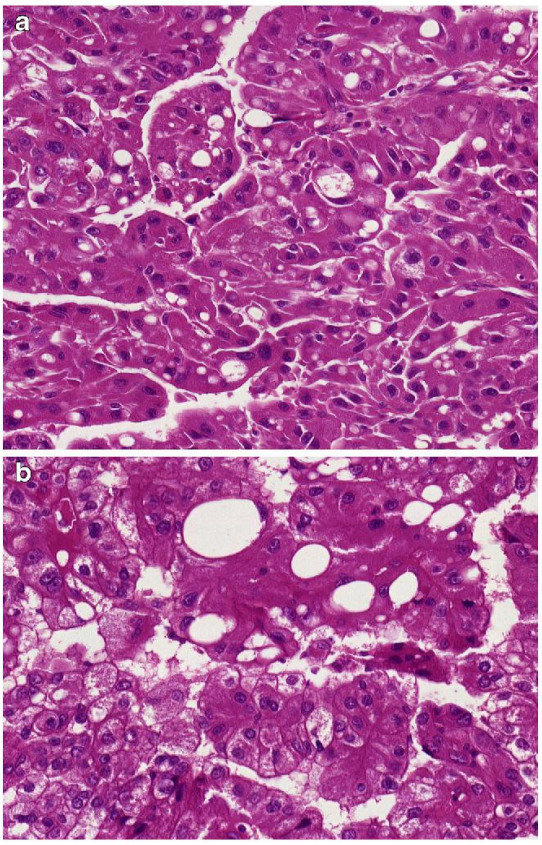

Fig. 4 As intracellular production was considered presence of the same material within cytoplasm in form of larger or smaller vacuoles. Some such cells reached the shape and characteristics of signet-ring cells (**a+b**)

Immunohistochemical analysis

Results of immunohistochemical examination are summarized in Table 3. All tumors were positive for AMACR, vimentin, and OSCAR. Keratin AE1-AE3 was diffusely positive in five tumors. CK 7 was diffusely positive in three (Fig. 8), focally in one case, and was negative in three cases. CK 20 was focally moderately positive in one tumor (CK 7 was negative in this case). Carbonic anhydrase IX was focally moderately positive in one case. PAX 8 was positive in six tumors, five strongly and diffuse, one focally. All tumors were negative for CDX2.

Mucin-like deposits were examined using a panel of antibodies against different MUC antigens (Table 4). MUC 1 was diffusely strongly positive in two cases and focally in three cases (two strongly and one moderately) (Fig. 9). None of the tumors were reactive for MUC 2, MUC 4, and MUC 6. Two cases were weakly positive for MUC 5 AC.

Molecular genetic analysis

Results of molecular genetic analyses are summarized in Table 5. Array CGH analysis was performed on one case (case

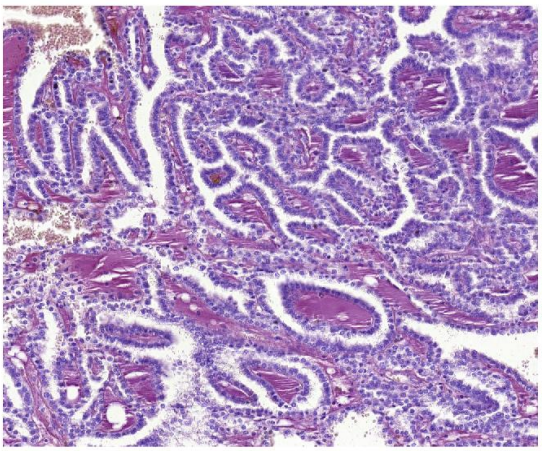

Fig. 5 Interstitial mucin-like material was positive for mucicarmin

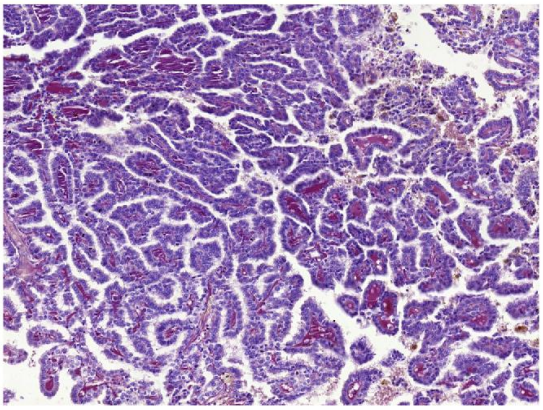

Fig. 6 The same interstitial deposition was positive for PAS

2), which showed gain of chromosomes 7, 16, and 17 and loss of chromosome Y. FISH was performed on four cases. Polysomy of chromosomes 7 and 17 was found in two cases. In one case, polysomy of only chromosome 17 was present. One case (case 1) was disomic for both chromosomes 7 and 17. Loss of heterozygosity (LOH) of chromosome 3p was assessed in five cases and was positive in one case (case 5), which also showed polysomy of chromosomes 7 and 17. In none of the six cases analyzed were mutations found in the *VHL* gene. We found no methylation of *VHL* gene promoter in the six cases analyzed.

Discussion

RCC with mucin or mucin-like secretion was initially published in 1963 by Foster and Levine [10], who reported Mayer's mucicarmine positive material in 2 out of 71 renal cell carcinomas. Their description unfortunately does not allow any conclusion as to the histological type according to current classifications [11]. Grignon et al. [12] described an RCC with luminal and cytoplasmic presence of mucin, reactive with Mayer's mucicarmine and Alcian blue. The documentation allows to conclude that this tumor was a papillary RCC with mucin/mucin-like secretion [12].

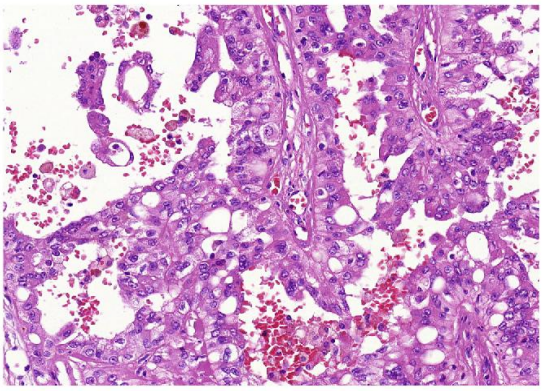

Fig. 7 Focally, cells had foamy cytoplasm and microvacuolated appearance resembling macrophages or hibernoma cells

The term "mucin" encompasses a large family of glycoproteins expressed by many normal and neoplastic cell types. Two main classes are distinguished: membrane-bound and secreted or gel forming [13]. Mucin can be stained empirically with mucicarmine, historically regarded as highly sensitive [14]. Recent studies correlating the results of mucicarmine staining with immunohistochemical staining for various antigens specific for individual mucin subtypes are lacking. Staining with PAS and Alcian blue might be more sensitive as they cover both neutral and acidic mucins, produced by epithelial or mesenchymal cells. However, these stains lack specificity as they also bind to other substances such as glycosylated proteins.

Of the MUC family, only MUC1 is expressed in normal epithelial cells of the kidney. MUC2, a secreted gel-forming mucin, is typically secreted by goblet cells of the gastrointestinal and respiratory tract [15]. MUC4 is a transmembrane glycoprotein, which provides a protective layer of mucus to epithelial cells of the intestine, airways, and mammary ducts [16]. MUC5AC is found mainly in the mucosal layer of the stomach, while MUC6 is located principally in gastric pyloric glands [17]. MUC 1 is expressed in convoluted distal tubules and in collecting ducts in normal renal tissue, with a polar apical distribution [18–20]. Leroy et al. reported that MUC1 is expressed in 54 % of PRCC. They found that MUC1 is predominantly expressed in type 1 PRCC and only rarely in type 2 PRCC [21].

The most frequent type of renal cell carcinoma with mucin production is MTS RCC, which is composed of tubules, many of which are elongated and merge into cord-like structures with transitions into spindle cells. Weakly basophilic mucin is present at least focally in most tumors [22], located mostly in the interstitium, and a proper term for such a finding would be myxoid rather than mucinous. Fine et al. mapped the histologic spectrum of MTS RCC and documented cases of MTS RCC without conspicuous extracellular mucin in H&E-stained sections [23]. However, scant mucinous material within cellular areas has been reported in these "mucin-poor" MTS RCC [24].

Our cases were completely different from MTS RCC. Tumors from our series lacked typical dual architecture; tubules lined by cuboidal cells were not encountered nor a spindle cell component with characteristic myxoid changes in the stroma. Immunohistochemical staining does not distinguish between PRCC and MTS RCC because of an overlapping

Table 3 Immunohistochemical examination

Case	AMACR	CANH9	VIM	OSCAR	AE1/3	PAX8	CK7	CK20	CDX2
1	+++	−	+++	+++	++	+++	++	−	−
2	+++	++ Foc.	+++	+++	++	+++	+++	−	−
3	+++	−	+++	+++	++	+++	+++ Foc.	−	−
4	++	−	+++	+++	+++	+++	+++	−	−
5	+++	−	+++	+++	+++	+++	−	−	−
6	++	−	+++	+	−	++ Foc.	−	−	−
7	+++	−	++	+	−	−	−	++ Foc.	−

Foc. = < 50 % cells staining, − = negative, + = weak positivity, ++ = moderate positivity, +++ = strong positivity, *AMACR* racemase, *CANH9* carbonic anhydrase, *AE1/3* cytokeratin AE1-AE3, *vim* vimentin

marker profile. However, a molecular genetic profile might help to differentiate between these entities. We have documented gain of chromosomes 7, 16, and 17 and loss of chromosome Y using array CGH analysis, confirmed subsequently by FISH. The pattern of these numerical chromosomal aberrations is not compatible with that of MTS RCC, which shows disomy of chromosomes 7 and 17 and chromosomal loss, notably of chromosomes 1, 4, 6, 8, 9, 13, 14, 15, and 22, regardless of grade [23].

Mucin production has been described in three primary papillary RCCs, which showed eosinophilic cuboidal to columnar cells and extensive luminal or intracytoplasmic acid mucin deposition, including sulphomucins as indicated by mucicarmine, Alcian blue (at pH 2.5), and high-iron diamine staining. Furthermore, foam cells (in two cases), hemosiderin, and siderophages (in two cases), calcification (in one case), and an incomplete fibrous capsule were described [2] [3]. Mucin production has also been reported in four papillary adenomas. Mucin was of acid type, as indicated by mucicarmine, Alcian blue (at pH 2.5), and Mowry's colloidal iron staining, intracellular in numerous scattered tumor cells in two cases, focal luminal in one case, and mixed intracellular and luminal in another case [4].

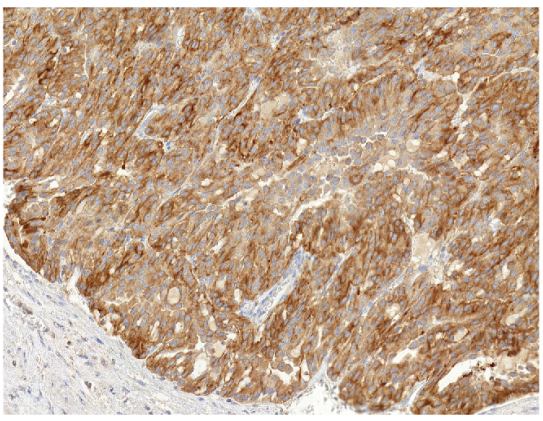

Fig. 8 CK 7 was diffusely positive in three cases

In this study, all tumors were classified as PRCC. Morphological and immunohistochemical features were mostly compatible with type 1 PRCC; however, some morphologic variability was noted [25]. All tumors expressed AMACR, vimentin, and OSCAR while four cases expressed CK 7. Architecture was predominantly papillary, even in CK 7-negative tumors. CK 7-negative PRCC has been reported notably by Langner et al. who described variable CK 7 reactivity in renal cell carcinoma subtypes, including PRCC [9]. Morphology and marker expression pattern (coexpression of AMACR, vimentin, and CK 7-among others) of our case 1 was typical of PRCC. However, for PRCC disomy of chromosomes 7, 17, and Y is unusual. Case 5 showed polysomy of chromosomes 7 and 17, supernumerary chromosome X, and LOH3p, compatible with both PRCC and clear cell RCC but morphology was consistent with PRCC. The marker expression pattern (CK 7 and carbonic anhydrase IX both negative) in this case was unusual for PRCC. We used morphology as ultimate criterion and considered the case as PRCC. Two more cases were not entirely typical of PRCC (cases 6 and 7) because they were negative for CK 7. Genetic analysis could not be performed on case 7 due to low quality of DNA. In case 6, status of the *VHL* gene (mutations, LOH3p, and methylation status) was normal but it showed loss of chromosome Y, which fits with PRCC. However, analysis of chromosomes 7 and 17 failed because of low-quality DNA.

We introduced the term "mucin-like" instead of "mucinous" because of the results of immunohistochemical staining for MUC antigens. The MUC antigens most commonly expressed in human mucinous carcinomas are MUC1, MUC2, MUC4, MUC5AC, and MUC6. Lack of expression of these antigens raises questions as to specificity of traditional stains (mucicarmine, PAS, Alcian blue) used to detect mucin. Reports on mucin deposits in tumors based only on traditional stains should be interpreted with caution when the results are not corroborated by immunohistochemistry. In all our cases, in H&E-stained sections, mucin-like material was present. Mucin-like material was

Table 4 Mucin staining

Case	Mucicarmine	Periodic Acid Schiff	Alcian blue	MUC1	MUC2	MUC4	MUC5AC	MUC6
1	+	++	−	+++ Foc.	−	−	−	−
2	+++ Foc.	+	+	+++ Foc.	−	−	+	−
3	+ Foc.	++	−	++ Foc.	−	−	−	−
4	+	−	+	+++	−	−	−	−
5	+	++	+	+++	−	−	+ Foc.	−
6	+ Foc.	+ Foc.	−	−	−	−	−	−
7	+ Foc.	+ Foc.	−	−	−	−	−	−

Foc. = < 50 % cells staining, − = negative, + = weak positivity, ++ = moderate positivity, +++ = strong positivity

intracytoplasmic in six cases, extracellular (intraluminal or in the stroma) in four cases. The interstitial myxoid changes were exclusively found in the core of papillae. Areas with diffuse myxoid changes which are seen in MTS RCC were absent. In five cases, we found cells with signet-ring morphology. Signet-ring cells are tumor cells with intracytoplasmic mucin that displaces the nucleus and their presence favors a diagnosis of signet-ring cell carcinoma regardless of site [26]. In two of our cases, mucicarmine or PAS-positive cells with signet-ring morphology were found which we considered as signet-ring cells. In three other cases, the cells with signet-ring morphology were negative for mucicarmine and PAS.

In the differential diagnosis of MTS RCC, several entities should be considered.

1. Hereditary leiomyomatosis renal cell carcinoma syndrome-associated renal cell carcinoma (HLRCC) arises in patients with a germline mutation in the *fumarate hydratase* (*FH*) gene. These tumors often have a papillary architecture but can be tubulopapillary, cribriform, or solid [22]. Even though the morphology of our tumors was not entirely compatible with HLRCC, we tested four cases for *FH* gene mutation but all of them showed a wild type *FH* gene.
2. Val-Bernal described a case of RO, composed of typical oncocytes in a predominantly tubular pattern and scattered tubules containing basophilic mucin (positive with Alcian blue at pH 2.5 and Mayer's mucicarmin), in the lumen but not intracytoplasmic. Immunohistochemistry was not reported. Tumor cells did not show gain of chromosomes 7 and 17 [6]. Our cases differed from RO in terms of morphology and marker profile, being mostly papillary and with expression of different markers. Chromosomal analysis with polysomy of chromosomes 7 and 17 supports our diagnosis of RCC. An oncocytic variant of PRCC has been reported but with morphologic characteristics different from our cases.
3. Val-Bernal also reported extracellular mucin within alveoli in CCRCC but only occasionally in the cytoplasm of neoplastic cells [24]. The mucin stained with Mayer's mucicarmine, Alcian blue-PAS (at pH 2.5), and Mowry's colloidal iron. Staining with Alcian blue at pH 0.4 indicated the presence of strongly acidic sulphated mucosubstances [5]. Our cases showed characteristic papillary architecture without clear cell elements. The marker profile was typical of PRCC only in four cases, with coexpression of vimentin and AMACR even in CK 7-negative tumors. Moreover, *VHL* was not mutated and its promoter not methylated. LOH of 3p was observed in one out of five analyzable cases. The latter case showed polysomy of chromosomes 7 and 17 and an unusual XXY pattern of sex chromosomes.

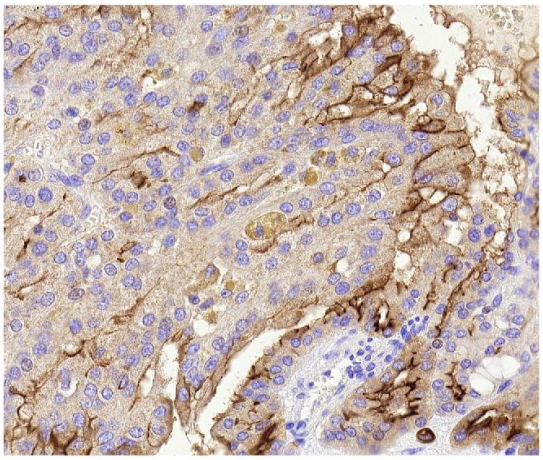

Fig. 9 MUC 1 was diffusely strongly positive in two cases and focally in three cases

Mucin/mucin-like secretion along with papillary architecture is more common in urothelial carcinomas (UC). Primary adenocarcinoma, UC with signet-ring cells, UC with gland-like lumina, and colonic types (villous

Table 5 Results of molecular genetic analyses

Case	Array CGH	LOH3p	TFE3F	TFEBF	VHL	VHLM	FISH 7	FISH16	FISH17	FISH Y	FH
1	NA	−	−	NA	−	−	D	−	D	XY	−
2	+7, +16, +17, −Y	−	−	NA	−	−	P	P	P	−Y	−
3	NA	NP	−	NA	−	−	NA	NA	NA	−Y	NA
4	NA	−	−	−	−	−	D	NA	P	−Y	−
5	NA	+	NA	NA	−	−	P	NA	P	XXY	NA
6	NA	−	NA	NA	−	−	NA	NA	NA	−Y	−
7	NA	NA	NA	NA	NA	NA	NA	NA	NA	NA	NA

− = negative, + = positive, *NA* not analyzable, *NP* not performed, − *Y* loss of chromosome Y, *VHL VHL* mutation, *VHLM VHL* methylation, *FH fumarate hydratase gene* mutation, *P* polysomy, *D* disomy

adenomas, villous carcinomas) are not extremely rare subtypes, and several reports have been published of such tumors in the whole urinary tract [27] [28]. Morphology of UC can be polymorphic and histochemical features and marker profile may vary. Glandular differentiation is observed in less than 10 % of urothelial carcinomas, usually in the form of small tubular or gland-like spaces in conventional urothelial carcinoma [29] [30]. Less frequently, foci similar to colonic-type adenocarcinoma can be found in otherwise typical UC and, rarely, a signet-ring cell or a mucinous component [31]. Primary adenocarcinoma is extremely rare in the renal pelvis, while at approximately 2 % of primary epithelial malignancies in the urinary bladder [6,8]. This entity includes primary bladder adenocarcinoma (non-urachal adenocarcinoma) and urachal carcinoma. Primary bladder adenocarcinoma develops in transitional epithelium through gradual changes (intestinal metaplasia) initiated by chronic inflammation [32]. Urachal carcinoma is less common than non-urachal adenocarcinoma of the bladder and arises from urachal remnants [10] [33]. Colonic-type villous adenoma and adenocarcinoma of the urinary tract are rare. Villous adenoma is characterized by papillary structures covered by columnar mucinous epithelium, as in colonic villous adenoma. Often an infiltrating adenocarcinoma coexists, which emphasizes the need to adequate sampling of any lesion diagnosed by biopsy as villous adenoma [28]. Our cases were located in the renal cortex or paracortex, without any connection with pelvic-calyceal system. No signs of urothelial differentiation were found, marker pattern was also unlike UC. One case was focally positive for CK 20 but not for CK 7.

The patient of case 7 died of metastatic colorectal carcinoma. In this case, the architecture of renal tumor was papillary, without tubules or dirty necrosis. Although the renal tumor was focally positive for CK 20, it also expressed vimentin and AMACR, which would be extremely unusual for metastasis of colorectal adenocarcinoma.

Conclusions

1. PRCCs with mucin/mucin-like secretion are rare (<0.5 % of all PRCC), and defining their morphology, immunohistochemical, and molecular genetic profile remains a challenge.
2. Mucicarmine-positive secretion does not rule out a diagnosis of PRCC.
3. A genuine mucin nature of the secreted material still needs to be confirmed by immunohistochemical analysis. Whether what is secreted in these PRCC cases is mucin or mucin-like remains to be clarified.
4. In the differential diagnosis of RCC with mucin/mucin-like secretion, in addition to tumors originating in renal parenchyma, also, lesions of urothelial origin should be considered, as they are more often mucicarmine positive.
5. PRCCs with mucin/mucin-like secretion have metastatic potential.

Acknowledgments The authors thank Dr. Ivan Damjanov for his help with the editing of our paper and for the constructive discussion.

Compliance with ethical standards The study was approved by local Ethics Committee (Medical Teaching Hospital and Medical School of Charles University in Plzen).

Funding The study was supported by the Charles University Research Fund (project number P36), by the project CZ.1.05/2.1.00/03.0076 from European Regional Development Fund, and by SVV 260283.

Conflict of interest The authors declare no conflict of interest.

References

1. Hes O, Hora M, Perez-Montiel DM, Suster S, Curik R, Sokol L, Ondic O, Mikulastik J, Betlach J, Peychl L, Hrabal P, Kodet R, Straka L, Ferak I, Vrabec V, Michal M (2002) Spindle and cuboidal renal cell carcinoma, a tumour having frequent association with nephrolithiasis: report of 11 cases including a case with hybrid conventional renal cell carcinoma/spindle and cuboidal renal cell carcinoma components. Histopathology 41:549–555

2. Val-Bernal JF, Gomez-Roman JJ, Vallina T, Villoria F, Mayorga M, Garcia-Arranz P (1999) Papillary (chromophil) renal cell carcinoma with mucinous secretion. Pathol Res Pract 195:11–17
3. Val-Bernal JF, Mayorga M, Garcia-Arranz P, Gomez-Roman JJ (1998) Mucin secretion in papillary (chromophil) renal cell carcinoma. Am J Surg Pathol 22:1037–1040
4. Val-Bernal JF, Pinto J, Gomez-Roman JJ, Mayorga M, Villoria F (2001) Papillary adenoma of the kidney with mucinous secretion. Histol Histopathol 16:387–392
5. Val-Bernal JF, Salcedo W, Val D, Parra A, Garijo MF (2013) Mucin-secreting clear cell renal cell carcinoma. A rare variant of conventional renal cell carcinoma. Ann Diagn Pathol 17:226–229
6. Val-Bernal JF, Val D, Garijo MF (2011) Mucin-producing renal oncocytoma. An undescribed variant of oncocytoma. Pathol Res Pract 207:271–274
7. A Renshaw, Fine needle aspiration of the kidney, In: Bostwick D, Cheng L. (eds) Urologic Surgical Pathology (2st ed), (2008) 196–213.
8. van Dongen JJ, Langerak AW, Bruggemann M, Evans PA, Hummel M, Lavender FL, Delabesse E, Davi F, Schuuring E, Garcia-Sanz R, van Krieken JH, Droese J, Gonzalez D, Bastard C, White HE, Spaargaren M, Gonzalez M, Parreira A, Smith JL, Morgan GJ, Kneba M, Macintyre EA (2003) Design and standardization of PCR primers and protocols for detection of clonal immunoglobulin and T-cell receptor gene recombinations in suspect lymphoproliferations: report of the BIOMED-2 Concerted Action BMH4-CT98–3936. Leukemia 17:2257–2317
9. Sperga M, Martinek P, Vanecek T, Grossmann P, Bauleth K, Perez-Montiel D, Alvarado-Cabrero I, Nevidovska K, Lietuvietis V, Hora M, Michal M, Petersson F, Kuroda N, Suster S, Branzovsky J, Hes O (2013) Chromophobe renal cell carcinoma–chromosomal aberration variability and its relation to Paner grading system: an array CGH and FISH analysis of 37 cases. Virchows Archiv: Int J Pathol 463:563–573
10. Gopalan A, Sharp DS, Fine SW, Tickoo SK, Herr HW, Reuter VE, Olgac S (2009) Urachal carcinoma: a clinicopathologic analysis of 24 cases with outcome correlation. Am J Surg Pathol 33:659–668
11. Foster EA, Levine AJ (1963) Mucin production in metastatic carcinomas. Cancer 16:506–509
12. Grignon DJ, Ro JY, Ayala AG (1988) Primary mucin-secreting adenocarcinoma of the kidney. Archiv Pathol Laboratory Med 112:847–849
13. Fowler J, Vinall L, Swallow D (2001) Polymorphism of the human muc genes. Front Biosci J Virtual Library 6:D1207–D1215
14. Lauren PA, Sorvari TE (1969) The histochemical specificity of mucicarmine staining in the identification of epithelial mucosubstances. Acta Histochem 34:263–272
15. Gum JR Jr, Hicks JW, Toribara NW, Siddiki B, Kim YS (1994) Molecular cloning of human intestinal mucin (MUC2) cDNA. Identification of the amino terminus and overall sequence similarity to prepro-von Willebrand factor. J Biol Chem 269:2440–2446
16. Jonckheere N, Van Seuningen I (2010) The membrane-bound mucins: from cell signalling to transcriptional regulation and expression in epithelial cancers. Biochimie 92:1–11
17. Ho SB, Shekels LL, Toribara NW, Kim YS, Lyftogt C, Cherwitz DL, Niehans GA (1995) Mucin gene expression in normal, preneoplastic, and neoplastic human gastric epithelium. Cancer Res 55:2681–2690
18. Cao Y, Karsten U, Zerban H, Bannasch P (2000) Expression of MUC1, Thomsen-Friedenreich-related antigens, and cytokeratin 19 in human renal cell carcinomas and tubular clear cell lesions. Virchows Archiv Int J Pathol 436:119–126
19. Kraus S, Abel PD, Nachtmann C, Linsenmann HJ, Weidner W, Stamp GW, Chaudhary KS, Mitchell SE, Franke FE, el Lalani N (2002) MUC1 mucin and trefoil factor 1 protein expression in renal cell carcinoma: correlation with prognosis. Human Pathol 33:60–67.
20. Leroy X, Copin MC, Devisme L, Buisine MP, Aubert JP, Gosselin B, Porchet N (2002) Expression of human mucin genes in normal kidney and renal cell carcinoma. Histopathology 40:450–457
21. Leroy X, Zini L, Leteurtre E, Zerimech F, Porchet N, Aubert JP, Gosselin B, Copin MC (2002) Morphologic subtyping of papillary renal cell carcinoma: correlation with prognosis and differential expression of MUC1 between the two subtypes. Modern Pathol Off J United States Canadian Acad Pathol Inc 15:1126–1130
22. Srigley JR, Delahunt B, Eble JN, Egevad L, Epstein JI, Grignon D, Hes O, Moch H, Montironi R, Tickoo SK, Zhou M, Argani P, Panel IRT (2013) The International Society of Urological Pathology (ISUP) Vancouver Classification of renal Neoplasia. Am J Surg Pathol 37:1469–1489
23. Peckova K, Martinek P, Sperga M, Montiel DP, Daum O, Rotterova P, Kalusova K, Hora M, Pivovarcikova K, Rychly B, Vranic S, Davidson W, Vodicka J, Dubova M, Michal M, Hes O (2015) Mucinous spindle and tubular renal cell carcinoma: analysis of chromosomal aberration pattern of low-grade, high-grade, and overlapping morphologic variant with papillary renal cell carcinoma. Ann Diagn Pathol 19:226–231
24. Fine SW, Argani P, DeMarzo AM, Delahunt B, Sebo TJ, Reuter VE, Epstein JI (2006) Expanding the histologic spectrum of mucinous tubular and spindle cell carcinoma of the kidney. Am J Surg Pathol 30:1554–1560
25. Delahunt B, Eble JN (1997) Papillary renal cell carcinoma: a clinicopathologic and immunohistochemical study of 105 tumors. Modern Pathol Off J United States and Canadian Acad Pathol Inc 10:537–544
26. Sung CO, Seo JW, Kim KM, Do IG, Kim SW, Park CK (2008) Clinical significance of signet-ring cells in colorectal mucinous adenocarcinoma. Modern Pathol Off J United States and Canadian Acad Pathol Inc 21:1533–1541
27. Alvarado-Cabrero D, Perez-Montiel O (2008) Hes, Multicystic urothelial carcinoma of the bladder with gland-like lumina and with signet-ring cells. A case report. Diagn Pathol 3:36
28. Seibel JL, Prasad S, Weiss RE, Bancila E, Epstein JI (2002) Villous adenoma of the urinary tract: a lesion frequently associated with malignancy. Hum Pathol 33:236–241
29. Lopez-Beltran L (2006) Cheng, histologic variants of urothelial carcinoma: differential diagnosis and clinical implications. Hum Pathol 37:1371–1388
30. Black PC, Brown GA, Dinney CP (2009) The impact of variant histology on the outcome of bladder cancer treated with curative intent. Urol Oncol 27:3–7
31. Amin MB (2009) Histological variants of urothelial carcinoma: diagnostic, therapeutic and prognostic implications. Modern Pathol Off J United States and Canadian Acad Pathol Inc 22(Suppl 2):S96–S118
32. Thomas DG, Ward AM, Williams JL (1971) A study of 52 cases of adenocarcinoma of the bladder. Br J Urol 43:4–15
33. Paner GP, Barkan GA, Mehta V, Sirintrapun SJ, Tsuzuki T, Sebo TJ, Jimenez RE (2012) Urachal carcinomas of the nonglandular type: salient features and considerations in pathologic diagnosis. Am J Surg Pathol 36:432–442

WARTHINOVU TUMORU PODOBNÝ PAPILÁRNÍ RENÁLNÍ KARCINOM: KLINICKOPATOLOGICKÁ, MORFOLOGICKÁ, IMUNOHISTOCHEMICKÁ A MOLEKULÁRNĚ GENETICKÁ ANALÝZA 11 PŘÍPADŮ

Renální karcinom je velmi heterogenní skupina tumorů, nově vydaná WHO klasifikace (2016) čítá na 14 typů jednotek [4] a, zvláště díky rychlému rozvoji genetických metod, nové rychle přibývají. Papilární renální karcinom (PRK) se tradičně dělí na typ 1 a 2, přičemž typ 1 je poměrně uniformní skupina, zatímco typ 2 je ve více aspektech značně heterogenní. Jako příklad poslouží nedávno popsané jednotky jako onkocytický, „mucin"-secernující, solidní, se světlobuněčnými znaky či bifazický alveoloskvamoidní karcinom [22-26],které se všechny řadí pod typ 2 PRK. Onkocytický papilární renální karcinom (OPRK) je v současné WHO klasifikaci zařazen jako další potencionální podtyp PRK. Histologicky je OPRK charakterizován proliferací velkých eosinofilních buněk podobných renálnímu onkocytomu (RO), uspořádáných nejčastěji papilárně, vzácněji tubulárně nebo solidně.

Do studie bylo zařazeno 11 případů OPRK, které vykazovaly výraznou denzní lymfocytární stromální infiltraci a napodobovaly tak Warthinův tumor slinných žláz nebo Warthin-like variantu papilárního karcinomu štítné žlázy. Imunoprofil renálních tumorů však odpovídal PRK a reakce s TTF-1 byla negativní, což metastatický původ vyloučilo.

Tumor infiltrující lymfocyty (TIL) a peritumorální lymfocyty jsou častým doprovodným znakem karcinomů spojených s Lynchovým syndromem. Imunohistochemická nukleární exprese tzv. mismatch repair proteinů MLH1 a PMS2 byla zachována ve všech případech Warthin-like PRK (WPRK), MSH2 a MSH6 byly v 1/11 případů negativní. Tento případ byl následně geneticky otestován na přítomnost mikrosatelitní instability, metylaci MLH1 promotoru a mutaci genu *BRAF V600E*, vše s negativním výsledkem, což nepoukazuje na spojitost TIL v WPRK s Lynchovým syndromem a zároveň i vylučuje účast vyšetřovaných *MMR* genů na tumorigenezi WPRK.

Cílem naší práce bylo rozšířit řady heterogenní skupiny PRK o další podtyp. Prognóza a léčba pacientů samozřejmě odvisí hlavně od stadia (stage) tumoru v době diagnózy, avšak rozpoznat, že se jedná o PRK, je důležité a povědomí o spektru morfologických variant PRK má tak klinický význam.

Annals of Diagnostic Pathology 27 (2017) 48–56

Contents lists available at ScienceDirect

Annals of Diagnostic Pathology

Warthin-like papillary renal cell carcinoma: Clinicopathologic, morphologic, immunohistochemical and molecular genetic analysis of 11 cases☆

Faruk Skenderi [a], Monika Ulamec [b], Tomas Vanecek [c], Petr Martinek [c], Reza Alaghehbandan [d], Maria Pane Foix [e], Iva Babankova [f], Delia Perez Montiel [g], Isabel Alvarado-Cabrero [h], Marian Svajdler [c], Pavol Dubinský [i], Dana Cempirkova [j], Michal Pavlovsky [k], Semir Vranic [a], Ondrej Daum [c], Ondrej Ondic [c], Kristyna Pivovarcikova [c], Kvetoslava Michalova [c], Milan Hora [l], Pavla Rotterova [m], Adela Stehlikova [c], Martin Dusek [c], Michal Michal [c], Ondrej Hes [c,*]

[a] Department of Pathology, University of Sarajevo Clinical Center, Sarajevo, Bosnia and Herzegovina
[b] "Ljudevit Jurak" Pathology Department, Clinical Hospital Center "Sestre milosrdnice", Zagreb, Croatia
[c] Department of Pathology, Charles University, Medical Faculty and Charles University Hospital Plzen, Czech Republic
[d] Department of Pathology, University of British Columbia, Royal Columbian Hospital, Vancouver, BC, Canada
[e] Department of Pathology, Bellvitge University Hospital, Barcelona, Spain
[f] Department of Pathology, Masaryk's Oncologic Institute, University Hospital Brno, Czech Republic
[g] Department of Pathology, Instituto Nacional de Cancerologia, Mexico City, Mexico
[h] Department of Pathology, Centro Medico, Mexico City, Mexico
[i] Department of Radiation Oncology, Oncology Institute, Kosice, Slovakia
[j] Department Pathology, Regional Hospital Jindrichuv Hradec, Czech Republic
[k] Department Pathology, Regional Hospital Most, Czech Republic
[l] Department of Urology, Charles University, Medical Faculty and Charles University Hospital Plzen, Czech Republic
[m] Biopticka Laboratory, Pilsen, Czech Republic

ARTICLE INFO

Available online xxxx

Keywords:
Kidney
Oncocytic papillary renal cell carcinoma
Warthin's tumor
Warthin-like
Lymphoid stroma
Immunohistochemistry
Chromosomal aberration pattern

ABSTRACT

Oncocytic papillary renal cell carcinoma (PRCC) is a distinct subtype of PRCC, listed as a possible new variant of PRCC in the 2016 WHO classification. It is composed of papillae aligned by large single-layered eosinophilic cells showing linearly arranged oncocytoma-like nuclei.

We analyzed clinicopathologic, morphologic, immunohistochemical and molecular-genetic characteristics of 11 oncocytic PRCCs with prominent tumor lymphocytic infiltrate, morphologically resembling Warthin's tumor.

The patients were predominantly males (8/11, 73%), with an average age of 59 years (range 14–76), and a mean tumor size of 7 cm (range 1–22 cm). Tumors had the features of oncocytic PRCCs with focal pseudostratification in 8/11 cases and showed dense stromal inflammatory infiltration in all cases. Papillary growth pattern was predominant, comprising more than 60% of tumor volume. Tubular and solid components were present in 5 and 3 cases, respectively. Uniform immunohistochemical positivity was found for AMACR, PAX-8, MIA, vimentin, and OSCAR. Tumors were mostly negative for carboanhydrase 9, CD117, CK20, and TTF-1. Immunohistochemical stains for DNA mismatch repair proteins MLH1 and PMS2 were retained in all cases, while MSH2 and MSH6 were negative in 1 case. Tumor infiltrating lymphocytes (TILs) consisted of both B and T cells. Chromosomal copy number variation analysis showed great variability in 5 cases, ranging from a loss of one single chromosome to complex genome rearrangements. Only one case showed gains of chromosomes 7 and 17, among other aberrations. In 4 cases no numerical imbalance was found. Follow up data was available for 9 patients (median 47.6 months, range 1–132). In 6 patients no lethal progression was noted, while 3 died of disease.

In conclusion, Warthin-like PRCC is morphologically very close to oncocytic PRCC, from which it differs by the presence of dense lymphoid stroma. Chromosomal numerical aberration pattern of these tumors is variable;

☆ The study was supported by the Charles University Research Fund (project number P36) and by the grant of Ministry of Health of the Czech Republic - Conceptual Development of Research Organization (Faculty Hospital in Pilsen – FN Pl, 00669806).

* Corresponding author at: Department of Pathology, Charles University, Medical Faculty and Charles University Hospital Plzen, Alej Svobody 80, 304 60 Pilsen, Czech Republic.
E-mail address: hes@medima.cz (O. Hes).

http://dx.doi.org/10.1016/j.anndiagpath.2017.01.005
1092-9134/

only one case showed gains of chromosomes 7 and 17. Warthin-like PRCC is a potentially aggressive tumor since a lethal outcome was recorded in 3/9 cases.

1. Introduction

Renal cell carcinoma (RCC) is a highly heterogeneous group of tumors, consisting of at least 14 subtypes recognized in the latest WHO classification, and several additional tentatively distinct variants [1-3]. The subgroup of papillary renal cell carcinoma (PRCC) is further divided into type 1 and 2. Recently, a number of studies have described a small series of morphologically distinctive PRCCs, such as oncocytic, solid, biphasic squamoid alveolar, "mucin"-secreting, or clear cell types, not belonging to any of the two main types [4-9]. These tumors may be associated with foci of type 2-resembling areas and are thus often designated as such, which may contribute to the molecular-genetic heterogeneity of PRCC type 2 tumors [10]. Some of these tumors are even designated as unclassified [11]. Even though the tumor stage remains the best determinant for the survival of patients after nephron sparing surgery within the PRCC group [12], the histological variants of PRCC are important to recognize. This is due to the fact that the papillary morphology is also seen in other RCC subtypes, and thus the treatment and outcome may significantly differ in patients with variant tumors as compared with those who have two classical forms of PRCC.

Oncocytic PRCC [4,13,14] is mentioned in the 2016 WHO classification as a tumor that has a papillary architecture, and is composed of large cells with finely granular eosinophilic cytoplasm, mostly single-layered, and linearly aligned oncocytoma-like nuclei [3]. Such morphology, with addition of a prominent lymphocytic infiltrate in stroma, may commonly be seen in the papillary cystadenoma lymphomatosum (Warthin's tumor) of the salivary glands. To the best of our knowledge, carcinomas resembling benign Warthin's tumor have been described in salivary glands [15] and thyroid [16], but not in the kidney. Tumor infiltrating lymphocytes (TILs) may have prognostic value and that with the advent of novel immune mediated therapies [17], tumors with TILs could be considered for potential immunotherapy in the future. Of note, lymphoid infiltrates are frequently found in tumors of other organs associated with Lynch syndrome. However, a potential link between this hereditary syndrome and lymphoid infiltrates in some renal tumors has not been explored.

The aim of this study was to analyze the clinicopathologic, morphologic, immunohistochemical and molecular-genetic characteristics of 11 oncocytic PRCCs with prominent lymphoid stroma (Warthin-like papillary renal cell carcinoma - WPRCC), morphologically reminiscent of Warthin's tumor.

2. Materials and methods

2.1. Case selection and routine microscopy

There were 1147 in-house and consultation cases of PRCC in Plzen Tumor Registry. We searched the database for keywords "oncocytic, papillary, kidney, lymphoid stroma", and reviewed 147 tumors. We subsequently selected 11 cases with predominant oncocytic cytology and abundant intratumoral lymphocytic infiltrate. All the cases were reviewed by three pathologists (FS, MU, OH). There were 1–10 tissue blocks available for each case, and 1–2 representative blocks were selected for immunohistochemical and molecular–genetic studies. Clinical, gross and follow-up data were collected by review of the institutional medical records and by contacting the consulting pathologists.

Tissue for light microscopy was fixed in 4% formaldehyde, embedded in paraffin using routine procedures. 5 μm thin sections were cut and stained with hematoxylin and eosin. Special stain technique for evaluation of mucin was performed using mucicarmine, periodic acid - Schiff (PAS) and alcian blue at pH 2.5. We evaluated percentages of papillary, tubular, cystic, and solid architectural patterns, abundance of TIL with reference to index case, nuclear grade according to the guidelines of ISUP (International Society of Urologic Pathology), nuclear pseudostratification, single versus multiple cell layers forming papillae, presence of foamy macrophages, and microscopic necrosis.

2.2. Immunohistochemistry

Immunohistochemical study was performed using primary antibodies recognizing following antigens: racemase/AMACR (13H4, monoclonal, Dako, Glostrup, Denmark, 1:200), carbonic anhydrase IX (rhCA9, monoclonal, RD systems, Abingdon, GB, 1:100), vimentin (D9, monoclonal, NeoMarkers, Westinghouse, CA, 1:1000), OSCAR (OSCAR, monoclonal, Covance-SpinChem, San Diego, CA, 1:500), PAX-8 (polyclonal, Cell Marque, Rocklin, CA, 1:25), cytokeratin 7 (OV-TL12/30, monoclonal, Dako, 1:200), cytokeratin 20 (M7019, monoclonal, Dako, 1:100), cytokeratins (AE1-AE3, monoclonal, BioGenex, San Ramon, CA, 1:1000), CD117 (CD117, polyclonal; Dako, Glostrup, Denmark; RTU), EMA (E29, monoclonal; DakoCytomation, Carpinteria, CA; 1:1000), CD10 (56C6, monoclonal; Novocastra, Newcastle upon Tyne, UK; 1:50), TTF-1 (SPT24, monoclonal; Novocastra, 1:400), *anti*-mitochondrial antigen (MIA, monoclonal; BioGenex; 1:100), CD3 (monoclonal, LN10, Novocastra, 1:50), CD5 (monoclonal, 4C7, Novocastra, 1:50), CD20 (monoclonal, L26, DakoCytomation, RTU), MSH2 (monoclonal, G219-1129, Cell Marque, RTU), MSH6 (monoclonal, 44, Ventana, Manheim, Germany, RTU), PMS2 (monoclonal, EPR 3947, Cell Marque, RTU), MLH1 (monoclonal, G168-728, Cell Marque, RTU). The primary antibodies were visualized using the supersensitive streptavidin-biotin-peroxidase complex (BioGenex). Appropriate positive controls were employed for all assays. Immunohistochemical staining was recorded negative if no staining, or less than 5% of staining was observed; as weak (+) for staining of up to 25% of tumor cells; moderate (++) for staining 25–50% of tumor cells; and strong (+++) for staining in more than 50% of tumor cells.

2.3. DNA extraction

DNA was extracted using the QIAsymphony DSP DNA Mini Kit on automated extraction system QIAsymphony SP (QIAGEN, Hilden, Germany) according to the manufacturer's supplementary protocol for FFPE samples. Concentration and purity of isolated DNA were measured using the NanoDrop ND-1000 (NanoDrop Technologies, Inc., Wilmington, DE, USA). DNA integrity was examined by multiplex PCR amplification of five fragments of lengths ranging from 100 to 600 base pairs (bp) [18].

2.4. Low pass whole genome analysis

All samples were tested for copy number variations (CNV) in all chromosomes using low pass whole genome sequencing on Ion Torrent PGM platform using kits and software from Life Technologies (Thermo Fisher Scientific, Waltham, MA USA). The extracted DNA (100 ng) was enzymatically fragmented using a shear enzyme mix contained in Ion Xpress Plus Fragment Library Kit. Samples with DNA integrity control result of 600 bp were sheared 10 min, and samples with lower integrity were sheared 5 min. Sequencing adapters were ligated and the sequencing library was size-selected for 200 bp. Final libraries were

Table 1
Clinicopathological data on Warthin-like papillary renal cell carcinoma.

Case No.	Age	Sex	Size (cm)	TNM stage	Follow-up (months)
Case 1	48	M	1.0[a]	–	DUD 1 months, autopsy, no generalization
Case 2	64	M	6.0	pT3	DOD 9 m, generalization, retroperitoneal lymph nodes, liver, lung, bones
Case 3	69	F	3.0	pT1	AW 12
Case 4	76	M	22[b]	pT3	DOD 12
Case 5	45	M	2.8	pT1	AW 108, then LFU
Case 6	64	M	14.5	pT2	LFU
Case 7	14	M	12.5	pT2	DOD 36
Case 8	NA	M	NA	NA	LFU
Case 9	59	M	2.5	pT1	AW 108
Case 10	74	F	4.2	pT1	AW 132
Case 11	75	F	1.5	pT1	AW 10

DUD = death of unrelated disease.
DOD = death of disease.
AW = alive and well.
LFU = lost to follow up.
NA = not available.
[a] Associated with renal oncocytoma 3.0 cm.
[b] Sarcomatoid component.

pooled and templating and enrichment steps were performed using Hi-Q Template OT2 200 Kit. Sequencing was performed on a 316v2 chip using Hi-Q Sequencing kit according to manufacturer's protocols aiming to obtain minimum of 100 000 reads per sample. Signal processing, mapping and quality control was performed with Torrent Suite v.5.0. CNVs were called and visualized using Ion Reporter v5.2 using low-pass whole-genome aneuploidy workflow. The Median of the Absolute values of all Pairwise Differences (MAPD) score filter was set to 0.3. The called CNVs passing the confidence filter (≥1) were annotated using ISCN cytogenetic coordinates and sequence positions using Hg19 genome assembly and reported in the Table 4. The aneuploidies of gonosomes were adjusted manually regarding the sex of the patient. For each sample several detected CNVs were confirmed by FISH using enumeration probes as described elsewhere [19].

2.5. Mutation analysis of MLH1, MSH2 and MSH6 genes

Mutation analysis of the MLH1, MSH2 and MSH6 genes was performed using PCR and Sanger sequencing as previously described in Kacerovska et al. 2016 [20]. Whole coding sequences (including exon-intron junctions) of the MLH1, MSH2 and MSH6 genes were obtained and compared to the appropriate reference sequences.

2.6. Microsatellite instability (MSI) analysis

Five mononucleotide markers (BAT-25, BAT-26, NR-21, NR-24, and MONO-27) were analyzed using the "MSI Analysis System" kit (Promega, Madison, WI) according to the manufacturer's instructions. The PCR products were separated by capillary electrophoresis using ABI 3130XL Genetic Analyzer (Applied Biosystems), and the output data were analyzed with GeneMapper software (Applied Biosystems).

2.7. MLH1 promoter methylation analysis

To perform methylation analysis, the bisulfite conversion ("EZ DNA Methylation-Gold Kit;" Zymo Research, Burlington, ON, Canada) was followed by the methylation-specific PCR targeting the MLH1 promoter according to Chan et al. [21].

2.8. BRAF V600E mutation analysis

Presence of the BRAF V600E mutation status was tested using the real-time PCR kit Cobas® 4800 BRAF V600 Mutation Test (Roche; Mannheim, Germany) according to the manufacturer's instructions.

3. Results

3.1. Clinicopathologic data

Clinical and pathologic data were available for 10 of 11 cases and are summarized in Tables 1 and 2. The patients were predominantly males (73%) with male to female ratio of 3:1. Average age was 59 years (range 14–76). One half of all tumors were at pT1 stage. The mean size of tumors was 7 cm (range 1–22 cm).

Table 2
Morphological data on Warthin-like papillary renal cell carcinoma.

Case No.	ISUP grade	Foamy macrophages	Architectural pattern[a]	TIL abundance[b]	Cell layers	Nuclear pseudostr.[c]	Necrosis
Case 1	2	+	P	++	SI	+	−
Case 2	2	−	S/P/T	+++	MU	−	+++
Case 3	2	−	P/T	+++	SI	+	+
Case 4	4	−	P	+++	SI	+	+
Case 5	3	−	P	++	SI	+++	−
Case 6	2	−	T	++	SI	+	−
Case 7	3	−	P/T	++	SI	++	−
Case 8	2	+	S/P	++	MU	−	−
Case 9	3	−	P/S	+++	SI	+	+
Case 10	2	+	S/TA	++	SI	+	−
Case 11	2	−	P	+++	SI	−	−

SI – single cell layer; MU – multiple cell layers.
[a] Architectural pattern: P-papillary, S-solid, T-tubular.
[b] TIL - tumor infiltrating lymphocytes: abundance was assessed both on HE and CD3, CD5, and CD20 stained slides, in reference to index case which was designated as +++.
[c] Nuclear pseudostratification was assessed as negative (−), sparse (+), moderate (++), prominent (+++), in reference to index case.

Fig. 1. On cross section the tumors were mostly brown to grey, compact, and well-circumscribed.

In cases when gross description was available (8 of 11 cases), the tumors were brown to grey, compact, and well-circumscribed (Fig. 1). Grossly visible necroses or hemorrhages were not reported.

Follow up information was available for 9/11 patients. Follow up period ranged from 1 to 132 months (median range 47.6 months). In 6 patients, there were no records about aggressive behavior or disease progression. However, 3 patients died of disease 9–36 months after resection. Metastatic spreading was documented to lymph nodes, liver, lung and bones. Sarcomatoid tumor differentiation was present in one case with a lethal outcome.

3.2. Morphologic characteristics

Basic morphologic characteristics are summarized in Table 2. Most of the tumors showed papillary growth pattern in more than 60% of tumor volume (Fig. 2). However, tubular and solid/compressed papillary components were also present in smaller volume percentages, in the majority of the cases (Fig. 3). The tumors were composed of medium to large eosinophilic cells, most of them had visible nucleoli at high magnification, corresponding to ISUP grade 2 (Fig. 4). Two cases were ISUP grade 3 and one was grade 4. Nuclear pseudostratification was present in 8/11 (Fig. 5A), however it was not prominent in the majority of cases (Fig. 5B). Foamy macrophages were seen in 3/11 cases (Fig. 6 and Table 2). Prominent feature in all cases was moderate to strong stromal inflammatory infiltration, predominantly composed of lymphocytes (Fig. 7A and B). The stroma was mostly loose, located within papillary tufts and also in some cases within areas with tubulocystic architecture. Desmoplastic stroma was not seen in any of the cases. Necrotic foci were present in 4/11 cases.

One WPRCC contained in addition to the papillary architecture, oncocytic cells and dense lymphoid stroma, a large component showing nondescript spindle cell sarcomatoid differentiation. Clinically, this tumor had an aggressive course and caused patient's death.

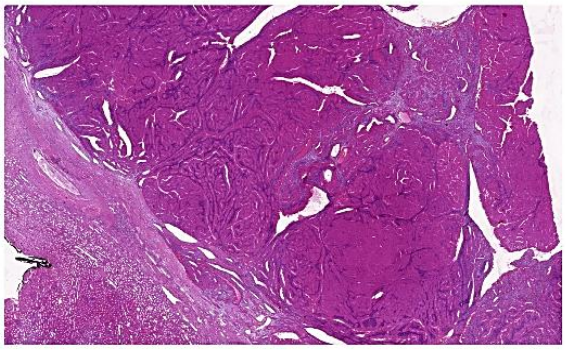

Fig. 3. Tubular and solid components. These were also present in smaller volume percentages in the majority of cases.

3.3. Immunohistochemical examinations

The results of the immunohistochemistry evaluation are summarized in Table 3. Briefly, the tumor cells were positive for PAX-8 (11/11, 100%), MIA (11/11, 100%) (Fig. 8A and B), vimentin (10/11, 91%) and OSCAR (11/11, 100%); variable for AMACR (10/11, 91%), CK7 (5/11, 54%) (Fig. 9 A + B), EMA (5/11, 45%), CD10 (7/11, 63%), and AE1/3 (4/11, 36%); mostly negative for carboanhydrase 9 (0/11, 0%), CD117

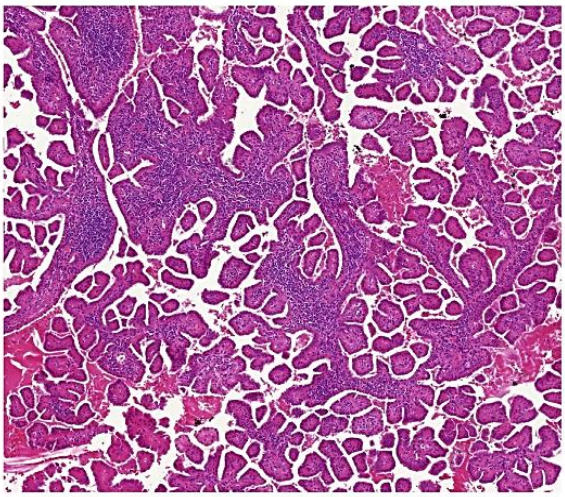

Fig. 2. Papillary growth pattern. It was seen in more than 60% of tumor volume in most tumors.

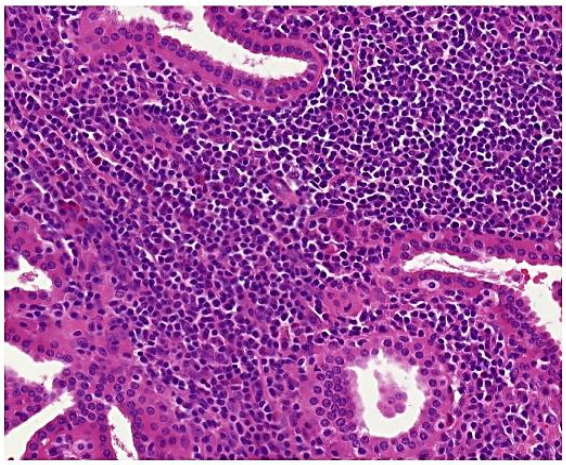

Fig. 4. Medium to large eosinophilic cells. Most of these cells had visible nucleoli at high magnification and corresponded to ISUP grade 2.

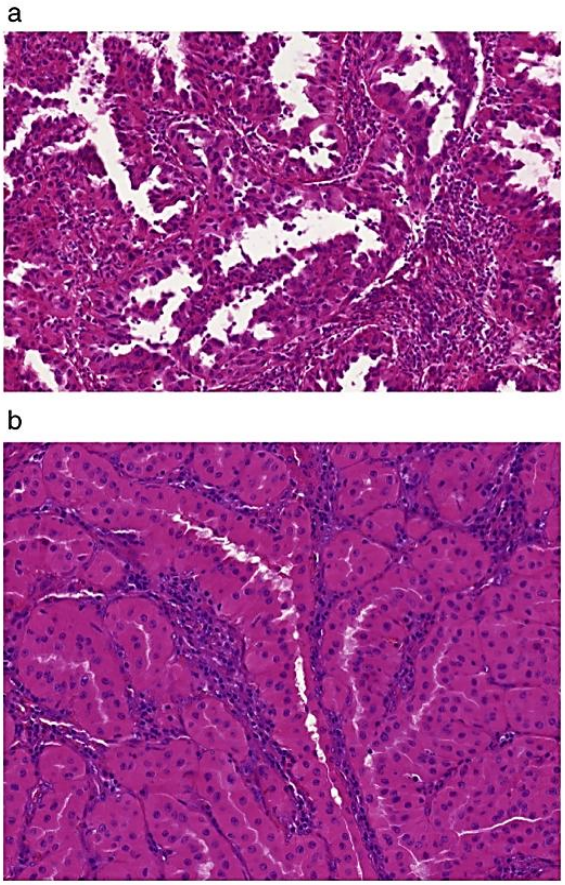

Fig. 5. Nuclear pseudostratification. It was present in 8/11 (A), however it was not prominent in the majority of cases (B).

(0/11, 0%), CK20 (1/11, 9%) and TTF-1 (0/11, 0%). DNA mismatch repair proteins (MLH1, MSH2, MSH6, PMS2) were retained in all cases except one case that exhibited a loss of MSH2 and MSH6 proteins (case no. 4).

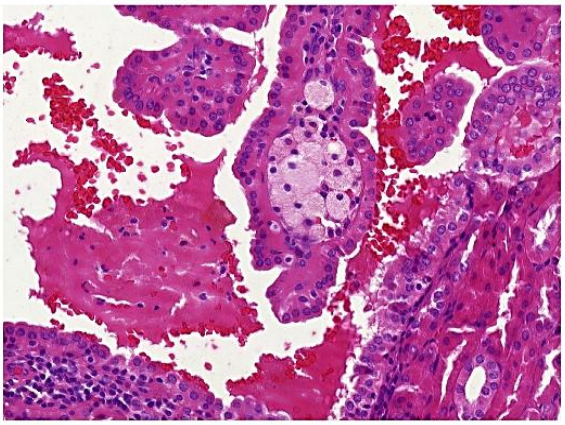

Fig. 6. Foamy macrophages. These cells were seen in 3/11 cases.

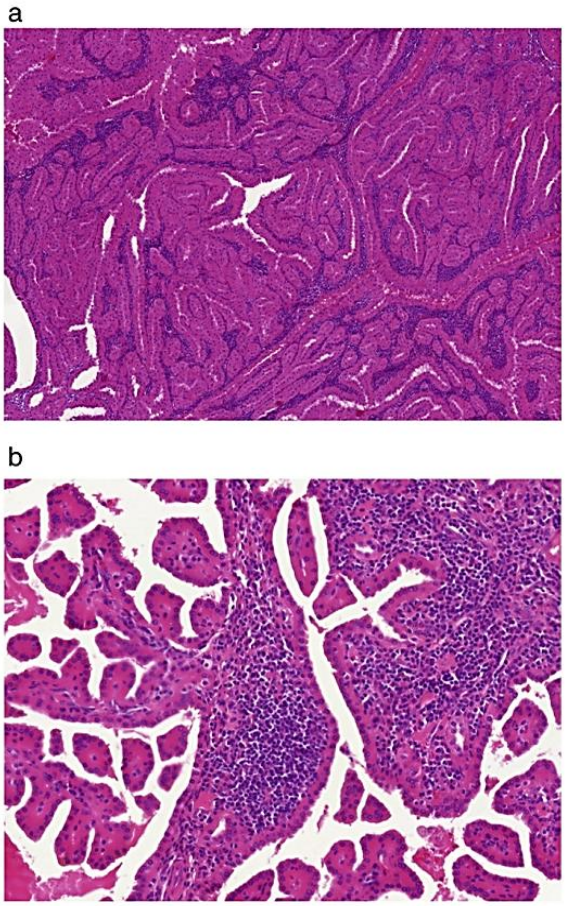

Fig. 7. A + B: lymphoid infiltration of the stroma. Moderate to strong stromal lymphoid infiltration was seen in all tumors.

TILs consisted of both B and T cells, mostly CD5 and CD3 positive, while in two cases CD20 positive lymphocytes were predominant.

3.4. Molecular genetic analysis

Nine cases produced good quality libraries and were successfully sequenced, while the remaining two samples were not analyzable. No CNV were found in four samples. The remaining five samples showed great variability in detected CNV ranging from loss of one chromosome to complex genome rearrangements including gains and losses of various parts of chromosomes as summarized in Table 4 and visualized in Fig. 10. Only one of the cases showed gain of chromosomes 7 and 17 (among the other aberrations). The range and quality of every detected CNV is summarized in Table 5.

Analyses of MMS and *BRAF V600E* were performed in one case (case 4), due to the loss of immunohistochemical reactivity with MSH2 and MSH6.

In the DNA purified from FFPE sample no microsatellite instability (MSI), no aberrant methylation of MLH1 promoter and no mutations in MLH1, MSH2 and MSH6 genes were found. Also *BRAF V600E* mutation was absent.

Table 3
Immunohistochemistry profile of Warthin-like papillary renal cell carcinoma.

Case No.	AMACR	PAX-8	Vimentin	MIA	CD10	CD117	CANH9	CK7	CK20	OSCAR	AE1/AE3	EMA	TTF-1	MSH2	MSH6	MLH1	PMS2
Case 1	+++	+++	+++	+++	+	−	−	−	−	+++	−	−	−	+++	+++	+++	+++
Case 2	−	+++	+++	+++	±	−	−	++	−	+++	+++	∓	−	+++	+++	+++	+++
Case 3	+++	+++	+++	+++	++	−	−	+++	−	+++	+++	+++	−	+++	+	+++	+++
Case 4	++	+++	−	+++	++	−	−	+	−	+++	−	+++	−	−	−	+++	+++
Case 5	+++	+++	++	+++	+++	−	−	−	−	+++	−	−	−	+++	+	+++	+++
Case 6	+++	++	+++	+++	++	−	−	−	−	+++	−	−	−	+++	++	+++	+++
Case 7	+++	+++	+++	+++	−	−	−	−	−	+	−	++	−	+++	+++	+++	+++
Case 8	+++	+++	+++	+++	++	−	−	+	−	+++	−	+	−	+++	+++	+++	+++
Case 9	+++	+++	+++	+++	++	−	−	−	+++	+++	−	−	−	+++	+	+++	+++
Case 10	+++	+++	+++	+++	−	−	−	+	−	+	+	−	−	+++	+++	+++	+++
Case 11	++	+++	+++	+++	−	−	−	+++	−	+++	+++	+++	−	+++	+++	+++	+++
	10/11 (91%)	11/11 (100%)	10/11 (91%)	11/11 (100%)	7/11 (63%)	0/11 (0%)	0/11 (0%)	6/11 (54%)	1/11 (9%)	11/11 (100%)	4/11 (36%)	5/11 (45%)	0/11 (0%)	10/11 (91%)	10/11 (91%)	11/11 (100%)	11/11 (100%)

Intensity and percentage of positive tumor cells were scored as: negative (−) if no staining or less than 5% staining was observed; weakly positive (+), if focal positivity seen in up to 25% of tumor cells; moderate (++), if positivity observed in 25–50% of tumor cells; diffuse (+++), if more than 50% of tumor cells positive. AMACR – alpha-methylacyl-CoA racemase; CANH9 – carboanhydrase 9; MIA – antimitochondrial antigen; MSH2, MSH6, PMS2, MLH1 – DNA mismatch repair enzymes/proteins.

4. Discussion

There are ongoing debates over the PRCC classification. Traditionally these carcinomas have been classified morphologically as type 1 and type 2. However, many cases of PRCC show only a part of the diagnostic criteria or overlapping morphology between both of the types. Results of immunohistochemical analyses are also more compact for type 1 PRCC and rather variable for type 2 PRCC [2]. Recent large multicentric studies from The Cancer Genome Atlas group and Marsaud et al. reported the genetic profile of large number of PRCCs and found that type 1 and type 2 are genetically distinct entities, but type 2 tumors may further be genetically subdivided into three groups [10,11].

Herein we report the clinicopathologic, morphological, immunohistochemical and molecular genetic profile of a distinct variant of renal carcinoma, showing predominantly papillary architecture, oncocytic cytology, and abundant tumor infiltrating lymphocytes, resembling benign Warthin's tumors of the parotid gland.

A series of so-called oncocytic PRCC (OPRCC) and several case reports of these tumors were previously published [4,13,22-25]. All of the studies reported similar morphological characteristics of the tumors, which are arranged mostly in papillary, but also tubular and solid architecture, with deeply eosinophilic cells, arranged in a single layer or in multiple layers, in some cases with pseudostratification. Nuclei are described mostly as bland and round, however, tumors with a nuclear grade 3 were also reported. Necrosis is recorded rarely. Foamy macrophages were occasionally present [13,25].

Our cohort of WPRCC was composed of tumors with similar morphology, however there were some substantial differences. The most striking feature was the presence of dense lymphocytic infiltration of the stroma within core of the papillae or stroma interspersed among tubular component. OPRCC are described mostly as tumors without pseudostratification [25,26], however this feature is mentioned in some papers [4,25]. In WPRCC series nuclear pseudostratification was detected in 8 cases, whereas in 2 cases was prominent and in 6 cases focal.

An interesting finding in our study was that of 10 cases with available follow-up data, 3 had an aggressive clinical course. Furthermore, one tumor with characteristic morphology (papillary architecture, oncocytic cells and dense lymphoid stroma) was associated with sarcomatoid differentiation. Remaining 2 aggressive cases were graded as grade 2 and 3 according ISUP grading system. Of note, the tumor with grade 2 was staged as pT3 according to the TNM 2009.

Immunohistochemical profile of OPRCCs has been reported in several studies [4,13,27]. In the current study, we found the immunoprofile of WPRCC almost identical to previously reported immunoprofile of OPRCC. However, vimentin was diffusely positive in 91% of cases in the current study, while it was variable in the OPRCC. WPRCCs were diffusely positive for AMACR, PAX-8, vimentin, MIA, and OSCAR, variably for cytokeratin AE1/AE3, CK7, CD10, EMA. Tumors were negative for carboanhydrase 9, CD117, CK20 and TTF-1.

Copy number variation analysis was successful in 9/11 cases. No numerical chromosomal aberrations were found in 4 tumors. The remaining 5 cases revealed variable chromosomal gains and losses. Such CNV variability is known in chromophobe RCC, in which, besides frequently encountered multiple loses, variable CNV pattern has been documented [19,28,29]. Only 1 of these 5 cases showed, among other chromosomal abnormalities, a polysomy of chromosomes 7 and 17, which is believed to be characteristic for PRCC. Given significant morphologic and genetic heterogeneity of the PRCC, even within type 2 category, these results are not too surprising. Recent large study from The Cancer Genome Atlas group identified genomic profile of PRCC, concluding that type 1 and 2 PRCC are distinctly different entities, and that type 2 PRCC is a heterogeneous disease with multiple distinct subgroups [10]. These results were also supported by previous studies comprising fewer cases [4,11,13,30,31].

The role of TILs is currently investigated by numerous research groups. Present data suggest that specific TIL phenotypes may have prognostic, predictive, or therapeutic value, however, this is yet to be clarified [17,32]. TIL and peritumoral lymphocytes are commonly found in carcinomas associated with Lynch syndrome (LS). LS is a hereditary cancer syndrome caused by mutations in DNA mismatch repair (MMR) proteins, resulting in deficient DNA repair machinery, eventually leading to a hypermutational phenotype and development of neoplasms in other organs. It is believed that renal cell carcinoma (in contrast to urothelial carcinoma of the renal pelvis) is not associated with LS. To find out whether WPRCC with its TILs could be associated with LS, we analyzed immunoreactivity of four MMR proteins, namely the MSH2, MSH6, PMS2, and MLH1. Except one case, we found in all tumors moderate to strong nuclear expression of investigated proteins, both in the tumor tissue and adjacent normal kidney tissue. In case with lost of MSH2 and MSH6 staining, microsatellite instability (MSI) and methylation of MLH1 promoter analyses, as well as mutations analysis in MLH1, MSH2 and MSH6 genes and *BRAF V600E* mutation were performed, which showed no abnormalities. Our results suggest no relationship between TILs in WPRCC and Lynch syndrome, and possibly, exclude the involvement of investigated MMR genes in tumorigenesis of WPRCC. The expression of MMR proteins was previously evaluated in clear cell RCC [33,34], but this is a first report of such in this unusual variant of PRCC.

Diagnostic features of WPRCC are not highly specific, and that several entities should be considered in the differential diagnosis. The most important one is a metastasis. Oncocytic variant of papillary thyroid

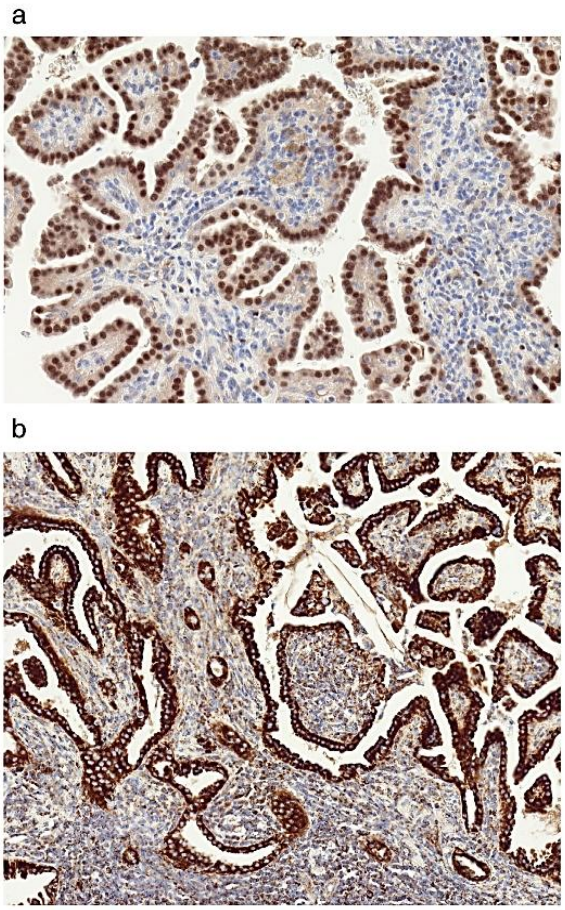

Fig. 8. Immunohistochemistry for PAX8 (A) and antimitochondrial antigen (B)·These immunostainings were positive in n all cases.

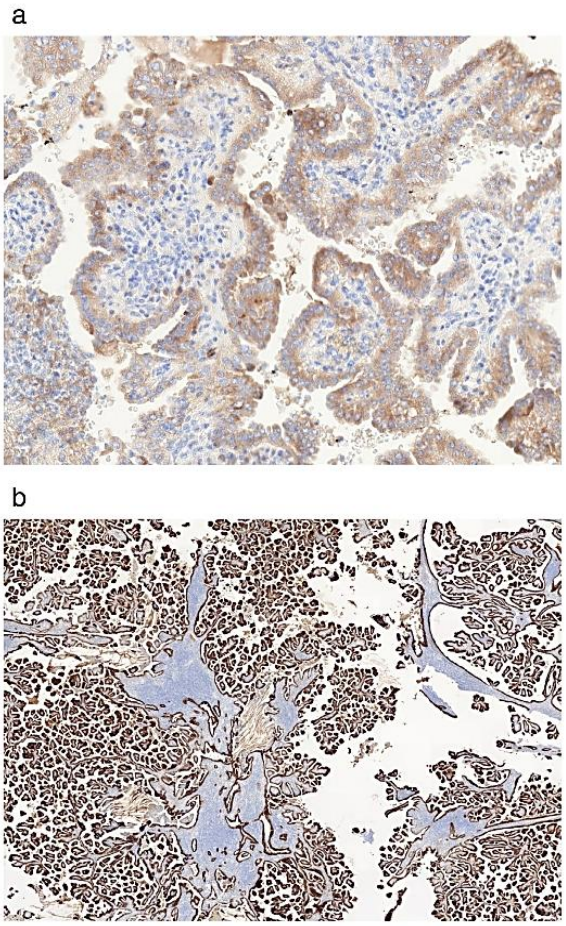

Fig. 9. Immunohistochemistry for AMACR (A) and CK 7 (B). All but one case (case 2) were positive for AMACR, 6 cases were immunoreactive for CK 7.

carcinoma with lymphocytic stroma (Warthin-like variant) is a rare tumor, generally reported to have a favorable prognosis but it may show aggressive clinical behavior [35]. The possibility of a renal metastasis of such a tumor was excluded in our series both clinically and by the fact that TTF-1 was negative in all tumors.

All eosinophilic subtypes of RCC may be considered in the differential diagnosis of Warthin-like PRCC. Oncocytoma and chromophobe RCC may rarely present with architecture mimicking PRCC, however true papillae are not part of the morphologic spectrum of these tumors [2]. Lymphocytic infiltrate in these tumors would be a highly unusual morphologic feature as well.

Another morphologically similar, but much more aggressive entity to be excluded is hereditary leiomyomatosis and renal cell carcinoma (HLRCC)-associated RCC/fumarate hydratase-deficient RCC [2,36,37]. This tumor can be papillary/tubulocystic, composed of eosinophilic cells with high grade nuclei and prominent deep red nucleoli. These tumors are characterized by mutation of the *fumarate hydratase gene* (*FH*). Oncocytic characteristics of cell population in these tumors are not mentioned in the literature. In contrast to HLRCC-associated RCC, we were not able to find typical large nuclei with red nucleoli and perinucleolar halo resembling cytomegalovirus inclusions. Moreover prominent TILs are not described in kidney tumors related to hereditary leiomyomatosis [37]. MiT family translocation carcinomas (namely spectrum of Xp11.2 RCC) may also be considered in the differential diagnosis, as they have papillary growth pattern, and may show areas composed of eosinophilic

Table 4
Summary of copy number variations of chromosomes.

Case No.	Gains	Loses
Case 1	None	None
Case 2	5	1, 3, Y
Case 3	None	None
Case 4	None	None
Case 5	NA	NA
Case 6	None	None
Case 7	None	1, 14, 18, 22
Case 8	1, 2, 5, 21	1, 3, 14, 15, Y
Case 9	7, 8, 12, 17	None
Case 10	None	x
Case 11	NA	NA

NA – not analyzable.

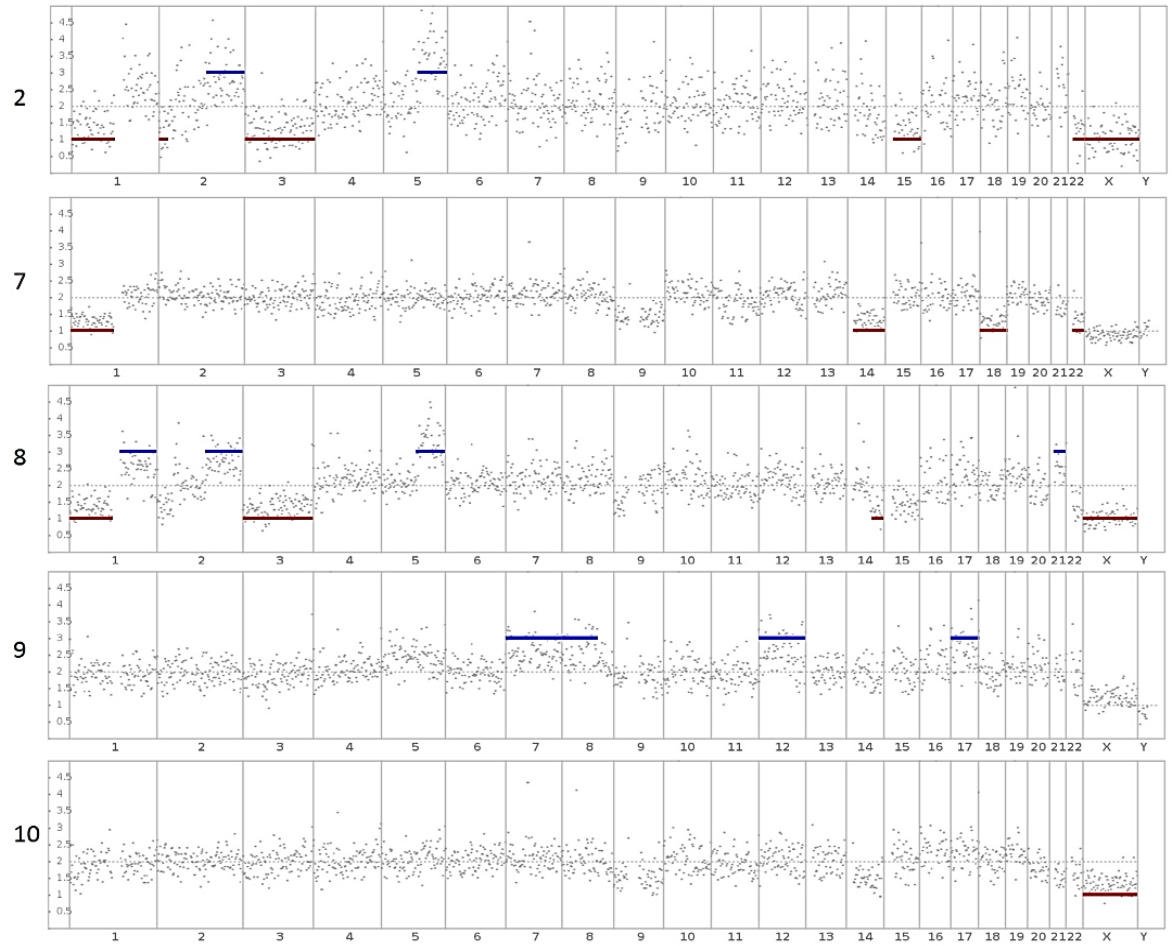

Fig. 10. Chromosome aberration patterns. CNV ranged from loss of one chromosome to complex genome rearrangements including gains and losses of various parts of chromosomes.

cells. Our cases were uniformly composed of oncocytic cells and did not show hyaline bodies, typical microcalcifications and areas with larger pale/clear cells [2].

Tubulocystic RCC may also be considered in the differential diagnosis, mainly because some of our cases did not display CNV. However, our cases differed from tubulocystic RCC by predominantly papillary architecture. No single case from our series showed a predominant tubulocystic growth pattern [38-40].

Succinate dehydrogenase-deficient RCC (SC-RCC) can be in the differential diagnosis as it includes tumors composed of vacuolated eosinophilic to clear cells with inconspicuous nucleoli, usually with a solid growth pattern, but rarely/less frequently showing a tubular or even papillary pattern. This tumor is characterized by the presence of cells with bubbly appearing eosinophilic cytoplasm. In addition to morphological differences, SC-RCC has different imunohistochemical and molecular hallmarks [2,41].

RCC in acquired cystic disease of the kidney (ACDK) is observed exclusively in patients with end-stage renal disease. All our patients had normal renal function, no one was dialyzed or had transplant kidney. Histologically, a variety of RCC types can be found in ACDK patients, including RCC with papillary and tubulopapillary architectures. The tumor cells always have acidophilic cytoplasm with oncocytic features and prominent nucleoli [2]. The presence of mostly abundant oxalate crystalloids is considered to be a typical morphologic feature. We were not able to find oxalate crystals in our cases.

In summary, we analyzed a cohort of PRCCs with oncocytic morphology and dense lymphoid stroma. While the immunohistochemical profile was consistent with PRCC, molecular genetic analysis revealed variable chromosomal abnormalities, indicating that they do not belong to neither type 1, nor type 2 PRCC. Nevertheless, due to the mophological resemblance to the OPRCC, we believe that WPRCC can be considered as part of the spectrum of this variant of papillary renal cell carcinoma group. Since 3/11 cases of WPRCC appeared to have metastatic potential, additional cases need to be studied to elucidate the true malignant potential of these tumors.

Conflict of interest

All authors declare no conflict of interest.

Table 5
Details of detected copy number variations.

Case No.	chr No.	ISCN	Hg19	Copies	Confidence
2	1	1p36.33p11.2	521368-120697156	1	10.02
	2	2p25.3p23.3	10000-25207815	1	1.50
	2	2q22.1q37.3	137858809-243102476	3	2.66
	3	3p26.3q29	60000-197962430	1	27.37
	5	5q21.1q35.3	99536286-180905260	3	13.43
	15	15q11.2q26.3	23564853-102521392	1	8.91
	22	22q11.1q13.33	16847850-50364777	1	5.59
	X	Xp22.33q28	2699520-154931044	1	57.92
7	1	1p36.33p11.2	521368-120697156	1	23.06
	14	14q11.1q32.33	19020000-107289540	1	11.64
	18	18p11.32q23	10000-78017248	1	12.69
	22	22q11.1q13.33	16847850-50364777	1	2.65
8	1	1p36.33p11.2	521368-120697156	1	12.12
	1	1q21.1q44	144810724-248908210	3	4.95
	2	2q22.1q37.3	139830771-243102476	3	14.84
	3	3p26.3q29	60000-197962430	1	24.09
	5	5q21.1q35.3	101498825-180905260	3	35.77
	14	14q24.3q32.33	75191525-107289540	1	1.22
	21	21q11.2q22.3	14338129-48119895	3	2.39
	X	Xp22.33q28	2699520-154931044	1	104.37
9	7	7p22.3q36.3	282484-159128663	3	11.13
	8	8p23.3q22.2	10000-100736467	3	5.95
	12	12p13.33q24.33	145739-133841895	3	8.85
	17	17p13.3q25.3	396626-81195210	3	6.32
10	X	Xp22.33q28	2699520-154931044	1	20.43

chr = chromosome, ISCN = International System for Human Cytogenetic Nomenclature.

Acknowledgement

We would like to thank our friend Ivan Damjanov, MD, PhD (University of Kansas), for all his critical and constructive comments and his assistance with editing of the manuscript.

References

[1] Kuroda N, Hess O, Zhou M. New and emerging renal tumour entities. Diagn Histopathol 2016;22:47–56.
[2] Moch H, Cubilla AL, Humphrey PA, Reuter VE, Ulbright TM. The 2016 WHO classification of tumours of the urinary system and male genital organs-part a: renal, penile, and testicular tumours. Eur Urol 2016;70:93–105.
[3] Moch H, Humphrey PA, Ulbright TM, Reuter VE. WHO classification of tumours of the urinary system and male genital organs. 4th ed. Lyon: IARC; 2016.
[4] Hes O, Brunelli M, Michal M, Cossu Rocca P, Hora M, Chilosi M, et al. Oncocytic papillary renal cell carcinoma: a clinicopathologic, immunohistochemical, ultrastructural, and interphase cytogenetic study of 12 cases. Ann Diagn Pathol 2006;10:133–9.
[5] Hes O, Condom Mundo E, Peckova K, Lopez JI, Martinek P, Vanecek T, et al. Biphasic squamoid alveolar renal cell carcinoma: a distinctive subtype of papillary renal cell carcinoma? Am J Surg Pathol 2016;40:664–75.
[6] Ulamec M, Skenderi F, Trpkov K, Kruslin B, Vranic S, Bulimbasic S, et al. Solid papillary renal cell carcinoma: clinicopathologic, morphologic, and immunohistochemical analysis of 10 cases and review of the literature. Ann Diagn Pathol 2016;23:51–7.
[7] Pivovarcikova K, Peckova K, Martinek P, Montiel DP, Kalusova K, Pitra T, et al. "Mucin"-secreting papillary renal cell carcinoma: clinicopathological, immunohistochemical, and molecular genetic analysis of seven cases. Virchows Arch 2016;469:71–80.
[8] Klatte T, Said JW, Seligson DB, Rao PN, de Martino M, Shuch B, et al. Pathological, immunohistochemical and cytogenetic features of papillary renal cell carcinoma with clear cell features. J Urol 2011;185:30–5.
[9] Ross H, Martignoni G, Argani P. Renal cell carcinoma with clear cell and papillary features. Arch Pathol Lab Med 2012;136:391–9.
[10] Cancer Genome Atlas Research N, Linehan WM, Spellman PT, Ricketts CJ, Creighton CJ, Fei SS, et al. Comprehensive molecular characterization of papillary renal-cell carcinoma. N Engl J Med 2016;374:135–45.
[11] Marsaud A, Dadone B, Ambrosetti D, Baudoin C, Chamorey E, Rouleau E, et al. Dismantling papillary renal cell carcinoma classification: the heterogeneity of genetic profiles suggests several independent diseases. Genes Chromosomes Cancer 2015;54:369–82.
[12] Bigot P, Bernhard JC, Gill IS, Vuong NS, Verhoest G, Flamand V, et al. The subclassification of papillary renal cell carcinoma does not affect oncological outcomes after nephron sparing surgery. World J Urol 2016;34:347–52.
[13] Xia QY, Rao Q, Shen Q, Shi SS, Li L, Liu B, et al. Oncocytic papillary renal cell carcinoma: a clinicopathological study emphasizing distinct morphology, extended immunohistochemical profile and cytogenetic features. Int J Clin Exp Pathol 2013;6:1392–9.
[14] Lefevre M, Couturier J, Sibony M, Bazille C, Boyer K, Callard P, et al. Adult papillary renal tumor with oncocytic cells: clinicopathologic, immunohistochemical, and cytogenetic features of 10 cases. Am J Surg Pathol 2005;29:1576–81.
[15] Ishibashi K, Ito Y, Masaki A, Fujii K, Beppu S, Sakakibara T, et al. Warthin-like mucoepidermoid carcinoma: a combined study of fluorescence in situ hybridization and whole-slide imaging. Am J Surg Pathol 2015;39:1479–87.
[16] Yeo MK, Bae JS, Lee S, Kim MH, Lim DJ, Lee YS, et al. The Warthin-like variant of papillary thyroid carcinoma: a comparison with classic type in the patients with coexisting Hashimoto's thyroiditis. Int J Endocrinol 2015;2015:456027.
[17] Festino L, Botti G, Lorigan P, Masucci GV, Hipp JD, Horak CE, et al. Cancer treatment with anti-PD-1/PD-L1 agents: is PD-L1 expression a biomarker for patient selection? Drugs 2016;76:925–45.
[18] van Dongen JJ, Langerak AW, Bruggemann M, Evans PA, Hummel M, Lavender FL, et al. Design and standardization of PCR primers and protocols for detection of clonal immunoglobulin and T-cell receptor gene recombinations in suspect lymphoproliferations: report of the BIOMED-2 concerted action BMH4-CT98-3936. Leukemia 2003;17:2257–317.
[19] Sperga M, Martinek P, Vanecek T, Grossmann P, Bauleth K, Perez-Montiel D, et al. Chromophobe renal cell carcinomas—chromosomal aberration variability and its relation to Paner grading system: an array CGH and FISH analysis of 37 cases. Virchows Archiv 2013;463:563–73.
[20] Kacerovska D, Drlik L, Slezakova L, Michal M, Stehlik J, Sedivcova M, et al. Cutaneous sebaceous lesions in a patient with MUTYH-associated polyposis mimicking Muir-Torre syndrome. Am J Dermatopathol 2016;38:915–23.
[21] Chan AO, Broaddus RR, Houlihan PS, Issa JP, Hamilton SR, Rashid A. CpG island methylation in aberrant crypt foci of the colorectum. Am J Pathol 2002;160:1823–30.
[22] Matsuoka T, Ichikawa C, Fukunaga A, Yano T, Sugino Y, Okada T, et al. Two cases of oncocytic papillary renal cell carcinoma. Hinyokika kiyo Acta Urol Jpn 2016;62:187–91.
[23] Masuzawa N, Kishimoto M, Nishimura A, Shichiri Y, Yanagisawa A. Oncocytic renal cell carcinoma having papillotubular growth: rare morphological variant of papillary renal cell carcinoma. Pathol Int 2008;58:300–5.
[24] Mai KT, Kohler DM, Robertson SJ, Belanger EC, Marginean EC. Oncocytic papillary renal cell carcinoma with solid architecture: mimic of renal oncocytoma. Pathol Int 2008;58:164–8.
[25] Kunju LP, Wojno K, Wolf Jr JS, Cheng L, Shah RB. Papillary renal cell carcinoma with oncocytic cells and nonoverlapping low grade nuclei: expanding the morphologic spectrum with emphasis on clinicopathologic, immunohistochemical and molecular features. Hum Pathol 2008;39:96–101.
[26] Kim JY. Oncocytic papillary renal cell carcinoma in the background of renal adenomatosis: a case report. Int J Surg Pathol 2016.
[27] Han G, Yu W, Chu J, Liu Y, Jiang Y, Li Y, et al. Oncocytic papillary renal cell carcinoma: a clinicopathological and genetic analysis and indolent clinical course in 14 cases. Pathol Res Pract 2017;213:1–6.
[28] Krill-Burger JM, Lyons MA, Kelly LA, Sciulli CM, Petrosko P, Chandran UR, et al. Renal cell neoplasms contain shared tumor type-specific copy number variations. Am J Pathol 2012;180:2427–39.
[29] Brunelli M, Eble JN, Zhang S, Martignoni G, Delahunt B, Cheng L. Eosinophilic and classic chromophobe renal cell carcinomas have similar frequent losses of multiple chromosomes from among chromosomes 1, 2, 6, 10, and 17, and this pattern of genetic abnormality is not present in renal oncocytoma. Mod Pathol 2005;18:161–9.
[30] Durinck S, Stawiski EW, Pavia-Jimenez A, Modrusan Z, Kapur P, Jaiswal BS, et al. Spectrum of diverse genomic alterations define non-clear cell renal carcinoma subtypes. Nat Genet 2015;47:13–21.
[31] Kovac M, Navas C, Horswell S, Salm M, Bardella C, Rowan A, et al. Recurrent chromosomal gains and heterogeneous driver mutations characterise papillary renal cancer evolution. Nat Commun 2015;6:6336.
[32] Massari F, Santoni M, Ciccarese C, Santini D, Alfieri S, Martignoni G, et al. PD-1 blockade therapy in renal cell carcinoma: current studies and future promises. Cancer Treat Rev 2015;41:114–21.
[33] Yoo KH, Won KY, Lim SJ, Park YK, Chang SG. Deficiency of MSH2 expression is associated with clear cell renal cell carcinoma. Oncol Lett 2014;8:2135–9.
[34] Petersson F, Sima R, Sperga M, Kazakov DV, Michal M, Hora M, et al. Lymphocyte-rich renal cell carcinoma: an unusual histomorphologic manifestation of a tumor that is not part of lynch syndrome. Appl Immunohistochem Mol Morphol 2011;19:519–27.
[35] Gross M, Eliashar R, Ben-Yaakov A, Weinberger JM, Maly B. Clinicopathologic features and outcome of the oncocytic variant of papillary thyroid carcinoma. Ann Otol Rhinol Laryngol 2009;118:374–81.
[36] Smith SC, Trpkov K, Chen YB, Mehra R, Sirohi D, Ohe C, et al. Tubulocystic carcinoma of the kidney with poorly differentiated foci: a frequent morphologic pattern of fumarate hydratase-deficient renal cell carcinoma. Am J Surg Pathol 2016;40:1457–72.
[37] Trpkov K, Hes O, Agaimy A, Bonert M, Martinek P, Magi-Galluzzi C, et al. Fumarate hydratase-deficient renal cell carcinoma is strongly correlated with fumarate hydratase mutation and hereditary leiomyomatosis and renal cell carcinoma syndrome. Am J Surg Pathol 2016;40:865–75.
[38] Tran T, Jones CL, Williamson SR, Eble JN, Grignon DJ, Zhang S, et al. Tubulocystic renal cell carcinoma is an entity that is immunohistochemically and genetically distinct from papillary renal cell carcinoma. Histopathology 2016;68:850–7.
[39] Ulamec M, Skenderi F, Zhou M, Kruslin B, Martinek P, Grossmann P, et al. Molecular genetic alterations in renal cell carcinomas with tubulocystic pattern: tubulocystic renal cell carcinoma, tubulocystic renal cell carcinoma with heterogenous component and familial leiomyomatosis-associated renal cell carcinoma. clinicopathologic and molecular genetic analysis of 15 cases. Appl Immunohistochem Mol Morphol 2016;24:521–30.
[40] Banerjee I, Yadav SS, Tomar V, Yadav S, Talreja S. Tubulocystic renal cell carcinoma: a great imitator. Rev Urol 2016;18:118–21.
[41] Kuroda N, Yorita K, Nagasaki M, Harada Y, Ohe C, Jeruc J, et al. Review of succinate dehydrogenase-deficient renal cell carcinoma with focus on clinical and pathobiological aspects. Pol J Pathol 2016;67:3–7.

BIFAZICKÝ SKVAMOIDNÍ ALVEOLÁRNÍ RENÁLNÍ KARCINOM. ZVLÁŠTNÍ PODTYP PAPILÁRNÍHO RENÁLNÍHO KARCINOMU?

Bifazický skvamoidní alveolární renální karcinom (BSARK) byl v nedávné době popsán naši institucí v sérii dvou případů [27]. Histologicky je charakterizován nápadným solidně-alveolárním uspořádáním, přičemž tumor se skládá z duální populace buněk ve variabilním poměru: 1) malé blandní nádorové buňky chudé na cytoplazmu, které lemují vnitřní stranu alveolárních struktur; 2) větší skvamoidní buňky s objemnější cytoplazmou a větším měchýřkovitým jádrem, které jsou uspořádané do kompaktních hnízd. Nepodařilo se nám morfologicky prokázat pravou skvamocelulární diferenciaci (intercelulární můstky a/nebo keratinové perly), považujeme proto za vhodnější druhou skupinu buněk nazývat skvamoidními namísto skvamózními. Dalším nepřehlédnutelným znakem v obou tumorech byla přítomnost emperipolézy. V žádném z případů jsme nezastihli jiné struktury, než výše zmíněné, proto jsme tyto tumory prohlásili za unikátní a dříve nepopsané a navrhli jsme pro tuto potencionálně novou jednotku deskriptivní termín bifazický skvamoidní alveolární renální karcinom.

Od té doby jsme shromáždili dalších 20 případů, které jsme zařadili do této studie (jeden případ byl po molekulárně genetickém otestování vyřazen), jejímž cílem bylo tuto jednotku lépe histopatologicky a biologicky definovat. Všechny případy jsme hodnotili morfologicky, za použití IHC a molekulární genetiky (aCGH, FISH). Histologicky jsme v 9/21 tumorech identifikovali přechod skvamoalveolárních struktur do partií vzhledu papilárního renálního karcinomu (PRK) (papilární uspořádání, pěnité makrofágy, psammomatózní tělíska). Konstantní byla přítomnost emperipolézy (ve všech případech). IHC byly všechny tumory pozitivní s CK7, EMA, vimentinem a cyklinem D1. Molekulárně geneticky jsme ve všech analyzovatelných tumorech detekovali nadbytečné chromozomy 7 a 17.

Z dostupných klinických dat je zřejmé, že BSARK má metastatický potenciál (metastazovalo 5 případů), nicméně na odhad prognózy je zatím sesbíráno málo případů.

Nález histologických znaků charakteristických pro PRK společně s imunoprofilem a molekulární genetikou podporují domněnku, že BSARK patří do morfologického spektra PRK a není samostatnou jednotkou. Naše studie přispívá k nyní stále více uznávanému pohledu, že PRK nelze striktně dělit na typ 1, 2 a potencionální typ 3 (onkocytický PRK), ale že jeho morfologické spektrum se s novými poznatky stále rozšiřuje.

Biphasic Squamoid Alveolar Renal Cell Carcinoma

A Distinctive Subtype of Papillary Renal Cell Carcinoma?

Ondrej Hes, MD, PhD, Enric Condom Mundo, MD, PhD,†‡ Kvetoslava Peckova, MD,* Jose I. Lopez, MD,§ Petr Martinek, PhD,* Tomas Vanecek, PhD,* Giovanni Falconieri, MD,‖ Abbas Agaimy, MD,¶ Whitney Davidson, MD,# Fredrik Petersson, MD, PhD,** Stela Bulimbasic, MD, PhD,†† Ivan Damjanov, MD, PhD,# Mireya Jimeno, MD,‡‡ Monika Ulamec, MD, PhD,§§ Miroslav Podhola, MD, PhD,‖‖ Maris Sperga, MD,¶¶ Maria Pane Foix, MD,†‡ Ksenya Shelekhova, MD, PhD,## Kristyna Kalusova, MD,*** Milan Hora, MD, PhD,*** Pavla Rotterova, MD, PhD,* Ondrej Daum, MD, PhD,* Kristyna Pivovarcikova, MD,* and Michal Michal, MD**

Abstract: Biphasic squamoid alveolar renal cell carcinoma (BSARCC) has been recently described as a distinct neoplasm. Twenty-one cases from 12 institutions were analyzed using routine histology, immunohistochemistry, array comparative genomic hybridization (aCGH) and fluorescence in situ hybridization. Tumors were removed from 11 male and 10 female patients, whose age ranged from 53 to 79 years. The size of tumors ranged from 1.5 to 16 cm. Follow-up information was available for 14 patients (range, 1 to 96 mo), and metastatic spread was found in 5 cases. All tumors comprised 2 cell populations arranged in organoid structures: small, low-grade neoplastic cells with scant cytoplasm usually lining the inside of alveolar structures, and larger squamoid cells with more prominent cytoplasm and larger vesicular nuclei arranged in compact nests. In 9/21 tumors there was a visible transition from such solid and alveolar areas into papillary components. Areas composed of large squamoid cells comprised 10% to 80% of total tumor volume. Emperipolesis was present in all (21/21) tumors. Immunohistochemically, all cases were positive for cytokeratin 7, EMA, vimentin, and cyclin D1. aCGH (confirmed by fluorescence in situ hybridization) in 5 analyzable cases revealed multiple numerical chromosomal changes including gains of chromosomes 7 and 17 in all cases. These changes were further disclosed in 6 additional cases, which were unsuitable for aCGH. We conclude that tumors show a morphologic spectrum ranging from RCC with papillary architecture and large squamoid cells to fully developed BSARCC. Emperipolesis in squamoid cells was a constant finding. All BSARCCs expressed CK7, EMA, vimentin, and cyclin D1. Antibody to cyclin D1 showed a unique and previously not recognized pattern of immunohistochemical staining. Multiple chromosomal aberrations were identified in all analyzable cases including gains of chromosomes 7 and 17, indicating that they are akin to papillary RCC. Some BSARCCs were clinically aggressive, but their prognosis could not be predicted from currently available data. Present microscopic, immunohistochemical, and molecular genetic data strongly support the view that BSARCC is a distinctive and peculiar morphologic variant of papillary RCC.

Key Words: kidney, biphasic squamoid alveolar renal cell carcinoma, papillary renal cell carcinoma, immunohistochemistry, aCGH, FISH

(*Am J Surg Pathol* 2016;40:664–675)

From the Departments of *Pathology; ***Urology, Charles University, Medical Faculty and Charles University Hospital Plzen; ‖‖Department of Pathology, Charles University, Medical Faculty and Charles University Hospital Hradec Kralove, Czech Republic; †Department of Pathology, Bellvitge University Hospital, Bellvitge Biomedical Research Institute (IDIBELL); ‡Department of Pathology and Experimental Therapeutics, University of Barcelona School of Medicine; ‡‡Department of Pathology, Consorci Sanitari Integral, Barcelona; §Department of Pathology, Cruces University Hospital, Biocruces Research Institute, University of the Basque Country, Barakaldo, Spain; ‖Department of Pathology, University of Trieste, Trieste, Italy; ¶Department of Pathology, University Hospital Erlangen, Erlangen, Germany; #Department of Pathology, The University of Kansas School of Medicine, Kansas City, KS; **Department of Pathology, National University Health System, Singapore, Singapore; ††Department of Pathology, Clinical Hospital Center Zagreb; §§"Ljudevit Jurak" Pathology Department, Clinical Hospital Center "Sestre milosrdnice", Zagreb, Croatia; ¶¶Department of Pathology, East University, Riga, Latvia; and ##Department of Pathology, Petrov's Research Institute of Oncology, St Petersburg, Russia.

Conflicts of Interest and Source of Funding: Supported by the Charles University Research Fund (project number P36) and by the project CZ.1.05/2.1.00/03.0076 from European Regional Development Fund (O.H.). The authors have disclosed that they have no significant relationships with, or financial interest in, any commercial companies pertaining to this article.

Correspondence: Ondrej Hes, MD, PhD, Department of Pathology, Charles University, Medical Faculty and Charles University Hospital Plzen, Alej Svobody 80, 304 60 Pilsen, Czech Republic (e-mail: hes@medima.cz).

Three years ago we reported 2 renal cell carcinomas (RCCs) that we thought had unique and previously unrecognized histopathologic features.[1] We named that neoplasm descriptively as a biphasic alveolo-squamoid renal cell carcinoma (BSARCC). Unique to this tumor

were organoid structures composed of centrally located solid nests of large squamoid cells surrounded in an alveolar manner by smaller cuboidal and flattened cells reminiscent of dilated tubules or cysts. The squamoid cells had vesicular large nuclei, which were surrounded by eosinophilic cytoplasm with distinct cell borders. The alveolar cells were smaller and mostly cuboidal displaying a high nuclear to cytoplasmic ratio.[1] The clinicopathologic significance of these histopathologic data was not addressed, and thus we decided to assemble a much larger number of similar cases.

In the present paper we present 20 additional cases of this tumor type, providing evidence that BSARCCs are histogenetically closely related to papillary RCC (PRCC). Clinical follow-up shows that some of these cases had an adverse outcome. We hope that our study will stimulate other uropathologists to review their databases and further contribute to the characterization of BSARCC as a clinicopathologic entity.

MATERIALS AND METHODS

A search algorithm including the keywords "unclassified, squamoid, squamous, glomeruloid" was used to identify renal tumors from the Plzen Tumor Registry and multiple other institutional archives and consult files of the other authors. All cases were reviewed by 3 pathologists (O.H., K.Pe., M.M.) and compared with the index case to identify matching features. One or more hematoxylin and eosin–stained slides were available for review in all cases (1 to 23 slides/case). Altogether 21 cases were identified from a total of 18,500 cases. Three cases have already been published previously and were included into the present study (cases 7, 14, and 15). These cases are marked by the sign § in Table 1.[1,2]

Light Microscopy

Tissue for light microscopy had been fixed in 4% formaldehyde and embedded in paraffin using routine procedures. Sections of 5 μm thickness were cut and stained with hematoxylin and eosin.

Immunohistochemistry

A relatively broad panel of antibodies was used for complex analysis of tumors with apparently dual population. All staining analyses were performed in 1 institution (University Hospital Plzen). The immunohistochemical study was performed using a Ventana Benchmark XT automated stainer (Ventana Medical System Inc., Tucson, AZ).

The following primary antibodies were used: epithelial membrane antigen (EMA) (E29, monoclonal; DakoCytomation, Carpinteria, CA; 1:1000), cytokeratins (AE1-AE3, monoclonal; BioGenex, San Ramon, CA; 1:1000), CK5/6 (D5/16B4, monoclonal; DakoCytomation; 1:100), CD10 (56C6; Novocastra, Burlingame, CA; 1:20), cytokeratin 7 (OV-TL12/30, monoclonal;

TABLE 1. Basic Clinicopathologic Data

Case	Sex	Age	Size (cm)	Side	Follow-up (mo)	Squamoid Area-extend in %	Emperipolesis
1	M	65	10 × 9.5 × 7	R	24, AWD*	10	Yes
2	M	57	6 × 5 × 4	UN	ND	20	Yes
3	F	60	10.5	L	29, DOD	20	Yes
4	F	53	3.2	R	1, DUN†	10	Yes
5	F	70	UN	UN	UN	40	Yes
6	M	66	3.5	R	6, AWD, then ND‡	10	Yes
7§	F	54	3	R	72, AW, then ND	100 (minimal papillary focus)	Yes
8	F	54	1.9 × 1.4 × 2	R	24, AW	40	Yes
9	M	63	3.5	UN	UN	60	Yes
10	M	57	3	UN	ND	45	Yes
11	F	79	4.5	UN	ND	30	Yes
12	F	70	2.9 × 1.7 × 1.5	R	18, AW	30	Yes
13	F	62	2.8 × 1.9 × 2	L	13, AW‖	35	Yes
14§	M	55	2	R	48, AW, then DUN¶	30	Yes
15§	F	54	2.2	R	96, AW, then DUN#	20	Yes
16	M	46	1.5	R	UN	40	Yes
17	M	60	2	R	24, AW	40	Yes
18	M	78	16.0	L	45, DOD**	45	Yes
19	M	53	3.0	R	6, AWD‡	5	Yes
20	M	65	5	UN	ND	30	Yes
21	F	72	6	L	3, AW	40	Yes

*pT3, pN2: lymph nodes paracaval (TNM 09).
†Dead of hemorrhagic shock 3 weeks after surgery, 18 years on hemodialysis.
‡6 months after nephrectomy, multiple bilateral lung metastases, lymph node metastases.
§Previously published cases.[1,2]
‖Ductal invasive carcinoma of breast treated 1 year before nephrectomy.
¶Dead of small cell carcinoma of the lung.
#Dead of cholangiogenic carcinoma of the liver.
**Metastases in mediastinal lymph nodes.
AW indicates alive and well; AWD, alive with disease; DOD, dead of disease; DUN, dead of unrelated condition; F, female; L, left; M, male; ND, not documented; R, right; UN, unknown.

FIGURE 1. Grossly, tumors are solid.

FIGURE 3. Some tumors were solid, firm with whitish color.

DakoCytomation; 1:200), cytokeratin 20 (M7019, monoclonal; DakoCytomation; 1:100), racemase/AMACR (P504S, monoclonal; Zeta, Sierra Madre, CA; 1:50), vimentin (D9, monoclonal; NeoMarkers, Westinghouse, CA; 1:1000), parvalbumin (PA-235, monoclonal; Sigma Aldrich, St Luis, MO; 1:500), Ki-67 (MIB1, monoclonal; Dako, Glostrup, Denmark; 1:1000), c-kit (CD117, polyclonal, Dako, Glostrup, Denmark, 1:300), CD10 (monoclonal, Sp67; Ventana, RTU), E-cadherin (12H6, monoclonal; Zymed, San Francisco, CA; 1:200), carbonic anhydrase IX (rhCA9, monoclonal; RD systems, Abingdon, GB; 1:100), p63 (4A4, monoclonal; Ventana, Tucson, AZ, RTU), p53 (DO-7, monoclonal; DakoCytomation; 1:30), antimelanosome (HMB45, monoclonal; DakoCytomation; 1:200), TFE3 (polyclonal; Abcam; 1:100), cathepsin K (3F9, monoclonal; Abcam; 1:100), WT1 (GF-H2, monoclonal; DakoCytomation; 1:150), TTF-1 (SPT24, monoclonal; Novocastra, Newcastle, UK; 1:400), antibody against cyclin D1-M 30 (M30 monoclonal; Lobome, Enzo Life Sciences, Ann Arbor, MI; 1:100), bcl-2 (monoclonal, 124; Cell Marque, Rocklin, CA; 1:100), cyclin D1 (SP4-R, monoclonal; Cell Marque; 1:100), (SP4-R, monoclonal; Ventana, RTU), (polyclonal; NeoMarkers, Fremont, CA; 1:100), and PAX-8 (polyclonal; Cell Marque; 1: 25). The primary antibodies were visualized using the supersensitive streptavidin-biotin-peroxidase complex (BioGenex). Appropriate positive controls were used.

FIGURE 2. Color ranges from whitish to tan/brown. Tan color of the gross section seen on a formalin-fixed tissue/specimen.

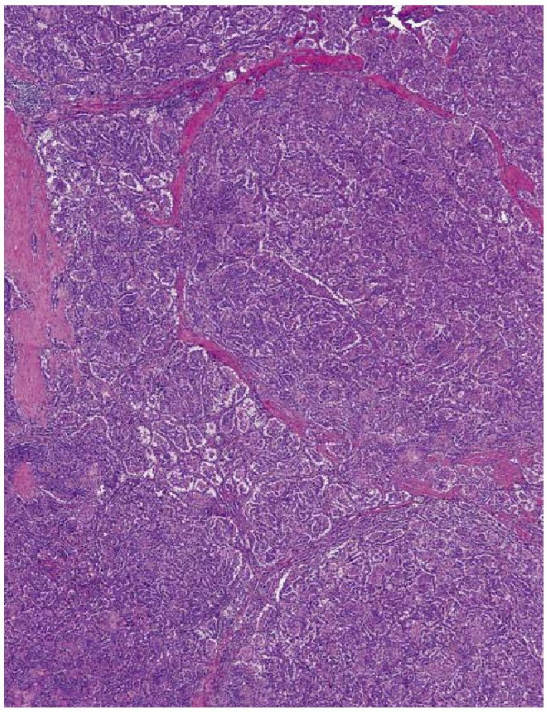

FIGURE 4. Well-developed BSARCC in which squamoid cells forming the majority of the tumors mass.

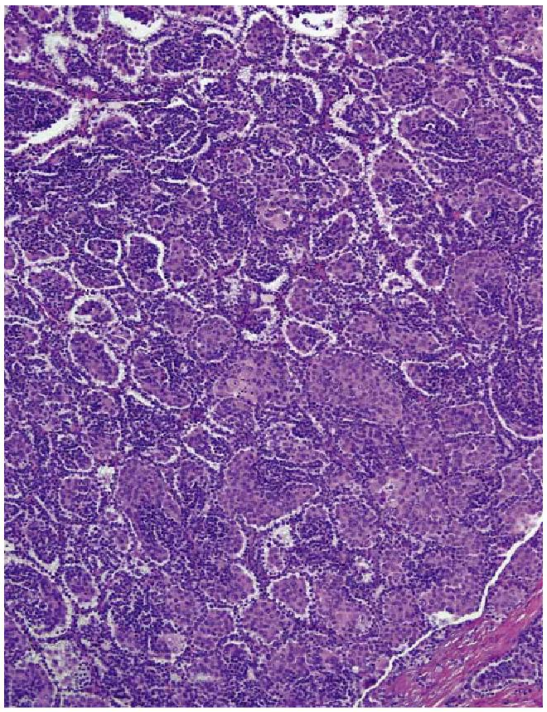

FIGURE 5. Solid-alveolar pattern of BSARCC is clearly seen.

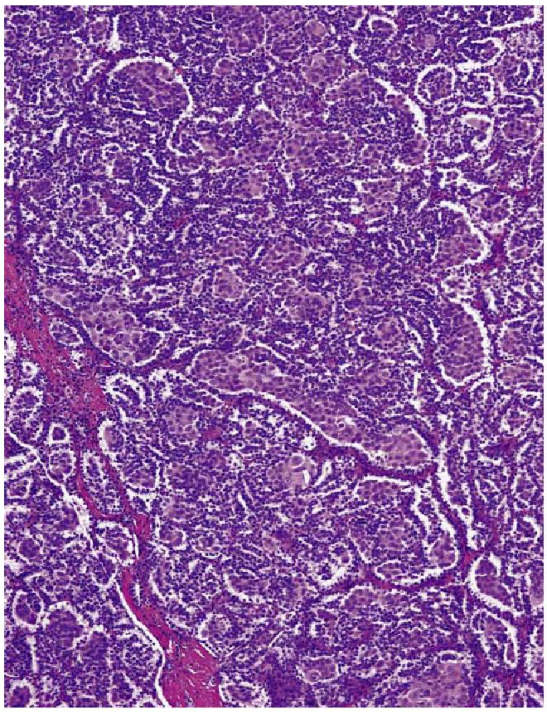

FIGURE 6. Squamoid areas surrounded by smaller cells with scant cytoplasm.

DNA Extraction

DNA from macrodissected formalin-fixed paraffin-embedded (FFPE) tissue was extracted using a QIAsymphony DNA Mini Kit (Qiagen, Hilden, Germany) on automated system (QIAsymphony SP, Qiagen) according to the manufacturer's supplementary protocol for FFPE samples (purification of genomic DNA from FFPE tissue using the QIAamp DNA FFPE Tissue Kit and Deparaffinization Solution). Samples were then purified using Qiaquick kit (Qiagen) and eluted in EB buffer (Qiagen). Concentration and purity of isolated DNA was measured using NanoDrop ND-1000 (NanoDrop Technologies Inc., Wilmington, DE). DNA integrity was examined by amplification of control genes in a multiplex polymerase chain reaction.[3]

Array Comparative Genomic Hybridization

Five cases (no 3, 9, 12, 13, 14) were suitable for analysis using array comparative genomic hybridization (aCGH).

CytoChip Focus Constitutional (BlueGnome Ltd, Cambridge, UK) array was used for aCGH analysis. It uses BAC technology and covers 143 regions of known significance with 1 Mb spacing across a genome. Probes are spotted in triplicates. First, 400 ng of DNA was labeled using the Fluorescent Labeling System (BlueGnome Ltd). The procedure included Cy3 labeling of a test sample and Cy5 labeling of a reference sample. Commercially produced reference of opposite sex was used in cases in which no reference sample was available (MegaPool Reference DNA Male/Female, Kreatech Diagnostics, Amsterdam, Netherlands). The labeled reference and the test sample were mixed, dried, and hybridized overnight at 47°C using Arrayit hybridization cassette (Arrayit Corporation, CA). Posthybridization washing was done using SSC buffers with increasing stringency. Dried microarray was scanned with InnoScan 900 (Innopsys, France) at a resolution of 5 μm. Scanned image was analyzed and quantified by BlueFuse Multi software (BlueGnome Ltd). The software uses Bayesian algorithms to generate intensity values for each Cy5 and Cy3 labeled spot on the array according an appropriate.gal file. Cutoff values for log 2 ratio are preset to −0.3 for loss and to 0.3 for gain by BlueFuse software.

Fluorescence In Situ Hybridization

Eleven cases were suitable for fluorescence in situ hybridization (FISH) analysis. A 4-μm-thick FFPE tissue section was placed onto a positively charged slide. The target area was circled with a diamond pen according to the corresponding hematoxylin and eosin–stained slide. The slide was routinely deparaffinized, incubated in the ×1 Target Retrieval Solution Citrate pH 6 (Dako) for 40 minutes at 95°C, then cooled for 20 minutes at room

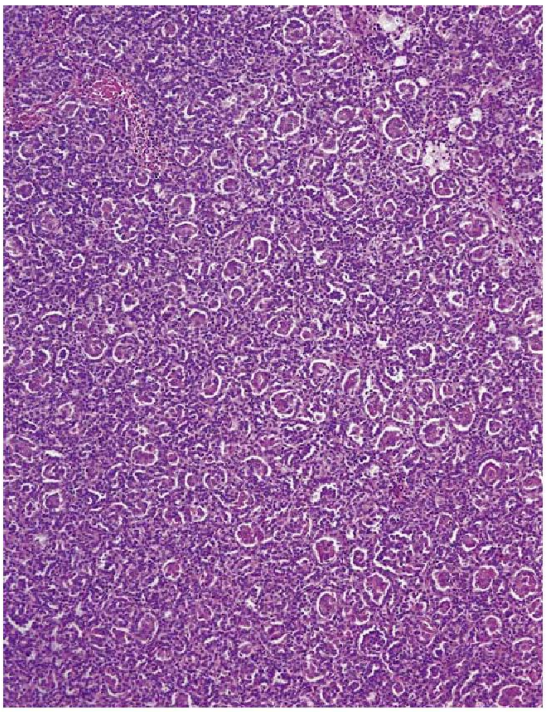

FIGURE 7. Scanning, low-power magnification shows RCC with papillary architecture comprising areas composed of large squamoid cells.

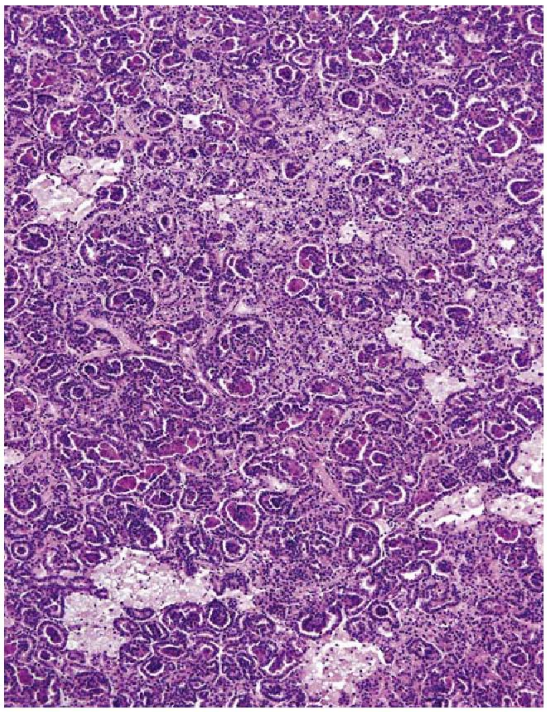

FIGURE 8. In some areas, foci of foam cells are present.

temperature in the same solution. The slide was washed in deionized water and digested in protease solution with pepsin (0.5 mg/mL) (Sigma Aldrich) in 0.01 M HCl at 37°C for 15 minutes. The slide was then immersed in deionized water for 5 minutes, dehydrated in a series of ethanol solutions (70%, 85%, and 96% for 2 min each) and air-dried. FISH probes CEP 7 Spectrum Orange (D7Z1), CEP 17 Spectrum Orange, CEP X (DXZ1) Spectrum Green/CEP Y (DYZ3) Spectrum Orange (Vysis/Abbott Molecular, Des Plaines, IL) were mixed with water and hybridization buffers according to manufacturer's protocol. The slide was incubated in a ThermoBrite instrument (StatSpin/Iris Sample Processing, Westwood, MA) with codenaturation at 85°C for 8 minutes and hybridization at 37°C for 16 hours. Posthybridization wash was performed in 2 × SSC/0.3% NP-40 solution at 72°C for 2 minutes. The slide was counterstained with DAPI I (Vysis) and stored in the dark at −20°C until examined. FISH signals were assessed using an Olympus BX51 fluorescence microscope. Scoring of aneuploidy was performed by counting the number of fluorescent signals in 100 randomly selected, nonoverlapping tumor cell nuclei. The slide was independently enumerated by 2 observers (P.M., T.V.). Cutoff values were set for each probe as shown in previous study.[4]

RESULTS

The clinicopathologic features of 21 cases of BSARCC are summarized in Table 1. Eleven of the patients were male and 10 were female; their ages ranged from 53 to 79 years (mean, 61.57 y). Tumor size ranged from 1.5 to 16 cm in greatest dimension (mean, 4.63 cm; median, 3.1 cm). All cases were solitary lesions. Follow-up data were available for 14/21 patients, with follow-up period ranging from 1 to 96 months (mean, 29.21 mo; median, 24 mo); metastatic spread was confirmed in 5 cases.

Three patients were alive with disease (lymph node involvement and bilateral lung metastases) after periods ranging from 6 to 24 months. However, 1 patient from this group (lung and lymph node metastases) was lost to follow-up 6 months after nephrectomy. Two patients died of widespread metastatic disease 29 and 45 months status post nephrectomy. Six patients were alive and well 3 to 72 months after diagnosis, whereas another 3 patients were without evidence of disease at 1, 48, and 96 months after surgery but died of unrelated diseases or conditions.

On gross examination the tumors were described as solid with color varying from whitish to tan or light brown (Figs. 1–3). Small areas of hemorrhage were reported in 4 cases with grossly visible necrotic foci noted in a single case.

All tumors were composed of a distinctly dual cell population. The first contained relatively uniform, small, low-grade neoplastic cells with scant cytoplasm. Such

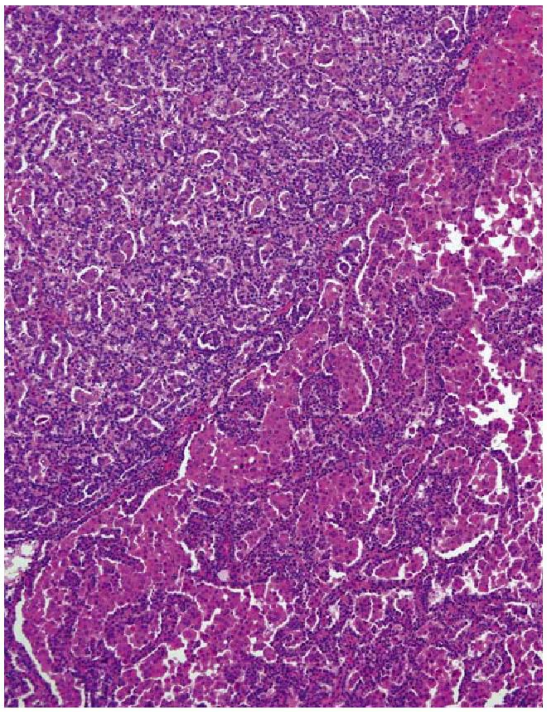

FIGURE 9. Transition between areas composed nearly exclusively of large squamoid cells and an area of more typical PRCC.

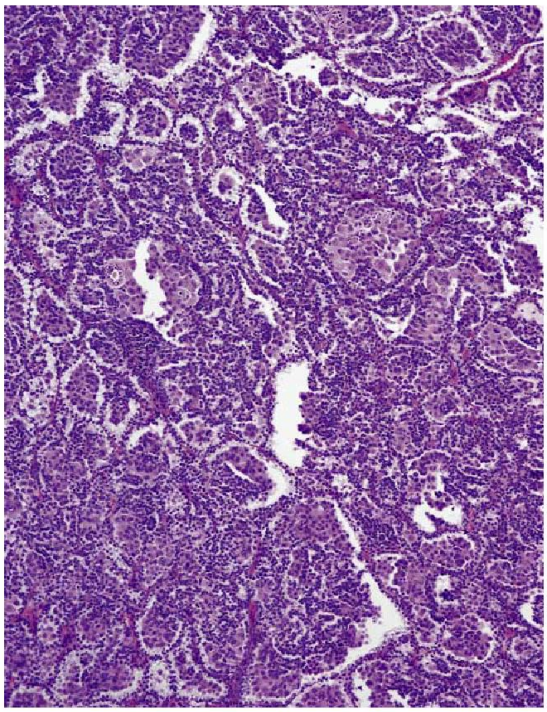

FIGURE 10. Emperipolesis was present in 21/21 tumors. This was found in large cells within squamoid areas. Scanning low-power magnification showing numerous foci of emperipolesis within squamoid areas.

small cells with scant cytoplasm had mostly round slightly elongated nuclei, resembling those of normal lymphocytes. These cells were arranged in rows forming alveolar-like structures, reminiscent of dilated tubules, microcystic structures, or Bowman capsular spaces. Alveolar spaces were often attached to the vascular septa contributing to their walls. Alveolar cells were separated by a slit space from the solid nests composed of larger squamoid cell, which formed the second cell population of all tumors. This second population was made up of large cells containing voluminous pink cytoplasm and large nuclei with prominent nucleoli. These eosinophilic cells were arranged in solid islands, forming the centers of alveolar structures and often revealing retraction artifacts, most likely related to the biphasic cell populations that were so closely intermixed. A retraction from the walls of the alveoli formed by smaller cells with scant cytoplasm may be seen in Figures 4–6. Neither the keratin pearls nor the intercellular bridges observed in true squamous epithelium were noted in any case. Large squamoid cells formed between 5% and 100% of the total tumor volume. Small foci of necrosis were identified on histologic examination in 3/21 cases, and a larger necrotic area was seen in just 1 case. Rare psammoma bodies were present in 7 tumors.

A visible transition from areas with a papillary pattern containing groups of large squamoid cells (Figs. 7, 8) to a fully developed solid-alveolar pattern was seen in 9 tumors (Fig. 9). These former areas were characterized by the presence of well-developed papillae and tubules all lined by mostly cuboidal low-grade epithelial cells with round nuclei. Focally, tubulopapillary formations with glomeruloid morphology were also noted.

Of particular note was the presence of emperipolesis, a highly unusual phenomenon among renal cell tumors. It was easily identified in all 21 cases. Emperipolesis was present only in large squamoid cells and was a very prominent feature within solid squamoid islands in some cases (Figs. 10–12). In fact, it was a conspicuous morphologic feature in a majority of the cases.

One case (case 3) included metastatic neoplastic tissue from multiple foci on the peritoneal surface and omentum. The metastatic deposits showed a mostly solid-alveolar pattern with large squamoid cells (Fig. 13), rare psammoma bodies (Fig. 14), and absent emperipolesis.

Immunohistochemical data are summarized in Table 2. One of the cases were not available for immunohistochemical examination. All analyzable tumors were positive for CK7 (Fig. 15), EMA, and vimentin in

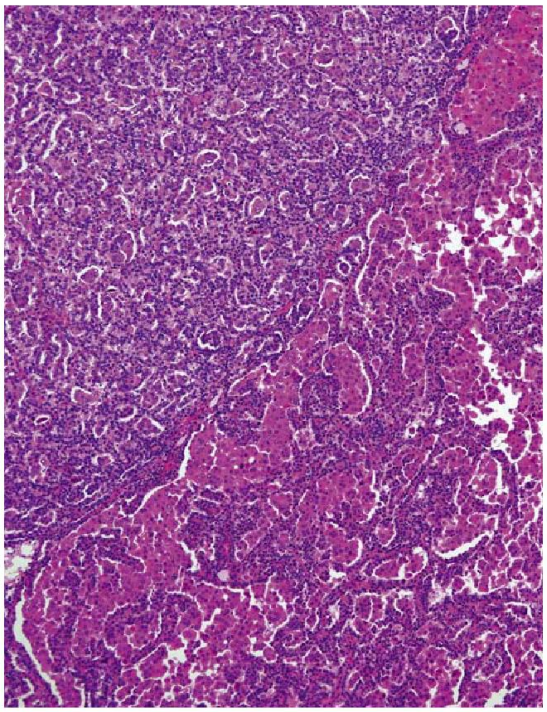

FIGURE 9. Transition between areas composed nearly exclusively of large squamoid cells and an area of more typical PRCC.

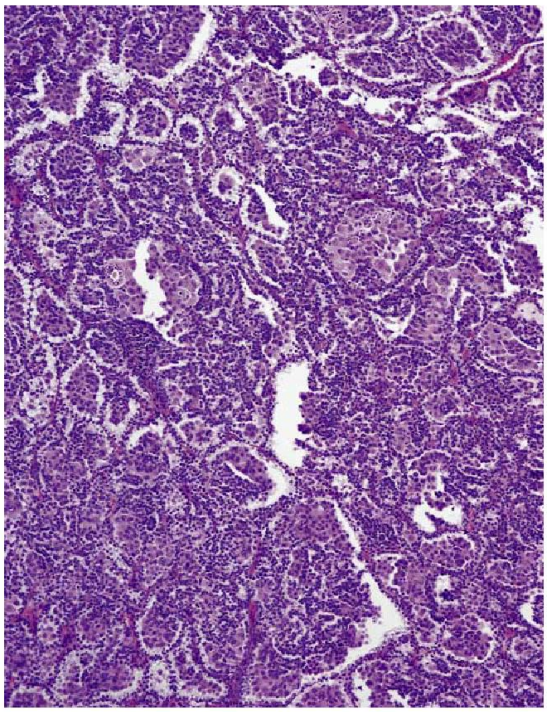

FIGURE 10. Emperipolesis was present in 21/21 tumors. This was found in large cells within squamoid areas. Scanning low-power magnification showing numerous foci of emperipolesis within squamoid areas.

small cells with scant cytoplasm had mostly round slightly elongated nuclei, resembling those of normal lymphocytes. These cells were arranged in rows forming alveolar-like structures, reminiscent of dilated tubules, microcystic structures, or Bowman capsular spaces. Alveolar spaces were often attached to the vascular septa contributing to their walls. Alveolar cells were separated by a slit space from the solid nests composed of larger squamoid cell, which formed the second cell population of all tumors. This second population was made up of large cells containing voluminous pink cytoplasm and large nuclei with prominent nucleoli. These eosinophilic cells were arranged in solid islands, forming the centers of alveolar structures and often revealing retraction artifacts, most likely related to the biphasic cell populations that were so closely intermixed. A retraction from the walls of the alveoli formed by smaller cells with scant cytoplasm may be seen in Figures 4–6. Neither the keratin pearls nor the intercellular bridges observed in true squamous epithelium were noted in any case. Large squamoid cells formed between 5% and 100% of the total tumor volume. Small foci of necrosis were identified on histologic examination in 3/21 cases, and a larger necrotic area was seen in just 1 case. Rare psammoma bodies were present in 7 tumors.

A visible transition from areas with a papillary pattern containing groups of large squamoid cells (Figs. 7, 8) to a fully developed solid-alveolar pattern was seen in 9 tumors (Fig. 9). These former areas were characterized by the presence of well-developed papillae and tubules all lined by mostly cuboidal low-grade epithelial cells with round nuclei. Focally, tubulopapillary formations with glomeruloid morphology were also noted.

Of particular note was the presence of emperipolesis, a highly unusual phenomenon among renal cell tumors. It was easily identified in all 21 cases. Emperipolesis was present only in large squamoid cells and was a very prominent feature within solid squamoid islands in some cases (Figs. 10–12). In fact, it was a conspicuous morphologic feature in a majority of the cases.

One case (case 3) included metastatic neoplastic tissue from multiple foci on the peritoneal surface and omentum. The metastatic deposits showed a mostly solid-alveolar pattern with large squamoid cells (Fig. 13), rare psammoma bodies (Fig. 14), and absent emperipolesis.

Immunohistochemical data are summarized in Table 2. One of the cases were not available for immunohistochemical examination. All analyzable tumors were positive for CK7 (Fig. 15), EMA, and vimentin in

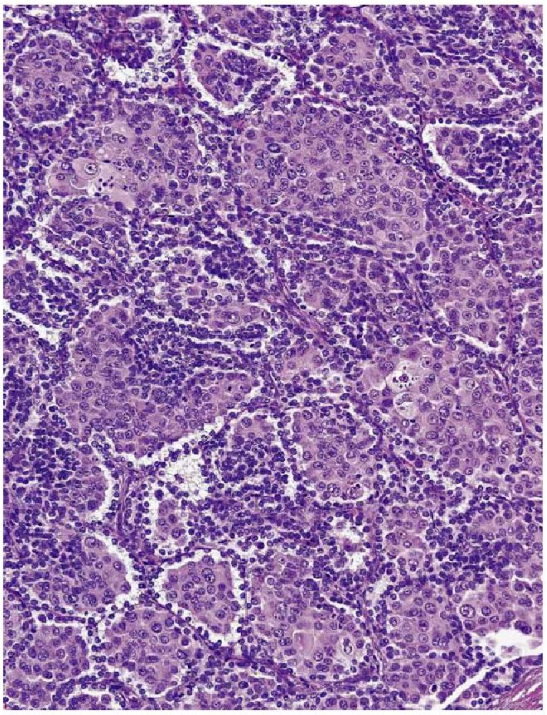

FIGURE 11. High-power magnification of squamoid cells with emperipolesis.

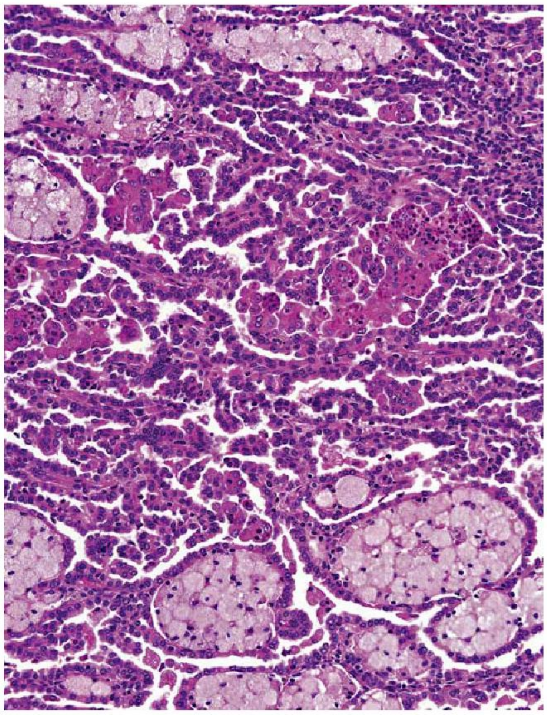

FIGURE 12. Similar to Figure 10. Emperipolesis in squamoid cells seen with foam cell macrophages intermingled among large squamoid cells.

both types of neoplastic cells. Nineteen of 21 cases were positive for cytokeratin AE1-AE3, and racemase (AMACR). All large squamoid cells expressed cyclin D1. There were no major differences among all 3 different antibodies against cyclin D1 (2 monoclonal and 1 polyclonal) (Figs. 16, 17). Large squamoid cells weakly expressed M30. All tumors were completely negative for TTF1, TFE 3, HMB45, and parvalbumin. Nineteen of 21 tumors were negative for CK 20, and 17/21 were negative for CD117 with documented positivity being focal, weak, and within the small-cell component.

Molecular-Genetic Data

Complete results of molecular genetic analyses, that is, aCGH and FISH, are summarized in Table 3. All analyzed samples (11/21) showed gains of chromosomes 7 and 17 (Fig. 18). Four of 5 analyzed male samples showed loss of chromosome Y. Additional gains of chromosome 20 were found in 3 of 5 analyzable cases using aCGH. Further chromosomal numerical changes including gain of chromosomes 16 and 12, loss of chromosome 21, and a loss of Xp22.33 were found in a single case.

DISCUSSION

Two cases of the so-called biphasic alveolo-squamoid renal carcinoma were reported in 2013.[1] Subsequently, 3 additional cases of the same tumor type were published in an abstract form in 2014.[1,2] The described tumors were composed of a distinctly dual cell population in which the larger tumor cells displayed squamoid features and formed round well-demarcated solid alveolar areas that, in large part, were surrounded by smaller neoplastic cells. Since publication of the above-mentioned paper, we have collected 20 additional cases from 12 institutions worldwide. In case 1 from Petersson et al's[1] paper, there was a very small, inconspicuous focus of papillary formation within the tumor. However, there were no other distinctive features to suggest the diagnosis of PRCC. Still we thought that the link of BSARCC and PRCC deserves to be explored.

PRCC is the second most frequently diagnosed RCC and is usually defined as a tumor derived from renal tubular epithelium with either papillary or tubule-papillary architecture. PRCC has traditionally been divided into 2 types. Type 1 PRCCs are mostly papillary, wherein the papillae are covered by cells with nuclei arranged in a single cell layer. The cells are relatively uniform with scant, pale, or basophilic cytoplasm and round nuclei. Type 2 is more polymorphic. Pseudostratification of nuclei is the key feature distinguishing type 2 from type 1 PRCC. PRCC type 2 usually has a higher nuclear grade, and cytoplasm is frequently eosinophilic.[5–7] A so-called

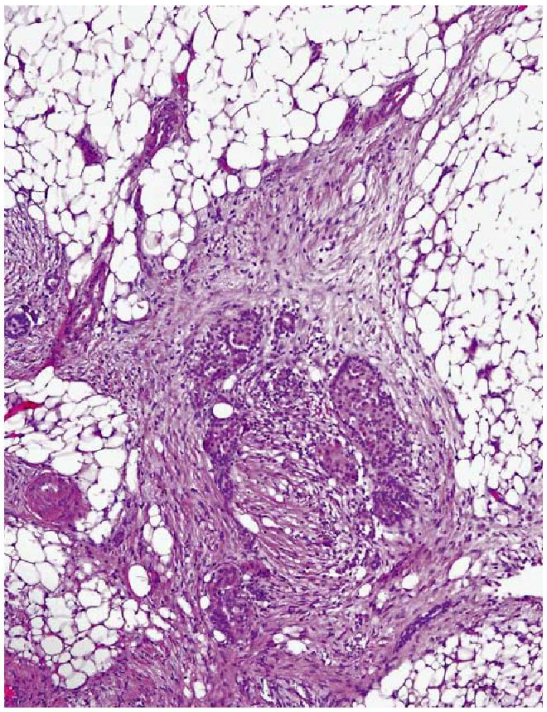

FIGURE 13. The metastatic deposits displayed a mostly solid alveolar pattern with large squamoid cells.

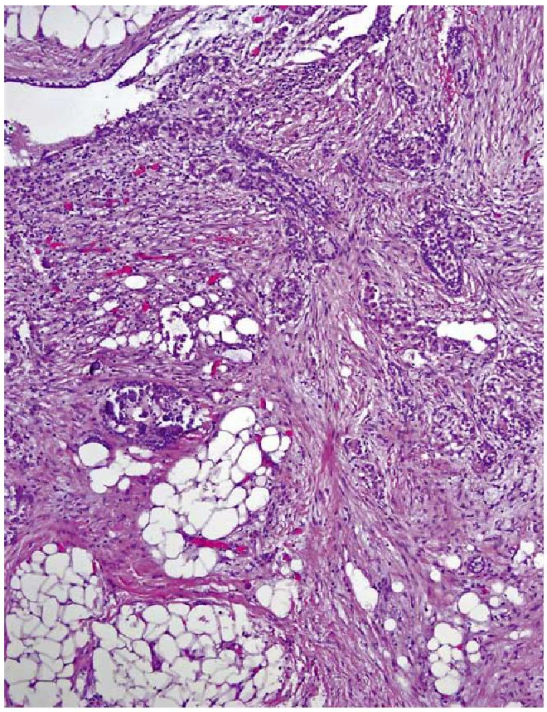

FIGURE 14. Rare psammoma bodies were present in metastases.

oncocytic variant of PRCC has also been described in the literature. These tumors are composed of cells with eosinophilic oncocytic cytoplasm, usually without pseudostratification of nuclei.[7–9] Some PRCCs are not easy to characterize as type 1, type 2, or oncocytic, and in such cases the diagnosis of PRCC, not otherwise specified, is usually established.

The fact that 10/21 cases of BSARCC exhibited components of classical PRCC suggests that BSARCC may be closely related to PRCC, or it may be a variant thereof with a peculiar and unusual morphology. The identified papillary component in these tumors was mostly compatible with type 1 PRCC according to Delahunt classification[5]; most papillae were covered by a single layer of smaller cells that had regular nuclei and scant cytoplasm.

In some areas the compression of papillae leads to the formation of tubulopapillary structures. Groups of larger, more pleomorphic cells with eosinophilic cytoplasm were found with such a pattern in the background. These larger cells displayed the same squamoid features seen in classical BSARCC and were immunohistochemically positive for cyclin D1. These transitional areas were either intermingled with areas exhibiting a more prominent biphasic pattern and with large areas of squamoid cells showing prominent emperipolesis or the transition between both patterns was in some cases more abrupt. PRCC with large eosinophilic cells like the cases reported herein has been described in the literature previously. It is shown in Sternberg's Diagnostic Pathology textbook (page 1982, figure 42.20).[10] The same type of PRCC is illustrated for example in the paper written by Mantoan Padilha et al.[11] We believe that so-called PRCC with formation of glomeruloids could be an early stage and BSARCC late stage of 1 neoplastic lesion and that we can consider such morphology as opposite ends of the same morphologic spectrum.

FISH analysis showed gains of chromosomes 7 and 17 in all 11 analyzable cases. Loss of chromosome Y was detected in 4 of 5 male cases, which is in line with patterns found in PRCC.[12,13] aCGH revealed some additional chromosomal changes, the most frequent being gain of chromosome 20. Case 2, which has been presented by Petersson et al[1] revealed a different chromosomal aberration pattern (losses on chromosomes 2, 5, 6, 9, 12, 15,16, 17, 18, and 22, including biallelic loss of the CDKN2A locus, and gains on chromosomes 1, 5, 11, 12, and 13). This case, after careful reevaluation of all available blocks and materials, was excluded from the current study and was rediagnosed as unclassified RCC. Hence, the pattern of chromosomal numerical aberrations was very uniform in all analyzable cases in our current study and was fully compatible with a diagnosis of PRCC.[7,14]

TABLE 2. Results of Immunohistochemical Examinations

Case	CANH	MIB1/hpf	TTF1	WT1	Cath	TFE3	HMB45	p53	p63	AE1/3	EMA	CK7
1	+	2-3 SC 5-6 LC	–	–	–	–	–	–	–	–	+ + +	+ foc
2	–	0-1 SC 3-4 LC	–	–	–	–	–	–	–	+ + +	+ +	+ +
3	–	0-1 SC 4-6 LC	–	–	–	–	–	+ LC	–	+ + + foc	+ + + foc	+ + +
4	+	0-1	–	–	–	–	–	–	–	+ + +	+ + + foc	+ + +
5	NP	NP	NP	NP	NP	NP	NP	NP	NP	NP	NP	NP
6	+ +	0-1 SC 2-3 LC	–	–	–	–	–	–	–	+ + +	+ + +	+ + +
7	+	0-2	–	–	–	–	–	+ + LC	–	+ + + foc	+ + +	+ + +
8	+ +	0-1	–	+ foc.	–	–	–	–	–	+ + + foc	+ + +	+ + +
9	+ +	0-1	–	–	–	–	–	–	–	+ + +	+ + +	+ + +
10	+ +	0 SC 1-2 LC	–	–	–	–	–	–	–	+ + +	+ + +	+ + +
11	+ +	0 SC 1-2 LC	–	–	–	–	–	–	–	+ + +	+ + +	+ + +
12	–	0-1	–	–	–	–	–	–	–	+ + + foc	+ + +	+ + +
13	–	0 SC 3-6 LC	–	–	–	–	–	–	–	+ + +	+ + +	+ + +
14	–	0-1	–	–	–	–	–	–	–	+ + +	+ + +	+ + +
15	–	0-1	–	–	–	–	–	–	–	+ + +	+ + +	+ + +
16	+ + LC	1-2 SC 4-7 LC	–	+ foc.	–	–	–	+	+ foc	+ + +	+ + +	+ + +
17	–	0-1	–	–	+ + foc	–	–	+ foc	–	+ + +	+ + +	+ + +
18	–	0-1 SC 5-7 LC	–	–	–	–	–	+ LC	–	+ + +	+ + +	+ + +
19	–	0–1	–	–	–	–	–	–	–	+ + +	+ + +	+ +
20	–	0-1	–	–	–	–	–	+ foc	–	+ + +	+ + +	+ + +
21	–	0-1 SC, 2-3 LC	–	–	–	–	–	–	–	+ +	+ + +	+ +

+ + + indicates strong positivity; + +, intermediate positivity; +, weak positivity; –, negative; AE1/3, AE1-AE3; CANH, carbonic anhydrase 9; cath, cathepsin K; E-cadh, E-cadherin; foc, focal; hpf, high-power field (×400); LC, large cells (squamoid); NP, not performed; parval, parvalbumin; SC, small cells; vim, vimentin.

Like in previous reports, we were not able to identify definitive morphologic proof of full squamous differentiation by light microscopy (intercellular bridges and/or keratin pearl formation) in any case.[1] Immunohistochemically, the absence of nuclear expression of p63 and only focal positivity with CK5/6 in 3/21 cases is in line with the light microscopic impression of "squamoid" rather than true squamous differentiation.

The presence of emperipolesis within the large squamoid cells is a very interesting phenomenon. Emperipolesis is defined as the presence of a non-neoplastic cell within the cytoplasm of another cell. An example of an entity featuring prominent emperipolesis is Rosai Dorfman disease.[15] Although the presence of emperipolesis is well recognized in several different tumorous entities, it is a highly unusual finding within RCCs. Emperipolesis was noted in all 21 cases and was a very prominent feature in some tumors. Staining with cyclin D1 proved helpful in revealing cells with emperipolesis, and such positivity was found exclusively in the large squamoid cell areas. Interestingly, cyclin D1 immunostaining has also proven helpful in disclosing cells with emperipolesis in cases of myxoinflammatory fibroblastic sarcomas.[16] *Cyclin D1/PRAD 1*, a cell cycle-related gene mapped to chromosome 11q13, has been found to be amplified in some breast cancers, certain squamous cell carcinomas of the head and neck and esophagus, several different lymphomas, etc.[17] Expression of cyclin D1 in RCCs has only recently been studied; Leroy et al[18] described overexpression of cyclin D1 in clear cell PRCC. Lima et al[19] looked at the prognostic significance of cyclin D1 expression in RCCs and concluded that high expression is associated with favorable prognosis. In addition, cyclin D1 has been used as part of the immunohistochemical panel for distinguishing between chromophobe RCC (CHRCC), clear cell RCC, and renal oncocytoma.[20] It seems that cyclin D1 positivity is one of the characteristic features of BSARCC; however, expression of cyclin D1 is not a specific diagnostic marker for BSARCC.

Differential Diagnosis

Squamoid differentiation described in all the 21 tumors of this series is one of the defining morphologic features of BSARCC. Generally speaking, squamous differentiation in RCC occurs extremely rarely. If ever found it should raise the possibility that particular tumor might be of urothelial origin. There have been several reports describing urothelial carcinoma within the kidney displaying squamous or squamoid features and even typical morphology of squamous carcinoma.[21–26] The present tumors differ, however, from such urothelial carcinomas: they were located inside the kidney parenchyma, and none of them was related to the urothelium of the renal pelvis or calices. No urothelial carcinoma in situ or urothelial dysplasia was detected in any of the current 21 cases. Thus we have excluded the possibility that the squamoid differentiation in BSARCC was related to squamous metaplasia of the urothelium.

Further evidence supporting the above interpretation was derived from the immunohistochemical data. Coexpression of CK7 and CK20 was noted within some large cells of the squamoid component in 1 case (case 7), but the small cells were completely negative for CK20. The vast majority of analyzable tumors were negative for CK20 in both cell components. Finally, we are not aware of any urothelial lesions with such a distinctly biphasic population of neoplastic cells in an organoid arrangement as seen in these renal tumors. Moreover, the cases with well-preserved

TABLE 2. *(continued)*

CyclinD1	CK20	CK5/6	CD10	AMACR	E-cadh	vim	Parval	CD117	M30	bcl2	PAX8
+ + +	–	–	+ + +	+ +	–	+ + + foc	–	–	+ +	foc.	+ +
+ + +	–	–	–	+ + +	–	+ +	–	–	+ +	–	+
+ + +	–	–	+ foc	+ + +	+ foc.	+ + +	–	–	+ +	–	+ dif
+ + +	–	–	–	+ + +	+ foc.	+ + + foc	–	–	+ + +	–	–
NP	NP	NP	NP	NP	NP	NP	NP	NP	NP	NP	NP
+ + +	–	–	–	+ + +	–	+ + +	–	–	+ + +	–	–
+ + +	+ + foc LC	+ +	–	+ + +	–	+ + +	–	–	+ + +	+ SC	+ +
+ + +	–	–	–	+ + +	+ + foc.	+ + +	–	–	+ + +	–	+ dif.
+ + +	–	+ +	–	+ + +	+ + + foc.	+ + +	–	–	+	–	–
+ + + –	–	–	–	–	+ foc.	+ + +	–	–	+ + +	–	+ dif.
+ + +	–	–	–	+ + +	–	+ + +	–	–	+ + foc.	+	+
+ + +	–	+ +	–	+ + +	+ + foc.	+ + + foc	–	–	+ + +	–	+ foc.
+ + +	–	–	–	+ + +	+ + + foc.	+ + +		–	+ + +	+ + +	+ +
+ + +	–	–	–	+ + +	+ foc.	+ + +	–	–	+ + foc.	+ dif.	+ dif
+ + +	–	–	–	+ + +	+ foc.	+ + +	–	+	+ + +	–	+ + +
+ + +	–	–	+ foc + +	+ + +	+ +	+ + +	–	+ + foc SC	+ + +	+ foc.	+ + foc
+ + +	–	–	–	+ + +	+ + foc	+ + +	–	+ foc SC	+ + +	+	+ + +
+ + +	–	–	+ + foc	+ + +	+ + SC + + + LC	+ + +	–	–	+ + dif	–	+
+ + +	–	–	–	+ +	– SC + LC	+ + +	–	–	+ + + dif.	–	–
+ + +	–	–	–	+ + +	–	+ + +	–	–	Foc +	+ foc	+ +
+ + +	–	–	–	+ +	foc. +	+ + +	–	–	–	–	+ +

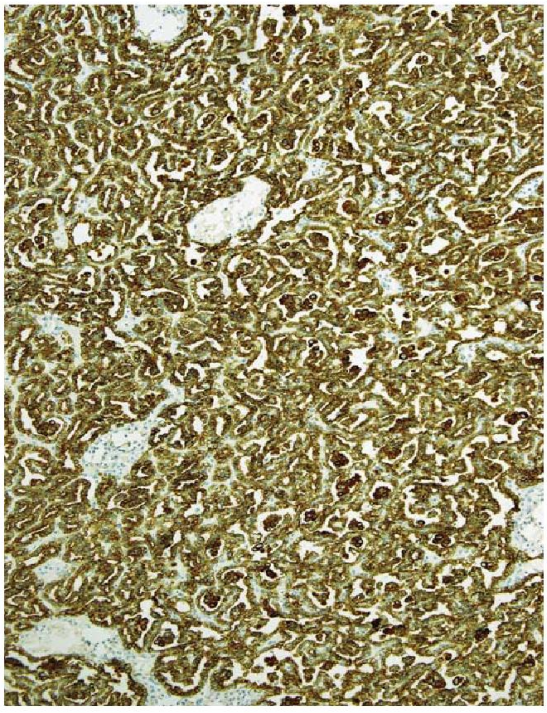

FIGURE 15. All tumors were positive for cytokeratin 7.

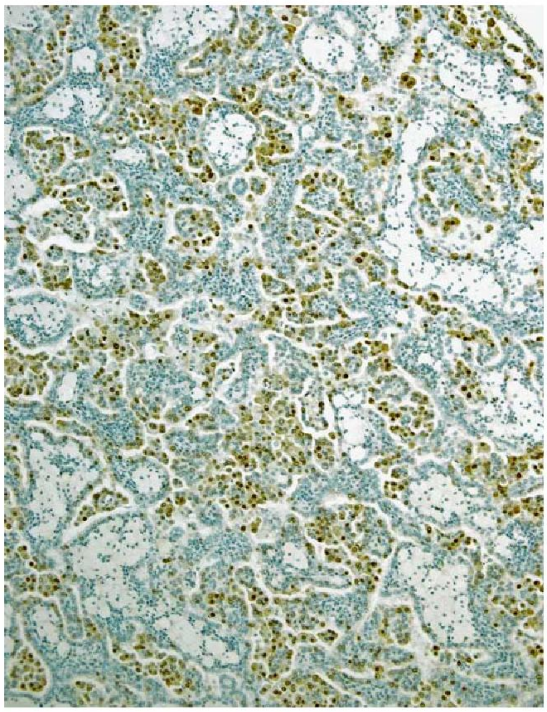

FIGURE 16. All large, squamoid cells expressed cyclin D1, reacting with both monoclonal antibodies (DAB-positive cells are brown).

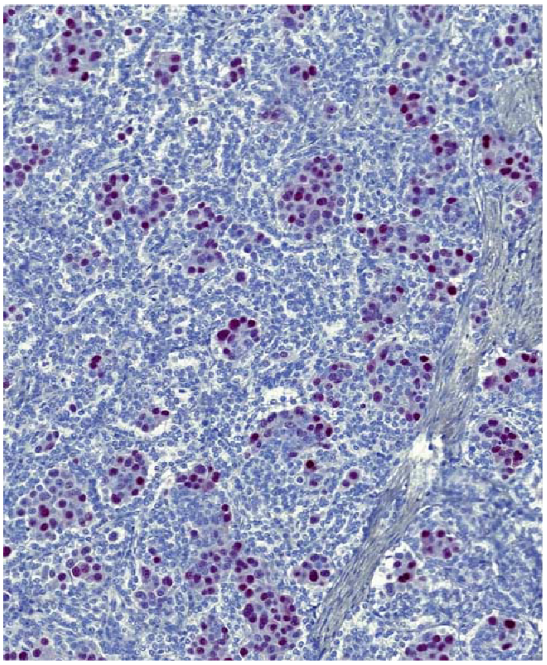

FIGURE 17. Squamoid cells were also positive with polyclonal antibody against cyclin D1 (alkaline phosphatase–positive cells are red).

DNA submitted to aCGH showed gains of chromosomes 7 and 17, which is suggestive of a connection to PRCC rather than urothelial carcinoma.

TABLE 3. Results of aCGH and FISH Analysis

Case	Sex	aCGH Result	CEP 7	CEP 17	CEP XY
1	M	NA	NA	NA	NA
2	M	NA	NA	NA	NA
3	F	+7, +17, +20, −21	P	P	XX
4	F	NA	P	P	XX
5	F	NA	NA	NA	NA
6	M	NA	NA	NA	NA
7	F	NA	P	P	XX
8	F	+7, +16, +17	P	P	XX
9	M	NA	NA	NA	NA
10	M	+7, +17, −Xp22.33, X-	P	P	X-
11	F	+7, +12, +17, +20	P	P	XX
12	F	+7, +17, +20	P	P	XX
13	F	NA	NA	NA	NA
14	M	NA	NA	NA	NA
15	F	NA	NA	NA	XX
16	M	NA	P	P	X-
17	M	NA	NA	NA	NA
18	M	NA	P	P	XY
19	M	NA	P	P	X-
20	M	NA	P	P	X-
21	F	NA	NA	NA	NA

CEP indicates centromeric probe; F, female; M, male; NA, not analyzable; P, polysomy; X-, loss of chromosome Y.

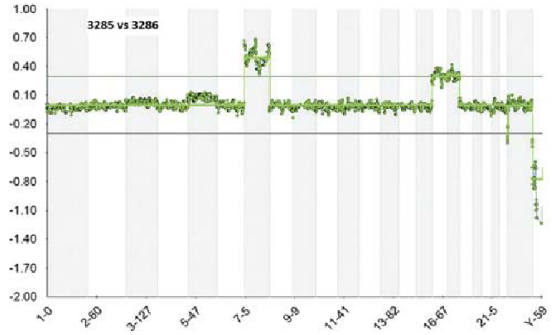

FIGURE 18. Gains of chromosomes 7 and 17 and losses of chromosomes 21 (variable) and Y were detected by aCGH analysis.

Squamous differentiation has been reported in RCC, but it seems to be a very rare phenomenon. Practically all RCCs with such morphology reported in the literature were CHRCCs with sarcomatoid transformation.[27–29] The cases presented here differ from CHRCC not only by morphology but also by their immunohistochemical and chromosomal profiles. There are 2 main variants of CHRCC that have been recognized: classical and eosinophilic.[30] Microscopically, these tumors are described as mostly solid or solid alveolar. However, the morphologic spectrum has been expanded to include microcystic, oncocytoma-like, adenomatoid, and tumors with neuroendocrine differentiation, and papillary arrangements.[31–37] There were no leaf-like cells or small eosinophilic cells present within the included tumors, and we were not able to identify raisinoid nuclei with perinuclear clearing typical of CHRCC. The sarcomatoid transformation seen in some CHRCCs has not been seen in our cases. The immunohistochemical profile of these cases differed from that of CHRCC. In this respect it is most important to note that CD117 was negative in 17/21 cases, and vimentin was positive in all analysable cases, which excludes the diagnosis of CHRCC. CD117 was only weakly positive within a small cell population of the 2 cases not counted above. CHRCCs are usually further characterized by multiple chromosomal losses of chromosomes 1, 2, 6, 10, 13, 17, and 21 in both classic and eosinophilic CHRCC.[30] Other studies also report numerical gains of chromosomes 4, 7, 15, 19, and 20,[4,38,39] but the significance of these findings is still a topic of discussion. The molecular genetic findings in all analyzed cases in this paper are completely different from the profiles identified in CHRCCs.

From the available clinical data, it is evident that BSARCC has metastatic potential. The morphology of the metastatic neoplasms did not differ significantly from that of the primary tumors, and it could be possible, albeit difficult, to recognize this unique pattern within a metastatic lesion even without information about the morphology of the primary tumor.

REFERENCES

1. Petersson F, Bulimbasic S, Hes O, et al. Biphasic alveolosquamoid renal carcinoma: a histomorphological, immunohistochemical, molecular genetic, and ultrastructural study of a distinctive morphologic variant of renal cell carcinoma. *Ann Diagn Pathol*. 2012;16:459–469.
2. Coromias Cishek A, Gonzalez M, Caamano V, et al. Biphasic alveolo-squamoid renal cell carcinoma (BASRC): light and immunohistochemical study of 3 cases. *Virchows Arch*. 2014;465(suppl 1): S157.
3. Van Dongen JJ, Langerak AW, Bruggemann M, et al. Design and standardization of PCR primers and protocols for detection of clonal immunoglobulin and T-cell receptor gene recombinations in suspect lymphoproliferations: report of the BIOMED-2 Concerted Action BMH4-CT98-3936. *Leukemia*. 2003;17:2257–2317.
4. Sperga M, Martinek P, Vanecek T, et al. Chromophobe renal cell carcinoma—chromosomal aberration variability and its relation to Paner grading system: an array CGH and FISH analysis of 37 cases. *Virchows Arch*. 2013;463:563–573.
5. Delahunt B, Eble JN. Papillary renal cell carcinoma: a clinicopathologic and immunohistochemical study of 105 tumors. *Mod Pathol*. 1997;10:537–544.
6. Delahunt B, Eble JN, McCredie MR, et al. Morphologic typing of papillary renal cell carcinoma: comparison of growth kinetics and patient survival in 66 cases. *Hum Pathol*. 2001;32:590–595.
7. Srigley JR, Delahunt B, Eble JN, et al. The International Society of Urological Pathology (ISUP) Vancouver Classification of Renal Neoplasia. *Am J Surg Pathol*. 2013;37:1469–1489.
8. Lefevre M, Couturier J, Sibony M, et al. Adult papillary renal tumor with oncocytic cells: clinicopathologic, immunohistochemical, and cytogenetic features of 10 cases. *Am J Surg Pathol*. 2005;29: 1576–1581.
9. Hes O, Brunelli M, Michal M, et al. Oncocytic papillary renal cell carcinoma: a clinicopathologic, immunohistochemical, ultrastructural, and interphase cytogenetic study of 12 cases. *Ann Diagn Pathol*. 2006;10:133–139.
10. Mills SE, Greenson JK, Hornick JL, et al, eds. *Sternberg's Diagnostic Surgical Pathology*, 6 ed. Philadelphia: Wolters Kluwer; 2015:2703.
11. Mantoan Padilha M, Billis A, Allende D, et al. Metanephric adenoma and solid variant of papillary renal cell carcinoma: common and distinctive features. *Histopathology*. 2013;62:941–953.
12. Kovacs G, Fuzesi L, Emanual A, et al. Cytogenetics of papillary renal cell tumors. *Genes Chromosomes Cancer*. 1991;3:249–255.
13. Jiang F, Richter J, Schraml P, et al. Chromosomal imbalances in papillary renal cell carcinoma: genetic differences between histological subtypes. *Am J Pathol*. 1998;153:1467–1473.
14. Eble JN, Sauter G, Epstein JI, et al. *WHO Classification of Tumours Tumours of the Urinary System and Male Genital Organs Pathology and Genetics*. Lyon: IARC Press; 2004:359.
15. Foucar E, Rosai J, Dorfman R. Sinus histiocytosis with massive lymphadenopathy (Rosai-Dorfman disease): review of the entity. *Semin Diagn Pathol*. 1990;7:19–73.
16. Michal M, Kazakov DV, Hadravsky L, et al. High-grade myxoinflammatory fibroblastic sarcoma: a report of 23 cases. *Ann Diagn Pathol*. 2015;19:157–163.
17. Zhang SY, Caamano J, Cooper F, et al. Immunohistochemistry of cyclin D1 in human breast cancer. *Am J Clin Pathol*. 1994;102: 695–698.
18. Leroy X, Camparo P, Gnemmi V, et al. Clear cell papillary renal cell carcinoma is an indolent and low-grade neoplasm with overexpression of cyclin-D1. *Histopathology*. 2014;64:1032–1036.
19. Lima MS, Pereira RA, Costa RS, et al. The prognostic value of cyclin D1 in renal cell carcinoma. *Int Urol Nephrol*. 2014;46: 905–913.
20. Zhao W, Tian B, Wu C, et al. DOG1, cyclin D1, CK7, CD117 and vimentin are useful immunohistochemical markers in distinguishing chromophobe renal cell carcinoma from clear cell renal cell carcinoma and renal oncocytoma. *Pathol Res Pract*. 2015;211: 303–307.
21. Mardi K, Kaushal V, Sharma V. Rare coexistence of keratinizing squamous cell carcinoma with xanthogranulomatous pyelonephritis in the same kidney: report of two cases. *J Cancer Res Ther*. 2010;6: 339–341.
22. Bhaijee F. Squamous cell carcinoma of the renal pelvis. *Ann Diagn Pathol*. 2012;16:124–127.
23. Zainuddin MA, Hong TY. Primary renal adenosquamous carcinoma. *Urol Ann*. 2010;2:122–124.
24. Terada T. Synchronous squamous cell carcinoma of the kidney, squamous cell carcinoma of the ureter, and sarcomatoid carcinoma of the urinary bladder: a case report. *Pathol Res Pract*. 2010; 206:379–383.
25. Holmang S, Lele SM, Johansson SL. Squamous cell carcinoma of the renal pelvis and ureter: incidence, symptoms, treatment and outcome. *J Urol*. 2007;178:51–56.
26. Perez-Montiel D, Wakely PE, Hes O, et al. High-grade urothelial carcinoma of the renal pelvis: clinicopathologic study of 108 cases with emphasis on unusual morphologic variants. *Mod Pathol*. 2006; 19:494–503.
27. Mete O, Kilicaslan I, Ozcan F, et al. Sarcomatoid chromophobe renal cell carcinoma with squamous differentiation. *Pathology*. 2007; 39:598–599.
28. Viswanathan S, Desai SB, Prabhu SR, et al. Squamous differentiation in a sarcomatoid chromophobe renal cell carcinoma: an unusual case report with review of the literature. *Arch Pathol Lab Med*. 2008;132:1672–1674.
29. Husain AEBJ, Trpkov K. Composite chromophobe renal cell carcinoma with sarcomatoid differentiation containing osteosarcoma, chondrosarcoma, squamous metaplasia and associated collecting duct carcinoma: a case report. *Anal Quant Cytopathol Histopathol*. 2014;36:235–240.
30. Brunelli M, Eble JN, Zhang S, et al. Eosinophilic and classic chromophobe renal cell carcinomas have similar frequent losses of multiple chromosomes from among chromosomes 1, 2, 6, 10, and 17, and this pattern of genetic abnormality is not present in renal oncocytoma. *Mod Pathol*. 2005;18:161–169.
31. Hes O, Vanecek T, Perez-Montiel DM, et al. Chromophobe renal cell carcinoma with microcystic and adenomatous arrangement and pigmentation—a diagnostic pitfall. Morphological, immunohistochemical, ultrastructural and molecular genetic report of 20 cases. *Virchows Arch*. 2005;446:383–393.
32. Dundr P, Pesl M, Povysil C, et al. Pigmented microcystic chromophobe renal cell carcinoma. *Pathol Res Pract*. 2007;203: 593–597.
33. Parada DD, Pena KB. Chromophobe renal cell carcinoma with neuroendocrine differentiation. *APMIS*. 2008;116:859–865.
34. Kuroda N, Tamura M, Hes O, et al. Chromophobe renal cell carcinoma with neuroendocrine differentiation and sarcomatoid change. *Pathol Int*. 2011;61:552–554.
35. Kuroda N, Liyama T, Moriki T, et al. Chromophobe renal cell carcinoma with focal papillary configuration, nuclear basaloid arrangement and stromal osseous metaplasia containing fatty bone marrow element. *Histopathology*. 2005;46:712–713.
36. Ohe C, Kuroda N, Keiko M, et al. Chromophobe renal cell carcinoma with neuroendocrine differentiation/morphology: a clinicopathological and genetic study of three cases. *Hum Pathol*. 2014;1:31–39.
37. Kuroda N, Tanaka A, Yamaguchi T, et al. Chromophobe renal cell carcinoma, oncocytic variant: a proposal of a new variant giving a critical diagnostic pitfall in diagnosing renal oncocytic tumors. *Med Mol Morphol*. 2013;46:49–55.
38. Vieira J, Henrique R, Ribeiro FR, et al. Feasibility of differential diagnosis of kidney tumors by comparative genomic hybridization of fine needle aspiration biopsies. *Genes Chromosomes Cancer*. 2010; 49:935–947.
39. Tan MH, Wong CF, Tan HL, et al. Genomic expression and single-nucleotide polymorphism profiling discriminates chromophobe renal cell carcinoma and oncocytoma. *BMC Cancer*. 2010;10:196.

SOLIDNÍ PAPILÁRNÍ RENÁLNÍ KARCINOM: KLINICKOPATOLOGICKÁ, MORFOLOGICKÁ A IMUNOHISTOCHEMICKÁ ANALÝZA 10 PŘÍPADŮ A PŘEHLED LITERATURY

Solidní papilární renální karcinom (SoPRK) je vzácný tumor s doposud popsanými pouze 53 případy. Histologicky je složen z malých epitelových buněk uspořádaných do stlačených tubulů a abortivních papil, které tumoru propůjčují solidní vzhled. Buňky s malými jádry a chudé na cytoplazmu by dovolovaly tento typ zařadit k papilárnímu renálnímu karcinomu typu 1, avšak architektonika SoPRK je zcela odlišná.

Do této studie jsme na podkladě morfologických znaků zařadili 10 případů SoPRK, které jsme vyšetřili imunohistochemicky a molekulárně geneticky a zaměřili jsme se zvláště na diferenciální diagnostiku tohoto vzácného typu PRK.

SoPRK postihuje častěji muže (poměr 3,5:1). Většina případů se diagnostikuje ve stadiu pT1 a ačkoliv klinická data jsou k dispozici zatím jen omezeně, SoPRK se zdá být indolentním tumorem. Imunohistochemicky (reaktivita s protilátkami CK7, AMACR, EMA) a molekulárně geneticky (polysomie/trisomie chromozomů 7 a 17, ztráta chromozomu Y) je SoPRK shodný s konvenčním PRK.

Diferenciálně diagnosticky je třeba vyloučit zvláště metanefrický adenom (MA), epiteloidní nefroblastom (EN), mucinózní tubulární a vřetenobuněčný renální karcinom (MTVRK) a solidní onkocytický renální karcinom (SoOPRK). MA se vyskytuje u mladších pacientů, převážně u žen. Ačkoliv oba typy tumorů se mohou morfologicky překrývat, imunoprofil a molekulárně genetické znaky se liší: MA adenom je typicky CK7 a AMACR negativní, WT1 a CD57 pozitivní a vykazuje mutace genu *BRAF V600E*. EN lze též snadno odlišit pomocí IHC a geneticky, navíc se tento typ tumoru jen velmi raritně vyskytuje u dospělých pacientů. Protože epitelové buňky u SoPRK mohou nabývat až vřetenitého vzhledu, v diferenciální diagnostice připadá v úvahu v MTVRK. Tento tumor dle své definice obsahuje myxoidní stroma. Existují však i na hlen chudé MTVRK a tomto případě může být odlišení svízelné. Doporučujeme důkladné zabločkování tumoru, po kterém jsou většinou partie typické pro MTVRK objeveny. SoOPRK uvádíme spíše z důvodu solidní architektoniky, jinak platí, že tento tumor může být bez nesnází od SoPRK odlišen na základě histologie.

Annals of Diagnostic Pathology 23 (2016) 51–57

Contents lists available at ScienceDirect

Annals of Diagnostic Pathology

Solid papillary renal cell carcinoma: clinicopathologic, morphologic, and immunohistochemical analysis of 10 cases and review of the literature

Monika Ulamec [a,b], Faruk Skenderi [c], Kiril Trpkov [d], Bozo Kruslin [a,b], Semir Vranic [c], Stela Bulimbasic [b,e], Sandra Trivunic [f], Delia Perez Montiel [g], Kvetoslava Peckova [h], Kristyna Pivovarcikova [h], Ondrej Ondic [h], Ondrej Daum [h], Pavla Rotterova [h], Martin Dusek [h], Milan Hora [i], Michal Michal [h], Ondrej Hes [h,*]

[a] Ljudevit Jurak Pathology Department, Clinical Hospital Center Sestre milosrdnice, Zagreb, Croatia
[b] Pathology Department, Medical University, Medical Faculty Zagreb, Croatia
[c] Department of Pathology, Clinical Centre of the University of Sarajevo, Sarajevo, Bosnia and Herzegovina
[d] Department of Pathology, Calgary Laboratory Services and University of Calgary, Calgary, AB, Canada
[e] Department of Pathology, Clinical Hospital Center Zagreb, Zagreb, Croatia
[f] Department of Pathology, Medical Faculty, University of Novi Sad, Serbia
[g] Department of Pathology, Institute Nacional de Cancerologia, Mexico City, Mexico
[h] Department of Pathology, Charles University, Medical Faculty and Charles University Hospital Plzen, Czech Republic
[i] Department of Urology, Charles University, Medical Faculty and Charles University Hospital Plzen, Czech Republic

ARTICLE INFO

Keywords:
Kidney
Solid
Papillary renal cell carcinoma
Review
Differential diagnosis

ABSTRACT

Solid papillary renal cell carcinoma is rarely reported in the literature, and its tumor characteristics are not entirely compatible with the concept of 2 histological subtypes of papillary renal cell carcinoma (PRCC). Tumor is composed mostly of small compressed tubules and short abortive papillae giving solid appearance of monomorphic epithelial cells with scanty cytoplasm and small nuclei, sometimes mimicking spindle cells, without or with sparse true papillae. It shows immunohistochemical (+CK7, +EMA, +AMACR) and genetic hallmarks (polysomy/trisomy 7/17, loss of Y) of conventional PRCC. About 53 cases have been described in the literature, with male predominance and age ranging from 17 to 82 years. By available follow-up data, solid PRCC has a favorable clinical course. We describe 10 cases compatible with the diagnosis of solid PRCC. All patients were males age range was from 34 to 70 years, and all but one were pT1 according to TNM 2009. On follow-up, 9 patients were without evidence of disease, and 1 had recurrent tumor. Size of the tumor ranged from 1.4 to 5.5 cm (mean, 3.32 cm). Tumors were well-circumscribed whitish to yellow masses with granular surface. Although solid architecture was a prominent morphologic feature, detailed analysis revealed that the tumors were composed of compressed short abortive papillae and compressed tubules admixed with true solid areas. Well-formed papillae were exceptionally present. All 10 cases were strongly and diffusely positive for CK7 and negative for WT-1. In conclusion, solid PRCC is a rare tumor with an incidence of less than 1% of all renal tumors. In majority of the cases, tumors were composed of tightly compressed tubular structures and short abortive papillae that render a solid morphologic appearance. Immunohistochemical and molecular features do not differ from conventional PRCC. Metanephric adenoma; epithelioid nephroblastoma; and, rarely, mucinous tubular and spindle cell carcinoma and oncocytic variant of PRCC should be considered in the differential diagnosis.

1. Introduction

Papillary renal cell carcinoma (PRCC) was first formally recognized as a specific entity in the Heidelberg classification, and then it was accepted in the 2004 World Health Organization (WHO) classification [1–2]. It was described as a malignant renal tumor with characteristic papillary or tubulopapillary architecture and with specific immunohistochemical and cytogenetic profile. PRCC is the second most common renal cell carcinoma (RCC) subtype occurring in up to 18.5% of all RCCs [3–5]. The description of PRCC dates back to 1974 in the study of Mancilla-Jimenez et al [6]. The authors reported in detail the ultrasonographic, macroscopic, and microscopic features of PRCC and recognized 2 consistent histologic patterns, namely, the papillae lined either by a single row of cells with scant cytoplasm or cells with pseudostratifed nuclei and abundant eosinophilic cytoplasm. Besides these 2 patterns,

Disclosure of conflict of interest: All authors declare no conflict of interest

The study was supported by the Charles University Research Fund (project number P36) and by project CZ.1.05/2.1.00/03.0076 from the European Regional Development Fund.

* Corresponding author at: Department of Pathology, Charles University, Medical Faculty and Charles University Hospital Plzen, Alej Svobody 80, 304 60 Pilsen, Czech Republic.
E-mail address: hes@medima.cz (O. Hes).

http://dx.doi.org/10.1016/j.anndiagpath.2016.04.008
1092-9134/

Table 1
Clinicopathological features and follow-up of solid PRCC

Case	Age (y)	Sex	Size (cm)	Follow-up
1	49	M	5.5	NED-8 y
2	70	M	1.5	DOC-3 y[a]
3	37	M	3.5	NED
4	66	M	2.5	NA
5	60	M	4.5	NED
6	54	M	2.8	NED-5 y
7	63	M	4	NED
8	34	M	2.5	NED-13 y
9	52	M	1.4	NED-9.5 y
10	48	M	5	AWD-8 y[b]

NED, no evidence of desease; DOC, dead for other reasons; NA, not available; AWD, alive with desease.
[a] Bilateral nephrectomy for PRCCs; dead for metastatic prostate cancer 3 years later; MSCT during follow-up diagnostics showed nephrectomy area without tumor.
[b] Only T3N0Mx tumor, recidivant tumor after 8 years, placed in the prior nephrectomy area.

they also reported papillary tumors with clear cells and other morphological features. PRCCs were later characterized in more details in several studies [7–9]. In 2004, the WHO classification adopted 2 types of PRCC: type 1, with papillae lined by a single cell layer of cuboidal cells with scant cytoplasm, and type 2, in which papillae are lined by large eosinophilic cells with pseudostratified nuclei [2]. Although less frequently encountered, several additional patterns were subsequently reported in the literature, including oncocytic [10–11], PRCC with clear cells [12], and solid PRCC. Solid variant of PRCC is composed of monomorphic epithelial cells with scant cytoplasm and small nuclei, arranged in tightly packed, ill-defined tubules or papillae and solid sheets [3,13–18]. It closely resembles metanephric adenoma (MA) and may share similar morphologic features with epitheloid nephroblastoma or mucinous tubular and spindle cell carcinoma (MTSC).

In this study, we describe a series of 10 cases collected from multiple institutions, and we discuss the diagnostic pitfalls and the differential diagnosis of the solid form of PRCC.

2. Material and methods

Ten cases compatible with the diagnosis of solid PRCC were retrieved out of 1311 papillary RCCs (including institutional, consultation, and archive cases) in the Pilsen Tumor Registry. Pathologic examination of all available hematoxylin and eosin–stained sections from each case (range, 1-18 slides) was performed by at least 3 pathologists (MU, FS, and OH). Cases were reevaluated, and solid, tubular, and papillary components were accessed as percentage of the tumor. Tissue for light microscopy was fixed in 4% formaldehyde and embedded in paraffin using routine procedures. Three-micrometer thin sections were cut and stained with hematoxylin and eosin to evaluate the architecture of the tumors. Basal membranes were highlighted by periodic acid Schiff (PAS) stain.

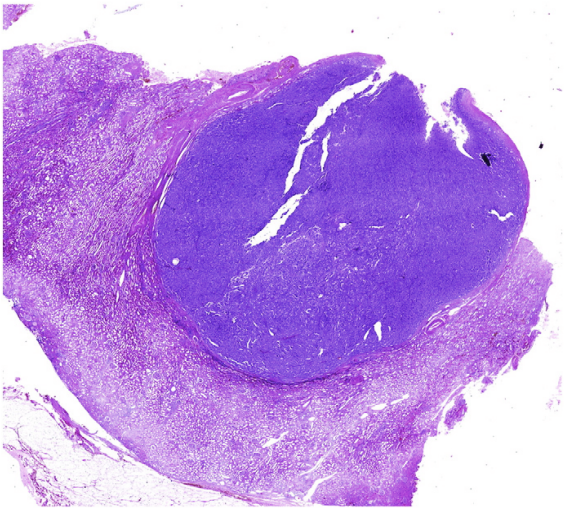

Fig. 1. Using scanning magnification, most of the tumors appeared completely solid.

The immunohistochemical study was performed using a Ventana Benchmark XT automated stainer (Ventana Medical System, Inc, Tucson, AZ).

The following primary antibodies were used in the immunohistochemical study: racemase/AMACR (13H4, monoclonal, DAKO, Glostrup, Denmark, 1:200), cytokeratin 7 (OV-TL12/30, monoclonal, DakoCytomation, Carpenteria CA, 1:200), epithelial membrane antigen (EMA) (E29, monoclonal, DakoCytomation, 1:1000), CD10 (monoclonal, Sp67, Ventana, RTU), CD34 (QBEnd-10, monoclonal, Dako, 1:100), CD57(NK 1, Leica Biosystems, Newcastle upon Tyne, UK, 1:200), WT1 (GF-H2, monoclonal, DakoCytomation, 1:150), Ki-67 (MIB1, monoclonal, Dako, 1:1000). Appropriate positive and negative controls were used. Immunostains were scored as 1 + (focal in small clusters of individual cells), 2 + (up to 50% positive cells), and 3 + (diffuse strong positivity in more than 50% of cells).

3. Results

The clinicopathologic data are summarized in Table 1. The age of the patients ranged from 34 to 70 years (mean age, 53.30); all patients were male. Size of the tumor in the largest diameter ranged from 1.4 to 5.5 cm (mean, 3.32 cm). Most of the cases were pT1 stage (TNM 09); 1 tumor was pT3. Most of the patients (8/10) were alive and well without signs of metastatic disease or relapse within follow-up period of 3-13 years. One patient was faced with recurrent tumor 8 years after resection. One patient had bilateral nephrectomy due to multiple small PRCCs and died of metastatic prostate cancer 3 years later.

Table 2
Gross and microscopic features of solid PRCC

Patient	Gross description	True solid (%)	Compressed tubuli (%)	Compressed abortive papillae; occasional glomeruloid formations (%)	True papillae (%)	Capsule	ISUP grade
1	Yellow well-circumscribed nodule	10	40	50	0	+	1
2	Yellow well-circumscribed nodule, bilateral papillary RCCs	20	70	10	0	+	1
3	Gray well-circumscribed nodule	5	80	10	5	+	2
4	Yellow well-circumscribed nodule	80	10	5	5	+	1
5	Gray well-circumscribed nodule	20	30	50	0	−	1
6	Yellow well-circumscribed nodule	5	10	80	5	+	1
7	Yellow well-circumscribed nodule	20	70	10	0	+	1
8	Yellow well-circumscribed nodule	10	50	40	0	−/+	1
9	Yellow well-circumscribed nodule	30	10	60	0	+	1
10	Yellow well-circumscribed nodule, necrotic −50%	60	20	20	0	+	2

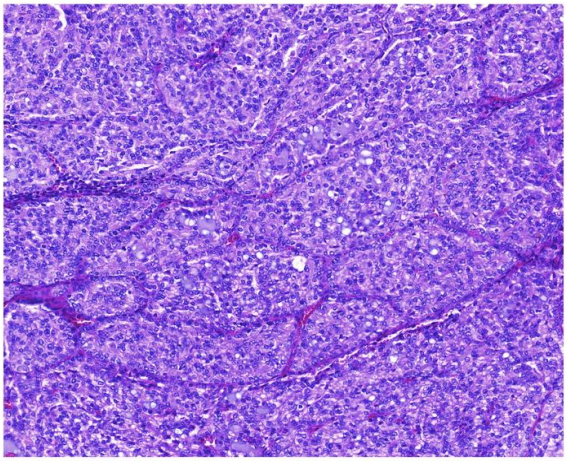

Fig. 2. Only 2 cases from our series were mostly arranged in solid-alveolar pattern.

Morphologic features are summarized in Table 2. Macroscopically, tumors were well-circumscribed yellow to white homogeneous nodules, sometimes with fine-granulated surface. One tumor showed necrotic area in up to 50% of the tumor.

Nine tumors were encapsulated. Using scanning magnification, most of the tumors appeared completely solid (Fig. 1), but on closer examination, true solid areas comprised 5% to 80% of the tumor. On high power and using PAS staining, only 2 tumors were mostly solid (60% and 80% of the tumors, respectively, comprised solid areas) (Fig. 2). Four tumors were composed mostly of compressed tubules (between 50% and 80% of the 2 tumors) (Fig. 3A and B), whereas the remaining 4 were composed mostly of compressed abortive papillae with occasional glomeruloid formations (between 50% and 80% of these contained compressed abortive papillae) (Fig. 4). True papillae with fibrovascular cores were found in 3 cases in up to 5% of the tumor. Tumor cells had scant cytoplasm and small, round to elongated nuclei with occasional nuclear grooves (International Society of Urological Pathology [ISUP] nucleolar grade was 1 or 2) (Fig. 5). In all but 1 case, the cells with scant but eosinophilic cytoplasm were also focally found. Small foci of tubules with cells showing sparse but clear cytoplasm were found in 2 cases.

The immunohistochemistry results are summarized in Table 3. All 10 cases were strongly and diffusely positive for CK7 (Fig. 6) and negative for WT-1. AMACR was diffusely positive in 9 cases (Fig. 7). EMA was positive diffusely in 8 cases and focally in 2. Vimentin was diffusely positive in 6 cases, and 4 were positive focally (less than 50% of cells). CD10 was focally positive in 4 cases. CD57 showed weak and focal positivity in 1 case. Proliferation activity was less than 2% in all tumors using Ki-67 labeling.

4. Discussion and review of the literature

4.1. Clinical and pathological characteristics

So-called solid PRCC, as a part of the morphologic PRCC spectrum, has been described for the first time by Renshaw et al [13]. The incidence was less than 1% of all renal tumors [3], and this estimation corresponds with the proportion of solid PRCCs in this series. In our study, the incidence was actually 0.76% of all PRCCs in the Pilsen Tumor Registry.

In toto, about 53 cases have been described in the literature with tumors showing distinctive solid PRCC features. The data from the English literature are summarized in Table 4. There is a male predominance, with a male to female ratio of 3.5:1. Age at time of diagnosis was from 17 to 82 years. The follow-up data are however limited, and it seems that solid PRCC has favorable clinical course. Most cases were classified as pT1 tumors, with nuclear grade up to 2, according to Fuhrman grading system [3,13–19]. In our study, the age range was from 34 to 70 years (mean age, 53.3), and all patients were male. The largest tumor size ranged from 1.4 to 5.5 cm (mean, 3.3 cm), which is similar to the previously published data. Nine of our cases were pT1 stage (TNM 09). One case was pT3 and demonstrated infiltration through the renal capsule with invasion into the perirenal fat. This patient had recurrent tumor after 8 years. Seven of the 10 cases were without evidence of disease during the follow-up from 3 to 13 years. One patient had multiple small PRCCs and died of metastatic prostate cancer 3 years later.

In the previous studies, the tumors were well-circumscribed, solid, homogeneous, and nodular masses, grayish white in color and located in the renal cortex. Hemorrhage and necrosis in the central areas were also described, as well as presence of multifocal tumors [13,16–17]. In this study, the tumors represented well-circumscribed solid nodules, mostly yellow in color and often showing finely granular cut surface. In 1 case, multifocal, bilateral PRCCs were found, together with the solid PRCC. Abundant necrosis was found in only 1 case.

Solid PRCC is typically composed of cells with scant cytoplasm and small, round to elongated nuclei, cytologically resembling type 1 PRCC. The cells are organized in solid sheets or tubular structures that are tightly packed, sometimes mimicking spindle cells, with no true papillae and lacking fibrovascular stalks. Some tumors may exhibit completely

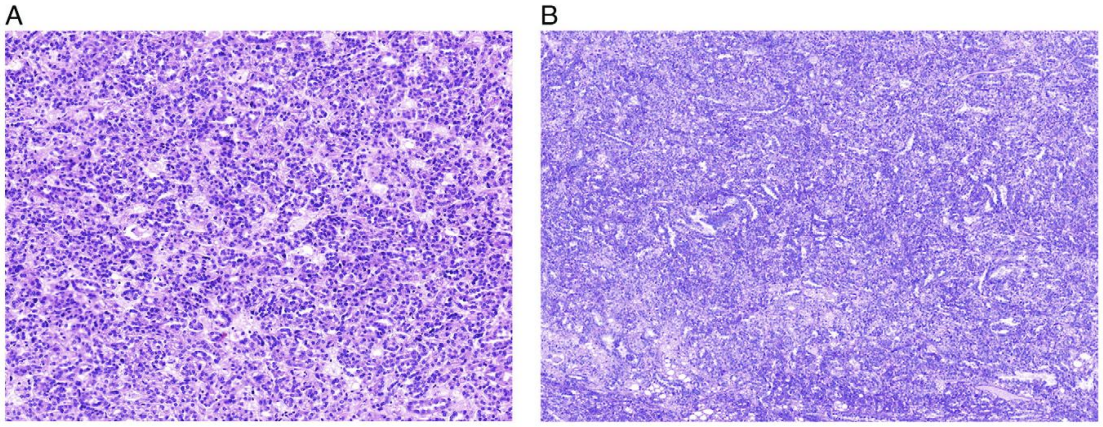

Fig. 3. (A) Four tumors were composed of small tubules. (B) Predominantly tubular architecture highlighted by PAS staining.

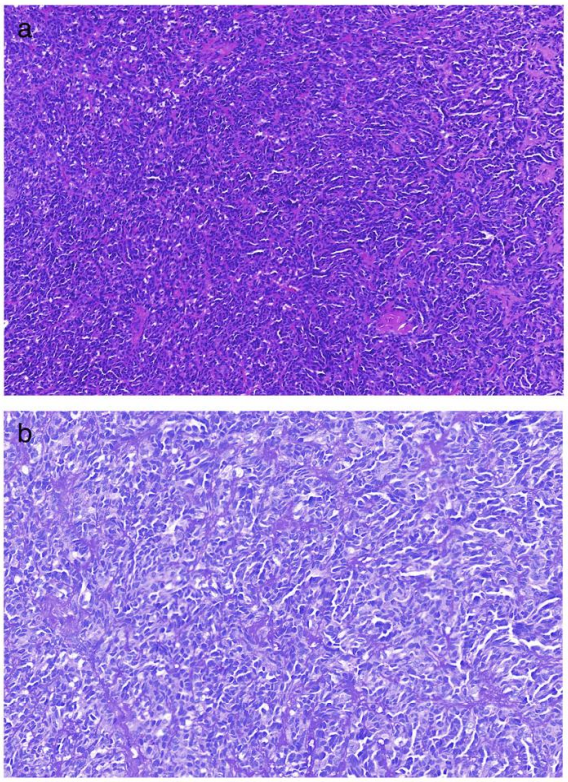

Fig. 4. (A-B) Four tumors in our series were composed of short compressed abortive papillae (hematoxylin and eosin = A, PAS = B).

solid morphology and distinct micronodules, with the cells showing eosinophilic cytoplasm. Abortive papillae are also frequently found.

In the current study, true solid areas comprised 5%-80% of the individual tumors; on high power and PAS stain, only 2 tumors had more than 50% solid pattern, without any visible tubules or papillae. Areas of compressed, tightly packed tubular structures and abortive papillae comprised the rest of the tumors, usually mimicking solid areas and rarely showing focal spindle cell appearance. Four tumors were mostly composed of compressed and abortive papillae, and 4 were composed

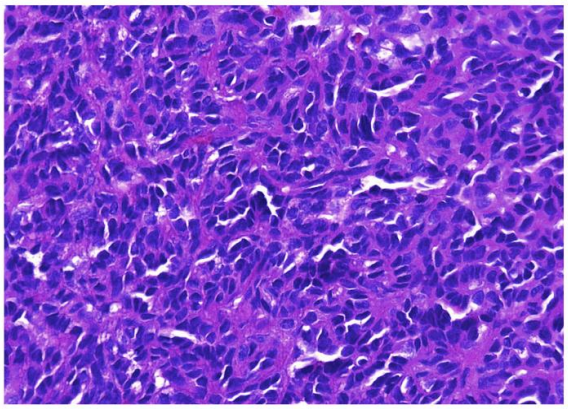

Fig. 5. Tumor cells had scant cytoplasm and small, round to elongated nuclei.

Table 3
Immunohistochemical staining results in solid PRCC

Patient	CK7	AMACR	EMA	WT-1	CD57	CD10	Vim	Ki-67
1	+++	+++	+++	−	+	−	+	≤1%
2	+++	+++	+++	−	−	+	+++	≤1%
3	+++	+++	+	−	−	−	++	≤1%
4	+++	+++	+++	−	−	++	++	≤1%
5	+++	+++	++	−	−	−	+++	≤1%
6	+++	+++	+++	−	−	−	+++	≤1%
7	+++	−	+++	−	−	−	+++	≤1%
8	+++	+++	+++	−	−	−	+++	≤1%
9	+++	+++	+++	−	−	+	+++	≤1%
10	+++	+++	+++	−	−	++	+	≤2%

+: focal positivity, in small clusters or single cells; ++: up to 50% of positive cells; +++: diffuse, strong positivity, more than 50% of positive cells. Vim, vimentin.

mostly of compressed tubules. True papillae with fibrovascular cores were found in 3 cases and formed up to 5% of the tumor volume.

The amount of cytoplasm in the neoplastic cells may be variable. In most of the cases, the cells had scant cytoplasm and appeared basophilic, but cells having more abundant cytoplasm and low-grade nuclear features were also noted. The spindle cell–like component was usually low grade with slightly elongated nuclei, moderate pleomorphism, finely dispersed chromatin, and distinct nucleoli. These cells were different from true sarcomatoid morphology and resembled the cells of mucinous tubular and spindle cell RCC. Mitoses were rarely found [3,13–19]. Cantley et al [16] described a case of a young male patient with renal tumor showing sarcomatoid RCC, with an epithelial component identical to the solid PRCC. In some cases, foamy macrophages and psammoma bodies were found in the stroma of the tumor [17]. Occasionally, isolated foam cells and psammoma bodies were also present in our cases, but mitotic figures were not found. Most of the neoplastic cells had scant cytoplasm and small, round to elongated nuclei, with ISUP nucleolar grade 1 and 2. In all cases, there were low-grade nuclei, except in 1 case in which cells showed scant eosinophilic cytoplasm.

Although small solid areas in conventional PRCC are compatible with the diagnosis of PRCC, specific criteria for the diagnosis of solid PRCC are not provided in the recent renal tumor classifications [5]. In published studies, however, variable percentages of solid architecture, compressed papillae, or tubules were used to define this entity. Some authors proposed that solid PRCC should not contain true papillae, whereas others suggested that true papillae could comprise up to 20% [3,16–17].

4.2. Immunohistochemical profile and genetics

PRCC usually stains positive for cytokeratin AE1/AE3, CAM5.2, high–molecular weight cytokeratins, CK7, EMA, vimentin, CD10, AMACR, and RCC [2,4–5,7–9]. Of note, CK7 positivity can be variable, and it is not a

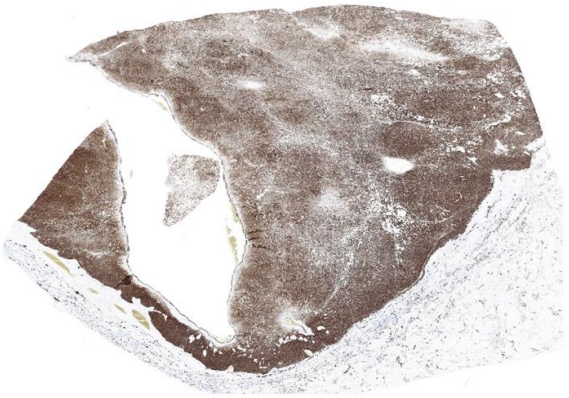

Fig. 6. All 10 cases were strongly and diffusely positive for CK7.

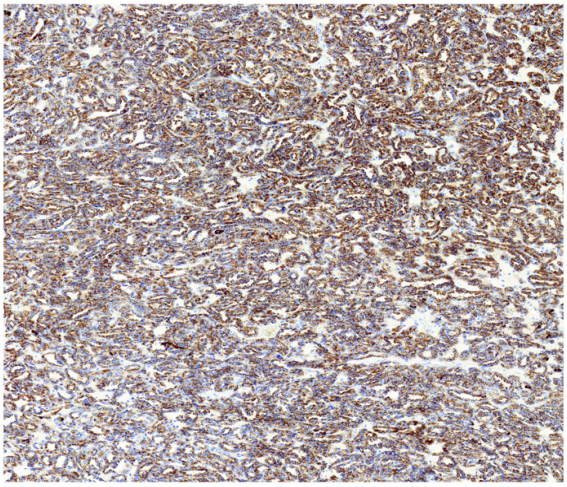

Fig. 7. Racemase (AMACR) was diffusely positive in 9 cases.

constant feature of PRCC; however, CK7 is frequently expressed in PRCC type 1. Solid PRCC shows immunoprofile similar to "conventional type" of PRCC, with strong, diffuse positivity for EMA, CK7, and AMACR and usually focal positivity for CD10 [3,13–19]. According to some studies, vimentin may be also focally positive.

In our experience, all10 evaluated cases were strongly and diffusely positive for CK7 and negative for WT-1. CK7 may in fact highlight the collapsed tubular architecture. AMACR was diffusely positive in 9 and EMA in 7 cases. CD10 was focally positive in 4 cases. CD57 showed weak and individual cell positivity in 9 cases. Proliferation activity, evaluated by Ki-67, was between 1% and 2% in all tumors.

4.3. Molecular genetic profile

Trisomy and tetrasomy of chromosome 7 and trisomy of 17, as well as loss of Y, are nearly pathognomic for PRCC. According to the published data, this also applies to solid PRCC [3,13–19]. According to WHO 2016, however, a wide variety of other chromosomal aberrations can be seen in PRCC, including trisomy 8, 12, 16, and 20 and loss of 1p, 4q, 6q, 7, 9p, 13q, Xp, and Xq, as well as amplification of 8q and overexpression of MYC. Thirteen percent of sporadic PRCCs demonstrate *MET* mutations. Loss of heterozygosity of *VHL* and *FHIT* can also be found. Type 1 PRCC shows gains of 7p and 17p, whereas LOH of 1p, 3p, 5q, 6, 8, 9p, 10, 11, 15, 18, and 22 was found in PRCC type 2. Allelic imbalance of 9q13 has been shown to be of prognostic significance in PRCC [5]. Renshaw et al [13] described cytogenetic changes in 1 case of solid PRCC, which demonstrated a karyotype of 45XXX, +X, +3, +5, +12, −14, +16, +17, −18, +20, and −21.

4.4. Pitfalls and differential diagnosis

Several entities should be considered in the differential diagnosis of solid PRCC, such as MA, epithelioid nephroblastoma, MTSC, and solid oncocytic PRCC (Table 5).

Metanephric adenoma of the kidney is a benign tumor usually found in younger patients, predominantly in women. It accounts for 0.2%-0.7% of adult renal epithelial neoplasms. It is sharply demarcated without a distinct pseudocapsule and consists of bland, small blue cells forming small, tightly packed tubular structures and acini but infrequently may also show more solid growth. Some tubules are typically elongated and branching. Both PRCC and MA may contain glomeruloid bodies with abortive papillae, tightly packed tubules, or solid tumor cell sheets. Psammoma bodies can be present in both MA and solid PRCC [20–22].

MA typically shows CK7−, AMACR−, WT1+, and CD57+ immunoprofile and does not exhibit the chromosomal changes typical of PRCC [20–25]. In fact, MA with polysomy 7 and 17 or loss of Y described in the literature most likely represents solid PRCC [20]. According to more recent data, BRAF V600E mutations were identified in nearly 90% of MAs, but similar BRAF exon 15 mutations are extremely rare in other renal tumors, including PRCCs. Immunohistochemistry for detection of BRAF V600E mutations was also validated, and it can be used as an additional tool in the differential diagnostic process [26]. According to the study of Yakirevich et al [27], majority of MAs are positive for kidney-specific catherin, whereas PRCCs and nephroblastomas are negative.

Table 4
Literature data

	Renshaw et al	Ngan et al	Argani et al	Zhang et al	Mantoan Padilha et al	Kinney et al	Cantley et al
No. cases	6[a]	1	5	2	23	15	1
Age	35-82	36	17-68	50-51	30-80	69-83	31
Sex (M/F)	4/2	1/0	1/0	2/0	15/8	11/?	1/0
Size (cm)	1-12	–	2.1-5.2	2-8	0.9-10	1.9-2	4.5
Nuclear grade 1/2/3/4	2/2/2/0	–	0/5/0/0	0/1/1/0	–	–	–
pTNM	2 T1, 4 T2	–	4T1a, 1T1b	1T1a, 1 T2	11T1a, 9T1b, 3 T2	–	T1b
Follow-up (mo)	2-108	–	Up to 8	8, 14	–	–	24
Follow-up	1 AWD (6 mo) 4 NED	–	5 NED	2 NED	–	–	NED
No. cases	6[a]	1	5	2	23	15	1
Papillae/solid encount	4-S	S	2-S[b]	2-T	10 S	–	T[c]
	2-T		3-T[b]		13 T		
CK7	6+	1+	5+	2+	23+	14+	1+
AMACAR	–	–	–	2+	23+	15+	–
EMA	6+	1+	–	2+	21+	–	1+
Vimentin	–	1−	–	2+	23−	–	1+
CD10	–	–	5+ (focal)	1 (focal)	–	–	–
WT-1	–	–	–	–	23−	15−	1−
CD57	–	–	–	–	16+ (focal)	14−; 1+	1−
Trisomy 7	2	–	5	2	14	8	1
Trisomy 17	3	–	3	2	15	8	–
Y loss	–	–	–	2	–	11	–

S, predominantly solid with small micronodules and abortive papillae; T, mostly tubular pattern and compressed tubules; –, no data; AWD, alive with disease; NED, no evidence of disease; M, male; F, female.
[a] Three were multifocal.
[b] Tumors with spindle cell foci.
[c] Foci with high-grade nuclei, with spindle cells.

Table 5
Differential diagnosis of solid PRCC

Characteristics	S PRCC	MA	EN	MTSC	OPRCC
Age (y)	17-83, average 54	Children, young adults, 5-83, average 49	Mostly children up to 6; in adult 21-67, average 32	32-79, average 56	40-82, average 67
Sex (M/F ratio)	M (3.5/1)	F (1/9)	Equal	F (1/1.5)	M (5/1)
Fibrous pseudocapsule	+	−	+	+	+
Multifocality	+	−	+	−	+
Cytology					
Cells with eosinophilic cytoplasm	+[a]	−	−	+[a]	+ (abundant)
Cells with scant cytoplasm	+	+	+	+	−
Nuclei	Low gr	Low gr	Low-high gr	Low gr	Low-high gr
True solid areas	+	+	+	+	+
Spindle cells with low-grade features	+	−	−	+	−
Compressed tubuli	+	+	+	+	+
Compressed abortive papillae (glomeruloid)	+	+	+	−	−
Real papillae with fibrovasc. CORE	+ (sparse)	+ (sparse)	−	−	+
Visible tubuli on LPF	+ (sparse)	+	+	+	+
Mucinous stroma	−	−	−	+	−
AE1/3	+	−	−	+	+
CK7	+	−	−	+	+
EMA	+	−	−	+	+
AMACAR	+	−	−	−	−
WT-1	−	+	+	−	−
CD57	−	+	+	−	−
Trisomy 7	Y	N	N	N	Y
Trisomy 17	Y	N	N	N	Y
Loss of Y	Y	N	N	N	Y

Y, yes; N, no; LPF, low-power field; SPRCC, solid PRCC; EN, epithelioid nephroblastoma; OPRCC, oncocytic PRCC; gr, grade; MA, metanephric adenoma; MTSC, mucinous tubulary and spindle cell carcinoma.
[a] Not so abundant cytoplasm as in oncocytic PRCC.

In a recently published study, 21 MAs and 23 solid PRCCs shared similar morphologic features. Eleven solid PRCCs lacked papillae completely but showed typical immunoprofile and genetic aberrations of PRCCs [3]. Some of these cases with solid and glomeruloid structures were composed of larger eosinophilic cells and resembled a renal tumor described by Petersson et al [28], provisionally named *biphasic alveolosquamoid renal carcinoma*. This entity was further analyzed in a larger cohort and was recently recognized as a subtype of PRCC. Therefore, a solid-alveolar morphology of this newly described PRCC variant should also be considered in the differential diagnosis of solid PRCC. However, it appears that there is little difference in the clinical management and the prognosis of this entity [29]. It is also worth mentioning that the diagnostic criteria for malignant MA described in the literature were never generally accepted, and likely all malignant MAs represent examples of extremely well-differentiated epithelioid nephroblastomas [20].

Nephroblastoma is very rare in adult patients, but adult nephroblastomas generally do not differ from their pediatric counterpart. Pure epithelioid nephroblastoma is exceptionally rarely seen in adult patients. However, this tumor type should also be considered in the differential diagnosis of solid PRCC. The morphology typically shows tubulopapillar and solid patterns; the cells are small and uniform with scant cytoplasm, and there are absent or very rare mitotic figures [18–19,30–32]. Kinney et al [18] analyzed 37 tumors originally diagnosed as MA, 13 solid PRCCs, and 20 epithelial-predominant nephroblastomas using immunohistochemistry and fluorescence in situ hybridization for trisomy of chromosomes 7 and 17 and loss of Y. All epithelial-predominant nephroblastomas were diffusely positive for WT-1, and only 1 was focally positive for CK7. All tumors showed disomy of chromosomes 7, 17, and Y present [18].

Another renal tumor which frequently shows solid architecture is MTSC. It is characterized by elongated and compressed tubules or cordlike formations of uniform, cuboidal cells with eosinophilic, focally vacuolated cytoplasm and distinct cell spindling, and usually demonstrates low-grade nuclei. The stroma is typically myxoid and contains variable amount of extracellular mucin. Focal clusters of foamy macrophages may also be seen. In cases with limited myxoid stroma (so-called mucin-poor variant) and limited presence of well-formed papillae, it may be difficult to distinguish MTSC from solid PRCC [33–34]. In rare examples of MTSC, the cells form solid and compact areas with minimal amount of interstitial mucin. Such cases can truly mimic solid PRCC, but in well-sampled tumors, more typical areas of MTSC are usually found. Both solid PRCC and MTSC can have tubular structures, papillary architecture, spindle cell appearance, psammoma bodies, foamy macrophages, and interstitial mucin and demonstrate positive staining for vimentin, CK7, CK19, EMA, AMACR, CD10, and RCC [15,17].

There are several studies that consider the issue of MTSC in the differential diagnosis of solid PRCC, raising the possibility that MTSC represents a subtype of PRCC [33–37]. Peckova et al [38] analyzed 54 MTSCs using array comparative genomic hybridization and divided the MTSCs into 3 categories: low grade, high grade, and MTSC overlapping with PRCC. They showed multiple chromosomal losses and no gains in low- and high-grade MTSC groups, supporting the concept that MTSC represents a distinct type of RCC. However, the group showing overlapping features with PRCC demonstrated more heterogeneous status, with frequent gains of chromosomes 7 and/or 17, suggesting that this MTSC subgroup should be considered in the spectrum of PRCC [38].

An oncocytic variant of PRCC different from PRCC type 1 and 2 was also reported, composed of papillae lined by single or rarely pseudostratified layers of cells with granular, deeply eosinophilic cytoplasm and round regular nuclei. In the new 2016 WHO classification of renal tumors, the oncocytic PRCC is considered as a possible new variant of PRCC [5]. This type of PRCC can also show solid pattern in up to 90% of the tumor. The immunoprofile and the genotype are compatible with PRCC [10–11,39–41]. Despite the solid architecture, oncocytic PRCC can be differentiated from solid PRCC mostly by histology. The oncocytic cells of oncocytic PRCC are eosinophilic and contain voluminous cytoplasm and differ from the smaller epithelial cells of solid PRCC which contain scanty cytoplasm.

5. Conclusion

In conclusion, solid PRCC is a rare tumor with an incidence less than 1% of all renal tumors. In the majority of cases, it is composed of solid areas and compressed tubular structures or short abortive papillae that result in a solid appearance. The immunohistochemical and molecular genetic features do not differ from conventional PRCC. Metanephric

adenoma, epithelioid nephroblastoma, and less often MTSC and an oncocytic variant of PRCC should all be considered in the differential diagnosis of solid PRCC.

References

[1] Kovacs G, Akhtar M, Beckwith BJ, Bugert P, Cooper CS, Delahunt B, et al. The Heidelberg classification of renal cell tumours. J Pathol 1997;183(2):131–3.
[2] Eble JN, Sauter G, Epstein JI, Sesterhenn IA, editors. Tumours of the urinary system andmale genital organs. World Health Organization classification of tumours. Press LI; 2004. p. 27–9.
[3] Mantoan Padilha M, Billis A, Allende D, Zhou M, Magi-Galluzzi C. Metanephric adenoma and solid variant of papillary renal cell carcinoma: common and distinctive features. Histopathology 2013;62(6):941–53.
[4] Klatte T, Said JW, Seligson DB, Rao PN, de Martino M, Shuch B, et al. Pathological, immunohistochemical and cytogenetic features of papillary renal cell carcinoma with clear cell features. J Urol 2011;185(1):30–5.
[5] Moch H, Humphrey PA, Ulbright TM, Reuter VE, editors. WHO classification of tumours of the urinary system and male genital organs. 4th ed. Lyon: IARC; 2016.
[6] Mancilla-Jimenez R, Stanley RJ, Blath RA. Papillary renal cell carcinoma: a clinical, radiologic, and pathologic study of 34 cases. Cancer 1976;38(6):2469–80.
[7] Delahunt B, Eble JN. Papillary renal cell carcinoma: a clinicopathologic and immunohistochemical study of 105 tumors. Mod Pathol 1997;10(6):537–44.
[8] Amin MB, Corless CL, Renshaw AA, Tickoo SK, Kubus JK, Schultz DS. Papillary (chromophil) renal cell carcinoma (PRCC): evaluation of conventional pathologic prognostic parameters in 62 cases. Am J Surg Pathol 1997;21:621–35.
[9] Delahunt B, Eble JN, McCredie MR, Bethwaite PB, Stewart JH, Bilous AM. Morphologic typing of papillary renal cell carcinoma: comparison of growth kinetics and patient survival in 66 cases. Hum Pathol 2001;32(6):590–5.
[10] Lefevre M, Couturier J, Sibony M, Bazille C, Boyer K, Callard P, et al. Adult papillary renal tumor with oncocytic cells: clinicopathologic, immunohistochemical, and cytogenetic features of 10 cases. Am J Surg Pathol 2005;29(12):1576–81.
[11] Hes O, Brunelli M, Michal M, Cossu Rocca P, Hora M, Chilosi M, et al. Oncocytic papillary renal cell carcinoma: a clinicopathologic, immunohistochemical, ultrastructural, and interphase cytogenetic study of 12 cases. Ann Diagn Pathol 2006;10(3):133–9.
[12] Gobbo S, Eble JN, Maclennan GT, Grignon DJ, Shah RB, Zhang S, et al. Renal cell carcinomas with papillary architecture and clear cell components: the utility of immunohistochemical and cytogenetical analyses in differential diagnosis. Am J Surg Pathol 2008;32(12):1780–6.
[13] Renshaw AA, Zhang H, Corless CL, Fletcher JA, Pins MR. Solid variants of papillary (chromophil) renal cell carcinoma: clinicopathologic and genetic features. Am J Surg Pathol 1997;21(10):1203–9.
[14] Ngan KW, Ng KF, Chuang CK. Solid variant of papillary renal cell carcinoma. Chang Gung Med J 2001;24(9):582–6.
[15] Argani P, Netto GJ, Parwani AV. Papillary renal cell carcinoma with low-grade spindle cell foci: a mimic of mucinous tubular and spindle cell carcinoma. Am J Surg Pathol 2008;32(9):1353–9.
[16] Cantley R, Gattuso P, Cimbaluk D. Solid variant of papillary renal cell carcinoma with spindle cell and tubular components. Arch Pathol Lab Med 2010;134(8):1210–4.
[17] Zhang Y, Yong X, Wu Q, Wang X, Zhang Q, Wu S, et al. Mucinous tubular and spindle cell carcinoma and solid variant papillary renal cell carcinoma: a clinicopathologic comparative analysis of four cases with similar molecular genetics datum. Diagn Pathol 2014;9:194.
[18] Kinney SN, Eble JN, Hes O, Williamson SR, Grignon DJ, Wang M, et al. Metanephric adenoma: the utility of immunohistochemical and cytogenetic analyses in differential diagnosis, including solid variant papillary renal cell carcinoma and epithelial-predominant nephroblastoma. Mod Pathol 2015 Sep;28(9):1236–48.
[19] Chen L, Deng FM, Melamed J, Zhou M. Differential diagnosis of renal tumors with tubulopapillary architecture in children and young adults: a case report and review of literature. Am J Clin Exp Urol 2014;2(3):266–72.
[20] Arroyo MR, Green DM, Perlman EJ, Beckwith JB, Argani P. The spectrum of metanephric adenofibroma and related lesions: clinicopathologic study of 25 cases from the National Wilms Tumor Study Group Pathology Center. Am J Surg Pathol 2001;25(4):433–44.
[21] Gatalica Z, Grujic S, Kovatich A, Petersen RO. Metanephric adenoma: histology, immunophenotype, cytogenetics, ultrastructure. Mod Pathol 1996;9(3):329–33.
[22] Jones EC, Pins M, Dickersin GR, Young RH. Metanephric adenoma of the kidney. A clinicopathological, immunohistochemical, flow cytometric, cytogenetic, and electron microscopic study of seven cases. Am J Surg Pathol 1995;19(6):615–26.
[23] Brown JA, Anderl KL, Borell TJ, Qian J, Bostwick DG, Jenkins RB. Simultaneous chromosome 7 and 17 gain and sex chromosome loss provide evidence that renal metanephric adenoma is related to papillary renal cell carcinoma. J Urol 1997;158(2):370–4.
[24] Brunelli M, Eble JN, Zhang S, Martignoni G, Cheng L. Metanephric adenoma lacks the gains of chromosomes 7 and 17 and loss of Y that are typical of papillary renal cell carcinoma and papillary adenoma. Mod Pathol 2003;16(10):1060–3.
[25] Obulareddy SJ, Xin J, Truskinovsky AM, Anderson JK, Franklin MJ, Dudek AZ. Metanephric adenoma of the kidney: an unusual diagnostic challenge. Rare Tumors 2010;2(2), e38.
[26] Udager AM, Pan J, Magers MJ, Palapattu GS, Morgan TM, Montgomery JS, et al. Molecular and immunohistochemical characterization reveals novel BRAF mutations in metanephric adenoma. Am J Surg Pathol 2015;39(4):549–57.
[27] Yakirevich E, Magi-Galluzzi C, Grada Z, Lu S, Resnick MB, Mangray S. Cadherin 17 is a sensitive and specific marker for metanephric adenoma. Am J Surg Pathol 2015;39(4):479–86.
[28] Petersson F, Bulimbasic S, Hes O, Slavik P, Martinek P, Michal M, et al. Biphasic alveolosquamoid renal carcinoma: a histomorphological, immunohistochemical, molecular genetic, and ultrastructural study of a distinctive morphologic variant of renal cell carcinoma. Ann Diagn Pathol 2012;16(6):459–69.
[29] Hes O, Condom Mundo E, Peckova K, Lopez JI, Martinek P, Vanecek T, et al. Biphasic Squamoid alveolar renal cell carcinoma: a distinctive subtype of papillary renal cell carcinoma? Am J Surg Pathol 2016;40(5):664–75.
[30] Huser J, Grignon DJ, Ro JY, Ayala AG, Shannon RL, Papadopoulos NJ. Adult Wilms' tumor: a clinicopathologic study of 11 cases. Mod Pathol 1990;3(3):321–6.
[31] Muir TE, Cheville JC, Lager DJ. Metanephric adenoma, nephrogenic rests, and Wilms' tumor: a histologic and immunophenotypic comparison. Am J Surg Pathol 2001;25(10):1290–6.
[32] Reinhard H, Aliani S, Ruebe C, Stockle M, Leuschner I, Graf N. Wilms' tumor in adults: results of the Society of Pediatric Oncology (SIOP) 93-01/Society for Pediatric Oncology and Hematology (GPOH) study. J Clin Oncol 2004;22(22):4500–6.
[33] Fine SW, Argani P, DeMarzo AM, Delahunt B, Sebo TJ, Reuter VE, et al. Expanding the histologic spectrum of mucinous tubular and spindle cell carcinoma of the kidney. Am J Surg Pathol 2006;30(12):1554–60.
[34] Paner GP, Srigley JR, Radhakrishnan A, Cohen C, Skinnider BF, Tickoo SK, et al. Immunohistochemical analysis of mucinous tubular and spindle cell carcinoma and papillary renal cell carcinoma of the kidney: significant immunophenotypic overlap warrants diagnostic caution. Am J Surg Pathol 2006;30(1):13–9.
[35] Alexiev BA, Burke AP, Drachenberg CB, Richards SM, Zou YS. Mucinous tubular and spindle cell carcinoma of the kidney with prominent papillary component, a non-classic morphologic variant. A histologic, immunohistochemical, electron microscopic and fluorescence in situ hybridization study. Pathol Res Pract 2014;210(7):454–8.
[36] Cossu-Rocca P, Eble JN, Delahunt B, Zhang S, Martignoni G, Brunelli M, et al. Renal mucinous tubular and spindle carcinoma lacks the gains of chromosomes 7 and 17 and losses of chromosome Y that are prevalent in papillary renal cell carcinoma. Mod Pathol 2006;19(4):488–93.
[37] Shen SS, Ro JY, Tamboli P, Truong LD, Zhai Q, Jung SJ, et al. Mucinous tubular and spindle cell carcinoma of kidney is probably a variant of papillary renal cell carcinoma with spindle cell features. Ann Diagn Pathol 2007;11(1):13–21.
[38] Peckova K, Martinek P, Sperga M, Montiel DP, Daum O, Rotterova P, et al. Mucinous spindle and tubular renal cell carcinoma: analysis of chromosomal aberration pattern of low-grade, high-grade, and overlapping morphologic variant with papillary renal cell carcinoma. Ann Diagn Pathol 2015;19(4):226–31.
[39] Allory Y, Ouazana D, Boucher E, Thiounn N, Vieillefond A. Papillary renal cell carcinoma. Prognostic value of morphological subtypes in a clinicopathologic study of 43 cases. Virchows Arch 2003;442(4):336–42.
[40] Kunju LP, Wojno K, Wolf Jr JS, Cheng L, Shah RB. Papillary renal cell carcinoma with oncocytic cells and nonoverlapping low grade nuclei: expanding the morphologic spectrum with emphasis on clinicopathologic, immunohistochemical and molecular features. Hum Pathol 2008 Jan;39(1):96–101.
[41] Mai KT, Kohler DM, Robertson SJ, Belanger EC, Marginean EC. Oncocytic papillary renal cell carcinoma with solid architecture: mimic of renal oncocytoma. Pathol Int 2008;58(3):164–8.

[20] Delahunt B. Advances and controversies in grading and staging of renal cell carcinoma. Mod Pathol 2009;22(Suppl. 2):S24–36.
[21] Delahunt B, Bethwaite PB, Nacey JN. Outcome prediction for renal cell carcinoma: evaluation of prognostic factors for tumours divided according to histological subtype. Pathology 2007;39:459–65.
[22] Delahunt B, Bethwaite PB, Miller RJ, Sika-Paotonu D, Srigley JR. Re: Fuhrman grade provides higher prognostic accuracy than nucleolar grade for papillary renal cell carcinoma: T. Klatte, C. Anterasian, J. W. Said, M. de Martino, F. F. Kabbinavar, A. S. Belldegrun and A. J. Pantuck. *J Urol* 2010;183:2143-2147. J Urol 2011;185:356–7 [author reply 357-358].
[23] Kumar V, Abbas AK, Fausto N, Aster JC. Robbins and Cotran pathologic basis of diseases. , 3-42 Philadelpia: Saunders Elsevier; 2010.
[24] Sukov WR, Lohse CM, Leibovich BC, Thompson RH, Cheville JC. Clinical and pathological features associated with prognosis in patients with papillary renal cell carcinoma. J Urol 2012;187:54–9.
[25] Onishi T, Ohishi Y, Goto H, Suzuki M, Miyazawa Y. Papillary renal cell carcinoma: clinicopathological characteristics and evaluation of prognosis in 42 patients. BJU Int 1999;83:937–43.
[26] Moch H, Gasser T, Amin MB, Torhorst J, Sauter G, Mihatsch MJ. Prognostic utility of the recently recommended histologic classification and revised TNM staging system of renal cell carcinoma: a Swiss experience with 588 tumors. Cancer 2000;89:604–14.
[27] Kim H, Cho NH, Kim DS, Kwon YM, Kim EK, Rha SH, et al. Renal cell carcinoma in South Korea: a multicenter study. Hum Pathol 2004;35:1556–63.
[28] Cheville JC, Lohse CM, Zincke H, Weaver AL, Blute ML. Comparisons of outcome and prognostic features among histologic subtypes of renal cell carcinoma. Am J Surg Pathol 2003;27:612–24.
[29] Fu Z, Sun L, Huang Y, Zhang J, Zhang Z, Wang L, et al. A type 2 papillary renal cell carcinoma presenting as an intracystic necrotic lesion: a case report. Mol Clin Oncol 2013;1:318–20.
[30] Pichler M, Hutterer GC, Chromecki TF, Pummer K, Mannweiler S, Zigeuner R. Presence and extent of histological tumour necrosis is an adverse prognostic factor in papillary type 1 but not in papillary type 2 renal cell carcinoma. Histopathology 2013;62:219–28.
[31] Pichler M, Hutterer GC, Chromecki TF, Jesche J, Kampel-Kettner K, Rehak P, et al. Histologic tumor necrosis is an independent prognostic indicator for clear cell and papillary renal cell carcinoma. Am J Clin Pathol 2012;137:283–9.
[32] Klatte T, Remzi M, Zigeuner RE, Mannweiler S, Said JW, Kabbinavar FF, et al. Development and external validation of a nomogram predicting disease specific survival after nephrectomy for papillary renal cell carcinoma. J Urol 2010;184:53–8.
[33] Chan JK, Cheuk W, Shimizu M. Anaplastic lymphoma kinase expression in inflammatory pseudotumors. Am J Surg Pathol 2001;25:761–8.
[34] Roquero L, Kryvenko ON, Gupta NS, Lee MW. Characterization of fibromuscular pseudocapsule in renal cell carcinoma. Int J Surg Pathol 2015;23:359–63.

MOLEKULÁRNĚ GENETICKÁ ANALÝZA JE NEZBYTNÁ PRO SPRÁVNOU DIAGNÓZU RENÁLNÍHO KARCINOMU NAPODOBUJÍCÍHO Xp11.2 TRANSLOKAČNÍ RENÁLNÍ KARCINOM

Xp11.2 translokační renální karcinom (TRK) je definován translokacemi chromosomu Xp11.2 vedoucí ke genové fúzi části krátkého raménka chromosomu X v lokusu 11.2 zahrnující *TFE3* gen. *TFE3* fúzuje s různými partnery, jmenovitě *ASPL*, *PRCC*, *PSF*, *CLTC*, *NONO*, přičemž fúze *TFE3-ASPL* je zdaleka nejčastější [4]. V době své iniciální deskripce byl Xp11.2 TRK morfologicky charakterizován světlými buňkami s objemnou cytoplazmou, uspořádanými převážně do papilárních struktur [28]. Jako další vodítka ke správné diagnóze jsou uváděna psammomatózní tělíska, hyalinní globule a příměs eosinofilních buněk. Nicméně, s přibývajícími publikacemi na toto téma se morfologické spektrum Xp11.2 TRK značně rozšířilo; byly popsány případy rostoucí částečně solidně, alveolárně, papilárně nebo v hnízdech [29, 30] a též se vyskytly případy histologicky napodobující PECom, melanom anebo alveolární sarkom měkkých tkání [31]. Imunohistochemicky jsou Xp11.2 TRK negativní nebo jen fokálně pozitivní v reakci s cytokeratiny a EMA a negativní v průkazu CANH-9 a AMACR, což je důležité v diferenciální diagnostice se světlobuněčným a papilárním reálním karcinomem (SRK;PRK). Specifická pro Xp11.2 TRK je nukleární, respektive cytoplazmatická pozitivita s TFE3 a cathepsinem K, ačkoliv z technických důvodů jsou tyto reakce často falešně pozitivní či falešně negativní a nelze na ně s jistotou spoléhat [32].

Do nynější studie jsme vybrali 20 případů morfologicky suspektních (avšak necharakteristických) z Xp11.2 TRK. Devět případů bylo díky break-apart FISH analýze potvrzeno jako Xp11.2 TRK. 9/11 zbývajících případů bylo geneticky analyzovatelných a tyto se staly předmětem dalšího zkoumání. Zmíněné tumory se vyznačovaly diverzní morfologií, často bylo možno v jednom tumoru zastihnout rysy SRK i PRK dohromady. Heterogenita byla patrná i imunohistochemicky. Například, z 5 případů, které byly převážně papilární, pouze 1 reagoval s CK7 a tento byl zároveň pozitivní s CANH-9 (marker SRK). Tumory morfologicky odpovídající SRK byly pozitivní s AMACR (marker PRK). Dva případy byly pozitivní v reakci s TFE3 a dva v cathepsinu K. Z uvedených příkladů vyplývá, že ke správnému zařazení podobných tumorů je molekulárně genetické vyšetření zásadní (případy byly finálně klasifikovány na základě genetických znaků).

Závěrem našeho výzkumu lze říci, že v případě TRK je cytogenetická analýza nadřazena morfologickým znakům a IHC průkazu TFE3 a cathepsinu K. Obzvláště důležité je si uvědomit, že pokud narazíme na morfologicky neklasifikovatelný tumor, který by potencionálně mohl spadat do kategorie TRK, je imunohistochemické vyšetření značně nespolehlivé a ve snaze o zařazení takového tumoru do jednoho ze subtypů RK spíše zmate, než pomůže. V tomto případě doporučujeme aplikovat FISH, konkrétně break-apart TFE3 analýzu k vyloučení Xp11.2 TRK. Díky současné éře cílené terapie a jejímu raketovému rozvoji považujeme diagnostiku translokačních karcinomů za důležitou.

Virchows Arch (2015) 466:313–322
DOI 10.1007/s00428-014-1702-7

ORIGINAL ARTICLE

Molecular-genetic analysis is essential for accurate classification of renal carcinoma resembling Xp11.2 translocation carcinoma

Malcolm Hayes · Kvetoslava Peckova · Petr Martinek · Milan Hora · Kristyna Kalusova · Lubomir Straka · Ondrej Daum · Bohuslava Kokoskova · Pavla Rotterova · Kristyna Pivovarčikova · Jindrich Branzovsky · Magdalena Dubova · Pavla Vesela · Michal Michal · Ondrej Hes

Received: 21 August 2014 / Revised: 26 October 2014 / Accepted: 1 December 2014 / Published online: 28 December 2014

Abstract Xp11.2-translocation renal carcinoma (TRCC) is suspected when a renal carcinoma occurs in young patients, patients with a prior history of exposure to chemotherapy and when the neoplasm has morphological features suggestive of that entity. We retrieved 20 renal tumours (from 17,500 archival cases) of which morphology arose suspicion for TRCC. In nine cases, TFE3 translocation was confirmed by fluorescence in situ hybridisation analysis. In 9 of the remaining 11 TRCC-like cases (7 male, 4 female, aged 22–84 years), material was available for further study. The morphological spectrum was diverse. Six tumours showed a mixture of cells with eosinophilic or clear cytoplasm in tubular, acinar and papillary architecture. One case was high grade with epithelioid, spindle cell and sarcomatoid areas. Another showed tubular, solid, and papillary areas and foci containing spindle cells reminiscent of mucinous tubular and spindle cell carcinoma. The third showed dyscohesive nests of large epithelioid and histiocytoid cells in a background of dense lymphoplasmacytic infiltrate. By immunohistochemistry, keratin AE1/AE3 was diffusely positive in three tumours, while CK7 strongly stained one tumour and another focally and weakly. CD10 and Pax8 were expressed by eight, AMACR and vimentin by seven, CA-IX by four and TFE3 and cathepsin K by two tumours. Of the two TFE3-positive tumours, one showed polysomy of chromosome 7 and the other of 17; they were *VHL* normal and diagnosed as unclassifiable RCC. Of the seven TFE3-negative tumours, three showed polysomy of 7/17 and *VHL* abnormality and were diagnosed as combined clear cell RCC/papillary RCC. One TFE3-negative tumour with normal 7/17 but LOH 3p (*VHL* abnormality) was diagnosed as clear cell RCC. One TFE3-negative tumour with polysomy 7/17 but normal *VHL* was diagnosed as papillary RCC, and two with normal chromosomes 7/17 and *VHL* gene were considered unclassifiable. As morphological features and IHC are heterogeneous, TRCC-like renal tumours can only be sub-classified accurately by multi-parameter molecular-genetic analysis.

Keywords Translocation · Renal cell carcinoma · TFE3 · Xp11 · FISH · Molecular genetics · MiTF · Immunohistochemistry

M. Hayes
Department of Pathology, BC Cancer Agency and Clinical Professor of Pathology, University of British Columbia, Vancouver, Canada

K. Peckova · P. Martinek · O. Daum · B. Kokoskova · P. Rotterova · K. Pivovarčikova · J. Branzovsky · M. Dubova · P. Vesela · M. Michal · O. Hes (✉)
Department of Pathology, Medical Faculty, Charles University and Charles University Hospital Plzen, Alej Svobody 80, 304 60 Plzen, Czech Republic
e-mail: hes@medima.cz

M. Hora · K. Kalusova
Department of Urology, Medical Faculty, Charles University and Charles University Hospital Plzen, Plzen, Czech Republic

L. Straka
Klinicka Patologia Presov, Presov, Slovak Republic

Introduction

Translocation-associated renal cell carcinoma (TRCC) resulting from Xp11.2 (TFE3) translocation was recognised first in paediatric and young adult patients [30, 41]. Subsequently TRCC was documented in older adults, and its frequency in the adult population is probably underestimated [8, 13, 20, 25, 48]. While TRCC has a favourable prognosis in children, these neoplasms may be aggressive in adults [24, 27, 31, 40].

Several variants of TRCC with translocation of TFE3 to different partner genes are now described [1, 2, 6, 7, 17, 42,

43]. The more common partners are *ASPL* and *PRCC* genes. TFE3 translocation also occurs in other neoplasms including alveolar soft-part sarcoma and some forms of PEComa [3, 22, 47]. TRCC involving the closely related *TFEB gene*, which is also part of the MiTF gene family, is rarer than TFE3-TRCC but has a similar clinical presentation and may have overlapping morphology [4, 9, 18, 38]. The two variants of MiTF-TRCC lack a familial history and are not multifocal, in contrast to renal cancers of the hereditary CCRCC syndrome associated with chromosome 3 translocations, and the hereditary PRCC associated with c-MET mutations [46].

Renal carcinoma occurring in a child, or in a patient exposed to chemotherapy for an earlier cancer, suggests the possibility of TRCC. Morphological studies of TRCC delineated an association with histological features that include a mixed papillary and alveolar architecture, a mixture of cells with clear and eosinophilic cytoplasm and clear cells with abundant voluminous cytoplasm. Presence of blood lakes, psammoma bodies, stromal hyaline globules and eosinophilic cytoplasmic inclusions are additional features described in TRCC. None of these morphological features is specific for TRCC, and some of the features depend on the precise translocation partner of the *TFE3 gene* fusion. Demonstration of the TFE3 translocation is the defining characteristic of TRCC. This is best demonstrated by break-apart fluorescence in situ hybridisation (FISH) [32]. Over-expression of the TFE3 protein can be shown by immunohistochemistry, but the test requires careful calibration and adherence to strict standards of fixation and controls to avoid false results. Furthermore, TRCC has relatively specific immunohistochemical and gene expression profiles that assist in its distinction from CRCC and PRCC [5, 14, 38].

The present study was performed on a group of 20 renal neoplasms selected for their unusual morphology or clinical presentation, which were considered suspicious for TRCC. Having excluded the bona fide cases of TFE3-TRCC by FISH testing, the remaining nine TRCC-like cases with adequate material were studied further in an attempt to classify them in terms of the currently accepted Vancouver classification. This exercise entailed the development of an investigative algorithm for future recommendation.

Materials and methods

Twenty tumours suspect for TRCC based mostly on morphological features were identified in the Plzen archive of 17,500 renal neoplasms. Haematoxylin and eosin-stained (H&E) glass slides and formalin-fixed paraffin embedded blocks were retrieved, and the pathology reports and clinical records were studied to obtain demographic and follow-up data of the patients and for gross descriptions of the tumours. In addition to the original archival slides, standard 4-μm sections were cut from formalin-fixed, paraffin-embedded blocks selected from the tumours. These were stained with H&E for light microscopic examination using standard methodology and spare sections were cut for IHC. The number of blocks per case ranged from 3 to 30.

All H&E-stained sections and IHC stains were reviewed by three authors of this paper (MH, KP and OH).

The immunohistochemical study was performed using a Ventana Benchmark XT automated stainer (Ventana Medical System, Inc., Tucson, AZ, USA). Antibodies against CK7 (monoclonal, OV-TL 12/30, 1:200, Dako, Glostrup, Denmark), pan keratin (polyclonal, AE1-AE3/PCK26, RTU, Ventana-Roche), CD10 (monoclonal, 56C6, 1:20, Novocastra, Burlingame, CA, USA), AMACR (monoclonal, 13H4, 1:200, Dako), TFE3 (polyclonal, Abcam, 1:100, Cambridge, UK), vimentin (D9, monoclonal, Neomarkers, Westinghouse, CA, USA, 1:1000), CA-IX (monoclonal, 303123, 1:100, RD systems, Minneapolis, MN, USA), cathepsin K (monoclonal, 3F9, Abcam, 1:100), PAX-8 (polyclonal, Abcam, Cambridge, UK, 1:100) and anti-melanosome (monoclonal, HMB45, DakoCytomation, 1:200) were applied to all cases. Selected cases were also stained for S-100 protein (polyclonal, DakoCytomation, 1:400), wide spectrum keratin (OSCAR, monoclonal, Covance, Princetown, NJ, 1:2000), cytokeratin 20 (M7019, monoclonal, DakoCytomation, 1:100) and cytokeratin (CAM 5,2 monoclonal, Becton-Dickinson, San Jose, CA, USA, 1:200) as part of their initial diagnostic work-up.

For each case, 3–30 blocks were available; for immunohistochemical study, 1–2 selected blocks were used per case.

Molecular genetic study

FISH analysis was performed for *TFE3* break and for enumeration of chromosomes X, Y, 7 and 17. The FISH procedure using centromeric probes for chromosomes 7 and 17 was described in paper of Petersson et al. [34]. The same technique of analysis and cut-off setting was used with probes CEP X/CEP Y (VYSIS/Abbott Molecular, Des Plaines, IL, USA) and ZytoLight® SPEC TFE3 Dual Color Break Apart Probe (ZytoVision GmbH, Bremerhaven, Germany). Monosomy and polysomy for chromosomes X and Y was defined as the presence of one signal per cell in >45 % and three and more signals in >10 % of cells, respectively. The cut-off value for TFE3 break was set to more than 10 % of nuclei with break signals. Mutation analysis of the *VHL* gene and loss of heterozygosity for chromosome 3p region (LOH3p) were studied by PCR and sequencing and fragmentation analysis, respectively. Methylation of the promoter of the VHL gene was analysed by methylation-specific PCR. All these methods were thoroughly described in paper of Petersson et al. [34].

Results

Clinical and gross findings

The patients, six male and three female, ranged in age from 43 to 84 years, 7 exceeding 50 years of age (Table 1). Tumour size ranged from 2.6 to 13 cm with six cases equal to or exceeding 5 cm in greatest dimension. Six cases were stage pT1 according TNM 09, two cases pT2 and one pT3. Four were from the left kidney and five from the right kidney. Most tumours were tan coloured with areas of brown, yellow to tan (Fig. 1a), white or grey with occasional, grossly visible necroses (Fig. 1b).

Follow-up was available in six cases. This ranged from 1 to 3 years. One patient died 1 year after diagnosis, and the other five patients are alive and well.

Histological findings

Three tumours had a prominent tubulopapillary architecture admixed with some solid nests of cells (Fig. 2a, b). Two tumours had a predominantly nested and alveolar pattern with alveolar spaces filled with eosinophilic secretions reminiscent of thyroid follicles (Fig. 3). One of these tumours contained small foci with a papillary architecture. Blood lakes were prominent in these two tumours and were seen focally in six other tumours. These two tumours and one of the neoplasms with a tubulopapillary architecture contained abundant clear cells with voluminous cytoplasm, prominent lateral cell borders and irregular apical cytoplasmic borders (so-called "blister" cells; Fig. 4). Such cells were seen focally in three other tumours. A population of cells with abundant eosinophilic (oncocyte-like) cytoplasm was also present in four of these tumours and predominated in two of the neoplasms (Fig. 5). One tumour with a nested and alveolar architecture mostly resembled CCRCC but had focal papillary architecture and some cells with eosinophilic granular cytoplasm (Fig. 6). Three of the above tumours contained varying numbers of psammoma bodies and one demonstrated prominent eosinophilic hyaline cytoplasmic inclusion bodies. None showed extracellular hyaline nodules of the type descried in some cases of TRCC. These six tumours were within the classically described morphological spectrum of TFE3-TRCC. Nuclei were Fuhrman grade 2 in three tumours and grade 3 in the other 3 tumours. Necrosis was seen in four of the six tumours.

Three tumours had unusual morphology. One unusual tumour exhibited a mixture of compressed tubules, papillary structures and spindle cells associated with a myxoid stroma that in places resembled the mucinous tubular and spindle cell renal carcinoma. Other areas had a so-called "solid papillary" pattern. The spindle cells in this neoplasm had eosinophilic cytoplasm imparting a myoid appearance. Nuclei were predominantly grade 2, but focally nuclei were highly pleomorphic; grade 3–4 and necrosis was identified in several foci (Fig. 7). Mitoses were scanty and not atypical. Therefore, in our opinion, this tumour did not represent sarcomatoid carcinoma but was too atypical to be considered mucinous tubular and spindle cell renal carcinoma. The second showed poorly cohesive nests of large plump polygonal cells some with abundant eosinophilic cytoplasm imparting a histiocytoid and rhabdoid appearance. Some cells showed peripheral clearing and vacuolation of their cytoplasm resembling that seen in Touton giant cells. In many areas, the neoplastic cells were overrun by numerous lymphocytes and plasma cells simulating a lymphoepithelial carcinoma or recalling the morphology of Hashimoto's thyroiditis. The third unusual tumour was composed predominantly of markedly atypical spindle cells arranged in poorly cohesive nests lying within a background of myxoid collagen imparting a sarcomatoid appearance. Focally, the spindle cell component was associated with intercellular eosinophilic matrix resembling osteoid. Elsewhere, this neoplasm showed poorly cohesive nests of large epithelioid cells with large vesicular nuclei containing macronucleoli suggesting melanoma or alveolar soft-part sarcoma. This

Table 1 Clinicopathologic data

Case	Sex	Age	Site	Size (cm)	pT TNM09	Color	Follow-up
1	M	51	Left	13	pT2	Yellowish	NA
2	M	80	Left	10×6×3	pT3a	Tan to brown	DOD 1 year after dg
3	F	60	Right	6×4×3	pT1b	Whitish	3 years AW
4	F	75	Right	2.6×2×2	pT1a	Gray to tan	1 year AW
5	F	84	Left	Diam. 5	pT1b	Gray to tan	NA
6	M	57	Right	2.5×2.7×2.9	pT1a	Yellowish	2 years AW
7	M	48	Right	9×8×7	pT2	Brownish-yellow	NA
8	M	72	Left	5×4.5×3.5	pT1b	Tan to brow	1 year AW, CRI, HT
9	M	43	Right	5.5×4.5×3	pT1b	Tan	1 year AW

M male, *F* female, *NA* not available, *DOD* dead of disease, *AW* alive and well, *CRI* chronic renal insufficiency, *HT* hypertension, *dg* diagnosis

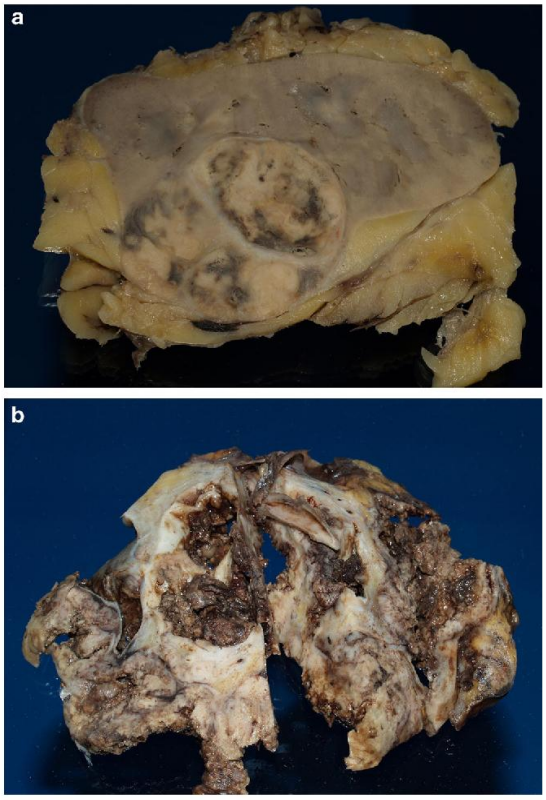

Fig. 1 Tumours were mostly yellow to tan on gross section (**a**) with foci of grossly visible necrosis (**b**)

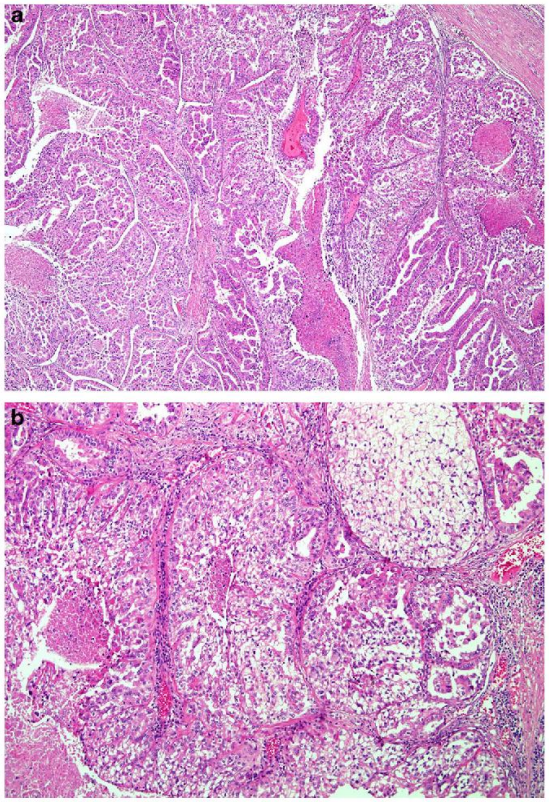

Fig. 2 Some tumours had a prominent tubulopapillary architecture admixed with solid nests of cells admixed with solid nests of cells(**a**, **b**)

tumour contained extensive necrosis, numerous mitoses and some atypical mitoses. It was invasive into perinephric fat and exhibited extensive lymphovascular invasion. This tumour was initially considered to potentially fall within the spectrum of ASPL-TFE3 or TFEB-TRCC and required exclusion of metastatic melanoma.

Immunohistochemical analysis

Results of the immunohistochemical analysis are listed in Table 2. None of the tumours showed an immunoprofile diagnostic of any particular type of RCC. Importantly, TFE3 was positive in two tumours neither of which was strongly positive for cathepsin K. A third tumour was initially interpreted as positive for TFE3 but presence of staining in adjacent benign tissues prompted repeat of the stain, which was negative. None of the tumours was positive for HMB45. Cathepsin K was positive in two tumours but one showed only weak focal staining. The latter tumour was positive for TFE3 by IHC but not FISH (Fig. 8). All but one of the nine TRCC-like tumours were positive for CD10, seven were positive for vimentin and four for carbonic anhydrase-IX (CA-IX). Seven were positive for AMACR. Keratin AE1/AE3 was diffusely positive in three tumours and was negative in six. CK7

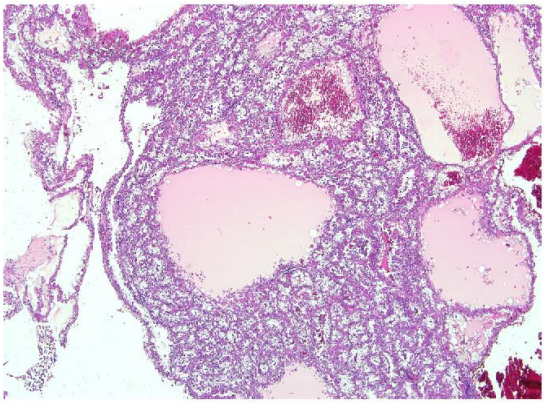

Fig. 3 Two tumours had a predominantly nested and alveolar pattern with alveolar spaces filled with eosinophilic secretions reminiscent of thyroid follicles

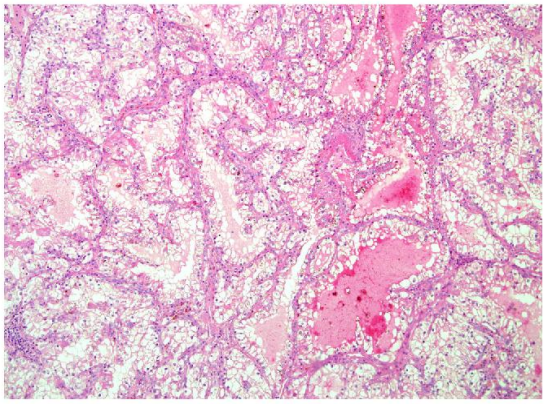

Fig. 4 Tumours with tubulopapillary architecture contained abundant clear cells with voluminous cytoplasm, prominent lateral cell borders and irregular apical cytoplasmic borders (so-called "blister" cells)

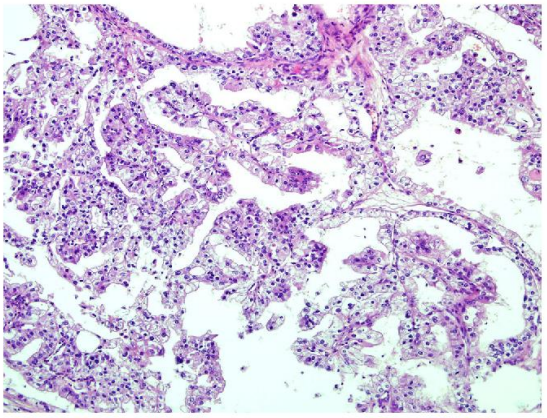

Fig. 6 One tumour with a nested and alveolar architecture mostly resembled CCRCC but had focal papillary architecture and some cells with eosinophilic granular cytoplasm

strongly stained one tumour, was weakly and focally positive in 1 and was negative in six cases. Pax 8 was positive in all but one case.

Molecular and cytogenetic analysis

One TFE3-negative tumour (case 8) showed normal copy numbers of 7,17 and LOH 3p (*VHL* abnormality) (Table 3). This tumour was diagnosed as clear cell RCC (CCRCC). One TFE3-negative tumour (case 1) with polysomy 7 and 17 but normal *VHL* status was diagnosed as papillary RCC (PRCC). Two TFE3-negative tumours (cases 4 and 6) had a normal complement of chromosomes 7 and 17 and no abnormality of the *VHL* gene. These tumours were considered unclassifiable. Three TFE3-negative tumours (cases 5, 7 and 9) that showed both polysomy of 7 and 17 and *VHL* abnormality were regarded as composite or combined CRCC/PRCC (unclassifiable). One of the two TFE3-IHC positive tumours (cases 2 and 3) showed only polysomy 7 and the other only polysomy 17, and both were negative for *VHL* gene abnormalities. These were also regarded as unclassifiable RCC.

Discussion

RCCs associated with TFE3 gene fusions are relatively rare tumours in adults but comprise approximately 30–50 % of renal cell carcinomas in children. There is an established association between TRCC and prior exposure to chemotherapy [14, 39]. The rarity of TRCC cases in our archive could be explained by the fact that a large majority of the renal neoplasms in the archive were obtained from hospitals concentrating on adult clinical practice (age of the patients is over 18 years). TFE3 translocation can occur to several different

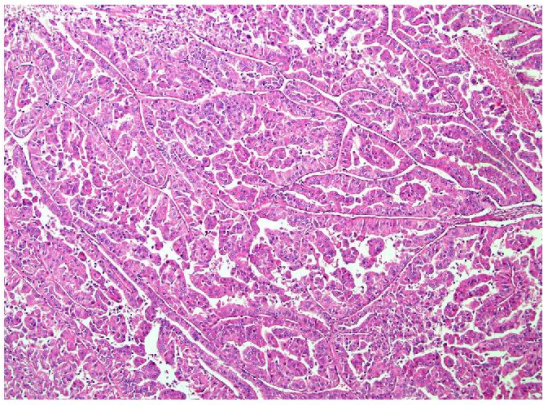

Fig. 5 A population of cells with abundant eosinophilic cytoplasm was also present in four of these tumours

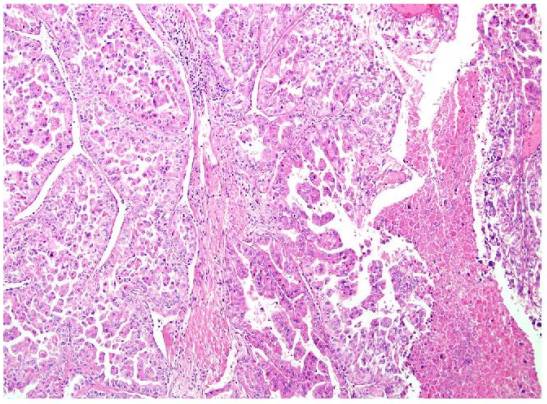

Fig. 7 Areas of necrosis were noted in the vicinity of papillary and micropapillary structures

Table 2 Immunohistochemical examination

Case:	TFE3	CANH9	CD10	Vim	AMACR	Cathep.	HMB45	AE1–AE3	CK7	Pax8
1	−	−	+++	+++	++	−	−	−	−	++
2	+++	−	++ foc	+++	−	−	−	−	+ foc	−
3	+++	−	+++ foc	+++	−	+ foc	−	−	−	+
4	−	−	++ foc	−	+++	+++	−	−	−	+
5	−	−	−	+++	+++	−	−	++	−	+
6	−	++ foc	+++	+++	+++	−	−	−	−	++
7	−	++ foc	+++	−	+++ foc	−	−	+++	−	++
8	−	++ foc	+++	+++	+++	−	−	++	+++	+
9	−	+++	+++	+++	+++ foc	−	−	−	−	+

foc=<25 % cells staining

CANH9 carbonic anhydrase IX, *Vim* Vimentin, *AMACR* alpha-methylacyl-CoA racemase, *Cathep*. cathepsin K, (−) negative, (+) weak, (++) moderate, (+++) strong

partner genes including *ASPL*, *PRCC*, *PSF*, *CLTC*, *NonO*, and others not yet fully clarified [7, 8, 10, 11, 19]. Prior to the recognition of translocation carcinomas of the kidney, most of these tumours were classified in the categories of clear cell renal cell carcinoma and papillary renal cell carcinoma [15, 35, 37]. Young age at presentation is one of the main indicators of a possible translocation-associated renal carcinoma and prompts the pathologist to consider such a diagnosis. However, since classical CCRCC and PRCC comprise the most common renal neoplasms in adults, the possibility of TRCC is seldom considered in that age group so the incidence of TFE3 translocation carcinomas in adults aged >50 years is not known but is likely underestimated. Recent studies have shown that TRCC occurs in younger adults who typically present a higher clinical stage than in paediatric patients. The more aggressive behaviour of TRCC in adults may also be explained by the progressive acquisition of chromosomal copy number alterations [33]. The importance of recognising TRCC is increasing in the era of potential targeted therapy [23, 28].

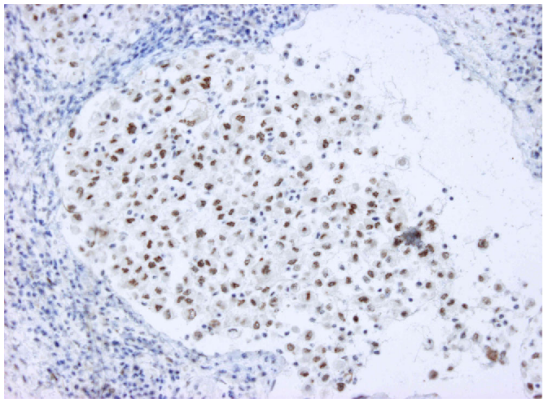

Fig. 8 Strong nuclear TFE3 positivity was noted in two tumours

At the time of initial description, TRCC was noted to have mostly papillary architecture and to be composed of cells with voluminous clear cytoplasm. Additional histological pointers to possible TRCC include an admixture of cells with clear and eosinophilic cytoplasm, presence of psammoma bodies and hyaline stromal globules [2, 44]. However, larger studies have expanded the histological profile to include mixed solid, nested, alveolar and papillary patterns such that accurate distinction from CCRCC and PRCC is impossible based only on morphology [1, 45]. The cells may have clear or eosinophilic cytoplasm, which may or may not be voluminous. Rare cases of TRCC contain melanin, express melanocytic markers by immunohistochemistry and exhibit a morphology that overlaps with PEComa, melanoma and even alveolar soft part sarcoma [3]. Different variants of TFE3 translocation were thought to result in different morphological appearances, but cases with overlapping morphological features were described later. Furthermore, a closely related form of TRCC involving the TFEB gene, another member of the MiTF gene family, was likewise initially thought to have a distinctive morphology but more experience with larger numbers of cases has shown morphological overlap with the more common TFE3 neoplasms and the more usual variants of renal carcinoma [8, 14, 18].

Immunohistochemical analysis may be helpful in differentiating TRCC from PRCC in that TRCC is negative or only weakly and focally positive for keratins and EMA, and is negative for racemase (AMACR) [1, 2, 12, 14]. Similar to clear cell carcinoma, TRCC is positive with the antibody to vimentin and strongly positive with CD10. However, vimentin staining is patchy in TRCC but diffuse in CCRCC, and TRCC is negative for carbonic anhydrase-9 (CA-IX). Positive nuclear staining for TFE3 protein and cytoplasmic staining for cathepsin K have been regarded as specific for

Table 3 Results of molecular and cytogenetic analyses

Case	TFE3 ba	CEP 7	CEP 17	X/Y	LOH3p	Mut VHL	Methyl VHL	Diag
1	Neg	Polysomy[a]	Polysomy[a]	4~5X/0Y; 2X/1Y[b]	Neg	Neg	Neg	PRCC
2	Neg	Polysomy	Disomy	NA	NA	Neg	NA	UNC
3	Neg	Disomy	Polysomy[a]	NP	Neg	Neg	Neg	UNC
4	Neg	Disomy	Disomy	NP	Neg	Neg	Neg	UNC
5	Neg	Polysomy[a]	Polysomy[a]	NP	Pos	Neg	Neg	CRCC/PRCC
6	Neg	Disomy	Disomy	2X/1Y	Neg	Neg	Neg	UNC
7	Neg	Polysomy	Polysomy	2X/2Y	Pos	Pos[c]	Neg	CRCC/PRCC
8	Neg	Disomy	Disomy	2X/0Y	Pos	Neg	Neg	CCRCC
9	Neg	Polysomy[a]	Polysomy[a]	Neg	Pos	Pos[d]	Neg	CRCC/PRCC

Pos positive, *Neg* negative, *NA* not analysable, *NP* not performed, *PRCC* papillary renal cell carcinoma, *UNC* unclassified renal cell carcinoma, *CRCC* clear cell renal cell carcinoma, *Mut VHL* mutation of *VHL gene, Methyl VHL* methylation status of *VHL gene*, *Diag* diagnosis

[a] Polysomy in large nuclei only

[b] Gain X, loss Y (4~5X/0Y) in large nuclei; gain X (2X/1Y) in small nuclei

[c] Somatic mutation c.504_508del/p.Leu168GlnfsTer3

[d] Somatic mutation c.393C>G/p.Asn131Lys

TRCC [5, 29, 38], but false positive and negative results have been reported in several studies not all of which have been explained on the basis of technical problems [21]. Indeed, it seems that over-expression of wild-typeTFE3 protein transcript may occur as a result of up-regulation of the normal gene, or as the result of increased gene copy number due to polysomy or amplification particularly in high grade CCRCC and in carcinomas with sarcomatoid and cystic features [26, 48]. Similarly, positive immunostains for melanocytic markers such as HMB45 may be seen in some variants of TFE3-TRCC, in the TFEB-TRCC and in PEComas [14, 16].

In the present study of 20 cases of RCC in which there was a suspicion of TRCC, nine cases were confirmed as X11.2-TRCC by break-apart FISH analysis. The remaining TRCC-like carcinomas showed a diverse morphology that precluded definite classification of these tumours on morphological grounds. Thus, many showed a mixture of papillary and CCRCC patterns. Seven cases contained clear cells with voluminous cytoplasm, so-called "blister" cells, a well-known feature of TRCC. IHC was also contradictory to the morphology in many cases, again suggesting possible TRCC. Of five cases exhibiting a predominantly papillary architecture, only one was strongly positive for CK7 and that tumour was also positive for CA-IX, a marker of CCRCC. Those tumours with morphology similar to CCRCC were all positive for AMACR, a marker of PRCC. The sarcomatoid tumour with morphology suggestive of melanoma or APSL-TFE3 TRCC posed a diagnostic challenge. It was positive for TFE3 by IHC, negative for HMB45 and showed only focal weak staining for cathepsin K. Although the stain for Pax-8 was negative, there was no clinical history of prior cutaneous melanoma or other visceral malignancy. Furthermore, metastatic melanoma was excluded by negative immunostaining for S-100 protein and diffusely positive staining for wide spectrum keratin (OSCAR). Positive immunostaining for TFE3 in the absence of the translocation has been described previously in sarcomatoid and other high-grade RCCs sometimes explained by gene polysomy or amplification [26]. Because of the contradictory morphological and immunohistochemical profiles of these TRCC-like neoplasms, we conclude that molecular/genetic analysis is the most reliable method extant to classify this group of unusual renal tumours.

The final molecular/genetic diagnosis did not correlate exactly with the histomorphology and immunoprofile in some cases (Table 4). In the case diagnosed as CCRCC on the basis of isolated abnormality of the *VHL* locus, the histology showed a prominent papillary architecture and alveolar nests with a micropapillary pattern within them. Immunostains for CK7 and AMACR were strongly positive. However, CA-IX was also positive. The case diagnosed as PRCC on the basis of polysomy of chromosomes 7 and 17 in the absence of *VHL* abnormality had prominent papillary architecture but showed a predominance of clear cells with voluminous vacuolated cytoplasm suggesting TRCC. On IHC, the tumour was negative for CK7 and positive for CD10 and vimentin. However, the stain for AMACR was positive. One of the three tumours diagnosed as combined PRCC–CCRCC on the basis of morphology, immunohistochemical examination and polysomy of chromosomes 7 and 17 and *VHL* abnormality showed a combined papillary, tubular and nested architecture and a predominance of cells with eosinophilic cytoplasm and scanty clear cells. One PRCC–CCRCC did not contain papillary structures and had a morphology most consistent with CCRCC but with clear cells showing voluminous cytoplasm suggesting TRCC. The third PRCC–CCRCC was the unusual tumour with a solid papillary pattern and areas of spindle cells in a mucinous

Table 4 Summary of unusual features

Molecular category	Case	Unusual features
CRCC	8	Papillary architecture AMACR and CK 7 strongly positive
PRCC	1	Clear cells with voluminous cytoplasm Glassy hyaline intra-cytoplasmic globules CK 7 negative
Combined PRCC-CCRCC	5, 7, 9	Spindle cell component and myxoid stroma and no alveolar or solid nest patterns in 1 case Papillary pattern absent in 1 case Very scanty clear cell component in 2 cases CK 7 negative in all AMACR positive in all CA-IX positive in 2 cases
Unclassifiable NOS	4, 6 2 3	2 cases had mixed PRCC and CCRCC morphology. Both contained clear cells with voluminous cytoplasm CK 7 negative but AMACR and cathepsin K positive Strong TFE3 positivity (by IHC), not confirmed by FISH

CRCC clear cell renal cell carcinoma, *PRCC* papillary renal cell carcinoma, *NOS* not otherwise specified, *IHC* Immunohistochemistry

stroma described above. By IHC, all three tumours were negative for CK7, positive for AMACR, and two were positive for CA-IX.

The study reported herein confirms the conclusion of other workers [36] that cytogenetic analysis is preferable to morphology and immunostains for TFE3 and cathepsin K in the diagnosis of TRCC. Furthermore, when TRCC-like tumours are selected on the basis of histological changes that do not conform to those classically described for other subtypes of RCC, immunohistochemistry is shown to be especially unreliable in further classifying these unusual renal neoplasms.

In conclusion, the molecular/genetic algorithm used herein is recommended for tumours with a TRCC-like morphology. This algorithm could also be applied in the investigation of unclassifiable RCC. Firstly, break-apart FISH analysis for TFE3 is performed and true cases of X11.2 translocation separated out. Next, numerical analysis of chromosomes 7 and 17 is performed together with thorough investigation of the status of the *VHL* gene on chromosome 3p using PCR for mutation analysis and LOH and methylation-specific PCR for the methylation analysis of the promoter region of the *VHL* gene. This enables true CCRCC and PRCC to be separated from the tumours that have combined features of CCRCC–PRCC. The remainder of unclassifiable RCCs may contain rare cases of TFEB–TRCC. These tumours are usually positive for cathepsin K and melanocytic markers on immunohistochemistry and can be confirmed by break-apart FISH analysis for the t(6;11) TFEB translocation [9]. Further, such unclassifiable cases may benefit from whole genome sequencing studies. Molecular features are indeed one of the characteristics useful for classification of unusual renal tumours. However, in group of TRCC and TRCC-like cases, it seems that they play a key role in the differential diagnostic process.

Acknowledgements The study was supported by the Charles University Research Fund (project number P36), by the project by the project CZ.1.05/2.1.00/03.0076 from European Regional Development Fund and by Ministry of Health, Czech Republic—conceptual development of research organization (Faculty Hospital in Pilsen—FNPl, 00669806).

Conflict of interest All authors declare no conflict of interest.

References

1. Argani P, Antonescu CR, Couturier J, Fournet JC, Sciot R, Debiec-Rychter M, Hutchinson B, Reuter VE, Boccon-Gibod L, Timmons C, Hafez N, Ladanyi M (2002) PRCC-TFE3 renal carcinomas: morphologic, immunohistochemical, ultrastructural, and molecular analysis of an entity associated with the t(X;1)(p11.2;q21). Am J Surg Pathol 26:1553–1566
2. Argani P, Antonescu CR, Illei PB, Lui MY, Timmons CF, Newbury R, Reuter VE, Garvin AJ, Perez-Atayde AR, Fletcher JA, Beckwith JB, Bridge JA, Ladanyi M (2001) Primary renal neoplasms with the ASPL-TFE3 gene fusion of alveolar soft part sarcoma: a distinctive tumor entity previously included among renal cell carcinomas of children and adolescents. Am J Pathol 159:179–192. doi:10.1016/S0002-9440(10)61684-7
3. Argani P, Aulmann S, Illei PB, Netto GJ, Ro J, Cho HY, Dogan S, Ladanyi M, Martignoni G, Goldblum JR, Weiss SW (2010) A distinctive subset of PEComas harbors TFE3 gene fusions. Am J Surg Pathol 34:1395–1406. doi:10.1097/PAS.0b013e3181f17ac0

4. Argani P, Hawkins A, Griffin CA, Goldstein JD, Haas M, Beckwith JB, Mankinen CB, Perlman EJ (2001) A distinctive pediatric renal neoplasm characterized by epithelioid morphology, basement membrane production, focal HMB45 immunoreactivity, and t(6;11)(p21.1;q12) chromosome translocation. Am J Pathol 158:2089–2096. doi:10.1016/S0002-9440(10)64680-9
5. Argani P, Hicks J, De Marzo AM, Albadine R, Illei PB, Ladanyi M, Reuter VE, Netto GJ (2010) Xp11 translocation renal cell carcinoma (RCC): extended immunohistochemical profile emphasizing novel RCC markers. Am J Surg Pathol 34:1295–1303. doi:10.1097/PAS.0b013e3181e8ce5b
6. Argani P, Ladanyi M (2005) Translocation carcinomas of the kidney. Clin Lab Med 25:363–378. doi:10.1016/j.cll.2005.01.008
7. Argani P, Lui MY, Couturier J, Bouvier R, Fournet JC, Ladanyi M (2003) A novel CLTC-TFE3 gene fusion in pediatric renal adenocarcinoma with t(X;17)(p11.2;q23). Oncogene 22:5374–5378. doi:10.1038/sj.onc.1206686
8. Argani P, Olgac S, Tickoo SK, Goldfischer M, Moch H, Chan DY, Eble JN, Bonsib SM, Jimeno M, Lloreta J, Billis A, Hicks J, De Marzo AM, Reuter VE, Ladanyi M (2007) Xp11 translocation renal cell carcinoma in adults: expanded clinical, pathologic, and genetic spectrum. Am J Surg Pathol 31:1149–1160. doi:10.1097/PAS.0b013e318031ffff
9. Argani P, Yonescu R, Morsberger L, Morris K, Netto GJ, Smith N, Gonzalez N, Illei PB, Ladanyi M, Griffin CA (2012) Molecular confirmation of t(6;11)(p21;q12) renal cell carcinoma in archival paraffin-embedded material using a break-apart TFEB FISH assay expands its clinicopathologic spectrum. Am J Surg Pathol 36:1516–1526. doi:10.1097/PAS.0b013e3182613d8f
10. Armah HB, Parwani AV (2010) Xp11.2 translocation renal cell carcinoma. Arch Pathol Lab Med 134:124–129. doi:10.1043/2008-0391-RSR.1
11. Armah HB, Parwani AV, Surti U, Bastacky SI (2009) Xp11.2 translocation renal cell carcinoma occurring during pregnancy with a novel translocation involving chromosome 19: a case report with review of the literature. Diagn Pathol 4:15. doi:10.1186/1746-1596-4-15
12. Bazille C, Allory Y, Molinie V, Vieillefond A, Cochand-Priollet B, Cussenot O, Callard P, Sibony M (2004) Immunohistochemical characterisation of the main histologic subtypes of epithelial renal tumours on tissue-microarrays. Study of 310 cases. Ann Pathol 24:395–406
13. Bruder E, Moch H (2004) [Pediatric renal cell carcinoma] Der Pathologe 25:324–327. doi:10.1007/s00292-004-0699-0
14. Camparo P, Vasiliu V, Molinie V, Couturier J, Dykema KJ, Petillo D, Furge KA, Comperat EM, Lae M, Bouvier R, Boccon-Gibod L, Denoux Y, Ferlicot S, Forest E, Fromont G, Hintzy MC, Laghouati M, Sibony M, Tucker ML, Weber N, Teh BT, Vieillefond A (2008) Renal translocation carcinomas: clinicopathologic, immunohistochemical, and gene expression profiling analysis of 31 cases with a review of the literature. Am J Surg Pathol 32:656–670. doi:10.1097/PAS.0b013e3181609914
15. Cao Y, Paner GP, Perry KT, Flanigan RC, Campbell SC, Picken MM (2005) Renal neoplasms in younger adults: analysis of 112 tumors from a single institution according to the new 2004 World Health Organization classification and 2002 American Joint Committee on Cancer Staging System. Arch Pathol Lab Med 129:487–491. doi:10.1043/1543-2165(2005)129<487:RNIYAA>2.0.CO;2
16. Chang IW, Huang HY, Sung MT (2009) Melanotic Xp11 translocation renal cancer: a case with PSF-TFE3 gene fusion and up-regulation of melanogenetic transcripts. Am J Surg Pathol 33:1894–1901. doi:10.1097/PAS.0b013e3181ba7a5f
17. Clark J, Lu YJ, Sidhar SK, Parker C, Gill S, Smedley D, Hamoudi R, Linehan WM, Shipley J, Cooper CS (1997) Fusion of splicing factor genes PSF and NonO (p54nrb) to the TFE3 gene in papillary renal cell carcinoma. Oncogene 15:2233–2239. doi:10.1038/sj.onc.1201394
18. Davis IJ, Hsi BL, Arroyo JD, Vargas SO, Yeh YA, Motyckova G, Valencia P, Perez-Atayde AR, Argani P, Ladanyi M, Fletcher JA, Fisher DE (2003) Cloning of an Alpha-TFEB fusion in renal tumors harboring the t(6;11)(p21;q13) chromosome translocation. Proc Natl Acad Sci U S A 100:6051–6056. doi:10.1073/pnas.0931430100
19. Dijkhuizen T, van den Berg E, Wilbrink M, Weterman M, GeurtsvanKessel A, Storkel S, Folkers RP, Braam A, de Jong B (1995) Distinct Xp11.2 breakpoints in two renal cell carcinomas exhibiting X;autosome translocations. Gene Chromosome Cancer 14:43–50
20. Eble JN, Sauter G, Epstein JI, Sesterhenn I, WHO Classification of Tumours (2004) Tumours of the urinary system and male genital organs. Pathology and genetics. IARC Press, Lyon
21. Gaillot-Durand L, Chevallier M, Colombel M, Couturier J, Pierron G, Scoazec JY, Mege-Lechevallier F (2013) Diagnosis of Xp11 translocation renal cell carcinomas in adult patients under 50 years: interest and pitfalls of automated immunohistochemical detection of TFE3 protein. Pathol Res Pract 209:83–89. doi:10.1016/j.prp.2012.10.013
22. Hodge JC, Pearce KE, Wang X, Wiktor AE, Oliveira AM, Greipp PT (2014) Molecular cytogenetic analysis for TFE3 rearrangement in Xp11.2 renal cell carcinoma and alveolar soft part sarcoma: validation and clinical experience with 75 cases. Mod Pathol 27:113–127. doi:10.1038/modpathol.2013.83
23. Hora M, Urge T, Travnicek I, Ferda J, Chudacek Z, Vanecek T, Michal M, Petersson F, Kuroda N, Hes O (2014) MiT translocation renal cell carcinomas: two subgroups of tumours with translocations involving 6p21 [t (6; 11)] and Xp11.2 [t (X;1 or X or 17)]. SpringerPlus 3:245. doi:10.1186/2193-1801-3-245
24. Klatte T, Streubel B, Wrba F, Remzi M, Krammer B, de Martino M, Waldert M, Marberger M, Susani M, Haitel A (2012) Renal cell carcinoma associated with transcription factor E3 expression and Xp11.2 translocation: incidence, characteristics, and prognosis. Am J Clin Pathol 137:761–768. doi:10.1309/AJCPQ6LLFMC4OXGC
25. Komai Y, Fujiwara M, Fujii Y, Mukai H, Yonese J, Kawakami S, Yamamoto S, Migita T, Ishikawa Y, Kurata M, Nakamura T, Fukui I (2009) Adult Xp11 translocation renal cell carcinoma diagnosed by cytogenetics and immunohistochemistry. Clin Cancer Res: Off J Am Assoc Cancer Res 15:1170–1176. doi:10.1158/1078-0432.CCR-08-1183
26. Macher-Goeppinger S, Roth W, Wagener N, Hohenfellner M, Penzel R, Haferkamp A, Schirmacher P, Aulmann S (2012) Molecular heterogeneity of TFE3 activation in renal cell carcinomas. Mod Pathol: Off J U S Can Acad Pathol Inc 25:308–315. doi:10.1038/modpathol.2011.169
27. Malouf GG, Camparo P, Molinie V, Dedet G, Oudard S, Schleiermacher G, Theodore C, Dutcher J, Billemont B, Bompas E, Guillot A, Boccon-Gibod L, Couturier J, Escudier B (2011) Transcription factor E3 and transcription factor EB renal cell carcinomas: clinical features, biological behavior and prognostic factors. J Urol 185:24–29. doi:10.1016/j.juro.2010.08.092
28. Malouf GG, Camparo P, Oudard S, Schleiermacher G, Theodore C, Rustine A, Dutcher J, Billemont B, Rixe O, Bompas E, Guillot A, Boccon-Gibod L, Couturier J, Molinie V, Escudier B (2010) Targeted agents in metastatic Xp11 translocation/TFE3 gene fusion renal cell carcinoma (RCC): a report from the Juvenile RCC Network. Ann Oncol: Off J Eur Soc Med Oncol / ESMO 21:1834–1838. doi:10.1093/annonc/mdq029
29. Martignoni G, Pea M, Gobbo S, Brunelli M, Bonetti F, Segala D, Pan CC, Netto G, Doglioni C, Hes O, Argani P, Chilosi M (2009) Cathepsin-K immunoreactivity distinguishes MiTF/TFE family renal translocation carcinomas from other renal carcinomas. Mod Pathol: Off J U S Can Acad Pathol Inc 22:1016–1022. doi:10.1038/modpathol.2009.58

30. Meloni AM, Sandberg AA, Pontes JE, Dobbs RM Jr (1992) Translocation (X;1)(p11.2;q21). A subtype of renal adenocarcinomas. Cancer Genet Cytogenet 63:100–101
31. Meyer PN, Clark JI, Flanigan RC, Picken MM (2007) Xp11.2 translocation renal cell carcinoma with very aggressive course in five adults. Am J Clin Pathol 128:70–79. doi:10.1309/LR5G1VMXPY3G0CUK
32. Mosquera JM, Dal Cin P, Mertz KD, Perner S, Davis IJ, Fisher DE, Rubin MA, Hirsch MS (2011) Validation of a TFE3 break-apart FISH assay for Xp11.2 translocation renal cell carcinomas. Diagn Mol Pathol: Am J Surg Pathol B 20:129–137. doi:10.1097/PDM.0b013e31820e9c67
33. Pan CC, Sung MT, Huang HY, Yeh KT (2013) High chromosomal copy number alterations in Xp11 translocation renal cell carcinomas detected by array comparative genomic hybridization are associated with aggressive behavior. Am J Surg Pathol 37:1116–1119. doi:10.1097/PAS.0b013e318293d872
34. Petersson F, Grossmann P, Hora M, Sperga M, Montiel DP, Martinek P, Gutierrez ME, Bulimbasic S, Michal M, Branzovsky J, Hes O (2013) Renal cell carcinoma with areas mimicking renal angiomyoadenomatous tumor/clear cell papillary renal cell carcinoma. Hum Pathol. doi:10.1016/j.humpath.2012.11.019
35. Ramphal R, Pappo A, Zielenska M, Grant R, Ngan BY (2006) Pediatric renal cell carcinoma: clinical, pathologic, and molecular abnormalities associated with the members of the mit transcription factor family. Am J Clin Pathol 126:349–364. doi:10.1309/98YE9E442AR7LX2X
36. Rao Q, Williamson SR, Zhang S, Eble JN, Grignon DJ, Wang M, Zhou XJ, Huang W, Tan PH, Maclennan GT, Cheng L (2013) TFE3 break-apart FISH has a higher sensitivity for Xp11.2 translocation-associated renal cell carcinoma compared with TFE3 or cathepsin K immunohistochemical staining alone: expanding the morphologic spectrum. Am J Surg Pathol 37:804–815. doi:10.1097/PAS.0b013e31827e17cb
37. Renshaw AA, Zhang H, Corless CL, Fletcher JA, Pins MR (1997) Solid variants of papillary (chromophil) renal cell carcinoma: clinicopathologic and genetic features. Am J Surg Pathol 21:1203–1209
38. Smith NE, Illei PB, Allaf M, Gonzalez N, Morris K, Hicks J, Demarzo A, Reuter VE, Amin MB, Epstein JI, Netto GJ, Argani P (2014) t(6;11) renal cell carcinoma (RCC): expanded immunohistochemical profile emphasizing novel RCC markers and report of 10 new genetically confirmed cases. Am J Surg Pathol 38:604–614. doi:10.1097/PAS.0000000000000203
39. Srigley JR, Delahunt B, Eble JN, Egevad L, Epstein JI, Grignon D, Hes O, Moch H, Montironi R, Tickoo SK, Zhou M, Argani P, Panel IRT (2013) The International Society of Urological Pathology (ISUP) Vancouver classification of renal neoplasia. Am J Surg Pathol 37:1469–1489. doi:10.1097/PAS.0b013e318299f2d1
40. Sukov WR, Hodge JC, Lohse CM, Leibovich BC, Thompson RH, Pearce KE, Wiktor AE, Cheville JC (2012) TFE3 rearrangements in adult renal cell carcinoma: clinical and pathologic features with outcome in a large series of consecutively treated patients. Am J Surg Pathol 36:663–670. doi:10.1097/PAS.0b013e31824dd972
41. Tomlinson DC, L'Hote CG, Kennedy W, Pitt E, Knowles MA (2005) Alternative splicing of fibroblast growth factor receptor 3 produces a secreted isoform that inhibits fibroblast growth factor-induced proliferation and is repressed in urothelial carcinoma cell lines. Cancer Res 65:10441–10449. doi:10.1158/0008-5472.CAN-05-1718
42. Tonk V, Wilson KS, Timmons CF, Schneider NR, Tomlinson GE (1995) Renal cell carcinoma with translocation (X;1). Further evidence for a cytogenetically defined subtype. Cancer Genet Cytogenet 81:72–75
43. Weterman MA, Wilbrink M, Geurts van Kessel A (1996) Fusion of the transcription factor TFE3 gene to a novel gene, PRCC, in t(X;1)(p11;q21)-positive papillary renal cell carcinomas. Proc Natl Acad Sci U S A 93:15294–15298
44. Winarti NW, Argani P, De Marzo AM, Hicks J, Mulyadi K (2008) Pediatric renal cell carcinoma associated with Xp11.2 translocation/TFE3 gene fusion. Int J Surg Pathol 16:66–72. doi:10.1177/1066896907304994
45. Wu A, Kunju LP, Cheng L, Shah RB (2008) Renal cell carcinoma in children and young adults: analysis of clinicopathological, immunohistochemical and molecular characteristics with an emphasis on the spectrum of Xp11.2 translocation-associated and unusual clear cell subtypes. Histopathology 53:533–544. doi:10.1111/j.1365-2559.2008.03151.x
46. Yan BC, Mackinnon AC, Al-Ahmadie HA (2009) Recent developments in the pathology of renal tumors: morphology and molecular characteristics of select entities. Arch Pathol Lab Med 133:1026–1032. doi:10.1043/1543-2165-133.7.1026
47. Zhong M, De Angelo P, Osborne L, Keane-Tarchichi M, Goldfischer M, Edelmann L, Yang Y, Linehan WM, Merino MJ, Aisner S, Hameed M (2010) Dual-color, break-apart FISH assay on paraffin-embedded tissues as an adjunct to diagnosis of Xp11 translocation renal cell carcinoma and alveolar soft part sarcoma. Am J Surg Pathol 34:757–766. doi:10.1097/PAS.0b013e3181dd577e
48. Zhong M, De Angelo P, Osborne L, Paniz-Mondolfi AE, Geller M, Yang Y, Linehan WM, Merino MJ, Cordon-Cardo C, Cai D (2012) Translocation renal cell carcinomas in adults: a single-institution experience. Am J Surg Pathol 36:654–662. doi:10.1097/PAS.0b013e31824f24a6

MORFOLOGICKÁ, IMUNOHISTOCHEMICKÁ A CHROMOZOMÁLNÍ ANALÝZA MULTICYSTICKÉHO CHROMOFOBNÍHO RENÁLNÍHO KARCINOMU, ARCHITEKTONICKY NEOBVYKLÉHO A DIAGNOSTICKY OBTÍŽNÉHO PODTYPU

Chromofobní renální karcinom (CHRK) je uspořádán většinou solidně nebo solidně alveolárně, přičemž se skládá ze směsi větších buněk s listovitým tvarem a světlou cytoplazmou a menších onkocytických buněk. Rozeznávají se dvě základní varianty: klasická a eosinofilní [4]. Morfologické spektrum je však značně širší a již bylo popsáno několik morfologických variant, jmenovitě mikrocystická adenomatoidní pigmentovaná, s neuroendokrinními znaky, s fokální papilární proliferací a varianta napodobující renální onkocytom [12, 14, 33-38].

Tento projekt si klade za cíl rozšířit výše zmíněnou množinu o dalšího člena: multicystickou variantu CHRK. Do studie bylo na základě morfologického obrazu zařazeno 10 případů CHRK s příznačným multicystickým uspořádáním, které byly následně vyšetřeny za pomoci imunohistochemie (IHC) a array komparativní genové hybridizace. Histologicky vykazovaly všechny tumory růstové uspořádání dvojího typu: 1) různě velké cysty budící dojem multilokulární cystické neoplazie nízkého maligního potenciálu a 2) stlačené cysty a tubuly se štěrbinovitými prostory. Ve všech vyšetřených tumorech byla konzistentně přítomna hrozinkovitě tvarovaná jádra patognomická pro CHRK a ve čtyřech případech jsme zastihly depozita lipochromu. IHC vyšetření (pozitivita s EMA, CK7, OSCAR, CD117, parvalbuminem, MIA, PAX8 a negativita s vimentinem, TFE3, CANH9, HMB45, cathepsinem K, AMACR a Ki-67) bylo kompatibilní s diagnózou CHRK, stejně tak jako molekulárně genetická analýza (2/5 analyzovatelných případů vykazovalo mnohočetné choromozomální ztráty a zbývající 3 byly bez numerických aberací).

Dříve popsaná adenomatoidně mikrocystická pigmentovaná varianta CHRK [33, 35, 36], jak už deskriptivní název napovídá, roste adenomatoidně a mikrocysticky a obsahuje hnědý pigment odpovídající lipochromu. Na základě nálezu lipochromu u téměř poloviny případů a architektoniky spadající do „cystického“ spektra (multicystický růst ve formě „opravdových“ či zkolabovaných, stlačených cyst) vnímáme multicystické CHRK jako extrémní formu adenomatoidně mikrocystické pigmentované varianty CHRK. IHC i molekulárně jsou zde popisované tumory kompatibilní s konvenčním CHRK, avšak diferenciálně diagnosticky je třeba zvažovat odlišné jednotky, jmenovitě cystickou/multicystickou variantu renálního onkocytomu, multilokulární cystickou neoplazii nízkého maligního potenciálu, granulární/eosinofilní high grade variantu světlobuněčného renálního karcinomu, tubulocystický renální karcinom nebo smíšený epiteliální a stromální tumor ledviny.

Virchows Arch
DOI 10.1007/s00428-016-2022-x

ORIGINAL ARTICLE

Morphological, immunohistochemical, and chromosomal analysis of multicystic chromophobe renal cell carcinoma, an architecturally unusual challenging variant

Maria Pané Foix[1,2] · Ana Dunatov[3] · Petr Martinek[4] · Enric Condom Mundó[1,2] · Saul Suster[5] · Maris Sperga[6] · Jose I. Lopez[7] · Monika Ulamec[8] · Stela Bulimbasic[9] · Delia Perez Montiel[10] · Reza Alaghehbandan[11] · Kvetoslava Peckova[4] · Krystina Pivovarcikova[4] · Daum Ondrej[4] · Pavla Rotterova[4] · Faruk Skenderi[12] · Kristyna Prochazkova[13] · Martin Dusek[4] · Milan Hora[13] · Michal Michal[4] · Ondrej Hes[4,14]

Received: 26 May 2016 / Revised: 27 July 2016 / Accepted: 5 September 2016

Abstract Chromophobe renal cell carcinoma (ChRCC) is typically composed of large leaf-like cells and smaller eosinophilic cells arranged in a solid-alveolar pattern. Eosinophilic, adenomatoid/pigmented, or neuroendocrine variants have also been described. We collected 10 cases of ChRCC with a distinct multicystic pattern out of 733 ChRCCs from our registry, and subsequently analyzed these by morphology, immunohistochemistry, and array comparative genomic hybridization. Of the 10 patients, 6 were males with an age range of 50–89 years (mean 68, median 69). Tumor size ranged between 1.2 and 20 cm (mean 5.32, median 3). Clinical follow-up was available for seven patients, ranging 1–19 years (mean 7.2, median 2.5). No aggressive behavior was documented. We observed two growth patterns, which were similar in all tumors: (1) variable-sized cysts, resembling multilocular cystic neoplasm of low malignant potential and (2) compressed cystic and tubular pattern with slit-like spaces. Raisinoid nuclei were consistently present while necrosis was absent in all cases. Half of the cases showed eosinophilic/oncocytic cytology, deposits of pigment (lipochrome) and microcalcifications. The other half was composed of pale or mixed cell populations. Immunostains for epithelial membrane antigen (EMA), CK7, OSCAR, CD117, parvalbumin, MIA, and Pax 8 were positive in all tumors while negative for vimentin, TFE3, CANH 9, HMB45, cathepsin K, and AMACR. Ki67 immunostain was positive in up to 1 % of neoplastic cells. Molecular genetic

✉ Ondrej Hes
hes@medima.cz

[1] Department of Pathology, Bellvitge University Hospital, Bellvitge Biomedical Research Institute (IDIBELL), Barcelona, Spain

[2] Department of Pathology and Experimental Therapeutics, School of Medicine, University of Barcelona, Barcelona, Spain

[3] Department of Pathology, University of Split, Split, Croatia

[4] Department of Pathology, , Medical Faculty and Charles University Hospital Plzen, Charles University, Alej Svobody 80, 304 60 Pilsen, Czech Republic

[5] Department of Pathology, Medical College of Wisconsin, Milwaukee, WI, USA

[6] Department of Pathology, East University, Riga, Latvia

[7] Department of Pathology, Cruces University Hospital, Biocruces Research Institute, University of the Basque Country, Barakaldo, Spain

[8] "Ljudevit Jurak" Pathology Department, Clinical Hospital Center "Sestre milosrdnice", Zagreb, Croatia

[9] Department of Pathology, Clinical Hospital Center Zagreb, Zagreb, Croatia

[10] Department of Pathology, Instituto Nacional de Cancerologia, Mexico City, Mexico

[11] Department of Pathology, Faculty of Medicine, Royal Columbian Hospital, University of British Columbia, Vancouver, BC, Canada

[12] Department of Pathology, Clinical Center of the University of Srajevo, Sarajevo, Bosnia and Herzegovina

[13] Department of Urology, Medical Faculty and Charles University Hospital, Charles University, Plzen, Czech Republic

[14] Biomedical Centre, Faculty of Medicine in Lzen, Charles University in Prague, Plzen, Czech Republic

Published online: 15 September 2016

examination revealed multiple chromosomal losses in two fifths analyzable tumors, while three cases showed no chromosomal numerical aberrations. ChRCC are rarely arranged in a prominent multicystic pattern, which is probably an extreme form of the microcystic adenomatoid pigmented variant of ChRCC. The spectrum of tumors entering the differential diagnosis of ChRCC is quite different from that of conventional ChRCC. The immunophenotype of ChRCC is identical with that of conventional ChRCC. Chromosomal numerical aberration pattern was variable; no chromosomal numerical aberrations were found in three cases. All the cases in this series have shown an indolent and non-aggressive behavior.

Keywords Kidney · Chromophobe renal cell carcinoma · Multicystic · Immunohistochemistry · ArrayCGH

Introduction

Chromophobe renal cell carcinoma (ChRCC) is the third most common type of adult renal epithelial tumor, accounting for approximately 5 % of renal carcinomas [1, 2]. ChRCC usually carries a more favorable prognosis than clear cell renal cell carcinoma (CCRCC). However, sarcomatoid differentiation, which is associated with worse prognosis, is found in approximately 8 % of ChRCC [2].

ChRCC usually shows solid or solid-alveolar architectural patterns, composed of a combination of cells with leaf-like morphology and pale cytoplasm, and smaller eosinophilic cells with oncocytic cytoplasm. The two main recognized ChRCC morphologic variants are classic and eosinophilic. However, the morphological spectrum has expanded to pigmented microcystic adenomatoid, oncocytoma-like, ChRCC with neuroendocrine differentiation, and ChRCC with focal papillary proliferations [3–10].

In this study, we describe a subset of ChRCC tumors with a pure multicystic architecture using morphologic, immunohistochemical, and array comparative genomic hybridization (aCGH) features.

Material and methods

From 733 ChRCCs in the Plzen Tumor Registry, 10 cases of ChRCC with a multicystic pattern were selected. The tissues had been fixed in neutral formalin, embedded in paraffin, cut into 4–5-μm-thin sections and stained with hematoxylin and eosin (H&E). One to seven paraffin blocks were available for each case. All tumors were independently reviewed by two pathologists (MPF and OH). Clinicopathologic and follow-up data were collected using medical records available from each participating institution. Selected cases were further analyzed using immunohistochemistry and aCGH.

Immunohistochemistry

The immunohistochemical study was performed using a Ventana Benchmark XT automated immunostainer (Ventana Medical System, Inc., Tucson, AZ, USA) on formalin fixed, paraffin embedded tissue. Primary antibodies against the following antigens were employed: epithelial membrane antigen (EMA) (E29, monoclonal, DakoCytomation, Carpinteria CA, 1:1000); cytokeratin 7 (OV-TL12/30, monoclonal, DakoCytomation, 1:200); OSCAR (OSCAR, 1:500, Covance, Herts, UK, 1:500), racemase/AMACR (P504S, monoclonal, Zeta, Sierra Madre, CA, 1:50); vimentin (D9, monoclonal, NeoMarkers, Westinghouse, CA, 1:1000); parvalbumin (PA-235, monoclonal, Sigma Aldrich, St. Luis, MO, 1:500): antimelanosome (HMB45, monoclonal, DakoCytomation, 1:200); Ki-67 (MIB1, monoclonal, Dako, Glostrup, Denmark, 1:1000); c-kit (CD117, polyclonal, Dako, Glostrup, Denmark, 1:300); carbonic anhydrase IX (rhCA9, monoclonal, RD systems, Abingdon, GB, 1:100); TFE3 (polyclonal, Abcam, Cambridge, UK, 1:100), cathepsin K (3F9, monoclonal, Abcam, 1:100); progesterone receptor (monoclonal, 1E2, Ventana, RTU); estrogen receptor (monoclonal, SP1, Ventana, RTU); antimitochondrial antigen (113-1, monoclonal, Biogenex, Fremont, CA, 1:500); smooth muscle actin (1A4, monoclonal, DakoCytomation, 1:1000); desmin (D33, monoclonal, Dako, 1:100); CD31 (JC70A, monoclonal, DakoCytomation, 1:50); CD34 (QBEnd-10, monoclonal, Dako, 1:100); and PAX-8 (polyclonal, Cell Marque, Rocklin, CA, 1: 25). The primary antibodies were visualized using the supersensitive streptavidin-biotin-peroxidase complex (BioGenex). Appropriate positive controls were employed.

Molecular genetic methods

DNA extraction

DNA was extracted from formalin-fixed paraffin-embedded (FFPE) tumor and non-tumor tissues (when available) of each case using QIAsymphony DNA Mini Kit (QIAGEN, Hilden, Germany) on an automated extraction system (QIAsymphony SP, QIAGEN) according to the manufacturer's supplementary protocol for FFPE samples (purification of genomic DNA from FFPE tissue using the QIAamp DNA FFPE Tissue Kit and Deparaffinization Solution). Concentration and purity of isolated DNA were measured using NanoDrop ND1000 (NanoDrop Technologies Inc., Wilmington, DE, USA). DNA integrity was examined by amplification of control genes in multiplex PCR, producing fragments from 100 to

600 base pairs. Only cases with DNA integrity equal to or higher than 400 bp were used for further analysis by aCGH.

Array comparative genomic hybridization

A CytoChip Focus Constitutional (BlueGnome Ltd., Cambridge, UK) microarray processor was used for analysis. CytoChip Focus Constitutional uses BAC technology and covers 143 regions of known significance with 1-Mb spacing across a genome. Probes were spotted in triplicate. First, 400 ng of gDNA was labeled using the Fluorescent Labeling System (BlueGnome Ltd., Cambridge, UK). The procedure consisted of Cy3 labeling of a test sample and Cy5 labeling of a reference sample. MegaPool Reference DNA of opposite sex was used as a reference sample (Kreatech Diagnostics, Amsterdam, Netherlands). Each labeled pair was mixed, dried, and hybridized overnight at 47 °C using ArrayIt hybridization cassettes (Arrayit Corporation, CA, USA). Posthybridization washing was done using SSC buffers with increasing stringency. Dried microarrays were scanned with InnoScan 900 (Innopsys, France) at a resolution of 5 μm.

Image and data analysis: scanned images were analyzed and quantified using BlueFuse Multi software (BlueGnome Ltd., Cambridge, UK). BlueFuse Multi uses Bayesian algorithms to generate intensity values for each Cy5 and Cy3 labeled spot on the array according to an appropriate .gal file. The reported changes were browsed and interpreted using BlueFuse Multi as well. Cutoff values were set to a log 2 ratio of −0.193 for loss and 0.170 for gain.

Results

The clinicopathological features of the 10 selected cases are summarized in Table 1. Six patients were male with an age range of 50–89 years (mean 68, median 69). Tumor size ranged between 1.2 and 20 cm (mean 5.32, median 3.7). Clinical follow-up was available for seven patients, ranging 1–19 years (mean 7.2, median 2.5). An aggressive clinical course was not observed in any of these patients.

At gross examination, tumors were relatively well-demarcated. No grossly visible angioinvasion or invasion into the renal sinus, pelvicalyceal system, or perirenal fat was encountered. The tumor cut surface was brown in three cases, tan/yellow in three cases, and tan to gray in one case. Gross information on color and consistency of the tumor was not available in three cases.

Morphologic features are presented in Table 2. The majority of the tumors showed predominantly eosinophilic/oncocytic morphology (6/10), a smaller proportion of cases demonstrating a pale and leaf-like neoplastic cell population (3/10) and one case a mixture of both. Raisinoid nuclei with perinuclear halo were present in all cases, with occasional binucleated cells. All cases were low grade according to the Paner grading system (grade 1 or 2). No cases with grade 3 or sarcomatoid differentiation were noted.

By histology, we separated the cases into two groups based on architectural pattern. The first group of seven cases included tumors showing a prominent multicystic pattern (Fig. 1). These were all demarcated, three with a fibrous pseudocapsule. Cysts were irregular in shape and size. Glands appeared cribriform focally in some tumors. Septa of the cysts were thin, mostly lined by a single layer of neoplastic cells. However, larger aggregates of mostly eosinophilic/oncocytic cells were present within the septa. Deposits of dark brown pigment (lipofuscin and hemosiderin) were focally present in four cases. Dystrophic calcification was noted in four cases. Necrosis was not present.

Tumors in the second group (3/10) had a more solid appearance due to arrangement of neoplastic cells in compressed elongated tubules resembling a solid architectural appearance (no true solid areas were seen) (Fig. 2). The whole tumor was

Table 1 Clinicopathologic data

Case	Age (years)	Sex	Size (cm)	Site	color	FU (years)
1	56	F	4.0	L	Brown/yellow	19 AW
2	68	F	3.0	L	Yellow	6 AW
3	70	M	5.0	R	Pink/yellow	4 AW
4	64	F	1.2	R	NA	LFU
5	72	M	2.5	R	Brown	2.5 AW
6	50	M	20.0	NA	NA	LFU
7	74	M	NA	NA	NA	LFU
8	67	M	3.7	R	Dark brown	15 NED, then DOD
9	89	F	7.0	R	Tan	1 AW
10	70	M	1.5	R	Tan/gray	3 AW

M male, *F* female, *L* left, *R* right, *FU* follow-up, *AW* alive and well, *LFU* lost for follow-up, *NED* no evidence of disease, *DOD* death of other disease, *NA* not available

Table 2 Basic morphological features

Case	Architecture	Percentage of cysctic component (%)	Cell type (predominant)	Capsule	Calcifications	Necrosis	Pigment	*P* grade
1	cystic	80	Eosinophil	P	P	A	P	1
2	cystic	100	Pale cells	A	A	A	P	1
3	Cystic/aden	60	Pale cells	A	A	A	P	2
4	Slit-like	100	Eosinophil	A	A	A	A	1
5	Cystic	100	Pale cells	A	P	A	A	2
6	Cystic/aden	80	Eosinophil	P	P	A	A	2
7	Cystic	100	Eosinophil	P	P	A	P	2
8	Slit-like	100	Eosinophil	A	A	A	A	2
9	Cystic/aden	70	Pale/Eosinophil	A	A	A	A	2
10	Slit-like/cyst	100	Eosinophil	A	A	A	P	1

P grade Paner grading, *P* present, *A* absent, *aden* adenomatous, *eosinophil* eosiniphilic cells

exclusively composed of tubules. Lumina of compressed elongated tubules displayed a slit-like pattern. In all three cases, the tumors were well-demarcated and without pseudocapsule. None of the cases showed necrosis or calcification, while focal pigment deposits were present in one case (Fig. 3).

Results of immunohistochemical examinations are summarized in Table 3. All tumors were positive for CK 7, OSCAR, CD117, EMA, parvalbumin, antimitochondrial antigen, and Pax 8. It should be noted that CK 7 positivity was moderate to strong with a rather patchy pattern in seven cases. Immunoreactivity for CD117 was diffuse but varied in intensity, ranging from weak (three cases) to strong (four cases). Proliferative activity as indicated by nuclear Ki67 staining was low (<1 %) in all cases. All tumors were negative for vimentin, AMACR, CANH IX, estrogen and progesterone receptors, TFE3, HMB45, cathepsin K, CD31, and CD34.

Table 4 presents aCGH results of the five cases suitable for aCGH analysis. Multiple losses of chromosomes 1p, 2q, 6, 13, 17, 21, and X were found in two cases. Three cases showed no numerical chromosomal aberrations.

Discussion

Chromophobe renal cell carcinomas represent approximately 5 % of all renal cell carcinomas. They are usually well-demarcated and composed of an admixture of smaller eosinophilic cells and larger clear cells with prominent cell membranes (leaf-like cells) (Fig. 4). The nuclei are usually irregular, with a raisinoid appearance and perinuclear clearing (halo) (Fig. 5). Binucleated cells are not rare. Tumors are typically arranged in a solid sheet-like pattern, separated by incomplete vascular septa [11].

Two main morphological variants are traditionally recognized: the classical variant demonstrating both cell types with

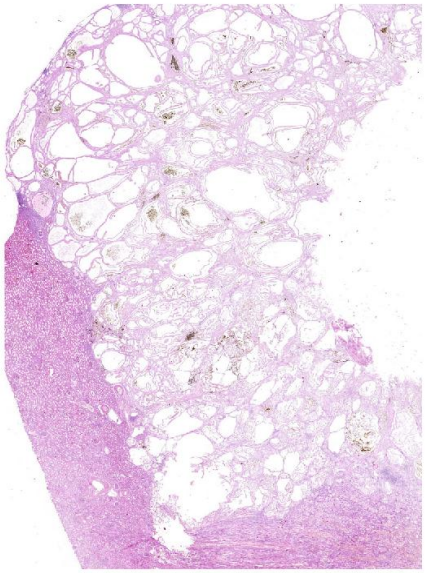

Fig. 1 Histotopogram showing multicystic nature of this rare morphologic variant of chromophobe RCC

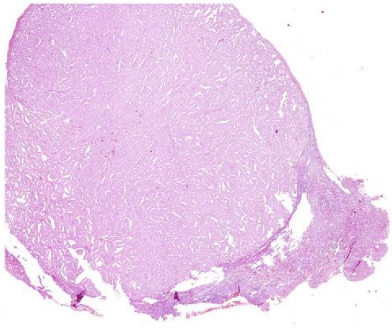

Fig. 2 Three tumors were composed of compressed cystic spaces/large tubules

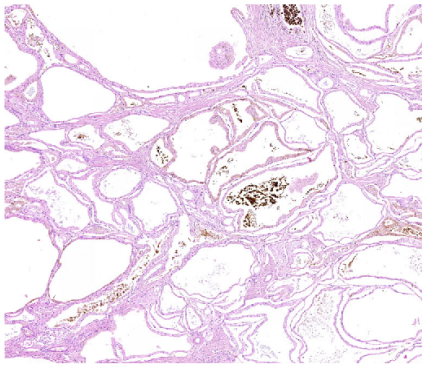

Fig. 3 Deposits of dark brown pigment (lipochrome) were seen in 5/10 tumors

a solid-alveolar growth pattern and the eosinophilic variant composed almost exclusively of smaller eosinophilic cells [2]. Several additional morphological variants have been described. The oncocytic variant is characterized by a solid mass of proliferating cells with typical oncocytic cytoplasm and minimal variation in size. Nuclei are round and centrally located and a perinucelar halo is mostly absent. Nonetheless, the immunohistochemical marker profile and pattern of numerical chromosomal aberrations are characteristic of ChRCC [4].

The adenomatoid microcystic pigmented variant of ChRCC has some features similar to those seen in our cases [3, 5, 6]. The cystic areas contain a mixture of eosinophilic and paler cells, both with the typical raisinoid nuclei and a perinuclear halo. The adenomatous structures in the adenomatoid microcystic pigmented variant are lined by smaller cylindrical cells with basal nuclei. Complex architecture and cribriform formations, similar to those seen in intraductal carcinoma of the breast, can also be observed in the adenomatoid microcystic pigmented variant of ChRCC, as well as areas with prominent fibrous stroma. Raisinoid nuclear shape has also been described in this variant. These cases characteristically contain areas with light to dark brown pigmentation corresponding to lipochrome [5]. Tumors in our series were multicystic even at low magnification. No compact solid areas were noted and lipochrome deposits were seen in four cases. We perceive multicystic ChRCC as the extreme end of the morphologic spectrum of ChRCC with adenomatoid microcystic pattern.

ChRCCs with neuroendocrine differentiation have been recently described [8, 9, 12]. Although many cases of ChRCC may show a neurondocrine-like morphological pattern, few show true neuroendocrine differentiation by immunohistochemical staining for neuroendocrine markers (chromogranin, synaptophysin, CD56 and neuron-specific enolase) or electron microscopy confirming neuroendocrine granules. Cytologic features are not remarkably different from classic ChRCC and from cases examined in this study.

Table 3 Results of immunohistochemical examination

Case	Vim	CK 7	OSC	EMA	CD117	AMACR	CAN	PAX8	Parv	PR/ER	TFE3	HMB	Cath	MIA	SMA	Des	CD31/34	Ki67 (%)
1	–	+++	+++	+++	+	–	–	+	+++	–	–	–	–	+++	Stroma+	–	–	~1
2	–	++	+++	+++	++	–	–	+	+	–	–	–	–	+++	Stroma+++	–	–	~1
3	–	Patchy++	+++	++	++	–	–	+	++	–	–	–	–	+++	–	–	–	~1
4	–	+++	+++	+++	+++	–	–	+	+++	–	–	–	–	+++	–	–	–	~1
5	–	Patchy+++	++	+++	+	–	–	+	+++	–	–	–	–	++	–	–	–	~1
6	–	Patchy+++	++	+++	+++	–	–	+	+++	–	–	–	–	+++	Capsule+	Stroma foc+	–	~1
7	–	Patchy+++	+++	+++	+	–	–	++	+++	–	–	–	–	+++	Stroma++	–	–	~1
8	–	Patchy+++	+++	+++	+++	–	–	++	+++	–	–	–	–	+++	Stroma+	–	–	~1
9	–	Patchy++	++	+++	+++	–	–	++	+++	–	–	–	–	++	Stroma+	–	–	~1
10	–	Patchy++	+++	+++	++	–	–	++	+++	–	–	–	–	+++	–	–	–	~1

VIM vimentin, *OSC* OSCAR, *CAN* carbonic anhydrase 9, *Parv* parvalbumin, *HMB* HMB45, *Cath* cathepsin K, *MIA* antimitochondrial antigen, *SMA* smooth muscle actin, *Des* desmin, – negative, + weak positivity, ++ moderate positivity, +++ strong positivity, *foc* focal

Table 4 Results of arrayCGH

Case	kgd	aCGH
1	300	NP
2	300	NP
3	200	NP
4	400	Normal
5	400	−1p, −2q, −6
6	600	Normal
7	200	NP
8	100	NP
9	600	−1p, −6, −13, −17, −21, −*X*
10	600	Normal

aCGH array comparative genomic hybridisation, *NP* not performed, *Normal* no chromosomal numerical abberations

Chromophobe carcinomas occasionally undergo sarcomatoid differentiation, with high-grade transformation associated with aggressive clinical course and unfavorable prognosis [13]. Histologically, these lesions can differentiate into heterologous elements such as osteosarcoma, rhabdomyosarcoma, chondrosarcoma, or even liposarcoma [14–19]. No sarcomatoid differentiation was identified in our series.

Architecturally, our cases were all multicystic without solid component but two different patterns emerged. A multicystic appearance, with large cystic spaces, slightly irregular in shape and size was found in seven cases while the other three appeared rather compact at low magnification but at higher magnification appeared to be composed of elongated compressed tubules and cysts, resulting in growth pattern with slit-like spaces. Raisinoid shape of nuclei, considered as landmark of all ChRCC, with perinuclear clearing (halo) was a constant finding in all our cases. Hence, cytologic features in were not different between the two patterns (large cysts and slit-like cysts) and similar to those of conventional ChRCC (Fig. 6).

Immunohistochemical stains performed in this series showed a profile similar to that of conventional ChRCC [20–22]. Our cases were positive for PAX 8, parvalbumin, antimitochondrial antigen, and CD117. The latter has been suggested as a useful

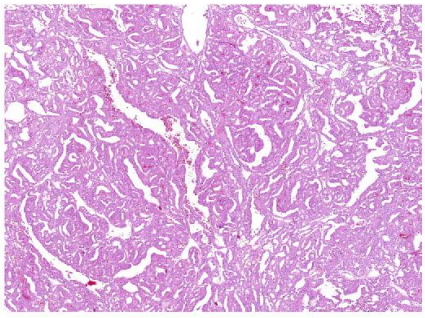

Fig. 4 Tumor composed of predominantly eosinophilic neoplastic cells

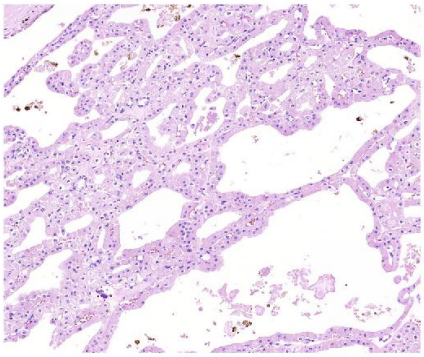

Fig. 5 Tumor composed of large pale cells with perinuclear halo and raisinoid nuclei

stain to differentiate ChRCCs and oncocytomas from other renal neoplasms [23] and was at least weakly positive in all cases. CK 7 staining was patchy in 30 % and diffuse in 70 % but strong in all cases. Of seven multicystic CHRCC with patchy CK 7 staining 2 were weakly but diffusely positive for CD117 while the remaining cases were diffusely and strongly positive (Fig. 7). These results are in concordance with those of previous studies reporting CK 7 staining in approximately 76 % of ChRCC (range 50–100 %). Focal CK 7 staining therefore does not exclude a diagnosis of CHRCC [22, 24–26].

EMA and OSCAR were diffusely positive in all cases. Actin staining was positive in the stroma of six tumors.

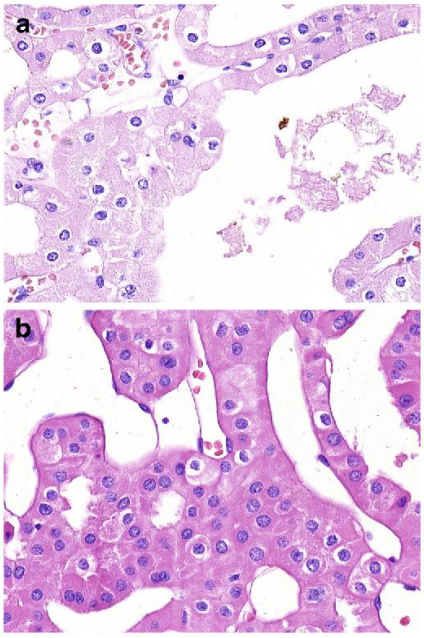

Fig. 6 **a**, **b** Large nuclei with wrinkled edge were constant finding in all 10 cases

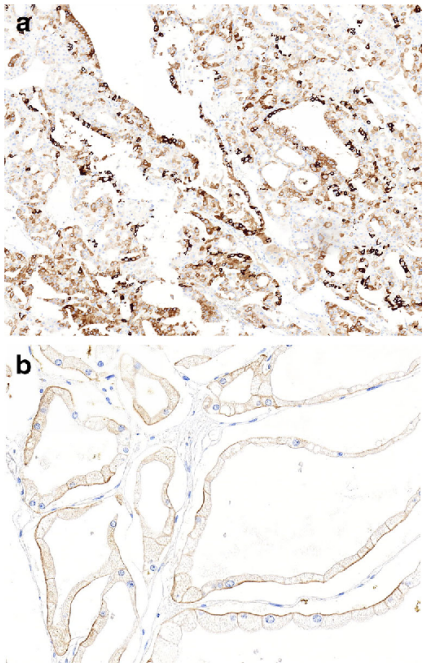

Fig. 7 **a**, **b** All tumors were positive for CK 7, as well as for CD117

Ki67-based proliferation index was low (<1 %) in all cases. Reactivity for other markers including hormone receptors (ER/PR), melanocytic markers, TFE3, cathepsin K, and endothelial markers was not observed in any case.

Previous molecular genetic studies performed on ChRCC revealed some recurrent alterations which are now considered a genetic hallmark for this entity. Multiple losses of chromosomes 1, 2, 6, 10, 13, 17, and 21 are usually detected in both classic and eosinophilic ChRCC [27]. Furthermore, some studies showed gains in chromosomes 4, 7, 15, 19, and 20 [28–31], but the significance of these numerical chromosomal aberrations is not entirely clear. These findings do suggest, however, that the spectrum of chromosomal anomalies of ChRCC may be broader than as yet reported. In two of our five cases suitable for arrayCGH analysis, we found multiple losses of chromosomes 1p, 2q, 6, 13, 17, 21, and X while the remaining three showed no numerical chromosomal aberrations. Absence of chromosomal aberrations has been reported for renal oncocytomas. Our three cases without chromosomal aberrations were predominantly composed of eosinophilic cells but raisinoid nuclei with perinuclear clearing were also present and the immunohistochemical marker pattern these cases was consistent with CHRCC. We emphasize that cases of ChRCC with a normal numerical chromosomal status have been reported previously in the literature [27, 32–36].

In the differential diagnosis of multicystic ChRCC, the following diagnoses should be considered: cystic/multicystic variant of renal oncocytoma, multilocular cystic clear cell carcinoma/neoplasm of low malignant potential (MCCCC), granular/eosinophilic high-grade variant of clear renal cell carcinoma (CCRCC), tubulocystic renal cell carcinoma (TCRCC), and mixed epithelial stromal tumor (MEST)/cystic nephroma (CN).

The cystic/multicystic variant of renal oncocytoma has been reported recently and also is included in the most recent WHO classification [11, 37, 38]. Although such cases occasionally show prominent cystic areas, foci of solid tumor with the typical islets of oncocytic cells in a background of fibrotic stroma can be easily identified, if sampling is adequate. Furthermore, cytomorphologic features, notably raisinoid nuclei, perinuclear clearing, and at least focal presence of a dual cell population strongly point towards the diagnosis of ChRCC.

Multilocular cystic clear cell carcinoma/neoplasm of low malignant potential (MCCCC) typically presents as a multicystic lesion without conspicuous solid areas [11, 39]. The cysts are lined by low-grade clear cells (maximum grade 2 according to the ISUP grading system) with a variable amount of usually pale cytoplasm or atrophic flattened epithelium. Architecture of multilocular cystic clear cell carcinoma/neoplasm is very similar to that of our tumors and yet, cytologically, our cases differ significantly from MCCCC. Pale, leaf-like cells as well as smaller oncocytic cells are completely different from clear cell elements characteristic of MCCCC. Further, raisinoid nuclei, which we easily encountered in our cases, have never been described in MCCCC. In addition, MCCCC expresses vimentin and CANH 9 but, as a rule, not CK 7, parvalbumin, antimitochondrial antigen, or CD117 [11].

The granular/eosinophilic high grade variant of clear renal cell carcinoma (CCRCC) are occasionally, at least focally, arranged in a multicystic pattern. High-grade CCRCCs usually have architectural and cytological features different from multicystic ChRCC. They mostly show alveolar or acinar growth patterns with delicate thin-walled blood vessels and abundant cytoplasmic lipid vacuoles and glycogen deposits [2, 40]. On the other hand, the typical ChRCC morphology (i.e., raisinoid nuclei with perinuclear clearing) is usually not observed in typical CCRCC. Marker profiles are also different, CCRCC expressing CANH 9, CD10, and vimentin, while CD117 and CK 7 are usually negative, although CK7 can be focally positive in up to 15 % of CCRCC.

Tubulocystic renal cell carcinoma (TCRCC) presents grossly as a solid or spongy mass. On microscopic examination, the lesion shows multiple cystic spaces lined by a single layer of flat, cuboidal, or low columnar cells. These cells have a moderate amount of eosinophilic cytoplasm and can show a hobnail appearance [41–43]. In contrast, the cystic areas in cystic ChRCC are lined by larger cells with wide, usually eosinophilic cytoplasm and typical irregular nuclei. The neoplastic cells in TCRCC are usually monotonous while tumor cells in ChRCC can show some degree of polymorphism, with

presence of both eosinophilic and leaf-like cells. TCRCC is usually positive for CK 18, CK 19, EMA, CD10, high molecular weight cytokeratin 34betaE12, and vimentin, while negative for CK7 [44]. Genome abnormalities of both entities are also different, TCRCC displaying mainly gains of chromosomes 7 and 17 [11, 45] although TCRCC with normal numerical chromosomal status have been reported recently [46].

Another renal tumor presenting with predominantly cystic morphology is mixed epithelial stromal tumor (MEST)/cystic nephroma (CN) [47, 48]. The currently accepted concept is that CN of adult onset and MEST are the same tumor at the two ends of the morphological spectrum of a single entity. This concept is supported not only by clinical data but also by morphology and molecular genetic analyses [11]. These tumors mostly occur in perimenopausal women. Histologically, MEST is defined as a dimorphic tumor with an epithelial component lining cystic structures embedded in a spindle cell Mullerian type of stroma [49]. The stromal component is usually of ovarian type and typically expresses estrogen and progesterone receptors, as well as desmin, smooth muscle actin, and vimentin. Of note, pediatric CN is a completely different tumor, unrelated to MEST. Of our 10 patients, 4 were female and none of the tumors showed morphologic features resembling Mullerian differentiation. In addition, the cytological features of cystic ChRCC in our series were different from the cell populations described in MEST. Immunoreactivity for estrogen or progesterone receptors was not noted.

We conclude that in rare cases, ChRCC displays a prominent multicystic pattern which we perceive as an extreme form of the microcystic adenomatoid pigmented variant of ChRCC. The immunophenotype of multicystic ChRCC is identical to that of conventional ChRCC but its differential diagnosis is quite different from that of conventional ChRCC. Its pattern of numerical chromosomal aberrations is variable and in three cases, none were found. All our cases have shown an indolent, non-aggressive behavior.

Compliance with ethical standards Study design has been approved by local ethical committee (Charles University, Medical School Plzen) LEK FN Plzeň.

Funding The study was supported by the Charles University Research Fund (project number P36), by the project FN 00669806, and by SVV 260283.

Conflict of interest All authors declare no conflict of interest

References

1. Amin MB, Amin MB, Tamboli P, Javidan J, Stricker H, de-Peralta Venturina M, Deshpande A, Menon M (2002) Prognostic impact of histologic subtyping of adult renal epithelial neoplasms: an experience of 405 cases. Am J Surg Pathol 26(3):281–291
2. Amin MB, Paner GP, Alvarado-Cabrero I, Young AN, Stricker HJ, Lyles RH, Moch H (2008) Chromophobe renal cell carcinoma: histomorphologic characteristics and evaluation of conventional pathologic prognostic parameters in 145 cases. Am J Surg Pathol 32(12):1822–1834. doi:10.1097/PAS.0b013e3181831e68
3. Michal M, Hes O, Svec A, Ludvikova M (1998) Pigmented microcystic chromophobe cell carcinoma: a unique variant of renal cell carcinoma. Ann Diagn Pathol 2(3):149–153
4. Kuroda N, Tanaka A, Yamaguchi T, Kasahara K, Naruse K, Yamada Y, Hatanaka K, Shinohara N, Nagashima Y, Mikami S, Oya M, Hamashima T, Michal M, Hes O (2013) Chromophobe renal cell carcinoma, oncocytic variant: a proposal of a new variant giving a critical diagnostic pitfall in diagnosing renal oncocytic tumors. Medical molecular morphology 46(1):49–55. doi:10.1007/s00795-012-0007-7
5. Hes O, Vanecek T, Perez-Montiel DM, Alvarado Cabrero I, Hora M, Suster S, Lamovec J, Curik R, Mandys V, Michal M (2005) Chromophobe renal cell carcinoma with microcystic and adenomatous arrangement and pigmentation—a diagnostic pitfall. Morphological, immunohistochemical, ultrastructural and molecular genetic report of 20 cases. Virchows Archiv: an international journal of pathology 446(4):383–393. doi:10.1007/s00428-004-1187-x
6. Dundr P, Pesl M, Povysil C, Tvrdik D, Pavlik I, Soukup V, Dvoracek J (2007) Pigmented microcystic chromophobe renal cell carcinoma. Pathol Res Pract 203(8):593–597. doi:10.1016/j.prp.2007.05.005
7. Kuroda N, Iiyama T, Moriki T, Shuin T, Enzan H (2005) Chromophobe renal cell carcinoma with focal papillary configuration, nuclear basaloid arrangement and stromal osseous metaplasia containing fatty bone marrow element. Histopathology 46(6):712–713. doi:10.1111/j.1365-2559.2005.02032.x
8. Parada DD, Pena KB (2008) Chromophobe renal cell carcinoma with neuroendocrine differentiation. APMIS 116(9):859–865
9. Kuroda N, Tamura M, Hes O, Michal M, Gatalica Z (2011) Chromophobe renal cell carcinoma with neuroendocrine differentiation and sarcomatoid change. Pathol Int 61(9):552–554. doi:10.1111/j.1440-1827.2011.02689.x
10. Thoenes W, Storkel S, Rumpelt HJ, Moll R, Baum HP, Werner S (1988) Chromophobe cell renal carcinoma and its variants—a report on 32 cases. J Pathol 155(4):277–287. doi:10.1002/path.1711550402
11. Moch H, Humphrey PA, Ulbright TM, Reuter VE (2016) WHO classification of tumours of the urinary system and male genital organs (World Health Organization classification of tumours). IARC Press, Lyon, 356 pp
12. Peckova K, Martinek P, Ohe C, Kuroda N, Bulimbasic S, Condom Mundo E, Perez Montiel D, Lopez JI, Daum O, Rotterova P, Kokoskova B, Dubova M, Pivovarcikova K, Bauleth K, Grossmann P, Hora M, Kalusova K, Davidson W, Slouka D, Miroslav S, Buzrla P, Hynek M, Michal M, Hes O (2015) Chromophobe renal cell carcinoma with neuroendocrine and neuroendocrine-like features. Morphologic, immunohistochemical, ultrastructural, and array comparative genomic hybridization analysis of 18 cases and review of the literature. Ann Diagn Pathol 19(4):261–268. doi:10.1016/j.anndiagpath.2015.05.001
13. Akhtar M, Tulbah A, Kardar AH, Ali MA (1997) Sarcomatoid renal cell carcinoma: the chromophobe connection. Am J Surg Pathol 21(10):1188–1195
14. Itoh T, Chikai K, Ota S, Nakagawa T, Takiyama A, Mouri G, Shinohara N, Yamashita T, Suzuki S, Koyanagi T, Nagashima K (2002) Chromophobe renal cell carcinoma with osteosarcoma-like differentiation. Am J Surg Pathol 26(10):1358–1362
15. Magro G, Lopes M, Amico P, Puzzo L (2005) Chromophobe renal cell carcinoma with extensive rhabdomyosarcomatous component.

Virchows Archiv: an international journal of pathology 447(5): 894–896. doi:10.1007/s00428-005-0026-z

16. Quiroga-Garza G, Khurana H, Shen S, Ayala AG, Ro JY (2009) Sarcomatoid chromophobe renal cell carcinoma with heterologous sarcomatoid elements. A case report and review of the literature. Archives of pathology & laboratory medicine 133(11):1857–1860. doi:10.1043/1543-2165-133.11.1857
17. Anila KR, Mathew AP, Somanathan T, Mathews A, Jayasree K (2012) Chromophobe renal cell carcinoma with heterologous (liposarcomatous) differentiation: a case report. Int J Surg Pathol 20(4):416–419. doi:10.1177/1066896911429298
18. Petersson F, Michal M, Franco M, Hes O (2010) Chromophobe renal cell carcinoma with liposarcomatous dedifferentiation—report of a unique case. International journal of clinical and experimental pathology 3(5):534–540
19. Husain A, Eigl BJ, Trpkov K (2014) Composite chromophobe renal cell carcinoma with sarcomatoid differentiation containing osteosarcoma, chondrosarcoma, squamous metaplasia and associated collecting duct carcinoma: a case report. Analytical and quantitative cytopathology and histopathology 36(4):235–240
20. Cochand-Priollet B, Molinie V, Bougaran J, Bouvier R, Dauge-Geffroy MC, Deslignieres S, Fournet JC, Gros P, Lesourd A, Saint-Andre JP, Toublanc M, Vieillefond A, Wassef M, Fontaine A, Groleau L (1997) Renal chromophobe cell carcinoma and oncocytoma. A comparative morphologic, histochemical, and immunohistochemical study of 124 cases. Archives of pathology & laboratory medicine 121(10):1081–1086
21. DeLong W, Sakr W (1996) Chromophobe renal cell carcinoma: a comparative histochemical and immunohistochemical study. J Urol Pathol 4:1–8
22. Taki A, Nakatani Y, Misugi K, Yao M, Nagashima Y (1999) Chromophobe renal cell carcinoma: an immunohistochemical study of 21 Japanese cases. Modern pathology: an official journal of the United States and Canadian Academy of Pathology, Inc 12(3):310–317
23. Petit A, Castillo M, Santos M, Mellado B, Alcover JB, Mallofre C (2004) KIT expression in chromophobe renal cell carcinoma: comparative immunohistochemical analysis of KIT expression in different renal cell neoplasms. Am J Surg Pathol 28(5):676–678
24. Wu SL, Kothari P, Wheeler TM, Reese T, Connelly JH (2002) Cytokeratins 7 and 20 Immunoreactivity in chromophobe renal cell carcinomas and renal oncocytomas. Modern pathology: an official journal of the United States and Canadian Academy of Pathology, Inc 15(7):712–717
25. Mathers ME, Pollock AM, Marsh C, O'Donnell M (2002) Cytokeratin 7: a useful adjunct in the diagnosis of chromophobe renal cell carcinoma. Histopathology 40(6):563–567. doi:10.1046/j.1365-2559.2002.01397.x
26. Liu L, Qian J, Singh H, Meiers I, Zhou X, Bostwick DG (2007) Immunohistochemical analysis of chromophobe renal cell carcinoma, renal oncocytoma, and clear cell carcinoma: an optimal and practical panel for differential diagnosis. Archives of pathology & laboratory medicine 131(8):1290–1297. doi:10.1043/1543-2165(2007)131[1290:IAOCRC]2.0.CO;2
27. Brunelli M, Eble JN, Zhang S, Martignoni G, Delahunt B, Cheng L (2005) Eosinophilic and classic chromophobe renal cell carcinomas have similar frequent losses of multiple chromosomes from among chromosomes 1, 2, 6, 10, and 17, and this pattern of genetic abnormality is not present in renal oncocytoma. Modern pathology: an official journal of the United States and Canadian Academy of Pathology, Inc 18(2):161–169. doi:10.1038/modpathol.3800286
28. Gunawan B, Bergmann F, Braun S, Hemmerlein B, Ringert RH, Jakse G, Fuzesi L (1999) Polyploidization and losses of chromosomes 1, 2, 6, 10, 13, and 17 in three cases of chromophobe renal cell carcinomas. Cancer Genet Cytogenet 110(1):57–61
29. Brunelli M, Gobbo S, Cossu-Rocca P, Cheng L, Hes O, Delahunt B, Pea M, Bonetti F, Mina MM, Ficarra V, Chilosi M, Eble JN, Menestrina F, Martignoni G (2007) Chromosomal gains in the sarcomatoid transformation of chromophobe renal cell carcinoma. Modern pathology: an official journal of the United States and Canadian Academy of Pathology, Inc 20(3):303–309. doi:10.1038/modpathol.3800739
30. Tan MH, Wong CF, Tan HL, Yang XJ, Ditlev J, Matsuda D, Khoo SK, Sugimura J, Fujioka T, Furge KA, Kort E, Giraud S, Ferlicot S, Vielh P, Amsellem-Ouazana D, Debre B, Flam T, Thiounn N, Zerbib M, Benoit G, Droupy S, Molinie V, Vieillefond A, Tan PH, Richard S, Teh BT (2010) Genomic expression and single-nucleotide polymorphism profiling discriminates chromophobe renal cell carcinoma and oncocytoma. BMC Cancer 10:196. doi:10.1186/1471-2407-10-196
31. Vieira J, Henrique R, Ribeiro FR, Barros-Silva JD, Peixoto A, Santos C, Pinheiro M, Costa VL, Soares MJ, Oliveira J, Jeronimo C, Teixeira MR (2010) Feasibility of differential diagnosis of kidney tumors by comparative genomic hybridization of fine needle aspiration biopsies. Genes, chromosomes & cancer 49(10):935–947. doi:10.1002/gcc.20805
32. Speicher MR, Schoell B, du Manoir S, Schrock E, Ried T, Cremer T, Storkel S, Kovacs A, Kovacs G (1994) Specific loss of chromosomes 1, 2, 6, 10, 13, 17, and 21 in chromophobe renal cell carcinomas revealed by comparative genomic hybridization. Am J Pathol 145(2):356–364
33. Verdorfer I, Hobisch A, Hittmair A, Duba HC, Bartsch G, Utermann G, Erdel M (1999) Cytogenetic characterization of 22 human renal cell tumors in relation to a histopathological classification. Cancer Genet Cytogenet 111:61–70
34. Bugert P, Gaul C, Weber K, Herbers J, Akhtar M, Ljungberg B, Kovacs G (1997) Specific genetic changes of diagnostic importance in chromophobe renal cell carcinomas. Laboratory investigation; a journal of technical methods and pathology 76(2):203–208
35. Iqbal MA, Akhtar M, Ali MA (1996) Cytogenetic findings in renal cell carcinoma. Hum Pathol 27(9):949–954
36. Sperga M, Martinek P, Vanecek T, Grossmann P, Bauleth K, Perez-Montiel D, Alvarado-Cabrero I, Nevidovska K, Lietuvietis V, Hora M, Michal M, Petersson F, Kuroda N, Suster S, Branzovsky J, Hes O (2013) Chromophobe renal cell carcinoma—chromosomal aberration variability and its relation to Paner grading system: an array CGH and FISH analysis of 37 cases. Virchows Archiv: an international journal of pathology 463(4):563–573. doi:10.1007/s00428-013-1457-6
37. Zhang Q, Ma J, Wu CY, Zhang DH, Zhao M (2015) Tubulocystic oncocytoma of the kidney: a case study and review of literature with focus on implications for differential diagnosis. International journal of clinical and experimental pathology 8(11):14786–14792
38. Skenderi F, Ulamec M, Vranic S, Bilalovic N, Peckova K, Rotterova P, Kokoskova B, Trpkov K, Vesela P, Hora M, Kalusova K, Sperga M, Perez Montiel D, Alvarado Cabrero I, Bulimbasic S, Branzovsky J, Michal M, Hes O (2016) Cystic renal oncocytoma and tubulocystic renal cell carcinoma: morphologic and immunohistochemical comparative study. Applied immunohistochemistry & molecular morphology: AIMM / official publication of the Society for Applied Immunohistochemistry 24(2):112–119. doi:10.1097/pai.0000000000000156
39. Eble JN, Bonsib SM (1998) Extensively cystic renal neoplasms: cystic nephroma, cystic partially differentiated nephroblastoma, multilocular cystic renal cell carcinoma, and cystic hamartoma of renal pelvis. Semin Diagn Pathol 15(1):2–20
40. Tickoo SK, Lee MW, Eble JN, Amin M, Christopherson T, Zarbo RJ, Amin MB (2000) Ultrastructural observations on mitochondria and microvesicles in renal oncocytoma, chromophobe renal cell carcinoma, and eosinophilic variant of conventional (clear cell) renal cell carcinoma. Am J Surg Pathol 24(9):1247–1256

41. MacLennan GT, Farrow GM, Bostwick DG (1997) Low-grade collecting duct carcinoma of the kidney: report of 13 cases of low-grade mucinous tubulocystic renal carcinoma of possible collecting duct origin. Urology 50(5):679–684. doi:10.1016/s0090-4295(97)00335-x
42. MacLennan GT, Bostwick DG (2005) Tubulocystic carcinoma, mucinous tubular and spindle cell carcinoma, and other recently described rare renal tumors. Clin Lab Med 25(2):393–416. doi:10.1016/j.cll.2005.01.005
43. Hora M, Urge T, Eret V, Stransky P, Klecka J, Kreuzberg B, Ferda J, Hyrsl L, Breza J, Holeckova P, Mego M, Michal M, Petersson F, Hes O (2011) Tubulocystic renal carcinoma: a clinical perspective. World J Urol 29(3):349–354. doi:10.1007/s00345-010-0614-7
44. Khalaf I, El-Badawy N, Shawarby MA (2013) Tubulocystic renal cell carcinoma, a rare tumor entity: review of literature and report of a case. Afr J Urol 19(1):1–6. doi:10.1016/j.afju.2012.12.001
45. Tran T, Jones CL, Williamson SR, Eble JN, Grignon DJ, Zhang S, Wang M, Baldridge LA, Wang L, Montironi R, Scarpelli M, Tan PH, Simper NB, Comperat E, Cheng L (2015) Tubulocystic renal cell carcinoma is an entity that is immunohistochemically and genetically distinct from papillary renal cell carcinoma. Histopathology. doi:10.1111/his.12840
46. Michal M, Syrucek M (1998) Benign mixed epithelial and stromal tumor of the kidney. Pathol Res Pract 194(6):445–448. doi:10.1016/s0344-0338(98)80038-1
47. Adsay NV, Eble JN, Srigley JR, Jones EC, Grignon DJ (2000) Mixed epithelial and stromal tumor of the kidney. Am J Surg Pathol 24(7):958–970
48. Kum JB, Grignon DJ, Wang M, Zhou M, Montironi R, Shen SS, Zhang S, Lopez-Beltran A, Eble JN, Cheng L (2011) Mixed epithelial and stromal tumors of the kidney: evidence for a single cell of origin with capacity for epithelial and stromal differentiation. Am J Surg Pathol 35(8):1114–1122. doi:10.1097/PAS.0b013e3182233fb6
49. Zhou M, Yang XJ, Lopez JI, Shah RB, Hes O, Shen SS, Li R, Yang Y, Lin F, Elson P, Sercia L, Magi-Galluzzi C, Tubbs R (2009) Renal tubulocystic carcinoma is closely related to papillary renal cell carcinoma: implications for pathologic classification. Am J Surg Pathol 33(12):1840–1849. doi:10.1097/PAS.0b013e3181be22d1

KOMPARATIVNÍ STUDIE MUTAČNÍ ANALÝZY GENU *TERT* MEZI VZORKY MOČI ZPRACOVANÝMI METODOU LIQUID BASED CYTOLOGIE A VZORKY TUMORŮ MOČOVÉHO MĚCHÝŘE ZPRACOVANÝMI STANDARDNÍ PARAFINOVOU TECHNIKOU

Karcinom močového měchýře je známý svoji tendencí k recidivám. Standardní follow-up metodu představuje cytologie, ultrasonografie a cystoskopie. Detekce mutace genu *TERT* v relativně vysokém počtu uroteliálních karcinomů různého typu zpracovaných parafinovou technikou nahrává myšlence, že by tyto mutace mohly být rozpoznány i v neoplastických buňkách zachycených v moči odebrané na cytologické vyšetření, tedy pro pacienta méně zatěžující neinvazivní procedury.

Účelem našeho výzkumu bylo porovnat záchyt mutace genu *TERT* ve vzorcích moči zpracovaných metodou liquid based cytologie (LBC) s následně odebranými vzorky tumoru močového měchýře zpracovanými parafinovou technikou. Do studie bylo zařazeno 29 pacientů, od kterých jsme měli k dispozici LBC moči a parafinové bloky neoplastické tkáně močového měchýře získané transuretrální resekcí. Mutace genu *TERT* byla v obou typech vzorků vyšetřena za použití Sanger sekvenovaní a next generation sequencing (NGS; sekvenování nové generace).

Výsledkem naší studie byla 100% shoda mezi LBC odběrem a parafinovým vzorkem u high grade uroteliálních karcinomů, avšak u low grade lézí byla komparativní analýza nespolehlivá. Naše výsledky nasvědčují tomu, že analýza mutace genu *TERT* (z LBC) může být spíše prospěšná pro screening pacientů s již diagnostikovaným *TERT* pozitivním (detekce z histologického vzorku) uroteliálním karcinomem, než jako spolehlivá metoda pro prvozáchyt uroteliální malignity. Zároveň je třeba zdůraznit, že nikoliv u všech uroteliálních karcinomů byla prokázána mutace genu *TERT* (pouze u 72% uroteliálních karcinomů zařazených do této studie bylo *TERT* mutovaných) a negativní výsledek mutační analýzy *TERT* tak nevylučuje přítomnost uroteliální neoplastické léze.

Annals of Diagnostic Pathology 24 (2016) 7–10

Contents lists available at ScienceDirect

Annals of Diagnostic Pathology

Comparative study of *TERT* gene mutation analysis on voided liquid-based urine cytology and paraffin-embedded tumorous tissue☆,☆☆

Kristyna Pivovarcikova, MD [a], Tomas Pitra, MD [b], Tomas Vanecek, PhD [a], Reza Alaghehbandan, MD [c], Barbora Gomolcakova, MSc [a], Ondrej Ondic, MD [a], Kvetoslava Peckova, MD [a], Pavla Rotterova, MD, PhD [a], Milan Hora, MD, PhD [b], Martin Dusek, MD [a], Michal Michal, MD [a], Ondrej Hes, MD, PhD [a,d,*]

[a] Department of Pathology, Charles University, Medical Faculty and Charles University Hospital Plzen, Pilsen, Czech Republic
[b] Department of Urology, Charles University, Medical Faculty and Charles University Hospital Plzen, Pilsen, Czech Republic
[c] Department of Pathology, Faculty of Medicine, University of British Columbia, Royal Columbia Hospital, Vancouver, BC, Canada
[d] Biomedical Centre, Charles University, Medical Faculty and Charles University Hospital Plzen, Pilsen, Czech Republic

ARTICLE INFO

Keywords:
Voided urine cytology
liquid-based cytology
Histology
Urothelial carcinoma
TERT gene mutation analysis

ABSTRACT

Noninvasive reliable urine-based screening method for detection of urothelial carcinoma (UC) is still highly elusive. Recently, studies have shown the presence of telomerase reverse transcriptase (*TERT*) gene mutation in a high number of UCs. This finding can be used as a marker in screening voided urine samples. The aim of this study was to assess sensitivity of *TERT* mutation in detecting UC between liquid-based cytology (LBC) voided urine and formalin-fixed, paraffin-embedded neoplastic tissue (FFPE). Voided urine of 29 patients was collected before surgery via LBC. Subsequently, neoplastic tissue from transurethrally resected tumors of the same patients was analyzed. Both LBC and paraffin-embedded tissues were analyzed independently for the *TERT* gene mutation using Sanger sequencing and next-generation sequencing. Using Sanger sequencing, *TERT* mutation was detected in 17 of 29 samples of voided urine, whereas 4 cases showed weak positivity. Of 17 patients with *TERT* mutation, 6 had mutation in C250T and 11 in C228T. Using next-generation sequencing, 19 of 28 LBC (1 case was not suitable for analysis) were positive for *TERT* mutation, of which 5 contained C250T mutation and 14 had C228T mutation. Sanger sequencing was performed in all 29 resected UC cases. *TERT* gene mutation was found in 21 cases in FFPE, for which 6 tumors had mutation in C250T, and C228T mutation was found in the remaining 15 tumors. *TERT* promoter mutation is not positive in all UCs, and that negative result in LBC samples does not exclude the possibility of UC. It is evident from our results that there is 100% agreement of results between the material from FFPE and the corresponding LBC material in cases of high-grade UC. In contrary, the agreement rate between results of FFPE and LBC material (analyzed by Sanger sequencing or next-generation sequencing) varied in low-grade lesions. The use of such a test is more clinically relevant for detecting recurrence in the surveillance setting such as known UC patients with associated *TERT* promoter mutation (from routine-processed histologic samples).

1. Introduction

Voided urine cytology is used for screening patients with hematuria, follow-up in patients with known urothelial carcinoma (UC), and detection of "flat" lesions (ie, UC in situ). Two types of cytologic techniques used for voided urine screening include conventional cytology (CC) and the relatively new technique liquid-based cytology (LBC). The main difference between the 2 methods is in processing of the material. Both methods serve, among others, to detect neoplastic cells in urine, but their predictive value is very limited, especially for detecting low-grade UC. Therefore, cystoscopy still remains the standard method for the detection of early low-grade bladder neoplasms.

Great efforts have been expended on exploring urine-based tests/biomarkers for the noninvasive detection of UC, with particular success being achieved measuring tumor-specific nucleic acid variants. Two of the most frequently mutated genes in bladder cancer with point mutation hotspots are *FGFR3* and *TERT*, which have been assessed as biomarkers for detecting UC in urinary DNA in different studies [1]. The *TERT* promoter is mutated in approximately 65% of bladder tumors regardless of stage and grade and represents the best single biomarker for UC for detecting primary bladder tumors [1].

☆ The study was supported by the Charles University Research Fund (project number P36) and by Institutional Research Fund FN 00669806.
☆☆ Disclosure of conflict of interest: All authors declare no conflict of interest.
* Corresponding author at: Department of Pathology, Charles University, Medical Faculty and Charles University Hospital Plzen, Alej Svobody 80, 304 60, Pilsen, Czech Republic.
E-mail address: hes@medima.cz (O. Hes).

http://dx.doi.org/10.1016/j.anndiagpath.2016.06.002
1092-9134/

We designed a comparative study to assess sensitivity of *TERT* mutation in detecting UC between LBC voided urine and formalin-fixed, paraffin-embedded (FFPE) neoplastic tissue.

2. Materials and methods

Twenty-nine patients who suspected to have either primary or recurrence UC were prospectively enrolled in the study. These patients had abnormal finding during dispensary cystoscopy (patients with recurrent UC) and/or had positive findings on ultrasonography or computed tomographic scan with initial presentation of macroscopic hematuria.

Voided urine was collected before surgery and fixed using LBC technique. Subsequently, transurethral resection of neoplastic tissue was performed and was fixed in 4% formaldehyde and embedded in paraffin using routine procedures. Two-micrometer-thin sections were cut and stained with hematoxylin and eosin. Grading system according to the 1973 World Health Organization (WHO) as well as the most recent 2016 WHO classification was used in all cases [2,3].

Both samples from LBC and FFPE tissues were analyzed independently for the *TERT* gene mutation using Sanger sequencing (SS) and next generation sequencing (NGS).

2.1. DNA extraction and quality control

DNA from FFPE tissue was extracted using a QIAsymphony DNA Mini Kit (Qiagen, Hilden, Germany) on the automated extraction system (QIAsymphony SP; Qiagen) according to the manufacturer's supplementary protocol for FFPE samples (purification of genomic DNA from FFPE tissue using the QIAamp DNA FFPE Tissue Kit and Deparaffinization Solution). The content of each LBC vial was centrifuged at 600*g* for 10 minutes, the pellet was resuspended in 600 μL of phosphate-buffered saline, and DNA was isolated using the QIAsymphony DNA DSP mini kit. Concentration and purity of isolated DNA were measured using NanoDrop ND-1000 (NanoDrop Technologies Inc, Wilmington, Delaware). DNA integrity was examined by amplification of control genes in a multiplex polymerase chain reaction (PCR) [4].

2.2. Mutation analysis by SS

Mutation analysis of part of *TERT* promoter was performed using PCR and direct sequencing. Polymerase chain reaction was carried out using primers shown in Table 1. The reaction conditions were as follows: 12.5 μL of HotStar Taq PCR Master Mix (Qiagen), 10 pmol of each primer (Table 1), 10 ng of template DNA, and distilled water up to 25 μL. The amplification program consisted of denaturation at 95°C for 15 minutes and then 40 cycles of denaturation at 95°C for 1 minute, annealing at 65°C for 1 minute, and extension at 72°C for 1 minute. The program was finished with 72°C incubation for 7 minutes. The PCR products were checked on 2% agarose gel electrophoresis. Successfully amplified PCR products were purified with magnetic particules Agencourt AMPure (Agencourt Bioscience Corporation, A Beckman Coulter Company, Beverly, Massachusetts). Products were then bidirectionally sequenced using Big Dye Terminator Sequencing kit (Life Technologies, Foster City, California), purified with magnetic particules Agencourt CleanSEQ (Agencourt Bioscience Corporation), all according to the manufacturer's protocol, and run on an automated sequencer ABI Prism 3130xl (Life Technologies) at a constant voltage of 13.2 kV for 11 minutes.

Table 1
Primers used for amplification of hotspot *TERT* mutation [23]

Name	Primer sequence 5′-3′
TERT-F2	CACCCGTCCTGCCCCTTCACCTT
TERT-R2	GGCTTCCCACGTGCGCAGCAGGA

2.3. Mutation analysis by NGS

Targeted sequencing of LBC urine samples was performed on the Ion Torrent PGM platform (Life Technologies) with Hi-Q Sequencing Kit (Life Technologies). Sequencing library was prepared by ligation of adapters to the same PCR products that were used for SS using Ion Plus Fragment Library Kit (Life Technologies).

Sequencing data were processed by the Torrent Suite Software V5.0.2 and analyzed via the Integrative Genomics Viewer. The minimum coverage depth for each sample was set to 500× with the cutoff value for positive samples set to 2.5% [1].

3. Results

Table 2 presents clinicopathologic data on 29 patients enrolled in this study. Thirteen patients had recurrent UC, whereas 16 were newly diagnosed UC cases. Patients' age ranged from 35.2 to 87.4 (median, 69 years; mean, 68.6 years), with 26 being male and 3 female.

Urothelial carcinoma was confirmed histologically in all 29 cases. Pathologic staging included pTa in 19 cases, pT1 in 9 cases, and pT2a in 1 case. Grade 1 (WHO 1973) or low-grade (WHO 2016) was found in 14 cases, grade 2 (WHO 1973) or low-grade (WHO 2016) in 5 cases, and grade 3 (WHO 1973) or high-grade (WHO 2016) in 10 cases [2,3].

Results of molecular genetic analyses are summarized in Table 3. Detection of *TERT* mutation in LBC was performed in all 29 cases—using both SS and NGS methods. Sanger sequencing detected *TERT* mutation in 17 of 29 cases (4 case with weak positivity). Six of 17 mutation C250T, and 11 of 17 had mutation C228T. Analysis with NGS methods was performed in 28 LBC (1 case was not suitable for analysis), which demonstrated positivity in 19 cases. Five of 19 LBC contained C250T mutation and 14 of 19 had C228T mutation. Sanger sequencing of FFPE was performed in all 29 cases and showed *TERT* gene mutation in 21 cases. Six of 21 tumors had mutation in C250T, and C228T mutation was found in 15 of 21 tumors.

Among the low-grade UC cases, *TERT* mutation was detected in 13 of 19 FFPE specimens, with concurrently positive cases in 9 of 19 LBC samples (using SS), and 11/18 LBC specimens (using NGS). Among the high-grade UC patients, positive *TERT* mutation was found in 8 of 10 cases, with similar findings for corresponding LBC materials.

Among the newly diagnosed low-grade UC cases, *TERT* mutation was found in 7 of 12 cases using FFPE tissue. Concurrent positive with *TERT* mutation were identified in 6 of 12 LBC samples using SS and 6 of 11 LBC materials using NGS. For low-grade recurrent UC cases, 6 of 7 patients were found to have *TERT* mutation using FFPE tissue. This corresponds to 3 of 7 LBC materials using SS and 5 of 7 LBC samples using NGS, concurrently. Furthermore, *TERT* mutation was found in 3 of 4 newly detected high-grade UC and in 5 of 6 cases of recurrent high-grade UC via FFPE tissue as well as corresponding LBC materials.

4. Discussion

Urothelial carcinoma is the seventh most common neoplasm worldwide, with an estimated global incidence of 330 380 new cases in 2012. Mortality rate differs by sex, with 2 to 10 deaths per 100 000 males per year and 0.5 to 4 deaths per 100 000 females per year [3]. The high recurrence rate of UC presents constant challenge for urologists and stress for the patients. Standard follow-up procedure comprises voided urine cytology, ultrasonography, and cystoscopy. However, less invasive procedures are highly in demand for years. Conventional cytology provides relatively good results in the diagnosis of high-grade tumors, with a sensitivity of 79% and a much higher specificity up to 100%. Conventional cytology in cases of low-grade UC has a sensitivity of 25% to 45% and a specificity of 98% [5-7]. Despite this, more sensitive and reliable methods, which would be comparable to cystoscopic findings, are desirable.

In recent years, attention has been directed toward *TERT* gene mutation. The mutations of *TERT* gene have been detected in several human

Table 2
Clinicopathologic information of patients with UC

Case	Sex	Age (y)	Newly detected UC/recurrence of UC	Clinical presentation	WHO 1973/WHO 2016: grade	TNM 09: stage
1	M	69	Newly detected UC	MAH	2/LG	pT1
2	M	69	Newly detected UC	MAH, CSK	3/HG	pTa
3	M	35	Newly detected UC	USG	1/LG	pTa
4	M	76	Recurrence	MAH, USG	3/HG	pT1
5	M	67	Recurrence	USG, CSK	3/HG	pT1
6	M	62	Newly detected UC	MAH, USG	1/LG	pTa
7	M	84	Recurrence	CSK	3/HG	pT1
8	M	87	Recurrence	CSK	3/HG	pT2a
9	M	75	Recurrence	Miction impairment, USG	3/HG	pT1
10	M	72	Newly detected UC	MAH, CSK	1/LG	pTa
11	M	66	Newly detected UC	MAH, MRI with tumorous mass	2/LG	pTa
12	M	64	Recurrence	MAH, USG	1/LG	pTa
13	M	77	Recurrence	MAH, CSK	1/LG	pT1
14	F	62	Newly detected UC	MAH, USG	3/HG	pT1
15	M	75	Recurrence	AC	1/LG	pTa
16	M	63	Recurrence	MAH, USG	1/LG	pTa
17	F	58	Newly detected UC	MAH, USG	2/LG	pTa
18	M	69	Recurrence	MAH, CSK	2/LG	pT1
19	M	65	Newly detected UC	MAH, USG, CSK	1/LG	pTa
20	M	74	Recurrence	MAH, CSK	1/LG	pTa
21	M	72	Newly detected UC	Dysuria, MAH, CT	3/HG	pT1
22	M	74	Newly detected UC	MAH, CSK	1/LG	pTa
23	M	58	Newly detected UC	CSK	3/HG	pTa
24	M	69	Recurrence	MAH, USG	1/LG	pTa
25	F	62	Newly detected UC	MAH, USG, CSK	1/LG	pTa
26	M	86	Newly detected UC	USG	2/LG	pTa
27	M	84	Recurrence	MAH	3/HG	pTa
28	M	62	Newly detected UC	USG	1/LG	pTa
29	M	54	Newly detected UC	USG, CSK	1/LG	pTa

Abbreviations: AC, abnormal cytologic finding; CSK, abnormal cystoscopy findings; CT, computed tomography; F, female; HG, high grade; LG, low grade; M, male; MAH, macroscopic hematuria; MRI, magnetic resonance imaging; USG, suspect ultrasonography finding.

neoplasms including sporadic and familial melanoma, gliomas, thyroid, and bladder cancer [8]. Telomerase is an RNA-dependent DNA polymerase that synthesizes telomeric DNA [9]. The main function of telomeres is to preserve chromosome integrity and genome stability by preventing the chromosome end from degradation. Telomerase activity is reactivated in up to 90% of human cancers, and it allows proliferating cancer cells to maintain telomere length [10]. TERT is catalytic subunit of telomerase complex, and the TERT protein is limiting for activity of telomerase [8,9,11,12]. The *TERT* gene consists of 16 exons spanning 35 kb [9], located on chromosome 5 [8].

Table 3
Results of molecular genetic analyses of FFPE and LBC samples

Case	SS of FFPE	SS of LBC material	NGS of LBC material
1	+C250T	+C250T	+C250T (18%)
2	+C250T	+C250T	+C250T (58%)
3	−	−	−
4	+C250T	+C250T	+C250T (66%)
5	+C228T	+C228T[a]	+C228T (15%)
6	+C228T	+ C228T[a]	+C228T (14%)
7	+C228T	+C228T	+C228T (63%)
8	+C228T	+ C228T[a]	+C228T (13%)
9	+C228T	+C228T	+C228T (57%)
10	−	−	−
11	+C228T	+C228T	+C228T (42%)
12	+C228T	+C228T	+C228T (41%)
13	+C228T	+C228T	+C228T (66%)
14	−	−	−
15	−	−	−
16	+C228T	−	+C228T (4%)
17	+C228T	+C228T[a]	+C228T (12%)
18	+C228T	+C228T	+C228T (45%)
19	+C250T	+C250T	+C250T (25%)
20	+C228T	−	+C228T (4%)
21	+C228T	+C228T	+C228T (63%)
22	+C228T	−	+C228T (7%)
23	+C250T	+C250T	+C250T (80%)
24	+C228T	−	−
25	−	−	−
26	−	−	−
27	−	−	−
28	−	−	−
29	+C250T	+C250T	NP

Abbreviation: NP, not performed.
[a] Weak positivity, − negative, + positive.

The *TERT* gene mutations seem to be the most frequent somatic mutations in tumors of the urinary bladder. The mutations occur with similar frequency, regardless of stage or grade, and are not associated with prognosis [8,13,14]. The presence of the *TERT* promoter mutations was shown in different subtypes of UC such as small cell carcinoma of the bladder [15], the nested variant of UC [16], UC with glandular differentiation [17], and squamous carcinoma of the urinary bladder [18]. A recent study also described the presence of *TERT* promoter mutation in a small percentage (15%) of inverted papillomas [19]. On the other hand, the *TERT* promoter mutation was not found in other benign lesions of the urinary bladder [16,17]. Similarly, the *TERT* promoter mutation was not identified in primary bladder adenocarcinoma [17].

Disclosure of *TERT* gene mutation in a relatively high number of UCs and their different subtypes raised the possibility of detecting the *TERT* gene mutation in neoplastic cells present in voided urine in patients with bladder cancer.

Conventional cytology is widely used as a noninvasive diagnostic/screening test. It is used for long-term observation of patients after transurethral resection of bladder tumor or as a screening test for patients presenting with microscopic/macroscopic hematuria. This test has high specificity, but its sensitivity is limited [20,21]. The sensitivity and even specificity of CC are very high in high-grade urothelial lesions; however, it poorly performs in identifying low-grade urothelial neoplasms. There are studies that investigated the detection of *TERT* mutation in voided urine processed via conventional cytologic techniques. Allory et al [9] showed that urine can be used for the detection of *TERT* mutation, with a sensitivity of 62% at initial diagnosis and 42% at

recurrence. This high frequency of hotspot mutations renders *TERT* a very attractive target for diagnosis of bladder tumors, using voided urine [1,13].

Liquid-based cytology is a more efficient alternative cytologic method to CC. The second most commonly used platforms for urine LBC are ThinPrep and MonoPrep2. The LBC urine sample is processed differently from voided urine by preparing a uniform thin cellular monolayer with no cellular overlap. This method also provides a relatively clean background without obscuring elements and enhanced cellular preservation [21]. Because the urine sample is placed directly in cytofixative, it provides better preservation of the cellular material which can be further used for immunohistochemical and/or molecular genetic testing [22].

Laucirica et al [22] reported statistically higher detection rate of UC using ThinPrep cytology compared with conventional preparation.

We used ThinPrep LBC urine samples to detect *TERT* promoter mutation and subsequently compared it with *TERT* promoter mutation in FFPE neoplastic tissues. Sanger sequencing on FFPE and LBC samples demonstrated *TERT* gene mutation in 21 (72.4%) of 29 FFPE samples and 17 (58.6%) of 29 LBC materials, respectively. The NGS method showed positive *TERT* mutation in 19 (67.8%) of 28 LBC samples. We compared the results of SS on FFPE with that of NGS on LBC materials (which is of course more sensitive than SS of LBC), demonstrating an agreement of 95% between these 2 different types of materials. This led us to conclude that in tumors with previously demonstrated *TERT* mutation, NSG of LBC material can be used as a noninvasive method for dispensary of patients with recurrent UC.

In our study, we detected *TERT* mutation in 13 of 19 cases in FFPE tissue, 9 of 19 of LBC specimens using SS, and 11 of 18 LBC specimens using NGS in patients with low-grade lesions. Positivity of *TERT* mutation was confirmed in 8 of 10 cases of high-grade UC (in FFPE tissue and LBC material). Two of 10 cases of high-grade UC were negative for *TERT* mutation.

This study faced a number of limitations. We examined a relatively small number of patients with narrow spectrum of examined types of the lesions. We did not use series of samples from healthy patients as negative control, considering that the aim of the study was to compare sensitivity of examining LBC vs FFPE material in detecting UC. Nevertheless, our findings clearly showed that not only there are differences between LBC and FFPE materials, but also the quality of test results is influenced by method of sequencing (SS vs NGS).

In conclusion, it is very crucial to note that not all UCs are positive for *TERT* promoter mutation (in our study, 72% of UC had the mutation) and that a negative finding does not exclude the possibility of UC.

It is evident from our results that there is 100% agreement of results between the material from FFPE and the corresponding LBC material in cases of high-grade UC. In contrary, the agreement rate between results of FFPE and LBC material (analyzed by SS or NGS) varied in low-grade lesions.

Furthermore, our findings suggest that *TERT* promoter mutation can be helpful in screening known UC patients with associated *TERT* promoter mutation from a routine-processed histologic sample. In other words, the use of such a test is more clinically relevant for detecting recurrence in the surveillance setting.

References

[1] Ward DG, Baxter L, Gordon NS, Ott S, Savage RS, Beggs AD, et al. Multiplex PCR and Next Generation Sequencing for the Non-Invasive Detection of Bladder Cancer. PLoS One 2016;11:e0149756.

[2] Mostofi FK, Sobin LH, Torloni H. International histological classification of tumors. Geneva: World Health Organization; 1973.

[3] Moch H, Humphrey PA, Ulbright TM, Reuter VE. WHO classification of tumours of the urinary system and male genital organs. Lyon: IARC; 2016.

[4] van Dongen JJ, Langerak AW, Brüggemann M, Evans PA, Hummel M, Lavender FL, et al. Design and standardization of PCR primers and protocols for detection of clonal immunoglobulin and T-cell receptor gene recombinations in suspect lymphoproliferations: report of the BIOMED-2 Concerted Action BMH4-CT98-3936. Leukemia 2003;17:2257–317.

[5] Bastacky S, Ibrahim S, Wilczynski SP, Murphy WM. The accuracy of urinary cytology in daily practice. Cancer 1999;87:118–28.

[6] Koss LG, Deitch D, Ramanathan R, Sherman AB. Diagnostic value of cytology of voided urine. Acta Cytol 1985;29:810–6.

[7] Raab SS, Lenel JC, Cohen MB. Low grade transitional cell carcinoma of the bladder. Cytologic diagnosis by key features as identified by logistic regression analysis. Cancer 1994;74:1621–6.

[8] Vinagre J, Pinto V, Celestino R, Reis M, Pópulo H, Boaventura P, et al. Telomerase promoter mutations in cancer: an emerging molecular biomarker? Virchows Arch 2014;465:119–33.

[9] Cong YS, Wen J, Bacchetti S. The human telomerase catalytic subunit hTERT: organization of the gene and characterization of the promoter. Hum Mol Genet 1999;8:137–42.

[10] Kyo S, Takakura M, Fujiwara T, Inoue M. Understanding and exploiting hTERT promoter regulation for diagnosis and treatment of human cancers. Cancer Sci 2008;99:1528–38.

[11] Nandakumar J, Cech TR. Finding the end: recruitment of telomerase to telomeres. Nat Rev Mol Cell Biol 2013;14:69–82.

[12] Cifuentes-Rojas C, Shippen DE. Telomerase regulation. Mutat Res 2012;730:20–7.

[13] Allory Y, Beukers W, Sagrera A, Flández M, Marqués M, Márquez M, et al. Telomerase reverse transcriptase promoter mutations in bladder cancer: high frequency across stages, detection in urine, and lack of association with outcome. Eur Urol 2014;65:360–6.

[14] Hurst CD, Platt FM, Knowles MA. Comprehensive mutation analysis of the TERT promoter in bladder cancer and detection of mutations in voided urine. Eur Urol 2014;65:367–9.

[15] Zheng X, Zhuge J, Bezerra SM, Faraj SF, Munari E, Fallon III JT, et al. High frequency of TERT promoter mutation in small cell carcinoma of bladder, but not in small cell carcinoma of other origins. J Hematol Oncol 2014;7:47.

[16] Zhong M, Tian W, Zhuge J, et al. Distinguishing nested variants of urothelial carcinoma from benign mimickers by TERT promoter mutation. Am J Surg Pathol 2015;39:127–31.

[17] Vail E, Zheng X, Zhou M, et al. Telomerase reverse transcriptase promoter mutations in glandular lesions of the urinary bladder. Ann Diagn Pathol 2015;19:301–5.

[18] Cowan M, Springer S, Nguyen D, et al. High prevalence of TERT promoter mutations in primary squamous cell carcinoma of the urinary bladder. Mod Pathol 2016;29:511–5.

[19] Cheng L, Davidson DD, Wang M, et al. Telomerase reverse transcriptase (TERT) promoter mutation analysis of benign, malignant and reactive urothelial lesions reveals a subpopulation of inverted papilloma with immortalizing genetic change. Histopathology 2015.

[20] Lotan Y, Roehrborn CG. Sensitivity and specificity of commonly available bladder tumor markers versus cytology: results of a comprehensive literature review and meta-analyses. Urology 2003;61:109–18 [discussion 118].

[21] Hwang EC, Park SH, Jung SI, Kwon DD, Park K, Ryu SB, et al. Usefulness of liquid-based preparation in urine cytology. Int J Urol 2007;14:626–9.

[22] Laucirica R, Bentz JS, Souers RJ, Wasserman PG, Crothers BA, Clayton AC, et al. Do liquid-based preparations of urinary cytology perform differently than classically prepared cases? Observations from the College of American Pathologists Interlaboratory Comparison Program in Nongynecologic Cytology. Arch Pathol Lab Med 2010;134:19–22.

[23] Wang K, Liu T, Ge N, Liu L, Yuan X, Liu J, et al. TERT promoter mutations are associated with distant metastases in upper tract urothelial carcinomas and serve as urinary biomarkers detected by a sensitive cast PCR. Oncotarget 2014;5:12428–39.

PŘÍTOMNOST PĚNITÝCH BUNĚK (NAPODOBUJÍCÍCH HIBERNOM) JE VZÁCNÝM RYSEM RENÁLNÍCH KARCINOMŮ

Pěnité buňky nebo mikrovakuolizace cytoplazmy prototypické pro hibernom se mohou vyskytnout v širokém okruhu různých neoplazií, nejčastěji v prostatickém adenokarcinomu, sebaceózních a adrenokortikálních tumorech, pleomorfním xantoastrocytomu, vzácně i v mnoha dalších tumorech.

V naší studii přinášíme popis devíti hibernomu podobných renálních karcinomů (RK) se signifikantní komponentou neoplastických epitelových buněk s nápadnou mikrovakuolizovanou cytoplazmou. Sedm tumorů bylo klasifikováno jako papilární RK, NOS, zbývající 2 byly zařazeny jako neklasifikované RK. Všechny tumory byly vyšetřeny elektronovou mikroskopií, imunohistochemicky (např. adipophilin, MIA, CD68, CK7, AMACR, CANH, CD10, HMB45) a molekulárně geneticky (analýza *SDHB* genové mutace pomocí PCR a následného přímého sekvenování). Ultrasktukturálně jsme v cytoplazmě hibernoma-like buněk mohli pozorovat mitochondrie a mikrovezikly. Všechny případy vykazovaly signifikantní IHC pozitivitu s adipophilinem a antimitochondriální protilátkou (MIA), zároveň bylo potvrzeno, že hibernoma-like buňky jsou epitelie a nikoliv makrofágy (pozitivní, resp. negativní reakce s cytokeratiny a CD68). Jelikož 2/9 tumorů, diagnostikované jako neklasifikované RK, vykazovaly solidně alveolární a nikoliv papilární architektoniku, společně s přítomností bublinovité cytoplazmy se nabízela možnost, že by se mohlo jednat SDHB deficientní RK. Avšak IHC ani molekulární analýza tuto domněnku nepotvrdily.

Na základě našich výsledků se domníváme, že mikrocystický, hibernoma-like vzhled popisovaných RK je dán abnormálním intracelulárním zpracováním lipidů. IHC byly všechny tumory kompatibilní s renální neoplazií a jednalo se o malé tumory (průměrná velikost 4,2 cm) omezené na ledvinu, což vylučuje, že by zde prezentované případy mohly být zaměněny za sekundární infiltraci parenchymu ledviny primárním retroperitoneálním dobře diferencovaným liposarkomem či adrenálním kortikálním karcinomem.

Virchows Arch (2014) 465:215–224
DOI 10.1007/s00428-014-1600-z

ORIGINAL ARTICLE

Foamy cell (hibernoma-like) change is a rare histopathological feature in renal cell carcinoma

Fredrik Petersson · Maris Sperga · Stela Bulimbasic · Petr Martinek · Marian Svajdler · Naoto Kuroda · Milan Hora · Roderick Simpson · Tomáš Tichy · Kvetoslava Peckova · Jindrich Branzovsky · Kristyna Pivovarcikova · Pavla Rotterova · Bohuslava Kokoskova · Kevin Bauleth · Dusan Martincok · Vincent Nagy · Michal Michal · Ondrej Hes

Received: 11 January 2014 / Revised: 28 February 2014 / Accepted: 22 May 2014 / Published online: 6 June 2014

Abstract We report nine patients (seven males and two females, median age 64 years (range 51–79 years)) with a renal cell carcinoma, each of which contained a significant component of neoplastic epithelial cells with a striking microvacuolated (hibernoma-like) cytoplasmic appearance. Tumor sizes ranged from 1.5 to 8.0 cm (mean 4.2 cm, median 4.3 cm). The basic architecture of the tumors was solid-alveolar in two cases (classified as renal cell carcinoma-not otherwise specified (NOS)) and papillary in seven cases (classified as papillary renal cell carcinoma NOS). The nuclear grade according to the Fuhrman grading system was three in all cases. By immunohistochemistry, the cells with microvacuolated cytopasm and significantly expressed adipophilin and anti-mitochondrial antigen in a similar cytoplasmic pattern. On ultrastructural examination, the cytoplasm of the neoplastic epithelial cells was packed with distended mitochondria, most of which displayed lamellated cristae. Numerous microvesicles were dispersed between the mitochondria. No mutations in the *succinate dehydrogenase B* gene were identified. Based on our findings, we propose that the mechanism behind this phenomenon is an abnormal intracellular processing of lipids. No aggressive behavior was observed in six out of nine patients with available follow-up information.

F. Petersson
Department of Pathology, National University Health System, Singapore, Singapore

F. Petersson · P. Martinek · M. Svajdler · K. Peckova · J. Branzovsky · K. Pivovarcikova · P. Rotterova · B. Kokoskova · K. Bauleth · M. Michal · O. Hes (✉)
Department of Pathology, Faculty of Medicine, University Hospital in Plzen, Charles University in Prague, Alej Svobody 80, 304 60 Pilsen, Czech Republic
e-mail: hes@medima.cz

M. Sperga
Department of Pathology, East University, Riga, Latvia

S. Bulimbasic
Department of Pathology, University Hospital Dubrava, Zagreb, Croatia

M. Svajdler
Department of Pathology, Louis Pasteur University Hospital, Kosice, Slovakia

N. Kuroda
Department of Pathology, Red Cross Hospital Kochi, Kochi, Japan

M. Hora
Department of Urology, Faculty of Medicine, University Hospital in Plzen, Charles University in Prague, Prague, Czech Republic

R. Simpson
Department of Anatomical Pathology, University of Calgary, Calgary, Alberta, Canada

T. Tichy
Department of Pathology, Palacky's University Hospital Olomouc, Olomouc, Czech Republic

D. Martincok
Department of Urology, Louis Pasteur University Hospital, Kosice, Slovakia

V. Nagy
Clinic of Urology, Faculty of Medicine, PJ Safarik University in Kosice and Louis Pasteur University Hospital, Kosice, Slovakia

O. Hes
Biomedical Centre, Faculty of Medicine in Plzen, Charles University in Prague, Plzen, Czech Republic

Keywords Kidney · Renal cell carcinoma · Hibernoma-like · Lipoma-like · Papillary renal cell carcinoma · Clear cell renal cell carcinoma · Unclassified renal cell carcinoma

Introduction

Foamy or microvacuolated cytoplasmic features have been described in a wide range of different neoplasms. Most commonly, this is present in some prostatic adenocarcinomas, hibernoma, sebaceous and adrenocortical tumors, pleomorphic xanthoastrocytoma, and Erdheim-Chester disease. On rare occasions, it can also be seen in ductal adenocarcinoma and endocrine neoplasms of the pancreas [3, 4], pancreatic intraepithelial neoplasia [2], neuroendocrine tumors of the appendix [5], cutaneous angiosarcoma [18], hepatocellular carcinoma [13], acquired cystic disease-associated (ACDA) renal cell carcinoma (RCC) [1], and sclerosing polycystic adenosis of salivary glands [15]. We report nine cases of non-ACDA-RCC which displayed a significant component of neoplastic epithelial cells with a striking microvacuolated (hibernoma-like) cytoplasmic appearance. Such structures are highly unusual for renal cell carcinomas. The cytoplasm of all nine cases contained a similar type of microvacuoles, which have been studied in detail by electron microscopy. Results were further validated using immunohistochemical examination (antibodies against mitochondrial antigen (MIA) and adipophilin among others). Adipophilin has been used as a marker for lipid droplet accumulation. MIA (113–1) recognizes a 60-kD antigen of human mitochondria and has been useful in identification of mitochondria.

Material and methods

Out of 17,000 renal tumors and tumor-like lesions in the institutional and consultation files of Sikl's Department of Pathology, Charles' University, Plzen, Czech Republic, nine cases of RCC displayed a significant component of neoplastic cells with a distinct foamy, microvacuolated character of the cytoplasm. Of these nine cases, seven cases had been diagnosed as papillary renal cell carcinoma NOS (PRCC) and two cases as unclassified RCC. The tissue had been fixed in neutral formalin and embedded in paraffin; 4- to 5-μm thick sections were cut and stained with hematoxylin and eosin (H&E).

Immunohistochemistry

The following primary antibodies were employed: cytokeratins (CAM 5,2, monoclonal, Becton-Dickinson, San Jose, CA, USA, 1:200; AE1–AE3, monoclonal, Biogenex, San Ramon, CA, USA, 1:1,000; cytokeratin 7 OV-TL12/30, monoclonal, DakoCytomation, 1:200; OSCAR, monoclonal, Covance, Herts, UK, 1:500), CD10 (56C6, Novocastra, Burlingame, CA, USA, 1:20), racemase/AMACR (P504S, monoclonal, Zeta, Sierra Madre, CA, USA, 1:50), vimentin (D9, monoclonal, Neomarkers, Westinghouse, CA, USA, 1:1,000), anti-mitochondrial antigen (113–1, monoclonal, Biogenex, 1:800), Ki-67 (MIB1, monoclonal, Dako, Glostrup, Denmark, 1:1,000), carbonic anhydrase IX (rhCA9, monoclonal, RD systems, Abingdon, GB, UK 1:100), anti-melanosome (HMB45, monoclonal, DakoCytomation, 1:200), TFE3 (polyclonal, Abcam, 1:100), cathepsin K (3F9, monoclonal, Abcam, 1:100), S100 (polyclonal, DakoCytomation, 1:400), PAX 2 (polyclonal, Invitrogen, Camarillo, CA, USA 1:100), adipophilin (ADFP 5–27, monoclonal, ACRIS, Herford, Germany, 1:20), and CD68 (KP1, monoclonal, NeoMarkers, 1:200).

Binding of primary antibodies was visualized using the supersensitive streptavidin-biotin-peroxidase complex (Biogenex). Appropriate positive controls were employed.

Ultrastructural study

Neoplastic, paraffin embedded tissue from six cases was deparaffinized and was further routinely processed for electron microscopy.

Molecular genetic analysis of SDHB

DNA extraction

DNA from formalin-fixed paraffin-embedded (FFPE) tumor tissue was extracted using QIAsymphony DNA Mini Kit (Qiagen, Hilden, Germany) on an automated extraction system (QIAsymphony SP, Qiagen) according to the manufacturer's supplementary protocol for FFPE samples (Purification of genomic DNA from FFPE tissue using the QIAamp DNA FFPE Tissue Kit and Deparaffinization Solution). Concentration and purity of isolated DNA was measured using NanoDrop ND-1000 (NanoDrop Technologies Inc., Wilmington, DE, USA). DNA integrity was examined by amplification of control genes in a multiplex PCR [19].

Analysis of *SDHB* gene mutation

Mutational analysis of complete CDS and exon-intron junctions of the *succinate dehydrogenase B* (*SDHB*) gene was performed using PCR and direct sequencing. Briefly, a 100-ng DNA was added to a reaction mixture consisting of 12.5 μl of FastStart PCR Master (*Roche* Diagnostic, Mannheim, Germany), 10 pmol of forward and reverse primers (Table 1), and distilled water up to 25 μl. The amplification program comprised denaturation at 95 °C for 9 min, 35 cycles of denaturation at 95 °C for 1 min, annealing 62 °C for 1 min, and extension at 72 °C for 1 min. The program was terminated by

Table 1 Basic clinicopathological data

Cases	Sex	Age	Site	Size (cm)	Color	Follow-up (years)	Diagnosis
1	M[a]	64	Left	Diameter 1.5	Yellow/tan	AW (2.5)	Unclass RCC
2	M	74	NA	Diameter 4.5	NA	LE	PRCC NOS
3	M	52	Right	8×7.5×4	Yellowish	AW (11)	PRCC NOS
4	F	79	NA	5×5×4.5	Gray to brown	LE	Unclass RCC
5	M	66	Right	4.3×4×3.5	Yellowish	AW (1), then LE	PRCC NOS
6	M	70	Right	3.5	Yellowish	LE	PRCC NOS
7	M[b]	58	Left	3.1×2.2×2	Gray	AW (8)	PRCC NOS
8	F[c]	51	Right	4.5×3.5×2	Yellow	AW (11)	PRCC NOS
9	M	58	NA	3	NA	AW (10)	PRCC NOS

PRCC NOS papillary renal cell carcinoma-not otherwise specified, *Unclass RCC* unclassified renal cell carcinoma, *AW* alive and well, *LE* loss of evidence, *NA* not available

[a] History of radical prostatectomy

[b] Bilateral tumors, contralateral kidney-clear cell renal cell carcinoma, pT1a

[c] History of idiopathic thrombocytopenic purpura

incubation at 72 °C for 7 min. The PCR products were separated by electrophoresis through a 2 % agarose gel.

Successfully amplified PCR products selected for sequencing analysis were purified with magnetic particles Agencourt® AMPure® (Agencourt Bioscience Corporation, A Beckman Coulter Company, Beverly, MA, USA), both sides sequenced using Big Dye Terminator Sequencing kit (Applied Biosystems) and purified with magnetic particles Agencourt® CleanSEQ® (AgencourtBioscience Corporation, A Beckman Coulter Company), all according to the manufacturer's protocol. Samples were then run on an automated sequencer ABI Prism 3130xl (Applied Biosystems) at a constant voltage of 13.2 kV for 20 min.

Results

The clinicopathological features are summarized in Table 1. Briefly, there were seven males and two females. The median age was 64 years (range 51–79 years). Follow-up was available for five out of nine patients. The follow-up period ranged from 1 to 11 years (mean 7.25 years, median 11 years). The tumor size ranged from 1.5 to 8.0 cm (mean 4.2 cm, median 4.3 cm). The cut surface was yellowish to tan in five cases, and in two cases, the color was grayish (Fig. 1). Information about the color and consistency was not available in the other two cases. No aggressive behavior was observed in six out of nine patients with available follow-up information.

Histology

All cases displayed a significant component of neoplastic epithelial cells with a striking microvacuolated appearance of the cytoplasm, reminiscent of the neoplastic cells in hibernomas (Fig. 2a, b).

The basic architecture of the tumors was solid-alveolated in two cases and papillary in seven cases. The nuclear grading according to the Fuhrman nucleolar grading system was 3 in all cases. The seven cases with papillary architecture (cases 2, 3, 5–9) (Fig. 3) were composed of epithelial cells with microvacuoles (Fig. 4) as described above, and they also contained non-epithelial, macrophage-type foam cells (confirmed immunohistochemically; cytokeratin-negative, CD68-positive) within the fibrovascular stalks; these tumors were classified as PRCCs. However, the architecture resembled type 2 PRCC; cells were mostly different with eosinophilic to clear cell appearance. A majority of the cells displayed the above-mentioned microvacuolated pattern. We classified these tumors as papillary renal cell

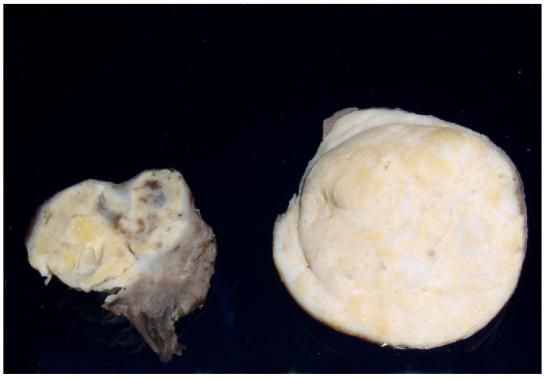

Fig. 1 The cut surface was yellowish in five cases (case 7)

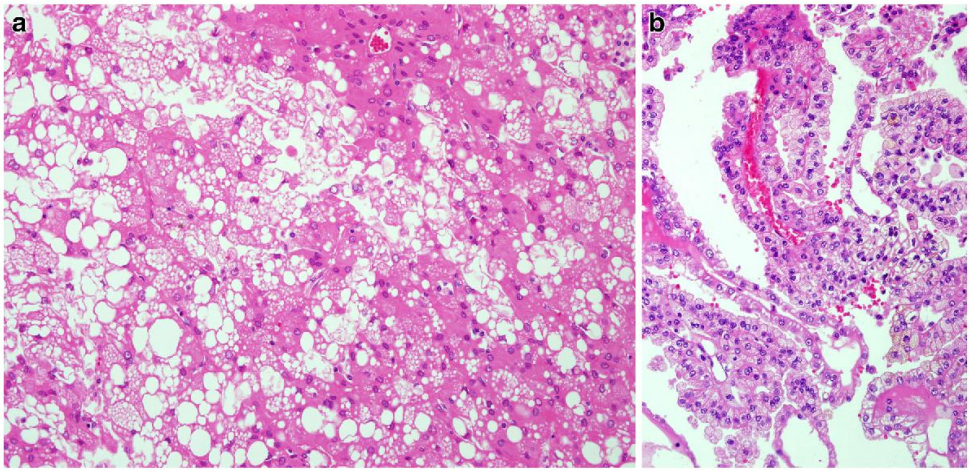

Fig. 2 Neoplastic epithelial cells with a striking microvacuolated appearance of the cytoplasm, reminiscent of the neoplastic cells in hibernomas, **a** case 1 and **b** case 2

carcinoma NOS. The other two tumors (cases 1 and 4) displayed a solid-alveolar architecture (Fig. 5). Small tubules were focally present within some of these tumors which were composed of slightly eosinophilic cells with microvacuolated/bubbly cytoplasm (Fig. 6a, b). Occasional tumor cells formed larger cytoplasmic vacuoles. The nuclear grading according to the Fuhrman nucleolar grading system was 3 in both cases. Based on the histological features, immunohistochemical, and molecular genetic findings (vide infra), these tumors were labeled as unclassified renal cell carcinomas.

Immunohistochemistry

The findings of the immunohistochemical study are summarized in Table 2. Briefly, all tumors exhibited significant expression of adipophilin located to the cells with microvacuolated cytoplasm. The expression of anti-mitochondrial antigen (Fig. 7a) showed a similar pattern as that of adipophilin (Fig. 7b). Interestingly, the neoplastic epithelial cells with foam cell morphology exhibited weak cytoplasmic expression of CD68. In contrast, the non-neoplastic macrophage-type foam cells were strongly positive

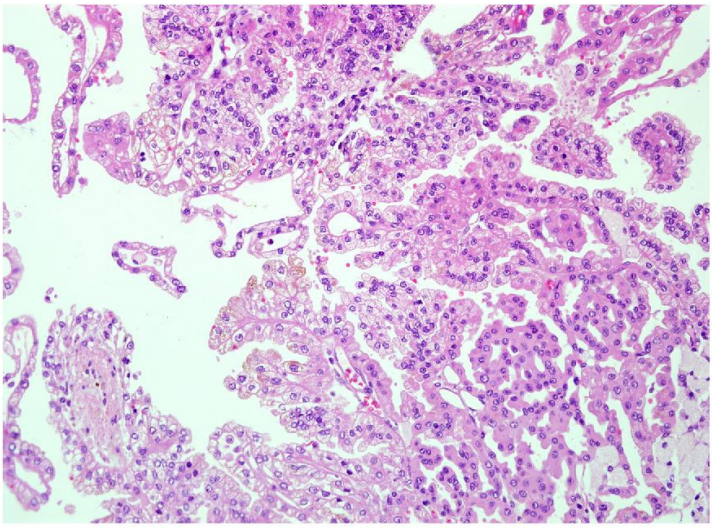

Fig. 3 The basic architecture of the tumors was papillary in seven out of nine cases. A small group of foam macrophages is located in the right lower corner of the image

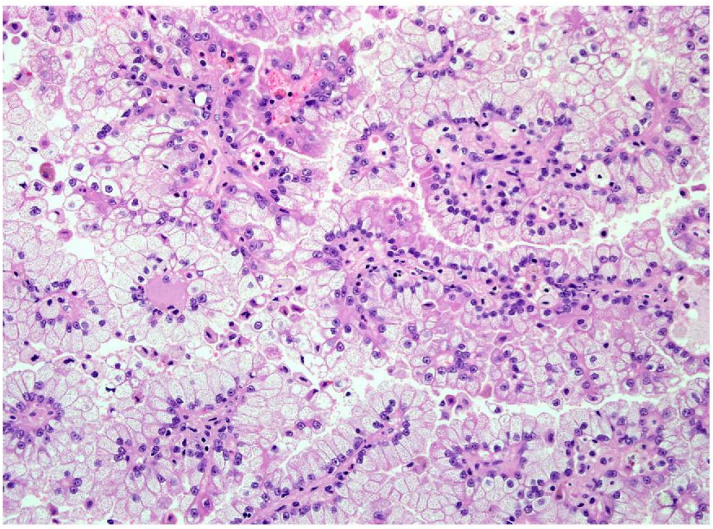

Fig. 4 Papillary tumors were composed of epithelial cells with microvacuoles

for CD68. The neoplastic epithelial cells were also strongly positive for vimentin and various cytokeratins (Fig. 8). All tumors were completely negative for cathepsin K and TFE3.

Ultrastructure

Six cases were examined by electron microscopy. The cytoplasm of the neoplastic epithelial cells was packed with distended mitochondria, most of which displayed lamellated cristae. Numerous microvesicles were dispersed between the mitochondria. No other prominent organelles were found within the cytoplasm (Fig. 9).

Molecular genetic analysis of *succinate dehydrogenase B* (*SDHB*) gene mutations

DNA sequences were compared to the reference sequence (http://www.ncbi.nlm.nih.gov) by the online program BLAST (http://blast.ncbi.nlm.nih.gov/Blast.cgi). No mutations were detected in any of the studied samples.

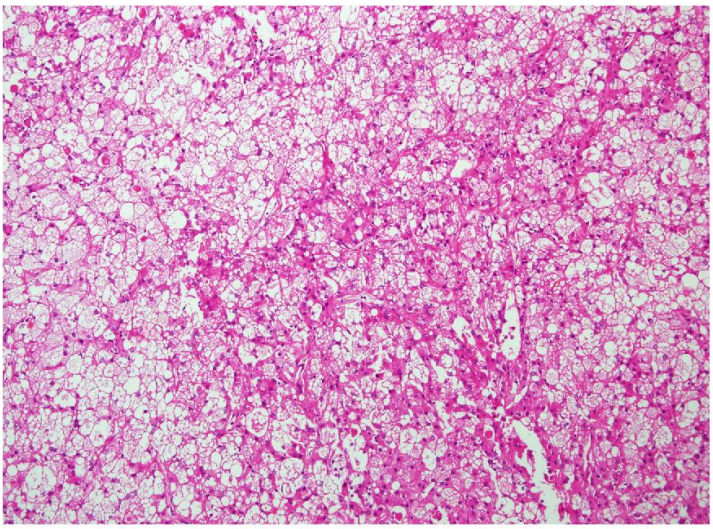

Fig. 5 Two out of nine tumors displayed mostly solid architecture

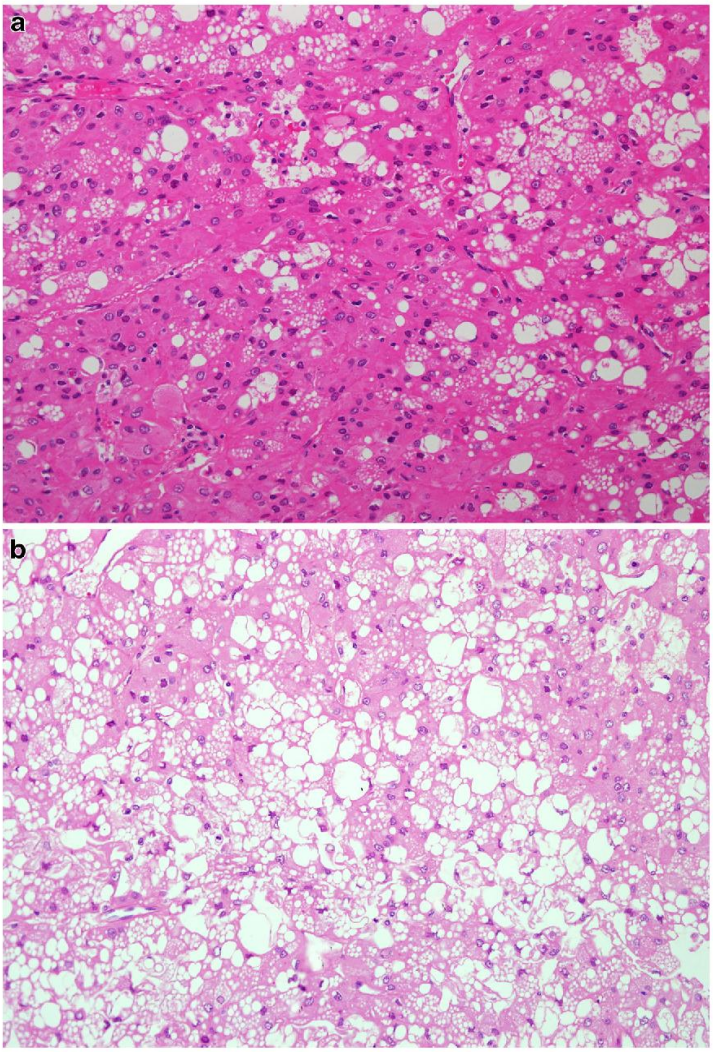

Fig. 6 Solid unclassified RCC were composed of eosinophilic cells with prominent microvacuolated cytoplasm (**a**, **b**)

Discussion

In this paper, we present a series of renal cell carcinomas with a significant component of neoplastic epithelial cells with a striking microvacuolated cytoplasmic appearance reminiscent of that encountered in hibernomas. In addition to hibernomas, a wide range of other neoplasms (as listed in "Introduction") may on occasion display a similar light-microscopic appearance. The mechanism behind the development of this microvacuolated cytoplasmic appearance is most probably the result of the accumulation of various membrane-bound molecules. This in turn may be caused by disturbance(s) in one or more cellular processes involved in the degradation, transport, synthesis, or endocytosis of lipids and/or various proteins.

Adipophilin is a protein that coats intracellular lipids and is, together with perilipin, a tail-interacting protein crucial for the maintenance of the integrity of intracellular lipid droplets [12]. As such, it is a good immunohistochemical marker for abnormal accumulation of intracytoplasmic fat as seen, for example, in neoplasms with sebaceous differentiation, and in secretory carcinomas of mammary and salivary glands, liposarcomas, and several different pathologic situations, like in atheroma, etc. [11, 14]. All our cases exhibited significant cytoplasmic immunohistochemical expression of adipophilin thus supporting the concept that the microvacuoles in the

Table 2 Results of immunohistochemical staining

Case	AE1.3	Cam 5.2	CK7	OSC	AMACR	CANH	CD10	CD68	PAX2	adi	HMB45	S100	MIA
1	<5 %, +	30 %, +	0	100 %, ++ to +++	100 %, +++	90 %, + to ++	90 %, +++	50 %, ++	5 %, ++	100 %+++	0	0	100 %++
2	5 %, ++	0	30 %, + to +++	50 %, + to +++	90 %, +++	90 %, ++	90 %, +++	90 %, + to +++	5 %, ++	100 %, +++	0	0	100 %+++
3	100 %, ++ to +++	75 %, + to +++	100 %, +++	100 %, +++	100 %, +++	100 %, + to ++	5 %, +	75 %, + to ++	0	40 %+++	0	0	100 %+++
4	0	Single cells +++	0	20 %, +	10 %, focal +++	90–100 %, + to +++ (foc)	90 %, ++ to +++	30 %, +	0	5 %, +++ (foc)	0	0	100 %, ++ to +++
5	NA	NA	NA	NA	NA	NA	NA	NA	NA	NA	NA	NA	
6	90–100 %, + to +++	80–90 %, + to +++	90–100 %, +++	100 %, ++ to +++	80 %, ++ to +++	20 %, + to +++	25 %, +++	25–50 %, +	0	100 %++	0	0	70 %+++
7	75–100 %, + to ++	75–100 %, ++	100 %, ++ to +++	+++	100 %, ++ to +++	75–100 %, +	<5 %, +	25–50 %, + to ++ (foc)	0	40 %+++	0	0	100 %+++
8	25 %, + to ++	20 %, +++	30 %+++	75–100 %, + to +++	75–100 %, ++ to +++	<5 %, +++ (foc)	50–75 %, +++	50–75 %, + to ++	10 %, ++ (foc)	100 %, +++	0	0	100 %, +++

0 negative, *foc* focally, + weak positivity, ++ moderate positivity, +++ strong positivity, *CK* cytokeratin, *AE1-AE3* cytokeratin, *OSC* Oscar, *CAM 5.2* cytokeratin, *AMACR* racemase, *vim* vimentin, *CANH* carboanhydrase IX, *adi* adipophilin, *HMB45* melanocytic marker, *MIA* anti-mitochondrial antigen, *NA* not available

cytoplasm can be attributed to abnormal accumulation of lipids in the tumor cells.

The immunohistochemical study clearly confirmed the light-microscopic impression in that the microvacuolated cells were epithelial in nature and not macrophages. In the ultrastructural study, we found the cytoplasm of the hibernoma-like cells to be filled with distended mitochondria and microvesicles. The former finding was corroborated by the findings in the immunohistochemical study, i.e., diffuse and strong expression of anti-mitochondrial antibody (MIA). Whether the presumed abnormally accumulated lipid material is compartmentalized to the mitochondria or the microvesicles cannot be clearly inferred from our findings, but intuitively, involvement of the latter structures (microvesicles) seems to be the more plausible alternative.

Regarding the histopathological differential diagnosis, the microvacuolated morphology of the cancer cells may present particular problems, especially when confronted with limited material on a core- or fine-needle aspiration biopsy. Papillary renal cell carcinoma frequently contains macrophages with foamy cytoplasm. However, these are always in a minority, whereas the malignant epithelial cells constitute the majority of the cellular population. Interestingly, in our cases (but perhaps not surprisingly) was the detection of weak expression of CD68 in the neoplastic foam cells. CD68 is present in all cell types with a significant component of lyso-/endosomes and is not restricted to macrophages. That these cells were epithelial in nature was substantiated by the finding of cytokeratin expression. Moreover, the true macrophage-type foam cells exhibited significantly stronger immunohistochemical staining for CD68 compared to the neoplastic epithelial cells with similar cytoplasmic features.

Very rarely, lipomatous neoplasms (lipomas and hibernoma) may appear as primary renal masses [6, 17]. With large tumors, the exact primary site may be difficult to determine. For example, a locally advanced primary retroperitoneal (well-differentiated liposarcoma) or adrenal tumor (mainly cortical carcinoma) with involvement of the kidney may be radiologically and even grossly almost impossible to separate from a primary renal neoplasm with extension outside the confines of the kidney [9]. However, our cases were undoubtedly intrarenal tumors with no involvement of the retroperitoneal space or surrounding structures.

Other tumors to consider are renal angiomyolipoma (AML), which can include vacuolated cells; similarly, extrarenal AML may very rarely contain cells with foamy cytoplasm. In both instances, a limited immunohistochemical panel (cytokeratins, smooth muscle actin, and HMB-45) will aid in the differential diagnosis.

Even clear cell RCC may very rarely contain lipomatous tissue and can mimic (at least radiologically) a true lipomatous tumor [16]. None of our cases displayed any histomorphological features of clear cell RCC.

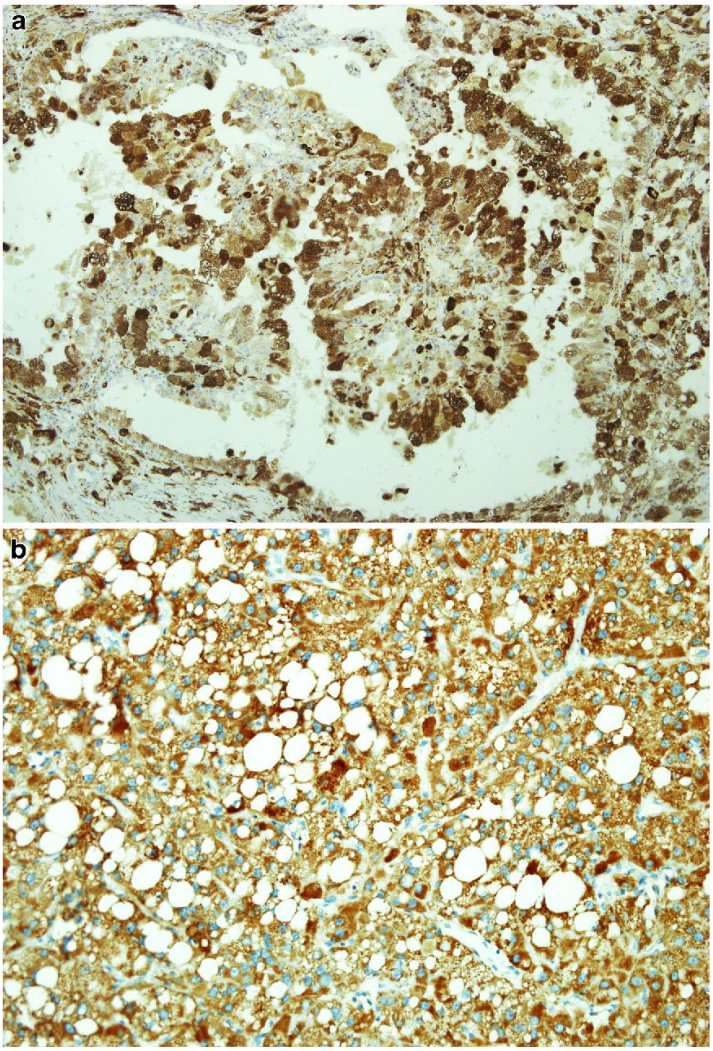

Fig. 7 The expression of anti-mitochondrial antigen (**a**) showed a similar pattern as that of adipophilin (**b**)

Another differential diagnostic problem is those renal cell carcinomas of which the architecture is papillary and the tumor cells exhibit clearing of the cytoplasm, i.e., not with the basophilic or eosinophilic/oncocytic cytoplasm that characterizes type 1, type 2, and oncocytic PRCC. Studies dealing with tumors composed of more or less clear cells arranged in a papillary pattern have been published [8, 10]. Our cases differed from these tumors on a cytologic (cytoplasmic) level. However, the light-microscopic appearance on low-power magnification of these papillary carcinomas with clear cells is somewhat similar to our cases. On high-power magnification, however, the distinction is easy, given the prominent cytoplasmic vacuolization in our tumors. Moreover, a similar combination of papillary architecture and cells with clear to pale cytoplasm is frequently encountered in the Mit-family-related RCC. To resolve this, an immunohistochemical study with TFE3/B and in selected cases performing a molecular genetic with eventually FISH and/or RT PCR examination would be instrumental. All cases in our study (nine out of nine) were completely TFE3 negative.

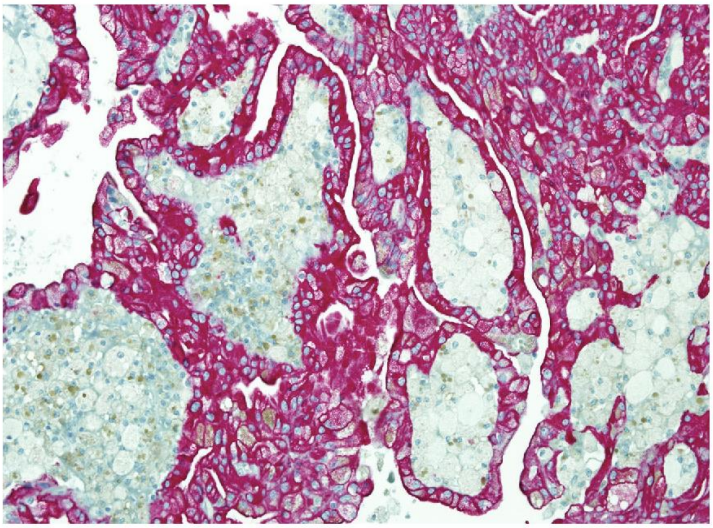

Fig. 8 The neoplastic epithelial cells were also strongly positive for various cytokeratins. Positivity for OSCAR is shown

Two of our nine cases showed light-microscopic features that distinguished them from the other seven tumors. These cases (no. 1 and 4) exhibited a non-papillary, solid-alveolar architecture and were composed of neoplastic cells resembling hibernoma cells. In this setting, i.e., faced with a renal tumor with a solid-alveolar architecture and where the tumor cells display a bubble-like cytoplasm, one should bear in mind the possibility of a renal tumor with *SDH* gene mutations [7]. This group of tumors occurs in patients which frequently also develop pheochromocytomas/paragangliomas and lack immunohistochemically detectable succinate dehydrogenase B (SDHB). None of our patients had a documented history of any paraganglioma/pheochromocytoma. Moreover, both our tumors were clearly positive for with SDHB. In addition, the SDHB-deficient renal neoplasms generally display tumor cells with an eosinophilic cytoplasmic appearance (in addition to the "bubbly" appearance) which was conspicuously absent in all our cases. Exclusion of this diagnosis in our cases was further supported by the results of molecular analysis of the *SDHB* gene status, in which no mutations in the *SDHB* gene were identified. Modified Fuhrman nucleolar grading system was easily applicable to all cases used in our study. The nuclear grade was 3 in nine out of nine cases. Apparently, the above discussed "hibernoma-like" cytoplasmic change had no influence on grade.

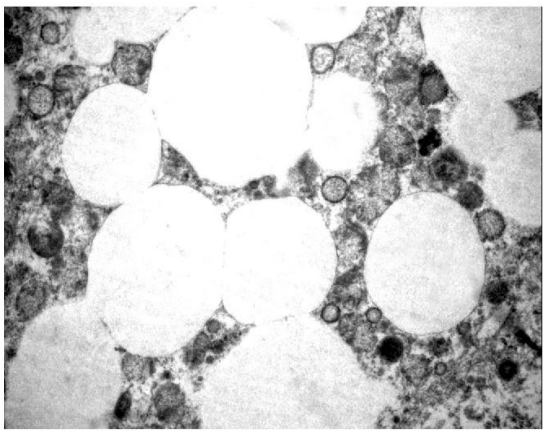

Fig. 9 The cytoplasm of the neoplastic epithelial cells was packed with distended mitochondria, most of which displayed concentric or lamellated cristae. Numerous microvesicles were dispersed between the mitochondria

In summary, we describe nine cases of renal cell carcinoma with a highly unusual cytomorphological, foamy cytoplasmic (hibernoma-like) appearance. Based on our findings, we propose that the mechanism behind this phenomenon is abnormal intracellular processing of lipids.

Acknowledgments The study was supported by the Charles University Research Fund (project number P36), by the project CZ.1.05/2.1.00/03.0076 from European Regional Development Fund, and by the Ministry of Health, Czech Republic—conceptual development of research organization (Faculty Hospital in Pilsen—FNPl, 00669806)

Conflict of interest All authors declare no conflict of interest.

References

1. Ahn S, Kwon GY, Cho YM, Jun SY, Choi C, Kim HJ, Park YW, Park WS, Shim JW (2013) Acquired cystic disease-associated renal cell carcinoma: further characterization of the morphologic and immunopathologic features. Med Mol Morphol 46(4):225–32
2. Albores-Saavedra J, Weimersheimer-Sandoval M, Chable-Montero F, Montante-Montes de Oca D, Hruban RH, Henson DE (2008) The foamy variant of pancreatic intraepithelial neoplasia. Ann Diagn Pathol 12:252–259
3. Ayub SB, Dodge J (2010) Lipid-rich variant of pancreatic endocrine neoplasms: a case report. Acta Cytol 54:829–834
4. Bellevicine C, Malapelle U, Iaccarino A, Schettino P, Napolitano V, Zeppa P, Troncone G (2013) Foamy gland pancreatic ductal adenocarcinoma diagnosed on EUS-FNA: a histochemical, immunohistochemical, and molecular report. Diagn Cytopathol 41:77–80
5. Chetty R, Serra S (2010) Lipid-rich and clear cell neuroendocrine tumors ("carcinoids") of the appendix: potential confusion with goblet cell carcinoid. Am J Surg Pathol 34:401–404
6. Delsignore A, Ranzoni S, Arancio M, Marchetti C, Landi G, Mina A, Marcato M, Martinengo C (2010) Kidney hibernoma: case report and literature review. Arch Ital Urol Androl 82:189–191
7. Gill AJ, Pachter NS, Chou A, Young B, Clarkson A, Tucker KM, Winship IM, Earls P, Benn DE, Robinson BG, Fleming S, Clifton-Bligh RJ (2011) Renal tumors associated with germline SDHB mutation show distinctive morphology. Am J Surg Pathol 35:1578–1585. doi:10.1097/PAS.0b013e318227e7f4
8. Haudebourg J, Hoch B, Fabas T, Cardot-Leccia N, Burel-Vandenbos F, Vieillefond A, Amiel J, Michiels JF, Pedeutour F (2010) Strength of molecular cytogenetic analyses for adjusting the diagnosis of renal cell carcinomas with both clear cells and papillary features: a study of three cases. Virchows Arch 457:397–404. doi:10.1007/s00428-010-0937-1
9. Katabathina VS, Vikram R, Nagar AM, Tamboli P, Menias CO, Prasad SR (2010) Mesenchymal neoplasms of the kidney in adults: imaging spectrum with radiologic-pathologic correlation. Radiographics 30:1525–1540. doi:10.1148/rg.306105517
10. Mai KT, Kohler DM, Roustan Delatour NL, Veinot JP (2006) Cytohistopathologic hybrid renal cell carcinoma with papillary and clear cell features. Pathol Res Pract 202:863–868
11. Mariano FV, Dos Santos HT, Azanero WD, da Cunha IW, Coutinho-Camilo CM, de Almeida OP, Kowalski LP, Altemani A (2013) Mammary analogue secretory carcinoma of salivary glands is a lipid-rich tumour, and adipophilin can be valuable in its identification. Histopathology. doi:10.1111/his.12192
12. Miura S, Gan JW, Brzostowski J, Parisi MJ, Schultz CJ, Londos C, Oliver B, Kimmel AR (2002) Functional conservation for lipid storage droplet association among Perilipin, ADRP, and TIP47 (PAT)-related proteins in mammals, *Drosophila*, and *Dictyostelium*. J Biol Chem 277:32253–32257
13. Noro T, Gotohda N, Kojima M, Konishi M, Nakaghori T, Takahashi S, Hasebe T, Kinoshita T (2010) Hepatocellular carcinoma with foamy histiocyte-like appearance: a deceptively clear cell carcinoma appearing variant. Case Rep Gastroenterol 4:286–292. doi:10.1159/000319545
14. Osako T, Takeuchi K, Horii R, Iwase T, Akiyama F (2013) Secretory carcinoma of the breast and its histopathological mimics: value of markers for differential diagnosis. Histopathology 63:509–1
15. Petersson F (2013) Sclerosing polycystic adenosis of salivary glands: a review with some emphasis on intraductal epithelial proliferations. Head Neck Pathol 7(Suppl 1):S97–106
16. Strotzer M, Lehner KB, Becker K (1993) Detection of fat in a renal cell carcinoma mimicking angiomyolipoma. Radiology 188:427–428
17. Tamboli P, Ro JY, Amin MB, Ligato S, Ayala AG (2000) Benign tumors and tumor-like lesions of the adult kidney. Part II: benign mesenchymal and mixed neoplasms, and tumor-like lesions. Adv Anat Pathol 7:47–66
18. Tatsas AD, Keedy VL, Florell SR, Simpson JF, Coffin CM, Kelley MC, Cates JM (2010) Foamy cell angiosarcoma: a rare and deceptively bland variant of cutaneous angiosarcoma. J Cutan Pathol 37:901–906
19. van Dongen JJ, Langerak AW, Bruggemann M, Evans PA, Hummel M, Lavender FL, Delabesse E, Davi F, Schuuring E, Garcia-Sanz R, van Krieken JH, Droese J, Gonzalez D, Bastard C, White HE, Spaargaren M, Gonzalez M, Parreira A, Smith JL, Morgan GJ, Kneba M, Macintyre EA (2003) Design and standardization of PCR primers and protocols for detection of clonal immunoglobulin and T-cell receptor gene recombinations in suspect lymphoproliferations: report of the BIOMED-2 Concerted Action BMH4-CT98-3936. Leukemia 17:2257–2317

MOLEKULÁRNĚ GENETICKÉ ALTERACE V RENÁLNÍCH KARCINOMECH S TUBULOCYSTICKOU ARCHITEKTONIKOU: TUBULOCYSTICKÝ RENÁLNÍ KARCINOM, TUBULOCYSTICKÝ RENÁLNÍ KARCINOM S HETEROGENNÍ KOMPONENTOU A RENÁLNÍ KARCINOM ASOCIOVANÝ S HEREDITÁRNÍ LEIOMYOMATÓZOU. KLINICKOPATOLOGICKÁ A MOLEKULÁRNĚ GENETICKÁ STUDIE 15 PŘÍPADŮ.

Tubulocystický renální karcinom (TCRK) byl v roce 2012 mezinárodní společností uropatologů (ISUP, International Society of Urological Pathology) označen za samostatnou jednotku [16] a toto označení bylo akceptováno ve WHO klasifikaci 2016 [4]. Histologicky je charakterizován tubulárně cystickým uspořádáním, přičemž tyto struktury jsou lemované atypickými cvočkovitými buňkami často vysokého nukleolárního grade. Morfologie TCRK se může překrývat s papilárním renálním karcinomem (PRK) v tom smyslu, že některé případy TCRK v sobě mohou skrývat struktury napodobující PRK. V některých případech lze nalézt typický TCRK s dobře ohraničeným ložiskem „pravého“ PRK: tato situace stále dovoluje tumor diagnostikovat jako TCRK. Tumory se složkami TCRK a PRK bez ostrého ohraničení promíchané mezi sebou však již nejsou kompatibilní s diagnózou TCRK. TCRK však může být morfologicky pestřejší a obsahovat i příměsi jiných tumorů než PRK. Molekulárně geneticky není TCRK zatím nijak obšírně prozkoumán, nejčastěji pozorované abnormality zahrnují trisomii chromozomů 7 a 17, společně se ztrátou chromozomu Y, což je sbližuje s PRK [4].

Naše studie zahrnuje 15 případů renálních karcinomů (RK) s tubulocystickým uspořádáním: 6 TCRK, 1 high-grade RK s tubulocystickou architekturou, 5 TCRK s dobře ohraničenými ložisky PRK, 2 high-grade RK, NOS a 1 RK s komponentu napodobující světlobuněčný papilární RK/renální angiomyoadenomatózní tumor (RAT). Molekulárně geneticky jsme vyšetřili aberace numerické aberace chromozomů 7, 17 a Y, mutaci genu *VHL* a *fumarát hydratázy (FH)*, ztrátu heterozygozity krátkého raménka 3. chromozomu (3p).

Z našeho výzkumu plyne, že TCRK má variabilní status chromozomů 7, 17 a Y, a to dokonce i v morfologicky uniformních případech. Biologické chování tumorů s úseky napodobujícími PRK/high-grade RK není zatím zcela zřetelné. Naše výsledky naznačují, že TCRK s heterogenní komponentou spíše nepatří do této jednotky, protože se chovají agresivněji než „čisté“ TCRK. Tyto případy dle našeho názoru nejlépe spadají do kategorie neklasifikovatelných RK. Jelikož jsme v jednom případě high-grade tubulocysticky uspořádaného RK detekovali mutaci genu *FH*, je zřejmé, že v některých případech může být morfologicky velice heterogenní RK spojený s hereditární leiomyomatózou ukryt i v kategorii TCRK. Navrhujeme proto, aby všechny „high-grade“ TCRK byly geneticky otestovány na přítomnost mutace genu *FH* a případně prediagnostikovány.

Molecular Genetic Alterations in Renal Cell Carcinomas With Tubulocystic Pattern: Tubulocystic Renal Cell Carcinoma, Tubulocystic Renal Cell Carcinoma With Heterogenous Component and Familial Leiomyomatosis-associated Renal Cell Carcinoma. Clinicopathologic and Molecular Genetic Analysis of 15 Cases

Monika Ulamec, MD, PhD,† Faruk Skenderi, MD, MSc,‡ Ming Zhou, MD, PhD,§ Božo Krušlin, MD, PhD,*† Petr Martínek, MSc,‖ Petr Grossmann, PhD,‖ Kvetoslava Peckova, MD,‖ Isabel Alvarado-Cabrero, MD,¶ Kristyna Kalusova, MSc, MD,# Bohuslava Kokoskova, MD,‖ Pavla Rotterova, MD, PhD,‖ Milan Hora, MD, PhD,# Ondrej Daum, MD, PhD,‖ Magdalena Dubova, MD,‖ Kevin Bauleth, MD,‖ David Slouka, MD, PhD,** Maris Sperga, MD,†† Whitney Davidson, BS, PSF,‡‡ Boris Rychly, MD,§§ Delia Perez Montiel, MD,‖‖ Michal Michal, MD,‖ and Ondrej Hes, MD, PhD‖¶¶*

Abstract: The characteristic morphologic spectrum of tubulocystic renal cell carcinoma (TC-RCC) may include areas resembling papillary RCC (PRCC). Our study includes 15 RCCs with tubulocystic pattern: 6 TC-RCCs, 1 RCC-high grade with tubulocystic architecture, 5 TC-RCCs with foci of PRCC, 2 with high-grade RCC (HGRCC) not otherwise specified, and 1 with a clear cell papillary RCC/renal angiomyoadenomatous tumor-like component. We analyzed aberrations of chromosomes 7, 17, and Y; mutations of *VHL* and *FH* genes; and loss of heterozygosity at chromosome 3p. Genetic analysis was performed separately in areas of classic TC-RCC and in those with other histologic patterns. The TC-RCC component demonstrated disomy of chromosome 7 in 9/15 cases, polysomy of chromosome 17 in 7/15 cases, and loss of Y in 1 case. In the PRCC component, 2/3 analyzable cases showed disomy of chromosome 7 and polysomy of chromosome 17 with normal Y. One case with focal HGRCC exhibited only disomy 7, whereas the case with clear cell papillary RCC/renal angiomyoadenomatous tumor-like pattern showed polysomies of 7 and 17, mutation of *VHL*, and loss of heterozygosity 3p. *FH* gene mutation was identified in a single case with an aggressive clinical course and predominant TC-RCC pattern. The following conclusions were drawn: (1) TC-RCC demonstrates variable status of chromosomes 7, 17, and Y even in cases with typical/uniform morphology. (2) The biological nature of PRCC/HGRCC-like areas within TC-RCC remains unclear. Our data suggest that heterogenous TC-RCCs may be associated with an adverse clinical outcome. (3) Hereditary leiomyomatosis-associated RCC can be morphologically indistinguishable from "high-grade" TC-RCC; therefore, in TC-RCC with high-grade features *FH* gene status should be tested.

Key Words: kidney, tubulocystic renal cell carcinoma, papillary renal cell carcinoma, hereditary leiomyomatosis-associated renal cell carcinoma, chromosomal aberration

(*Appl Immunohistochem Mol Morphol* 2016;24:521–530)

Received for publication February 13, 2015; accepted April 6, 2015.

From the *Ljudevit Jurak Department of Pathology, Sestre milosrdnice Clinical Hospital Center; †Department of Pathology, School of Medicine, University of Zagreb, Zagreb, Croatia; ‡Department of Pathology and Cytology, Clinical Center of the University of Sarajevo, Sarajevo, Bosnia and Hercegovina; §Department of Pathology, New York School of Medicine, NYU Langone Medical Center, New York, NY; ‡‡Department of Pathology and Laboratory Medicine, University of Kansas Medical Center, Kansas City, KS; Departments of ‖Pathology; #Urology; **Otorhinolaryngology, Charles University, Medical Faculty and Charles University Hospital Plzen; ¶¶Biomedical Centre, Faculty of Medicine in Plzen, Charles University in Prague, Plzen, Czech Republic; ¶Department of Pathology, Centro Medico; ‖‖Department of Pathology, Institute Nacional de Cancerologia, Mexico City, Mexico; ††Department of Pathology, East University, Riga, Latvia; and §§Department of Pathology, Cytopathos, Bratislava, Slovakia.

Supported by the Charles University Research Fund (project number P36), by the project CZ.1.05/2.1.00/03.0076 from European Regional Development Fund, and by Charles University Grant SVV 2015-260172.

The authors declare no conflict of interest.

Reprints: Ondrej Hes, MD, PhD, Department of Pathology, Charles University, Medical Faculty and Charles University Hospital Plzen, Alej Svobody 80, 304 60 Pilsen, Czech Republic (e-mail:hes@medima.cz).

Renal neoplasms constitute a wide spectrum of entities with an extensive array of morphologic features and molecular alterations. Genetic alterations in many tumor

subgroups remain unknown. The most frequently studied genetic alterations in renal neoplasms include chromosome 3p abnormalities, *VHL* gene changes, and, in cases of papillary renal cell carcinoma (PRCC), the status of chromosomes 7 and 17. Alteration of many other genes is also seen in these tumors, as well as in other infrequent histologic subtypes of renal cell carcinoma (RCC), suggesting that multiple molecular pathways are involved in their pathogenesis.

Tubulocystic RCC (TC-RCC) is recognized as a distinct epithelial neoplasm by the Vancouver International Society of Urological Pathology Classification 2012 (ISUP).[1] Up to 100 cases of this rare tumor have been reported in the literature. TC-RCC has a characteristic macroscopic and microscopic appearance. It is a well-circumscribed, encapsulated, gray-colored tumor with multiple cysts of varying size, giving it a bubble wrap appearance. Histologically, it is composed of well-formed tubules and cysts lined by atypical cells with abundant eosinophilic cytoplasm, often having a hobnail appearance. The nuclei are usually high grade, enlarged, with prominent nucleoli, although mitoses are rarely seen. The intervening stroma is fibrotic.[1–8]

The morphology of TC-RCC may overlap with PRCC, given that, in some cases, PRCC-like areas are found in TC-RCC. Small foci of high-grade RCC (HGRCC) not otherwise specified (NOS) areas have also been described in the literature and are, according to these studies, compatible with a TC-RCC diagnosis.[8–14] Occasionally, it is possible to find cases of otherwise typical TC-RCC with well-formed, circumscribed areas of PRCC or, more rarely, of different types of RCC[9–15]

The most frequently observed cytogenetic abnormalities in PRCC include trisomy of chromosomes 7 and 17 with loss of the Y chromosome in male individuals.[15–19] As a result of these findings, some authors suggest there is a relationship between PRCC and TC-RCC.[6,8–10,15]

However, the status of tumors with otherwise typical TC-RCC morphology admixed and intermingled with PRCC-like/other RCC-like areas is not entirely elucidated.

In this study we investigated the status of chromosomes 7, 17, and Y in 15 tumors initially diagnosed as TC-RCC, of which 7 presented with foci of PRCC-like morphology, 2 contained areas of HGRCC NOS, and 1 showed a clear cell papillary RCC/renal angiomyoadenomatous tumor-like component (CCPRCC/RAT). *FH* gene analysis was performed in 3 cases with an earlier age of onset, followed by a more aggressive clinical course.

MATERIALS AND METHODS

Fifteen cases were retrieved from the >17,500 renal tumors (institutional, consultation cases, and archive cases from other institutions) in the Pilsen Tumor Registry. Pathologic examination of routine hematoxylin-eosin–stained sections was performed in each case by at least 3 pathologists (M.U., F.S., and O.H.). Cases were reevaluated and further histologic patterns were described (PRCC, CCPRCC/RAT-like pattern, and solid HGRCC). The extent of the heterogenous component was assessed as a percentage of the tumor. In 2 cases, separate structures of papillary adenomas were found in the adjacent kidney parenchyma but were not analyzed further.

Molecular Genetic Methods

Heterogenous structures (PRCC, CCPRCC/RAT-like pattern, and HGRCC) were analyzed separately from areas of typical TC-RCC. Chromosomal aberrations were determined independently in areas with classic TC-RCC and in those with other histologic patterns.

Fluorescence In Situ Hybridization (FISH)

For each case a 4-μm-thick section was placed onto a positively charged slide. Hematoxylin-eosin–stained slides were examined for determination of areas for cell counting. The unstained slide was routinely deparaffinized and incubated in the 1× Target Retrieval Solution Citrate pH 6 (Dako, Glostrup, Denmark) for 40 minutes at 95°C and subsequently cooled for 20 minutes at room temperature in the same solution. The slide was washed in deionized water for 5 minutes and digested in protease solution with pepsin (0.5 mg/mL) (Sigma Aldrich, St Louis, MO) in 0.01 M HCl at 37°C for 20 minutes. The slide was then placed into deionized water for 5 minutes, dehydrated in a series of ethanol solutions (70%, 85%, 96% for 2 min each), and air-dried. Probes for aneuploidy detection of chromosomes 7, 17, and Y (Vysis/Abbott Molecular, IL) (Table 1) were mixed with water and CEP Hybridization buffer (Vysis) in a 1:2:7 ratio. An appropriate amount of probe mix and factory premixed XY probe was applied to each specimen, which was then covered with a glass coverslip and sealed with rubber cement. The slide was incubated in the ThermoBrite instrument (StatSpin/Iris Sample Processing, Westwood, MA) with codenaturation parameters of 85°C for 8 minutes and hybridization parameters of 37°C for 16 hours. The rubber cemented coverslip was then removed and the slide was placed in posthybridization wash solution (2× SSC/0.3% NP-40) at 72°C for 2 minutes. The slide was air-dried in the dark, counterstained with 4, 6-diamidino-2-phenylindole (DAPI) (Vysis), coverslipped, and examined immediately.

The sections were examined with an Olympus BX51 fluorescence microscope (Olympus Corporation, Tokyo, Japan) using a ×100 objective with Triple Band Pass (DAPI/SpectrumGreen/SpectrumOrange) and Single Band Pass (SpectrumGreen/SpectrumOrange) filter sets.

TABLE 1. FISH Probes for Detection of Aneuploidy of Chromosomes 7, 17, and Y

Chromosome	Probe
7	CEP 7 (D7Z1)/7p11.1-q11.1 Alpha Satellite DNA
17	CEP 17 (D17Z1)/17p11.1-q11.1 Alpha Satellite DNA
Y	CEP X (DXZ1) SpectrumGreen/CEP Y (DYZ3)//Yp11.1-q11.1 Alpha Satellite DNA/Xp11.1-q11.1 Alpha Satellite DNA

FISH indicates fluorescence in situ hybridization.

Scoring of aneuploidy was performed by counting the number of fluorescent signals in 100 randomly selected, nonoverlapping tumor cell nuclei. The slides were independently enumerated by 2 observers (P.M. and P.G.). Monosomy and polysomy for chromosomes 7 and 17 were defined as the presence of 1 signal in >45% and 3 or more signals in >10% of nuclei (mean+3 SD in normal non-neoplastic control tissues), respectively. Samples showing 2 signals between these cutoffs (<45% of 1 signal and <10% of 3 or more signals per nucleus) were considered disomic. In male cases, aneuploidies of chromosome X and Y were defined as the absence of signal in >45% or presence of 2 or more signals in >10% of nuclei (mean+3 SD in normal non-neoplastic control tissues).

DNA Extraction

DNA for molecular genetic investigation was extracted from formalin-fixed, paraffin-embedded (FFPE) tissue. Several 5-μm-thick sections were placed on each slide. Hematoxylin-eosin–stained slides were examined for identification of neoplastic tissue. Subsequently, neoplastic and non-neoplastic tissue was scraped from unstained slides and DNA was isolated by the NucleoSpin Tissue Kit (Macherey-Nagel, Düren, Germany). All procedures were performed according to the manufacturer's protocols.

VHL Gene Analysis

Mutation analysis of exons 1, 2, and 3 of the *VHL* gene was performed using polymerase chain reaction (PCR) and direct sequencing. PCR was carried out using the primers shown in Table 2. The reaction conditions were as follows: 12.5 μL of HotStar Taq PCR Master Mix (Qiagen), 10 pmoL of each primer, 100 ng of template DNA, and distilled water up to 25 μL. The amplification program consisted of denaturation at 95°C for 15 minutes and then 40 cycles of denaturation at 95°C for 1 minute, annealing at 55°C for 1 minute, and extension at 72°C for 1.5 minutes for all amplicons. The program was finished by 72°C incubation for 7 minutes. The PCR products were checked on 2% agarose gel electrophoresis. Successfully amplified PCR products were purified with magnetic particles Agencourt AMPure (Agencourt Bioscience Corporation, A Beckman Coulter Company, Beverly, MA), both side sequenced using Big Dye Terminator Sequencing Kit (Applied Biosystems, Foster City, CA) and purified with magnetic particles Agencourt CleanSEQ (Agencourt Bioscince Corporation) all according to the manufacturers' protocol. The samples were subsequently run on an automated sequencer ABI Prism 3130xl (Applied Biosystems) at a constant voltage of 13.2 kV for 20 minutes. All samples were analyzed in duplicates and analysis of positive samples was repeated. For 3p loss of heterozygosity (LOH) analysis of neoplastic tissue DNA, 10 STR (short tandem repeats) markers: D3S666, D3S1270, D3S1300, D3S1581, D3S1597, D3S1600, D3S1603, D3S1768, D3S2338, and D3S3630 located on the short arm of chromosome 3 (3p) were chosen from the database (Gene Bank UniSTS). The primers are listed in Table 3. PCR conditions were the same as mentioned above. Successfully amplified PCR products were mixed with GeneScan 500 LIZ dye Size Standard (Applied Biosystems) and run on an automated genetic analyzer ABI Prism 3130xl (Applied Biosystems) at a constant voltage of 15 kV for 20 minutes. A sample was considered LOH positive if the ratio of nontumor DNA to tumor DNA was >1.5 or <0.66. All samples were analyzed in duplicates.

TABLE 2. PCR Primers Used in Mutation Analysis of the *VHL* Gene and Designed in Primer3 Software

Gene/Exon	Name	Primers (Sequence 5′→3′)
VHL/exon 1	VHL e1-1	CGCGAAGACTACGGAGGT
	VHL e1-2	GTCTTCTTCAGGGCCGTA
	VHL e1-3	GAGGCAGGCGTCGAAGAG
	VHL e1-4	GCGATTGCAGAAGATGACCT
	VHL e1-5	GCCGAGGAGGAGATGGAG
	VHL e1-6	CCCGTACCTCGGTAGCTGT
	VHL e1-7	CCGTATGGCTCAACTTCGAC
	VHL e1-8	GCTTCAGACCGTGCTATCGT
VHL/exon 2	VHL e2-1	ACCGGTGTGGCTCTTTAACA
	VHL e2-2	TCCTGTACTTACCACAACAACCTT
VHL/exon 3	VHL e3-1	GCAAAGCCTCTTGTTCGTTC
	VHL e3-2	ACATTTGGGTGGTCTTCCAG
	VHL e3-3	CAGGAGACTGGACATCGTCA
	VHL e3-4C	CCATCAAAAGCTGAGATGAAAC

PCR indicates polymerase chain reaction.

FH Gene Mutation Analysis

Three cases occurring in young patients (29, 31, 44 y) were further analyzed. DNA from FFPE tissue was extracted using a QIAsymphony DNA Mini Kit (Qiagen) on the automated extraction system (QIAsymphonySP, Qiagen) according to the manufacturer's supplementary protocol for FFPE samples (Purification of genomic DNA from FFPE tissue using the QIAamp DNA FFPE Tissue Kit and Deparaffinization Solution). Mutation analysis of

TABLE 3. PCR Primers Used in LOH Analysis of Chromosome 3p

Marker	Name	Primers (Sequence 5′→3′)
D3S666	D3S666-SK#15	CAAGGCATTAAAGTGGCCACGC
	D3S666-SK#16	GTTTGAACCAGTTTCCTACTGAG
D3S1270	D3S1270-F	TGGAACTGTATCAAAGGCTC
	D3S1270-R	TTGCATTAGNATTCTCCAGA
D3S1300	D3S1300SF	AGCTCACATTCTAGTCAGCCT
	D3S1300A	GCCAATTCCCCAGATG
D3S1581	D3S1581-F	CAGAACTGCCAAACCA
	D3S1581-R	GGGTAACAGGAGCGAG
D3S1597	D3S1597-F	AGTACAAATACACACAAATGTCTC
	D3S1597-R	GCAAATCGTTCATTGCT
D3S1600	D3S1600-F	ATCACCATCATCTGCCTGTC
	D3S1600-R	TGCTTGCCTTGGGATTTA
D3S1603	D3S1603-F	CCCTAACTCCACTTGAAAGC
	D3S1603-R	TCAGCGAACAGCAACAAAT
D3S1768	D3S1768SF	GGTTGCTGCCAAAGATTAGA
	D3S1768A	CACTGTGATTTGCTGTTGGA
D3S2338	D3S2338-F	GAAGCCAGCAGTTTCTC
	D3S2338-R	CTGTATTGTTTTCCAGGATAAG
D3S3630	D3S3630-F	AAGGGATAAGCTGCAAATCA
	D3S3630-R	ACCAAATACAATTCATGAGACCTGA

LOH indicates loss of heterozygosity; PCR, polymerase chain reaction.

the whole coding sequence of the *FH* gene was performed using PCR and direct sequencing. PCR was carried out using the primers shown in Table 4. The reaction conditions were as follows: 12.5 μL of HotStar Taq PCR Master Mix (Qiagen), 10 pmoL of each primer (Table 4), 100 ng of template DNA, and distilled water up to 25 μL. The amplification program consisted of denaturation at 95°C for 15 minutes and then 40 cycles of denaturation at 95°C for 1 minute, annealing at 60°C for 1 minute, and extension at 72°C for 1.5 minutes for all amplicons. The program was finished with 72°C incubation for 7 minutes. The PCR products were checked on 2% agarose gel electrophoresis.

Successfully amplified PCR products were purified with the magnetic particles Agencourt AMPure (Agencourt Bioscience Corporation, A Beckman Coulter Company), both side sequenced using the Big Dye Terminator Sequencing Kit (Applied Biosystems) and purified with the magnetic particles Agencourt CleanSEQ (Agencourt) all according to the manufacturers' protocol. Subsequently, the sequencing products were run on an automated sequencer ABI Prism 3130xl (Applied Biosystems) at a constant voltage of 13.2 kV for 20 minutes.

RESULTS

The clinical data and pathologic features of 15 cases are summarized in Table 5. The age of the patients ranged from 29 to 78 (mean = 59.53). There were 10 men and 5 women (male to female ratio 2:1). Size of the tumor, in the greatest dimension, ranged from 2 to 10 cm (mean = 5.21 cm). Fourteen patients were treated by radical nephrectomy and 1 underwent partial nephrectomy. All of the tumors presented as a solitary mass; 11 were in stage pT1, 3 in pT2, and a single case in pT3. Six of the cases were pure TC-RCCs that formed well-circumscribed masses with classic histologic features—closely packed well-formed tubules and cysts separated by thin fibrous septa (Figs. 1A, B). The epithelial cells lining the cysts were eosinophilic with a cuboidal or flattened appearance and hobnail cells were commonly found. The lining cells contained prominent nucleoli, mostly equivalent to ISUP nucleolar grade 3. Six of the 15 patients with TC-RCC had associated PRCC-like areas (Figs. 2A, B). In 1 case, the PRCC-like pattern was present in close proximity to the principle lesion, whereas in the others it was an integral part of the main tumor mass. However, PRCC-like component was well-separated from main TC-RCC areas. There were 2 cases with small foci of solid tumor, which were designated as HGRCC NOS (Fig. 3). One of these also contained well-circumscribed PRCC-like areas. In another case, a highly unusual histologic picture was found: typical TC-RCC with areas containing CCPRCC/RAT-like features. This case was particularly interesting because of its advanced stage at the time of presentation and further aggressive course; the patient died of metastatic disease 1 year after surgery. An autopsy was not performed.

One case, in which the lesion was mostly arranged in a tubulocystic pattern (cells were mostly large and eosinophilic with prominent nuclei and conspicuous red nucleoli), was later diagnosed as hereditary leiomyomatosis-associated RCC (HLRCC) using molecular genetic testing (Fig. 4).

Ten of 15 patients were alive and well after a 1.5- to 9-year follow-up period. Four of 15 had died of the disease (metastatic dissemination, cachexia, or other complications). Two of the deceased patients were under the age of 45 (1 male; 29 y and 1 female; 31 y) as was another with metastatic disease (male; 44). Three of the 4 deceased patients had heterogenous components within the TC-RCC. In 2 patients, the period from establishing of diagnosis to death was 1 and 2 years. Information about delay between cancer detection and death was not available in remaining 2 patients. The patient whose tumor was later designated as HLRCC was a 44-year-old man. His tumor was composed of 95% TC-RCC-like areas and 5% PRCC-like areas. The patient is alive with regressive changed metastases in lung and mediastinum (after sunitinib treatment) 7 years after surgery. Patients with pure TC-RCC who were over 45 years of age showed no evidence of residual disease after treatment.

TABLE 4. PCR Primers Used in *FH* Gene Mutation Analysis

Primer Name	Sequence 5′→3′	Product Size (bp)
FH-e1-F	GCGGAACGGTTTCTGACA	263
FH-e1-R	CAGGAGGGCTGAAGGTCACT	
FH-e2-F	GATGCGATTACTTTTGATCCTG	235
FH-e2-R	CCAAAATAGCCAACATTTCCA	
FH-e3-F	GCCAAAATAATAAACTTCCATGC	230
FH-e3-R	AGTATGGCATGGGTCTGAGG	
FH-e4-F	GGCATAATCAGCATTATTATTTCCTT	262
FH-e4-R	AAAAACAGCAAAGCTCACATACTG	
FH-e5a-F	TTTGTTTTTGTTGCCTCTGATTT	169
FH-e5a-R	GGATTTTGCATCAAGAGCATC	
FH-e5b-F	CTTTTCCCACAGCAATGCAC	218
FH-e5b-R	CATTTGTACCAAGCTCTAAATTGAA	
FH-e6a-F	CTTTGCTCATCATAAGATTTGAAGT	262
FH-e6a-R	CAACAGCAGTGCCTCCAG	
FH-e6b-F	TCAGGAATTTAGTGGTTATGTTCAA	224
FH-e6b-R	CAGACCACGTATAATGAGAAATGAA	
FH-e7a-F	TTGCTAATGGTAGAAAAATGTT TAGTT	200
FH-e7a-R	CCCAAAAATCGAATATCATTTGC	
FH-e7b-F	CTCATGACGCTCTGGTTGAG	197
FH-e7b-R	CAAGTTTTAGCTCCAACATTTAC TAGC	
FH-e8-F	TTTCTTTATTCTCCTGATTATTTGCAT	249
FH-e8-R	CCAAGATAATAAGCCTTTGGTCA	
FH-e9-F	CTCTCTCTCTCTCTCTCTCTCACTCAC	244
FH-e9-R	TGGTTTAGCTTTTTAATTTTGCATT	
FH-e10-F	AACCCATATGTCGTCTTTTTATTTTT	245
FH-e10-R	TTTTTAAGAAATGGGAGTCTGTTTTT	

PCR indicates polymerase chain reaction.

Molecular Genetic Findings

The FISH results are reported in Table 6. Thirteen tumors were informative for FISH in TC-RCC areas for chromosome 7, and 14 were informative for chromosome 17. The remaining samples were not suitable for analysis. Nine cases had disomy and 4 had polysomy of chromo-

TABLE 5. Clinical and Histopathologic Data

Cases	TC-RCC (%)	PRCC (%)	HGRCC (%)	PA	RAT (%)	Age	Sex	Size (cm)	Nuclear Grade	TNM (7th ed. 2009)	Follow-up (y)
1	100	—	—	—	—	62	M	2.0	1	pT1a	9 NED
2	100	—	—	—	—	68	M	2.5	2	pT1aNxMx	6 NED
3	100	—	—	—	—	31	F	5.1	2	pT1bNxMx	DOD UKP
4	100	—	—	—	—	49	F	3.0	3	pT1aNxMx	4 NED
5	100	—	—	—	—	75	M	9.0	3	pT2NxMx	3 NED
6	100*	—	—	3 mm focus	—	71	F	4.5	3	pT1bNxMx	1.5 NED
7	95*	5*	—	—	—	44	M	8.0	3	pT2NxMx	7 AWD
8	60*	40*	—	—	—	68	M	6.5	2	pT1bNxMx	4 NED
9	90*	10*	—	—	—	29	M	6.0	3	pT1bNxM1	DOD 1 AD
10	95*	5*	—	2 mm focus	—	60	M	2.2	3	pT1aNxMx	4 NED
11	99*	1*	—	—	—	60	M	2.5	2	pT1aNxMx	1 NED†
12	99*	1*	—	—	—	61	F	5.0	3	pT1bpN0Mx	3 NED
13	70*	25*	5*	—	—	63	M	9.0	2	pT2, cN0,cMX	3 NED
14	95*	—	5*	—	—	78	M	2.8	1	pT1a, NX, MX	DOD UKP
15	50*	—	—	—	50*	74	F	10.0	2	pT3NxMx	DOD‡ 2AD

*Both components were separated from each other, no intermingled areas were encountered.
†Radical prostatectomy performed 1 year after nephrectomy.
‡Metastases to the bones.
AD indicates after establishing of diagnosis; AWD, alive with disease; DOD, dead of disease; HGRCC, high-grade RCC, not otherwise specified; NED, no evidence of disease; PA, papillary adenoma in the adjacent kidney; PRCC, papillary renal cell carcinoma; RAT, clear cell (tubulo) papillary renal cell carcinoma/renal angiomyoadenomatous tumor-like area; TC-RCC, tubulocystic renal cell carcinoma; UKP, unknown period.

TABLE 6. FISH Analyses for Different Patterns of the Tumor

Number	Histologic Pattern (%)	Chromosome 7	Chromosome 17	Chromosome Y	*FH* Mutation
1	TC-RCC (100)	Polysomy	Disomy	Normal (XY)	NP
2*	TC-RCC (100)	NA	Polysomy	NA	NP
3	TC-RCC (100)	Disomy	Polysomy	NP	Negative
4	TC-RCC (100)	Disomy	Polysomy	NP	NP
5	TC-RCC (100)	Disomy	Disomy	NP	NP
6	TC-RCC (100)	Disomy	Disomy	Loss of Y (X0)	NP
7	TC-RCC (95)	Polysomy	Polysomy	Polysomy of Y (XYY)	mut†
	PRCC (5)	Disomy	Polysomy	Normal (XY)	
8	TC-RCC (60)	Disomy	Polysomy	Normal (XY)	NP
	PRCC (40)	Polysomy	Polysomy	Polysomy of X (XXY)	
9	TC-RCC (90)	Disomy	Disomy	NA	NA
	PRCC (10)	NA	NA	NA	
10	TC-RCC (95)	Disomy	Polysomy	NA	NP
	PRCC (5)	NA	NA	NA	
11	TC-RCC (99)	Polysomy	Disomy	Normal (XY)	NP
	PRCC (1)	NA	NA	NA	
12	TC-RCC (99)	Disomy	Disomy	NP	NP
	PRCC (1)	NA	NA	NP	
13	TC-RCC (70)	Disomy	Polysomy	NA	NP
	PRCC (25)	Disomy	Polysomy	Normal (XY)	
	HGRCC (5)	Disomy	Polysomy	Normal (XY)	
14	TC-RCC (95)	NA	NA	NA	NP
	HGRCC (5)	NA	NA	NA	
15‡	TC-RCC (50)	Polysomy	Polysomy	NP	NP
	RAT (50)	Polysomy	Polysomy	NP	

*4.M74431/08- NA for *VHL* and LOH3p.
†FH mutation in exon 7: c.911_917delCTTTTGT/p.(Phe305Leufs*22).
‡15. M27460/13(RAT)- *VHL*- mutation in exon 1c.202T > A, p.(S68T); LOH3p-positive.
FISH indicates fluorescence in situ hybridization; HGRCC, high-grade RCC, not otherwise specified; NA, not analyzable; NP, not performed; PRCC, papillary renal cell carcinoma; RAT, clear cell (tubulo) papillary renal cell carcinoma/renal angiomyoadenomatous tumor-like area; TC-RCC, tubulocystic renal cell carcinoma.

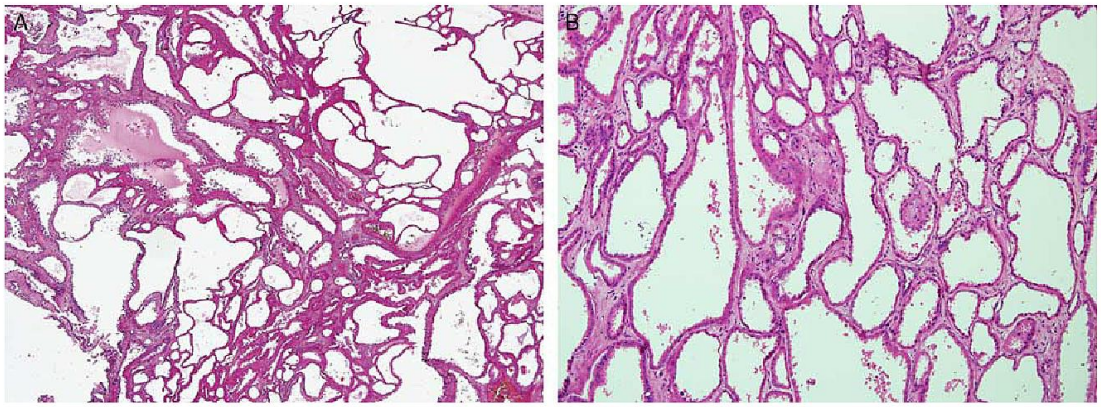

FIGURE 1. A, Scanning magnification showed typical tubulocystic renal cell carcinoma. B, The same tumor in detail. Cysts were lined mostly by low cylindrical epithelial cells.

some 7, 8 cases had polysomy and 6 had disomy of chromosome 17. Chromosome Y showed polysomy in 1 case and loss in another case; 3 cases had normal status of chromosome Y. In the whole cohort, the most frequent aberrancies were disomy of chromosome 7 and polysomy of chromosome 17.

Three tumors were informative for FISH in PRCC areas and others were not analyzable due to low DNA quality. In 2 cases, disomy of chromosome 7, gain of chromosome 17, and normal Y was found. The case later proven to be HLRCC had polysomy of 7 and 17 with gain of Y in TC-RCC-like areas and disomy of 7 and gain of 17 with normal Y in PRCC-like areas. One of the 2 tumors containing a small focus of HGRCC was not analyzable due to the small number of tumor cells present in the area of interest. The focus of HGRCC in the second tumor showed disomy of chromosome 7, polysomy of chromosome 17, and normal Y. This tumor also contained a PRCC focus that showed the same status of chromosomes 7 and Y with gain of chromosome 17. The TC-RCC component in the aforementioned tumor showed disomy of chromosome 7 and polysomy of chromosome 17.

In the single case with a CCPRCC/RAT-like pattern, both components (CCPRCC/RAT and TC-RCC) showed gains of chromosomes 7 and 17. In addition, mutation of the *VHL* gene and LOH 3p were found in the CCPRCC/RAT-like area.

Three cases with aggressive forms of TC-RCC (patients being younger than 45 at the time of diagnosis) were analyzed for mutations of the *FH* gene. One was not

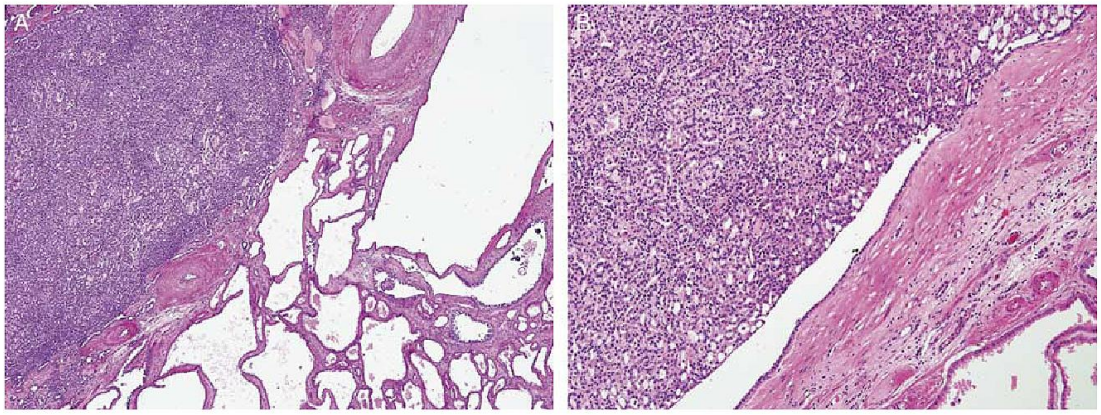

FIGURE 2. A, Well-demarcated focus of papillary renal cell carcinoma is clearly visible on the left part of the photo, whereas on the right side is the tubulocystic renal cell carcinoma component. B, Papillary renal cell carcinoma component, corresponding mostly with type 1.

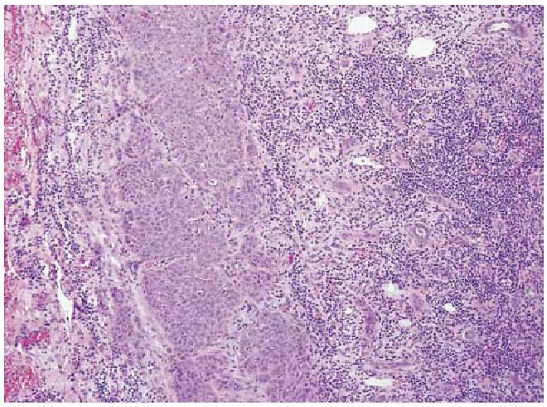

FIGURE 3. There were 2 cases with small foci of solid tumor that were designated as high-grade renal cell carcinoma not otherwise specified.

analyzable due to low quality of DNA, 1 was negative for mutations, and 1 showed a deletion of exon 7 of the *FH* gene: c.911_917delCTTTTGT, p.(Phe305Leufs*22).

DISCUSSION

TC-RCC is a rare tumor with characteristic features, which were first described by MacLennan and colleagues in 1997. The original name for the tumor was "low-grade collecting duct carcinoma," suggesting an origin in the cells of the collecting ducts. However, part of the original series was later recognized as mucinous tubular and spindle cell carcinoma.[20–23] Ultrastructural studies and immunohistochemical results showed mixed features of proximal and distal tubules.[1,4–8] Numerical chromosomal aberrations, mostly gains of chromosomes 7 and/or 17, have been studied and considered to be characteristic for TC-RCC.[3,6–8,13]

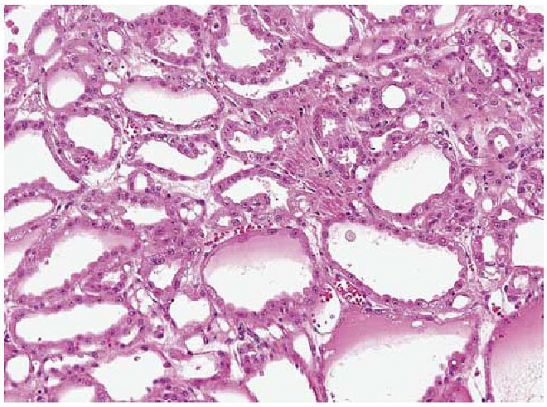

FIGURE 4. One case, in which the lesion was mostly arranged in a tubulocystic pattern, was later diagnosed as hereditary leiomyomatosis-associated renal cell carcinoma using molecular genetic testing.

To our knowledge, up to 100 cases of TC-RCC have been published previously, with few studies suggesting a relationship between TC-RCC and PRCC.[9,10] However, there were neither discriminating immunohistochemical markers nor conclusive evidence to identify a specific lineage of histogenesis for TC-RCC. Unfortunately, the immunohistochemical profiles of TC-RCC and PRCC are also very similar. AMACR is usually diffusely and strongly positive in both TC-RCC and PRCC. Other stains, including PAX-2, CD10, 34bE12, cytokeratin 19, and cytokeratin 7, mostly exhibited heterogenous patterns and it is extremely difficult to use immunohistochemical examination for establishing a correct diagnosis in complicated cases.[9]

The ultrastructural features are distinctive and show characteristics of both proximal convoluted tubules and intercalated cells. Tumor cells exhibit short microvilli with brush border organization, cytoplasmic interdigitation, and abundant mitochondria.[4]

In our series, 15 cases of tumors with a tubulocystic pattern were analyzed, including 7 with well-demarcated foci of PRCC-like features and 1 with PRCC/RAT-like features. There were other 2 cases with small areas of HGRCC NOS and 1 of these also contained PRCC-like areas. All of the distinct histologic components were analyzed separately. FISH results for chromosomes 7, 17, and Y were variable. The majority of cases showed disomy of chromosome 7, whereas half of the cases showed polysomy or gain of chromosome 17 and 1 showed loss of Y chromosome within the TC-RCC pattern. Three of 7 possible cases with PRCC components were suitable for analysis and revealed different profiles than the "host" TC-RCC tumors. All 3 cases showed polysomies of chromosome 17 and 1 showed polysomy of chromosome 7. In 1 case polysomy of chromosome X (XXY) was found. The case later proven to be HLRCC showed polysomy of 7, 17, and Y in TC-RCC-like areas and disomy of 7 and polysomy of 17 with disomy of Y in PRCC-like areas.

Yang and colleagues demonstrated a unique molecular signature of TC-RCC in comparison with other renal tumors using comparative genomic microarray analysis. TC-RCC showed gains of chromosome 17 but not chromosome 7, whereas most PRCCs showed chromosomal gains in both chromosomes 7 and 17.[3] Chen and colleagues described 2 cases, 1 was pure TC-RCC and the other was TC-RCC with foci of PRCC. Both components in the described cases showed gains of chromosomes 7 and 17, affirming the theory about the relationship between PRCC and TC-RCC.[8] Identical findings have been published in the paper of Kong et al[7] describing a unique case of bilateral TC-RCC in a background of diabetic end-stage renal disease.

Amin and colleagues studied 31 TC-RCC cases and showed that immunohistochemistry and ultrastructural examination reveal features of proximal convoluted tubules and distal nephron. Gene expression profiling showed that tubulocystic carcinoma displays a distinct

molecular signature compared with clear cell and chromophobe carcinoma. Amin and colleagues also performed microarray analysis that revealed 53 overexpressed and 126 underexpressed transcripts from different gene loci. Only 1 of the proteins (ubiquitin-specific protease 36) was located on chromosome 17 and it was underexpressed, whereas none of the studied gene products was found on chromosomes 7 or Y.[4] Zhou and colleagues included 20 cases of renal tumors comprising partially or exclusively TC-RCC in their study. Ten of 12 TC-RCCs had a chromosome 7 gain, 8 of 12 cases had a chromosome 17 gain, and 8 of 9 cases had a loss of the Y chromosome. Six of 9 cases in which all 3 chromosomes were studied showed a gain of chromosomes 7 and 17 and a loss of Y. On the basis of these results, they concluded that these tumors are closely related entities.[9]

Results of our study differ slightly from those in the series of Zhou et al.[9] It is possible to consider genetic changes found in our cases as compatible with results of the study performed by Yang et al.[3] Our study emphasizes the importance of good tissue sampling and careful morphologic evaluation of the given tumor. According to ISUP Vancouver Classification Criteria, cases that display a tubulocystic pattern admixed with the usual elements of PRCC [or collecting duct carcinoma (CDC)] should not be diagnosed as TC-RCC, whereas cases with focal, well-circumscribed PRCC-like areas allow for a diagnosis of TC-RCC.[1] Cases examined in our study were typical TC-RCC with well-demarcated foci of PRCC-like areas. No RCCs with intermingled areas of TC-RCC and PRCC component were involved in our series (Figs. 5A–C).

The pattern of chromosomal aberration present in our cases demonstrates the heterogenic nature of TC-RCC even within single tumorous lesions. Moreover, gains of chromosomes 7 and 17 were found in only 1 case with areas morphologically resembling PRCC. Results of our FISH analysis raised the question of whether PRCC-like areas are simply an illustration of morphologic heterogeneity or whether they represent legitimate differentiation toward PRCC. Unfortunately, the number of analyzable cases in our study is limited and we are, therefore, unable to further elucidate this phenomenon.

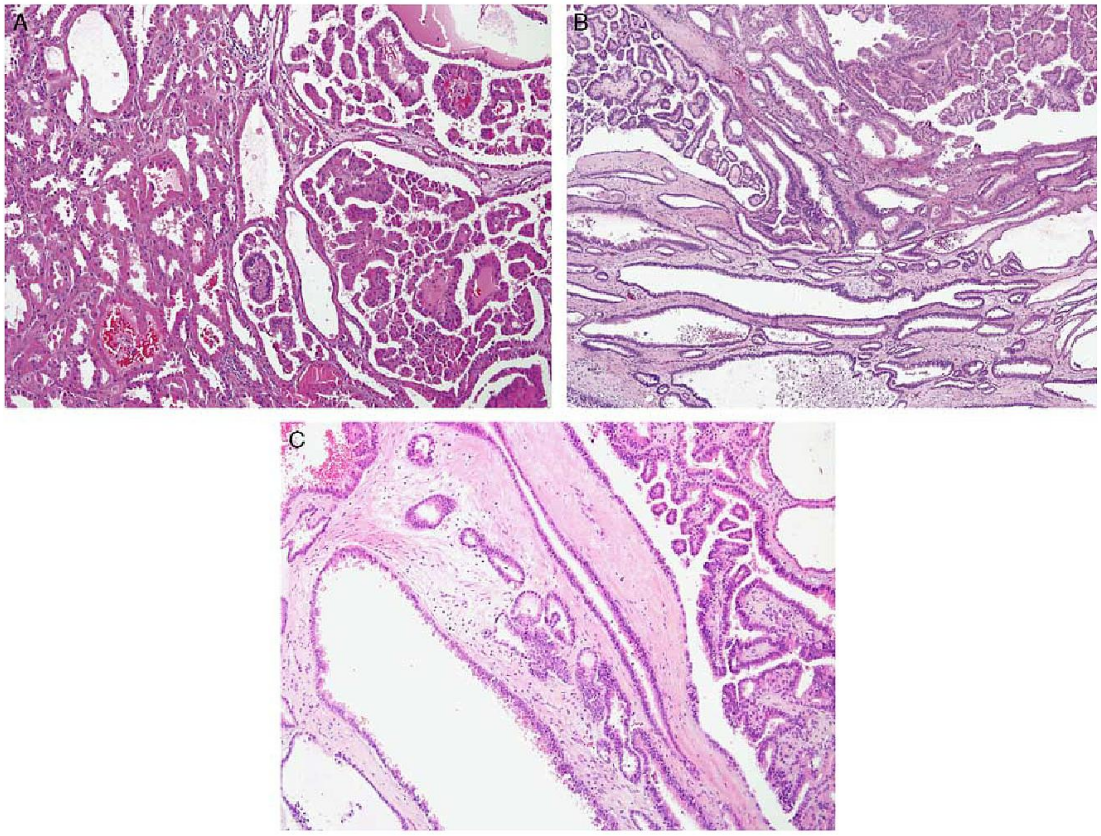

FIGURE 5. A-C, In some tumors it is possible to find areas where structures characteristic for tubulocystic carcinoma are admixed with those typical for papillary renal cell carcinoma. Such cases were not included into our study and should not be classified as tubulocystic renal cell carcinoma according International Society of Urological Pathology recommendations.

In the case with CCPRCC/RAT-like areas (case 15), results of FISH analysis were particularly interesting. Both components showed the same genetic profile, that is, gains of chromosomes 7 and 17, whereas *VHL* gene mutation and LOH 3p were identified in the heterologous (CCPRCC/RAT-like areas) component only. Al-Hussain and colleagues also described 3 cases of TC-RCC with a high-grade component using the term "dedifferentiated foci." The authors performed FISH on 2 of these tumors and their results showed the same genetic aberrations in the TC-RCC component and the dedifferentiated component. Both cases exhibited disomy of chromosome 7 and trisomy of chromosome 17, whereas only 1 of the 2 showed disomy of chromosome Y.[12]

An aggressive form of RCC, which is mostly consistent with PRCC type 2 according to WHO 2004, can also be found in hereditary leiomyomatosis—characterized by a germline mutation of the gene encoding for the tricarboxylic acid cycle enzyme fumarate hydratase (*FH*). Hereditary leiomyomatosis is a tumor predisposition syndrome that increases the risk for a triad of features: cutaneous leiomyomas, uterine leiomyomas, and RCCs. Usually it is diagnosed early in life and 50% of patients have metastatic disease at the time of diagnosis.[24,25]

Merino and colleagues described the morphologic spectrum of RCC in hereditary leiomyomatosis. Of 40 tumors reviewed, besides papillary architecture, several different patterns were recognized: tubulo-papillary (8 cases), tubular (2 cases), and solid (1 case).[26] In the study of Chen and colleagues, the clinicopathologic features of 9 patients with renal tumors presenting as sporadic cases but later proven to have *FH* germline mutations were reviewed. Similar morphologic features to those observed in a previous study were disclosed.[27]

In our study, 3 cases with an aggressive form of TC-RCC in patients under 45 years of age were analyzed for possible *FH* gene mutation. One tumor (case 7), which showed a predominantly tubulocystic pattern (95%) with only a small area of papillary architecture (5%), was positive for *FH* gene mutation. The second case demonstrated classic TC-RCC only and was negative for *FH* mutation, and a third case could not be analyzed due to insufficient quality of DNA.

Genetic heterogeneity and clinical data—fatal outcomes in 3 of 9 patients with heterogenous tumors—raise questions about diagnosing TC-RCC in cases with heterogenous histologic patterns. On the basis of our results, TC-RCCs have variable status of chromosomes 7 and 17, a characteristic that is also observed in other kidney tumors such as mucinous tubular and spindle cell tumors. The PRCC-like components exhibited chromosome 7 and 17 aberrancy patterns that were distinct from those of host TC-RCCs.

Recently, discussion about a possible relationship between TC-RCC and CDC has been revisited.[12] However, Osunkoya and colleagues has shown that TC-RCC is distinct from CDC based on immunohistochemical examination. TC-RCC was characterized by vimentin, p53, and α-methylacyl CoA racemase overexpression when compared with CDC.[26] Thus, at this point in time, there is an insufficient number of studies elucidating this possibility and further comparative studies are needed in the future.

CONCLUSIONS

(1) TC-RCC has variable status of chromosomes 7, 17, and Y even in morphologically uniform cases with typical morphology.
(2) The biological nature of PRCC/HGRCC-like areas within TC-RCC remains unclear. Our data support the notion that TC-RCCs with a heterogenous component should not be diagnosed as TC-RCC and can have an adverse outcome. For such cases, unclassified RCC is probably the best diagnostic category.
(3) HLRCC can be morphologically indistinguishable from "high-grade" TC-RCC; therefore, in cases of TC-RCC with high-grade features, the status of *FH* gene should be tested.

REFERENCES

1. Srigley JR, Delahunt B, Eble JN, et al. The International Society of Urological Pathology (ISUP) Vancouver Classification of Renal Neoplasia. *Am J Surg Pathol*. 2013;37:1469–1489.
2. Azoulay S, Vieillefond A, Paraf F, et al. Tubulocystic carcinoma of the kidney: a new entity among renal tumors. *Virchows Arch*. 2007;451:905–909.
3. Yang XJ, Zhou M, Hes O, et al. Tubulocystic carcinoma of the kidney: clinicopathologic and molecular characterization. *Am J Surg Pathol*. 2008;32:177–187.
4. Amin MB, MacLennan GT, Gupta R, et al. Tubulocystic carcinoma of the kidney: clinicopathologic analysis of 31 cases of a distinctive rare subtype of renal cell carcinoma. *Am J Surg Pathol*. 2009;33:384–392.
5. Alexiev BA, Drachenberg CB. Tubulocystic carcinoma of the kidney: a histologic, immunohistochemical, and ultrastructural study. *Virchows Arch*. 2013;462:575–581.
6. Kuroda N, Matsumoto H, Ohe C, et al. Review of tubulocystic carcinoma of the kidney with focus on clinical and pathobiological aspects. *Pol J Pathol*. 2013;64:233–237.
7. Kong MX, Hale C, Subietas-Mayol A, et al. Bilateral tubulocystic renal cell carcinomas in diabetic end-stage renal disease: first case report with cytogenetic and ultrastructural studies. *Rare Tumors*. 2013;5:e57.
8. Chen N, Nie L, Gong J, et al. Gains of chromosomes 7 and 17 in tubulocystic carcinoma of kidney: two cases with fluorescence in situ hybridisation analysis. *J Clin Pathol*. 2014;67:1006–1009.
9. Zhou M, Yang XJ, Lopez JI, et al. Renal tubulocystic carcinoma is closely related to papillary renal cell carcinoma: implications for pathologic classification. *Am J Surg Pathol*. 2009;33:1840–1849.
10. Deshmukh M, Shet T, Bakshi G, et al. Tubulocystic carcinoma of kidney associated with papillary renal cell carcinoma. *Indian J Pathol Microbiol*. 2011;54:127–130.
11. Bhullar JS, Thamboo T, Esuvaranathan K. Unique case of tubulocystic carcinoma of the kidney with sarcomatoid features: a new entity. *Urology*. 2011;78:1071–1072.
12. Al-Hussain TO, Cheng L, Zhang S, et al. Tubulocystic carcinoma of the kidney with poorly differentiated foci: a series of 3 cases with fluorescence in situ hybridization analysis. *Hum Pathol*. 2013;44:1406–1411.
13. Sangle NA, Mao R, Shetty S, et al. Novel molecular aberrations and pathologic findings in a tubulocystic variant of renal cell carcinoma. *Indian J Pathol Microbiol*. 2013;56:428–433.
14. Moses KA, Decaro JJ, Osunkoya AO, et al. Tubulocystic carcinoma of the kidney: a case report of natural history and long-term follow-up. *ScientificWorldJournal*. 2010;10:586–589.
15. Brennan C, Srigley JR, Whelan C, et al. Type 2 and clear cell papillary renal cell carcinoma, and tubulocystic carcinoma: a unifying concept. *Anticancer Res*. 2010;30:641–644.
16. Corless CL, Aburatani H, Fletcher JA, et al. Papillary renal cell carcinoma: quantitation of chromosomes 7 and 17 by FISH, analysis

of chromosome 3p for LOH, and DNA ploidy. *Diagn Mol Pathol*. 1996;5:53–64.
17. Jiang F, Richter J, Schraml P, et al. Chromosomal imbalances in papillary renal cell carcinoma: genetic differences between histological subtypes. *Am J Pathol*. 1998;153:1467–1473.
18. Klatte T, Pantuck AJ, Said JW, et al. Cytogenetic and molecular tumor profiling for type 1 and type 2 papillary renal cell carcinoma. *Clin Cancer Res*. 2009;15:1162–1169.
19. Yu W, Zhang W, Jiang Y, et al. Clinicopathological, genetic, ultrastructural characterizations and prognostic factors of papillary renal cell carcinoma: new diagnostic and prognostic information. *Acta Histochem*. 2013;115:452–459.
20. MacLennan GT, Farrow GM, Bostwick DG. Low-grade collecting duct carcinoma of the kidney: report of 13 cases of low-grade mucinous tubulocystic renal carcinoma of possible collecting duct origin. *Urology*. 1997;50:679–684.
21. MacLennan GT, Bostwick DG. Tubulocystic carcinoma, mucinous tubular and spindle cell carcinoma, and other recently described rare renal tumors. *Clin Lab Med*. 2005;25:393–416.
22. Murphy W, Beckwith JB, Farrow GM. Tumors of the kidney. In: Murphy W, Beckwith JB, Farrow GM, eds. *Atlas of the Tumour Pathology Tumour of the Kidney, Bladder, and Related Urinary Structures*, 3rd ed. Washington, DC: Armed Forces Institute of Pathology; 1994.
23. Osunkoya AO, Young AN, Wang W, et al. Comparison of gene expression profiles in tubulocystic carcinoma and collecting duct carcinoma of the kidney. *Am J Surg Pathol*. 2009;33:1103–1106.
24. Linehan WM, Rouault TA. Molecular pathways: Fumarate hydratase-deficient kidney cancer—targeting the Warburg effect in cancer. *Clin Cancer Res*. 2013;19:3345–3352.
25. Alam NA, Rowan AJ, Wortham NC, et al. Genetic and functional analyses of FH mutations in multiple cutaneous and uterine leiomyomatosis, hereditary leiomyomatosis and renal cancer, and fumarate hydratase deficiency. *Hum Mol Genet*. 2003;12:1241–1252.
26. Merino MJ, Torres-Cabala C, Pinto P, et al. The morphologic spectrum of kidney tumors in hereditary leiomyomatosis and renal cell carcinoma (HLRCC) syndrome. *Am J Surg Pathol*. 2007;31:1578–1585.
27. Chen YB, Brannon AR, Toubaji A, et al. Hereditary leiomyomatosis and renal cell carcinoma syndrome-associated renal cancer: recognition of the syndrome by pathologic features and the utility of detecting aberrant succination by immunohistochemistry. *Am J Surg Pathol*. 2014;38:627–637.

2. ČÁST

NÁDORY VARLAT

PRIMÁRNÍ STROMÁLNÍ TUMOR VARLETE Z PRSTENČITÝCH BUNĚK: STUDIE 13 PŘÍPADŮ DOKAZUJÍCÍ JEJICH FENOTYPICKOU A GENOTYPICKOU OBDOBU S PANKREATICKÝM SOLIDNÍM PSEUDOPAPILÁRNÍM TUMOREM.

Na myšlenku, že existuje spojitost mezi primárním stromálním tumorem varlete a solidním pseudopapilárním tumorem (SPT) pankreatu nás přivedl jeden případ, který se vyskytl v pravém varleti u 32 letého muže. Tumor měl rozměry 4,8x3x4 cm a histologicky byl velmi zajímavý. Skládal se ze dvou distinktních komponent: 1) solidní komponenta neodlišitelná od SPT pankreatu, složená z monomorfní populace epiteloidních buněk s pravidelnými kulatými jádry. V některých částech tumoru byla solidní komponenta uspořádaná i trabekulárně nebo do hnízd, 2) komponenta z prstenčitých buněk, která tvořila většinu objemu tumoru a byla histologicky charakterizována uniformními epiteloidními buňkami s velkou prázdnou cytoplazmatickou vakuolou, která odtlačovala jádro na periferii. Stejně jako solidní komponenta, i tato prstenčitá byla blandního vzhledu. V mnoha místech tumoru bylo patrné promíchání obou komponent, přecházely jedna v druhou. Další struktury, které jsme v tumoru viděli, byly hyalinní globule. Ačkoliv je nadnesené považovat je za specifické, je dobře známo, že jsou přítomny v podstatě ve 100% SPT pankreatu. Imunohistochemicky reagoval tumor pozitivně s β-kateninem, cyklinem D1 (nukleární pozitivita u obou protilátek), CD10, vimentinem, galektinem-3, klaudinem7, α-1-antitrypsinem, CD56, NSE a byl negativní v průkazu chromograninu, inhibinu, kalretininu, NANOG, OCT3/4 a SALL4. Molekulárně genetická analýza detekovala onkogenní somatickou mutaci v exonu 3 CTNNB1 genu kodujícího β-katenin. Jak imunoprofil, tak molekulárně genetické vlastnosti jsou shodné se SPT pankreatu, což jsme spolu s morfologickým překryvem považovali za průkaz, že jde o příbuzné tumory. Nazvali jsme tento tumor Pankreatický analog solidního pseudopapilárního tumoru paratestikulární oblasti (PA-SPT) a tento případ byl odpublikován jako case report [5]. Krátce na to jsme obdrželi 3 případy testikulárních tumorů, které se skládaly pouze ze solidní komponenty, jinými slovy, byly histologicky identické se SPT pankreatu. Zkoušeli jsme do v mikroskopu naslepo vkládat tyto testikulárními tumory a pankreatické SPT a nebyly jsme schopni je lokalizovat, tumory byly jednoduše identické. Tyto 3 případy nás ujistily, že PA-SPT není osamocen a že tyto případy vážně existují. Rozhodli jsme se proto dále podrobně zkoumat, co všechno ještě mají pankreatické SPT společného s testikulárními tumory. V plzeňském registru nádorů jsme nechali vyhledat všechny dostupné SPT pankreatu (22 případů) a všechny zrevidovali s cílem objevit další společné znaky. 19/22 SPT pankreatu obsahovalo prstenčité buňky, což dokazuje, že jde o jejich charakteristický, a dá se říci konstantní znak. Když jsme dali do souvislosti výše popsané postřehy, uvědomili jsme si, že PA-SPN je stejný jako SPT pankreatu, kromě toho, že obsahuje komponentu prstenčitých buněk. Nicméně, jak jsme se později přesvědčili, prstenčité buňky jsou charakteristické i pro SPT pankreatu. Nabízela se tedy hypotéza, že SPT pankreatu mají možná nějakou souvislost s primárními stromálními tumory varlete z prstenčitých buněk (PSTVPB).

Tato hypotéza se stala předmětem našeho výzkumu. Od dob popisu prvního případu PSTVPB [39] jsme nashromáždili 13 případů těchto tumorů, které jsme zařadili do studie. Velikost primárních tumorů se pohybovala mezi 0,5 a 2 cm (průměr 1,2). Histologicky by se daly rozdělit do dvou skupin: 7 případů se skládalo pouze z prstenčité komponenty, stejné, jakou disponoval PA-SPT (tzv. čisté tumory) a 6 případů vykazovalo jak komponentu prstenčitých buněk tak solidní, neprstenčitou. Jinými slovy, druhá skupina tumorů měla histologicky velmi blízko k PA-SPT. Všechny tumory byly vyšetřeny imunohistochemicky

(IHC) a molekulárně geneticky a výsledky následně porovnány s pankreatickými SPT a jedním případem PA-SPT. IHC reagovaly PSTVPB pozitivně s β-kateninem, cyklinem D1 (nukleární pozitivita u obou), CD10, vimentinem, galektinem-3, klaudinem7, α-1-antitrypsinem, CD56, NSE a negativně s chromograninem, sex-cor markery (inhibinem, kalretininem, SF-1 a FOXL2), NANOG, OCT3/4 a SALL4. Molekulárně genetická analýza u všech tumorů, které byly vyšetřitelné (10 případů), detekovala mutace v exonu 3 CTNNB1 genu kodujícího β-katenin. Z výsledků je zřejmé, že PA-SPT a PSTVPB reprezentují morfologické spektrum stejné jednotky a že obě skupiny mají vztah k SPT pankreatu. Otázkou zůstává, co znamená primární stromální tumor z prstenčitých buněk varlete a proč i tento nemá svůj protějšek v pankreatu? Rozdíl mezi testikulárními a pankreatickými tumory je v jejich velikosti: zatímco tumory varlete jsou malé (0,5-2 cm u tumorů v této studii), pankreatické tumory jsou typicky velké. Všechny „čisté“ tumory varlete z prstenčitých buněk měly nejmenší velikost (největší měřil 0,9 cm). Myslíme si, že „čisté“ tumory z prstenčitých buněk představují iniciální růstovou fázi a jak tumor roste, objevuje se i solidní komponenta, která se zvětšující se velikostí převažuje. Tato hypotéza může být podpořena jedním případem PA-SPT, který byl mnohem větší než PSTVPB (téměř 5 cm) a jak jsme demonstrovali, solidní komponenta byla velmi dobře vyvinuta. Protože SPT pankreatu jsou resekovány objemné, pravděpodobně u nich „prstenčité“ stadium mineme a vidíme pouze solidní komponentu. Nemáme osobně v registru jediný malý SPT pankreatu a tak naše domněnka nemůže být věrohodně doložena. SPT byl již popsán v i ovariu [40-43] a v nedávné době byl publikován jeden případ ovariálního stromálního ovariálního tumoru z prstenčitých buněk [44], který byl imunohistochemicky i geneticky identický s případy námi popisovanými testikulárními případy.

Na základě našich výsledků předpokládáme, že SPT pankreatu, ovaria, PA-SPT a primární stromální tumor z prstenčitých buněk varlete a ovaria představují identickou jednotku vyskytující se v různých orgánech. Domníváme se, že primární stromální tumor z prstenčitých buněk varlete, ovaria a pravděpodobně i pankreatu představuje iniciální růstovou fázi SPT.

Práce je přijata k publikaci v Human Pathology:

Date: Jul 04, 2017
To: "Kvetoslava Michalova" peckova.kveta@gmail.com
From: Vincenzo Eusebi eesserver@eesmail.elsevier.com
Reply To: Vincenzo Eusebi vincenzo.eusebi@unibo.it
Subject: Editor Decision YHUPA-D-17-00292R1

Ms. Ref. No.: YHUPA-D-17-00292R1
Title: Primary Signet Ring Stromal Tumor of the Testis: A Study of 13 Cases Indicating Their Phenotypic and Genotypic Analogy to Pancreatic Solid Pseudopapillary Neoplasm.
Human Pathology

Dear Dr. Michalova,

I am pleased to confirm that your paper "Primary Signet Ring Stromal Tumor of the Testis: A Study of 13 Cases Indicating Their Phenotypic and Genotypic Analogy to Pancreatic Solid Pseudopapillary Neoplasm." has been accepted for publication in Human Pathology.

Comments from the Editor and Reviewers are appended below if available.
You should receive galley proofs from the publisher in a few weeks.

Please have all authors sign and date the authors' signature form and send it to the editorial office via email (jmcostello2@wisc.edu) or fax (608-265-4393) as soon as possible. The form must be received before publication. A copy of the form can be downloaded at:
http://ees.elsevier.com/yhupa/img/Ethics_and_Financial_Conflict_Form.pdf

When your paper is published on ScienceDirect, you want to make sure it gets the attention it deserves. To help you get your message across, Elsevier has developed a new, free service called AudioSlides: brief, webcast -style presentations that are shown (publicly available) next to your published article. This format gives you the opportunity to explain your research in your own words and attract interest. You will receive an invitation email to create an AudioSlides presentation shortly. For more information and examples, please visit
http://www.elsevier.com/audioslides

Thank you for submitting your work to this journal.

With kind regards,

Vincenzo Eusebi, M.D.
Pathologist
Human Pathology

Comments from the Editors and Reviewers:

Elsevier Editorial System(tm) for Human Pathology

Manuscript Draft

Manuscript Number: YHUPA-D-17-00292R1

Title: Primary Signet Ring Stromal Tumor of the Testis: A Study of 13 Cases Indicating Their Phenotypic and Genotypic Analogy to Pancreatic Solid Pseudopapillary Neoplasm.

Article Type: Original Article

Keywords: testis; pancreas; primary signet ring stromal tumor; solid pseudopapillary neoplasm; analogue

Corresponding Author: Dr. Kvetoslava Michalova,

Corresponding Author's Institution:

First Author: Kvetoslava Michalova, M.D.

Order of Authors: Kvetoslava Michalova, M.D.; Kvetoslava Michalova; Michael Michal Jr., M.D.; Dmitry V Kazakov, M.D.; Monika Sedivcova; Ondrej Hes, M.D.; Ladislav Hadravsky, M.D.; Abbas Agaimy, M.D.; Maria Tretiakova, M.D.; Carlos Bacchi, M.D.; Arndt Hartmann, M.D.; Naoto Kuroda, M.D.; Stela Bulimbasic, M.D.; Marijana Coric, M.D.; Tatjana Antic, M.D.; Michal Michal, M.D.

Abstract: Primary signet ring stromal tumor of the testis (PSRSTT) is an extremely rare tumor described only twice in the literature. Pancreatic-analogue solid pseudopapillary neoplasm (SPN) of the testis is a recently reported entity with morphological overlap with PSRSTT. We reviewed our files to find all cases of PSRSTT in order to better characterize this entity. We studied 13 cases of PSRSTTs using histological, immunohistochemical (IHC) and molecular genetic methods and compared the results with pancreatic SPN. Grossly, the size of PSRSTTs ranged from 0.5 to 2 cm (mean 1.1). Microscopically, PSRSTTs predominantly showed a proliferation of low-grade epithelioid cells containing characteristic cytoplasmic vacuole dislodging the nucleus (signet ring cells) separated by fibrous septa into trabeculae and nests. The immunoprofile was characterized by immunoreactivity for β-catenin, cyclin D1 (nuclear positivity for both antibodies), CD10, vimentin, galectin 3, claudin7, α-1-antitrypsin, CD56, NSE and negativity with chromogranin, inhibin, calretinin, SF-1, NANOG, OCT3/4 and SALL4. In some cases, the IHC panel was restricted due to a limited amount of tissue. Molecular genetic analysis revealed mutations within exon 3 of the CTNNB1 encoding β-catenin in all analyzable cases. Based on histological similarities between pancreatic SPN and PSRSTT and their identical IHC and molecular genetic features, we assume that both neoplasms share the same pathogenesis and thus PSRSTT can be considered as a testicular analogue of pancreatic SPN.

Primary Signet Ring Stromal Tumor of the Testis: A Study of 13 Cases Indicating Their Phenotypic and Genotypic Analogy to Pancreatic Solid Pseudopapillary Neoplasm.

Running head: Primary Signet Ring Stromal Tumor of the Testis.

Kvetoslava Michalova, M.D. - Department of Pathology, Faculty of Medicine in Pilsen, Charles University, Biopticka laborator s.r.o., Plzen, Czech Republic

Michael Michal Jr, M.D. - Department of Pathology, Faculty of Medicine in Pilsen, Charles University, Biopticka laborator s.r.o., Plzen, Czech Republic, Prague and Biomedical Center, Faculty of Medicine in Pilsen, Charles University, Czech Republic

Dmitry V. Kazakov, M.D. - Department of Pathology, Faculty of Medicine in Pilsen, Charles University, Biopticka laborator s.r.o., Plzen, Czech Republic

Monika Sedivcova - Biopticka laborator s.r.o., Plzen, Czech Republic

Ondrej Hes, M.D. -Department of Pathology, Faculty of Medicine in Pilsen, Charles University, Biopticka laborator s.r.o., Plzen, Czech Republic

Ladislav Hadravsky, M.D. - Department of Pathology, Charles University, 3rd Medical Faculty and Charles University Hospital Royal Vineyards, Prague, Czech Republic

Abbas Agaimy, M.D. – Institute of Pathology, University Hospital Erlangen, Friedrich-Alexander University Erlangen-Nürnberg, Erlangen, Germany

Maria Tretiakova, M.D. -Department of Pathology, University of Washington, Seattle, USA

Carlos Bacchi, M.D. - Consultoria em Patologia, Botucatu, SP, Brazil

Arndt Hartmann, M.D. - Institute of Pathology, University Hospital Erlangen, Friedrich-Alexander University Erlangen-Nürnberg, Erlangen, Germany

Naoto Kuroda, M.D. -Department of Diagnostic Pathology, Kochi Red Cross Hospital, Kochi, Japan

Stela Bulimbasic, M.D. - Department of Pathology, University Hospital Centre, Zagreb, Croatia

Marijana Coric, M.D. -Department of Pathology, University Hospital Centre, Zagreb, Croatia

Tatjana Antic, M.D. - Department of Pathology, The University of Chicago, Chicago, USA

Michal Michal, M.D. - Department of Pathology, Faculty of Medicine in Pilsen, Charles University, Biopticka laborator s.r.o., Plzen, Czech Republic

Address for correspondence: Kvetoslava Michalova M.D., Department of Pathology, Charles University, Medical Faculty and Charles University Hospital Plzen, Alej Svobody 80, 304 60 Plzen, Czech Republic. Email: kveta.michalova@biopticka.cz

Abstract

Primary signet ring stromal tumor of the testis (PSRSTT) is an extremely rare tumor described only twice in the literature. Pancreatic-analogue solid pseudopapillary neoplasm (SPN) of the testis is a recently reported entity with morphological overlap with PSRSTT. We reviewed our files to find all cases of PSRSTT in order to better characterize this entity. We studied 13 cases of PSRSTTs using histological, immunohistochemical (IHC) and molecular genetic methods and compared the results with pancreatic SPN. Grossly, the size of PSRSTTs ranged from 0.5 to 2 cm (mean 1.1). Microscopically, PSRSTTs predominantly showed a proliferation of low-grade epithelioid cells containing characteristic cytoplasmic vacuole dislodging the nucleus (signet ring cells) separated by fibrous septa into trabeculae and nests. The immunoprofile was characterized by immunoreactivity for β-catenin, cyclin D1 (nuclear positivity for both antibodies), CD10, vimentin, galectin 3, claudin7, α-1-antitrypsin, CD56, NSE and negativity with chromogranin, inhibin, calretinin, SF-1, NANOG, OCT3/4 and SALL4. In some cases, the IHC panel was restricted due to a limited amount of tissue. Molecular genetic analysis revealed mutations within exon 3 of the *CTNNB1* encoding β-catenin in all analyzable cases. Based on histological similarities between pancreatic SPN and PSRSTT and their identical IHC and molecular genetic

features, we assume that both neoplasms share the same pathogenesis and thus PSRSTT can be considered as a testicular analogue of pancreatic SPN.

Introduction

Primary signet ring stromal tumor of the testis (PSRSTT) was first described in 2005 by Michal et al. [1] and subsequently by Kuo et al [2] as single case reports. Microscopically, both tumors were characterized by the proliferation of low-grade epithelioid cells containing characteristic cytoplasmic vacuole dislodging the nucleus to the periphery of the cells (signet ring cells) which were separated by fibrous septa resulting in a trabecular and/or nested architecture [1]. Pancreatic solid pseudopapillary neoplasm (SPN) is a rare tumor with uncertain histogenesis traditionally encountered in the pancreas [3]. However, recent small series and several case reports have described an ovarian tumor identical to that seen in the pancreas [4-8] and, most recently, a pancreatic analogue solid pseudopapillary neoplasm of the testis (PA-SPN) has been described by our group [9]. Microscopically, PA-SPN consisted of two distinct components: a signet ring cell component histologically identical to that seen in the primary signet ring stromal tumor of the testis blending with a component identical to pancreatic SPN by

showing a solid (and in minor parts also pseudopapillary) component comprised by poorly cohesive low grade cells with eosinophilic cytoplasm. The purpose of this study is to morphologically, immunohistochemically and molecular genetically investigate 13 cases of primary signet ring stromal tumors of the testis and compare their features with pancreatic SPN and with one published case of PA-SPN [9] in order to establish their possible pathogenetic relationship.

Materials and Methods

Cases cross-matching the keywords „testis“, „signet ring stromal tumor”, „ unclassified sex-cord tumor“, „male adnexal tumor of probable Wolffian origin“, „Sertoli cell tumor, benign, NOS“ were retrieved from the Plzen tumor registry; they came from the period 1993-2017. Additional cases were retrieved from the routine and consultation files of the authors. Upon reevaluation, 13 cases of primary testicular tumors that fulfilled the diagnostic criteria for this study were selected. The clinical information was extracted from the registry records, and follow-up data obtained from attending clinicians. In all but 2 cases, paraffin blocks or unstained reserve slides were available for the study. To compare PSRSTT with SPN we reviewed 20 pancreatic cases from Plzen tumor registry. For conventional microscopy, tissues were fixed in formalin, routinely processed and stained with hematoxylin-eosin (H&E).

Immunohistochemistry

The IHC analysis was performed using a Ventana BenchMark ULTRA (Ventana Medical System, Inc., Tucson, Arizona). The list of antibodies and basic technical specifications are summarized in the Table 1. Due to the limited amount of tissue blocks or reserve slides the utilization of the entire immunohistochemical panel was restricted. Following stains (β-catenin, CD10, CD56, NSE, inhibin, calretinin, S100, OSCAR) were performed on most cases, whereas additional stains (vimentin, synaptophysin, chromogranin, SF-1, OCT3/4, SALL4, NANOG, cyclin D1, AE1/3, galectin 3, MIB-1, claudin 5, claudin 7, α-1-antitrypsin) were applied in only a few of them. Antibodies were visualized using the enzymes alkaline phosphatase or peroxidase as detecting systems (both purchased from Ventana Medical System, Inc., Tucson, Arizona).

Molecular Genetic Analysis of the β-Catenin Gene

Mutational analysis of exon 3 of the CTNNB1 gene was performed via polymerase chain reaction and direct sequencing as described previously [10].

Results

Clinical features

The clinical features are summarized in the Table 2. The age of the patients at the time of diagnosis ranged from 23 to 58 years (mean 39, median 35). Follow-up was available for 5 patients. One patient died of unrelated disease (prostatic adenocarcinoma). The remaining patients were alive and well without progression, recurrence or evidence of metastatic disease. None of the patients had a tumor in the pancreas and/or suffered from familiar adenomatous polyposis (FAP).

Gross and microscopic findings

Grossly, the tumors were predominantly well circumscribed and encapsulated, solid and grey in color. No cystic or necrotic foci were noted. The size of the tumors ranged from 0.5 to 2 cm (mean 1.1, median 1). 12/13 tumors were located in the testis (Figure 1A), the remaining tumor was paratesticular. All tumors were unilateral. Microscopically, all of them showed a signet ring cell population. Signet ring cells were characterized as monomorphic rounded epithelioid cells which contained single, large cytoplasmic vacuoles (Figure 1B). These vacuoles compressed and displaced the nuclei, which caused some nuclei to acquire a crescent shape, while others retained an original round shape. Signet ring cells were separated by fibrous septa into trabeculae and nests, which sometimes resulted in an Indian file appearance reminiscent of metastatic signet ring cell carcinomas. Beside the signet ring cell proliferation, six tumors contained a trabecular, nested or solid, non-signet ring cell component consisting of benign looking cells with

eosinophilic cytoplasm (Figure 2A-E). Both components were often intermixed, with the signet ring cell component gradually blending with non-signet ring areas (Figure 2F). The smallest tumor containing both components measured 0.9 cm in largest dimension.

Cellular atypia was absent and mitoses were extremely rare in both components. Nuclei were uniform, with finely dispersed chromatin and occasional grooves. Focally, hyaline PAS-positive globules were intermingled within tumors in four cases (Figure 3). The adjacent non-neoplastic testis was devoid of germ cell neoplasia in situ or any other pathologic changes.

After reviewing of 20 cases of pancreatic SPN we found a signet ring cell component in 17 neoplasms and it was morphologically identical to the one seen in PSRSTT.

Immunohistochemistry

The IHC findings are summarized in Table 3. Neoplastic cells in all studied tumors reacted diffusely with antibodies to β-catenin, cyclin D1 (nuclear positivity for both antibodies) CD10, vimentin, galectin-3, claudin7 and α-1-antitrypsin (Fig 4A-C). CD56 was diffusely positive in 5/9 analyzable cases, whereas in the remaining 4 cases immunoreactivity was focal. Neuron specific enolase (NSE) was diffusely positive in 6/7 cases and reacted focally in the remaining case. Expression of synaptophysin, S100 protein, pan-cytokeratins (AE1/3, OSCAR), claudin 5 was

variable and there was no expression of chromogranin, inhibin, calretinin, SF-1, NANOG, OCT3/4, and SALL4 (Fig 4D).

Mutations in Exon 3 of the CTNNB1 gene

The molecular genetic features are summarized in Table 4 and examples are depicted in Figure 5A-C. In all (10/10) analyzable cases, a mutation was detected in exon 3 of the *CTNNB1*. 2 cases revealed mutation c.98C>G (p.Ser33Cys), 2 cases c.110C>T (p.Ser37Phe), 1 case c.110C>G (p.Ser37Cys), 1 case c.94G>T (p.Asp32Tyr), 1 case c.94G>C (p.Asp32His), 1 case c.94G>A (p.Asp32Asn), 1 case c.122C>T (p.Thr41Ile) and 1 case featured c.88_99del12 (p.Tyr30_Ser33del). The remaining 3 cases were not analyzable.

Discussion

Primary signet ring stromal tumor of the testis (PSRSTT) is an extremely rare tumor, with only 2 cases published so far. Both reported neoplasms were asymptomatic, unilateral and small in size (1 and 0.7 cm) and followed a benign clinical course without recurrence or metastasis [1, 2]. Histologically, both tumors were well circumscribed and demonstrated a monomorphic population of bland signet ring cells separated by fibrous septa into trabeculae and nests [1, 2]. Immunohistochemically, the tumor cells in both cases reacted with vimentin and

were negative with cytokeratin, epithelial membrane antigen (EMA), inhibin, estrogen and progesterone receptors.

Pancreatic solid pseudopapillary neoplasm (SPN) is a rare tumor [11] usually affecting young adults (mean age 28 y) with a striking female predominance (F:M ratio 10:1). When clinically apparent, it is usually large. Pancreatic SPN is generally considered as a tumor with an indolent behavior, although some neoplasms may pursue an aggressive course, causing on rare occasions death of the patients [12]. Microscopically, they are characterized by poorly cohesive monomorphic bland tumor cells growing in a solid, and focally, pseudopapillary fashion (as a result of cellular discohesion and necrosis). The diagnosis can be confirmed by the typical coexpression of β-catenin (nuclear positivity), CD10, vimentin, galectin-3, CD 56, NSE, cyclin D1 (nuclear positivity) and α -1-antitrypsin in addition to the negative reaction with chromogranin in most cases. Sex-cord markers and smooth muscle markers are not expressed by pancreatic SPN [13].

Extrapancreatic primary SPN is a rare entity. There have been few isolated case reports and one small series of SPN arising outside the pancreas and without the presence of an ectopic pancreatic tissue at the site of occurrence: 9 cases were recorded arising primarily in the ovary [4-7, 14], and one case of testicular tumor has recently been reported by our group [9]. The tumor was described under the

name “pancreatic analogue solid pseudopapillary neoplasm arising in paratesticular location”. In fact, although the bulk of the tumor originally seemed to be paratesticular in location, recently after making a large amount of recuts for educational purposes, in the deeper levels was evident that it originated in testicular parenchyma. Accordingly, we will use the name “pancreatic analogue solid pseudopapillary neoplasm of the testis” (PA-SPN) instead of the original term. Microscopically, PA-SPN exhibits two distinct components, namely a signet ring cell component indistinguishable from that occurring in the aforementioned PSRSTT and a solid (and in minor parts also pseudopapillary) component of poorly cohesive low grade cells with eosinophilic cytoplasm identical to that seen in pancreatic SPN. Clusters of foamy macrophages, deposits of hemosiderin, and small foci of oncocytic change were sporadically found within the solid areas and hyaline PAS-positive globules were scattered between tumor cells in both components. Such features are well described in the pancreatic SPN [15, 16]. Owing to the very pronounced signet ring cell component in the PA-SPN, we came to the idea that the PSRSTT might belong into the same category.

For this purpose, we have collected 13 cases of PSRSTT which are included in this study. While 7 of them featured only the signet ring component, the remaining 6 cases exhibited both signet ring cell and solid non-signet ring cell components in various proportions. These cases with both components were morphologically

similar to the PA-SPN. The immunoprofile of PSRSTT included positivity with β-catenin, cyclin D1 (both nuclear), CD10, NSE, CD56, α -1-antitrypsin, vimentin, galectin – 3, claudin 7 and negativity for chromogranin, sex-cord markers and germ cell markers. In some cases, the IHC panel was restricted due to a limited amount of tissue. These striking IHC similarities between PSRSTT and PA-SPN provide indirect evidence that these tumors are very closely related if not entirely identical.

An oncogenic somatic mutation in exon 3 of the *CTNNB1* (β-catenin) gene has been found in pancreatic SPN [17] and recently detected in ovarian solid pseudopapillary neoplasm [14] and PA-SPN [9], thus linking them at the molecular genetic level, in addition to morphological similarities. β-catenin is a key regulatory molecule of the Wnt signaling pathway, which is important for cell homeostasis, differentiation and proliferation and its activity is tightly regulated [18]. β-catenin is activated by Wnt binding, after which it is transferred to the nucleus where it works as a transcriptional cofactor. In the absence of Wnt, β-catenin remains in the cytoplasm where it is rapidly degraded by the destruction complex containing among others adenomatous polyposis coli (APC) protein [18]. Missense mutations of β-catenin lead to an abnormal stabilization and nuclear overexpression of its protein, which can be highlighted immunohistochemically. In the current study, all analyzable cases of PSRSTT revealed a mutation in exon 3 of the *CTNNB1* gene. The family of β-catenin driven neoplasia is gradually growing and include among

variety of epithelial neoplasms and continuously enlarging group of soft tissue neoplasms also parenchymal lesions of uncertain histogenesis. To the former category belong neuromuscular choristomas [19] and to the latter sclerosing hemangioma of the lung, calcifying nested stromal epithelial tumor of the liver, microcystic stromal tumor of the ovary [20, 21], and pancreatic SPN together with SPN of the ovary [18]. Our study adds to this list primary signet ring stromal tumor of the testis and PA-SPN.

We retrieved 20 pancreatic SPN from our files in order to determine the frequency of a signet ring cell component in these tumors. This was found in 17/20 cases, indicating that this feature is one of the morphological characteristics of pancreatic SPNs. Because all pure PSRSTTs were the smallest tumors in our series, we hypothesize that testicular examples that have mostly a signet ring cell component represent neoplasms in the incipient growth of phase, and as the lesions grow solid areas with trabecular or pseudopapillary arrangement typical for pancreatic SPN develop. This hypothesis can be further supported by the PA-SPN as its size (nearly 5 cm) was significantly larger than PSRSTTs and the solid, SPN-like component was here very well developed.

There is no consensus regarding the line of differentiation of pancreatic SPN. It is traditionally classified as an epithelial neoplasm, however, the cytokeratin expression is rare and mostly absent. Thus the origin and phenotypic relationship of

pancreatic SPN tumor cells to the pancreatic tissue still remains enigmatic [13]. Kosmahl et al in their study suggested an extrapancreatic origin of solid pseudopapillary neoplasms. Genital ridges are very close to the pancreatic anlage during embryogenesis, allowing the possibility that cells from the primitive gonads may migrate to the developing pancreas [13]. This theory has been discussed for mucinous cystic neoplasms and serous microcystic adenomas of the pancreas and may be also valid for pancreatic SPN [22, 23]. The occurrence of the herein discussed cases in the testicular area together with the previously published cases in the ovary may serve as arguments in favor for this theory.

In the differential diagnosis, distinction from Sertoli cell tumor NOS is the most interesting. It is our view that in the past PSRSTTs were diagnosed as Sertoli cell tumor NOS, as this category included even cases that were immunohistochemically negative for sex-cord markers inhibin, calretinin and SF-1 [24]. It seems to us that immunohistochemically inhibin, calretinin and SF-1 negative testicular tumors with signet ring cell histology that featured positive immunoreactivity for β-catenin, cyclin D1 (both nuclear), CD10, NSE, CD56, α -1-antitrypsin, vimentin, galectin – 3, claudin 7 and negativity for chromogranin represented in fact PSRSTTs and not Sertoli cell tumors of any kind. Real testicular tumors with Sertoli cell differentiation are in our view mostly immunohistochemically positive for sex-cord markers such as inhibin and calretinin ,SF-1 or FOXL2 [25].

It is not our intention to question the entity of Sertoli cell tumors, but rather to set apart morphologically well-defined group of tumors with consistent IHC and molecular characteristics which we think deserves separation from the rather heterogeneous category of Sertoli cell tumors, NOS.

In conclusion, we have described a series of primary signet ring stromal tumors of the testicular region showing morphologic, immunohistochemical and molecular genetic overlap with PA-SPN. We believe that primary signet ring stromal tumor of the testis and SPN of the pancreas, ovary and pancreatic analogue SPN of the testis are similar tumors probably represening a single entity occurring in different organs. We further think that the recently published case of a 1.1 cm large signet ring stromal cell tumor of the ovary with *CTNNB1* mutation and vimentin, cyclin D1, CD10, β-catenin immunohistochemical positivity and cytokeratins, calretinin, EMA and inhibin negativity is the ovarian counterpart of PSRSTT and represents incipient growth phase of ovarian SPN [26].

Our concept was further strengthened by a recently published letter to the editor by Mengoli et al. The authors reported another 2 identical cases with the same results and conclusion [27, 28]. Notwithstanding, we acknowledge that the final proof that PSRSTT is identical to pancreatic SPN will bring only the genetic comparison of these two entities.

It is not our intention to question the entity of Sertoli cell tumors, but rather to set apart morphologically well-defined group of tumors with consistent IHC and molecular characteristics which we think deserves separation from the rather heterogeneous category of Sertoli cell tumors, NOS.

In conclusion, we have described a series of primary signet ring stromal tumors of the testicular region showing morphologic, immunohistochemical and molecular genetic overlap with PA-SPN. We believe that primary signet ring stromal tumor of the testis and SPN of the pancreas, ovary and pancreatic analogue SPN of the testis are similar tumors probably represening a single entity occurring in different organs. We further think that the recently published case of a 1.1 cm large signet ring stromal cell tumor of the ovary with *CTNNB1* mutation and vimentin, cyclin D1, CD10, β-catenin immunohistochemical positivity and cytokeratins, calretinin, EMA and inhibin negativity is the ovarian counterpart of PSRSTT and represents incipient growth phase of ovarian SPN [26].

Our concept was further strengthened by a recently published letter to the editor by Mengoli et al. The authors reported another 2 identical cases with the same results and conclusion [27, 28]. Notwithstanding, we acknowledge that the final proof that PSRSTT is identical to pancreatic SPN will bring only the genetic comparison of these two entities.

References:

1. Michal M, Hes O, Kazakov DV. Primary signet-ring stromal tumor of the testis. Virchows Arch 2005; 447, 107-110.
2. Kuo CY, Wen MC, Wang J, Jan YJ. Signet-ring stromal tumor of the testis: a case report and literature review. Hum Pathol 2009; 40, 584-587.
3. Seo HE, Lee MK, Lee YD, et al. Solid-pseudopapillary tumor of the pancreas. J Clin Gastroenterol 2006; 40, 919-922.
4. Deshpande V, Oliva E, Young RH. Solid pseudopapillary neoplasm of the ovary: a report of 3 primary ovarian tumors resembling those of the pancreas. Am J Surg Pathol 2010; 34, 1514-1520.
5. Cheuk W, Beavon I, Chui DT, Chan JK. Extrapancreatic solid pseudopapillary neoplasm: report of a case of primary ovarian origin and review of the literature. Int J Gynecol Pathol 2011; 30, 539-543.
6. Stoll LM, Parvataneni R, Johnson MW, et al. Solid pseudopapillary neoplasm, pancreas type, presenting as a primary ovarian neoplasm. Hum Pathol 2012; 43, 1339-1343.
7. He S, Yang X, Zhou P, Cheng Y, Sun Q. Solid pseudopapillary tumor: an invasive case report of primary ovarian origin and review of the literature. Int J Clin Exp Pathol 2015; 8, 8645-8649.
8. Syriac S, Kesterson J, Izevbaye I, et al. Clinically aggressive primary solid pseudopapillary tumor of the ovary in a 45-year-old woman. Ann Diagn Pathol 2012; 16, 498-503.
9. Michal M, Bulimbasic S, Coric M, et al. Pancreatic analogue solid pseudopapillary neoplasm arising in the paratesticular location. The first case report. Hum Pathol 2016; 56, 52-56.
10. Kazakov DV, Sima R, Vanecek T, et al. Mutations in exon 3 of the CTNNB1 gene (beta-catenin gene) in cutaneous adnexal tumors. Am J Dermatopathol 2009; 31, 248-255.
11. Klimstra DS, Wenig BM, Heffess CS. Solid-pseudopapillary tumor of the pancreas: a typically cystic carcinoma of low malignant potential. Semin Diagn Pathol 2000; 17, 66-80.
12. Estrella JS, Li L, Rashid A, et al. Solid pseudopapillary neoplasm of the pancreas: clinicopathologic and survival analyses of 64 cases from a single institution. Am J Surg Pathol 2014; 38, 147-157.
13. Kosmahl M, Seada LS, Janig U, Harms D, Kloppel G. Solid-pseudopapillary tumor of the pancreas: its origin revisited. Virchows Arch 2000; 436, 473-480.
14. Kominami A, Fujino M, Murakami H, Ito M. beta-catenin mutation in ovarian solid pseudopapillary neoplasm. Pathol Int 2014; 64, 460-464.
15. Goldstein J, Benharroch D, Sion-Vardy N, et al. Solid cystic and papillary tumor of the pancreas with oncocytic differentiation. J Surg Oncol 1994; 56, 63-67.
16. Meriden Z, Shi C, Edil BH, et al. Hyaline globules in neuroendocrine and solid-pseudopapillary neoplasms of the pancreas: a clue to the diagnosis. Am J Surg Pathol 2011; 35, 981-988.
17. Abraham SC, Klimstra DS, Wilentz RE, et al. Solid-pseudopapillary tumors of the pancreas are genetically distinct from pancreatic ductal adenocarcinomas and almost always harbor beta-catenin mutations. Am J Pathol 2002; 160, 1361-1369.
18. Agaimy A, Haller F. CTNNB1 (beta-Catenin)-altered Neoplasia: A Review Focusing on Soft Tissue Neoplasms and Parenchymal Lesions of Uncertain Histogenesis. Adv Anat Pathol 2016; 23, 1-12.
19. Carter JM, Howe BM, Hawse JR, et al. CTNNB1 Mutations and Estrogen Receptor Expression in Neuromuscular Choristoma and Its Associated Fibromatosis. Am J Surg Pathol 2016; 40, 1368-1374.
20. Irving JA, Young RH. Microcystic stromal tumor of the ovary: report of 16 cases of a hitherto uncharacterized distinctive ovarian neoplasm. Am J Surg Pathol 2009; 33, 367-375.
21. Irving JA, Lee CH, Yip S, et al. Microcystic Stromal Tumor: A Distinctive Ovarian Sex Cord-Stromal Neoplasm Characterized by FOXL2, SF-1, WT-1, Cyclin D1, and beta-catenin Nuclear Expression and CTNNB1 Mutations. Am J Surg Pathol 2015; 39, 1420-1426.
22. Compagno J, Oertel JE. Microcystic adenomas of the pancreas (glycogen-rich cystadenomas): a clinicopathologic study of 34 cases. Am J Clin Pathol 1978; 69, 289-298.

23. Compagno J, Oertel JE. Mucinous cystic neoplasms of the pancreas with overt and latent malignancy (cystadenocarcinoma and cystadenoma). A clinicopathologic study of 41 cases. Am J Clin Pathol 1978; 69, 573-580.
24. Moch H, Humphrey, P.A., Ulbright, T.M., Reuter, V.E. WHO Classification of Tumours of the Urinary System and Male Genital Organs. Fourth edition. 2016, p. 400.
25. Perrone F, Bertolotti A, Montemurro G, et al. Frequent mutation and nuclear localization of beta-catenin in sertoli cell tumors of the testis. Am J Surg Pathol 2014; 38, 66-71.
26. Kopczynski J, Kowalik A, Chlopek M, et al. Oncogenic Activation of the Wnt/beta-Catenin Signaling Pathway in Signet Ring Stromal Cell Tumor of the Ovary. Appl Immunohistochem Mol Morphol 2016; 24, e28-33.
27. Mengoli MC, Bonetti LR, Intersimone D, Fedeli F, Rossi G. Solid pseudopapillary tumor: a new tumor entity in the testis? Hum Pathol 2016.
28. Michalova K, Michal M, Kazakov DV, Michal M. Solid pseudopapillary tumor: a new tumor entity in the testis?-reply. Hum Pathol 2016.

Legends to Figures:

Figure 1: The tumors were well circumscribed and small in size (A). Signet ring cells were characterized as monomorphic rounded epithelioid cells which contained single, large and clear cytoplasmic vacuole compressing and displacing the nucleus, which caused some nuclei to acquire a crescent shape, while others retained an original round shape (B).

Figure 2: Signet ring cells component was characteristic feature of every case. Small tumors were composed entirely of signet ring cells (A). Beside the signet ring cell proliferation, larger tumors contained additional non-signet ring cell component arranged in solid (B), nested (C) or trabecular (D and E) fashion. The

components were often intermixed with the signet ring cell component gradually blending with a non-signet ring area (F).

Figure 3: Focally, hyaline PAS-positive globules were intermingled within tumors in four cases.

Figure 4: The immunoreaction with β-catenin was relatively strong and diffuse (A) and the positivity with this antibody was nuclear (B). All tested cases were positive with CD10 (C) and negative with calretinin (D).

Figure 5: The sequenogram data involving mutations in exon 3 of *CTNNB1* gene; used nomenclature NM_001904.3. Substitution c.94G>T, p.Asp32Tyr (A), substitution c.98C>G, p.Ser33Cys (B), substitution c.110C>G, p.Ser37Cys (C).

Figure 1

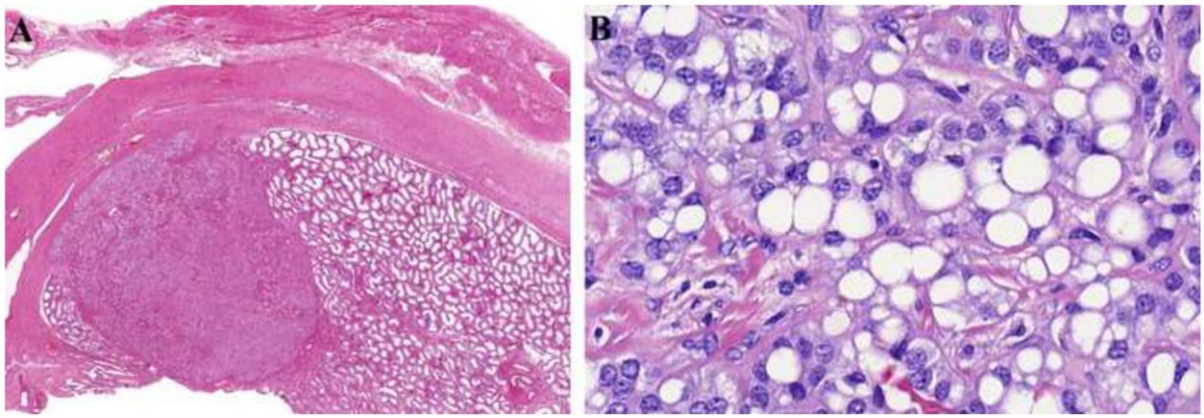

Figure 2

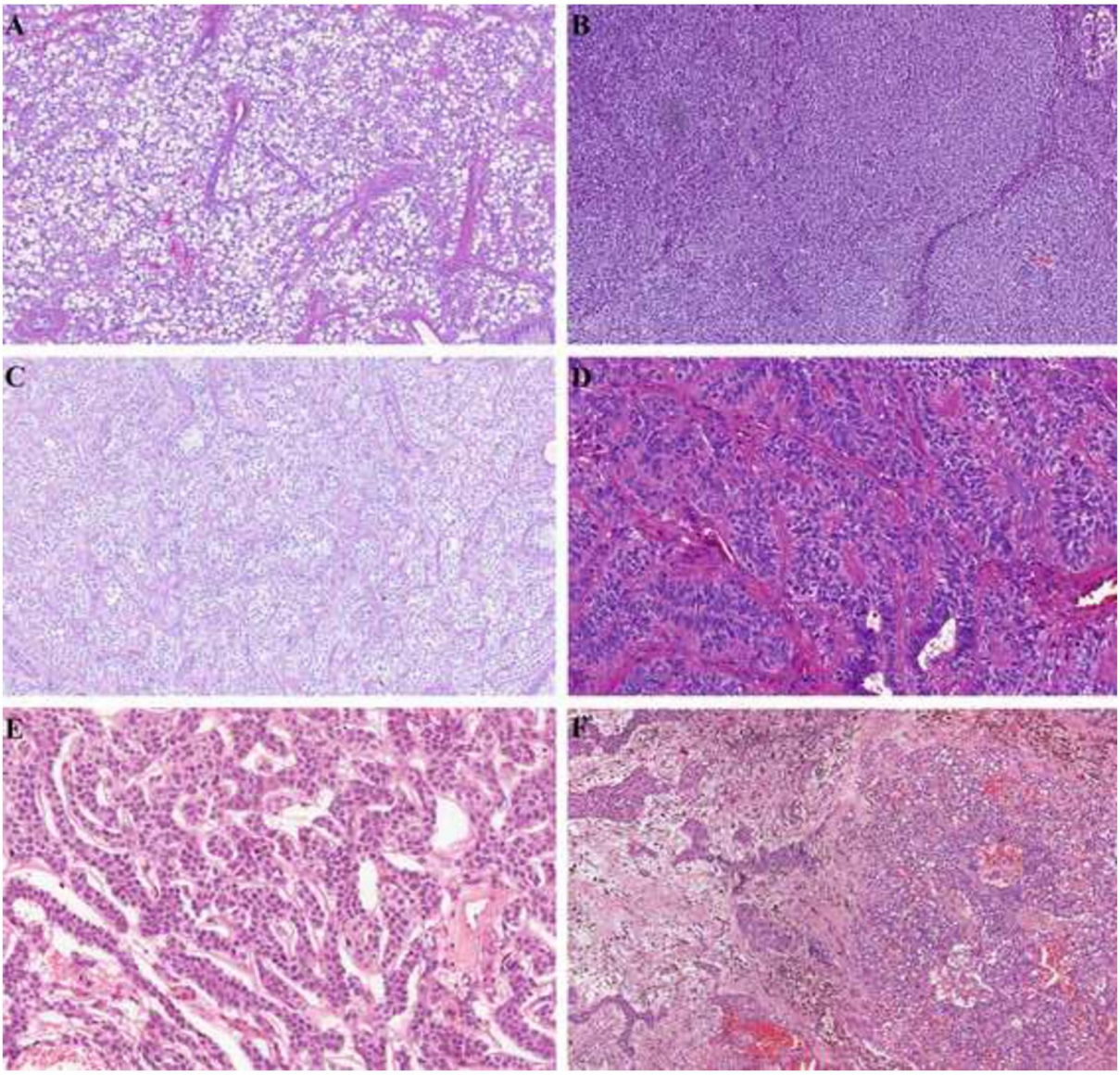

Figure 3

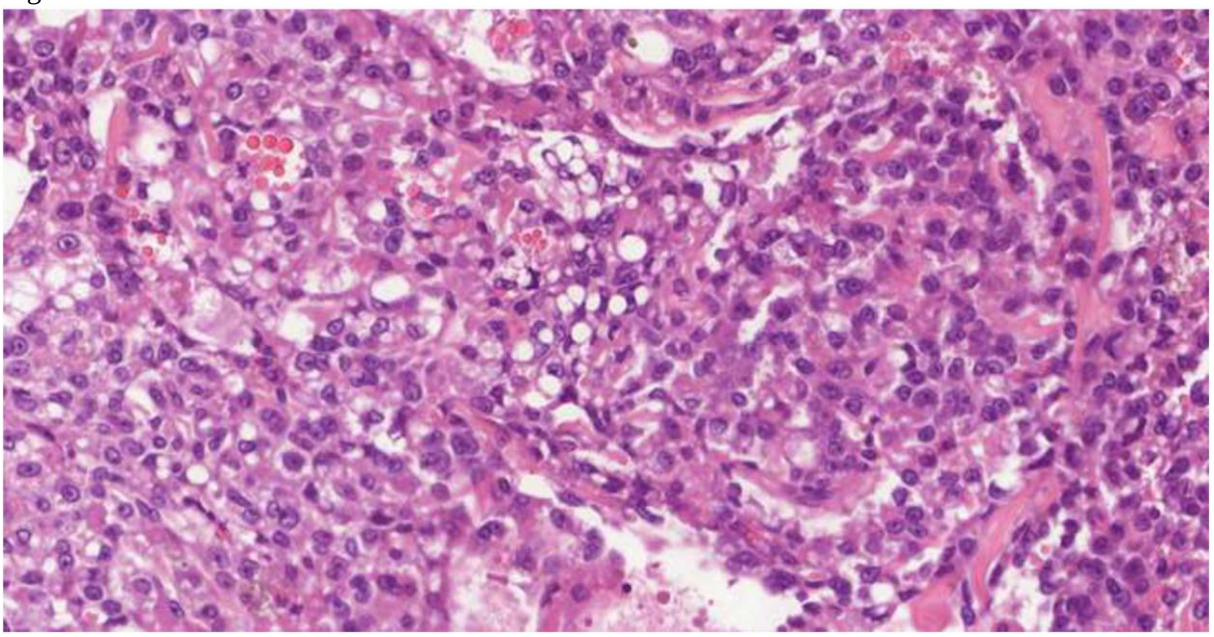

Figure 4

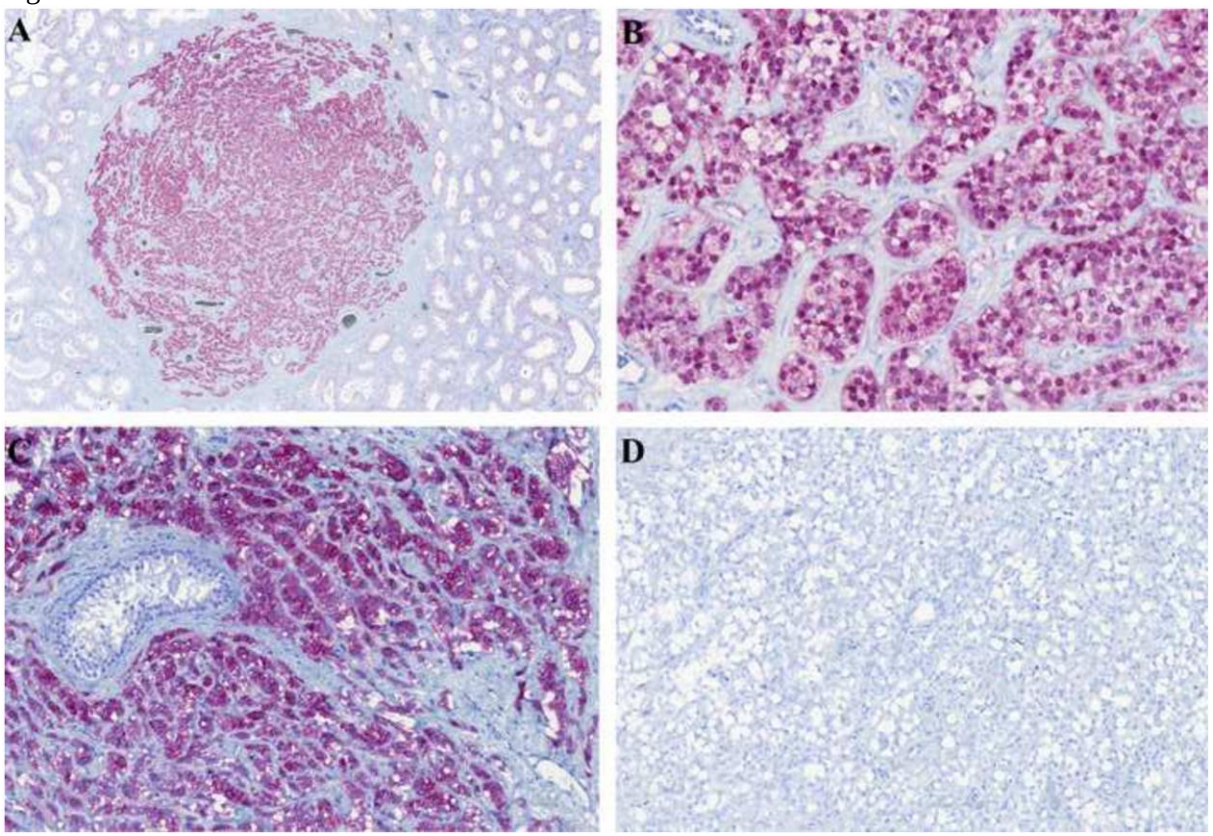

Figure 5

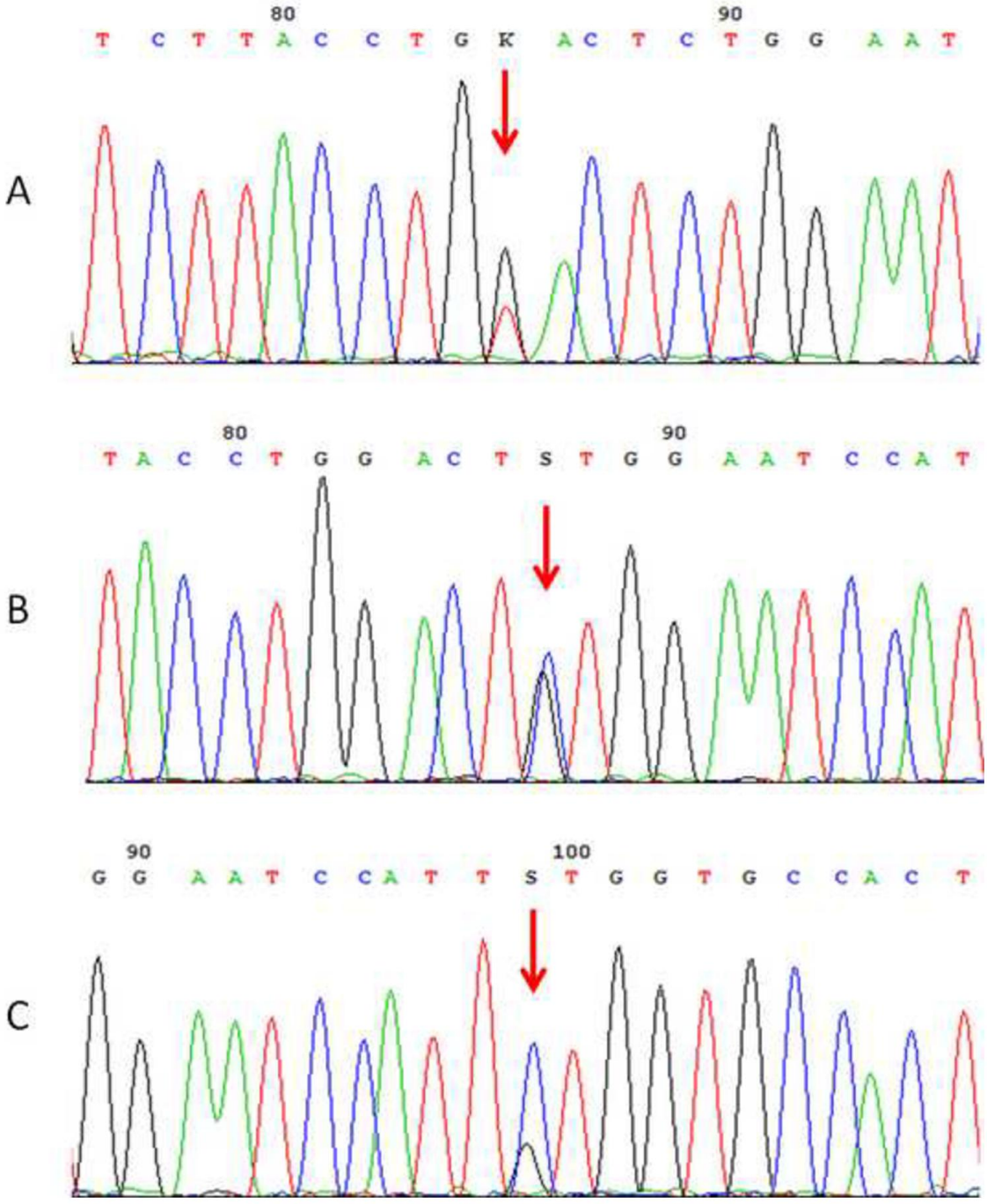
A
80
90
T C T T A C C T G K A C T C T G G A A T
B
80
90
T A C C T G G A C T S T G G A A T C C A T
C
90
100
G G A A T C C A T T S T G G T G C C A C T

Table 1: List of antibodies			
Antibody	**Clone**	**Manufacturer**	**Dilution**
β-catenin	polyclonal	Thermo Fischer Scientific, Freemont, CA, USA	1:150
CD10	SP67	Ventana Medical System, Inc., Tucson, Arizona, USA	RTU
Vimentin	V9	Cell Marque, Rocklin, CA, USA	RTU
CD56	MRQ-42	Cell Marque, Rocklin, CA, USA	RTU
Synaptophysin	SP11	Ventana Medical System, Inc., Tucson, Arizona, USA	RTU
Chromogranin	DAK-A3	Dako, Glostrup, Denmark	1:400
NSE	BBS/NC/VI-H14	Dako, Glostrup, Denmark	1:1000
Inhibin	R1	Ventana Medical System, Inc., Tucson, Arizona, USA	RTU
Calretinin	SP65	Ventana Medical System, Inc., Tucson, Arizona, USA	RTU
SF-1	N1665	R+D Systems, Minneapolis, Minnesota, USA	1:100
OCT3/4	N1NK	Novocastra, Newcastle, UK	RTU
SALL4	6,00E+03	Sigma-Aldrich, Saint Louis, MO, USA	1:800
NANOG	polyclonal	Abcam, Cambridge, UK	1:100
Cyclin D1	polyclonal	Thermo Fisher Scientific, Fremont, CA	1:100
S-100 protein	polyclonal	Ventana Medical System, Inc., Tucson, Arizona, USA	RTU
AE1-AE3	AE1/AE3/PCK26	Ventana Medical System, Inc., Tucson, Arizona, USA	RTU
OSCAR	IsoType:IgG2a	Covance, Emeryville, CA, USA	1:100
Galectin-3	9C4	Cell Marque, Rocklin, CA, USA	RTU
MIB 1	Ki-67	Dako, Glostrup, Denmark	1:400
Claudin 5	4C3C2	Invitrogen Corporation, Camarillo, CA, USA	1:100
Claudin 7	LS-B2918	LSBio, Seattle, WA, USA	1:200
α-1 -antitrypsin	polyclonal	Cell Marque, Rocklin, CA, USA	1: 200

Table 2: Clinicopathologic features				
Case	**Age**	**Size (cm)**	**Localisation**	**Follow-up**
PA-SPN	32	4,8x4x3	paratestis	AW in 1 yr FU
1	34	diam. 0.9	testis	NA
2	NA	diam. 0,5	testis	NA
3	NA	NA	testis	NA
4	55	2x1x1	paratestis	AW in 4 yrs FU
5	43	NA	testis	AW in 4 yrs FU
6	32	diam. 0.9	testis	AW in 6 yrs FU
7	57	NA	testis	NA
8	23	diam. 1	testis	NA
9	35	diam. 1	testis	NA
10	29	diam 1.2	testis	AW in 5 yrs FU
11	58	diam. 1	testis	Died from prostatic adenocarcinoma in 2001
12	29	diam. 2	testis	NA
13	35	0.8x0.7x0.6	testis	NA

Table 3: Immunohistochemical results

Case	β-cat	CD 10	Vim	CD 56	Syna	Chro	NSE	Inh	Calret	SF-1	OCT 3/4	SALL 4	NAN	Cyc D1	S100	AE1/3	OSC	Gal 3	MIB - 1	Clau 5	Clau 7	α-1-antitr
PA-SPN	+	+	+	Foc +	foc +	-	+	-	-	-	NP	-	-	+	+	foc +	+	+	NP	+	+	+
1	+	+	NP	foc +	+	NP	+	-	-	NP	NP	NP	NP	+	-	foc +	foc +	+	low	weak +	+	+
2	+	+	NP	foc +	-	-	NP	NP	NP	-	NP	NP	NP	NP	-	-	NP	NP	NP	NP	NP	NP
3	+	+	NP	foc +	-	NP	+	-	-	NP	NP	NP	NP	NP	-	NP	-	NP	NP	NP	NP	NP
4	+	+	NP	NP	-	NP	+	-	-	NP	NP	NP	NP	+	-	NP	foc +	NP	low	NP	NP	NP
5	NP	NP	NP	NP	NP	NP	NP	-	-	NP	-	-	-	NP	-	NP	NP	NP	NP	NP	NP	NP
6	+	+	+	+	NP	-	+	-	-	NP	NP	-	-	+	foc +	NP	foc +	NP	NP	NP	NP	NP
7	+	+	+	NP	+	NP	foc +	-	-	-	NP	NP	NP	NP	NP	NP	NP	NP	low	NP	NP	NP
8	NP	NP	NP	NP	NP	NP	NP	NP	NP	NP	NP	NP	NP	NP	NP	NP	NP	NP	NP	NP	NP	NP
9	+	+	NP	foc +	NP	NP	NP	-	-	NP	NP	NP	NP	NP	NP	NP	-	NP	NP	NP	NP	NP
10	+	+	+	+	NP	NP	NP	-	-	-	NP	NP	NP	NP	NP	NP	-	NP	NP	NP	NP	NP
11	+	+	+	+	-	NP	+	-	-	NP	NP	NP	NP	+	-	-	-	NP	NP	NP	NP	NP
12	+	weak +	+	+	NP	NP	NP	-	-	NP	NP	NP	NP	+	foc +	-	-	+	NP	-	+	+
13	+	+	NP	+	NP	NP	+	-	-	-	-	-	-	NP	NP	NP	foc +	NP	NP	NP	NP	NP

Table 4: Molecular genetic features	
Case	**Mutations in Exon 3 of the *CTNNB1* gene**
PA-SPN	c.101G>T (p.Gly34Val)

1	c.110C>T, p.Ser37Phe
2	c.88_99del12, p.Tyr30_Ser33del
3	c.122C>T, p.Thr41Ile
4	c.98C>G, p.Ser33Cys
5	c.110C>T, p.Ser37Phe
6	c.98C>G, p.Ser33Cys
7	NA
8	NA
9	c.110C>G, p.Ser37Cys
10	c.94G>T, p.Asp32Tyr
11	c.94G>C, p.Asp32His
12	NA
13	c.94G>A, p.Asp32Asn

SOLIDNÍ PSEUDOPAPILÁRNÍ TUMOR: NOVÁ NÁDOROVÁ JEDNOTKA VE VARLETI?

Koncept studie týkající se primárních stromálních tumorů varlete z prstenčitých buněk (popsáno v předchozí studii, str. 166) byl nedávno podpořen skupinou italských autorů, kteří reagovali na prvopopis PA-SPT. Formou dopisu editorovi přidali 2 případy testikulárních tumorů ve všech aspektech shodných s námi popisovanými případy a podpořili tak naši hypotézu, že PA-SPT a PSTVPB reprezentují distinktní jednotku analogickou SPT pankreatu.

Níže je přiložen jak dopis editorovi, tak naše odpověď na něj.

Human Pathology (2017) **62**, 242–247

ELSEVIER

Human PATHOLOGY

www.elsevier.com/locate/humpath

Correspondence

Solid pseudopapillary tumor: a new tumor entity in the testis?

To the Editor,

We greatly appreciated the case by Michal et al [1] reporting on a pancreatic analogue solid pseudopapillary tumor (SPT) of the paratesticular location. Analogously, we recently dealt with 2 cases arising in the right testis of a 60-year-old man and in the left testis of a 56-year-old man. The patients have an uneventful medical history, and the testicular nodules (1.5 and 3.2 cm, respectively) were incidentally disclosed during an ultrasound echosonography performed for hydrocele. Routine laboratory test results and serum tumor markers were unremarkable. The patients each underwent orchiectomies, grossly revealing a gray-brownish nodule with well-defined margins surrounded by normal testicular parenchyma.

At histology, the tumors showed a solid, cystic, and pseudopapillary growth pattern with myxohyaline core and microcystic spaces in the first case and a signet ring cell proliferation with nuclear grooves and pseudoinclusion in the second case (Figure). Mitotic activity was inconsistent, necrosis was absent, whereas hyaline periodic acid–Schiff–positive globules were intermingled within cells. Tumor cells strongly displayed nuclear and cytoplasmic expression for β-catenin (Figure E)

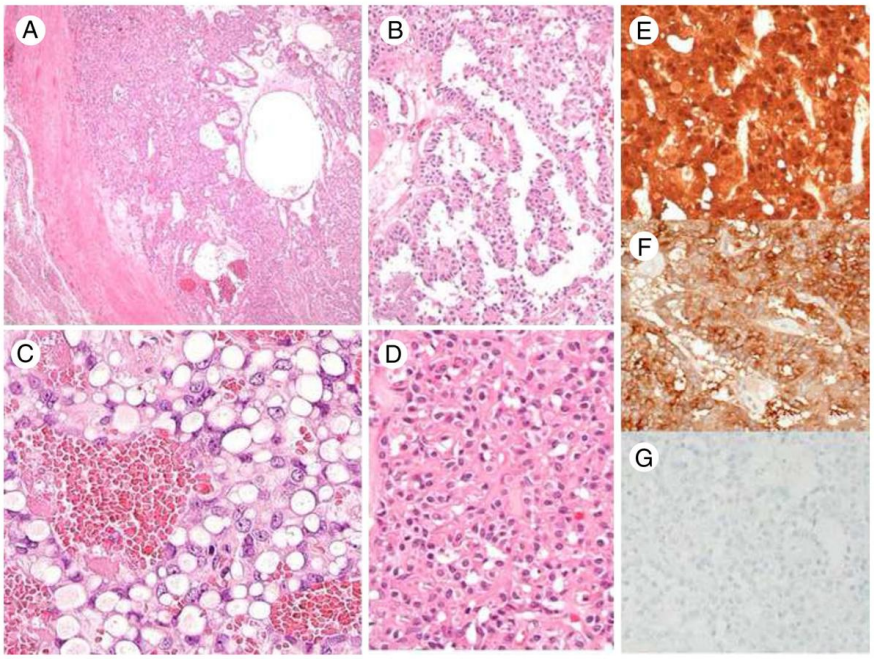

Figure The tumors appear as a well-defined lesion with a fibrous pseudocapsule (A), a pseudopapillary (B) and solid (C) growth pattern, fibrous septa, hemorrhagic foci, microcystic spaces, and signet ring cells (D) (hematoxylin and eosin stain). At immunohistochemistry, tumor cells express β-catenin (E, nuclear and cytoplasmic staining) and CD10 (F) but lack E-cadherin reactivity (G).

and diffusely stained with CD10 (Figure F), CD56, CD117, CD99, progesterone receptors, and cyclin D1 (Figure D). Negative staining was observed with α-inhibin, E-cadherin (Figure G), pan-cytokeratins, SALL-4, OCT-4, CDX2, α-fetoprotein, CD30, β-HCG, DOG-1, calretinin, chromogranin, synaptophysin, glypican-3, and SF1. Mutations in the *CTNNB1* gene exon 3 were identified by direct sequencing. An abdominal computed tomographic scan performed in both patients gave a negative result. These features consistently supported the diagnosis of SPT of the testis. No further therapy was performed after surgery, and the patients are alive and well at 15- and 27-month follow-up, respectively.

In 2010, Deshpande et al [2] first described 3 primary ovarian neoplasms histologically and immunohistochemically identical to SPT of the pancreas. Since then, different examples have been reported in the ovary, leading to the introduction of SPT as a distinct tumor entity in the last *WHO Classification of Tumours of Female Reproductive Organs* [3].

The main differential diagnosis in these cases is with Sertoli cell tumor (SCT), including its sclerosing-type variant, with which SPT may share some morphologic and immunohistochemical features. Interestingly, protein nuclear expression and mutations of *β*-catenin gene have been demonstrated in SCT [4], and signet ring cell stromal tumor is generally considered an uncommon variant of SCT [5]. However, we agree with Michal et al [1] that signet ring cell stromal tumor of the testis does represent an "orphan" neoplasm of uncertain histogenesis, possibly representing a peculiar morphologic variant of SPT in the testis. As in the ovary, the exact pathogenesis of SPT remains unclear, and the lack of a teratoma component does not support the possibility of a neoplastic transformation from ectopic pancreatic tissue. Because several other SPTs of the ovary have been published after the initial description by Deshpande et al [2], it will be not surprising to "officially" recognize the occurrence of SPT also in the testis among tumors showing solid, pseudopapillary, and signet ring cell growth pattern and *β*-catenin alterations.

Maria Cecilia Mengoli, MD
Luca Reggiani Bonetti, MD, PhD
Department of Anatomic Pathology, Azienda Ospedaliero-Universitaria Policlinico di Modena
71-41124 Modena, Italy
E-mail address: cecilia.mengoli@gmail.com

Donatella Intersimone, MD
Franco Fedeli, MD
Operative Unit of Pathologic Anatomy
Azienda Ospedaliera S. Andrea, 19121 La Spezia, Italy

Giulio Rossi, MD, PhD
Pathologic Anatomy, Hospital of Aosta, 11100 Aosta, Italy

http://dx.doi.org/10.1016/j.humpath.2016.08.011

References

[1] Michal M, Bulimbasic S, Coric M, et al. Pancreatic analogue solid pseudopapillary neoplasm arising in the paratesticular location. The first case report. Hum Pathol 2016;56:52-6.
[2] Deshpande V, Oliva E, Young RH. Solid pseudopapillary neoplasm of the ovary: a report of 3 primary ovarian tumors resembling those of the pancreas. Am J Surg Pathol 2010;34:1514-20.
[3] Kurman RJ, Carcangiu ML, Herrington CS, Young RH, editors. WHO classification of tumours of female reproductive organs. 4th ed. Lyon: IARC; 2014.
[4] Kuo CY, Wen MC, Wang J, Jan YJ. Signet-ring stromal tumor of the testis: a case report and literature review. Hum Pathol 2009;40:584-7.
[5] Perrone F, Bertolotti A, Montemurro G, et al. Frequent mutation and nuclear localization of *β*-catenin in Sertoli cell tumors of the testis. Am J Surg Pathol 2014;38:66-70.

Solid pseudopapillary tumor: a new tumor entity in the testis? Reply

To the Editor,

We would like to thank Dr Mengoli et al for their letter to the editor concerning our previously published article [1]. Their observations are valuable, and the authors confirm our suggestion that most signet ring cell tumors of testis [2] are an "orphan neoplasm" representing a peculiar variant of solid pseudopapillary neoplasm (SPN) known for the long time to occur in the pancreas and recently described in the ovary as well [3].

In the meantime, we have collected 13 cases of testicular tumors being entirely (Fig. 1) or partly composed of signet ring cells. Interestingly, the non–signetring cell component in some of these tumors appeared very distinctive. It contained areas characteristically seen in pancreatic SPN including solid, pseudopapillary, oncocytic (oxyphilic) areas, foamy cells, deposits of hemosiderin, trabecular areas, and hyaline globules (Fig. 2A-D). In addition, the immunohistochemical profile comprising CD10, synaptophysin, CD56, *β*-catenin, and neuron-specific enolase positivity and chromogranin, inhibin, calretinin, SF1, and FOXL2 negativity is entirely identical to SPN of the pancreas.

Signet ring cell stromal tumors of the testis were likely misdiagnosed as Sertoli cell tumors, not otherwise specified in the past [4]. It is our view that tumors with such an immunoprofile can hardly be regarded as any tumor with Sertoli cell differentiation, and a much simpler explanation is to consider them as the testicular analogue of SPN.

Kvetoslava Michalova, MD
Department of Pathology, Charles University Medical Faculty and Charles University Hospital Plzen
Pilsen 30460, Czech Republic

CHORIOGONADOTROPIN POZITIVNÍ SEMINOM – KLINICKOPATOLOGICKÁ A MOLEKULÁRNĚ GENETICKÁ STUDIE 15 PŘÍPADŮ

Klasické čisté seminomy jsou typicky negativní v imunohistochemickém (IHC) průkazu lidského choriogonadotropinu (hCG), avšak přítomnost syntitiotrofoblastů (ST), pozitivních v IHC reakci s hCG, je zde dobře doložená [45]. S klasickým seminomem s extenzivní IHC pozitivitou s hCG a zároveň bez přítomnosti ST se však setkáme zřídkakdy. Ze 168 klasických seminomů v plzeňském registrů nádorů jsme vybrali 15 takovýchto případů, které jsme následně rozdělili do 2 skupin:

1. 10 případů s extenzivní imunoreakcí s hCG ve více než 60% nádorových buněk a signifikantní expresí mRNA beta pojednotky hCG (detekováno pomocí RT-PCR). Osm případů bylo stage pT1 a dva pT3a. 6/10 pacientů mělo zvýšenou krevní hladinu hCG.
2. 5 případů s hCG imunoreaktivitou pouze v roztroušených nádorových buňkách a se slabou expresí mRNA beta pojednotky hCG (BCG). Čtyři případy byly stage pT1 a jeden pT2. Jeden pacient měl zvýšené krevní testy na hCG.

Jako negativní kontrolu jsme použili 4 případy klasických seminomů areaktivních s hCG, které jsme již dále nevyšetřovali molekulárně a označili je pracovně jako skupina 3.

Přibližně 7-25% pacientů s klasickým seminomem má v době diagnózy zvýšené krevní hodnoty hCG, což je přičítáno přítomnosti ST [46-48] a/nebo vyššímu stage tumoru. Případy zařazené do této studie však byly prosty ST a většina tumorů byla pT1. Náš výzkum poukazuje na fakt, že IHC exprese hCG v klasických seminomech nemusí být omezena pouze na ST, ale může být produkována „typickými“ neoplastickými buňkami seminomu. IHC pozitivita s hCG může být v těchto tumorech buď difúzní (skupina 1 v naší studii) anebo omezena pouze na některé nadorové buňky (skupina 2 v naší studii). Zdá se, že hCG pozitivní seminomy bez syntitiotrofoblastů se svým biologickým chováním nijak neliší od častějších, hCG negativních seminomů, ačkoliv prognostické závěry se z takto malé studie nedají vyvozovat. Zároveň bychom chtěli zdůraznit již známou, ale často opomíjenou důležitost extenzivního zabločkování tumorů, které zůstává i přes rapidní rozvoj sofistikovaných diagnostických metod stále stěžejním diagnostickým pomocníkem v rukách patologa. Zvláště u pacientů se zvýšenými krevními hodnotami hCG by vždy měla být zvažována možnost přítomnosti neseminomové (zvláště choriokarcinomové) komponenty a vyloučena až na základě prohlednutí velkého množství bloků negativních na přítomnost neseminomové komponenty.

Annals of Diagnostic Pathology 18 (2014) 89–94

Contents lists available at ScienceDirect

Annals of Diagnostic Pathology

Choriogonadotropin positive seminoma—a clinicopathological and molecular genetic study of 15 cases☆,☆☆

Ondrej Hes, MD, PhD [a,b,*], Kristyna Pivovarcikova [a], Jan Stehlik, PhD [a], Petr Martinek, MSc [a], Tomas Vanecek, PhD [a], Kevin Bauleth [a], Olga Dolejsova, MD [c], Fredrik Petersson, MD, PhD [a,d], Milan Hora, MD, PhD [c], Delia Perez Montiel, MD [e], Kvetoslava Peckova, MD [a], Jindrich Branzovsky, MD [a], David Slouka, MD [f], Josef Vodicka, MD, PhD [g], Bohuslava Kokoskova, MSc [a], Radoslav Matej, MD, PhD [h], Michal Michal, MD [a]

[a] Department of Pathology, Charles University, Medical Faculty and Charles University Hospital Plzen, Czech Republic
[b] Biomedical Centre, Faculty of Medicine in Plzen, Charles University in Prague, Plzen, Czech Republic
[c] Department of Urology, Charles University, Medical Faculty and Charles University Hospital Plzen, Czech Republic
[d] Department of Pathology, National University Health System, Singapore
[e] Department of Pathology, Institute Nacional de Cancerologia, Mexico City, Mexico
[f] Department of Otorhinolaryngology, Charles University, Medical Faculty and Charles University Hospital Plzen, Czech Republic
[g] Department of Surgery, Charles University, Medical Faculty and Charles University Hospital Plzen, Czech Republic
[h] Department of Pathology and Molecular Medicine, Thomayer's Hospital, Prague, Czech Republic

ARTICLE INFO

Keywords:
Testis
Seminoma
Human chorionic gonadotropin
Immunohistochemistry
RT-PCR

ABSTRACT

The presence of human chorionic gonadotropin (hCG) positive syncytiotrophoblastic cells (STC) in classic seminoma (CS) is well documented. CS with extensive hCG positive, non-syncytiotrophoblastic tumour cells (without STC) is exceptionally rare. In this study, we present 15 such cases. 168 CSs were retrieved from the Plzen Tumor registry. Cases of mixed germ cell tumors (with CS) and CSs with typical STC were excluded. Cases with completely embedded tumor mass were selected for further study and immunohistochemically examined with anti-hCG. Positive cases were further analyzed by reverse transcriptase polymerase chain reaction. Two groups of hCG-positive CSs were identified. Group 1 comprised 10 patients with a mean patient age of 37.7 years and mean tumor size of 4.96 cm. Eight cases were pT1 (TMN 2009) and 2 cases pT3a. Blood levels of hCG were elevated in 6 of the 10 patients preoperatively. In 2 patients the blood level of hCG was not tested. Mean follow-up period was 6.1 years. No metastatic behavior was noted. All tumors were extensively immunoreactive for hCG in more than 60% of tumor cells. The expression of hCG beta subunit (CGB)—mRNA in tumor tissue was documented. Group 2: Comprised 5 patients with a mean age was 34 years. Mean tumor size was 4.7 cm. Four cases were stage pT1 and 1 case was pT2. The mean follow-up period was 3.1 years. No metastatic behavior was noted. Preoperative blood levels of hCG were elevated in 1/5 of the patient. Strong hCG positivity was limited to scattered single tumor cells distributed throughout the entire tumor. Only weak expression of CGB mRNA was detected. We can conclude that immunohistochemical detection of expression of hCG in CS is not limited to syncytiotrophoblastic cells. In this study, we report two immunohistochemical patterns of hCG expression in classic seminomas: diffuse hCG staining in the majority of tumor cells and scattered hCG-positive cells within the tumor.

1. Introduction

Seminoma is the most common type of testicular germ cell tumor. The peak incidence is around 40 years of age. Pure seminomas account for about 50% of all testicular germ cell tumors. Patients mostly present with a testicular mass. Only about 2% to 3% of seminomas are diagnosed because of symptoms attributed to metastatic disease [1]. Very rarely, gynecomastia occurs, most likely as a result of elevated levels of serum human chorionic gonadotropin (hCG). It is believed that elevated blood-levels of hCG are a result of the activity of intermingled syncytiotrophoblastic cells or large cell mono/multinucleated cells (STC) within the

☆ Disclosure of conflict of interest: All authors declare no conflict of interest.

☆☆ The study was supported by the Charles University Research Fund (project number P36) and by the project by the project CZ.1.05/2.1.00/03.0076 from European Regional Development Fund.

* Corresponding author. Department of Pathology, Charles University, Medical Faculty and Charles University Hospital Plzen, Alej Svobody 80, 304 60 Pilsen, Czech Republic. Tel.: +420 377104643; fax: +420 377104650.
E-mail address: hes@medima.cz (O. Hes).

1092-9134/$ – see front matter © 2014 Elsevier Inc. All rights reserved.
http://dx.doi.org/10.1016/j.anndiagpath.2013.12.004

tumor [2–4]. Such syncytiotrophoblastic cells are present in 10% to 20% of classic seminomas (CS) [5].

In this study, we present 15 cases of hCG positive CSs without typical syncytiotrophoblastic cells. The majority of the patients showed elevated level of hCG in blood preoperatively.

2. Material and methods

All cases that had been coded as seminoma during 1997 to 2013 were retrieved from the institutional archive of the Charles University Department of Pathology and University Hospital in Plzen and reviewed. All mixed germ cell tumors were excluded from the study. Total number of 168 CSs were found. Only cases where the tumorous mass was completely embedded were further examined. Seminomas with typical syncytiotrophoblastic elements were also excluded from the study. Hence, only cases with pure classic seminoma pattern were further submitted to immunohistochemical examination. The remaining cases consisted of 98 classic seminomas. The immunohistochemical study was performed using a Ventana Benchmark XT automated stainer (Ventana Medical System, Inc, Tucson, AZ, USA) on formalin-fixed, paraffin-embedded tissue. Antibody against hCG (polyclonal-isolated beta chain, 1:10 000, DakoCytomation, Glostrup, Denmark) was applied.

Blocks from human placental tissue were used as positive control. Non-neoplastic testicular or adnexal tissue was used as internal negative control in each case.

Slides from each case were evaluated as follows:

Negative = no cells expressed hCG; Focally positive = less than 60% of the tumor cells expressed hCG or when scattered single cell positivity were identified; Diffusely positive = more than 60% of the tumor cells expressed hCG.

2.1. Molecular genetic study (reverse transcriptase polymerase chain reaction)

15 cases of hCG positive seminomas were further examined by reverse transcriptase polymerase chain reaction (RT-PCR). Four immunohistochemically hCG negative seminomas were used as negative control. This cohort was labeled as Group 3 (see below).

RNA from tumor and non-tumor tissue was extracted and treated by DNase according to the manufacturer's instructions using the RecoverAll Total Nucleic Acid Isolation Kit (Ambion, Austin, TX, USA). cDNA was synthesized using the Transcriptor First Strand cDNA Synthesis Kit (RNA input 2 μg) (Roche Diagnostics, Mannheim, Germany).

Each PCR reaction consisted of 3.5 μL of sterile PCR water, 10 μL of "iQ SYBR Green Supermix" (Bio-Rad Laboratories, Alfred Nobel Drive, Hercules, CA, USA), 0.75 μL of each primer (10 μmol/L) and 5 μL of cDNA. All amplifications were carried out on a Rotor-Gene Q instrument (Qiagen, Hilden Germany) for 40 cycles (95°C for 20 seconds, 60°C for 30 seconds, and 72°C for 30 seconds) following an initial denaturation/Taq activation step (94°C for 4 minutes). Primers used for chorionic gonadotropin beta subunit (CGB) amplification (CGB-F1 5′-GCTACTGCCCCACCATGACC-3′ and CGB-R1 5′-GGACTC-GAAGCGCACATCG-3′) are specific and do not amplify sequentially very similar luteinizing hormone-B mRNA [6]. The abundance of B2M reference transcript (β2-microglobulin) was also quantified in each sample as described previously [7]; the following primers were used: B2M-F 5′-GTCTCGCTCCGTGGCCTTA-3′ and B2M-R 5′-TGAATCTTTG-GAGTACGCTGGATA-3′. To further prevent amplification of genomic DNA, CGB-F1 and B2M-R primers were designed to anneal specifically to a template corresponding to the spliced transcript only. Product sizes of specific PCR products (CGB = 92 bp, B2M = 81 bp) were confirmed by 2% agarose gel electrophoresis.

Rotor-gene Q series original software (version 1.7) was used for data analysis. First, efficiencies of individual primer pairs were calculated from slopes of PCR curves (CGB = 1.66 and B2M = 1.7) in "Comparative analysis" mode of the software. Then, expression ratio of target CGB mRNA to reference B2M mRNA was calculated for each sample from the respective PCR efficiencies and crossing points according to Pffafl [8].

2.2. Statistical analysis

Differences in CGB mRNA expression among each group [1–3] and between tumor and normal tissue within each group were analyzed with Kruskal-Wallis exact test and Wilcoxon exact test, respectively.

3. Results

Of the 168 cases that had been coded as "classic seminoma", which were retrieved and reviewed for the study, 10 cases of pure seminomas with extensive hCG positive areas were found (Group 1).

Basic clinicopathologic data for this group are summarized in Table 1.

The mean age of the patients was 37.7 years, median 36.5 years. Mean size of the tumors was 4.96 cm, median 3.8 cm.

Eight cases were stage pT1 (TNM 2009); 2 cases were pT3a. No distant metastases had been documented at the time of surgery and during the follow-up period. Six tumors were located in the right and 4 in the left testicle.

Table 1
Group 1—diffusely hCG positive seminomas—basic clinicopathological features

	Age	Side	Size (cm)	Stage (TNM 09)	hCG blood (IU/L)[+]	Recurrence/metastasis	Follow-up
Case 1	35	Sin.	0.8 × 0.5 × 0.6	pT1	2	0	2 m AW (0.2 y)
Case 2	33	Dx.	4.7 × 4 × 4	pT1	151	0	5.7 y AW
Case 3	35	Dx.	5.5 × 2.5 × 3	pT1	378	0	3 y AW[*]
Case 4	51	Dx.	4 × 2.1 × 2.2	pT1	NA	0	3.5 y AW
Case 5	23	Sin.	3.3 × 1.5 × 1	pT1	10	0	5.4 y AW
Case 6	44	Dx.	12.5 × 7 × 8	pT1	9	0	4 y AW
Case 7	42	Dx.	3.6 × 2.5 × 2	pT1	13	0	2 y AW
Case 8	46	Sin.	7 × 9 × 5	pT3, pN0	NA	0	12 y AW
Case 9	38	Dx.	3 × 2.5 × 1,5	pT3, pN0	142	0	12.5 y AW
Case 10	30	Sin.	3.2 × 2.2 × 2.5	pT1	Not elevated[§]	0	13 y AW

Dx, right; sin, left; AW, alive and well; LE, lost of evidence; NA, not available preoperatively; y, year/years; m, month.
[*] Patient underwent left radical orchidectomy for classic seminoma 9 years ago, no expression of hCG has been noted.
[+] Normal level: 0–5 IU/L.
[§] Not elevated, as was expressed in clinical record.

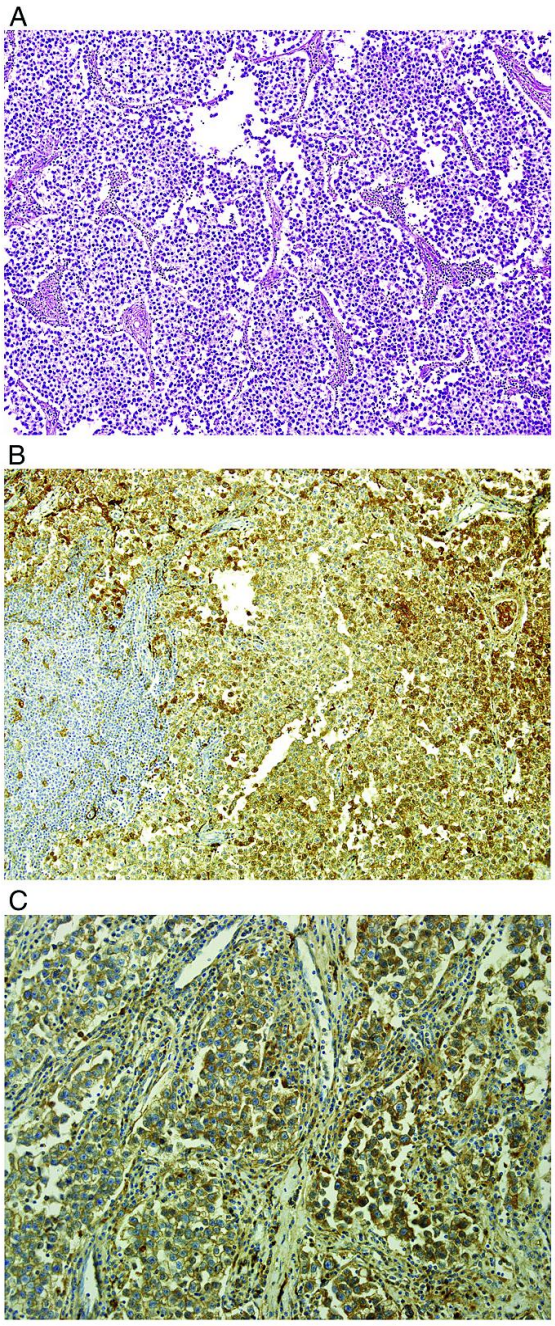

Fig. 1. Diffusely positive classic seminoma. A, Hematoxylin-eosin. B, Immunohistochemical staining with hCG. C, Detail of hCG diffusely positive area in classic seminoma.

Follow-up was available for 10/10 of the patients. The average follow-up was 6.13 years, median 4.7 years. No metastatic behavior was noted in any of the patients.

Serum levels of hCG were elevated in 6/10 of the patients at the time of diagnosis. In 2 patients, the preoperative blood level of hCG had not been analyzed.

Table 2
Group 1—diffusely hCG positive seminomas—morphology and immunoreactivity

	Pattern	Necrosis	Extend	Intensity
Case 1	Solid	0	Diffuse	Strong
Case 2	Solid	+	Diffuse	Moderate/strong
Case 3	Solid/tubular	0	Diffuse	Moderate/strong
Case 4	Solid	0	Diffuse	Moderate/strong
Case 5	Solid	0	Diffuse	Strong
Case 6	Solid	0	Focal	Strong
Case 7	Solid	0	Diffuse	Moderate/strong
Case 8	Solid	+	Focal	Strong
Case 9	Solid	0	Diffuse	Moderate/strong
Case 10	Solid/Tubular	+	Focal	Strong

Morphologically, all cases were exclusively composed of the characteristic monotonous, atypical, neoplastic seminoma-cells exhibiting clear cytoplasm with variable lymphocytic infiltration. Limited areas (<10% of tumor volume) of necrosis were present in 3 cases. The architecture was predominantly solid, with 2 cases (nos. 3 and 10) showing focal tubular pattern (Fig. 1A). The tubular architecture was most prominent in case 10. No typical syncytiotrophoblastic tumor cells were present in any of the cases.

Results of the immunohistochemical study are summarized in Table 2.

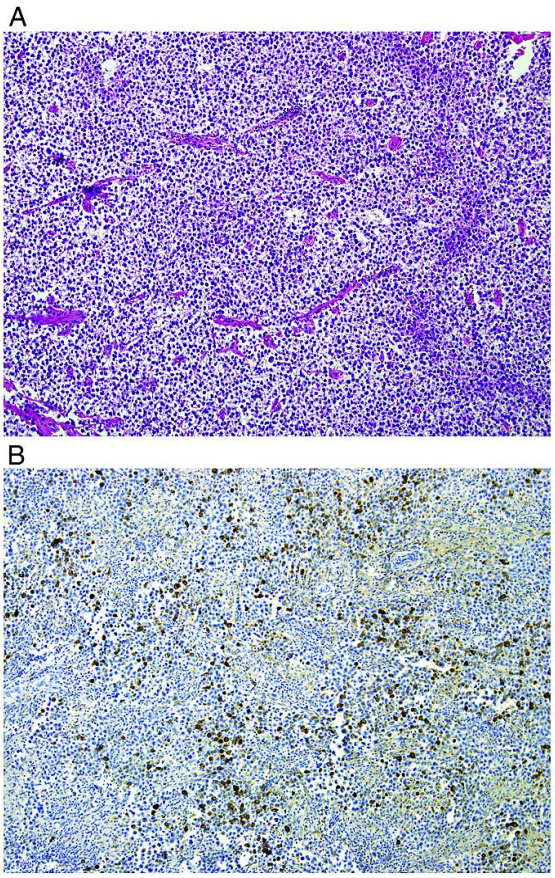

Fig. 2. Focally positive classic seminoma. A, Hematoxylin-eosin. B, Immunohistochemical staining with hCG showed scattered single strongly positive cells.

Table 3
Group 2—focally hCG positive seminomas—basic clinicopathological features

	Age	Side	Size (cm)	Stage (TNM 09)	hCG blood (IU/L)[+]	Recurrence/metastasis	Follow-up
Case 1	26	Dx.	4.5 × 4 × 3	pT1	2	LE	LE
Case 2	35	Dx.	6.5 × 4.5 × 4	pT1	3	0	2 y AW
Case 3	29	Dx.	9 × 4.5 × 4	pT2	17	0	1 y AW
Case 4	48	Dx.	2 × 1.5 × 1	pT1	0.5	0	1.3 y AW
Case 5	32	Sin.	1.5 × 1.3 × 1	pT1	0	0	8.3 y AW

Abbreviations: Dx, right; sin, left; AW, alive and well; LE, lost of evidence; y, year/years.
[+] Normal level: 0–5 IU/L.

Diffuse reactivity for/expression of hCG (more than 60% of the tumor cells was identified in 7 cases, focal immunoreactivity (<60%) was present in 3 cases. The immunohistochemically labeled hCG was cytoplasmatic (Fig. 1B and C).

A second group (5 cases) exhibited scattered strongly hCG-expressing tumor cells was also identified. Basic clinicopathologic data are summarized in the Table 3 (Group 2). The mean age of the patients was 34 years, median 32 years. The mean size of the tumors was 4.7 cm, median 4.5 cm. Four cases were of pT1 stage (according TNM 2009), 1 case of pT2. No distant metastases were noted at the time of surgery. Four cases were located in the right testicle, 1 case in the left testicle. Follow-up was available for 4 of the 5 patients, with an average period of 3.15 years, median 1.65 years. No metastatic behavior was noted in any patients. Serum level of hCG was elevated in 1 of the 5 patients at the time of diagnosis.

Morphologically, all cases in this group were exclusively composed of typical seminoma-cells with clear cytoplasm and with variable lymphocytic infiltration (Fig. 2A). Small foci of necrosis (<5% of tumor volume) were present in 1 case. The architecture was exclusively with no unusual patterns in any of the tumors. No typical syncytiotrophoblastic or giant cells were present.

All cases from this group showed identical pattern of immunoreactivity. Scattered single tumor cells with strong cytoplasmic immunoreactivity for hCG were present diffusely throughout the tumor (Fig. 2B).

Group 3 consisted of 4 patients with CS and was used as a negative control. Basic clinicopathologic data are shown in the Table 4. The mean age of the patients was 34.8 years, median 36 years. The mean size of the tumors was 7.3 cm, median 7.8 cm.

One case was pT1 (according TNM 2009), one case pT2, cN1, one case pT3, and one case pT3, cN2. Follow up was available for 4/4 of the patients, with an average period of 3.1 years. No progression of the disease was documented in any of the 4 patients. The architecture was mostly solid and/or alveolar. No expression of hCG was identified in any of the tumors.

Table 4
Group 3: hCG negative seminomas (negative control)- Basic clinicopathological features

	Age	Side	Size (cm)	Stage (TNM 09)	hCG blood (IU/L)[+]	Recurrence/metastasis	Follow-up
Case 1	30	Sin.	11 × 6 × 6	pT3N2	6.0	0	1.3 y AW
Case 2	37	Dx.	2.5 × 1.5 × 1.5	pT3	Not elevated[§]	0	6.8 y AW
Case 3	36	Sin.	8.5 × 3.5 × 4	pT1	5.0	0	1.4 y AW
Case 4	36	Dx.	7 × 4.2 × 4	pT2N1	NA	0	3 y AW

Dx, right; sin, left; AW, alive and well; LE, lost of evidence; NA, not available preoperatively; y, year/years.
[+] Normal level: 0–5 IU/L.
[§] Not elevated, as was expressed in clinical record.

3.1. Molecular genetics

Results of molecular genetics study are depicted in Table 5 and Fig. 3. In Group 1, expression of CGB was detected at mRNA level in tumor tissue and practically no expression was found in non-tumor tissue. In Group 2, weak expression of CGB was detected in tumor tissue and no expression was found in non-tumor tissue. In Group 3, no CGB transcript was observed.

3.2. Statistical analysis

Comparison of CGB mRNA expression among groups 1, 2, and 3 showed statistically significant differences ($P < .001$) (Fig. 4). Comparison of CGB mRNA expression between tumor and normal tissue within each group revealed statistically significant differences in Group 1 ($P < .001$) and Group 2 ($P = .0476$) while no significant change were found in Group 3 ($P = 1.0$).

4. Discussion

Pure CSs are generally believed to be immunohistochemically negative for hCG. However, it is well known that CSs with syncytiotrophoblasts are common and the syncytiotrophoblasts are indeed strongly immunoreactive for hCG. Moreover, there is a spectrum of trophoblastic cells within CSs ranging from large mono or binucleated cells to large, typical multinucleated syncytiotrophoblastic cells [9–11].

From our cohort of 168 cases of CS, all cases with mixed germ cell morphology and cases with typical well-recognizable

Table 5
Relative expression level of CGB mRNA in tumor and normal tissue of groups 1, 2, and 3

	Tumor tissue	Normal tissue
Group 1		
Case 1	0.0477199	0.0016174
Case 2	NA	0.0000000
Case 3	0.4502905	0.0025535
Case 4	0.0903906	0.0000000
Case 5	0.0289434	0.0000000
Case 6	0.0077732	0.0000000
Case 7	0.0296978	0.0000000
Case 8	0.0663216	0.0000000
Case 9	0.0702606	0.0000000
Case 10	0.0243507	0.0000000
Group 2		
Case 1	0.0000000	0.0000000
Case 2	0.0077106	0.0000000
Case 3	0.0051808	0.0000000
Case 4	0.0113600	0.0000000
Case 5	0.0542344	0.0000000
Group 3		
Case 1	0.0000000	0.0000000
Case 2	0.0000000	0.0000000
Case 3	0.0000000	0.0000000
Case 4	0.0000000	0.0000000

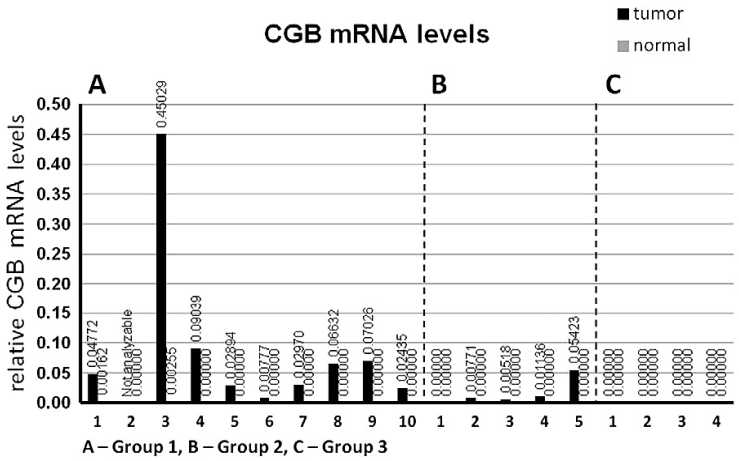

Fig. 3. Relative expression of CGB mRNA in tumor and non-tumor tissue.

syncytiotrophoblastic elements were excluded. The remaining cases consisted of 98 classic seminomas. Ten tumors displayed immunohistochemically extensively positive areas (>60% of tumor cells; group 1). Five cases contained scattered tumor cells which exhibited strong expression of hCG throughout the tumors (Group 2). Importantly, all cases were typical pure classic seminomas by morphology.

The immunohistochemically detected expression of hCG was confirmed with mRNA expression analysis. We detected statistically significant increased CGB levels in both group 1 and 2, although the magnitude of the increased of CGB level in group 2 was of borderline value when compared to non-neoplastic, testicular tissue. The molecular study also confirmed statistically significant differences in the extent of immunohistochemically detected hCG between groups 1, 2, and 3.

Increased CGB mRNA expression was demonstrated in most of the tumor tissue samples in both groups 1 and 2. As expected, no expression was found in group 3 and normal control tissue. However, a detailed analysis of RT-PCR results revealed the following: (1) case 2 in group 1 was not analyzable due to the low quality of RNA. (2) There were 2 cases in group 2 (cases 1 and 3) in which a negligible presence of CGB mRNA was found in normal tissue. The most probable explanation for this is minor contamination of normal tissue with infiltrating tumor cells. (3) The tumor tissue of Case 1 in Group 2 did not reveal any CGB mRNA expression even though the immunohistochemical result was positive. We cannot easily explain this, but this phenomenon may be due to very low levels of CGB expression, which were under detection limits of the method.

Approximately 7% to 25% of all patients with classic seminoma have elevated serum levels of hCG at the time of diagnosis. It is believed that higher stages and/or more voluminous tumor burden are associated with elevated hCG levels in the peripheral blood [12]. If blood is sampled from the testicular vein, 80% to 85% of patients have elevated hCG level [13,14]. In our series, 8 of 10 patients were of stage pT1 (TNM 2009); only 2 cases were pT3. The median size of our cases was 3.8 cm. In our series, all blood tests were taken routinely from the region of vena mediana cubiti. In 7 of our patients, elevated level of hCG was detected. Preoperative serum hCG levels were not available in 2 patients. Normal serum hCG levels (0-5 IU/L) was found in 6 of 15 patients.

In a group of 10 extensively hCG positive cases in our series (group 1), elevated blood level of hCG was noted preoperatively in 6 patients. In 2 patients, blood levels were within physiological limits. In 2 patients, preoperative blood levels were not available. Among 5 cases

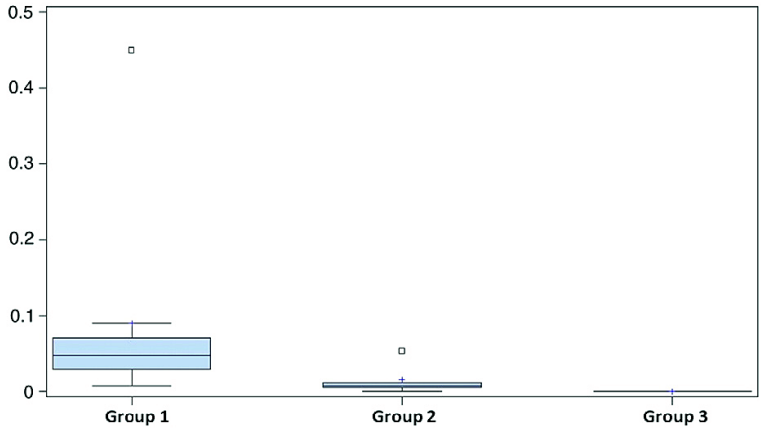

Fig. 4. Comparison of CGB mRNA expression among groups 1, 2, and 3.

with focal, scattered hCG expressing cells in the immunohistochemical study (group 2), only 1 patient presented with elevated preoperative blood level of hCG.

Seminomas without syncytiotrophoblastic cells producing hCG are known from previous studies. Hori et al. examined cohort of 45 patients with histologically confirmed seminomas. Eleven patients had elevated blood β-hCG level. In 24% of their cases, the seminomatous tumors contained syncytiotrophoblasts, in 80% of the tumors, mononuclear, β-hCG positive cells were detected. In their study, 22% of seminomas displayed both mononuclear β-hCG positive and syncytiotrophoblastic cells. Mononuclear beta-hCG positive cells were described as "…constituted a small proportion of mononuclear seminoma cells…" [15]. An identical pattern of hCG expression (single mononuclear cells diffusely distributed within tumor) was found in the seminomas of our group 2.

An interesting fact is the relatively high percentage of pure classic seminomas with hCG expressing, non-syncytiotrophoblastic cells in our series. Of the 168 analyzed cases, 10 (6%) were extensively positive for hCG and 5 cases (3%) were focally positive, which altogether reached 9%.

Finally we want to stress the importance of extensive sampling of germ cell tumors generally. Even in tumors with appearance of CS unusual findings (eg, minor non-seminomatous components) could be disclosed. Especially in patients with elevated blood levels of hCG, it is of critical importance to rule out the possibility of mixed germ cell tumor with a non-seminomatous component (especially choriocarcinoma) because of the different therapeutic approach. However, based on our results, we have clearly established that not all cases of germ cell tumors with elevated blood levels of hCG are of the mixed germ cell tumor category or CS containing syncitiotrophoblasts.

Based on the findings of our study, we can conclude that:

1. Immunohistochemically detected hCG expression in classic seminomas is not limited to the syncytiotrophoblastic or large mono-/multinucleated cells, but is produced by the "typical" seminoma-cells.
2. There are two immunohistochemical patterns of hCG expression in classic seminomas: (A) diffuse hCG staining in the majority of tumor cells and (B) scattered hCG-positive cells within the tumor.
3. Although our series contain a limited number of cases, the clinical behavior of extensively hCG positive seminomas appears not to differ significantly from the more common hCG-negative counterpart. This should, however, be investigated/confirmed in larger series.

References

[1] Ulbright TM, Amin MB, Young RH. Tumors of the testis, adnexa, spermatic cord, and scrotum. Washington D.C.: AFIP; 1999.
[2] Javadpour N. Human chorionic gonadotropin in seminoma. J Urol 1984;131:407.
[3] Mann K, Siddle K. Evidence for free beta-subunit secretion in so-called human chorionic gonadotropin-positive seminoma. Cancer 1988;62:2378–82.
[4] Scheiber K, Mikuz G, Frommhold H, Bartsch G. Human chorionic gonadotropin-positive seminoma: is this a special type of seminoma with a poor prognosis? Prog Clin Biol Res 1985;203:97–104.
[5] von Hochstetter AR, Sigg C, Saremaslani P, Hedinger C. The significance of giant cells in human testicular seminomas. A clinico-pathological study. Virchows Arch A Pathol Anat Histopathol 1985;407:309–22.
[6] Costa CJM, Benachi A, Olivi M, Dumez Y, Vidaud M, Gautier E. Fetal expressed gene analysis in maternal blood: a new tool for noninvasive study of the fetus. Clin Chem 2003;49:981–3.
[7] Cheng CJ, Wu YC, Shu JA, Ling TY, Kuo HC, Wu JY, et al. Aberrant expression and distribution of the OCT-4 transcription factor in seminomas. J Biomed Sci 2007;14:797–807.
[8] Pfaffl MW. A new mathematical model for relative quantification in real-time RT-PCR. Nucleic Acids Res 2001;29:e45.
[9] Eble JN, Sauter G, Epstein JI, Sesterhenn I. WHO Classification of Tumours. Tumours of the urinary system and male genital organs. Pathology and Genetics. Lyon: IARC Press; 2004.
[10] Sehested M, Jacobsen GK. Ultrastructure of syncytiotrophoblast-like cells in seminomas of the testis. Int J Androl 1987;10:121–6.
[11] Ulbright TM. Germ cell neoplasms of the testis. Am J Surg Pathol 1993;17:1075–91.
[12] Weissbach L, Bussar-Maatz R, Lohrs U, Schubert GE, Mann K, Hartmann M, et al. Prognostic factors in seminomas with special respect to HCG: results of a prospective multicenter study. Seminoma Study Group. Eur Urol 1999;36:601–8.
[13] Hartmann M, Pottek T, Bussar-Maatz R, Weissbach L. Elevated human chorionic gonadotropin concentrations in the testicular vein and in peripheral venous blood in seminoma patients. An analysis of various parameters. Eur Urol 1997;31:408–13.
[14] Mumperow E, Hartmann M. Spermatic cord beta-human chorionic gonadotropin levels in seminoma and their clinical implications. J Urol 1992;147:1041–3.
[15] Hori K, Uematsu K, Yasoshima H, Yamada A, Sakurai K, Ohya M. Testicular seminoma with human chorionic gonadotropin production. Pathol Int 1997;47:592–9.

ZÁVĚR

Doktorská dizertační práce uzavírá postgraduální studium z oboru patologie MUDr. Květoslavy Michalové (rozené Peckové). Během studia byly splněny požadované cíle. S pomocí spoluautorů jsme zdokumentovali biologické chování, morfologii a cytogenetiku některých neobvyklých tumorů urogenitálního traktu.

Výsledkem tříletého studia je 7 prvoautorských prací, z nichž 5 se týká nádorů ledvin a 2 nádorů varlat. Dále se autorka podílela jako spoluautor na 13 publikacích. Výsledky všech studií představených v doktorské dizertační práci byly publikovány v zahraničních odborných časopisech s impact faktorem.

PODĚKOVÁNÍ

Prof. MUDr. Ondřejovi Hesovi, Ph.D.
Prof. MUDr. Aleně Skálové, CsC.
Prof. MUDr. Michalovi Michalovi
Univerzitě Karlově v Praze, Lékařské fakultě v Plzni
Svým spolupracovníkům Šiklova ústavu patologie a Bioptické laboratoře, s.r.o. v Plzni
Své rodině a nejbližším

REFERENCE

1. David G. Bostwick JNE. Urologic Surgical Pathology. St.Louis: Mosby-Year Book, 1997.
2. Kovacs G, Akhtar M, Beckwith BJ, et al. The Heidelberg classification of renal cell tumours. J Pathol 1997; 183, 131-133.
3. Bianco R, Melisi D, Ciardiello F, Tortora G. Key cancer cell signal transduction pathways as therapeutic targets. Eur J Cancer 2006; 42, 290-294.
4. Moch H, Humphrey, P.A., Ulbright, T.M., Reuter, V.E. WHO Classification of Tumours of the Urinary System and Male Genital Organs. Fourth edition. 2016, p. 400.
5. Michal M, Bulimbasic S, Coric M, et al. Pancreatic analogue solid pseudopapillary neoplasm arising in the paratesticular location. The first case report. Hum Pathol 2016; 56, 52-56.
6. Canzonieri V, Volpe R, Gloghini A, Carbone A, Merlo A. Mixed renal tumor with carcinomatous and fibroleiomyomatous components, associated with angiomyolipoma in the same kidney. Pathol Res Pract 1993; 189, 951-956; discussion 957-959.
7. Petersson F, Branzovsky J, Martinek P, et al. The leiomyomatous stroma in renal cell carcinomas is polyclonal and not part of the neoplastic process. Virchows Arch 2014; 465, 89-96.
8. Hakimi AA, Tickoo SK, Jacobsen A, et al. TCEB1-mutated renal cell carcinoma: a distinct genomic and morphological subtype. Mod Pathol 2015; 28, 845-853.
9. Argani P, Hawkins A, Griffin CA, et al. A distinctive pediatric renal neoplasm characterized by epithelioid morphology, basement membrane production, focal HMB45 immunoreactivity, and t(6;11)(p21.1;q12) chromosome translocation. Am J Pathol 2001; 158, 2089-2096.
10. Argani P, Reuter VE, Zhang L, et al. TFEB-amplified Renal Cell Carcinomas: An Aggressive Molecular Subset Demonstrating Variable Melanocytic Marker Expression and Morphologic Heterogeneity. Am J Surg Pathol 2016; 40, 1484-1495.
11. Bulimbasic S, Ljubanovic D, Sima R, et al. Aggressive high-grade mucinous tubular and spindle cell carcinoma. Hum Pathol 2009; 40, 906-907.
12. Parada DD, Pena KB. Chromophobe renal cell carcinoma with neuroendocrine differentiation. Apmis 2008; 116, 859-865.
13. Mokhtar GA, Al-Zahrani R. Chromophobe renal cell carcinoma of the kidney with neuroendocrine differentiation: A case report with review of literature. Urol Ann 2015; 7, 383-386.
14. Kuroda N, Tamura M, Hes O, Michal M, Gatalica Z. Chromophobe renal cell carcinoma with neuroendocrine differentiation and sarcomatoid change. Pathol Int 2011; 61, 552-554.
15. Ohe C KN, Keiko M, Tomoki K, Masatsugu M, Shun S, Teharata S, Hosaka N, Hes O, Michal M, Mastsuda T, Uemura T. Chromophobe renal cell carcinoma with neuroendocrine differentiation/morphology: A clinicopathological and genetic study of three cases. Human Pathology: Case Reports 2014; 1, 31-39.
16. Srigley JR, Delahunt B, Eble JN, et al. The International Society of Urological Pathology (ISUP) Vancouver Classification of Renal Neoplasia. Am J Surg Pathol 2013; 37, 1469-1489.

17. Delahunt B. Advances and controversies in grading and staging of renal cell carcinoma. Mod Pathol 2009; 22 Suppl 2, S24-36.
18. Delahunt B, Bethwaite PB, Nacey JN. Outcome prediction for renal cell carcinoma: evaluation of prognostic factors for tumours divided according to histological subtype. Pathology 2007; 39, 459-465.
19. Doros LA, Rossi CT, Yang J, et al. DICER1 mutations in childhood cystic nephroma and its relationship to DICER1-renal sarcoma. Mod Pathol 2014; 27, 1267-1280.
20. Trpkov K, Yilmaz A, Uzer D, et al. Renal oncocytoma revisited: a clinicopathological study of 109 cases with emphasis on problematic diagnostic features. Histopathology 2010; 57, 893-906.
21. David Bostwick LC. Urologic Surgical Pathology. 2008.
22. Hes O, Brunelli M, Michal M, et al. Oncocytic papillary renal cell carcinoma: a clinicopathologic, immunohistochemical, ultrastructural, and interphase cytogenetic study of 12 cases. Ann Diagn Pathol 2006; 10, 133-139.
23. Pivovarcikova K, Peckova K, Martinek P, et al. "Mucin"-secreting papillary renal cell carcinoma: clinicopathological, immunohistochemical, and molecular genetic analysis of seven cases. Virchows Arch 2016; 469, 71-80.
24. Ulamec M, Skenderi F, Trpkov K, et al. Solid papillary renal cell carcinoma: clinicopathologic, morphologic, and immunohistochemical analysis of 10 cases and review of the literature. Ann Diagn Pathol 2016; 23, 51-57.
25. Klatte T, Said JW, Seligson DB, et al. Pathological, immunohistochemical and cytogenetic features of papillary renal cell carcinoma with clear cell features. J Urol 2011; 185, 30-35.
26. Hes O, Condom Mundo E, Peckova K, et al. Biphasic Squamoid Alveolar Renal Cell Carcinoma: A Distinctive Subtype of Papillary Renal Cell Carcinoma? Am J Surg Pathol 2016; 40, 664-675.
27. Petersson F, Bulimbasic S, Hes O, et al. Biphasic alveolosquamoid renal carcinoma: a histomorphological, immunohistochemical, molecular genetic, and ultrastructural study of a distinctive morphologic variant of renal cell carcinoma. Ann Diagn Pathol 2012; 16, 459-469.
28. Argani P, Antonescu CR, Illei PB, et al. Primary renal neoplasms with the ASPL-TFE3 gene fusion of alveolar soft part sarcoma: a distinctive tumor entity previously included among renal cell carcinomas of children and adolescents. Am J Pathol 2001; 159, 179-192.
29. Argani P, Antonescu CR, Couturier J, et al. PRCC-TFE3 renal carcinomas: morphologic, immunohistochemical, ultrastructural, and molecular analysis of an entity associated with the t(X;1)(p11.2;q21). Am J Surg Pathol 2002; 26, 1553-1566.
30. Wu A, Kunju LP, Cheng L, Shah RB. Renal cell carcinoma in children and young adults: analysis of clinicopathological, immunohistochemical and molecular characteristics with an emphasis on the spectrum of Xp11.2 translocation-associated and unusual clear cell subtypes. Histopathology 2008; 53, 533-544.
31. Argani P, Aulmann S, Illei PB, et al. A distinctive subset of PEComas harbors TFE3 gene fusions. Am J Surg Pathol 2010; 34, 1395-1406.
32. Gaillot-Durand L, Chevallier M, Colombel M, et al. Diagnosis of Xp11 translocation renal cell carcinomas in adult patients under 50 years: interest and pitfalls of automated immunohistochemical detection of TFE3 protein. Pathol Res Pract 2013; 209, 83-89.
33. Michal M, Hes O, Svec A, Ludvikova M. Pigmented microcystic chromophobe cell carcinoma: a unique variant of renal cell carcinoma. Ann Diagn Pathol 1998; 2, 149-153.
34. Kuroda N, Tanaka A, Yamaguchi T, et al. Chromophobe renal cell carcinoma, oncocytic variant: a proposal of a new variant giving a critical diagnostic pitfall in diagnosing renal oncocytic tumors. Med Mol Morphol 2013; 46, 49-55.

35. Hes O, Vanecek T, Perez-Montiel DM, et al. Chromophobe renal cell carcinoma with microcystic and adenomatous arrangement and pigmentation--a diagnostic pitfall. Morphological, immunohistochemical, ultrastructural and molecular genetic report of 20 cases. Virchows Arch 2005; 446, 383-393.
36. Dundr P, Pesl M, Povysil C, et al. Pigmented microcystic chromophobe renal cell carcinoma. Pathol Res Pract 2007; 203, 593-597.
37. Kuroda N, Iiyama T, Moriki T, Shuin T, Enzan H. Chromophobe renal cell carcinoma with focal papillary configuration, nuclear basaloid arrangement and stromal osseous metaplasia containing fatty bone marrow element. Histopathology 2005; 46, 712-713.
38. Thoenes W, Storkel S, Rumpelt HJ, et al. Chromophobe cell renal carcinoma and its variants--a report on 32 cases. J Pathol 1988; 155, 277-287.
39. Michal M, Hes O, Kazakov DV. Primary signet-ring stromal tumor of the testis. Virchows Arch 2005; 447, 107-110.
40. Deshpande V, Oliva E, Young RH. Solid pseudopapillary neoplasm of the ovary: a report of 3 primary ovarian tumors resembling those of the pancreas. Am J Surg Pathol 2010; 34, 1514-1520.
41. He S, Yang X, Zhou P, Cheng Y, Sun Q. Solid pseudopapillary tumor: an invasive case report of primary ovarian origin and review of the literature. Int J Clin Exp Pathol 2015; 8, 8645-8649.
42. Kominami A, Fujino M, Murakami H, Ito M. beta-catenin mutation in ovarian solid pseudopapillary neoplasm. Pathol Int 2014; 64, 460-464.
43. Cheuk W, Beavon I, Chui DT, Chan JK. Extrapancreatic solid pseudopapillary neoplasm: report of a case of primary ovarian origin and review of the literature. Int J Gynecol Pathol 2011; 30, 539-543.
44. Kopczynski J, Kowalik A, Chlopek M, et al. Oncogenic Activation of the Wnt/beta-Catenin Signaling Pathway in Signet Ring Stromal Cell Tumor of the Ovary. Appl Immunohistochem Mol Morphol 2016; 24, e28-33.
45. von Hochstetter AR, Sigg C, Saremaslani P, Hedinger C. The significance of giant cells in human testicular seminomas. A clinico-pathological study. Virchows Arch A Pathol Anat Histopathol 1985; 407, 309-322.
46. Javadpour N. Human chorionic gonadotropin in seminoma. J Urol 1984; 131, 407.
47. Mann K, Siddle K. Evidence for free beta-subunit secretion in so-called human chorionic gonadotropin-positive seminoma. Cancer 1988; 62, 2378-2382.
48. Scheiber K, Mikuz G, Frommhold H, Bartsch G. Human chorionic gonadotropin-positive seminoma: is this a special type of seminoma with a poor prognosis? Prog Clin Biol Res 1985; 203, 97-104.